

Blurb page here - a few paragraphs giving brief description of book

DRAFT

Copyright - Paul M. Bellan

September 30, 2004

⇒contents subject to change⇐

This draft copy is being submitted for evaluation of print quality and identification of any other issues-please do not use for final publication!! It was composed as follows:

1. Written using Scientific WorkPlace V5 (this produces Latex output and then a dvi file), Scientific WorkPlace web site is at <http://www.mackichan.com/>
2. A 'Style File' file was created using Style Editor in Scientific WorkPlace; this file has been continuously revised to improve the appearance (e.g., margins, headers, location of page numbers, etc.).

3. The dvi file created by Latex was then printed to a postscript file using AdobePS generic postscript driver on Windows 2000 operating system.

4. AdobePS was tweaked as suggested in the website <http://www.cs.biu.ac.il/~herzbea/makeP.htm> which stated following for maximizing quality of output:

"After you install the printer, you may want to fine-tune its properties. To do so, open again the Printers setting folder, and right click on the printer; select 'Properties'. Under 'Device Settings', set very low values (e.g. 5) to the following two parameters:

Minimum font size to download as outline

Maximum font size to download as bitmap

Next, go to the 'Advanced' tab, and from there, select 'Printing Defaults...'. In the window that opens, select 'Document options', then 'Postscript options'. Set the following two options:

PostScript Output Option: Optimize for Portability

TrueType Font Download Option: Outline"

Note: the above suggestions were for MS Imagesetter driver, but this driver failed to print some figures properly so the AdobePS was substituted instead and works much better.

5. The postscript file can be read with no difficulties using GhostScript 4.3 on my Pentium IV running Windows 2000 and gives good quality printed output from Ghostscript on my HP Laserjet 6MP postscript printer (600dpi).

Fundamentals of Plasma Physics

Paul M. Bellan

publisher's information page (page iv, but not numbered)
Contents includes:
Published by CUP

date

Library of Congress,

Composed using Scientific Workplace, Latex

to my parents

Contents

<i>Preface</i>	xi
1 Basic concepts	1
1.1 History of the term “plasma”	1
1.2 Brief history of plasma physics	1
1.3 Plasma parameters	3
1.4 Examples of plasmas	3
1.5 Logical framework of plasma physics	4
1.6 Debye shielding	7
1.7 Quasi-neutrality	9
1.8 Small v. large angle collisions in plasmas	11
1.9 Electron and ion collision frequencies	14
1.10 Collisions with neutrals	16
1.11 Simple transport phenomena	17
1.12 A quantitative perspective	20
1.13 Assignments	22
2 Derivation of fluid equations: Vlasov, 2-fluid, MHD	30
2.1 Phase-space	30
2.2 Distribution function and Vlasov equation	31
2.3 Moments of the distribution function	33
2.4 Two-fluid equations	36
2.5 Magnetohydrodynamic equations	46
2.6 Summary of MHD equations	52
2.7 Sheath physics and Langmuir probe theory	53
2.8 Assignments	58
3 Motion of a single plasma particle	62
3.1 Motivation	62
3.2 Hamilton-Lagrange formalism v. Lorentz equation	62
3.3 Adiabatic invariant of a pendulum	66
3.4 Extension of WKB method to general adiabatic invariant	68
3.5 Drift equations	73
3.6 Relation of Drift Equations to the Double Adiabatic MHD Equations	91
3.7 Non-adiabatic motion in symmetric geometry	95
3.8 Motion in small-amplitude oscillatory fields	108
3.9 Wave-particle energy transfer	110
3.10 Assignments	119

4	Elementary plasma waves	123
4.1	General method for analyzing small amplitude waves	123
4.2	Two-fluid theory of unmagnetized plasma waves	124
4.3	Low frequency magnetized plasma: Alfvén waves	131
4.4	Two-fluid model of Alfvén modes	138
4.5	Assignments	147
5	Streaming instabilities and the Landau problem	149
5.1	Streaming instabilities	149
5.2	The Landau problem	153
5.3	The Penrose criterion	172
5.4	Assignments	175
6	Cold plasma waves in a magnetized plasma	178
6.1	Redundancy of Poisson's equation in electromagnetic mode analysis	178
6.2	Dielectric tensor	179
6.3	Dispersion relation expressed as a relation between n_x^2 and n_z^2	193
6.4	A journey through parameter space	195
6.5	High frequency waves: Altar-Appleton-Hartree dispersion relation	197
6.6	Group velocity	201
6.7	Quasi-electrostatic cold plasma waves	203
6.8	Resonance cones	204
6.9	Assignments	208
7	Waves in inhomogeneous plasmas and wave energy relations	210
7.1	Wave propagation in inhomogeneous plasmas	210
7.2	Geometric optics	213
7.3	Surface waves - the plasma-filled waveguide	214
7.4	Plasma wave-energy equation	219
7.5	Cold-plasma wave energy equation	221
7.6	Finite-temperature plasma wave energy equation	224
7.7	Negative energy waves	225
7.8	Assignments	228
8	Vlasov theory of warm electrostatic waves in a magnetized plasma	229
8.1	Uniform plasma	229
8.2	Analysis of the warm plasma electrostatic dispersion relation	234
8.3	Bernstein waves	236
8.4	Warm, magnetized, electrostatic dispersion with small, but finite k_{\parallel}	239
8.5	Analysis of linear mode conversion	241
8.6	Drift waves	249
8.7	Assignments	263
9	MHD equilibria	264
9.1	Why use MHD?	264
9.2	Vacuum magnetic fields	265

9.3	Force-free fields	268
9.4	Magnetic pressure and tension	268
9.5	Magnetic stress tensor	271
9.6	Flux preservation, energy minimization, and inductance	272
9.7	Static versus dynamic equilibria	274
9.8	Static equilibria	275
9.9	Dynamic equilibria: flows	286
9.10	Assignments	295
10	Stability of static MHD equilibria	298
10.1	The Rayleigh-Taylor instability of hydrodynamics	299
10.2	MHD Rayleigh-Taylor instability	302
10.3	The MHD energy principle	306
10.4	Discussion of the energy principle	319
10.5	Current-driven instabilities and helicity	319
10.6	Magnetic helicity	320
10.7	Qualitative description of free-boundary instabilities	323
10.8	Analysis of free-boundary instabilities	326
10.9	Assignments	334
11	Magnetic helicity interpreted and Woltjer-Taylor relaxation	336
11.1	Introduction	336
11.2	Topological interpretation of magnetic helicity	336
11.3	Woltjer-Taylor relaxation	341
11.4	Kinking and magnetic helicity	345
11.5	Assignments	357
12	Magnetic reconnection	360
12.1	Introduction	360
12.2	Water-beading: an analogy to magnetic tearing and reconnection	361
12.3	Qualitative description of sheet current instability	362
12.4	Semi-quantitative estimate of the tearing process	364
12.5	Generalization of tearing to sheared magnetic fields	371
12.6	Magnetic islands	376
12.7	Assignments	378
13	Fokker-Planck theory of collisions	382
13.1	Introduction	382
13.2	Statistical argument for the development of the Fokker-Planck equation	384
13.3	Electrical resistivity	393
13.4	Runaway electric field	395
13.5	Assignments	395
14	Wave-particle nonlinearities	398
14.1	Introduction	398
14.2	Vlasov non-linearity and quasi-linear velocity space diffusion	399

14.3	Echoes	412
14.4	Assignments	426
15	Wave-wave nonlinearities	428
15.1	Introduction	428
15.2	Manley-Rowe relations	430
15.3	Application to waves	435
15.4	Non-linear dispersion formulation and instability threshold	444
15.5	Digging a hole in the plasma via ponderomotive force	448
15.6	Ion acoustic wave soliton	454
15.7	Assignments	457
16	Non-neutral plasmas	460
16.1	Introduction	460
16.2	Brillouin flow	460
16.3	Isomorphism to incompressible 2D hydrodynamics	463
16.4	Near perfect confinement	464
16.5	Diocotron modes	465
16.6	Assignments	476
17	Dusty plasmas	483
17.1	Introduction	483
17.2	Electron and ion current flow to a dust grain	484
17.3	Dust charge	486
17.4	Dusty plasma parameter space	490
17.5	Large P limit: dust acoustic waves	491
17.6	Dust ion acoustic waves	494
17.7	The strongly coupled regime: crystallization of a dusty plasma	495
17.8	Assignments	504
	<i>Bibliography and suggested reading</i>	507
	<i>References</i>	509
	<i>Appendix A: Intuitive method for vector calculus identities</i>	515
	<i>Appendix B: Vector calculus in orthogonal curvilinear coordinates</i>	518
	<i>Appendix C: Frequently used physical constants and formulae</i>	524
	<i>Index</i>	528

Preface

This text is based on a course I have taught for many years to first year graduate and senior-level undergraduate students at Caltech. One outcome of this teaching has been the realization that although students typically decide to study plasma physics as a means towards some larger goal, they often conclude that this study has an attraction and charm of its own; in a sense the journey becomes as enjoyable as the destination. This conclusion is shared by me and I feel that a delightful aspect of plasma physics is the frequent transferability of ideas between extremely different applications so, for example, a concept developed in the context of astrophysics might suddenly become relevant to fusion research or vice versa.

Applications of plasma physics are many and varied. Examples include controlled fusion research, ionospheric physics, magnetospheric physics, solar physics, astrophysics, plasma propulsion, semiconductor processing, and metals processing. Because plasma physics is rich in both concepts and regimes, it has also often served as an incubator for new ideas in applied mathematics. In recent years there has been an increased dialog regarding plasma physics among the various disciplines listed above and it is my hope that this text will help to promote this trend.

The prerequisites for this text are a reasonable familiarity with Maxwell's equations, classical mechanics, vector algebra, vector calculus, differential equations, and complex variables – i.e., the contents of a typical undergraduate physics or engineering curriculum. Experience has shown that because of the many different applications for plasma physics, students studying plasma physics have a diversity of preparation and not all are proficient in all prerequisites. Brief derivations of many basic concepts are included to accommodate this range of preparation; these derivations are intended to assist those students who may have had little or no exposure to the concept in question and to refresh the memory of other students. For example, rather than just invoke Hamilton-Lagrange methods or Laplace transforms, there is a quick derivation and then a considerable discussion showing how these concepts relate to plasma physics issues. These additional explanations make the book more self-contained and also provide a close contact with first principles.

The order of presentation and level of rigor have been chosen to establish a firm foundation and yet avoid unnecessary mathematical formalism or abstraction. In particular, the various fluid equations are derived from first principles rather than simply invoked and the consequences of the Hamiltonian nature of particle motion are emphasized early on and shown to lead to the powerful concepts of symmetry-induced constraint and adiabatic invariance. Symmetry turns out to be an essential feature of magnetohydrodynamic plasma confinement and adiabatic invariance turns out to be not only essential for understanding many types of particle motion, but also vital to many aspects of wave behavior.

The mathematical derivations have been presented with intermediate steps shown in as much detail as is reasonably possible. This occasionally leads to daunting-looking expressions, but it is my belief that it is preferable to see all the details rather than have them glossed over and then justified by an "it can be shown" statement.

The book is organized as follows: Chapters 1-3 lay out the foundation of the subject. Chapter 1 provides a brief introduction and overview of applications, discusses the logical framework of plasma physics, and begins the presentation by discussing Debye shielding and then showing that plasmas are quasi-neutral and nearly collisionless. Chapter 2 introduces phase-space concepts and derives the Vlasov equation and then, by taking moments of the Vlasov equation, derives the two-fluid and magnetohydrodynamic systems of equations. Chapter 2 also introduces the dichotomy between adiabatic and isothermal behavior which is a fundamental and recurrent theme in plasma physics. Chapter 3 considers plasmas from the point of view of the behavior of a single particle and develops both exact and approximate descriptions for particle motion. In particular, Chapter 3 includes a detailed discussion of the concept of adiabatic invariance with the aim of demonstrating that this important concept is a fundamental property of all nearly periodic Hamiltonian systems and so does not have to be explained anew each time it is encountered in a different situation. Chapter 3 also includes a discussion of particle motion in fixed frequency oscillatory fields; this discussion provides a foundation for later analysis of cold plasma waves and wave-particle energy transfer in warm plasma waves.

Chapters 4-8 discuss plasma waves; these are not only important in many practical situations, but also provide an excellent way for developing insight about plasma dynamics. Chapter 4 shows how linear wave dispersion relations can be deduced from systems of partial differential equations characterizing a physical system and then presents derivations for the elementary plasma waves, namely Langmuir waves, electromagnetic plasma waves, ion acoustic waves, and Alfvén waves. The beginning of Chapter 5 shows that when a plasma contains groups of particles streaming at different velocities, free energy exists which can drive an instability; the remainder of Chapter 5 then presents Landau damping and instability theory which reveals that surprisingly strong interactions between waves and particles can lead to either wave damping or wave instability depending on the shape of the velocity distribution of the particles. Chapter 6 describes cold plasma waves in a background magnetic field and discusses the Clemmow-Mullaly-Allis diagram, an elegant categorization scheme for the large number of qualitatively different types of cold plasma waves that exist in a magnetized plasma. Chapter 7 discusses certain additional subtle and practical aspects of wave propagation including propagation in an inhomogeneous plasma and how the energy content of a wave is related to its dispersion relation. Chapter 8 begins by showing that the combination of warm plasma effects and a background magnetic field leads to the existence of the Bernstein wave, an altogether different kind of wave which has an infinite number of branches, and shows how a cold plasma wave can ‘mode convert’ into a Bernstein wave in an inhomogeneous plasma. Chapter 8 concludes with a discussion of drift waves, ubiquitous low frequency waves which have important deleterious consequences for magnetic confinement.

Chapters 9-12 provide a description of plasmas from the magnetohydrodynamic point of view. Chapter 9 begins by presenting several basic magnetohydrodynamic concepts (vacuum and force-free fields, magnetic pressure and tension, frozen-in flux, and energy minimization) and then uses these concepts to develop an intuitive understanding for dynamic behavior. Chapter 9 then discusses magnetohydrodynamic equilibria and derives the Grad-Shafranov equation, an equation which depends on the existence of symmetry and which characterizes three-dimensional magnetohydrodynamic equilibria. Chapter 9 ends

with a discussion on magnetohydrodynamic flows such as occur in arcs and jets. Chapter 10 examines the stability of perfectly conducting (i.e., ideal) magnetohydrodynamic equilibria, derives the ‘energy principle’ method for analyzing stability, discusses kink and sausage instabilities, and introduces the concepts of magnetic helicity and force-free equilibria. Chapter 11 examines magnetic helicity from a topological point of view and shows how helicity conservation and energy minimization leads to the Woltjer-Taylor model for magnetohydrodynamic self-organization. Chapter 12 departs from the ideal models presented earlier and discusses magnetic reconnection, a non-ideal behavior which permits the magnetohydrodynamic plasma to alter its topology and thereby relax to a minimum-energy state.

Chapters 13-17 consist of various advanced topics. Chapter 13 considers collisions from a Fokker-Planck point of view and is essentially a revisiting of the issues in Chapter 1 using a more sophisticated point of view; the Fokker-Planck model is used to derive a more accurate model for plasma electrical resistivity and also to show the failure of Ohm’s law when the electric field exceeds a critical value called the Dreicer limit. Chapter 14 considers two manifestations of wave-particle nonlinearity: (i) quasi-linear velocity space diffusion due to weak turbulence and (ii) echoes, non-linear phenomena which validate the concepts underlying Landau damping. Chapter 15 discusses how nonlinear interactions enable energy and momentum to be transferred between waves, categorizes the large number of such wave-wave nonlinear interactions, and shows how these various interactions are all based on a few fundamental concepts. Chapter 16 discusses one-component plasmas (pure electron or pure ion plasmas) and shows how these plasmas have behaviors differing from conventional two-component, electron-ion plasmas. Chapter 17 discusses dusty plasmas which are three component plasmas (electrons, ions, and dust grains) and shows how the addition of a third component also introduces new behaviors, including the possibility of the dusty plasma condensing into a crystal. The analysis of condensation involves revisiting the Debye shielding concept and so corresponds, in a sense to having the book end on the same note it started on.

I would like to extend my grateful appreciation to Professor Michael Brown at Swarthmore College for providing helpful feedback obtained from using a draft version in a seminar course at Swarthmore and to Professor Roy Gould at Caltech for providing useful suggestions. I would also like to thank graduate students Deepak Kumar and Gunsu Yun for carefully scrutinizing the final drafts of the manuscript and pointing out both ambiguities in presentation and typographical errors. I would also like to thank the many students who, over the years, provided useful feedback on earlier drafts of this work when it was in the form of lecture notes. Finally, I would like to acknowledge and thank my own mentors and colleagues who have introduced me to the many fascinating ideas constituting the discipline of plasma physics and also the many scientists whose hard work over many decades has led to the development of this discipline.

Paul M. Bellan
Pasadena, California
September 30, 2004

Basic concepts

1.1 History of the term “plasma”

In the mid-19th century the Czech physiologist Jan Evangelista Purkinje introduced use of the Greek word plasma (meaning “formed or molded”) to denote the clear fluid which remains after removal of all the corpuscular material in blood. Half a century later, the American scientist Irving Langmuir proposed in 1922 that the electrons, ions and neutrals in an ionized gas could similarly be considered as corpuscular material entrained in some kind of fluid medium and called this entraining medium plasma. However it turned out that unlike blood where there really is a fluid medium carrying the corpuscular material, there actually is no “fluid medium” entraining the electrons, ions, and neutrals in an ionized gas. Ever since, plasma scientists have had to explain to friends and acquaintances that they were not studying blood!

1.2 Brief history of plasma physics

In the 1920’s and 1930’s a few isolated researchers, each motivated by a specific practical problem, began the study of what is now called plasma physics. This work was mainly directed towards understanding (i) the effect of ionospheric plasma on long distance *short-wave radio* propagation and (ii) *gaseous electron tubes* used for rectification, switching and voltage regulation in the pre-semiconductor era of electronics. In the 1940’s Hannes Alfvén developed a theory of hydromagnetic waves (now called Alfvén waves) and proposed that these waves would be important in astrophysical plasmas. In the early 1950’s large-scale plasma physics based *magnetic fusion energy* research started simultaneously in the USA, Britain and the then Soviet Union. Since this work was an offshoot of thermonuclear weapon research, it was initially classified but because of scant progress in each country’s effort and the realization that controlled fusion research was unlikely to be of military value, all three countries declassified their efforts in 1958 and have cooperated since. Many other countries now participate in fusion research as well.

Fusion progress was slow through most of the 1960’s, but by the end of that decade the

empirically developed Russian *tokamak* configuration began producing plasmas with parameters far better than the lackluster results of the previous two decades. By the 1970's and 80's many tokamaks with progressively improved performance were constructed and at the end of the 20th century fusion break-even had nearly been achieved in tokamaks. International agreement was reached in the early 21st century to build the International Thermonuclear Experimental Reactor (ITER), a break-even tokamak designed to produce 500 megawatts of fusion output power. Non-tokamak approaches to fusion have also been pursued with varying degrees of success; many involve magnetic confinement schemes related to that used in tokamaks. In contrast to fusion schemes based on magnetic confinement, inertial confinement schemes were also developed in which high power lasers or similarly intense power sources bombard millimeter diameter pellets of thermonuclear fuel with ultra-short, extremely powerful pulses of strongly focused directed energy. The intense incident power causes the pellet surface to ablate and in so doing, act like a rocket exhaust pointing radially outwards from the pellet. The resulting radially inwards force compresses the pellet adiabatically, making it both denser and hotter; with sufficient adiabatic compression, fusion ignition conditions are predicted to be achieved.

Simultaneous with the fusion effort, there has been an equally important and extensive study of space plasmas. Measurements of near-Earth space plasmas such as the aurora and the ionosphere have been obtained by ground-based instruments since the late 19th century. Space plasma research was greatly stimulated when it became possible to use spacecraft to make routine *in situ* plasma measurements of the Earth's *magnetosphere*, the *solar wind*, and the magnetospheres of other planets. Additional interest has resulted from ground-based and spacecraft measurements of topologically complex, dramatic structures sometimes having explosive dynamics in the *solar corona*. Using radio telescopes, optical telescopes, Very Long Baseline Interferometry and most recently the Hubble and Spitzer spacecraft, large numbers of *astrophysical jets* shooting out from magnetized objects such as stars, active galactic nuclei, and black holes have been observed. Space plasmas often behave in a manner qualitatively similar to laboratory plasmas, but have a much grander scale.

Since the 1960's an important effort has been directed towards using plasmas for *space propulsion*. Plasma thrusters have been developed ranging from small *ion thrusters* for spacecraft attitude correction to powerful *magnetoplasmadynamic thrusters* that –given an adequate power supply – could be used for interplanetary missions. Plasma thrusters are now in use on some spacecraft and are under serious consideration for new and more ambitious spacecraft designs.

Starting in the late 1980's a new application of plasma physics appeared – *plasma processing* – a critical aspect of the fabrication of the tiny, complex integrated circuits used in modern electronic devices. This application is now of great economic importance.

In the 1990's studies began on *dusty plasmas*. Dust grains immersed in a plasma can become electrically charged and then act as an additional charged particle species. Because dust grains are massive compared to electrons or ions and can be charged to varying amounts, new physical behavior occurs that is sometimes an extension of what happens in a regular plasma and sometimes altogether new. In the 1980's and 90's there has also been investigation of *non-neutral plasmas*; these mimic the equations of incompressible hydrodynamics and so provide a compelling analog computer for problems in incompressible hydrodynamics. Both dusty plasmas and non-neutral plasmas can also form bizarre strongly coupled collective states where the plasma resembles a solid (e.g., forms quasi-crystalline structures). Another application of non-neutral plasmas is as a means to store

large quantities of positrons.

In addition to the above activities there have been continuing investigations of industrially relevant plasmas such as *arcs*, *plasma torches*, and *laser plasmas*. In particular, approximately 40% of the steel manufactured in the United States is recycled in huge electric arc furnaces capable of melting over 100 tons of scrap steel in a few minutes. Plasma displays are used for flat panel televisions and of course there are naturally-occurring terrestrial plasmas such as *lightning*.

1.3 Plasma parameters

Three fundamental parameters¹ characterize a plasma:

1. the particle density n (measured in particles per cubic meter),
2. the temperature T of each species (usually measured in eV, where 1 eV=11,605 K),
3. the steady state magnetic field B (measured in Tesla).

A host of subsidiary parameters (e.g., Debye length, Larmor radius, plasma frequency, cyclotron frequency, thermal velocity) can be derived from these three fundamental parameters. For partially-ionized plasmas, the fractional ionization and cross-sections of neutrals are also important.

1.4 Examples of plasmas

1.4.1 Non-fusion terrestrial plasmas

It takes considerable resources and skill to make a hot, fully ionized plasma and so, except for the specialized fusion plasmas, most terrestrial plasmas (e.g., arcs, neon signs, fluorescent lamps, processing plasmas, welding arcs, and lightning) have electron temperatures of a few eV, and for reasons given later, have ion temperatures that are colder, often at room temperature. These ‘everyday’ plasmas usually have no imposed steady state magnetic field and do not produce significant self magnetic fields. Typically, these plasmas are weakly ionized and dominated by collisional and radiative processes. Densities in these plasmas range from 10^{14} to 10^{22}m^{-3} (for comparison, the density of air at STP is $2.7 \times 10^{25}\text{m}^{-3}$).

1.4.2 Fusion-grade terrestrial plasmas

Using carefully designed, expensive, and often large plasma confinement systems together with high heating power and obsessive attention to purity, fusion researchers have succeeded in creating fully ionized hydrogen or deuterium plasmas which attain temperatures

¹In older plasma literature, density and magnetic fields are often expressed in cgs units, i.e., densities are given in particles per cubic centimeter, and magnetic fields are given in Gauss. Since the 1990’s there has been general agreement to use SI units when possible. SI units have the distinct advantage that electrical units are in terms of familiar quantities such as amps, volts, and ohms and so a model prediction in SI units can much more easily be compared to the results of an experiment than a prediction given in cgs units.

in the range from 10's of eV to *tens of thousands* of eV. In typical magnetic confinement devices (e.g., tokamaks, stellarators, reversed field pinches, mirror devices) an externally produced 1-10 Tesla magnetic field of carefully chosen geometry is imposed on the plasma. Magnetic confinement devices generally have densities in the range $10^{19} - 10^{21} \text{m}^{-3}$. Plasmas used in inertial fusion are much more dense; the goal is to attain for a brief instant densities one or two orders of magnitude larger than solid density ($\sim 10^{27} \text{m}^{-3}$).

1.4.3 Space plasmas

The parameters of these plasmas cover an enormous range. For example the density of space plasmas vary from 10^6m^{-3} in interstellar space, to 10^{20}m^{-3} in the solar atmosphere. Most of the astrophysical plasmas that have been investigated have temperatures in the range of 1-100 eV and these plasmas are usually fully ionized.

1.5 Logical framework of plasma physics

Plasmas are complex and exist in a wide variety of situations differing by many orders of magnitude. An important situation where plasmas do not normally exist is ordinary human experience. Consequently, people do not have the sort of intuition for plasma behavior that they have for solids, liquids or gases. Although plasma behavior seems non- or counter-intuitive at first, with suitable effort a good intuition for plasma behavior can be developed. This intuition can be helpful for making initial predictions about plasma behavior in a new situation, because plasmas have the remarkable property of being extremely *scalable*; i.e., the same qualitative phenomena often occur in plasmas differing by many orders of magnitude. Plasma physics is usually not a precise science. It is rather a web of overlapping points of view, each modeling a limited range of behavior. Understanding of plasmas is developed by studying these various points of view, all the while keeping in mind the linkages between the points of view.

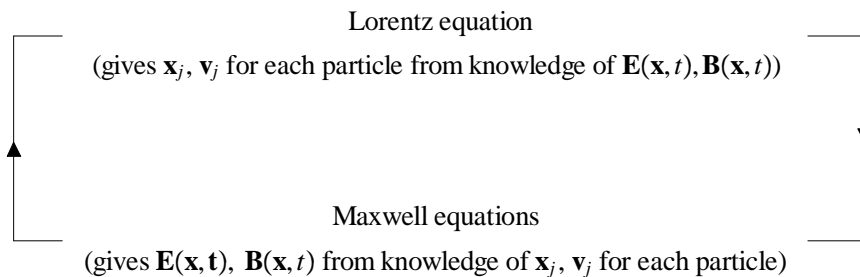


Figure 1.1: Interrelation between Maxwell's equations and the Lorentz equation

Plasma dynamics is determined by the *self-consistent interaction between electromagnetic fields and statistically large numbers of charged particles* as shown schematically in

Fig.1.1. In principle, the time evolution of a plasma can be calculated as follows:

1. given the trajectory $\mathbf{x}_j(t)$ and velocity $\mathbf{v}_j(t)$ of each and every particle j , the electric field $\mathbf{E}(\mathbf{x},t)$ and magnetic field $\mathbf{B}(\mathbf{x},t)$ can be evaluated using Maxwell's equations, and simultaneously,
2. given the instantaneous electric and magnetic fields $\mathbf{E}(\mathbf{x},t)$ and $\mathbf{B}(\mathbf{x},t)$, the forces on each and every particle j can be evaluated using the Lorentz equation and then used to update the trajectory $\mathbf{x}_j(t)$ and velocity $\mathbf{v}_j(t)$ of each particle.

While this approach is conceptually easy to understand, it is normally impractical to implement because of the extremely large number of particles and to a lesser extent, because of the complexity of the electromagnetic field. To gain a practical understanding, we therefore do not attempt to evaluate the entire complex behavior all at once but, instead, study plasmas by considering specific phenomena. For each phenomenon under immediate consideration, appropriate simplifying approximations are made, leading to a more tractable problem and hopefully revealing the essence of what is going on. A situation where a certain set of approximations is valid and provides a self-consistent description is called a regime. There are a number of general categories of simplifying approximations, namely:

1. *Approximations involving the electromagnetic field:*
 - (a) assuming the magnetic field is zero (unmagnetized plasma)
 - (b) assuming there are no inductive electric fields (electrostatic approximation)
 - (c) neglecting the displacement current in Ampere's law (suitable for phenomena having characteristic velocities much slower than the speed of light)
 - (d) assuming that all magnetic fields are produced by conductors external to the plasma
 - (e) various assumptions regarding geometric symmetry (e.g., spatially uniform, uniform in a particular direction, azimuthally symmetric about an axis)
2. *Approximations involving the particle description:*
 - (a) averaging of the Lorentz force over some sub-group of particles:
 - i. Vlasov theory: average over all particles of a given species (electrons or ions) having the same velocity at a given location and characterize the plasma using the distribution function $f_\sigma(\mathbf{x}, \mathbf{v}, t)$ which gives the density of particles of species σ having velocity \mathbf{v} at position \mathbf{x} at time t
 - ii. two-fluid theory: average velocities over all particles of a given species at a given location and characterize the plasma using the species density $n_\sigma(\mathbf{x}, t)$, mean velocity $\mathbf{u}_\sigma(\mathbf{x}, t)$, and pressure $P_\sigma(\mathbf{x}, t)$ defined relative to the species mean velocity
 - iii. magnetohydrodynamic theory: average momentum over all particles of all species and characterize the plasma using the center of mass density $\rho(\mathbf{x}, t)$, center of mass velocity $\mathbf{U}(\mathbf{x}, t)$, and pressure $P(\mathbf{x}, t)$ defined relative to the center of mass velocity
 - (b) assumptions about time (e.g., assume the phenomenon under consideration is fast or slow compared to some characteristic frequency of the particles such as the cyclotron frequency)

- (c) assumptions about space (e.g., assume the scale length of the phenomenon under consideration is large or small compared to some characteristic plasma length such as the cyclotron radius)
- (d) assumptions about velocity (e.g., assume the phenomenon under consideration is fast or slow compared to the thermal velocity $v_{T\sigma}$ of a particular species σ)

The large number of possible permutations and combinations that can be constructed from the above list means that there will be a large number of regimes. Since developing an intuitive understanding requires making approximations of the sort listed above and since these approximations lack an obvious hierarchy, it is not clear where to begin. In fact, as sketched in Fig.1.2, the models for particle motion (Vlasov, 2-fluid, MHD) involve a circular argument. Wherever we start on this circle, we are always forced to take at least one new concept on trust and hope that its validity will be established later. The reader is encouraged to refer to Fig.1.2 as its various components are examined so that the logic of this circle will eventually become clear.

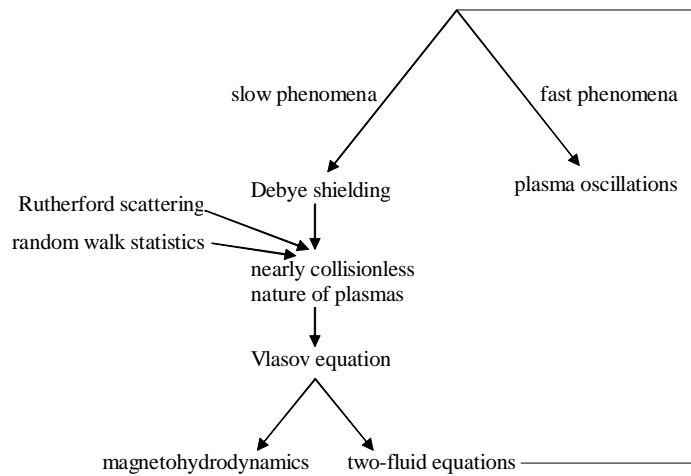


Figure 1.2: Hierarchy of models of plasmas showing circular nature of logic.

Because the argument is circular, the starting point is at the author's discretion, and for good (but not overwhelming reasons), this author has decided that the optimum starting point on Fig.1.2 is the subject of *Debye shielding*. Debye concepts, the Rutherford model for how charged particles scatter from each other, and some elementary statistics will be combined to construct an argument showing that plasmas are *weakly collisional*. We will then discuss *phase-space* concepts and introduce the *Vlasov equation* for the phase-space density. Averages of the Vlasov equation will provide *two-fluid equations* and also the *magnetohydrodynamic* (MHD) equations. Having established this framework, we will then return to study features of these points of view in more detail, often tying up loose ends that

occurred in our initial derivation of the framework. Somewhat separate from the study of Vlasov, two-fluid and MHD equations (which all attempt to give a self-consistent picture of the plasma) is the study of *single particle orbits in prescribed fields*. This provides useful intuition on the behavior of a typical particle in a plasma, and can provide important inputs or constraints for the self-consistent theories.

1.6 Debye shielding

We begin our study of plasmas by examining Debye shielding, a concept originating from the theory of liquid electrolytes (Debye and Huckel 1923). Consider a finite-temperature plasma consisting of a statistically large number of electrons and ions and assume that the ion and electron densities are initially equal and spatially uniform. As will be seen later, the ions and electrons need not be in thermal equilibrium with each other, and so the ions and electrons will be allowed to have separate temperatures denoted by T_i, T_e .

Since the ions and electrons have random thermal motion, thermally induced perturbations about the equilibrium will cause small, transient spatial variations of the electrostatic potential ϕ . In the spirit of circular argument the following assumptions are now invoked without proof:

1. The plasma is assumed to be nearly collisionless so that collisions between particles may be neglected to first approximation.
2. Each species, denoted as σ , may be considered as a ‘fluid’ having a density n_σ , a temperature T_σ , a pressure $P_\sigma = n_\sigma \kappa T_\sigma$ (κ is Boltzmann’s constant), and a mean velocity \mathbf{u}_σ so that the collisionless equation of motion for each fluid is

$$m_\sigma \frac{d\mathbf{u}_\sigma}{dt} = q_\sigma \mathbf{E} - \frac{1}{n_\sigma} \nabla P_\sigma \quad (1.1)$$

where m_σ is the particle mass, q_σ is the charge of a particle, and \mathbf{E} is the electric field.

Now consider a perturbation with a sufficiently *slow* time dependence to allow the following assumptions:

1. The inertial term $\sim d/dt$ on the left hand side of Eq.(1.1) is negligible and may be dropped.
2. Inductive electric fields are negligible so the electric field is almost entirely electrostatic, i.e., $\mathbf{E} \sim -\nabla\phi$.
3. All temperature gradients are smeared out by thermal particle motion so that the temperature of each species is spatially uniform.
4. The plasma remains in thermal equilibrium throughout the perturbation (i.e., can always be characterized by a temperature).

Invoking these approximations, Eq.(1.1) reduces to

$$0 \approx -n_\sigma q_\sigma \nabla\phi - \kappa T_\sigma \nabla n_\sigma, \quad (1.2)$$

a simple balance between the force due to the electrostatic electric field and the force due to the isothermal pressure gradient. Equation (1.2) is readily solved to give the *Boltzmann relation*

$$n_\sigma = n_{\sigma 0} \exp(-q_\sigma \phi / \kappa T_\sigma) \quad (1.3)$$

where $n_{\sigma 0}$ is a constant. It is important to emphasize that the Boltzmann relation results from the assumption that the perturbation is *very slow*; if this is not the case, then inertial effects, inductive electric fields, or temperature gradient effects will cause the plasma to have a completely different behavior from the Boltzmann relation. Situations exist where this ‘slowness’ assumption is valid for electron dynamics but not for ion dynamics, in which case the Boltzmann condition will apply only to the electrons but not to the ions (the converse situation does not normally occur, because ions, being heavier, are always more sluggish than electrons and so it is only possible for a phenomena to appear slow to electrons but not to ions).

Let us now imagine slowly inserting a single additional particle (so-called “test” particle) with charge q_T into an initially unperturbed, spatially uniform neutral plasma. To keep the algebra simple, we define the origin of our coordinate system to be at the location of the test particle. Before insertion of the test particle, the plasma potential was $\phi = 0$ everywhere because the ion and electron densities were spatially uniform and equal, but now the ions and electrons will be perturbed because of their interaction with the test particle. Particles having the same polarity as q_T will be slightly repelled whereas particles of opposite polarity will be slightly attracted. The slight displacements resulting from these repulsions and attractions will result in a small, but finite potential in the plasma. This potential will be the superposition of the test particle’s own potential and the potential of the plasma particles that have moved slightly in response to the test particle.

This slight displacement of plasma particles is called *shielding* or *screening* of the test particle because the displacement tends to reduce the effectiveness of the test particle field. To see this, suppose the test particle is a positively charged ion. When immersed in the plasma it will attract nearby electrons and repel nearby ions; the net result is an effectively negative charge cloud surrounding the test particle. An observer located far from the test particle and its surrounding cloud would see the combined potential of the test particle and its associated cloud. Because the cloud has the opposite polarity of the test particle, the cloud potential will partially cancel (i.e., *shield* or *screen*) the test particle potential.

Screening is calculated using Poisson’s equation with the source terms being the test particle and its associated cloud. The cloud contribution is determined using the Boltzmann relation for the particles that participate in the screening. This is a ‘self-consistent’ calculation for the potential because the shielding cloud is affected by its self-potential.

Thus, Poisson’s equation becomes

$$\nabla^2 \phi = -\frac{1}{\varepsilon_0} \left[q_T \delta(\mathbf{r}) + \sum_{\sigma} n_{\sigma}(\mathbf{r}) q_{\sigma} \right] \quad (1.4)$$

where the term $q_T \delta(\mathbf{r})$ on the right hand side represents the charge density due to the test particle and the term $\sum_{\sigma} n_{\sigma}(\mathbf{r}) q_{\sigma}$ represents the charge density of all plasma particles that participate in the screening (i.e., everything except the test particle). Before the test particle was inserted $\sum_{\sigma=i,e} n_{\sigma}(\mathbf{r}) q_{\sigma}$ vanished because the plasma was assumed to be initially neutral.

Since the test particle was inserted slowly, the plasma response will be Boltzmann-like and we may substitute for $n_{\sigma}(\mathbf{r})$ using Eq.(1.3). Furthermore, because the perturbation due to a single test particle is infinitesimal, we can safely assume that $|q_{\sigma} \phi| \ll \kappa T_{\sigma}$, in which case Eq.(1.3) becomes simply $n_{\sigma} \approx n_{\sigma 0} (1 - q_{\sigma} \phi / \kappa T_{\sigma})$. The assumption of initial

neutrality means that $\sum_{\sigma=i,e} n_{\sigma 0} q_{\sigma} = 0$ causing the terms independent of ϕ to cancel in Eq.(1.4) which thus reduces to

$$\nabla^2 \phi - \frac{1}{\lambda_D^2} \phi = -\frac{q_T}{\epsilon_0} \delta(\mathbf{r}) \quad (1.5)$$

where the effective Debye length is defined by

$$\frac{1}{\lambda_D^2} = \sum_{\sigma} \frac{1}{\lambda_{\sigma}^2} \quad (1.6)$$

and the species Debye length λ_{σ} is

$$\lambda_{\sigma}^2 = \frac{\epsilon_0 \kappa T_{\sigma}}{n_{0\sigma} q_{\sigma}^2}. \quad (1.7)$$

The second term on the left hand side of Eq.(1.5) is just the negative of the shielding cloud charge density. The summation in Eq.(1.6) is over all species that participate in the shielding. Since ions cannot move fast enough to keep up with an electron test charge which would be moving at the nominal electron thermal velocity, the shielding of electrons is only by other electrons, whereas the shielding of ions is by both ions and electrons.

Equation (1.5) can be solved using standard mathematical techniques (cf. assignments) to give

$$\phi(\mathbf{r}) = \frac{q_T}{4\pi\epsilon_0 r} e^{-r/\lambda_D}. \quad (1.8)$$

For $r \ll \lambda_D$ the potential $\phi(\mathbf{r})$ is identical to the potential of a test particle in vacuum whereas for $r \gg \lambda_D$ the test charge is completely screened by its surrounding shielding cloud. The nominal radius of the shielding cloud is λ_D . Because the test particle is completely screened for $r \gg \lambda_D$, the total shielding cloud charge is equal in magnitude to the charge on the test particle and opposite in sign. This test-particle/shielding-cloud analysis makes sense only if there is a macroscopically large number of plasma particles in the shielding cloud; i.e., the analysis makes sense only if $4\pi n_0 \lambda_D^3 / 3 \gg 1$. This will be seen later to be the condition for the plasma to be nearly collisionless and so validate assumption #1 in Sec.1.6.

In order for shielding to be a relevant issue, the Debye length must be small compared to the overall dimensions of the plasma, because otherwise no point in the plasma could be outside the shielding cloud. Finally, it should be realized that *any* particle could have been construed as being ‘the’ test particle and so we conclude that the time-averaged effective potential of any selected particle in the plasma is given by Eq. (1.8) (from a statistical point of view, selecting a particle means that it no longer is assumed to have a random thermal velocity and its effective potential is due to its own charge and to the time average of the random motions of the other particles).

1.7 Quasi-neutrality

The Debye shielding analysis above assumed that the plasma was initially neutral, i.e., that the initial electron and ion densities were equal. We now demonstrate that if the Debye

length is a microscopic length, then it is indeed an excellent assumption that plasmas remain extremely close to neutrality, while not being exactly neutral. It is found that the electrostatic electric field associated with any reasonable configuration is easily produced by having only a tiny deviation from perfect neutrality. This tendency to be *quasi-neutral* occurs because a conventional plasma does not have sufficient internal energy to become substantially non-neutral for distances greater than a Debye length (there do exist non-neutral plasmas which violate this concept, but these involve rotation of plasma in a background magnetic field which effectively plays the neutralizing role of ions in a conventional plasma).

To prove the assertion that plasmas tend to be quasi-neutral, we consider an initially neutral plasma with temperature T and calculate the largest radius sphere that could spontaneously become depleted of electrons due to thermal fluctuations. Let r_{\max} be the radius of this presumed sphere. Complete depletion (i.e., maximum non-neutrality) would occur if a random thermal fluctuation caused all the electrons originally in the sphere to vacate the volume of the sphere and move to its surface. The electrons would have to come to rest on the surface of the presumed sphere because if they did not, they would still have available kinetic energy which could be used to move out to an even larger radius, violating the assumption that the sphere was the largest radius sphere which could become fully depleted of electrons. This situation is of course extremely artificial and likely to be so rare as to be essentially negligible because it requires all the electrons to be moving radially relative to some origin. In reality, the electrons would be moving in random directions.

When the electrons exit the sphere they leave behind an equal number of ions. The remnant ions produce a radial electric field which pulls the electrons back towards the center of the sphere. One way of calculating the energy stored in this system is to calculate the work done by the electrons as they leave the sphere and collect on the surface, but a simpler way is to calculate the energy stored in the electrostatic electric field produced by the ions remaining in the sphere. This electrostatic energy did not exist when the electrons were initially in the sphere and balanced the ion charge and so it must be equivalent to the work done by the electrons on leaving the sphere.

The energy density of an electric field is $\epsilon_0 E^2/2$ and because of the spherical symmetry assumed here the electric field produced by the remnant ions must be in the radial direction. The ion charge in a sphere of radius r is $Q = 4\pi n e r^3/3$ and so after all the electrons have vacated the sphere, the electric field at radius r is $E_r = Q/4\pi\epsilon_0 r^2 = n e r/3\epsilon_0$. Thus the energy stored in the electrostatic field resulting from complete lack of neutralization of ions in a sphere of radius r_{\max} is

$$W = \int_0^{r_{\max}} \frac{\epsilon_0 E_r^2}{2} 4\pi r^2 dr = \pi r_{\max}^5 \frac{2n_e^2 e^2}{45\epsilon_0}. \quad (1.9)$$

Equating this potential energy to the initial electron thermal kinetic energy $W_{kinetic}$ gives

$$\pi r_{\max}^5 \frac{2n_e^2 e^2}{45\epsilon_0} = \frac{3}{2} n \kappa T \times \frac{4}{3} \pi r_{\max}^3 \quad (1.10)$$

which may be solved to give

$$r_{\max}^2 = 45 \frac{\epsilon_0 \kappa T}{n_e e^2} \quad (1.11)$$

so that $r_{\max} \simeq 7\lambda_D$.

Thus, the largest spherical volume that could spontaneously become fully depleted of electrons has a radius of a few Debye lengths, but this would require the highly unlikely situation of having all the electrons initially moving in the outward radial direction. We conclude that *the plasma is quasi-neutral over scale lengths much larger than the Debye length*. When a biased electrode such as a wire probe is inserted into a plasma, the plasma screens the field due to the potential on the electrode in the same way that the test charge potential was screened. The screening region is called the *sheath*, which is a region of non-neutrality having an extent of the order of a Debye length.

1.8 Small v. large angle collisions in plasmas

We now consider what happens to the momentum and energy of a test particle of charge q_T and mass m_T that is injected with velocity \mathbf{v}_T into a plasma. This test particle will make a sequence of random collisions with the plasma particles (called “field” particles and denoted by subscript F); these collisions will alter both the momentum and energy of the test particle.

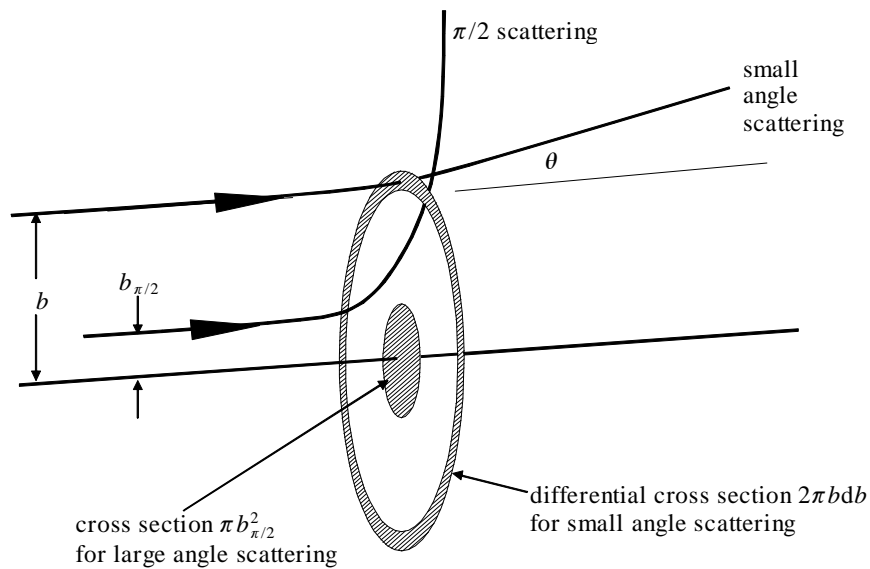


Figure 1.3: Differential scattering cross sections for large and small deflections

Solution of the Rutherford scattering problem in the center of mass frame shows (see

assignment 1, this chapter) that the scattering angle θ is given by

$$\tan\left(\frac{\theta}{2}\right) = \frac{q_T q_F}{4\pi\epsilon_0 b \mu v_0^2} \sim \frac{\text{Coulomb interaction energy}}{\text{kinetic energy}} \quad (1.12)$$

where $\mu^{-1} = m_T^{-1} + m_F^{-1}$ is the reduced mass, b is the impact parameter, and v_0 is the initial relative velocity. It is useful to separate scattering events (i.e., collisions) into two approximate categories, namely (1) large angle collisions where $\pi/2 \leq \theta \leq \pi$ and (2) small angle (grazing) collisions where $\theta \ll \pi/2$.

Let us denote $b_{\pi/2}$ as the impact parameter for 90 degree collisions; from Eq.(1.12) this is

$$b_{\pi/2} = \frac{q_T q_F}{4\pi\epsilon_0 \mu v_0^2} \quad (1.13)$$

and is the radius of the inner (small) shaded circle in Fig.1.3. Large angle scatterings will occur if the test particle is incident anywhere within this circle and so the total cross section for *all* large angle collisions is

$$\begin{aligned} \sigma_{\text{large}} &\approx \pi b_{\pi/2}^2 \\ &= \pi \left(\frac{q_T q_F}{4\pi\epsilon_0 \mu v_0^2} \right)^2. \end{aligned} \quad (1.14)$$

Grazing (small angle) collisions occur when the test particle impinges *outside* the shaded circle and so *occur much more frequently* than large angle collisions. Although each grazing collision does not scatter the test particle by much, there are far more grazing collisions than large angle collisions and so it is important to compare the *cumulative* effect of grazing collisions with the *cumulative* effect of large angle collisions.

To make matters even more complicated, the effective cross-section of grazing collisions depends on impact parameter, since the larger b is, the smaller the scattering. To take this weighting of impact parameters into account, the area outside the shaded circle is subdivided into a set of concentric annuli, called differential cross-sections. If the test particle impinges on the differential cross-section having radii between b and $b + db$, then the test particle will be scattered by an angle lying between $\theta(b)$ and $\theta(b + db)$ as determined by Eq.(1.12). The area of the differential cross-section is $2\pi b db$ which is therefore the effective cross-section for scattering between $\theta(b)$ and $\theta(b + db)$. Because the azimuthal angle about the direction of incidence is random, the simple average of N small angle scatterings vanishes, i.e., $N^{-1} \sum_{i=1}^N \theta_i = 0$ where θ_i is the scattering due to the i^{th} collision and N is a large number.

Random walk statistics must therefore be used to describe the cumulative effect of small angle scatterings and so we will use the *square* of the scattering angle, i.e. θ_i^2 , as the quantity for comparing the cumulative effects of small (grazing) and large angle collisions. Thus, scattering is a diffusive process.

To compare the respective cumulative effects of grazing and large angle collisions we calculate how many small angle scatterings must occur to be equivalent to a single large angle scattering (i.e. $\theta_{\text{large}}^2 \approx 1$); here we pick the nominal value of the large angle scattering to be 1 radian. In other words, we ask what must N be in order to have $\sum_{i=1}^N \theta_i^2 \approx 1$ where each θ_i represents an individual small angle scattering event. Equivalently, we may

ask what time t do we have to wait for the cumulative effect of the grazing collisions on a test particle to give an effective scattering equivalent to a single large angle scattering?

To calculate this, let us imagine we are “sitting” on the test particle. In this test particle frame the field particles approach the test particle with the velocity v_{rel} and so the apparent flux of field particles is $\Gamma = n_F v_{rel}$ where v_{rel} is the relative velocity between the test and field particles. The number of small angle scattering events in time t for impact parameters between b and $b + db$ is $\Gamma t 2\pi b db$ and so the time required for the cumulative effect of small angle collisions to be equivalent to a large angle collision is given by

$$1 \approx \sum_{i=1}^N \theta_i^2 = \Gamma t \int 2\pi b db [\theta(b)]^2. \quad (1.15)$$

The definitions of scattering theory show (see assignment 9) that $\sigma \Gamma = t^{-1}$ where σ is the cross section for an event and t is the time one has to wait for the event to occur. Substituting for Γt in Eq.(1.15) gives the cross-section σ^* for the cumulative effect of grazing collisions to be equivalent to a single large angle scattering event,

$$\sigma^* = \int 2\pi b db [\theta(b)]^2. \quad (1.16)$$

The appropriate lower limit for the integral in Eq.(1.16) is $b_{\pi/2}$, since impact parameters smaller than this value produce large angle collisions. What should the upper limit of the integral be? We recall from our Debye discussion that the field of the scattering center is *screened out* for distances greater than λ_D . Hence, small angle collisions occur *only* for impact parameters in the range $b_{\pi/2} < b < \lambda_D$ because the scattering potential is non-existent for distances larger than λ_D .

For small angle collisions, Eq.(1.12) gives

$$\theta(b) = \frac{q_T q_F}{2\pi \epsilon_0 \mu v_0^2 b}. \quad (1.17)$$

so that Eq. (1.7.3) becomes

$$\sigma^* = \int_{b_{\pi/2}}^{\lambda_D} 2\pi b db \left(\frac{q_T q_F}{2\pi \epsilon_0 \mu v_0^2 b} \right)^2 \quad (1.18)$$

or

$$\sigma^* = 8 \ln \left(\frac{\lambda_D}{b_{\pi/2}} \right) \sigma_{\text{large}}. \quad (1.19)$$

Thus, if $\lambda_D/b_{\pi/2} \gg 1$ the cross section σ^* will significantly exceed σ_{large} . Since $b_{\pi/2} = 1/2n\lambda_D^2$, the condition $\lambda_D \gg b_{\pi/2}$ is equivalent to $n\lambda_D^3 \gg 1$, which is just the criterion for there to be a large number of particles in a sphere having radius λ_D (a so-called *Debye sphere*). This was the condition for the Debye shielding cloud argument to make sense. We conclude that the criterion for an ionized gas to behave as a plasma (i.e., Debye shielding is important and grazing collisions dominate large angle collisions) is the condition that $n\lambda_D^3 \gg 1$. For most plasmas $n\lambda_D^3$ is a large number with natural logarithm of order 10; typically, when making rough estimates of σ^* , one uses $\ln(\lambda_D/b_{\pi/2}) \approx 10$. The reader may have developed a concern about the seeming arbitrary nature of the choice of $b_{\pi/2}$ as the ‘dividing line’ between large angle and grazing collisions. This arbitrariness

is of no consequence since the logarithmic dependence means that any other choice having the same order of magnitude for the ‘dividing line’ would give essentially the same result.

By substituting for $b_{\pi/2}$ the cross section can be re-written as

$$\sigma^* = \frac{1}{2\pi} \left(\frac{q_T q_f}{\epsilon_0 \mu v_0^2} \right)^2 \ln \left(\frac{\lambda_D}{b_{\pi/2}} \right). \quad (1.20)$$

Thus, σ^* decreases approximately as the fourth power of the relative velocity. In a hot plasma where v_0 is large, σ^* will be *very small* and so scattering by Coulomb collisions is often much less important than other phenomena. A useful way to decide whether Coulomb collisions are important is to compare the collision frequency $\nu = \sigma^* n v$ with the frequency of other effects, or equivalently the mean free path of collisions $l_{mfp} = 1/\sigma^* n$ with the characteristic length of other effects. If the collision frequency is small, or the mean free path is large (in comparison to other effects) collisions may be neglected to first approximation, in which case the plasma under consideration is called a collisionless or ‘‘ideal’’ plasma. The effective Coulomb cross section σ^* and its related parameters ν and l_{mfp} can be used to evaluate transport properties such as electrical resistivity, mobility, and diffusion.

1.9 Electron and ion collision frequencies

One of the fundamental physical constants influencing plasma behavior is the ion to electron mass ratio. The large value of this ratio often causes electrons and ions to experience qualitatively distinct dynamics. In some situations, one species may determine the essential character of a particular plasma behavior while the other species has little or no effect. Let us now examine how mass ratio affects:

1. Momentum change (scattering) of a given incident particle due to collision between
 - (a) like particles (i.e., electron-electron or ion-ion collisions, denoted ee or ii),
 - (b) unlike particles (i.e., electrons scattering from ions denoted ei or ions scattering from electrons denoted ie),
2. Kinetic energy change (scattering) of a given incident particle due to collisions between like or unlike particles.

Momentum scattering is characterized by the time required for collisions to deflect the incident particle by an angle $\pi/2$ from its initial direction, or more commonly, by the inverse of this time, called the collision frequency. The momentum scattering collision frequencies are denoted as $\nu_{ee}, \nu_{ii}, \nu_{ei}, \nu_{ie}$ for the various possible interactions between species and the corresponding times as τ_{ee} , etc. Energy scattering is characterized by the time required for an incident particle to transfer all its kinetic energy to the target particle. Energy transfer collision frequencies are denoted respectively by $\nu_{Eee}, \nu_{Eii}, \nu_{Eei}, \nu_{Eie}$.

We now show that these frequencies separate into categories having *three distinct orders of magnitude* having relative scalings $1 : (m_i/m_e)^{1/2} : m_i/m_e$. In order to estimate the orders of magnitude of the collision frequencies we assume the incident particle is ‘typical’ for its species and so take its incident velocity to be the species thermal velocity $v_{T\sigma} = (2\kappa T_\sigma/m_\sigma)^{1/2}$. While this is reasonable for a rough estimate, it should be realized that, because of the v^{-4} dependence in σ^* , a more careful averaging over all particles in the

thermal distribution will differ somewhat. This careful averaging is rather involved and will be deferred to Chapter 13.

We normalize all collision frequencies to ν_{ee} , and for further simplification assume that the ion and electron temperatures are of the same order of magnitude. First consider ν_{ei} : the reduced mass for ei collisions is the same as for ee collisions (except for a factor of 2 which we neglect), the relative velocity is the same — hence, we conclude that $\nu_{ei} \sim \nu_{ee}$. Now consider ν_{ii} : because the temperatures were assumed equal, $\sigma_{ii}^* \approx \sigma_{ee}^*$ and so the collision frequencies will differ only because of the different velocities in the expression $\nu = n\sigma v$. The ion thermal velocity is lower by an amount $(m_e/m_i)^{1/2}$ giving $\nu_{ii} \approx (m_e/m_i)^{1/2}\nu_{ee}$.

Care is required when calculating ν_{ie} . Strictly speaking, this calculation should be done in the center of mass frame and then transformed back to the lab frame, but an easy way to estimate ν_{ie} using lab-frame calculations is to note that momentum is conserved in a collision so that in the lab frame $m_i\Delta\mathbf{v}_i = -m_e\Delta\mathbf{v}_e$ where Δ means the change in a quantity as a result of the collision. If the collision of an ion head-on with a stationary electron is taken as an example, then the electron bounces off forward with twice the ion's velocity (corresponding to a specular reflection of the electron in a frame where the ion is stationary); this gives $\Delta\mathbf{v}_e = 2\mathbf{v}_i$ and $|\Delta\mathbf{v}_i|/|\mathbf{v}_i| = 2m_e/m_i$. Thus, in order to have $|\Delta\mathbf{v}_i|/|\mathbf{v}_i|$ of order unity, it is necessary to have m_i/m_e head-on collisions of an ion with electrons whereas in order to have $|\Delta\mathbf{v}_e|/|\mathbf{v}_e|$ of order unity it is only necessary to have one collision of an electron with an ion. Hence $\nu_{ie} \sim (m_e/m_i)\nu_{ee}$.

Now consider energy changes in collisions. If a moving electron makes a head-on collision with an electron at rest, then the incident electron stops (loses all its momentum and energy) while the originally stationary electron flies off with the same momentum and energy that the incident electron had. A similar picture holds for an ion hitting an ion. Thus, like-particle collisions transfer energy at the same rate as momentum so $\nu_{Eee} \sim \nu_{ee}$ and $\nu_{Eii} \sim \nu_{ii}$.

Inter-species collisions are more complicated. Consider an electron hitting a stationary ion head-on. Because the ion is massive, it barely recoils and the electron reflects with a velocity nearly equal in magnitude to its incident velocity. Thus, the change in electron momentum is $-2m_e\mathbf{v}_e$. From conservation of momentum, the momentum of the recoiling ion must be $m_i\mathbf{v}_i = 2m_e\mathbf{v}_e$. The energy transferred to the ion in this collision is $m_iv_i^2/2 = 4(m_e/m_i)m_ev_e^2/2$. Thus, an electron has to make $\sim m_i/m_e$ such collisions in order to transfer all its energy to ions. Hence, $\nu_{Eei} = (m_e/m_i)\nu_{ee}$.

Similarly, if an incident ion hits an electron at rest the electron will fly off with twice the incident ion velocity (in the center of mass frame, the electron is reflecting from the ion). The electron gains energy $m_ev_i^2/2$ so that again $\sim m_i/m_e$ collisions are required for the ion to transfer all its energy to electrons.

We now summarize the orders of magnitudes of collision frequencies in the table below.

~ 1	$\sim (m_e/m_i)^{1/2}$	$\sim m_e/m_i$
ν_{ee}	ν_{ii}	ν_{ie}
ν_{ei}	ν_{Eii}	ν_{Eei}
ν_{Eee}		ν_{Eie}

Although collisions are typically unimportant for fast transient processes, they may eventually determine many properties of a given plasma. The wide disparity of collision

frequencies shows that one has to be careful when determining which collisional process is relevant to a given phenomenon. Perhaps the best way to illustrate how collisions must be considered is by an example, such as the following:

Suppose half the electrons in a plasma initially have a directed velocity v_0 while the other half of the electrons and all the ions are initially at rest. This may be thought of as a high density beam of electrons passing through a cold plasma. On the fast (i.e., ν_{ee}) time scale the beam electrons will:

(i) collide with the stationary electrons and share their momentum and energy so that after a time of order ν_{ee}^{-1} the beam will become indistinguishable from the background electrons. Since momentum must be conserved, the combined electrons will have a mean velocity $v_0/2$.

(ii) collide with the stationary ions which will act as nearly fixed scattering centers so that the beam electrons will scatter in direction but not transfer significant energy to the ions.

Both the above processes will randomize the velocity distribution of the electrons until this distribution becomes Maxwellian (the maximum entropy distribution); the Maxwellian will be centered about the average velocity discussed in (i) above.

On the very slow ν_{Eei} time scale (down by a factor m_i/m_e) the electrons will transfer momentum to the ions, so on this time scale the electrons will share their momentum with the ions, in which case the electrons will slow down and the ions will speed up until eventually electrons and ions have the same momentum. Similarly the electrons will share energy with the ions in which case the ions will heat up while the electrons will cool.

If, instead, a beam of ions were injected into the plasma, the ion beam would thermalize and share momentum with the background ions on the intermediate ν_{ii} time scale, and then only share momentum and energy with the electrons on the very slow ν_{Eie} time scale.

This collisional sharing of momentum and energy and thermalization of velocity distribution functions to make Maxwellians is the process by which thermodynamic equilibrium is achieved. Collision frequencies vary as $T^{-3/2}$ and so, for hot plasmas, collision processes are often slower than many other phenomena. Since collisions are the means by which thermodynamic equilibrium is achieved, plasmas are typically *not in thermodynamic equilibrium*, although some components of the plasma may be in a partial equilibrium (for example, the electrons may be in thermal equilibrium with each other but not with the ions). Hence, thermodynamically based descriptions of the plasma are often inappropriate. It is not unusual, for example, to have a plasma where the electron and ion temperatures differ by more than an order of magnitude. This can occur when one species or the other has been subject to heating and the plasma lifetime is shorter than the interspecies energy equilibration time $\sim \nu_{Eei}^{-1}$.

1.10 Collisions with neutrals

If a plasma is weakly ionized then collisions with neutrals must be considered. These collisions differ fundamentally from collisions between charged particles because now the interaction forces are short-range (unlike the long-range Coulomb interaction) and so the neutral can be considered simply as a hard body with cross-section of the order of its actual geometrical size. All atoms have radii of the order of 10^{-10} m so the typical neutral cross

section is $\sigma_{\text{neut}} \sim 3 \times 10^{-20} \text{ m}^2$. When a particle hits a neutral it can simply scatter with no change in the internal energy of the neutral; this is called *elastic scattering*. It can also transfer energy to the structure of the neutral and so cause an internal change in the neutral; this is called *inelastic scattering*. Inelastic scattering includes ionization and excitation of atomic level transitions (with accompanying optical radiation).

Another process can occur when ions collide with neutrals — the incident ion can capture an electron from the neutral and become neutralized while simultaneously ionizing the original neutral. This process, called *charge exchange* is used for producing energetic neutral beams. In this process a high energy beam of ions is injected into a gas of neutrals, captures electrons, and exits as a high energy beam of neutrals.

Because ions have approximately the same mass as neutrals, ions rapidly exchange energy with neutrals and tend to be in thermal equilibrium with the neutrals if the plasma is weakly ionized. As a consequence, ions are typically cold in weakly ionized plasmas, because the neutrals are in thermal equilibrium with the walls of the container.

1.11 Simple transport phenomena

1. Electrical resistivity- When a uniform electric field \mathbf{E} exists in a plasma, the electrons and ions are accelerated in opposite directions creating a relative momentum between the two species. At the same time electron-ion collisions dissipate this relative momentum so it is possible to achieve a steady state where relative momentum creation (i.e., acceleration due to the \mathbf{E} field) is balanced by relative momentum dissipation due to interspecies collisions (this dissipation of relative momentum is known as ‘drag’). The balance of forces on the electrons gives

$$0 = -\frac{e}{m_e}\mathbf{E} - v_{ei}\mathbf{u}_{\text{rel}} \quad (1.21)$$

since the drag is proportional to the *relative* velocity \mathbf{u}_{rel} between electrons and ions. However, the electric current is just $\mathbf{J} = -n_e e \mathbf{u}_{\text{rel}}$ so that Eq.(1.21) can be re-written as

$$\mathbf{E} = \eta \mathbf{J} \quad (1.22)$$

where

$$\eta = \frac{m_e v_{ei}}{n_e e^2} \quad (1.23)$$

is the plasma electrical resistivity. Substituting $v_{ei} = \sigma^* n_i v_{Te}$ and noting from quasi-neutrality that $Z n_i = n_e$ the plasma electrical resistivity is

$$\eta = \frac{Z e^2}{2\pi m_e \epsilon_0^2 v_{Te}^3} \ln \left(\frac{\lambda_D}{b_{\pi/2}} \right) \quad (1.24)$$

from which we see that resistivity is independent of density, proportional to $T_e^{-3/2}$, and also proportional to the ion charge Z . This expression for the resistivity is only approximate since we did not properly average over the electron velocity distribution (a more accurate expression, differing by a factor of order unity, will be derived in Chapter 13). Resistivity resulting from grazing collisions between electrons and ions as given by Eq.(1.24) is known as Spitzer resistivity (Spitzer and Harm 1953). It

should be emphasized that although this discussion assumes existence of a *uniform* electric field in the plasma, a uniform field will not exist in what naively appears to be the most obvious geometry, namely a plasma between two parallel plates charged to different potentials. This is because Debye shielding will concentrate virtually all the potential drop into thin sheaths adjacent to the electrodes, resulting in near-zero electric field inside the plasma. A practical way to obtain a uniform electric field is to create the field by induction so that there are no electrodes that can be screened out.

2. Diffusion and ambipolar diffusion- Standard random walk arguments show that particle diffusion coefficients scale as $D \sim (\Delta x)^2 / \tau$ where Δx is the characteristic step size in the random walk and τ is the time between steps. This can also be expressed as $D \sim v_T^2 / \nu$ where $\nu = \tau^{-1}$ is the collision frequency and $v_T = \Delta x / \tau = \nu \Delta x$ is the thermal velocity. Since the random step size for particle collisions is the mean free path and the time between steps is the inverse of the collision frequency, the electron diffusion coefficient in an unmagnetized plasma scales as

$$D_e = \nu_e l_{mfp,e}^2 = \frac{\kappa T_e}{m_e \nu_e} \quad (1.25)$$

where $\nu_e = \nu_{ee} + \nu_{ei} \sim \nu_{ee}$ is the 90° scattering rate for electrons and $l_{mfp,e} = \sqrt{\kappa T_e / m_e \nu_e^2}$ is the electron mean free path. Similarly, the ion diffusion coefficient in an unmagnetized plasma is

$$D_i = \nu_i l_{mfp,i}^2 = \frac{\kappa T_i}{m_i \nu_i} \quad (1.26)$$

where $\nu_i = \nu_{ii} + \nu_{ie} \sim \nu_{ii}$ is the effective ion collision frequency. The electron diffusion coefficient is typically much larger than the ion diffusion coefficient in an unmagnetized plasma (it is the other way around for diffusion across a magnetic field in a magnetized plasma where the step size is the Larmor radius). However, if the electrons in an unmagnetized plasma did in fact diffuse across a density gradient at a rate two orders of magnitude faster than the ions, the ions would be left behind and the plasma would no longer be quasi-neutral. What actually happens is that the electrons try to diffuse faster than the ions, but an electrostatic electric field is established which decelerates the electrons and accelerates the ions until the electron and ion fluxes become equalized. This results in an effective diffusion, called the ambipolar diffusion, which is less than the electron rate, but greater than the ion rate. Equation (1.21) shows that an electric field establishes an average electron momentum $m_e \mathbf{u}_e = -e\mathbf{E} / \nu_e$ where ν_e is the rate at which the average electron loses momentum due to collisions with ions or neutrals. Electron-electron collisions are excluded from this calculation because the average electron under consideration here cannot lose momentum due to collisions with other electrons, because the other electrons have on average the same momentum as this average electron. Since the electric field cannot impart momentum to the plasma as a whole, the momentum imparted to ions must be equal and opposite so $m_i \mathbf{u}_i = e\mathbf{E} / \nu_e$. Because diffusion in the presence of a density gradient produces an electron flux $-D_e \nabla n_e$, the net electron flux resulting from both an electric field and a diffusion across a density gradient is

$$\mathbf{\Gamma}_e = n_e \mu_e \mathbf{E} - D_e \nabla n_e \quad (1.27)$$

where

$$\mu_e = -\frac{e}{m_e v_e} \quad (1.28)$$

is called the electron mobility. Similarly, the net ion flux is

$$\mathbf{\Gamma}_i = n_i \mu_i \mathbf{E} - D_i \nabla n_i \quad (1.29)$$

where

$$\mu_i = \frac{e}{m_i v_i} \quad (1.30)$$

is the ion mobility. In order to maintain quasineutrality, the electric field automatically adjusts itself to give $\mathbf{\Gamma}_e = \mathbf{\Gamma}_i = \mathbf{\Gamma}_{ambipolar}$ and $n_i = n_e = n$; this ambipolar electric field is

$$\begin{aligned} \mathbf{E}_{ambipolar} &= \frac{(D_e - D_i)}{(\mu_e - \mu_i)} \nabla \ln n \\ &\simeq \frac{D_e}{\mu_e} \nabla \ln n \\ &= \frac{\kappa T_e}{e} \nabla \ln n \end{aligned} \quad (1.31)$$

Substitution for \mathbf{E} gives the ambipolar diffusion to be

$$\mathbf{\Gamma}_{ambipolar} = - \left(\frac{\mu_e D_i - D_e \mu_i}{\mu_e - \mu_i} \right) \nabla n \quad (1.32)$$

so the ambipolar diffusion coefficient is

$$\begin{aligned} D_{ambipolar} &= \frac{\mu_e D_i - D_e \mu_i}{\mu_e - \mu_i} \\ &= \frac{\frac{D_i}{\mu_i} - \frac{D_e}{\mu_e}}{\frac{1}{\mu_i} - \frac{1}{\mu_e}} \\ &= \frac{D_i \frac{m_i v_i}{e} + D_e \frac{m_e v_e}{e}}{\frac{m_i v_i}{e} + \frac{m_e v_e}{e}} \\ &= \frac{\kappa (T_i + T_e)}{m_i v_i} \end{aligned} \quad (1.33)$$

where Eqs.(1.25) and (1.26) have been used as well as the relation $v_i \sim (m_e/m_i)^{1/2} v_e$. If the electrons are much hotter than the ions, then for a given ion temperature, the ambipolar diffusion scales as T_e/m_i . The situation is a little like that of a small child tugging on his/her parent (the energy of the small child is like the electron temperature, the parental mass is like the ion mass, and the tension in the arm which accelerates the parent and decelerates the child is like the ambipolar electric field); the resulting motion (parent and child move together faster than the parent would like and slower than the child would like) is analogous to electrons being retarded and ions being accelerated by the ambipolar electric field in such a way as to maintain quasineutrality.

1.12 A quantitative perspective

Relevant physical constants are

$$\begin{aligned} e &= 1.6 \times 10^{-19} \text{ Coulombs} \\ m_e &= 9.1 \times 10^{-31} \text{ kg} \\ m_p/m_e &= 1836 \\ \varepsilon_0 &= 8.85 \times 10^{-12} \text{ Farads/meter.} \end{aligned}$$

The temperature is measured in units of electron volts, so that $\kappa = 1.6 \times 10^{-19}$ Joules/volt; i.e., $\kappa = e$. Thus, the Debye length is

$$\begin{aligned} \lambda_D &= \sqrt{\frac{\varepsilon_0 \kappa T}{ne^2}} \\ &= \sqrt{\frac{\varepsilon_0}{e}} \sqrt{\frac{T_{eV}}{n}} \\ &= 7.4 \times 10^3 \sqrt{\frac{T_{eV}}{n}} \text{ meters.} \end{aligned} \quad (1.34)$$

We will assume that the typical velocity is related to the temperature by

$$\frac{1}{2}mv^2 = \frac{3}{2}\kappa T. \quad (1.35)$$

For electron-electron scattering $\mu = m_e/2$ so that the small angle scattering cross-section is

$$\begin{aligned} \sigma^* &= \frac{1}{2\pi} \left(\frac{e^2}{\varepsilon_0 mv^2/2} \right)^2 \ln(\lambda_D/b_{\pi/2}) \\ &= \frac{1}{2\pi} \left(\frac{e^2}{3\varepsilon_0 \kappa T} \right)^2 \ln \Lambda \end{aligned} \quad (1.36)$$

where

$$\begin{aligned} \Lambda &= \frac{\lambda_D}{b_{\pi/2}} \\ &= \sqrt{\frac{\varepsilon_0 \kappa T}{ne^2}} \frac{4\pi\varepsilon_0 mv^2/2}{e^2} \\ &= 6\pi n \lambda_D^3 \end{aligned} \quad (1.37)$$

is typically a very large number corresponding to there being a macroscopically large number of particles in a sphere having a radius equal to a Debye length; different authors will have slightly different numerical coefficients, depending on how they identify velocity with temperature. This difference is of no significance because one is taking the logarithm.

The collision frequency is $\nu = \sigma^* n v$ so

$$\begin{aligned}
 \nu_{ee} &= \frac{n}{2\pi} \left(\frac{e^2}{3\varepsilon_0 \kappa T} \right)^2 \sqrt{\frac{3\kappa T}{m_e}} \ln \Lambda \\
 &= \frac{e^{5/2}}{2 \times 3^{3/2} \pi \varepsilon_0^2 m_e^{1/2}} \frac{n \ln \Lambda}{T_{eV}^{3/2}} \\
 &= 4 \times 10^{-12} \frac{n \ln \Lambda}{T_{eV}^{3/2}}.
 \end{aligned} \tag{1.38}$$

Typically $\ln \Lambda$ lies in the range 8-25 for most plasmas.

Table 1.1 lists nominal parameters for several plasmas of interest and shows these plasmas have an enormous range of densities, temperatures, scale lengths, mean free paths, and collision frequencies. The crucial issue is the ratio of the mean free path to the characteristic scale length.

Arc plasmas and magnetoplasmadynamic thrusters are in the category of dense lab plasmas; these plasmas are very collisional (the mean free path is much smaller than the characteristic scale length). The plasmas used in semiconductor processing and many research plasmas are in the diffuse lab plasma category; these plasmas are collisionless. It is possible to make both collisional and collisionless lab plasmas, and in fact if there is are large temperature or density gradients it is possible to have both collisional and collisionless behavior in the same device.

	n	T	λ_D	$n\lambda_D^3$	$\ln\Lambda$	ν_{ee}	l_{mfp}	L
units	m^{-3}	eV	m			s^{-1}	m	m
Solar corona (loops)	10^{15}	100	10^{-3}	10^7	19	10^2	10^5	10^8
Solar wind (near earth)	10^7	10	10	10^9	25	10^{-5}	10^{11}	10^{11}
Magnetosphere (tail lobe)	10^4	10	10^2	10^{11}	28	10^{-8}	10^{14}	10^8
Ionosphere	10^{11}	0.1	10^{-2}	10^4	14	10^2	10^3	10^5
Mag. fusion (tokamak)	10^{20}	10^4	10^{-4}	10^7	20	10^4	10^4	10
Inertial fusion (imploded)	10^{31}	10^4	10^{-10}	10^2	8	10^{14}	10^{-7}	10^{-5}
Lab plasma (dense)	10^{20}	5	10^{-6}	10^3	9	10^8	10^{-2}	10^{-1}
Lab plasma (diffuse)	10^{16}	5	10^{-4}	10^5	14	10^4	10^1	10^{-1}

Table 1.1: Comparison of parameters for a wide variety of plasmas

1.13 Assignments

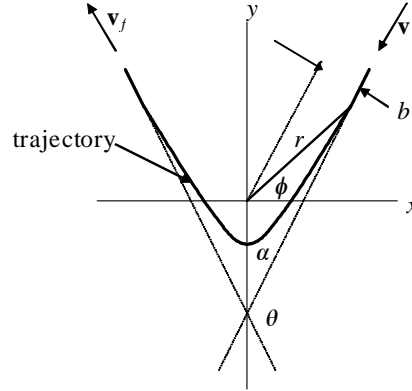


Figure 1.4: Geometry of scattering in center of mass frame. Scattering center is at the origin and θ is the scattering angle. Note symmetries of velocities before and after scattering.

1. Rutherford Scattering: This assignment involves developing a derivation for Rutherford scattering which uses geometrical arguments to take advantage of the symmetry of the scattering trajectory.
 - (a) Show that the equation of motion in the center of mass frame is

$$\mu \frac{d\mathbf{v}}{dt} = \frac{q_1 q_2}{4\pi\epsilon_0 r^2} \hat{r}.$$

The calculations will be done using the center of mass frame geometry shown in Fig.1.4 which consists of a cylindrical coordinate system r, ϕ, z with origin at the scattering center. Let θ be the scattering angle, and let b be the impact parameter as indicated in Fig.1.4. Also, define a Cartesian coordinate system x, y so that $y = r \sin \phi$ etc.; these Cartesian coordinates are also shown in Fig.1.4.

- (b) By taking the time derivative of $\mathbf{r} \times \dot{\mathbf{r}}$ show that the angular momentum $L = \mu \mathbf{r} \times \dot{\mathbf{r}}$ is a constant of the motion. Show that $L = \mu b v_\infty = \mu r^2 \dot{\phi}$ so that $\dot{\phi} = b v_\infty / r^2$.
- (c) Let \mathbf{v}_i and \mathbf{v}_f be the initial and final velocities as shown in Fig.1.4. Since energy is conserved during scattering the magnitudes of these two velocities must be the same, i.e., $|\mathbf{v}_i| = |\mathbf{v}_f| = v_\infty$. From the symmetry of the figure it is seen that the x component of velocity at infinity is the same before and after the collision, even though it is altered during the collision. However, it is seen that the y component of the velocity reverses direction as a result of the collision. Let Δv_y

be the net change in the y velocity over the entire collision. Express Δv_y in terms of v_{yi} , the y component of \mathbf{v}_i .

- (d) Using the y component of the equation of motion, obtain a relationship between dv_y and $d \cos \phi$. (Hint: it is useful to use conservation of angular momentum to eliminate dt in favor of $d\phi$.) Let ϕ_i and ϕ_f be the initial and final values of ϕ . By integrating dv_y , calculate Δv_y over the entire collision. How is ϕ_f related to ϕ_i and to α (refer to figure)?
- (e) How is v_{yi} related to ϕ_i and v_∞ ? How is θ related to α ? Use the expressions for Δv_y obtained in parts (c) and (d) above to obtain the Rutherford scattering formula

$$\tan\left(\frac{\theta}{2}\right) = \frac{q_1 q_2}{4\pi\epsilon_0 \mu b v_\infty^2}$$

What is the scattering angle for grazing (small angle collisions) and how does this small angle scattering relate to the initial center of mass kinetic energy and to the potential energy at distance b ? For grazing collisions how does b relate to the distance of closest approach? What impact parameter gives 90 degree scattering?

2. *One-dimensional Scattering relations:* The separation of collision types according to m_e/m_i can also be understood by considering how the combination of conservation of momentum and of energy together constrain certain properties of collisions. Suppose that a particle with mass m_1 and incident velocity v_1 makes a head-on collision with a stationary target particle having mass m_2 . The conservation equations for momentum and energy can be written as

$$\begin{aligned} m_1 v_1 &= m_1 v_1' + m_2 v_2' \\ \frac{1}{2} m_1 v_1^2 &= \frac{1}{2} m_1 v_1'^2 + \frac{1}{2} m_2 v_2'^2. \end{aligned}$$

where prime refers to the value after the collision. By eliminating v_1' between these two equations obtain v_2' as a function of v_1 . Use this to construct an expression showing the ratio $m_2 v_2'^2 / m_1 v_1^2$, i.e., the fraction of the incident particle energy is transferred to the target particle per collision. How does this fraction depend on m_1/m_2 when m_1/m_2 is equal to unity, very large, or very small? If m_1/m_2 is very large or very small how many collisions are required to transfer approximately all of the incident particle energy to target particles?

3. *Some basic facts you should know:* Memorize the value of ϵ_0 (or else arrange for the value to be close at hand). What is the value of Boltzmann's constant when temperatures are measured in electron volts? What is the density of the air you are breathing, measured in particles per cubic meter? What is the density of particles in solid copper, measured in particles per cubic meter? What is room temperature, expressed in electron volts? What is the ionization potential (in eV) of a hydrogen atom? What is the mass of an electron and of an ion (in kilograms)? What is the strength of the Earth's magnetic field at your location, expressed in Tesla? What is the strength of the magnetic field produced by a straight wire carrying 1 ampere as measured by an observer located 1 meter from the wire and what is the direction of the magnetic field? What

is the relationship between Tesla and Gauss, between particles per cubic centimeter and particles per cubic meter? What is magnetic flux? If a circular loop of wire with a break in it links a magnetic flux of 29.83 Weber which increases at a constant rate to a flux of 30.83 Weber in one second, what voltage appears across the break?

4. Solve Eq.(1.5) the ‘easy’ way by first proving using Gauss’ law to show that the solution of

$$\nabla^2 \phi = -\frac{1}{\epsilon_0} \delta(\mathbf{r})$$

is

$$\phi = \frac{1}{4\pi\epsilon_0 r}.$$

Show that this implies

$$\nabla^2 \frac{1}{4\pi r} = -\delta(\mathbf{r}) \quad (1.39)$$

is a representation for the delta function. Then, use spherical polar coordinates and symmetry to show that the Laplacian reduces to

$$\nabla^2 \phi = \frac{1}{r^2} \frac{\partial}{\partial r} \left(r^2 \frac{\partial \phi}{\partial r} \right).$$

Explicitly calculate $\nabla^2(1/r)$ and then reconcile your result with Eq.(1.39). Using these results guess that the solution to Eq.(1.5) has the form

$$\phi = \frac{g(r)}{4\pi\epsilon_0 r}.$$

Substitute this guess into Eq.(1.5) to obtain a differential equation for g which is trivial to solve.

5. Solve Eq.(1.5) for $\phi(\mathbf{r})$ using a more general method which illustrates several important mathematical techniques and formalisms. Begin by defining the 3D Fourier transform

$$\tilde{\phi}(\mathbf{k}) = \int d\mathbf{r} \phi(\mathbf{r}) e^{-i\mathbf{k} \cdot \mathbf{r}} \quad (1.40)$$

in which case the inverse transform is

$$\phi(\mathbf{r}) = \frac{1}{(2\pi)^3} \int d\mathbf{k} \tilde{\phi}(\mathbf{k}) e^{i\mathbf{k} \cdot \mathbf{r}} \quad (1.41)$$

and note that the Dirac delta function can be expressed as

$$\delta(\mathbf{r}) = \frac{1}{(2\pi)^3} \int d\mathbf{k} e^{i\mathbf{k} \cdot \mathbf{r}}. \quad (1.42)$$

Now multiply Eq.(1.5) by $\exp(-i\mathbf{k} \cdot \mathbf{r})$ and then integrate over all \mathbf{r} , i.e. operate with $\int d\mathbf{r}$. The term involving ∇^2 is integrated by parts, which effectively replaces the ∇ operator with $i\mathbf{k}$.

Show that the Fourier transform of the potential is

$$\tilde{\phi}(\mathbf{k}) = \frac{q_T}{\epsilon_0(k^2 + \lambda_D^{-2})}. \quad (1.43)$$

and use this in Eq. (1.41).

Because of spherical symmetry use spherical polar coordinates for the k space integral. The only fixed direction is the \mathbf{r} direction so choose the polar axis of the \mathbf{k} coordinate system to be parallel to \mathbf{r} . Thus $\mathbf{k} \cdot \mathbf{r} = kr\alpha$ where $\alpha = \cos \theta$ and θ is the polar angle. Also, $d\mathbf{k} = -d\phi k^2 d\alpha dk$ where ϕ is the azimuthal angle. What are the limits of the respective ϕ , α , and k integrals? In answering this, you should first obtain an integral of the form

$$\phi(\mathbf{r}) \sim \int_{\phi=?}^? d\phi \int_{\alpha=?}^? d\alpha \int_{k=?}^? k^2 dk \times (?) \quad (1.44)$$

where the limits and the integrand with appropriate coefficients are specified (i.e., replace all the question marks and \sim by the correct quantities). Upon evaluation of the ϕ and α integrals Eq.(1.44) becomes an even function of k so that the range of integration can be extended to $-\infty$ providing the overall integral is multiplied by $1/2$. Realizing that $\sin kr = \text{Im}[e^{ikr}]$, derive an expression of the general form

$$\phi(\mathbf{r}) \sim \text{Im} \int_{-\infty}^{\infty} k dk \frac{e^{ikr}}{f(k^2)}. \quad (1.45)$$

but specify the coefficient and exact form of $f(k^2)$. Explain why the integration contour (which is along the real k axis) can be completed in the upper half complex k plane. Complete the contour in the upper half plane and show that the integrand has a single pole in the upper half plane at $k = ?$ Use the method of residues to obtain $\phi(\mathbf{r})$.

6. Make sure you know how to evaluate quickly $\mathbf{A} \times (\mathbf{B} \times \mathbf{C})$ and $(\mathbf{A} \times \mathbf{B}) \times \mathbf{C}$. A useful mnemonic which works for both cases is: “Both variations = Middle (dot other two) - Outer (dot other two)”, where outer refers to the outer vector of the parentheses (furthest from the center of the triad), and middle refers to the middle vector in the triad of vectors.
7. Particle Integrator scheme (Birdsall and Langdon 1985)-In this assignment you will develop a simple, but powerful “leap-frog” numerical integration scheme. This is a type of “implicit” numerical integration scheme. This numerical scheme can later be used to evaluate particle orbits in time-dependent fields having complex topology. These calculations can be considered as numerical experiments used in conjunction with the analytic theory we will develop. This combined analytical/numerical approach provides a deeper insight into charged particle dynamics than does analysis alone.

Brief note on Implicit v. Explicit numerical integration schemes

Suppose it is desired use numerical methods to integrate the equation

$$\frac{dy}{dt} = f(y(t), t)$$

Unfortunately, since $y(t)$ is the sought-after quantity, we do not know what to use in the right hand side for $y(t)$. A naive choice would be to use the previous value of y in the RHS to get a scheme of the form

$$\frac{y_{\text{new}} - y_{\text{old}}}{\Delta t} = f(y_{\text{old}}, t)$$

which may be solved to give

$$y_{\text{new}} = y_{\text{old}} + \Delta t f(y_{\text{old}}, t)$$

Simple and appealing as this is, it does not work since it is numerically unstable.

However, if we use the following scheme we will get a stable result:

$$\frac{y_{\text{new}} - y_{\text{old}}}{\Delta t} = f((y_{\text{new}} + y_{\text{old}})/2, t) \quad (1.46)$$

In other words, we have used the average of the new and the old values of y in the RHS. This makes sense because the RHS is a function evaluated at time t whereas $y_{\text{new}} = y(t + \Delta t/2)$ and $y_{\text{old}} = y(t - \Delta t/2)$. If Taylor expand these last quantities are Taylor expanded, it is seen that to lowest order $y(t) = [y(t + \Delta t/2) + y(t - \Delta t/2)]/2$.

Since y_{new} occurs on both sides of the equation we will have to solve some sort of equation, or invert some sort of matrix to get y_{new} .

Start with

$$m \frac{d\mathbf{v}}{dt} = q(\mathbf{E} + \mathbf{v} \times \mathbf{B}).$$

Define, the angular cyclotron frequency vector $\boldsymbol{\Omega} = q\mathbf{B}/m$ and the normalized electric field $\boldsymbol{\Sigma} = q\mathbf{E}/m$ so that the above equation becomes

$$\frac{d\mathbf{v}}{dt} = \boldsymbol{\Sigma} + \mathbf{v} \times \boldsymbol{\Omega} \quad (1.47)$$

Using the implicit scheme of Eq.(1.46), show that Eq. (1.47) becomes

$$\mathbf{v}_{\text{new}} + \mathbf{A} \times \mathbf{v}_{\text{new}} = \mathbf{C}$$

where $\mathbf{A} = \boldsymbol{\Omega}\Delta t/2$ and $\mathbf{C} = \mathbf{v}_{\text{old}} + \Delta t (\boldsymbol{\Sigma} + \mathbf{v}_{\text{old}} \times \boldsymbol{\Omega}/2)$. By first dotting the above equation with \mathbf{A} and then crossing it with \mathbf{A} show that the new value of velocity is given by

$$\mathbf{v}_{\text{new}} = \frac{\mathbf{C} + \mathbf{A}\mathbf{A} \cdot \mathbf{C} - \mathbf{A} \times \mathbf{C}}{1 + A^2}.$$

The new position is simply given by

$$\mathbf{x}_{\text{new}} = \mathbf{x}_{\text{old}} + \mathbf{v}_{\text{new}} dt$$

The above two equations can be used to solve charged particle motion in complicated, 3D, time dependent fields. Use this particle integrator to calculate the trajectory of an electron moving in crossed electric and magnetic fields where the non-vanishing components are $E_x = 1$ volt/meter and $B_z = 1$ Tesla. Plot your result graphically on your computer monitor. Try varying the field strengths, polarities, and also try ions instead of electrons.

8. Use the leap-frog numerical integration scheme to demonstrate the Rutherford scattering problem:

(i) Define a characteristic length for this problem to be the impact parameter for a 90 degree scattering angle, $b_{\pi/2}$. A reasonable choice for the characteristic velocity is v_{∞} . What is the characteristic time?

(ii) Define a Cartesian coordinate system such that the z axis is parallel to the incident relative velocity vector \mathbf{v}_∞ and goes through the scattering center. Let the impact parameter be in the y direction so that the incident particle is traveling in the $y - z$ plane. Make the graphics display span $-50 \leq z/b_{\pi/2} \leq 50$ and $-50 \leq y/b_{\pi/2} \leq 50$.

(iii) Set the magnetic field to be zero, and let the electric field be

$$\mathbf{E} = -\nabla\phi$$

where $\phi = ?$ so $E_x = ?$ etc.

(iv) By using $r^2 = x^2 + y^2 + z^2$ calculate the electric field at each particle position, and so determine the particle trajectory.

(v) Demonstrate that the scattering is indeed at 90 degrees when $b = b_{\pi/2}$. What happens when b is much larger or much smaller than $b_{\pi/2}$? What happens when q_1, q_2 have the same or opposite signs?

(vi) Have your code draw the relevant theoretical scattering angle θ_s and show that the numerical result is in agreement.

9. Collision relations- Show that $\sigma n_t l_{mfp} = 1$ where σ is the cross-section for a collision, n_t is the density of target particles and l_{mfp} is the mean free path. Show also that the collision frequency is given by $\nu = \sigma n_t v$ where v is the velocity of the incident particle. Calculate the electron-electron collision frequency for the following plasmas: fusion ($n \sim 10^{20} \text{m}^{-3}$, $T \sim 10 \text{ keV}$), partially ionized discharge plasma ($n \sim 10^{16} \text{m}^{-3}$, $T \sim 10 \text{ eV}$). At what temperature does the conductivity of plasma equal that of copper, and of steel? Assume that $Z = 1$.
10. Cyclotron motion- Suppose that a particle is immersed in a uniform magnetic field $\mathbf{B} = B\hat{z}$ and there is no electric field. Suppose that at $t = 0$ the particle's initial position is at $\mathbf{x} = 0$ and its initial velocity is $\mathbf{v} = v_0\hat{x}$. Using the Lorentz equation, calculate the particle position and velocity as a function of time (be sure to take initial conditions into account). What is the direction of rotation for ions and for electrons (right handed or left handed with respect to the magnetic field)? If you had to make up a mnemonic for the sense of ion rotation, would it be Lions or Rions? Now, repeat the analysis but this time with an electric field $\mathbf{E} = \hat{x}E_0 \cos(\omega t)$. What happens in the limit where $\omega \rightarrow \Omega$ where $\Omega = qB/m$ is the cyclotron frequency? Assume that the particle is a proton and that $B = 1 \text{ Tesla}$, $v_0 = 10^5 \text{ m/s}$, and compare your results with direct numerical solution of the Lorentz equation. Use $E_0 = 10^4 \text{ V/m}$ for the electric field.
11. Space charge limited current- When a metal or metal oxide is heated to high temperatures it emits electrons from its surface. This process called *thermionic emission* is the basis of vacuum tube technology and is also essential when high currents are drawn from electrodes in a plasma. The electron emitting electrode is called a *cathode* while the electrode to which the electrons flow is called an *anode*. An idealized configuration is shown in Fig.1.5.

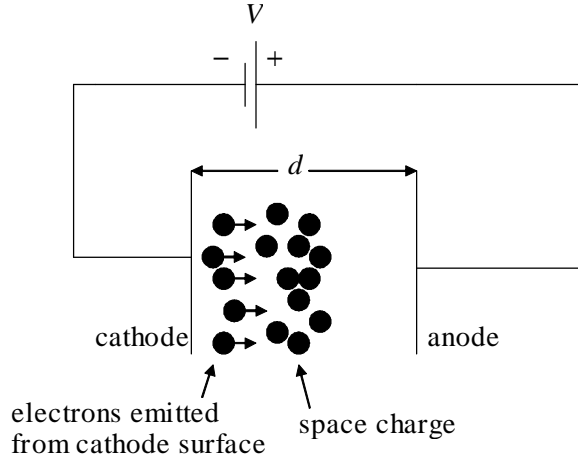


Figure 1.5: Electron cloud accelerated from cathode to anode encounters space charge of previously emitted electrons.

This configuration can operate in two regimes: (i) the *temperature limited* regime where the current is determined by the thermionic emission capability of the cathode, and (ii) the *space charge limited* regime, where the current is determined by a buildup of electron density in the region between cathode and anode (inter-electrode region). Let us now discuss this space charge limited regime: If the current is small then the number of electrons required to carry the current is small and so the inter-electrode region is nearly vacuum in which case the electric field in this region will be nearly uniform and be given by $E = V/d$ where V is the anode-cathode potential difference and d is the anode cathode separation. This electric field will accelerate the electrons from anode to cathode. However, if the current is large, there will be a significant electron density in the inter-electrode region. This space charge will create a localized depression in the potential (since electrons have negative charge). The result is that the electric field will be reduced in the region near the cathode. If the space charge is sufficiently large, the electric field at the cathode vanishes. In this situation attempting to increase the current by increasing the number of electrons ejected by the cathode will not succeed because an increase in current (which will give an increase in space charge) will produce a repulsive electric field which will prevent the additional electrons from leaving the cathode. Let us now calculate the space charge limited current and relate it to our discussion on Debye shielding. The current density in this system is

$$J = -n(x)ev(x) = \text{a negative constant}$$

Since potential is undefined with respect to a constant, let us choose this constant so

that the cathode potential is zero, in which case the anode potential is V_0 . Assuming that electrons leave the cathode with zero velocity, show that the electron velocity as a function of position is given by

$$v(x) = \sqrt{\frac{2eV(x)}{m_e}}.$$

Show that the above two equations, plus Poisson's equation, can be combined to give the following differential equation for the potential

$$\frac{d^2V}{dx^2} - \lambda V^{-1/2} = 0$$

where $\lambda = \epsilon_0^{-1} |J| \sqrt{m_e/2e}$. By multiplying this equation with the integrating factor dV/dx and using the space charge limited boundary condition that $E = 0$ at $x = 0$, solve for $V(x)$. By rearranging the expression for $V(x)$ show that the space charge limited current is

$$J = \frac{4}{9} \epsilon_0 \sqrt{\frac{2e}{m_e}} \frac{V^{3/2}}{d^2}.$$

This is called the Child-Langmuir space charge limited current. For reference the temperature limited current is given by the Richardson-Dushman law,

$$J = AT^2 e^{-\phi_0/\kappa T}$$

where coefficient A and the *work function* ϕ_0 are properties of the cathode material, while T is the cathode temperature. Thus, the actual cathode current will be whichever is the smaller of the above two expressions. Show there is a close relationship between the physics underlying the Child-Langmuir law and Debye shielding (hint-characterize the electron velocity as being a thermal velocity and its energy as being a thermal energy, show that the inter-electrode spacing corresponds to ?). Suppose that a cathode was operating in the space charge limited regime and that some positively charged ions were placed in the inter-electrode region. What would happen to the space charge-would it be possible to draw more or less current from the cathode? Suppose the entire inter-electrode region were filled with plasma with electron temperature T_e . What would be the appropriate value of d and how much current could be drawn from the cathode (assuming it were sufficiently hot)? Does this give you any ideas on why high current switch tubes (called ignitrons) use plasma to conduct the current?

Derivation of fluid equations: Vlasov, 2-fluid, MHD

2.1 Phase-space

Consider a particle moving in a one-dimensional space and let its position be described as $x = x(t)$ and its velocity as $v = v(t)$. A way to visualize the x and v trajectories simultaneously is to plot them on a 2-dimensional graph where the horizontal coordinate is given by $x(t)$ and the vertical coordinate is given by $v(t)$. This $x - v$ plane is called *phase-space*. The trajectory (or orbit) of several particles can be represented as a set of curves in phase-space as shown in Fig.2.1. Examples of a few qualitatively different phase-space orbits are shown in Fig.2.1.

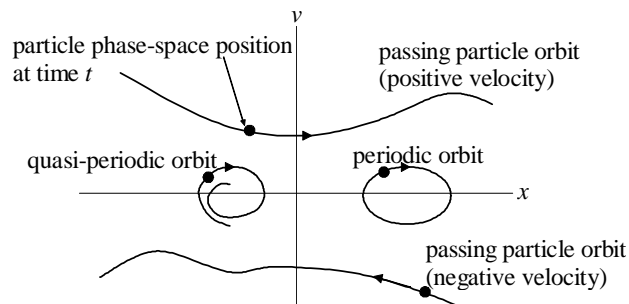


Figure 2.1: Phase space showing different types of possible particle orbits.

Particles in the upper half plane always move to the right since they have a positive velocity while those in the lower half plane always move to the left. Particles having exact periodic motion [e.g., $x = A \cos(\omega t)$, $v = -\omega A \sin(\omega t)$] alternate between moving to the right and the left and so describe an ellipse in phase-space. Particles with nearly periodic (quasi-periodic) motions will have near-ellipses or spiral orbits. A particle that does not

reverse direction is called a passing particle, while a particle confined to a certain region of phase-space (e.g., a particle with periodic motion) is called a trapped particle.

2.2 Distribution function and Vlasov equation

At any given time, each particle has a specific position and velocity. We can therefore characterize the instantaneous configuration of a large number of particles by specifying the density of particles at each point x, v in phase-space. The function prescribing the instantaneous density of particles in phase-space is called the *distribution function* and is denoted by $f(x, v, t)$. Thus, $f(x, v, t)dx dv$ is the number of particles at time t having positions in the range between x and $x + dx$ and velocities in the range between v and $v + dv$. As time progresses, the particle motion and acceleration causes the number of particles in these x and v ranges to change and so f will change. This temporal evolution of f gives a description of the system more detailed than a fluid description, but less detailed than following the trajectory of each individual particle. Using the evolution of f to characterize the system does not keep track of the trajectories of individual particles, but rather characterizes classes of particles having the same x, v .

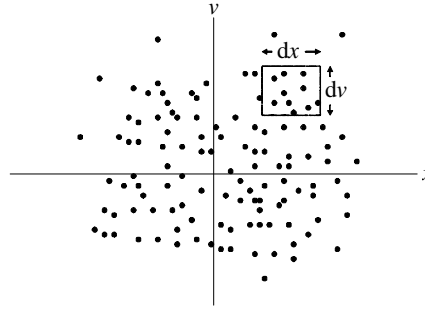


Figure 2.2: A box with in phase space having width dx and height dv .

Now consider the rate of change of the number of particles inside a small box in phase-space such as is shown in Fig.2.2. Defining $a(x, v, t)$ to be the acceleration of a particle, it is seen that the particle flux in the horizontal direction is fv and the particle flux in the vertical direction is fa . Thus, the particle fluxes into the four sides of the box are:

1. Flux into left side of box is $f(x, v, t)v dv$
2. Flux into right side of box is $-f(x + dx, v, t)v dv$
3. Flux into bottom of box is $f(x, v, t)a(x, v, t) dx$
4. Flux into top of box is $-f(x, v + dv, t)a(x, v + dv, t) dx$

The number of particles in the box is $f(x, v, t)dx dv$ so that the rate of change of particles in the box is

$$\frac{\partial f(x, v, t)}{\partial t} dx dv = -f(x + dx, v, t) v dv + f(x, v, t) v dv - f(x, v + dv, t) a(x, v + dv, t) dx + f(x, v, t) a(x, v, t) dx \quad (2.1)$$

or, on Taylor expanding the quantities on the right hand side, we obtain the one dimensional *Vlasov equation*,

$$\frac{\partial f}{\partial t} + v \frac{\partial f}{\partial x} + \frac{\partial}{\partial v} (af) = 0. \quad (2.2)$$

It is straightforward to generalize Eq.(2.2) to three dimensions and so obtain the three-dimensional Vlasov equation

$$\frac{\partial f}{\partial t} + \mathbf{v} \cdot \frac{\partial f}{\partial \mathbf{x}} + \frac{\partial}{\partial \mathbf{v}} \cdot (\mathbf{a}f) = 0. \quad (2.3)$$

Because \mathbf{x} , \mathbf{v} are independent quantities in phase-space, the spatial derivative term has the commutation property:

$$\mathbf{v} \cdot \frac{\partial f}{\partial \mathbf{x}} = \frac{\partial}{\partial \mathbf{x}} \cdot (\mathbf{v}f). \quad (2.4)$$

The particle acceleration is given by the Lorentz force

$$\mathbf{a} = \frac{q}{m} (\mathbf{E} + \mathbf{v} \times \mathbf{B}) \quad (2.5)$$

Because $(\mathbf{v} \times \mathbf{B})_i = v_j B_k - v_k B_j$ is independent of v_i , the term $\partial(\mathbf{v} \times \mathbf{B})_i / \partial v_i$ vanishes so that even though the acceleration \mathbf{a} is velocity-dependent, it nevertheless commutes with the vector velocity derivative as

$$\mathbf{a} \cdot \frac{\partial f}{\partial \mathbf{v}} = \frac{\partial}{\partial \mathbf{v}} \cdot (\mathbf{a}f) \quad (2.6)$$

Because of this commutation property the Vlasov equation can also be written as

$$\frac{\partial f}{\partial t} + \mathbf{v} \cdot \frac{\partial f}{\partial \mathbf{x}} + \mathbf{a} \cdot \frac{\partial f}{\partial \mathbf{v}} = 0 \quad (2.7)$$

If we “sit on top of” a particle moving in phase-space with trajectory $\mathbf{x} = \mathbf{x}(t)$, $\mathbf{v} = \mathbf{v}(t)$ and measure the distribution function as we are carried along by the particle, the observed rate of change of the distribution function will be $df(\mathbf{x}(t), \mathbf{v}(t), t)/dt$ where the d/dt means that the derivative is measured in the moving frame. Because $d\mathbf{x}/dt = \mathbf{v}$ and $d\mathbf{v}/dt = \mathbf{a}$, this observed rate of change is

$$\left(\frac{df(\mathbf{x}(t), \mathbf{v}(t), t)}{dt} \right)_{\text{orbit}} = \frac{\partial f}{\partial t} + \mathbf{v} \cdot \frac{\partial f}{\partial \mathbf{x}} + \mathbf{a} \cdot \frac{\partial f}{\partial \mathbf{v}} = 0. \quad (2.8)$$

Thus, the distribution function as measured when moving along a particle trajectory (orbit) is a *constant*. This gives a powerful method for finding solutions to the Vlasov equation. Since the distribution function is a constant when measured in the frame following an orbit, we can choose it to depend on *any quantity* that is constant along the orbit (Jeans 1915, Watson 1956).

For example, if the energy E of particles is constant along their orbits then $f = f(E)$ is a solution to the Vlasov equation. On the other hand, if both the energy and the momentum p are constant along particle orbits, then any distribution function with the functional dependence $f = f(E, p)$ is a solution to the Vlasov equation. Depending on the situation at hand, the energy and/or canonical momentum may or may not be constant along an orbit and so whether or not $f = f(E, p)$ is a solution to the Vlasov equation depends on the specific problem under consideration. However, there always exists at least one constant of the motion for any trajectory because, just like every human being has an invariant birthday, the initial conditions of a particle trajectory are invariant along its orbit. As a simple example, consider a situation where there is no electromagnetic field so that $\mathbf{a} = 0$ in which case the particle trajectories are simply $\mathbf{x}(t) = \mathbf{x}_0 + \mathbf{v}_0 t$, $\mathbf{v}(t) = \mathbf{v}_0$ where $\mathbf{x}_0, \mathbf{v}_0$ are the initial position and velocity. Let us check to see whether $f(\mathbf{x}_0)$ is indeed a solution to the Vlasov equation. Write $\mathbf{x}_0 = \mathbf{x}(t) - \mathbf{v}_0 t$ so $f(\mathbf{x}_0) = f(\mathbf{x}(t) - \mathbf{v}_0 t)$ and observe that

$$\frac{\partial f}{\partial t} + \mathbf{v} \cdot \frac{\partial f}{\partial \mathbf{x}} + \mathbf{a} \cdot \frac{\partial f}{\partial \mathbf{v}} = -\mathbf{v}_0 \cdot \frac{\partial f}{\partial \mathbf{x}} + \mathbf{v} \cdot \frac{\partial f}{\partial \mathbf{x}} = 0. \quad (2.9)$$

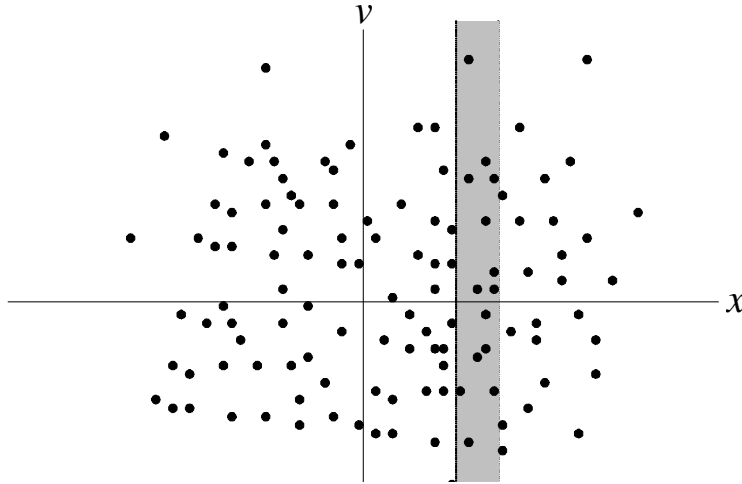


Figure 2.3: Moments give weighted averages of the particles in the shaded vertical strip

2.3 Moments of the distribution function

Let us count the particles in the shaded vertical strip in Fig.2.3. The number of particles in this strip is the number of particles lying between x and $x + dx$ where x is the location of the left hand side of the strip and $x + dx$ is the location of the right hand side. The number of particles in the strip is equivalently defined as $n(x, t)dx$ where $n(x, t)$ is the *density* of

particles at x . Thus we see that $\int f(x, v)dv = n(x)$; the transition from a phase-space description (i.e., x, v are dependent variables) to a normal space description (i.e., x is a dependent variable) involves “integrating out” the velocity dependence to obtain a quantity (e.g., density) depending only on position. Since the number of particles is finite, and since f is a positive quantity, we see that f must vanish as $v \rightarrow \infty$.

Another way of viewing f is to consider it as the probability that a randomly selected particle at position x has the velocity v . Using this point of view, we see that averaging over the velocities of all particles at x gives the mean velocity $u(x)$ determined by $n(x)u(x) = \int v f(x, v)dv$. Similarly, multiplying f by v^2 and integrating over velocity will give an expression for the mean energy of all the particles. This procedure of multiplying f by various powers of v and then integrating over velocity is called *taking moments of the distribution function*.

It is straightforward to generalize this “moment-taking” to three dimensional problems simply by taking integrals over three-dimensional velocity space. Thus, in three dimensions the density becomes

$$n(\mathbf{x}) = \int f(\mathbf{x}, \mathbf{v})d\mathbf{v} \quad (2.10)$$

and the mean velocity becomes

$$\mathbf{u}(\mathbf{x}) = \frac{\int \mathbf{v}f(\mathbf{x}, \mathbf{v})d\mathbf{v}}{n(\mathbf{x})}. \quad (2.11)$$

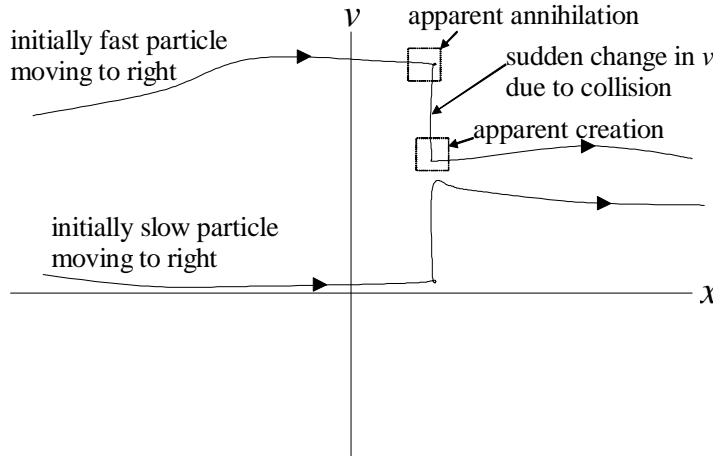


Figure 2.4: Detailed view of collisions causing ‘jumps’ in phase space

2.3.1 Treatment of collisions in the Vlasov equation

It was shown in Sec. 1.8 that the cumulative effect of grazing collisions dominates the

cumulative effect of the more infrequently occurring large angle collisions. In order to see how collisions affect the Vlasov equation, let us now temporarily imagine that the grazing collisions are replaced by an equivalent sequence of abrupt large scattering angle encounters as shown in Fig.2.4. Two particles involved in a collision do not significantly change their positions during the course of a collision, but they do substantially change their velocities. For example, a particle making a head-on collision with an equal mass stationary particle will stop after the collision, while the target particle will assume the velocity of the incident particle. If we draw the detailed phase-space trajectories characterized by a collision between two particles we see that each particle has a sudden change in its vertical coordinate (i.e., velocity) but no change in its horizontal coordinate (i.e., position). The collision-induced velocity jump occurs very fast so that if the phase-space trajectories were recorded with a “movie camera” having insufficient framing rate to catch the details of the jump the resulting movie would show particles being spontaneously created or annihilated within given volumes of phase-space (e.g., within the boxes shown in Fig. 2.4).

The details of these individual jumps in phase-space are complicated and yet of little interest since all we really want to know is the cumulative effect of many collisions. It is therefore both efficient and sufficient to follow the trajectories on the slow time scale while accounting for the apparent “creation” or “annihilation” of particles by inserting a *collision operator* on the right hand side of the Vlasov equation. In the example shown here it is seen that when a particle is apparently “created” in one box, another particle must be simultaneously “annihilated” in another box at the same x coordinate but a different v coordinate (of course, what is actually happening is that a single particle is suddenly moving from one box to the other). This coupling of the annihilation and creation rates in different boxes constrains the form of the collision operator. We will not attempt to derive collision operators in this chapter but will simply discuss the constraints on these operators. From a more formal point of view, collisions are characterized by constrained sources and sinks for particles in phase-space and inclusion of collisions in the Vlasov equation causes the Vlasov equation to assume the form

$$\frac{\partial f_\sigma}{\partial t} + \frac{\partial}{\partial \mathbf{x}} \cdot (\mathbf{v} f_\sigma) + \frac{\partial}{\partial \mathbf{v}} \cdot (\mathbf{a} f_\sigma) = \sum_\alpha C_{\sigma\alpha}(f_\sigma) \quad (2.12)$$

where $C_{\sigma\alpha}(f_\sigma)$ is the rate of change of f_σ due to collisions of species σ with species α .

Let us now list the constraints which must be satisfied by the collision operator $C_{\sigma\alpha}(f_\sigma)$ are as follows:

- (a) Conservation of particles – Collisions cannot change the total number of particles at a particular location so

$$\int d\mathbf{v} C_{\sigma\alpha}(f_\sigma) = 0. \quad (2.13)$$

- (b) Conservation of momentum – Collisions between particles of the same species cannot change the total momentum of that species so

$$\int d\mathbf{v} m_\sigma \mathbf{v} C_{\sigma\sigma}(f_\sigma) = 0 \quad (2.14)$$

while collisions between different species must conserve the total momentum of both species together so

$$\int d\mathbf{v} m_i \mathbf{v} C_{ie}(f_i) + \int d\mathbf{v} m_e \mathbf{v} C_{ei}(f_e) = 0. \quad (2.15)$$

- (c) Conservation of energy –Collisions between particles of the same species cannot change the total energy of that species so

$$\int d\mathbf{v} m_\sigma v^2 C_{\sigma\sigma}(f_\sigma) = 0 \quad (2.16)$$

while collisions between different species must conserve the total energy of both species together so

$$\int d\mathbf{v} m_i v^2 C_{ie}(f_i) + \int d\mathbf{v} m_e v^2 C_{ei}(f_e) = 0. \quad (2.17)$$

2.4 Two-fluid equations

Instead of just taking moments of the distribution function f itself, moments will now be taken of the entire Vlasov equation to obtain a set of partial differential equations relating the mean quantities $n(\mathbf{x})$, $\mathbf{u}(\mathbf{x})$, etc. We begin by integrating the Vlasov equation, Eq.(2.12), over velocity for each species. This first and simplest step in the procedure is often called taking the “zeroth” moment, since we are multiplying by unity which for consistency with later “moment-taking”, can be considered as multiplying the entire Vlasov equation by \mathbf{v} raised to the power zero. Multiplying the Vlasov equation by unity and then integrating over velocity gives

$$\int \left[\frac{\partial f_\sigma}{\partial t} + \frac{\partial}{\partial \mathbf{x}} \cdot (\mathbf{v} f_\sigma) + \frac{\partial}{\partial \mathbf{v}} \cdot (\mathbf{a} f_\sigma) \right] d\mathbf{v} = \sum_\alpha \int C_{\sigma\alpha}(f_\sigma) d\mathbf{v}. \quad (2.18)$$

The velocity integral commutes with both the time and space derivatives on the left hand side because \mathbf{x} , \mathbf{v} , and t are independent variables, while the third term on the left hand side is the volume integral of a divergence in velocity space. Gauss’s theorem [i.e., $\int_{vol} d\mathbf{x} \nabla \cdot \mathbf{Q} = \int_{sfc} ds \cdot \mathbf{Q}$] gives f_σ evaluated on a surface at $v = \infty$. However, because $f_\sigma \rightarrow 0$ as $v \rightarrow \infty$, this surface integral in velocity space vanishes. Using Eqs.(2.10), (2.11), and (2.13), we see that Eq.(2.18) becomes the species *continuity equation*

$$\frac{\partial n_\sigma}{\partial t} + \nabla \cdot (n_\sigma \mathbf{u}_\sigma) = 0. \quad (2.19)$$

Now let us multiply Eq.(2.12) by \mathbf{v} and integrate over velocity to take the “first moment”,

$$\int \mathbf{v} \left[\frac{\partial f_\sigma}{\partial t} + \frac{\partial}{\partial \mathbf{x}} \cdot (\mathbf{v} f_\sigma) + \frac{\partial}{\partial \mathbf{v}} \cdot (\mathbf{a} f_\sigma) \right] d\mathbf{v} = \sum_\alpha \int \mathbf{v} C_{\sigma\alpha}(f_\sigma) d\mathbf{v}. \quad (2.20)$$

This may be re-arranged in a more tractable form by:

- (i) “pulling” both the time and space derivatives out of the velocity integral,
- (ii) writing $\mathbf{v} = \mathbf{v}'(\mathbf{x}, t) + \mathbf{u}(\mathbf{x}, t)$ where $\mathbf{v}'(\mathbf{x}, t)$ is the *random* part of a given velocity, i.e., that part of the velocity which differs from the mean (note that \mathbf{v} is independent of both \mathbf{x} and t but \mathbf{v}' is not; also $d\mathbf{v} = d\mathbf{v}'$),
- (iii) integrating by parts in 3-D velocity space on the acceleration term and using

$$\left(\frac{\partial \mathbf{v}}{\partial \mathbf{v}}\right)_{ij} = \delta_{ij}.$$

After performing these manipulations, the first moment of the Vlasov equation becomes

$$\begin{aligned} \frac{\partial (n_\sigma \mathbf{u}_\sigma)}{\partial t} + \frac{\partial}{\partial \mathbf{x}} \cdot \int (\mathbf{v}' \mathbf{v}' + \mathbf{v}' \mathbf{u}_\sigma + \mathbf{u}_\sigma \mathbf{v}' + \mathbf{u}_\sigma \mathbf{u}_\sigma) f_\sigma d\mathbf{v}' \\ - \frac{q_\sigma}{m_\sigma} \int (\mathbf{E} + \mathbf{v} \times \mathbf{B}) f_\sigma d\mathbf{v}' = -\frac{1}{m_\sigma} \mathbf{R}_{\sigma\alpha} \end{aligned} \quad (2.21)$$

where $\mathbf{R}_{\sigma\alpha}$ is the net frictional drag force due to collisions of species σ with species α . Note that $\mathbf{R}_{\sigma\sigma} = 0$ since a species cannot exert net drag on itself (e.g., the totality of electrons cannot cause frictional drag on the totality of electrons). The frictional terms have the form

$$\mathbf{R}_{ei} = \nu_{ei} m_e n_e (\mathbf{u}_e - \mathbf{u}_i) \quad (2.22)$$

$$\mathbf{R}_{ie} = \nu_{ie} m_i n_i (\mathbf{u}_i - \mathbf{u}_e) \quad (2.23)$$

so that in the ion frame the drag on electrons is simply the total electron momentum $m_e n_e \mathbf{u}_e$ measured in this frame multiplied by the rate ν_{ei} at which this momentum is destroyed by collisions with ions. This form for frictional drag has the following properties: (i) $\mathbf{R}_{ei} + \mathbf{R}_{ie} = 0$ showing that the plasma cannot have a frictional drag on itself, (ii) friction causes the faster species to be slowed down by the slower species, and (iii) there is no friction between species if both have the same mean velocity.

Equation (2.21) can be further simplified by factoring \mathbf{u} out of the velocity integrals and recalling that by definition $\int \mathbf{v}' f_\sigma d\mathbf{v}' = 0$. Thus, Eq. (2.21) reduces to

$$m_\sigma \left[\frac{\partial (n_\sigma \mathbf{u}_\sigma)}{\partial t} + \frac{\partial}{\partial \mathbf{x}} \cdot (n_\sigma \mathbf{u}_\sigma \mathbf{u}_\sigma) \right] = n_\sigma q_\sigma (\mathbf{E} + \mathbf{u}_\sigma \times \mathbf{B}) - \frac{\partial}{\partial \mathbf{x}} \cdot \overleftrightarrow{\mathbf{P}}_\sigma - \mathbf{R}_{\sigma\alpha} \quad (2.24)$$

where the *pressure tensor* $\overleftrightarrow{\mathbf{P}}$ is defined by

$$\overleftrightarrow{\mathbf{P}}_\sigma = m_\sigma \int \mathbf{v}' \mathbf{v}' f_\sigma d\mathbf{v}'.$$

If f_σ is an isotropic function of \mathbf{v}' , then the off-diagonal terms in $\overleftrightarrow{\mathbf{P}}_\sigma$ vanish and the three diagonal terms are identical. In this case, it is useful to define the diagonal terms to be the *scalar pressure* P_σ , i.e.,

$$\begin{aligned} P_\sigma &= m_\sigma \int v'_x v'_x f_\sigma d\mathbf{v}' = m_\sigma \int v'_y v'_y f_\sigma d\mathbf{v}' = m_\sigma \int v'_z v'_z f_\sigma d\mathbf{v}' \\ &= \frac{m_\sigma}{3} \int \mathbf{v}' \cdot \mathbf{v}' f_\sigma d\mathbf{v}'. \end{aligned} \quad (2.25)$$

Equation (2.25) defines pressure for a three-dimensional isotropic system. However, we will often deal with systems of reduced dimensionality, i.e., systems with just one or two dimensions. Equation (2.25) can therefore be generalized to these other cases by introducing the general N -dimensional definition for scalar pressure

$$P_\sigma = \frac{m_\sigma}{N} \int \mathbf{v}' \cdot \mathbf{v}' f_\sigma d^N \mathbf{v}' = \frac{m_\sigma}{N} \int \sum_{j=1}^N v_j'^2 f_\sigma d^N \mathbf{v}' \quad (2.26)$$

where \mathbf{v}' is the N -dimensional random velocity.

It is important to emphasize that assuming isotropy is done largely for mathematical convenience and that in real systems the distribution function is often quite anisotropic. Collisions, being randomizing, drive the distribution function towards isotropy, while competing processes simultaneously drive it towards anisotropy. Thus, each situation must be considered individually in order to determine whether there is sufficient collisionality to make f isotropic. Because fully-ionized hot plasmas often have insufficient collisions to make f isotropic, the oft-used assumption of isotropy is an oversimplification which may or may not be acceptable depending on the phenomenon under consideration.

On expanding the derivatives on the left hand side of Eq.(2.24), it is seen that two of the terms combine to give \mathbf{u} times Eq. (2.19). After removing this embedded continuity equation, Eq.(2.24) reduces to

$$n_\sigma m_\sigma \frac{d\mathbf{u}_\sigma}{dt} = n_\sigma q_\sigma (\mathbf{E} + \mathbf{u}_\sigma \times \mathbf{B}) - \nabla P_\sigma - \mathbf{R}_{\sigma\alpha} \quad (2.27)$$

where the operator d/dt is defined to be the *convective derivative*

$$\frac{d}{dt} = \frac{\partial}{\partial t} + \mathbf{u}_\sigma \cdot \nabla \quad (2.28)$$

which characterizes the temporal rate of change seen by an observer *moving with the mean fluid velocity* \mathbf{u}_σ of species σ . An everyday example of the convective term would be the apparent temporal increase in density of automobiles seen by a motorcyclist who enters a traffic jam of stationary vehicles and is not impeded by the traffic jam.

At this point in the procedure it becomes evident that a certain pattern recurs for each successive moment of the Vlasov equation. When we took the zeroth moment, an equation for the density $\int f_\sigma d\mathbf{v}$ resulted, but this also introduced a term involving the next higher moment, namely the mean velocity $\sim \int \mathbf{v} f_\sigma d\mathbf{v}$. Then, when we took the first moment to get an equation for the velocity, an equation was obtained containing a term involving the next higher moment, namely the pressure $\sim \int \mathbf{v} \mathbf{v} f_\sigma d\mathbf{v}$. Thus, each time we take a moment of the Vlasov equation, an equation for the moment we want is obtained, but because of the $\mathbf{v} \cdot \nabla f$ term in the Vlasov equation, a next higher moment also appears. Thus, moment-taking never leads to a closed system of equations; there is always be a “loose end”, a highest moment for which there is no determining equation. Some sort of ad hoc closure procedure must always be invoked to terminate this chain (as seen below, typical closures involve invoking adiabatic or isothermal assumptions). Another feature of taking moments is that each higher moment has embedded in it a term which contains complete lower moment equations multiplied by some factor. Algebraic manipulation can identify these lower moment equations and eliminate them to give a simplified higher moment equation.

Let us now take the second moment of the Vlasov equation. Unlike the zeroth and first moments, here the dimensionality of the system enters explicitly so the more general pressure definition given by Eq. (2.26) will be used. Multiplying the Vlasov equation by $m_\sigma v^2/2$ and integrating over velocity gives

$$\left\{ \begin{array}{l} \frac{\partial}{\partial t} \int \frac{m_\sigma v^2}{2} f_\sigma d^N \mathbf{v} \\ + \frac{\partial}{\partial \mathbf{x}} \cdot \int \frac{m_\sigma v^2}{2} \mathbf{v} f_\sigma d^N \mathbf{v} \\ + q_\sigma \int \frac{v^2}{2} \frac{\partial}{\partial \mathbf{v}} \cdot (\mathbf{E} + \mathbf{v} \times \mathbf{B}) f_\sigma d^N \mathbf{v} \end{array} \right\} = \sum_\alpha \int m_\sigma \frac{v^2}{2} C_{\sigma\alpha} f_\sigma d^N \mathbf{v}. \quad (2.29)$$

We now consider each term of this equation separately as follows:

1. The time derivative term becomes

$$\frac{\partial}{\partial t} \int \frac{m_\sigma v^2}{2} f_\sigma d^N \mathbf{v} = \frac{\partial}{\partial t} \int \frac{m_\sigma (\mathbf{v}' + \mathbf{u}_\sigma)^2}{2} f_\sigma d^N \mathbf{v}' = \frac{\partial}{\partial t} \left(\frac{NP_\sigma}{2} + \frac{m_\sigma n_\sigma u_\sigma^2}{2} \right).$$

2. Again using $\mathbf{v} = \mathbf{v}' + \mathbf{u}_\sigma$ the space derivative term becomes

$$\frac{\partial}{\partial \mathbf{x}} \cdot \int \frac{m_\sigma v^2}{2} \mathbf{v} f_\sigma d^N \mathbf{v} = \nabla \cdot \left(\mathbf{Q}_\sigma + \frac{2+N}{2} P_\sigma \mathbf{u}_\sigma + \frac{m_\sigma n_\sigma u_\sigma^2}{2} \mathbf{u}_\sigma \right).$$

where $\mathbf{Q}_\sigma = \int \frac{m_\sigma v'^2}{2} \mathbf{v}' f_\sigma d^N \mathbf{v}$ is called the *heat flux*.

3. On integrating by parts, the acceleration term becomes

$$q_\sigma \int \frac{v^2}{2} \frac{\partial}{\partial \mathbf{v}} \cdot [(\mathbf{E} + \mathbf{v} \times \mathbf{B}) f_\sigma] d^N \mathbf{v} = -q_\sigma \int \mathbf{v} \cdot \mathbf{E} f_\sigma d\mathbf{v} = -q_\sigma n_\sigma \mathbf{u}_\sigma \cdot \mathbf{E}.$$

4. The collision term becomes (using Eq.(2.16))

$$\sum_\alpha \int m_\sigma \frac{v^2}{2} C_{\sigma\alpha} f_\sigma d\mathbf{v} = \int_{\alpha \neq \sigma} m_\sigma \frac{v^2}{2} C_{\sigma\alpha} f_\sigma d\mathbf{v} = - \left(\frac{\partial W}{\partial t} \right)_{E\sigma\alpha}.$$

where $(\partial W/\partial t)_{E\sigma\alpha}$ is the rate at which species σ collisionally transfers energy to species α .

Combining the above four relations, Eq.(2.29) becomes

$$\begin{aligned} \frac{\partial}{\partial t} \left(\frac{NP_\sigma}{2} + \frac{m_\sigma n_\sigma u_\sigma^2}{2} \right) + \nabla \cdot \left(\mathbf{Q}_\sigma + \frac{2+N}{2} P_\sigma \mathbf{u}_\sigma + \frac{m_\sigma n_\sigma u_\sigma^2}{2} \mathbf{u}_\sigma \right) - q_\sigma n_\sigma \mathbf{u}_\sigma \cdot \mathbf{E} \\ = - \left(\frac{\partial W}{\partial t} \right)_{E\sigma\alpha}. \end{aligned} \quad (2.30)$$

This equation can be simplified by invoking two mathematical identities, the first of which is

$$\frac{\partial}{\partial t} \left(\frac{m_\sigma n_\sigma u_\sigma^2}{2} \right) + \nabla \cdot \left(\frac{m_\sigma n_\sigma u_\sigma^2}{2} \mathbf{u}_\sigma \right) = n_\sigma \left(\frac{\partial}{\partial t} + \mathbf{u}_\sigma \cdot \nabla \right) \frac{m_\sigma u_\sigma^2}{2} = n_\sigma \frac{d}{dt} \left(\frac{m_\sigma u_\sigma^2}{2} \right). \quad (2.31)$$

The second identity is obtained by dotting the equation of motion with \mathbf{u}_σ and is

$$\begin{aligned} & n_\sigma m_\sigma \left[\frac{\partial}{\partial t} \left(\frac{u_\sigma^2}{2} \right) + \mathbf{u}_\sigma \cdot \left(\nabla \left(\frac{u_\sigma^2}{2} \right) - \mathbf{u}_\sigma \times \nabla \times \mathbf{u}_\sigma \right) \right] \\ &= n_\sigma q_\sigma \mathbf{u}_\sigma \cdot \mathbf{E} - \mathbf{u}_\sigma \cdot \nabla P_\sigma - \mathbf{R}_{\sigma\alpha} \cdot \mathbf{u}_\sigma \end{aligned}$$

or

$$n_\sigma \frac{d}{dt} \left(\frac{m_\sigma u_\sigma^2}{2} \right) = n_\sigma q_\sigma \mathbf{u}_\sigma \cdot \mathbf{E} - \mathbf{u}_\sigma \cdot \nabla P_\sigma - \mathbf{R}_{\sigma\alpha} \cdot \mathbf{u}_\sigma. \quad (2.32)$$

Inserting Eqs. (2.31) and (2.32) in Eq.(2.30) gives the energy evolution equation

$$\frac{N}{2} \frac{dP_\sigma}{dt} + \frac{2+N}{2} P \nabla \cdot \mathbf{u}_\sigma = -\nabla \cdot \mathbf{Q}_\sigma + \mathbf{R}_{\sigma\alpha} \cdot \mathbf{u}_\sigma - \left(\frac{\partial W}{\partial t} \right)_{E\sigma\alpha}. \quad (2.33)$$

The first term on the right hand side represents the heat flux, the second term gives the frictional heating of species σ due to frictional drag on species α , while the last term on the right hand side gives the rate at which species σ collisionally transfers energy to other species. Although Eq.(2.33) is complicated, two important limiting situations become evident if we let t be the characteristic time scale for a given phenomenon and l be its characteristic length scale. A characteristic velocity $V_{ph} \sim l/t$ may then be defined for the phenomenon and so, replacing temporal derivatives by t^{-1} and spatial derivatives by l^{-1} in Eq.(2.33), it is seen that the two limiting situations are:

1. *Isothermal limit* – The heat flux term dominates all other terms in which case the temperature becomes spatially uniform. This occurs if (i) $v_{T\sigma} \gg V_{ph}$ since the ratio of the left hand side terms to the heat flux term is $\sim V_{ph}/v_{T\sigma}$ and (ii) the collisional terms are small enough to be ignored.
2. *Adiabatic limit* – The heat flux terms and the collisional terms are small enough to be ignored compared to the left hand side terms; this occurs when $V_{ph} \gg v_{T\sigma}$. Adiabatic is a Greek word meaning ‘impassable’, and is used here to denote that no heat is flowing.

Both of these limits make it possible to avoid solving for \mathbf{Q}_σ which involves the third moment and so both the adiabatic and isothermal limit provide a closure to the moment equations.

The energy equation may be greatly simplified in the adiabatic limit by re-arranging the continuity equation to give

$$\nabla \cdot \mathbf{u}_\sigma = -\frac{1}{n_\sigma} \frac{dn_\sigma}{dt} \quad (2.34)$$

and then substituting this expression into the left hand side of Eq.(2.33) to obtain

$$\frac{1}{P_\sigma} \frac{dP_\sigma}{dt} = \frac{\gamma}{n_\sigma} \frac{dn_\sigma}{dt} \quad (2.35)$$

where

$$\gamma = \frac{N+2}{N}. \quad (2.36)$$

Equation (2.35) may be integrated to give the adiabatic equation of state

$$\frac{P_\sigma}{n_\sigma^\gamma} = \text{constant}; \quad (2.37)$$

this can be considered a derivation of adiabaticity based on geometry and statistical mechanics rather than on thermodynamic arguments.

2.4.1 Entropy of a distribution function

Collisions cause the distribution function to tend towards a simple final state characterized by having the maximum entropy for the given constraints (e.g., fixed total energy). To see this, we provide a brief discussion of entropy and show how it relates to a distribution function.

Suppose we throw two dice, labeled A and B , and let R denote the result of a throw. Thus R ranges from 2 through 12. The complete set of (A, B) combinations that give these R 's are listed below:

$$R = 2 \iff (1,1)$$

$$R = 3 \iff (1,2), (2,1)$$

$$R = 4 \iff (1,3), (3,1), (2,2)$$

$$R = 5 \iff (1,4), (4,1), (2,3), (3,2)$$

$$R = 6 \iff (1,5), (5,1), (2,4), (4,2), (3,3)$$

$$R = 7 \iff (1,6), (6,1), (2,5), (5,2), (3,4), (4,3)$$

$$R = 8 \iff (2,6), (6,2), (3,5), (5,3), (4,4)$$

$$R = 9 \iff (3,6), (6,3), (4,5), (5,4)$$

$$R = 10 \iff (4,6), (6,4), (5,5)$$

$$R = 11 \iff (5,6), (6,5)$$

$$R = 12 \iff (6,6)$$

There are six (A, B) pairs that give $R = 7$, but only one pair for $R = 2$ and only one pair for $R = 12$. Thus, there are six microscopic states [distinct (A, B) pairs] corresponding to $R = 7$ but only one microscopic state corresponding to each of $R = 2$ or $R = 12$. Thus, we *know more* about the microscopic state of the system if $R = 2$ or 12 than if $R = 7$. We define the entropy S to be the *natural logarithm of the number of microscopic states corresponding to a given macroscopic state*. Thus for the dice, the entropy would be the natural logarithm of the number of (A, B) pairs that correspond to a given R . The entropy for $R = 2$ or $R = 12$ would be zero since $S = \ln(1) = 0$, while the entropy for $R = 7$ would be $S = \ln(6)$ since there were six different ways of obtaining $R = 7$.

If the dice were to be thrown a statistically large number of times the most likely result for any throw is $R = 7$; this is the macroscopic state with the most number of microscopic states. Since any of the possible microscopic states is an equally likely outcome, the most likely macroscopic state after a large number of dice throws is the macroscopic state with the highest entropy.

Now consider a situation more closely related to the concept of a distribution function. In order to do this we first pose the following simple problem: Suppose we have a pegboard with \mathcal{N} holes, labeled $h_1, h_2, \dots, h_{\mathcal{N}}$ and we also have \mathcal{N} pegs labeled by $p_1, p_2, \dots, p_{\mathcal{N}}$. What are the number of ways of putting all the pegs in all the holes? Starting with hole h_1 , we have a choice of \mathcal{N} different pegs, but when we get to hole h_2 there are now only $\mathcal{N} - 1$ pegs remaining so that there are now only $\mathcal{N} - 1$ choices. Using this argument for

subsequent holes, we see there are $\mathcal{N}!$ ways of putting all the pegs in all the holes.

Let us complicate things further. Suppose that we arrange the holes in \mathcal{M} groups, say group G_1 has the first 10 holes, group G_2 has the next 19 holes, group G_3 has the next 4 holes and so on, up to group \mathcal{M} . We will use f to denote the number of holes in a group, thus $f(1) = 10$, $f(2) = 19$, $f(3) = 4$, etc. The number of ways of arranging pegs within a group is just the factorial of the number of pegs in the group, e.g., the number of ways of arranging the pegs within group 1 is just $10!$ and so in general the number of ways of arranging the pegs in the j^{th} group is $[f(j)]!$.

Let us denote C as the number of ways for putting all the pegs in all the groups *without caring* about the internal arrangement within groups. The number of ways of putting the pegs in all the groups *caring* about the internal arrangements in all the groups is $C \times f(1)! \times f(2)! \times \dots \times f(\mathcal{M})!$, but this is just the number of ways of putting all the pegs in all the holes, i.e.,

$$C \times f(1)! \times f(2)! \times \dots \times f(\mathcal{M})! = \mathcal{N}!$$

or

$$C = \frac{\mathcal{N}!}{f(1)! \times f(2)! \times \dots \times f(\mathcal{M})!}.$$

Now C is just the number of microscopic states corresponding to the macroscopic state of the prescribed grouping $f(1) = 10$, $f(2) = 19$, $f(3) = 4$, etc. so the entropy is just $S = \ln C$ or

$$\begin{aligned} S &= \ln \left(\frac{\mathcal{N}!}{f(1)! \times f(2)! \times \dots \times f(\mathcal{M})!} \right) \\ &= \ln \mathcal{N}! - \ln f(1)! - \ln f(2)! - \dots - \ln f(\mathcal{M})! \end{aligned} \quad (2.38)$$

Stirling's formula shows that the large argument asymptotic limit of the factorial function is

$$\lim_{k \rightarrow \text{large}} \ln k! = k \ln k - k. \quad (2.39)$$

Noting that $f(1) + f(2) + \dots + f(\mathcal{M}) = \mathcal{N}$ the entropy becomes

$$\begin{aligned} S &= \mathcal{N} \ln \mathcal{N} - f(1) \ln f(1) - f(2) \ln f(2) - \dots - f(\mathcal{M}) \ln f(\mathcal{M}) \\ &= \mathcal{N} \ln \mathcal{N} - \sum_{j=1}^{\mathcal{M}} f(j) \ln f(j) \end{aligned} \quad (2.40)$$

The constant $\mathcal{N} \ln \mathcal{N}$ is often dropped, giving

$$S = - \sum_{j=1}^{\mathcal{M}} f(j) \ln f(j). \quad (2.41)$$

If j is made into a continuous variable say, $j \rightarrow v$ so that $f(v)dv$ is the number of items in the group labeled by v , then the entropy can be written as

$$S = - \int dv f(v) \ln f(v). \quad (2.42)$$

By now, it is obvious that f could be the velocity distribution function in which case $f(v)dv$ is just the number of particles in the group having velocity between v and $v + dv$. Since the peg groups correspond to different velocity ranges coordinates, having more dimensions just means having more groups and so for three dimensions the entropy generalizes to

$$S = - \int d\mathbf{v} f(\mathbf{v}) \ln f(\mathbf{v}). \quad (2.43)$$

If the distribution function depends on position as well, this corresponds to still more peg groups, and so a distribution function which depends on both velocity and position will have the entropy

$$S = - \int dx \int d\mathbf{v} f(\mathbf{x}, \mathbf{v}) \ln f(\mathbf{x}, \mathbf{v}). \quad (2.44)$$

2.4.2 Effect of collisions on entropy

The highest entropy state is the most likely state of the system because the highest entropy state has the most number of microscopic states corresponding to the macroscopic state. Collisions (or other forms of randomization) will take some prescribed initial microscopic state where phase-space positions of all particles are individually specified and scramble these positions to give a new microscopic state. The new scrambled state could be any microscopic state, but is most likely to be a member of the class of microscopic states belonging to the highest entropy macroscopic state. Thus, any randomization process such as collisions will cause the system to evolve towards the maximum entropy macroscopic state.

An important shortcoming of this argument is that it neglects any conservation relations that have to be satisfied. To see this, note that the expression for entropy could be maximized if all the particles are put in one group, in which case $C = \mathcal{N}!$, which is the largest possible value for C . Thus, the maximum entropy configuration of \mathcal{N} plasma particles corresponds to all the particles having the same velocity. However, this would assign a specific energy to the system which would in general differ from the energy of the initial microstate. This maximum entropy state is therefore not accessible in isolated system, because energy would not be conserved if the system changed from its initial microstate to the maximum entropy state.

Thus, a qualification must be added to the argument. Randomizing processes will scramble the system to attain the state of maximum entropy state *consistent* with any constraints placed on the system. Examples of such constraints would be the requirements that the total system energy and the total number of particles must be conserved. We therefore re-formulate the problem as: given an isolated system with \mathcal{N} particles in a fixed volume V and initial average energy per particle $\langle E \rangle$, what is the maximum entropy state consistent with conservation of energy and conservation of number of particles? This is a variational problem because the goal is to maximize S subject to the constraint that both \mathcal{N} and $\mathcal{N} \langle E \rangle$ are fixed. The method of Lagrange multipliers can then be used to take into account these constraints. Using this method the variational problem becomes

$$\delta S - \lambda_1 \delta \mathcal{N} - \lambda_2 \delta (\mathcal{N} \langle E \rangle) = 0 \quad (2.45)$$

where λ_1 and λ_2 are as-yet undetermined Lagrange multipliers. The number of particles

is

$$\mathcal{N} = V \int f dv. \quad (2.46)$$

The energy of an individual particle is $E = mv^2/2$ where v is the velocity measured in the rest frame of the center of mass of the entire collection of \mathcal{N} particles. Thus, the total kinetic energy of all the particles in this rest frame is

$$\mathcal{N} \langle E \rangle = V \int \frac{mv^2}{2} f(v) dv \quad (2.47)$$

and so the variational problem becomes

$$\delta \int dv \left(f \ln f - \lambda_1 V f - \lambda_2 V \frac{mv^2}{2} f \right) = 0. \quad (2.48)$$

Incorporating the volume V into the Lagrange multipliers, and factoring out the coefficient δf this becomes

$$\int dv \delta f \left(1 + \ln f - \lambda_1 - \lambda_2 \frac{mv^2}{2} \right) = 0. \quad (2.49)$$

Since δf is arbitrary, the integrand must vanish, giving

$$\ln f = \lambda_2 \frac{mv^2}{2} - \lambda_1 \quad (2.50)$$

where the ‘1’ has been incorporated into λ_1 .

The maximum entropy distribution function of an isolated, energy and particle conserving system is therefore

$$f = \lambda_1 \exp(-\lambda_2 mv^2/2); \quad (2.51)$$

this is called a Maxwellian distribution function. We will often assume that the plasma is locally Maxwellian so that $\lambda_1 = \lambda_1(\mathbf{x}, t)$ and $\lambda_2 = \lambda_2(\mathbf{x}, t)$. We define the temperature to be

$$\kappa T_\sigma(\mathbf{x}, t) = \frac{1}{\lambda_2(\mathbf{x}, t)} \quad (2.52)$$

where Boltzmann’s factor κ allows temperature to be measured in various units. The normalization factor is set to be

$$\lambda_1(\mathbf{x}, t) = n(\mathbf{x}, t) \left(\frac{m_\sigma}{2\pi\kappa T_\sigma(\mathbf{x}, t)} \right)^{N/2} \quad (2.53)$$

where N is the dimensionality (1, 2, or 3) so that $\int f_\sigma(\mathbf{x}, \mathbf{v}, t) d^N \mathbf{v} = n_\sigma(\mathbf{x}, t)$. Because the kinetic energy of individual particles was defined in terms of velocities measured in the rest frame of the center of mass of the complete system of particles, if this center of mass is moving in the lab frame with a velocity \mathbf{u}_σ , then in the lab frame the Maxwellian will have the form

$$f_\sigma(\mathbf{x}, \mathbf{v}, t) = n_\sigma \left(\frac{m_\sigma}{2\pi\kappa T_\sigma} \right)^{N/2} \exp(-m_\sigma(\mathbf{v} - \mathbf{u}_\sigma)^2/2\kappa T_\sigma). \quad (2.54)$$

2.4.3 Relation between pressure and Maxwellian

The scalar pressure has a simple relation to the generalized Maxwellian as seen by recasting Eq.(2.26) as

$$\begin{aligned}
 P_\sigma &= -\frac{n_\sigma m_\sigma}{N} \left(\frac{\beta}{\pi}\right)^{N/2} \frac{d}{d\beta} \int e^{-\beta v^2} d\mathbf{v} \\
 &= -\frac{n_\sigma m_\sigma}{N} \left(\frac{\beta}{\pi}\right)^{N/2} \frac{d}{d\beta} \left(\frac{\beta}{\pi}\right)^{-N/2} \\
 &= n_\sigma \kappa T_\sigma,
 \end{aligned} \tag{2.55}$$

which is just the ideal gas law. Thus, the definitions that have been proposed for pressure and temperature are consistent with everyday notions for these quantities.

Clearly, neither the adiabatic nor the isothermal assumption will be appropriate when $V_{ph} \sim v_{T\sigma}$. The fluid description breaks down in this situation and the Vlasov description must be used. It must also be emphasized that the distribution function is Maxwellian only if there are sufficient collisions or some other randomizing process. Because of the weak collisionality of a plasma, this is often not the case. In particular, since the collision frequency scales as v^{-3} , fast particles take much longer to become Maxwellian than slow particles. It is not at all unusual for a plasma to be in a state where the low velocity particles have reached a Maxwellian distribution whereas the fast particles form a non-Maxwellian ‘‘tail’’.

We now summarize the two-fluid equations:

- continuity equation for each species

$$\frac{\partial n_\sigma}{\partial t} + \nabla \cdot (n_\sigma \mathbf{u}_\sigma) = 0 \tag{2.56}$$

- equation of motion for each species

$$n_\sigma m_\sigma \frac{d\mathbf{u}_\sigma}{dt} = n_\sigma q_\sigma (\mathbf{E} + \mathbf{u}_\sigma \times \mathbf{B}) - \nabla P_\sigma - \mathbf{R}_{\sigma\alpha} \tag{2.57}$$

- equation of state for each species

Regime	Equation of state	Name
$V_{ph} \gg v_{T\sigma}$	$P_\sigma \sim n_\sigma^\gamma$	adiabatic
$V_{ph} \ll v_{T\sigma}$	$P_\sigma = n_\sigma \kappa T_\sigma, T_\sigma = \text{constant}$	isothermal

- Maxwell’s equations

$$\nabla \times \mathbf{E} = -\frac{\partial \mathbf{B}}{\partial t} \tag{2.58}$$

$$\nabla \times \mathbf{B} = \mu_0 \sum_\sigma n_\sigma q_\sigma \mathbf{u}_\sigma + \mu_0 \varepsilon_0 \frac{\partial \mathbf{E}}{\partial t} \tag{2.59}$$

$$\nabla \cdot \mathbf{B} = 0 \tag{2.60}$$

$$\nabla \cdot \mathbf{E} = \frac{1}{\varepsilon_0} \sum_\sigma n_\sigma q \tag{2.61}$$

2.5 Magnetohydrodynamic equations

Particle motion in the two-fluid system was described by the individual species mean velocities \mathbf{u}_e , \mathbf{u}_i and by the pressures $\overleftrightarrow{\mathbf{P}}_e$, $\overleftrightarrow{\mathbf{P}}_i$ which gave information on the random deviation of the velocity from its mean value. Magnetohydrodynamics is an alternate description of the plasma where instead of using \mathbf{u}_e , \mathbf{u}_i to describe mean motion, two new velocity variables that are a linear combination of \mathbf{u}_e , \mathbf{u}_i are used. As will be seen below, this means a slightly different definition for pressure must also be used.

The new velocity-like variables are (i) the current density

$$\mathbf{J} = \sum_{\sigma} n_{\sigma} q_{\sigma} \mathbf{u}_{\sigma} \quad (2.62)$$

which is essentially the relative velocity between ions and electrons, and (ii) the center of mass velocity

$$\mathbf{U} = \frac{1}{\rho} \sum_{\sigma} m_{\sigma} n_{\sigma} \mathbf{u}_{\sigma}. \quad (2.63)$$

where

$$\rho = \sum_{\sigma} m_{\sigma} n_{\sigma} \quad (2.64)$$

is the total mass density. Magnetohydrodynamics is primarily concerned with low frequency, long wavelength, *magnetic* behavior of the plasma.

2.5.1 MHD continuity equation

Multiplying Eq.(2.19) by m_{σ} and summing over species gives the MHD continuity equation

$$\frac{\partial \rho}{\partial t} + \nabla \cdot (\rho \mathbf{U}) = 0. \quad (2.65)$$

2.5.2 MHD equation of motion

To obtain an equation of motion, we take the first moment of the Vlasov equation, then multiply by m_{σ} and sum over species to obtain

$$\frac{\partial}{\partial t} \sum_{\sigma} m_{\sigma} \int \mathbf{v} f_{\sigma} d\mathbf{v} + \frac{\partial}{\partial \mathbf{x}} \cdot \sum_{\sigma} \int m_{\sigma} \mathbf{v} \mathbf{v} f_{\sigma} d\mathbf{v} + \sum_{\sigma} q_{\sigma} \int \mathbf{v} \frac{\partial}{\partial \mathbf{v}} \cdot [(\mathbf{E} + \mathbf{v} \times \mathbf{B}) f_{\sigma}] = 0; \quad (2.66)$$

the right hand side is zero since $\mathbf{R}_{ei} + \mathbf{R}_{ie} = 0$, i.e., the total plasma cannot exert drag on itself. We now define random velocities relative to \mathbf{U} (rather than to \mathbf{u}_{σ} as was the case for the two-fluid equations) so that the second term can be written as

$$\sum_{\sigma} \int m_{\sigma} \mathbf{v} \mathbf{v} f_{\sigma} d\mathbf{v} = \sum_{\sigma} \int m_{\sigma} (\mathbf{v}' + \mathbf{U})(\mathbf{v}' + \mathbf{U}) f_{\sigma} d\mathbf{v} = \sum_{\sigma} \int m_{\sigma} \mathbf{v}' \mathbf{v}' f_{\sigma} d\mathbf{v} + \rho \mathbf{U} \mathbf{U} \quad (2.67)$$

where $\sum_{\sigma} \int m_{\sigma} \mathbf{v}' f_{\sigma} d\mathbf{v} = 0$ has been used to eliminate terms linear in \mathbf{v}' . The MHD pressure tensor is now defined in terms of the random velocities relative to \mathbf{U} and is given

by

$$\overleftarrow{\mathbf{P}}^{\text{MHD}} = \sum_{\sigma} \int m_{\sigma} \mathbf{v}' \mathbf{v}' f_{\sigma} d\mathbf{v}. \quad (2.68)$$

We insert Eqs.(2.67) and (2.68) in Eq.(2.66), integrate by parts on the acceleration term, and perform the summation over species to obtain the MHD equation of motion

$$\frac{\partial(\rho\mathbf{U})}{\partial t} + \nabla \cdot (\rho\mathbf{U}\mathbf{U}) = \left(\sum_{\sigma} n_{\sigma} q_{\sigma} \right) \mathbf{E} + \mathbf{J} \times \mathbf{B} - \nabla \cdot \overleftarrow{\mathbf{P}}^{\text{MHD}}. \quad (2.69)$$

MHD is typically used to describe phenomena with large spatial scales where the plasma is essentially neutral, so that $\sum_{\sigma} n_{\sigma} q_{\sigma} \approx 0$. Just as in the two-fluid situation, the left hand side of Eq.(2.69) contains a factor times the MHD continuity equation,

$$\frac{\partial(\rho\mathbf{U})}{\partial t} + \nabla \cdot (\rho\mathbf{U}\mathbf{U}) = \left[\frac{\partial\rho}{\partial t} + \nabla \cdot (\rho\mathbf{U}) \right] \mathbf{U} + \rho \frac{\partial\mathbf{U}}{\partial t} + \rho\mathbf{U}\nabla \cdot \mathbf{U}. \quad (2.70)$$

Using Eq.(2.65) leads to the standard form for the MHD equation of motion

$$\rho \frac{D\mathbf{U}}{Dt} = \mathbf{J} \times \mathbf{B} - \nabla \cdot \overleftarrow{\mathbf{P}}^{\text{MHD}} \quad (2.71)$$

where

$$\frac{D}{Dt} = \frac{\partial}{\partial t} + \mathbf{U} \cdot \nabla \quad (2.72)$$

is the convective derivative using the MHD center of mass velocity. Scalar approximations of the MHD pressure tensor will be postponed until after discussing implications of the MHD Ohm's law.

2.5.3 MHD Ohm's law

Equation (2.71) provides one equation relating \mathbf{J} and \mathbf{U} ; let us now find the other one. In order to find this second relation between \mathbf{J} and \mathbf{U} consider the two-fluid electron equation of motion:

$$m_e \frac{d\mathbf{u}_e}{dt} = -e(\mathbf{E} + \mathbf{u}_e \times \mathbf{B}) - \frac{1}{n_e} \nabla (n_e \kappa T_e) - v_{ei} m_e (\mathbf{u}_e - \mathbf{u}_i). \quad (2.73)$$

In MHD we are interested in low frequency phenomena with large spatial scales. If the characteristic time scale of the phenomenon is long compared to the electron cyclotron motion, then the electron inertia term $m_e d\mathbf{u}_e/dt$ can be dropped since it is small compared to the magnetic force term $-e(\mathbf{u}_e \times \mathbf{B})$. This assumption is reasonable for velocities perpendicular to \mathbf{B} , but can be a poor approximation for the velocity component parallel to \mathbf{B} , since parallel velocities do not provide a magnetic force. Since $\mathbf{u}_e - \mathbf{u}_i = -\mathbf{J}/n_e e$ and $\mathbf{u}_i \simeq \mathbf{U}$, Eq.(2.73) reduces to the generalized Ohm's law

$$\mathbf{E} + \mathbf{U} \times \mathbf{B} - \frac{1}{n_e e} \mathbf{J} \times \mathbf{B} + \frac{1}{n_e e} \nabla (n_e \kappa T_e) = \eta \mathbf{J}. \quad (2.74)$$

The term $-\mathbf{J} \times \mathbf{B}/n_e e$ on the left hand side of Eq.(2.74) is called the *Hall term* and can be neglected in either of the following two cases:

1. The pressure term in the MHD equation of motion, Eq.(2.71) is negligible compared to the other two terms which therefore must balance giving

$$|\mathbf{J}| \sim \omega \rho |\mathbf{U}| / |\mathbf{B}|;$$

here $\omega \sim D/Dt$ is the characteristic frequency of the phenomenon. In this case comparison of the Hall term with the $\mathbf{U} \times \mathbf{B}$ term shows that the Hall term is small by a factor $\sim \omega/\omega_{ci}$ where $\omega_{ci} = q_i B/m_i$ is the ion cyclotron frequency. Thus dropping the Hall term is justified for phenomena having characteristic frequencies small compared to ω_{ci} .

2. The electron-ion collision frequency is large compared to the electron cyclotron frequency $\omega_{ce} = q_e B/m_e$ in which case the Hall term may be dropped since it is small by a factor ω_{ce}/ν_{ei} compared to the right hand side resistive term $\eta \mathbf{J} = (m_e \nu_{ei}/n_e e^2) \mathbf{J}$.

From now on, when using MHD it will be assumed that one of these conditions is true and Hall terms will be dropped (if Hall terms are retained, the system is called Hall MHD). Typically, Eq. (2.74) will not be used directly; instead its curl will be used to provide the *induction* equation

$$-\frac{\partial \mathbf{B}}{\partial t} + \nabla \times (\mathbf{U} \times \mathbf{B}) - \frac{1}{n_e e} \nabla n_e \times \nabla \kappa T_e = \nabla \times \left(\frac{\eta}{\mu_0} \nabla \times \mathbf{B} \right). \quad (2.75)$$

Usually the density gradient is parallel to the temperature gradient so that the thermal electromotive force term $(n_e e)^{-1} \nabla n_e \times \nabla \kappa T_e$ can be dropped, in which case the induction equation reduces to

$$-\frac{\partial \mathbf{B}}{\partial t} + \nabla \times (\mathbf{U} \times \mathbf{B}) = \nabla \times \left(\frac{\eta}{\mu_0} \nabla \times \mathbf{B} \right). \quad (2.76)$$

The thermal term is often simply ignored in the MHD Ohm's law, which is written as

$$\mathbf{E} + \mathbf{U} \times \mathbf{B} = \eta \mathbf{J}; \quad (2.77)$$

this is only acceptable providing we intend to take the curl and providing $\nabla n_e \times \nabla \kappa T_e \simeq 0$.

2.5.4 Ideal MHD and frozen-in flux

If the resistive term $\eta \mathbf{J}$ is small compared to the other terms in Eq.(2.77), then the plasma is said to be *ideal* or *perfectly conducting*. From the Lorentz transformation of electromagnetic theory we realize that $\mathbf{E} + \mathbf{U} \times \mathbf{B} = \mathbf{E}'$ where \mathbf{E}' is the electric field observed in the frame moving with velocity \mathbf{U} . This implies that the magnetic flux in ideal plasmas is time-invariant in the frame moving with velocity \mathbf{U} , because otherwise Faraday's law would imply the existence of an electric field in the moving frame. In order to have the magnetic flux invariant in the moving frame, the magnetic field lines must convect with the velocity \mathbf{U} , i.e., the magnetic field lines are *frozen* into the plasma and *move with the plasma*. The frozen-in field concept is the essential "bed-rock" concept underlying ideal MHD. While this concept is often an excellent approximation, it must be kept in mind that the concept becomes invalid in situations when any one of the electron inertia, electron pressure, or Hall terms become important and lead to different, more complex behavior.

A formal proof of this frozen-in flux property will now be established by direct calculation of the rate of change of the magnetic flux through a surface $S(t)$ bounded by a material line $C(t)$, i.e., a closed contour which moves with the plasma. This magnetic flux is

$$\Phi(t) = \int_{S(t)} \mathbf{B}(\mathbf{x}, t) \cdot d\mathbf{s} \quad (2.78)$$

and the flux changes with respect to time due to either (i) the explicit time dependence of $\mathbf{B}(t)$ or (ii) changes in the surface $S(t)$ resulting from plasma motion. The rate of change of flux is thus

$$\frac{D\Phi}{Dt} = \lim_{\delta t \rightarrow 0} \left(\frac{\int_{S(t+\delta t)} \mathbf{B}(\mathbf{x}, t + \delta t) \cdot d\mathbf{s} - \int_{S(t)} \mathbf{B}(\mathbf{x}, t) \cdot d\mathbf{s}}{\delta t} \right). \quad (2.79)$$

The displacement of a segment $d\mathbf{l}$ of the bounding contour C is $\mathbf{U}\delta t$ where \mathbf{U} is the velocity of this segment. The incremental change in surface area due to this displacement is $\Delta S = \mathbf{U}\delta t \times d\mathbf{l}$. The rate of change of flux can thus be expressed as

$$\begin{aligned} \frac{D\Phi}{Dt} &= \lim_{\delta t \rightarrow 0} \frac{\int_{S(t+\delta t)} \left(\mathbf{B}(\mathbf{x}, t) + \delta t \frac{\partial \mathbf{B}}{\partial t} \right) \cdot d\mathbf{s} - \int_{S(t)} \mathbf{B}(\mathbf{x}, t) \cdot d\mathbf{s}}{\delta t} \\ &= \lim_{\delta t \rightarrow 0} \frac{\int_{S(t)} \left(\mathbf{B}(\mathbf{x}, t) + \delta t \frac{\partial \mathbf{B}}{\partial t} \right) \cdot d\mathbf{s} + \oint_C \mathbf{B}(\mathbf{x}, t) \cdot \mathbf{U}\delta t \times d\mathbf{l} - \int_{S(t)} \mathbf{B}(\mathbf{x}, t) \cdot d\mathbf{s}}{\delta t} \\ &= \int_{S(t)} \frac{\partial \mathbf{B}}{\partial t} \cdot d\mathbf{s} + \oint_C \mathbf{B}(\mathbf{x}, t) \cdot \mathbf{U} \times d\mathbf{l} \\ &= \int_{S(t)} \left[\frac{\partial \mathbf{B}}{\partial t} + \nabla \times (\mathbf{B} \times \mathbf{U}) \right] \cdot d\mathbf{s}. \end{aligned} \quad (2.80)$$

Thus, if

$$\frac{\partial \mathbf{B}}{\partial t} = \nabla \times (\mathbf{U} \times \mathbf{B}) \quad (2.81)$$

then

$$\frac{D\Phi}{Dt} = 0 \quad (2.82)$$

so that the magnetic flux linked by any closed material line is constant. Therefore, magnetic flux is frozen into an ideal plasma because Eq.(2.76) reduces to Eq.(2.81) if $\eta = 0$. Equation (2.81) is called the ideal MHD induction equation.

2.5.5 MHD equations of state

Double adiabatic laws A procedure analogous to that which led to Eq.(2.35) gives the MHD adiabatic relation

$$\frac{P^{MHD}}{\rho^\gamma} = \text{const.} \quad (2.83)$$

where again $\gamma = (N + 2)/N$ and N is the number of dimensions of the system. It was shown in the previous section that magnetic flux is conserved in the plasma frame.

This means that, as shown in Fig.2.5, a tube of plasma initially occupying the same volume as a magnetic flux tube is constrained to evolve in such a way that $\int \mathbf{B} \cdot d\mathbf{s}$ stays constant over the plasma tube cross-section. For a flux tube of infinitesimal cross-section, the magnetic field is approximately uniform over the cross-section and we may write this as $BA = \text{const.}$ where A is the cross-sectional area. Let us define two temperatures for this magnetized plasma, namely T_{\perp} the temperature corresponding to motions perpendicular to the magnetic field, and T_{\parallel} the temperature corresponding to motions parallel to the magnetic field. If for some reason (e.g., anisotropic heating or compression) the temperature develops an anisotropy such that $T_{\perp} \neq T_{\parallel}$ and if collisions are infrequent, this anisotropy will persist for a long time, since collisions are the means by which the two temperatures equilibrate. Thus, rather than assuming that the MHD pressure is fully isotropic, we consider the less restrictive situation where the MHD pressure tensor is given by

$$\overleftrightarrow{\mathbf{P}}^{\text{MHD}} = \begin{bmatrix} P_{\perp} & 0 & 0 \\ 0 & P_{\perp} & 0 \\ 0 & 0 & P_{\parallel} \end{bmatrix} = P_{\perp} \overleftrightarrow{\mathbf{I}} + (P_{\parallel} - P_{\perp}) \widehat{\mathbf{B}}\widehat{\mathbf{B}}. \quad (2.84)$$

The first two coordinates (x, y -like) in the above matrix refer to the directions perpendicular to the local magnetic field \mathbf{B} and the third coordinate (z -like) refers to the direction parallel to \mathbf{B} . The tensor expression on the right hand side is equivalent (here $\overleftrightarrow{\mathbf{I}}$ is the unit tensor) but allows for arbitrary, curvilinear geometry. We now develop separate adiabatic relations for the perpendicular and parallel directions:

- Parallel direction- Here the number of dimensions is $N = 1$ so that $\gamma = 3$ and so the adiabatic law gives

$$\frac{P_{\parallel}^{1D}}{\rho_{1D}^3} = \text{const.} \quad (2.85)$$

where ρ_{1D} is the *one-dimensional* mass density; i.e., $\rho_{1D} \sim 1/L$ where L is the length along the one-dimension, e.g. along the length of the flux tube in Fig.2.5. The three-dimensional mass density ρ , which has been used implicitly until now has the proportionality $\rho \sim 1/LA$ where A is the cross-section of the flux tube; similarly the three dimensional pressure has the proportionality $P_{\parallel} \sim \rho T_{\parallel}$. However, we must be careful to realize that $P_{\parallel}^{1D} \sim \rho_{1D} T_{\parallel}$ so, using $BA = \text{const.}$, Eq. (2.85) can be recast as

$$\text{const.} = \frac{P_{\parallel}^{1D}}{\rho_{1D}^3} \sim \frac{\rho_{1D} T_{\parallel}}{\rho_{1D}^3} \sim T_{\parallel} L^2 \sim \underbrace{\left(\frac{1}{LA}\right)}_{P_{\parallel}} \underbrace{(LA)^3}_{\rho^{-3}} B^2. \quad (2.86)$$

or

$$\frac{P_{\parallel} B^2}{\rho^3} = \text{const.} \quad (2.87)$$

- Perpendicular direction- Here the number of dimensions is $N = 2$ so that $\gamma = 2$ and the adiabatic law gives

$$\frac{P_{\perp}^{2D}}{\rho_{2D}^2} = \text{const.} \quad (2.88)$$

where P_{\perp}^{2D} is the 2-D perpendicular pressure, and has dimensions of energy per unit area, while ρ_{2D} is the 2-D mass density and has dimensions of mass per unit area. Thus, $\rho_{2D} \sim 1/A$ so that $P_{\perp}^{2D} \sim \rho_{2D} T_{\perp} \sim T_{\perp}/A$ in which case Eq.(2.88) can be re-written as

$$const. = \frac{P_{\perp}^{2D}}{\rho_{2D}^2} \sim T_{\perp} A \sim \left(\frac{1}{LA} \right) T_{\perp} \frac{LA}{B} \quad (2.89)$$

or

$$\frac{P_{\perp}}{\rho B} = const. \quad (2.90)$$

Equations (2.87) and (2.90) are called the double adiabatic or CGL laws after Chew, Goldberger and Low (1956) who first developed them using a Vlasov analysis).

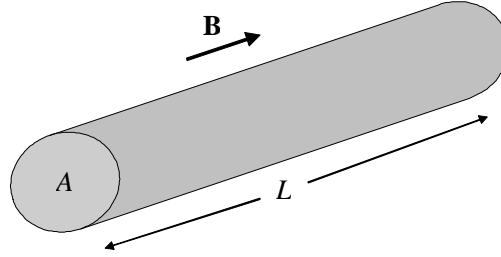


Figure 2.5: Magnetic flux tube with flux $\Phi = BA$.

Single adiabatic law If collisions are sufficiently frequent to equilibrate the perpendicular and parallel temperatures, then the pressure tensor becomes fully isotropic and the dimensionality of the system is $N = 3$ so that $\gamma = 5/3$. There is now just one pressure and temperature and the adiabatic relation becomes

$$\frac{P}{\rho^{5/3}} = const. \quad (2.91)$$

2.5.6 MHD approximations for Maxwell's equations

The various assumptions contained in MHD lead to a simplifying approximation of Maxwell's equations. In particular, the assumption of charge neutrality in MHD makes Poisson's equation superfluous because Poisson's equation prescribes the relationship between non-neutrality and the electrostatic component of the electric field. The assumption of charge neutrality has implications for the current density also. To see this, the 2-fluid continuity

equations is multiplied by q_σ and then summed over species to obtain the charge conservation equation

$$\frac{\partial}{\partial t} \left(\sum n_\sigma q_s \right) + \nabla \cdot \mathbf{J} = 0. \quad (2.92)$$

Thus, charge neutrality implies

$$\nabla \cdot \mathbf{J} = 0. \quad (2.93)$$

Let us now consider Ampere's law

$$\nabla \times \mathbf{B} = \mu_0 \mathbf{J} + \mu_0 \varepsilon_0 \frac{\partial \mathbf{E}}{\partial t}. \quad (2.94)$$

Taking the divergence gives

$$\nabla \cdot \mathbf{J} + \varepsilon_0 \frac{\partial \nabla \cdot \mathbf{E}}{\partial t} = 0$$

which is equivalent to Eq.(2.92) if Poisson's equation is invoked.

Finally, MHD is restricted to phenomena having characteristic velocities V_{ph} slow compared to the speed of light in vacuum $c = (\varepsilon_0 \mu_0)^{-1/2}$. Again t is assumed to represent the characteristic time scale for a given phenomenon and l is assumed to represent the corresponding characteristic length scale so that $V_{ph} \sim l/t$. Faraday's equation gives the scaling

$$\nabla \times \mathbf{E} = - \frac{\partial \mathbf{B}}{\partial t} \implies E \sim Bl/t. \quad (2.95)$$

On comparing the magnitude of the displacement current term in Eq.(2.94) to the left hand side it is seen that

$$\frac{\mu_0 \varepsilon_0 \left| \frac{\partial \mathbf{E}}{\partial t} \right|}{|\nabla \times \mathbf{B}|} \sim \frac{c^{-2} E/t}{B/l} \sim \left(\frac{V_{ph}}{c} \right)^2. \quad (2.96)$$

Thus, if $V_{ph} \ll c$ the displacement current term can be dropped from Ampere's law resulting in the so-called "pre-Maxwell" form

$$\nabla \times \mathbf{B} = \mu_0 \mathbf{J}. \quad (2.97)$$

The divergence of Eq. (2.97) gives Eq.(2.93) so it is unnecessary to specify Eq.(2.93) separately.

2.6 Summary of MHD equations

We may now summarize the MHD equations:

1. Mass conservation

$$\frac{\partial \rho}{\partial t} + \nabla \cdot (\rho \mathbf{U}) = 0. \quad (2.98)$$

2. Equation of state and associated equation of motion

- (a) Single adiabatic regime, collisions equilibrate perpendicular and parallel temperatures so that both pressure and temperature are isotropic

$$\frac{P}{\rho^{5/3}} = const. \quad (2.99)$$

and the equation of motion is

$$\rho \frac{D\mathbf{U}}{Dt} = \mathbf{J} \times \mathbf{B} - \nabla P. \quad (2.100)$$

- (b) Double adiabatic regime, the collision frequency is insufficient to equilibrate perpendicular and parallel temperatures so that

$$\frac{P_{\parallel} B^2}{\rho^3} = \text{const.}, \quad \frac{P_{\perp}}{\rho B} = \text{const.} \quad (2.101)$$

and the equation of motion is

$$\rho \frac{D\mathbf{U}}{Dt} = \mathbf{J} \times \mathbf{B} - \nabla \cdot \left[P_{\perp} \overleftrightarrow{\mathbf{T}} + (P_{\parallel} - P_{\perp}) \hat{\mathbf{B}} \hat{\mathbf{B}} \right]. \quad (2.102)$$

3. Faraday's Law

$$\nabla \times \mathbf{E} = - \frac{\partial \mathbf{B}}{\partial t}. \quad (2.103)$$

4. Ampere's Law

$$\nabla \times \mathbf{B} = \mu_0 \mathbf{J}. \quad (2.104)$$

5. Ohm's Law

$$\mathbf{E} + \mathbf{U} \times \mathbf{B} = \eta \mathbf{J}. \quad (2.105)$$

These equations provide a self-consistent description of phenomena that satisfy all the various assumptions we have made, namely:

- (i) The plasma is charge-neutral since characteristic lengths are much longer than a Debye length;
- (ii) The characteristic velocity of the phenomenon under consideration is slow compared to the speed of light;
- (iii) The pressure and density gradients are parallel, so there is no electrothermal EMF;
- (iv) The time scale is long compared to both the electron and ion cyclotron periods.

Even though these assumptions are self-consistent, they may not accurately portray a real plasma and so MHD models, while intuitively appealing, must be used with caution.

2.7 Sheath physics and Langmuir probe theory

Let us now turn attention back to Vlasov theory and discuss an immediate practical application of this theory. The properties of collisionless Vlasov equilibria can be combined with Poisson's equation to develop a model for the potential in the steady-state transition region between a plasma and a conducting wall; this region is known as a sheath and is important in many situations. The sheath is non-neutral and its width is of the order of a Debye length. The exact sheath potential profile must be solved numerically because of the transcendental nature of the relevant equations, but a useful approximate solution can be obtained by a simple analytic argument which will now be discussed. Sheath physics is of particular importance for interpreting the behavior of Langmuir probes which are small

metal wires used to diagnose low temperature plasmas. Biasing a Langmuir probe at a sequence of voltages and then measuring the resulting current provides a simple way to gauge both the plasma density and the electron temperature.

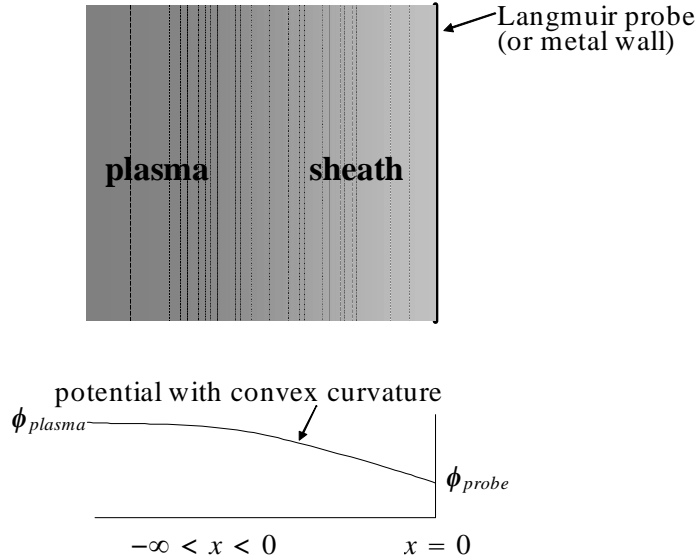


Figure 2.6: Sketch of sheath. Ions are accelerated in sheath to probe (wall) at $x = 0$ whereas electrons are repelled. Convex curvature of sheath requires $n_i(x)$ to always be greater than $n_e(x)$.

The model presented here is the simplest possible model for sheaths and Langmuir probes and is one-dimensional. The geometry, sketched in Fig.2.6, idealizes the Langmuir probe as a metal wall located at $x = 0$ and biased to a potential ϕ_{probe} ; this geometry could also be used to describe an actual biased metal wall at $x = 0$ in a two-dimensional plasma. The plasma is assumed to be collisionless and unmagnetized and to have an ambipolar potential ϕ_{plasma} which differs from the laboratory reference potential (so-called ground potential) because of a difference in the diffusion rates of electrons and ions out of the plasma. The plasma is assumed to extend into the semi-infinite left-hand half-plane $-\infty < x < 0$. If $\phi_{probe} = \phi_{plasma}$, then neither electrons nor ions will be accelerated or decelerated on leaving the plasma and so each species will strike the probe (or wall) at a rate given by its respective thermal velocity. Since $m_e \ll m_i$, the electron thermal velocity greatly exceeds the ion thermal velocity. Thus, for $\phi_{probe} = \phi_{plasma}$ the electron flux to the probe (or wall) greatly exceeds the ion flux and so the current collected by the probe (or wall) will be negative.

Now consider what happens to this electron flow if the probe (or wall) is biased *negative* with respect to the plasma as shown in Fig.2.6. To simplify the notation, a bar will be used

to denote a potential measured relative to the plasma potential, i.e.,

$$\bar{\phi}(x) = \phi(x) - \phi_{plasma}. \quad (2.106)$$

The bias potential imposed on the probe (or wall) will be shielded out by the plasma within a distance of the order of the Debye length; this region is the sheath. The relative potential $\bar{\phi}(x)$ varies within the sheath and has the two limiting behaviors:

$$\begin{aligned} \lim_{x \rightarrow 0} \bar{\phi}(x) &= \phi_{probe} - \phi_{plasma} \\ \lim_{|x| \gg \lambda_D} \bar{\phi}(x) &= 0. \end{aligned} \quad (2.107)$$

Inside the plasma, i.e., for $|x| \gg \lambda_D$, it is assumed that the electron distribution function is Maxwellian with temperature T_e . Since the distribution function depends only on constants of the motion, the one-dimensional electron velocity distribution function must depend only on the electron energy $mv^2/2 + q_e\bar{\phi}(x)$, a constant of the motion, and so must be of the form

$$f_e(v, x) = \frac{n_0}{\sqrt{\pi 2\kappa T_e/m_e}} \exp\left(-\left(\frac{mv^2/2 + q_e\bar{\phi}(x)}{\kappa T_e}\right)\right) \quad (2.108)$$

in order to be Maxwellian when $x \gg \lambda_D$.

The electron density is

$$n_e(x) = \int_{-\infty}^{\infty} dv f_e(v, 0) = n_0 e^{-q_e\bar{\phi}(x)/\kappa T_e}. \quad (2.109)$$

When the probe is biased negative with respect to the plasma, only those electrons with sufficient energy to overcome the negative potential barrier will be collected by the probe.

The ion dynamics is not a mirror image of the electron dynamics. This is because a repulsive potential prevents passage of particles having insufficient initial energy to climb over a potential barrier whereas an attractive potential allows passage of all particles entering a region of depressed potential. Particle density is reduced compared to the inlet density for both repulsive and attractive potentials but for different reasons. As shown in Eq.(2.109) a repulsive potential reduces the electron density exponentially (this is essentially the Boltzmann analysis developed in the theory of Debye shielding). Suppose the ions are cold and enter a region of attractive potential with velocity u_0 . Flux conservation shows that $n_0 u_0 = n_i(x) u_i(x)$ and since the ions accelerate to higher velocity when falling down the attractive potential, the ion density must also decrease. Thus the electron density scales as $\exp(-|q_e\bar{\phi}|/\kappa T_e)$ and so decreases upon approaching the wall in response to what is a repulsive potential for electrons whereas the ion density scales as $1/u_i(x)$ and also decreases upon approaching the wall in response to what is an attractive potential for ions.

Suppose the probe is biased negatively with respect to the plasma. Since quasi-neutrality within the plasma mandates that the electric field must vanish inside the plasma, the potential must have a downward slope on going from the plasma to the probe and the derivative of this slope must also be downward. This means that the potential $\bar{\phi}$ must have a convex curvature and a negative second derivative as indicated in Fig.2.6. However, the

one-dimensional Poisson's equation

$$\frac{d^2\bar{\phi}}{dx^2} = -\frac{e}{\varepsilon_0} (n_i(x) - n_e(x)) \quad (2.110)$$

shows that in order for $\bar{\phi}$ to have convex curvature, it is necessary to have $n_i(x) > n_e(x)$ everywhere. This condition will now be used to estimate the inflow velocity of the ions at the location where they enter the sheath from the bulk plasma.

Ion energy conservation gives

$$\frac{1}{2}m_i u^2(x) + e\bar{\phi}(x) = \frac{1}{2}m_i u_0^2 \quad (2.111)$$

which can be solved to give

$$u(x) = \sqrt{u_0^2 - 2e\bar{\phi}(x)/m_i}. \quad (2.112)$$

Using the ion flux conservation relation $n_0 u_0 = n_i(x) u_i(x)$ the local ion density is found to be

$$n_i(x) = \frac{n_0}{(1 - 2e\bar{\phi}(x)/m_i u_0^2)^{1/2}}. \quad (2.113)$$

The convexity requirement $n_i(x) > n_e(x)$ implies

$$(1 - 2e\bar{\phi}(x)/m_i u_0^2)^{-1/2} > e^{\bar{\phi}(x)/\kappa T_e}. \quad (2.114)$$

Bearing in mind that $\bar{\phi}(x)$ is negative, this can be re-arranged as

$$1 + \frac{2e|\bar{\phi}(x)|}{m_i u_0^2} < e^{2e|\bar{\phi}(x)|/\kappa T_e} \quad (2.115)$$

or

$$\frac{2e|\bar{\phi}(x)|}{m_i u_0^2} < \frac{2e|\bar{\phi}(x)|}{\kappa T_e} + \frac{1}{2} \left(\frac{2e|\bar{\phi}(x)|}{\kappa T_e} \right)^2 + \frac{1}{3!} \left(\frac{2e|\bar{\phi}(x)|}{\kappa T_e} \right)^3 + \dots \quad (2.116)$$

which can only be satisfied for arbitrary $|\bar{\phi}(x)|$ if

$$u_0^2 > 2\kappa T_e/m_i. \quad (2.117)$$

Thus, in order to be consistent with the assumption that the probe is more negative than the plasma to keep $d^2\bar{\phi}/dx^2$ negative and hence $\bar{\phi}$ convex, it is necessary to have the ions enter the region of non-neutrality with a velocity slightly larger than the so-called "ion acoustic" velocity $c_s = \sqrt{\kappa T_e/m_i}$.

The ion current collected by the probe is given by the ion flux times the probe area, i.e.,

$$\begin{aligned} I_i &= n_0 u_0 q_i A \\ &= n_0 c_s e A. \end{aligned} \quad (2.118)$$

The electron current density incident on the probe is

$$\begin{aligned} J_e(x) &= \int_0^\infty dv q_e v f_e(v, 0) \\ &= \frac{n_0 q_e e^{-q_e \bar{\phi}(x)/\kappa T_e}}{\sqrt{\pi 2\kappa T_e/m_e}} \int_0^\infty dv v e^{-mv^2/2\kappa T_e} \\ &= n_0 q_e \sqrt{\frac{\kappa T_e}{2\pi m_e}} e^{-e|\bar{\phi}(x)|/\kappa T_e} \end{aligned} \quad (2.119)$$

and so the electron current collected at the probe is

$$I_e = -n_0 e A \sqrt{\frac{\kappa T_e}{2\pi m_e}} e^{-e|\bar{\phi}(x)|/\kappa T_e}. \quad (2.120)$$

Thus, the combined electron and ion current collected by the probe is

$$\begin{aligned} I &= I_i + I_e \\ &= n_0 c_s e A - n_0 e A \sqrt{\frac{\kappa T_e}{2\pi m_e}} e^{-e|\bar{\phi}(x)|/\kappa T_e}. \end{aligned} \quad (2.121)$$

The electron and ion currents cancel each other when

$$\sqrt{\frac{2\kappa T_e}{m_i}} = \sqrt{\frac{\kappa T_e}{2\pi m_e}} e^{-e|\bar{\phi}(x)|/\kappa T_e} \quad (2.122)$$

i.e., when

$$\begin{aligned} e|\bar{\phi}_{probe}|/\kappa T_e &= \ln \sqrt{\frac{m_i}{4\pi m_e}} \\ &= 2.5 \text{ for hydrogen.} \end{aligned} \quad (2.123)$$

This can be expressed as

$$\phi_{probe} = \phi_{plasma} - \frac{\kappa T_e}{e} \ln \sqrt{\frac{m_i}{4\pi m_e}} \quad (2.124)$$

and shows that when the probe potential is more negative than the plasma potential by an amount $T_e \ln \sqrt{m_i/4\pi m_e}$ where T_e is expressed in electron volts, then no current flows to the probe. This potential is called the floating potential, because an insulated object immersed in the plasma will always charge up until it reaches the floating potential at which point no net current flows to the object.

These relationships can be used as simple diagnostic for the plasma density and temperature. If a probe is biased with a large negative potential, then no electrons are collected but an ion flux is collected. The collected current is called the ion saturation current and is given by $I_{sat} = n_0 c_s e A$. The ion saturation current is then subtracted from all subsequent measurements giving the electron current $I_e = I - I_{sat} = n_0 e A (\kappa T_e / 2\pi m_e)^{1/2} \exp(-e|\bar{\phi}(x)|/\kappa T_e)$. The slope of a logarithmic plot of I_e versus ϕ gives $1/\kappa T_e$ and can be used to measure the electron temperature. Once the electron temperature is known, c_s can be calculated. The plasma density can then be calculated from the ion saturation current measurement and knowledge of the probe area. Langmuir probe measurements are simple to implement but are not very precise, typically having an uncertainty of a factor of two or more.

2.8 Assignments

1. Prove Stirling's formula. To do this first show

$$\begin{aligned}\ln N! &= \ln 1 + \ln 2 + \ln 3 + \dots + \ln N \\ &= \sum_{j=1}^N \ln j\end{aligned}$$

Now assume N is large and, using a graphical argument, show that the above expression can be expressed as an integral

$$\ln N! \approx \int_{?}^{?} h(x) dx$$

where the form of $h(x)$ and the limits of integration are to be provided. Evaluate the integral and obtain Stirling's formula

$$\ln N! \simeq N \ln N - N \quad \text{for large } N$$

which is a way of calculating the values of factorials of large numbers. Check the accuracy of Stirling's formula by evaluating the left and right hand sides of Stirling's formula numerically and plot the results for $N = 1, 10, 100, 1000, 10^4$ and higher if possible.

2. Variational calculus and Lagrange multipliers- The entropy associated with a distribution function is

$$S = \int_{-\infty}^{\infty} f(v) \ln f(v) dv.$$

- Since $f(v)$ measures the number of particles that have velocity v , use physical arguments to explain what value $f(\pm\infty)$ must have.
- Suppose that $f_{ME}(v)$ is the distribution function having the maximum entropy out of all distribution functions allowed for the problem at hand. Let $\delta f(v)$ be some small arbitrary deviation from $f_{ME}(v)$. What is the entropy $S + \delta S$ associated with the distribution function $f_{ME}(v) + \delta f(v)$? What is the differential of entropy δS between the two situations?
- Each particle in the distribution function has a kinetic energy $mv^2/2$ and suppose that there are no external forces acting on the system of particles so that the potential energy of each particle is zero. Let E be the total energy of all the particles. How does E depend on the distribution function? If the system is isolated and the system changes from having a distribution function $f_{ME}(v)$ to having the distribution function $f_{ME}(v) + \delta f(v)$ what is the change in energy δE between these two cases?
- By now you should have integral expressions for δS and for δE . Both of these integrals should have what value? Make a rough sketch showing any possible, nontrivial v dependence of the integrands of these expressions (i.e., show whether the integrands are positive definite or not).
- Since δf was assumed to be arbitrary, what can you say about the ratio of the integrand in the expression for δS to the integrand in the expression for δE ? Is

this ratio constant or not (explain your answer)? Let this ratio be denoted by λ (this is called a Lagrange multiplier).

(f) Show that the conclusion reached in 'e' above lead to the $f_{ME}(v)$ having to be a Maxwellian.

3. Suppose that a group of N particles with charge q_σ and mass m_σ are located in an electrostatic potential $\phi(\mathbf{x})$. What is the maximum entropy distribution function for this situation (give a derivation)?

4. Prove that

$$\int_{-\infty}^{\infty} dx e^{-ax^2} = \sqrt{\frac{\pi}{a}} \quad (2.125)$$

Hint: Consider the integral

$$\int_{-\infty}^{\infty} dx e^{-x^2} \int_{-\infty}^{\infty} dy e^{-y^2} = \int_{-\infty}^{\infty} \int_{-\infty}^{\infty} dx dy e^{-(x^2+y^2)},$$

and note that $dx dy$ is an element of area. Then instead of using Cartesian coordinates for the integral over area, use cylindrical coordinates and express all quantities in the double integral in cylindrical coordinates.

5. Evaluate the integrals

$$\int_{-\infty}^{\infty} dx x^2 e^{-ax^2}, \int_{-\infty}^{\infty} dx x^4 e^{-ax^2}.$$

Hint: Take the derivative of both sides of Eq.(2.125) with respect to a .

6. Suppose that a particle starts at time $t = t_0$ with velocity \mathbf{v}_0 at location \mathbf{x}_0 and is located in a uniform, constant magnetic field $\mathbf{B} = B\hat{z}$. There is no electric field. Calculate its position and velocity as a function of time. Make sure that your solution satisfies the initial conditions on both velocity and position. Be careful to treat motion parallel to the magnetic field as well as perpendicular. Express your answer in vector form as much as possible; use the subscripts \parallel, \perp to denote directions parallel and perpendicular to the magnetic field, and use $\omega_c = qB/m$ to denote the cyclotron frequency. Show that $f(\mathbf{x}_0)$ is a solution of the Vlasov equation.

7. Thermal force (Braginskii 1965)- If there is a temperature gradient then because of the temperature dependence of collisions, there turns out to be an additional subtle drag force proportional to ∇T . To find this force, suppose a temperature gradient exists in the x direction, and consider the frictional drag on electrons passing a point $x = x_0$. The electrons moving to the right (positive velocity) at x_0 have travelled without collision from the point $x_0 - l_{mfp}$, where the temperature was $T(x_0 - l_{mfp})$, while those moving to the left (negative velocity) will have come collisionlessly from the point $x_0 + l_{mfp}$ where the temperature is $T(x_0 + l_{mfp})$. Suppose that both electrons and ions have no mean velocity at x_0 ; i.e., $u_e = u_i = 0$. Show that the total drag force on all the electrons at x_0 is

$$R_{thermal} = -2m_e n_e l_{mfp} \frac{\partial}{\partial x} (v_{ei} v_{Te}).$$

Normalize the collision frequency, thermal velocity, and mean free paths to their values at $x = x_0$ where $T = T_0$; e.g. $v_{Te}(T) = v_{Te0}(T/T_0)^{1/2}$. By writing $\partial/\partial x = (\partial T/\partial x) \partial/\partial T$ and using these normalized values show that

$$\mathbf{R}_{thermal} = -2n_e\kappa\nabla T_e.$$

A more accurate treatment which does a proper averaging over velocities gives

$$\mathbf{R}_{thermal} = -0.71n_e\kappa\nabla T_e.$$

8. MHD with neutrals- Suppose a plasma is partially (perhaps weakly) ionized so that besides moment equations for ions and electrons there will also be moment equations for neutrals. Now the constraints will be different since ionization and recombination will genuinely produce creation of plasma particles and also of neutrals. Construct a set of constraint equations on the collision operators which will now include ionization and recombination as well as scattering. Take the zeroth and first moment of the three Vlasov equations for ions, electrons, and neutrals and show that the continuity equation is formally the same as before, i.e.,

$$\frac{\partial\rho}{\partial t} + \nabla \cdot (\rho\mathbf{U}) = 0$$

providing ρ refers to the total mass density of the entire fluid (electrons, ions and neutrals) and \mathbf{U} refers to the center of mass velocity of the entire fluid. Show also that the equation of motion is formally the same as before, provided the pressure refers to the pressure of the entire configuration:

$$\rho\frac{D\mathbf{U}}{Dt} = -\nabla P + \mathbf{J} \times \mathbf{B}.$$

Show that Ohm's law will be the same as before, providing the plasma is sufficiently collisional so that the Hall term can be dropped, and so Ohm's law is

$$\mathbf{E} + \mathbf{U} \times \mathbf{B} = \eta\mathbf{J}$$

Explain how the neutral component of the plasma gets accelerated by the $\mathbf{J} \times \mathbf{B}$ force — this must happen since the inertial part of the equation of motion (i.e., $\rho D\mathbf{U}/Dt$) includes the acceleration on neutrals. Assume that electron temperature gradients are parallel to electron density gradients so that the electro-thermal force can be ignored.

9. MHD Heat Transport Equation- Define the MHD N -dimensional pressure

$$P = \frac{1}{N} \sum_{\sigma} m_{\sigma} \int \mathbf{v}' \cdot \mathbf{v}' f_{\sigma} d^N \mathbf{v}$$

where $\mathbf{v}' = \mathbf{v} - \mathbf{U}$ and N is the number of dimensions of motion (e.g., if only motion in one dimension is considered, then $N = 1$, and \mathbf{v}, \mathbf{U} are one dimensional, etc.). Also define the isotropic MHD heat flux

$$\mathbf{q} = \sum_{\sigma} m_{\sigma} \int \mathbf{v}' \frac{v'^2}{2} f d^N \mathbf{v}$$

(i) By taking the second moment of the Vlasov equation for each species (i.e., use $v^2/2$) and summing over species show that

$$\frac{N}{2} \frac{DP}{Dt} + \frac{N+2}{2} P \nabla \cdot \mathbf{U} = -\nabla \cdot \mathbf{q} + \mathbf{J} \cdot (\mathbf{E} + \mathbf{U} \times \mathbf{B})$$

Hints:

- (a) Prove that $\mathbf{U} \cdot (m_\sigma \sum \int \mathbf{v}' \mathbf{v}' f_\sigma d^N \mathbf{v}) = P \mathbf{U}$ assuming that f_σ is isotropic.
- (b) What happens to $\sum_\sigma m_\sigma \int v^2 C_{\sigma\alpha} f_\sigma d^N \mathbf{v}$?
- (c) Prove using the momentum and continuity equations that

$$\frac{\partial}{\partial t} \left(\frac{\rho U^2}{2} \right) + \nabla \cdot \left(\frac{\rho U^2}{2} \mathbf{U} \right) = -\mathbf{U} \cdot \nabla P + \mathbf{U} \cdot (\mathbf{J} \times \mathbf{B}).$$

(ii) Using the continuity equation and Ohm's law show that

$$\frac{N}{2} \frac{DP}{DT} - \frac{N+2}{2} \frac{P}{\rho} \frac{D\rho}{Dt} = -\nabla \cdot \mathbf{q} + \eta J^2$$

Show that if both the heat flux term $-\nabla \cdot \mathbf{q}$ and the Ohmic heating term ηJ^2 can be ignored, then the pressure and density are related by the adiabatic condition $P \sim \rho^\gamma$ where $\gamma = (N+2)/N$. By assuming that $D/Dt \sim \omega$ and that $\nabla \sim k$ show that the dropping of these two right hand terms is equivalent to assuming that $\omega \gg \nu_{ei}$ and that $\omega/k \gg v_T$. Explain why the phenomenon should be isothermal if $\omega/k \ll v_T$.

10. Sketch the current collected by a Langmuir probe as a function of the bias voltage and indicate the ion saturation current, the exponentially changing electron current, the floating potential, and the plasma potential. Calculate the ion saturation current collected by a 1 cm long, 0.25 mm diameter probe immersed in a 5 eV argon plasma which has a density $n = 10^{16} \text{ m}^{-3}$. Calculate the electron saturation current also (i.e., the current when the probe is at the plasma potential). What is the offset of the floating potential relative to the plasma potential?

Motion of a single plasma particle

3.1 Motivation

As discussed in the previous chapter, Maxwellian distributions result when collisions have maximized the local entropy. Since collisions occur infrequently in hot plasmas, many important phenomena have time scales much shorter than the time required for the plasma to relax to a Maxwellian. A collisionless model of the plasma is thus required to characterize these fast phenomena. Since randomization does not occur in collisionless plasmas, entropy is conserved and the distribution function is typically non-Maxwellian. Such a plasma is not in thermodynamic equilibrium and so thermodynamic concepts do not in general apply.

In Sect.2.2 it was shown that any function constructed from constants of the particle motion is a solution of the collisionless Vlasov equation. It is therefore worthwhile to develop a ‘repertoire’ of constants of the motion which can then be used to construct solutions to the Vlasov equation appropriate for various circumstances. Furthermore, the study of single particle motion is a worthy endeavor because it:

- (i) develops valuable intuition,
- (ii) highlights unusual situations requiring special treatment,
- (iii) gives valuable insight into fluid motion.

3.2 Hamilton-Lagrange formalism v. Lorentz equation

Two mathematically equivalent formalisms describe charged particle dynamics; these are (i) the Lorentz equation

$$m \frac{d\mathbf{v}}{dt} = q(\mathbf{E} + \mathbf{v} \times \mathbf{B}) \quad (3.1)$$

and (ii) Hamiltonian-Lagrangian dynamics.

The two formalisms are complementary: the Lorentz equation is intuitive and suitable for approximate methods, whereas the more abstract Hamiltonian-Lagrange formalism exploits time and space symmetries. A brief review of the Hamiltonian-Lagrangian formalism follows, emphasizing aspects relevant to dynamics of charged particles.

The starting point is to postulate the existence of a function L , called the Lagrangian, which:

1. contains *all* information about the particle dynamics for a given situation,
2. depends only on generalized coordinates $Q_i(t), \dot{Q}_i(t)$ appropriate to the problem,
3. possibly has an explicit dependence on time t .

If such a function $L(Q_i(t), \dot{Q}_i(t), t)$ exists, then information on particle dynamics is retrieved by manipulation of the *action integral*

$$S = \int_{t_1}^{t_2} L(Q_i(t), \dot{Q}_i(t), t) dt. \quad (3.2)$$

This manipulation is based on d'Alembert's principle of least action. According to this principle, one considers the infinity of possible trajectories a particle *could* follow to get from its initial position $Q_i(t_1)$ to its final position $Q_i(t_2)$, and postulates that the trajectory *actually* followed is the one which results in the *least* value of S . Thus, the value of S must be minimized (note that S here is action, and not entropy as in the previous chapter). Minimizing S does not give the actual trajectory directly, but rather gives equations of motion which can be solved to give the actual trajectory.

Minimizing S is accomplished by considering an arbitrary nearby *alternative* trajectory $Q_i(t) + \delta Q_i(t)$ having the *same* beginning and end points as the actual trajectory, i.e., $\delta Q_i(t_1) = \delta Q_i(t_2) = 0$. In order to make the variational argument more precise, δQ_i is expressed as

$$\delta Q_i(t) = \epsilon \eta_i(t) \quad (3.3)$$

where ϵ is an arbitrarily adjustable scalar assumed to be small so that $\epsilon^2 < \epsilon$ and $\eta_i(t)$ is a function of t which vanishes when $t = t_1$ or $t = t_2$ but is otherwise arbitrary. Calculating δS to second order in ϵ gives

$$\begin{aligned} \delta S &= \int_{t_1}^{t_2} L(Q_i + \delta Q_i, \dot{Q}_i + \delta \dot{Q}_i, t) dt - \int_{t_1}^{t_2} L(Q_i, \dot{Q}_i, t) dt \\ &= \int_{t_1}^{t_2} L(Q_i + \epsilon \eta_i, \dot{Q}_i + \epsilon \dot{\eta}_i, t) dt - \int_{t_1}^{t_2} L(Q_i, \dot{Q}_i, t) dt \\ &= \int_{t_1}^{t_2} \left(\epsilon \eta_i \frac{\partial L}{\partial Q_i} + \frac{(\epsilon \eta_i)^2}{2} \frac{\partial^2 L}{\partial Q_i^2} + \epsilon \dot{\eta}_i \frac{\partial L}{\partial \dot{Q}_i} + \frac{(\epsilon \dot{\eta}_i)^2}{2} \frac{\partial^2 L}{\partial \dot{Q}_i^2} \right) dt. \end{aligned} \quad (3.4)$$

Suppose that the trajectory $Q_i(t)$ is the one that minimizes S . Any other trajectory must lead to a higher value of S and so δS must be positive for any finite value of ϵ . If ϵ is chosen to be sufficiently small, then the absolute values of the terms of order ϵ^2 in Eq.(3.4) will be smaller than the absolute values of the terms linear in ϵ . The sign of ϵ could then be chosen to make δS negative, but this would violate the requirement that δS must be positive. The only way out of this dilemma is to insist that the sum of the terms linear in ϵ in Eq.(3.4) vanishes so that $\delta S \sim \epsilon^2$ and is therefore always positive as required. Insisting that the sum of terms linear in ϵ vanishes implies

$$0 = \int_{t_1}^{t_2} \left(\eta_i \frac{\partial L}{\partial Q_i} + \dot{\eta}_i \frac{\partial L}{\partial \dot{Q}_i} \right) dt. \quad (3.5)$$

Using $\dot{\eta}_i = d\eta_i/dt$ the above expression may be integrated by parts to obtain

$$\begin{aligned} 0 &= \int_{t_1}^{t_2} \left(\eta_i \frac{\partial L}{\partial Q_i} + \frac{d\eta_i}{dt} \frac{\partial L}{\partial \dot{Q}_i} \right) dt \\ &= \left[\eta_i \frac{\partial L}{\partial \dot{Q}_i} \right]_{t_1}^{t_2} + \int_{t_1}^{t_2} \left\{ \eta_i \frac{\partial L}{\partial Q_i} - \eta_i \frac{d}{dt} \left(\frac{\partial L}{\partial \dot{Q}_i} \right) \right\} dt. \end{aligned} \quad (3.6)$$

Since $\eta_i(t_{1,2}) = 0$ the integrated term vanishes and since η_i was an arbitrary function of t , the coefficient of η_i in the integrand must vanish, yielding *Lagrange's equation*

$$\frac{dP_i}{dt} = \frac{\partial L}{\partial Q_i} \quad (3.7)$$

where the *canonical momentum* P_i is defined as

$$P_i = \frac{\partial L}{\partial \dot{Q}_i}. \quad (3.8)$$

Equation (3.7) shows that if L does *not* depend on a particular generalized coordinate Q_j then $dP_j/dt = 0$ in which case the canonical momentum P_j is a *constant of the motion*; the coordinate Q_j is called a *cyclic* or *ignorable* coordinate. This is a very powerful and profound result. Saying that the Lagrangian function does not depend on a coordinate is equivalent to saying that the system is *symmetric* in that coordinate or translationally invariant with respect to that coordinate. The quantities P_j and Q_j are called conjugate and action has the dimensions of the product of these quantities.

Hamilton extended this formalism by introducing a new function related to the Lagrangian. This new function, called the Hamiltonian, provides further useful information and is defined as

$$H \equiv \left(\sum_i P_i \dot{Q}_i \right) - L. \quad (3.9)$$

Partial derivatives of H with respect to P_i and to Q_i give Hamilton's equations

$$\dot{Q}_i = \frac{\partial H}{\partial P_i} \quad \dot{P}_i = -\frac{\partial H}{\partial Q_i} \quad (3.10)$$

which are equations of motion having a close relation to phase-space concepts. The time derivative of the Hamiltonian is

$$\frac{dH}{dt} = \sum_i \frac{dP_i}{dt} \dot{Q}_i + \sum_i P_i \frac{d\dot{Q}_i}{dt} - \left(\sum_i \frac{\partial L}{\partial Q_i} \dot{Q}_i + \sum_i \frac{\partial L}{\partial \dot{Q}_i} \frac{d\dot{Q}_i}{dt} + \frac{\partial L}{\partial t} \right) = -\frac{\partial L}{\partial t}. \quad (3.11)$$

This shows that if L does not explicitly depend on time, i.e., $\partial L/\partial t = 0$, the Hamiltonian H is a *constant of the motion*. As will be shown later, H corresponds to the energy of the system, so if $\partial L/\partial t = 0$, the energy is a constant of the motion. Thus, energy is conjugate to time in analogy to canonical momentum being conjugate to position (note that energy \times time also has the units of action). If the Lagrangian does not explicitly depend on time, then the system can be thought of as being 'symmetric' with respect to time, or 'translationally' invariant with respect to time.

The Lagrangian for a charged particle in an electromagnetic field is

$$L = \frac{mv^2}{2} + q\mathbf{v} \cdot \mathbf{A}(\mathbf{x}, t) - q\phi(\mathbf{x}, t); \quad (3.12)$$

the validity of Eq.(3.12) will now be established by showing that it generates the Lorentz equation when inserted into Lagrange's equation. Since no symmetry is assumed, there is no reason to use any special coordinate system and so ordinary Cartesian coordinates will

be used as the canonical coordinates in which case Eq.(3.8) gives the canonical momentum as

$$\mathbf{P} = m\mathbf{v} + q\mathbf{A}(\mathbf{x},t). \quad (3.13)$$

The left hand side of Eq.(3.7) becomes

$$\frac{d\mathbf{P}}{dt} = m \frac{d\mathbf{v}}{dt} + q \left(\frac{\partial \mathbf{A}}{\partial t} + \mathbf{v} \cdot \nabla \mathbf{A} \right) \quad (3.14)$$

while the right hand side of Eq.(3.7) becomes

$$\begin{aligned} \frac{\partial L}{\partial \mathbf{x}} &= q \nabla (\mathbf{v} \cdot \mathbf{A}) - q \nabla \phi = q (\mathbf{v} \cdot \nabla \mathbf{A} + \mathbf{v} \times \nabla \times \mathbf{A}) - q \nabla \phi \\ &= q (\mathbf{v} \cdot \nabla \mathbf{A} + \mathbf{v} \times \mathbf{B}) - q \nabla \phi. \end{aligned} \quad (3.15)$$

Equating the above two expressions gives the Lorentz equation where the electric field is defined as $\mathbf{E} = -\partial \mathbf{A} / \partial t - \nabla \phi$ in accord with Faraday's law. This proves that Eq.(3.12) is mathematically equivalent to the Lorentz equation when used with the principle of least action.

The Hamiltonian associated with this Lagrangian is, in Cartesian coordinates,

$$\begin{aligned} H &= \mathbf{P} \cdot \mathbf{v} - L \\ &= \frac{mv^2}{2} + q\phi \\ &= \frac{(\mathbf{P} - q\mathbf{A}(\mathbf{x},t))^2}{2m} + q\phi(\mathbf{x},t) \end{aligned} \quad (3.16)$$

where the last line is the form more suitable for use with Hamilton's equations, i.e., $H = H(\mathbf{x}, \mathbf{P}, t)$. Equation (3.16) also shows that H is, as promised, the particle energy. If generalized coordinates are used, the energy can be written in a general form as $E = H(Q, P, t)$. Equation (3.11) showed that even though both Q and P depend on time, the energy depends on time only if H explicitly depends on time. Thus, in a situation where H does not explicitly depend on time, the energy would have the form $E = H(Q(t), P(t)) = \text{const.}$

It is important to realize that both canonical momentum and energy depend on the reference frame. For example, a bullet fired in an airplane in the direction opposite to the airplane motion and with a speed equal to the airplane's speed, has a large energy as measured in the airplane frame, but zero energy as measured by an observer on the ground. A more subtle example (of importance to later analysis of waves and Landau damping) occurs when \mathbf{A} and/or ϕ have a wave-like dependence, e.g. $\phi(\mathbf{x},t) = g(\mathbf{x} - \mathbf{V}_{ph}t)$ where \mathbf{V}_{ph} is the wave phase velocity. This potential is *time-dependent* in the lab frame and so the associated Lagrangian has an explicit dependence on time in the lab frame, which implies that *energy is not a constant of the motion in the lab frame*. In contrast, ϕ is *time-independent* in the wave frame and so the energy is a *constant of the motion in the wave frame*. Existence of a constant of the motion reduces the complexity of the system of equations and typically makes it possible to integrate at least one equation in closed form. Thus it is advantageous to analyze the system in the frame having the most constants of the motion.

3.3 Adiabatic invariant of a pendulum

Perfect symmetry is never attained in reality. This leads to the practical question of how constants of the motion behave when space and/or time symmetries are ‘good’, but not perfect. Does the utility of constants of the motion collapse abruptly when the slightest non-symmetrical blemish rears its ugly head, does the utility decay gracefully, or does something completely different happen? To answer these questions, we begin by considering the problem of a small-amplitude pendulum having a time-dependent, but *slowly changing* resonant frequency $\omega(t)$. Since $\omega^2 = g/l$, the time-dependence of the frequency might result from either a slow change in the gravitational acceleration g or else from a slow change in the pendulum length l . In both cases the pendulum equation of motion will be

$$\frac{d^2x}{dt^2} + \omega^2(t)x = 0. \quad (3.17)$$

This equation cannot be solved exactly for arbitrary $\omega(t)$ but for if a modest restriction is put on $\omega(t)$ the equation can be solved *approximately* using the WKB method (Wentzel 1926, Kramers 1926, Brillouin 1926). This method is based on the hypothesis that the solution for a time-dependent frequency is likely to be a generalization of the constant-frequency solution

$$x = \text{Re} [A \exp(i\omega t)], \quad (3.18)$$

where this generalization is guessed to be of the form

$$x(t) = \text{Re} \left[A(t) e^{i \int^t \omega(t') dt'} \right]. \quad (3.19)$$

Here $A(t)$ is an amplitude function determined as follows: calculate the first derivative of Eq. (3.19),

$$\frac{dx}{dt} = \text{Re} \left[i\omega A e^{i \int^t \omega(t') dt'} + \frac{dA}{dt} e^{i \int^t \omega(t') dt'} \right], \quad (3.20)$$

then the second derivative

$$\frac{d^2x}{dt^2} = \text{Re} \left[\left(i \frac{d\omega}{dt} A + 2i\omega \frac{dA}{dt} - \omega^2 A + \frac{d^2A}{dt^2} \right) e^{i \int^t \omega(t') dt'} \right], \quad (3.21)$$

and insert this last result into Eq. (3.17) which reduces to

$$i \frac{d\omega}{dt} A + 2i\omega \frac{dA}{dt} + \frac{d^2A}{dt^2} = 0, \quad (3.22)$$

since the terms involving ω^2 cancel exactly. To proceed further, we make an assumption – the validity of which is to be checked later – that the time dependence of dA/dt is *sufficiently slow* to allow dropping the last term in Eq. (3.22) relative to the middle term. The two terms that remain in Eq. (3.22) can then be re-arranged as

$$\frac{1}{\omega} \frac{d\omega}{dt} = -\frac{2}{A} \frac{dA}{dt} \quad (3.23)$$

which has the exact solution

$$A(t) \sim \frac{1}{\sqrt{\omega(t)}}. \quad (3.24)$$

The assumption of slowness is thus at least self-consistent, for if $\omega(t)$ is indeed slowly changing, Eq.(3.24) shows that $A(t)$ will also be slowly changing and the dropping of the last term in Eq.(3.22) is justified. The slowness requirement can be quantified by assuming that the frequency has an exponential dependence

$$\omega(t) = \omega_0 e^{\alpha t}. \quad (3.25)$$

Thus

$$\alpha = \frac{1}{\omega} \frac{d\omega}{dt} \quad (3.26)$$

is a measure of how fast the frequency is changing compared to the frequency itself. Hence dropping the last term in Eq.(3.22) is legitimate if

$$\alpha \ll 4\omega_0 \quad (3.27)$$

or

$$\frac{1}{\omega} \frac{d\omega}{dt} \ll 4\omega. \quad (3.28)$$

In other words, if Eq.(3.28) is satisfied, then the fractional change of the pendulum period per period is small.

Equation (3.24) indicates that when ω is time-dependent, the pendulum amplitude is not constant and so the pendulum energy is *not* conserved. It turns out that what *is* conserved is the *action integral*

$$S = \oint v dx \quad (3.29)$$

where the integration is over one period of oscillation. This integral can also be written in terms of time as

$$S = \int_{t_0}^{t_0+\tau} v \frac{dx}{dt} dt \quad (3.30)$$

where t_0 is a time when x is at an instantaneous maximum and τ , the period of a complete cycle, is defined as the interval between two successive times when $dx/dt = 0$ and d^2x/dt^2 has the same sign (e.g., for a pendulum, t_0 would be a time when the pendulum has swung all the way to the right and so is reversing its velocity while τ is the time one has to wait for this to happen again). To show that action is conserved, Eq. (3.29) can be integrated by parts as

$$\begin{aligned} S &= \int_{t_0}^{t_0+\tau} \left[\frac{d}{dt} \left(x \frac{dx}{dt} \right) - x \frac{d^2x}{dt^2} \right] dt \\ &= \left[x \frac{dx}{dt} \right]_{t_0}^{t_0+\tau} - \int_{t_0}^{t_0+\tau} x \frac{d^2x}{dt^2} dt \\ &= \int_{t_0}^{t_0+\tau} \omega^2 x^2 dt \end{aligned} \quad (3.31)$$

where (i) the integrated term has vanished by virtue of the definitions of t_0 and τ , and (ii) Eq.(3.17) has been used to substitute for d^2x/dt^2 . Equations (3.19) and (3.24) can be combined to give

$$x(t) = x(t_0) \sqrt{\frac{\omega(t_0)}{\omega(t)}} \cos \left(\int_{t_0}^t \omega(t') dt' \right) \quad (3.32)$$

so Eq.(3.31) becomes

$$\begin{aligned}
S &= \int_{t_0}^{t_0+\tau} \omega(t')^2 \left\{ x(t_0) \sqrt{\frac{\omega(t_0)}{\omega(t')}} \cos \left(\int_{t_0}^{t'} \omega(t'') dt'' \right) \right\}^2 dt' \\
&= [x(t_0)]^2 \omega(t_0) \int_{t_0}^{t_0+\tau} \omega(t') \cos^2 \left(\int_{t_0}^{t'} \omega(t'') dt'' \right) dt' \\
&= [x(t_0)]^2 \omega(t_0) \int_0^{2\pi} d\xi \cos^2 \xi = \pi [x(t_0)]^2 \omega(t_0) = \text{const.}
\end{aligned} \tag{3.33}$$

where $\xi = \int_{t_0}^{t'} \omega(t'') dt''$ and $d\xi = \omega(t') dt'$. Equation (3.29) shows that S is the area in phase-space enclosed by the trajectory $\{x(t), v(t)\}$ and Eq.(3.33) shows that for a slowly changing pendulum frequency, *this area is a constant of the motion*. Since the average energy of the pendulum scales as $\sim [\omega(t)x(t)]^2$, we see from Eq.(3.24) that the ratio

$$\frac{\text{energy}}{\text{frequency}} \sim \omega(t)x^2(t) \sim S \sim \text{const.} \tag{3.34}$$

The ratio in Eq.(3.34) is the classical equivalent of the quantum number N of a simple harmonic oscillator because in quantum mechanics the energy E of a simple harmonic oscillator is related to the frequency by the relation $E/h\omega = N + 1/2$.

This analysis clearly applies to *any* dynamical system having an equation of motion of the form of Eq.(3.17). Hence, if the dynamics of plasma particles happens to be of this form, then S can be added to our repertoire of constants of the motion.

3.4 Extension of WKB method to general adiabatic invariant

Action has the dimensions of (canonical momentum) \times (canonical coordinate) so we may anticipate that for general Hamiltonian systems, the action integral given in Eq.(3.29) is not an invariant because v is *not*, in general, proportional to P . We postulate that the general form for the action integral is

$$S = \oint P dQ \tag{3.35}$$

where the integral is over one period of the periodic motion and P, Q are the relevant canonical momentum-coordinate conjugate pair. The proof of adiabatic invariance used for Eq.(3.29) does not work directly for Eq.(3.35); we now present a slightly more involved proof to show that Eq.(3.35) is indeed the more general form of adiabatic invariant.

Let us define the radius vector in the $Q - P$ plane to be $\mathbf{R} = (Q, P)$ and define unit vectors in the Q and P directions by \hat{Q} and \hat{P} ; these definitions are shown in Fig.3.1. Furthermore we define the z direction as being normal to the $Q - P$ plane; thus the unit vector \hat{z} is 'out of the paper', i.e., $\hat{z} = \hat{Q} \times \hat{P}$. Hamilton's equations [i.e., $\dot{P} = -\partial H/\partial Q$, $\dot{Q} = \partial H/\partial P$] may be written in vector form as

$$\frac{d\mathbf{R}}{dt} = -\hat{z} \times \nabla H \tag{3.36}$$

where

$$\nabla = \hat{Q} \frac{\partial}{\partial Q} + \hat{P} \frac{\partial}{\partial P} \quad (3.37)$$

is the gradient operator in the $Q - P$ plane. Equation (3.36) shows that the phase-space ‘velocity’ $d\mathbf{R}/dt$ is *orthogonal* to ∇H . Hence, \mathbf{R} stays on a level contour of H . If H is constant, then, in order for the motion to be periodic, the path along this level contour must circle around and join itself, like a road of *constant elevation* around the rim of a mountain (or a crater). If H is not constant, but slowly changing in time, the contour will circle around and *nearly* join itself.

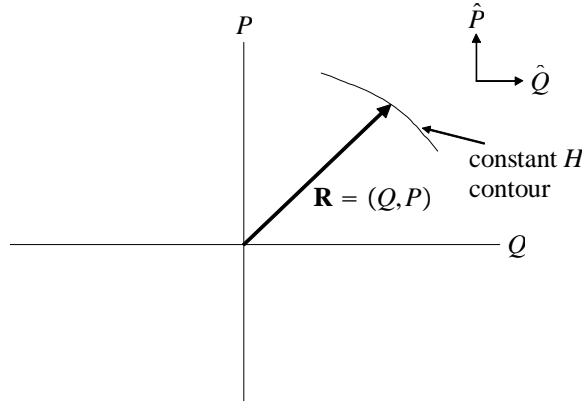


Figure 3.1: Q-P plane

Equation (3.36) can be inverted by crossing it with \hat{z} to give

$$\nabla H = \hat{z} \times \frac{d\mathbf{R}}{dt}. \quad (3.38)$$

For periodic and near-periodic motions, $d\mathbf{R}/dt$ is always in the same sense (always clockwise or always counterclockwise). Thus, Eq. (3.38) shows that an ‘observer’ following the path would always see that H is increasing on the left hand side of the path and decreasing on the right hand side (or vice versa). For clarity, the origin of the $Q - P$ plane is re-defined to be at a local maximum or minimum of H . Hence, near the extremum H must have the Taylor expansion

$$H(P, Q) = H_{extremum} + \frac{P^2}{2} \left[\frac{\partial^2 H}{\partial P^2} \right]_{P=0, Q=0} + \frac{Q^2}{2} \left[\frac{\partial^2 H}{\partial Q^2} \right]_{P=0, Q=0} \quad (3.39)$$

where $[\partial^2 H / \partial P^2]_{P=0, Q=0}$ and $[\partial^2 H / \partial Q^2]_{P=0, Q=0}$ are either both positive (valley) or both negative (hill). Since H is assumed to have a slow dependence on time, these second derivatives will be time-dependent so that Eq.(3.39) has the form

$$H = \alpha(t) \frac{P^2}{2} + \beta(t) \frac{Q^2}{2} \quad (3.40)$$

where $\alpha(t)$ and $\beta(t)$ have the same sign. The term $H_{extremum}$ in Eq.(3.39) has been dropped because it is just an additive constant to the energy and does not affect Hamilton's equations. From Eq. (3.36) the direction of rotation of \mathbf{R} is seen to be counterclockwise if the extremum of H is a hill, and clockwise if a valley.

Hamilton's equations operating on Eq.(3.40) give

$$\frac{dP}{dt} = -\beta Q, \quad \frac{dQ}{dt} = \alpha P. \quad (3.41)$$

These equations do not directly generate the simple harmonic oscillator equation because of the time dependence of α, β . However, if we define the auxiliary variable

$$\tau = \int^t \beta(t') dt' \quad (3.42)$$

then

$$\frac{d}{dt} = \frac{d\tau}{dt} \frac{d}{d\tau} = \beta \frac{d}{d\tau}$$

so Eq.(3.41) becomes

$$\frac{dP}{d\tau} = -Q, \quad \frac{dQ}{d\tau} = \frac{\alpha}{\beta} P. \quad (3.43)$$

Taking the τ derivative of the left equation above, and substituting the right hand equation gives

$$\frac{d^2 P}{d\tau^2} + \frac{\alpha}{\beta} P = 0 \quad (3.44)$$

which now is a simple harmonic oscillator with $\omega^2(\tau) = \alpha(\tau)/\beta(\tau)$. The action integral may be rewritten as

$$S = \int P \frac{dQ}{d\tau} d\tau \quad (3.45)$$

where the integral is over one period of the motion. Using Eqs.(3.43) and following the same procedure as was used with Eqs.(3.32) and Eq.(3.33), this becomes

$$S = \int P^2 \frac{\alpha}{\beta} d\tau = \lambda^2 \int \left[\left(\frac{\alpha(\tau')}{\beta(\tau')} \right)^{1/2} \cos^2 \left(\int^{\tau'} (\alpha/\beta)^{1/2} d\tau'' \right) \right] d\tau' \quad (3.46)$$

where λ is a constant dependent on initial conditions. By introducing the orbit phase $\phi = \int^{\tau} (\alpha/\beta)^{1/2} d\tau$, Eq.(3.46) becomes

$$S = \lambda^2 \int_0^{2\pi} d\phi \cos^2 \phi = const. \quad (3.47)$$

Thus, the general action integral is indeed an adiabatic invariant. This proof is of course only valid in the vicinity of an extremum of H , i.e., only where H can be adequately represented by Eq.(3.40).

3.4.1 General Proof for the General Adiabatic Invariant

We now develop a proof for the general adiabatic invariant. This proof is not restricted to small oscillations (i.e., being near an extremum of H) as was the previous discussion.

Let the Hamiltonian depend on time via a slowly changing parameter $\lambda(t)$, so that $H = H(P, Q, \lambda(t))$. From Eq.(3.16) the energy is given by

$$E(t) = H(P, Q, \lambda(t)) \quad (3.48)$$

and, in principle, this relation can be inverted to give $P = P(E(t), Q, \lambda(t))$. Suppose a particle is executing nearly periodic motion in the $Q - P$ plane. We define the turning point Q_{tp} as a position where $dQ/dt = 0$. Since Q is oscillating there will be a turning point associated with Q having its maximum value and a turning point associated with Q having its minimum value. From now on let us only consider turning points where Q has its maximum value, that is we only consider the turning points on the right hand side of the nearly periodic trajectories in the $Q - P$ plane shown in Fig.3.2.

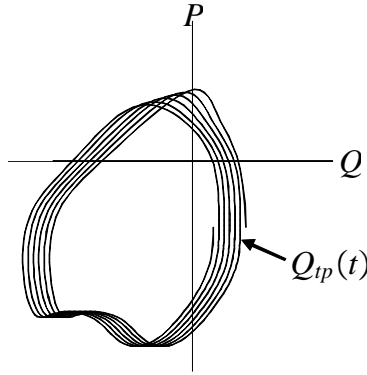


Figure 3.2: Nearly periodic phase space trajectory for slowly changing Hamiltonian. The turning $Q_{tp}(t)$ point is where Q is at its maximum.

If the motion is periodic, then the turning point for the $N + 1^{th}$ period will be the same as the turning point for the N^{th} period, but if the motion is only nearly periodic, there will be a slight difference as shown in Fig.3.2. This difference can be characterized by making the turning point a function of time so $Q_{tp} = Q_{tp}(t)$. This function is only defined for the times when $dQ/dt = 0$. When the motion is not exactly periodic, this turning point is such that $Q_{tp}(t + \tau) \neq Q_{tp}(t)$ where τ is the time interval required for the particle to go from the first turning point to the next turning point. The action integral is over one entire period of oscillation starting from a right hand turning point and then going to the next right hand turning point (cf. Fig. 3.2) and so can be written as

$$\begin{aligned} S &= \oint P dQ \\ &= \int_{Q_{tp}(t)}^{Q_{tp}(t+\tau)} P dQ. \end{aligned} \quad (3.49)$$

From Eq.(3.16) it is seen that P/m is not, in general, the velocity and so the velocity dQ/dt is not, in general, proportional to P . Thus, the turning points are not necessarily at the locations where P vanishes, and in fact P need not change sign during a period. However, S still corresponds to the area of phase-space enclosed by one period of the phase-space trajectory.

We can now calculate

$$\begin{aligned}
\frac{dS}{dt} &= \frac{d}{dt} \oint P dQ = \frac{d}{dt} \int_{Q_{tp}(t)}^{Q_{tp}(t+\tau)} P(E(t), Q, \lambda(t)) dQ \\
&= \left[P \frac{dQ}{dt} \right]_{Q_{tp}(t)}^{Q_{tp}(t+\tau)} + \int_{Q_{tp}(t)}^{Q_{tp}(t+\tau)} \left(\frac{\partial P}{\partial t} \right)_Q dQ \\
&= \int_{Q_{tp}(t)}^{Q_{tp}(t+\tau)} \left[\left(\frac{\partial P}{\partial E} \right)_{Q,\lambda} \frac{dE}{dt} + \left(\frac{\partial P}{\partial \lambda} \right)_{Q,E} \frac{d\lambda}{dt} \right] dQ.
\end{aligned} \tag{3.50}$$

Because $dQ/dt = 0$ at the turning point, the integrated term vanishes and so there is no contribution from motion of the turning point. From Eq.(3.48) we have

$$1 = \frac{\partial H}{\partial P} \left(\frac{\partial P}{\partial E} \right)_{Q,\lambda} \tag{3.51}$$

and

$$0 = \frac{\partial H}{\partial P} \left(\frac{\partial P}{\partial \lambda} \right)_{Q,E} + \frac{\partial H}{\partial \lambda} \tag{3.52}$$

so that Eq.(3.50) becomes

$$\frac{dS}{dt} = \oint \left(\frac{\partial H}{\partial P} \right)^{-1} \left[\frac{dE}{dt} - \frac{\partial H}{\partial \lambda} \frac{d\lambda}{dt} \right] dQ. \tag{3.53}$$

From Eq.(3.48) we have

$$\frac{dE}{dt} = \frac{\partial H}{\partial P} \frac{dP}{dt} + \frac{\partial H}{\partial Q} \frac{dQ}{dt} + \frac{\partial H}{\partial \lambda} \frac{d\lambda}{dt} = \frac{\partial H}{\partial \lambda} \frac{d\lambda}{dt} \tag{3.54}$$

since the first two terms cancelled due to Hamilton's equations. Substitution of Eq.(3.54) into Eq.(3.53) gives $dS/dt = 0$, completing the proof of adiabatic invariance. No assumption has been made here that P, Q are close to the values associated with an extremum of H .

This proof seems too neat, because it has established adiabatic invariance simply by careful use of the chain rule, and by taking partial derivatives. However, this observation reveals the underlying essence of adiabaticity, namely it is the differentiability of H, P with respect to λ from one period to the next and the Hamilton nature of the system which together provide the conditions for the adiabatic invariant to exist. If the motion had been such that after one cycle the motion had changed so drastically that taking a derivative of H or P with respect to λ would not make sense, then the adiabatic invariant would not exist.

3.5 Drift equations

We show in this section that it is possible to deduce intuitive and quite accurate analytic solutions for the velocity (drift) of charged particles in arbitrarily complicated electric and magnetic fields provided the fields are *slowly changing in both space and time* (this requirement is essentially the slowness requirement for adiabatic invariance). Drift solutions are obtained by solving the Lorentz equation

$$m \frac{d\mathbf{v}}{dt} = q(\mathbf{E} + \mathbf{v} \times \mathbf{B}) \quad (3.55)$$

iteratively, taking advantage of the assumed separation of scales between fast and slow motions.

3.5.1 Simple $E \times B$ and force drifts

Before developing the general method for analyzing drifts, a simple example illustrating the basic idea will now be discussed. This example consists of an ion starting at rest in a spatially uniform magnetic field $\mathbf{B} = B\hat{z}$ and a spatially uniform electric field $\mathbf{E} = E\hat{y}$. The origin is defined to be at the ion's starting position and both electric and magnetic fields are constant in time. The assumed spatial uniformity and time-independence of the fields represent the extreme limit of assuming that the fields are slowly changing in space and time.

Because the magnetic force $q\mathbf{v} \times \mathbf{B}$ is perpendicular to \mathbf{v} , the magnetic force does no work and so only the electric field can change the ion's energy (this can be seen by dotting Eq.(3.55) with \mathbf{v}). Also, because all fields are uniform and static the electric field can be expressed as $\mathbf{E} = -\nabla\phi$ where $\phi = -Ey$ is an electrostatic potential. Since the ion lowers its potential energy $q\phi$ on moving to larger y , motion in the positive y direction corresponds to the ion "falling downhill". Since the ion starts from rest at $y = 0$ where $\phi = 0$, the total energy $W = mv^2/2 + q\phi$ is initially zero. Furthermore, the time-independence of the fields implies that W must remain zero for all time. Because the kinetic energy $mv^2/2$ is positive-definite, the ion can only attain finite kinetic energy if it falls downhill, i.e., moves into regions of positive y . If for any reason the ion y -coordinate becomes zero at some later time, then at such a time the ion would again have to have $\mathbf{v} = 0$ because $W = mv^2 - qEy = 0$.

When the ion begins moving, it will initially experience mainly the electric force $qE\hat{y}$ because the magnetic force $q\mathbf{v} \times \mathbf{B}$, being proportional to velocity, is negligible. The electric force accelerates the ion in the y direction so the ion develops a positive v_y and also moves towards larger positive y as it "falls downhill" in the potential. As it develops a positive v_y , the ion starts to experience a magnetic force $qv_y\hat{y} \times B\hat{z} = v_yqB\hat{x}$ which accelerates the ion in the positive x -direction causing the ion to develop a positive v_x in addition. The trajectory now becomes curved as the ion veers in the x direction while moving towards larger y . The positive v_x continues to increase and as a consequence a new magnetic force $qv_x\hat{x} \times B\hat{z} = -v_xqB\hat{y}$ develops and, being in the negative y direction, this increasing magnetic force counteracts the steady electric force, eventually causing the ion to decelerate in the y direction. The velocity v_y now decreases and ultimately reverses so that the ion starts to head in the negative y direction back towards $y = 0$. As a consequence of the reversal of v_y , the magnetic force $qv_y\hat{y} \times B\hat{z}$ will become negative and so the ion

will also decelerate in the x -direction. Moving with negative v_y means the ion is going uphill in the electrostatic potential and when it reaches $y = 0$, its potential energy must go back to zero. As noted above, the ion must come to rest at this point, because its total energy is always zero. Because the x velocity was never negative, the result of all this is that the ion makes a net positive displacement in the x direction. The whole process then repeats with the result that the ion keeps advancing in x while making a sequence of semi-circles in which v_y oscillates in polarity while v_x is never negative. The ion consequently moves like a leap-frog which bounces up and down in the y direction while continuously advancing in the x direction. If an electron had been used instead of an ion, the sign of both the electric and magnetic forces would have reversed and the electron would have been confined to regions where $y \leq 0$. However, the net displacement would also be in the positive x direction (this is easily seen by repeating the above argument using an electron).

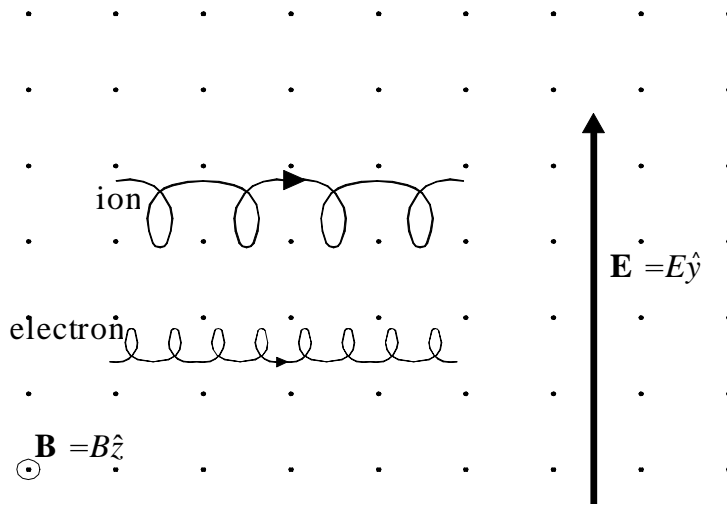


Figure 3.3: $\mathbf{E} \times \mathbf{B}$ drifts for particles having finite initial energy

If an ion starts with a finite rather than a zero velocity, it will execute cyclotron (also called Larmor) orbits which take the ion into regions of both positive and negative y . However, the ion will have a larger gyro-radius in its $y > 0$ orbit segment than in its $y < 0$ orbit segment resulting again in an average drift to the right as shown in Fig.3.3. Electrons have larger gyro-radii in the $y < 0$ portions of their orbit, but have a counterclockwise rotation so electrons *also* drift to the right. The magnitude of this steady drift is easily calculated by assuming the existence of a constant perpendicular drift velocity in the Lorentz equation, and then averaging out the cyclotron motion:

$$0 = \mathbf{E} + \langle \mathbf{v} \rangle \times \mathbf{B}. \quad (3.56)$$

This may be solved to give the average drift velocity

$$\mathbf{v}_E \equiv \langle \mathbf{v} \rangle = \frac{\mathbf{E} \times \mathbf{B}}{B^2}. \quad (3.57)$$

This steady ‘ E cross B ’ drift is independent of both the particle’s polarity and initial velocity. One way of interpreting this behavior is to recall that according to the theory of special relativity the electric field \mathbf{E}' observed in a frame moving with velocity \mathbf{u} is $\mathbf{E}' = \mathbf{E} + \mathbf{u} \times \mathbf{B}$ and so Eq. (3.56) is simply a statement that a particle drifts in such a way to ensure that the electric field seen in its own frame vanishes. The ‘ E cross B ’ drift analysis can be easily generalized to describe the effect on a charged particle of *any* force orthogonal to \mathbf{B} by simply making the replacement $\mathbf{E} \rightarrow \mathbf{F}/q$ in the Lorentz equation. Thus, any spatially uniform, temporally constant force orthogonal to \mathbf{B} will cause a drift

$$\mathbf{v}_F \equiv \langle \mathbf{v} \rangle = \frac{\mathbf{F} \times \mathbf{B}}{qB^2}. \quad (3.58)$$

Equations (3.57) and (3.58) lead to two counter-intuitive and important conclusions:

1. A steady-state electric field perpendicular to a magnetic field does not drive currents in a plasma, but instead causes a bulk motion of the entire plasma across the magnetic field with the velocity \mathbf{v}_E .
2. A steady-state *force* (e.g., gravity, centrifugal force, etc.) perpendicular to the magnetic field causes oppositely directed motions for electrons and ions and so drives a cross-field current

$$\mathbf{J}_F = \sum_{\sigma} n_{\sigma} \frac{\mathbf{F} \times \mathbf{B}}{B^2}. \quad (3.59)$$

3.5.2 Drifts in slowly changing arbitrary fields

We now consider charged particle motion in arbitrarily complicated but slowly changing fields subject to the following restrictions:

1. The time variation is so slow that the fields can be considered as approximately constant during each cyclotron period of the motion.
2. The fields vary so *gradually* in space that they are nearly uniform over the spatial extent of any single complete cyclotron orbit.
3. The electric and magnetic fields are related by Faraday’s law $\nabla \times \mathbf{E} = -\partial \mathbf{B} / \partial t$.
4. $E/B \ll c$ so that relativistic effects are unimportant (otherwise there would be a problem with v_E becoming faster than c).

In this more general situation a charged particle will gyrate about \mathbf{B} , stream parallel to \mathbf{B} , have ‘ $E \times B$ ’ drifts across \mathbf{B} , and may also have force-based drifts. The analysis is based on the assumption that all these various motions are well-separated (easily distinguishable from each other); this assumption is closely related to the requirement that the fields vary slowly and also to the concept of adiabatic invariance.

The assumed separation of scales is expressed by decomposing the particle motion into a fast, oscillatory component – the gyro-motion – and a slow component obtained by

averaging out the gyromotion. As sketched in Fig.3.4, the particle's position and velocity are each decomposed into two terms

$$\mathbf{x}(t) = \mathbf{x}_{gc}(t) + \mathbf{r}_L(t), \quad \mathbf{v}(t) = \frac{d\mathbf{x}}{dt} = \mathbf{v}_{gc}(t) + \mathbf{v}_L(t) \quad (3.60)$$

where $\mathbf{r}_L(t)$, $\mathbf{v}_L(t)$ give the *fast* gyration of the particle in a cyclotron orbit and $\mathbf{x}_{gc}(t)$, $\mathbf{v}_{gc}(t)$ are the *slowly* changing motion of the *guiding center* obtained after averaging out the cyclotron motion. Ignoring any time dependence of the fields for now, the magnetic field seen by the particle can be written as

$$\begin{aligned} \mathbf{B}(\mathbf{x}(t)) &= \mathbf{B}(\mathbf{x}_{gc}(t) + \mathbf{r}_L(t)) \\ &= \mathbf{B}(\mathbf{x}_{gc}(t)) + (\mathbf{r}_L(t) \cdot \nabla) \mathbf{B}. \end{aligned} \quad (3.61)$$

Because \mathbf{B} was assumed to be nearly uniform over the cyclotron orbit, it is sufficient to keep only the first term in the Taylor expansion of the magnetic field. The electric field may be expanded in a similar fashion.

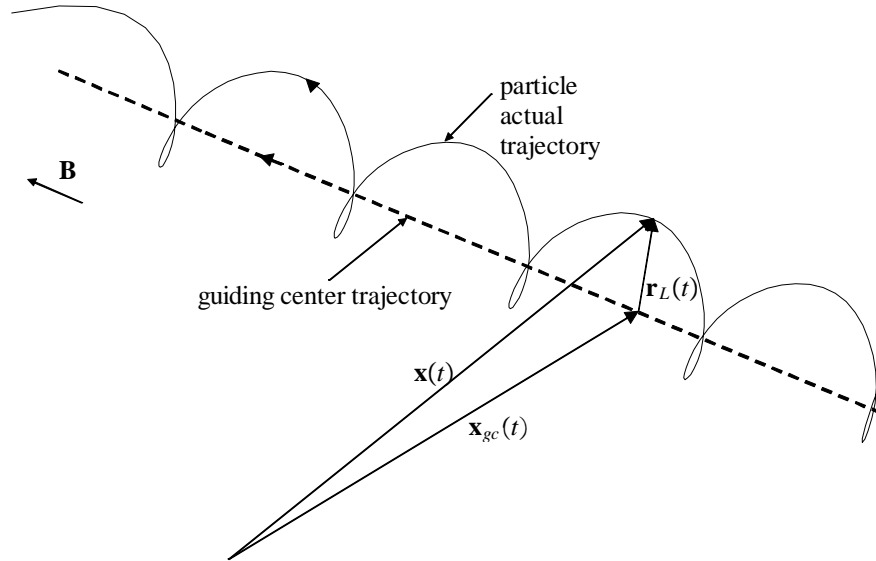


Figure 3.4: Drift in an arbitrarily complicated field

After insertion of these Taylor expansions for the non-uniform electric and magnetic

fields, the Lorentz equation becomes

$$\begin{aligned} m \frac{d[\mathbf{v}_{gc}(t) + \mathbf{v}_L(t)]}{dt} &= q \left[\mathbf{E}(\mathbf{x}_{gc}(t)) + (\mathbf{r}_L(t) \cdot \nabla) \mathbf{E} \right] \\ &\quad + q [\mathbf{v}_{gc}(t) + \mathbf{v}_L(t)] \times \left[\mathbf{B}(\mathbf{x}_{gc}(t)) + (\mathbf{r}_L(t) \cdot \nabla) \mathbf{B} \right]. \end{aligned} \quad (3.62)$$

The gyromotion (i.e., the fast cyclotron motion) is defined to be the solution of the equation

$$m \frac{d\mathbf{v}_L(t)}{dt} = q \mathbf{v}_L(t) \times \mathbf{B}(\mathbf{x}_{gc}(t)); \quad (3.63)$$

subtracting this fast motion equation from Eq.(3.62) leaves

$$\begin{aligned} m \frac{d\mathbf{v}_{gc}(t)}{dt} &= q \left[\mathbf{E}(\mathbf{x}_{gc}(t)) + (\mathbf{r}_L(t) \cdot \nabla) \mathbf{E} \right] \\ &\quad + q \left\{ \mathbf{v}_{gc}(t) \times \left[\mathbf{B}(\mathbf{x}_{gc}(t)) + (\mathbf{r}_L(t) \cdot \nabla) \mathbf{B} \right] + \mathbf{v}_L(t) \times (\mathbf{r}_L(t) \cdot \nabla) \mathbf{B} \right\}. \end{aligned} \quad (3.64)$$

Let us now average Eq.(3.64) over one gyroperiod in which case terms *linear* in gyromotion average to zero. What remains is an equation describing the slow quantities, namely

$$m \frac{d\mathbf{v}_{gc}(t)}{dt} = q \left\{ \mathbf{E}(\mathbf{x}_{gc}(t)) + \mathbf{v}_{gc}(t) \times \mathbf{B}(\mathbf{x}_{gc}(t)) + \langle \mathbf{v}_L(t) \times (\mathbf{r}_L(t) \cdot \nabla) \mathbf{B} \rangle \right\} \quad (3.65)$$

where $\langle \rangle$ means averaged over a cyclotron period. The guiding center velocity can now be decomposed into components perpendicular and parallel to \mathbf{B} ,

$$\mathbf{v}_{gc}(t) = \mathbf{v}_{\perp gc}(t) + v_{\parallel gc}(t) \hat{B} \quad (3.66)$$

so that

$$\frac{d\mathbf{v}_{gc}(t)}{dt} = \frac{d\mathbf{v}_{\perp gc}(t)}{dt} + \frac{d(v_{\parallel gc}(t) \hat{B})}{dt} = \frac{d\mathbf{v}_{\perp gc}(t)}{dt} + \frac{dv_{\parallel gc}(t)}{dt} \hat{B} + v_{\parallel gc}(t) \frac{d\hat{B}}{dt}. \quad (3.67)$$

Denoting the distance along the magnetic field by s , the derivative of the magnetic field unit vector can be written, to lowest order, as

$$\frac{d\hat{B}}{dt} = \frac{\partial \hat{B}}{\partial s} \frac{ds}{dt} = v_{\parallel gc} \hat{B} \cdot \nabla \hat{B}, \quad (3.68)$$

so Eq.(3.65) becomes

$$\begin{aligned} m \left[\frac{d\mathbf{v}_{\perp gc}(t)}{dt} + \frac{dv_{\parallel gc}(t)}{dt} \hat{B} + v_{\parallel gc}^2 \hat{B} \cdot \nabla \hat{B} \right] &= q \mathbf{E}(\mathbf{x}_{gc}(t)) \\ &\quad + q \mathbf{v}_{gc}(t) \times \mathbf{B}(\mathbf{x}_{gc}(t)) \\ &\quad + q \langle \mathbf{v}_L(t) \times (\mathbf{r}_L(t) \cdot \nabla) \mathbf{B} \rangle. \end{aligned} \quad (3.69)$$

The component of this equation along \mathbf{B} is

$$m \frac{dv_{\parallel gc}(t)}{dt} = q \left[E_{\parallel}(\mathbf{x}_{gc}(t)) + \langle \mathbf{v}_L(t) \times (\mathbf{r}_L(t) \cdot \nabla) \mathbf{B} \rangle_{\parallel} \right] \quad (3.70)$$

while the component perpendicular to \mathbf{B} is

$$m \left[\frac{d\mathbf{v}_{\perp gc}(t)}{dt} + v_{\parallel gc}^2 \widehat{B} \cdot \nabla \widehat{B} \right] = q \left[\begin{array}{l} \mathbf{E}_{\perp}(\mathbf{x}_{gc}(t)) \\ + \mathbf{v}_{gc}(t) \times \mathbf{B}(\mathbf{x}_{gc}(t)) \\ + \langle \mathbf{v}_L(t) \times (\mathbf{r}_L(t) \cdot \nabla) \mathbf{B} \rangle_{\perp} \end{array} \right]. \quad (3.71)$$

Equation (3.71) is of the generic form

$$m \frac{d\mathbf{v}_{\perp gc}}{dt} = \mathbf{F}_{\perp} + q\mathbf{v}_{gc} \times \mathbf{B} \quad (3.72)$$

where

$$\mathbf{F}_{\perp} = q \left[\begin{array}{l} \mathbf{E}_{\perp}(\mathbf{x}_{gc}(t)) + \langle \mathbf{v}_L(t) \times (\mathbf{r}_L(t) \cdot \nabla) \mathbf{B} \rangle_{\perp} \\ - m v_{\parallel gc}^2 \widehat{B} \cdot \nabla \widehat{B} \end{array} \right] \quad (3.73)$$

Equation (3.72) is solved iteratively based on the assumption that $\mathbf{v}_{\perp gc}$ has a slow time dependence. In the first iteration, the time dependence is neglected altogether so that the LHS of Eq.(3.72) is set to zero to obtain the ‘first guess’ for the perpendicular drift to be

$$\mathbf{v}_{\perp gc} \simeq \mathbf{v}_F \equiv \frac{\mathbf{F}_{\perp} \times \mathbf{B}}{qB^2}.$$

Next, \mathbf{v}_p is defined to be a correction to this first guess, where \mathbf{v}_p is assumed small and incorporates effects due to any time dependence of $\mathbf{v}_{\perp gc}$. To determine \mathbf{v}_p , we write $\mathbf{v}_{\perp gc} = \mathbf{v}_F + \mathbf{v}_P$ so, to second order Eq. (3.72) becomes,

$$m \frac{d(\mathbf{v}_F + \mathbf{v}_P)}{dt} = \mathbf{F}_{\perp} + q(\mathbf{v}_F + \mathbf{v}_P) \times \mathbf{B}. \quad (3.74)$$

In accordance with the slowness condition, it is assumed that $|d\mathbf{v}_P/dt| \ll |d\mathbf{v}_F/dt|$ so Eq.(3.74) becomes

$$0 = -m \frac{d\mathbf{v}_F}{dt} + q\mathbf{v}_P \times \mathbf{B}. \quad (3.75)$$

Crossing this equation with \mathbf{B} gives the general *polarization drift*

$$\mathbf{v}_P = -\frac{m}{qB^2} \frac{d\mathbf{v}_F}{dt} \times \mathbf{B}. \quad (3.76)$$

The most important example of the polarization drift is when \mathbf{v}_F is the $E \times B$ drift in a uniform, constant magnetic field so that

$$\begin{aligned} \mathbf{v}_P &= -\frac{m}{qB^2} \frac{d}{dt} \left(\frac{\mathbf{E} \times \mathbf{B}}{B^2} \right) \times \mathbf{B} \\ &= \frac{m}{qB^2} \frac{d\mathbf{E}}{dt}. \end{aligned} \quad (3.77)$$

To calculate the middle term on the RHS of Eq.(3.73), it is necessary to average over cyclotron orbits (also called gyro-orbits or Larmor orbits). This middle term is defined as the ‘grad B ’ force

$$\mathbf{F}_{\nabla B} = q \langle \mathbf{v}_L(t) \times (\mathbf{r}_L(t) \cdot \nabla) \mathbf{B} \rangle. \quad (3.78)$$

To simplify the algebra for the averaging, a local Cartesian coordinate system is used with x axis in the direction of the gyrovelocity at $t = 0$ and z axis in the direction of the magnetic field *at the gyrocenter*. Thus, the Larmor orbit velocity has the form

$$\mathbf{v}_L(t) = v_{L0} [\hat{x} \cos \omega_c t - \hat{y} \sin \omega_c t] \quad (3.79)$$

where

$$\omega_c = \frac{qB}{m} \quad (3.80)$$

is called the cyclotron frequency and the Larmor orbit position has the form

$$\mathbf{r}_L(t) = \frac{v_{L0}}{\omega_c} [\hat{x} \sin \omega_c t + \hat{y} \cos \omega_c t]. \quad (3.81)$$

Inserting the above two expressions in Eq.(3.78) gives

$$\mathbf{F}_{\nabla B} = q \frac{v_{L0}^2}{\omega_c} \langle [\hat{x} \cos \omega_c t - \hat{y} \sin \omega_c t] \times ([\hat{x} \sin \omega_c t + \hat{y} \cos \omega_c t] \cdot \nabla) \mathbf{B} \rangle. \quad (3.82)$$

Noting that $\langle \sin^2 \omega_c t \rangle = \langle \cos^2 \omega_c t \rangle = 1/2$ while $\langle \sin(\omega_c t) \cos(\omega_c t) \rangle = 0$, this reduces to

$$\begin{aligned} \mathbf{F}_{\nabla B} &= \frac{qv_{L0}^2}{2\omega_c} \left[\hat{x} \times \frac{\partial \mathbf{B}}{\partial y} - \hat{y} \times \frac{\partial \mathbf{B}}{\partial x} \right] \\ &= \frac{mv_{L0}^2}{2B} \left[\hat{x} \times \frac{\partial (B_y \hat{y} + B_z \hat{z})}{\partial y} - \hat{y} \times \frac{\partial (B_x \hat{x} + B_z \hat{z})}{\partial x} \right] \\ &= \frac{mv_{L0}^2}{2B} \left[\hat{z} \left(\frac{\partial B_y}{\partial y} + \frac{\partial B_x}{\partial x} \right) - \hat{y} \frac{\partial B_z}{\partial y} - \hat{x} \frac{\partial B_z}{\partial x} \right]. \end{aligned} \quad (3.83)$$

But from $\nabla \cdot \mathbf{B} = 0$, it is seen that $\frac{\partial B_y}{\partial y} + \frac{\partial B_x}{\partial x} = -\frac{\partial B_z}{\partial z}$ so the 'grad B ' force is

$$\mathbf{F}_{\nabla B} = -\frac{mv_{L0}^2}{2B} \nabla B \quad (3.84)$$

where the approximation $B_z \simeq B$ has been used since the magnetic field direction is mainly in the \hat{z} direction.

Let us now define

$$\mathbf{F}_c = -mv_{\parallel gc}^2 \hat{B} \cdot \nabla \hat{B} \quad (3.85)$$

and consider this force. Suppose that the magnetic field lines have curvature and consider a particular point on a specific field line. Define, as shown in Fig.3.5, a two-dimensional cylindrical coordinate system (R, ϕ) with origin at the field line center of curvature for this specific point and lying in the plane of the field line at this point. Then, the radial position of the chosen point in this cylindrical coordinate system is the local radius of curvature of the field line and, since $\hat{\phi} = \hat{B}$, it is seen that $\hat{B} \cdot \nabla \hat{B} = \hat{\phi} \cdot \nabla \hat{\phi} = -\hat{R}/R$. Thus, the force associated with curvature of a field line

$$\mathbf{F}_c = \frac{mv_{\parallel gc}^2 \hat{R}}{R} \quad (3.86)$$

is just the centrifugal force resulting from the motion along the curve of the particle's guiding center.

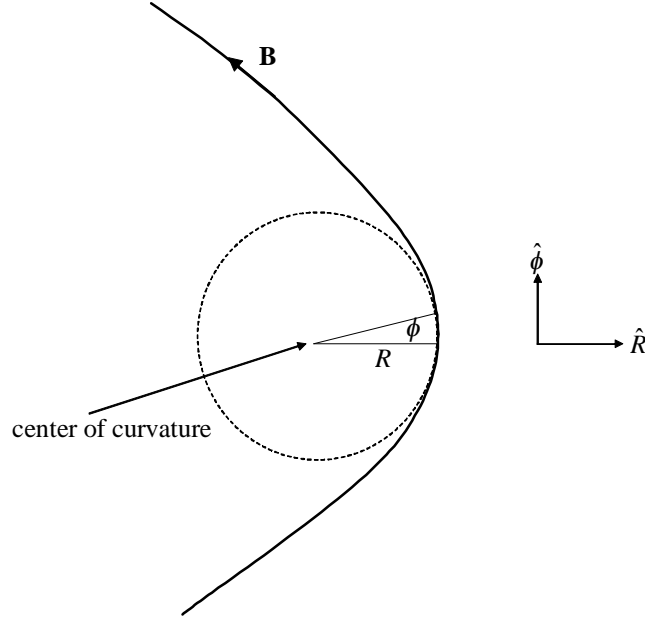


Figure 3.5: Local cylindrical coordinate system defined by curved magnetic field, $\hat{\phi} = \hat{B}$.

The drifts can be summarized as

$$\mathbf{v}_{\perp gc} = \mathbf{v}_E + \mathbf{v}_{\nabla B} + \mathbf{v}_c + \mathbf{v}_P \quad (3.87)$$

where

1. the ' E cross B ' drift is

$$\mathbf{v}_E = \frac{\mathbf{E} \times \mathbf{B}}{B^2} \quad (3.88)$$

2. the ' $\text{grad } B$ ' drift is

$$\mathbf{v}_{\nabla B} = -\frac{mv_{L0}^2}{2qB^3} \nabla B \times \mathbf{B} \quad (3.89)$$

3. the ' curvature ' drift is

$$\mathbf{v}_c = -\frac{mv_{\parallel gc}^2}{qB^2} \hat{B} \cdot \nabla \hat{B} \times \mathbf{B} = \frac{1}{qB^2} \left(\frac{mv_{\parallel gc}^2 \hat{R}}{R} \right) \times \mathbf{B} \quad (3.90)$$

4. the ' polarization ' drift is

$$\mathbf{v}_P = -\frac{m}{qB^2} \left[\frac{d}{dt} (\mathbf{v}_E + \mathbf{v}_{\nabla B} + \mathbf{v}_c) \right] \times \mathbf{B} \quad (3.91)$$

3.5.3 μ conservation

We now imagine being in a frame moving with the velocity $\mathbf{v}_{\perp gc}$; in this frame the only perpendicular velocity is the cyclotron velocity (Larmor motion). Since $\mathbf{v}_{\perp gc}$ is orthogonal to \mathbf{B} , the parallel equation of motion is not affected by this change of frame and using Eqs.(3.70) and (3.84) can be written as

$$m \frac{dv_{\parallel}}{dt} = qE_{\parallel} - \frac{mv_{L0}^2}{2B} \frac{\partial B}{\partial s} \quad (3.92)$$

where as before, s is the distance along the magnetic field. Multiplication by v_{\parallel} gives an energy relation

$$\frac{d}{dt} \left(\frac{mv_{\parallel}^2}{2} \right) = qE_{\parallel} v_{\parallel} - \frac{mv_{L0}^2}{2B} v_{\parallel} \frac{\partial B}{\partial s}. \quad (3.93)$$

The perpendicular force defined in Eq.(3.73) does not exist in this moving frame because it has been ‘transformed away’ by the change of frames. Also, recall that it was assumed that the characteristic scale lengths of \mathbf{E} and \mathbf{B} are large compared to the gyro radius (Larmor radius). However, if the magnetic field has an *absolute time derivative*, Faraday’s law states that there must be an inductive electric field, i.e., an electric field for which $\oint \mathbf{E} \cdot d\mathbf{l} \neq 0$. This is distinct from the static electric field that has been previously assumed and so its consequences must be explicitly taken into account.

To understand the effect of an inductive electric field, consider a specific particle, and dot the Lorentz equation with \mathbf{v} to obtain

$$\frac{d}{dt} \left(\frac{mv_{\parallel}^2}{2} + \frac{mv_{L0}^2}{2} \right) = qv_{\parallel} E_{\parallel} + q\mathbf{v}_{\perp} \cdot \mathbf{E}_{\perp} \quad (3.94)$$

where \mathbf{v}_{\perp} is the vector Larmor orbit velocity. Subtracting Eq.(3.93) from (3.94) gives

$$\frac{d}{dt} \left(\frac{mv_{L0}^2}{2} \right) = q\mathbf{v}_{\perp} \cdot \mathbf{E}_{\perp} + \frac{mv_{L0}^2}{2B} v_{\parallel} \frac{\partial B}{\partial s}. \quad (3.95)$$

Integration of Faraday’s law over the cross-section of the Larmor orbit gives

$$\int ds \cdot \nabla \times \mathbf{E} = - \int ds \cdot \frac{\partial \mathbf{B}}{\partial t} \quad (3.96)$$

or

$$\oint d\mathbf{l} \cdot \mathbf{E} = -\pi r_L^2 \frac{\partial B}{\partial t} \quad (3.97)$$

where it has been assumed that the magnetic field is changing sufficiently slowly for the orbit radius to be approximately constant during each orbit.

Equation (3.95) involves the local electric field \mathbf{E}_{\perp} but Eq.(3.97) only gives the line integral of the electric field. This line integral can still be used if Eq.(3.95) is averaged over a cyclotron period. The critical term is the time average over the Larmor orbit of $q\mathbf{v}_{\perp} \cdot \mathbf{E}_{\perp}$

(which gives the rate at which the perpendicular electric field does work on the particle),

$$\begin{aligned}
 \langle q\mathbf{v}_\perp \cdot \mathbf{E}_\perp \rangle_{orbit} &= \frac{\omega_c}{2\pi} \int dt q\mathbf{v}_\perp \cdot \mathbf{E}_\perp \\
 &= -\frac{q\omega_c}{2\pi} \oint d\mathbf{l} \cdot \mathbf{E}_\perp \\
 &= \frac{q\omega_c}{2} r_L^2 \frac{\partial B}{\partial t}.
 \end{aligned} \tag{3.98}$$

The substitution $\mathbf{v}_\perp dt = -d\mathbf{l}$ has been used and the minus sign is invoked because particle motion is diamagnetic (e.g., ions have a left-handed orbit, whereas in Stokes' theorem $d\mathbf{l}$ is assumed to be a right handed line element). Averaging of Eq. (3.95) gives

$$\left\langle \frac{d}{dt} \left(\frac{mv_{L0}^2}{2} \right) \right\rangle = \frac{mv_{L0}^2}{2B} \frac{\partial B}{\partial t} + \frac{mv_{L0}^2}{2B} v_\parallel \frac{\partial B}{\partial s} = \frac{mv_{L0}^2}{2B} \frac{dB}{dt} \tag{3.99}$$

where $dB/dt = \partial B/\partial t + v_\parallel \partial B/\partial s$ is the *total derivative* of the average magnetic field experienced by the particle over a Larmor orbit. Defining the Larmor orbit kinetic energy as $W_\perp = mv_{L0}^2/2$, Eq.(3.99) can be rewritten as

$$\frac{1}{W_\perp} \frac{dW_\perp}{dt} = \frac{1}{B} \frac{dB}{dt} \tag{3.100}$$

which has the solution

$$\frac{W_\perp}{B} \equiv \mu = \text{const.} \tag{3.101}$$

for magnetic fields that can be changing in *both* time and space. In plasma physics terminology, μ is called the 'first adiabatic' invariant, and the invariance of μ shows that the ratio of the kinetic energy of gyromotion to gyrofrequency is a conserved quantity. The derivation assumed the magnetic field changed sufficiently slowly for the instantaneous field strength $B(t)$ during an orbit to differ only slightly from the orbit-averaged field strength $\langle B \rangle$ the orbit, i.e., $|B(t) - \langle B \rangle| \ll \langle B \rangle$.

3.5.4 Relation of μ conservation to other conservation relations

μ conservation is both of fundamental importance and a prime example of the adiabatic invariance of the action integral associated with a periodic motion. The μ conservation concept unites together several seemingly disparate points of view:

1. Conservation of magnetic moment of a particle- According to electromagnetic theory the magnetic moment m of a current loop is $m = IA$ where I is the current carried in the loop and A is the area enclosed by the loop. Because a gyrating particle traces out a circular orbit at the frequency $\omega_c/2\pi$ and has a charge q , it effectively constitutes a current loop having $I = q\omega_c/2\pi$ and cross-sectional area $A = \pi r_L^2$. Thus, the magnetic moment of the gyrating particle is

$$m = \left(\frac{q\omega_c}{2\pi} \right) \pi r_L^2 = \frac{mv_{L0}^2}{2B} = \mu \tag{3.102}$$

and so the magnetic moment m is an adiabatically conserved quantity.

2. Conservation of magnetic flux enclosed by gyro-orbit- Because the magnetic flux Φ enclosed by the gyro-orbit is

$$\Phi = B\pi r_L^2 = \left(\frac{2m\pi}{q}\right)\mu, \quad (3.103)$$

μ conservation further implies conservation of the magnetic flux enclosed by a gyro-orbit. This is consistent with the concept that the magnetic flux is frozen into the plasma, since if the field is made stronger, the field lines squeeze together such that the density of field lines per area increases proportional to the field strength. As shown in Fig.3.6, the particle orbit area contracts in inverse proportion to the field strength so that after a compression of field, the particle orbit links the same number of field lines as before the compression.

3. Hamiltonian point of view (cylindrical geometry with azimuthal symmetry)- Define a cylindrical coordinate system (r, θ, z) with z axis along the axis of rotation of the gyrating particle. Since $B_z = r^{-1}\partial(rA_\theta)/\partial r$ the vector potential is $A_\theta = rB_z/2$. The velocity vector is $\mathbf{v} = \dot{r}\hat{r} + r\dot{\theta}\hat{\theta} + \dot{z}\hat{z}$ and the Lagrangian is

$$L = \frac{m}{2} (\dot{r}^2 + r^2\dot{\theta}^2 + \dot{z}^2) + qr\dot{\theta}A_\theta - q\phi \quad (3.104)$$

so that the canonical angular momentum is

$$P_\theta = mr^2\dot{\theta} + qrA_\theta = mr^2\dot{\theta} + qr^2B_z/2. \quad (3.105)$$

Since particles are diamagnetic, $\dot{\theta} = -\omega_c$. Because of the azimuthal symmetry, P_θ will be a constant of the motion and so

$$const. = P_\theta = -mr^2\omega_c + qr^2B/2 = -\frac{mv_{\dot{\theta}}^2}{2\omega_c} = -\frac{m}{q}\mu. \quad (3.106)$$

This shows that constancy of canonical angular momentum is equivalent to μ conservation. It is important to realize that constancy of angular momentum due to perfect axisymmetry is a much more restrictive assumption than the slowness assumption used for adiabatic invariance.

4. Adiabatic gas law- The pressure associated with gyrating particles has dimensionality $N = 2$, i.e., $P = (m/2) \int \mathbf{v}' \cdot \mathbf{v}' f d^2v$ where $\mathbf{v}' = v_x\hat{x} + v_y\hat{y}$ and the $x - y$ plane is the plane of the gyration. Also the density for a two dimensional system has units of particles/area, i.e. $n \sim 1/A$. Hence, the pressure will scale as $P \sim v_{T\perp}^2/A$. Since $\gamma = (N + 2)/N = 2$, the adiabatic law, Eq.(2.37), gives

$$const. \sim \frac{P}{n^2} \sim \frac{v_{T\perp}^2}{A} A^2; \quad (3.107)$$

but from the flux conservation property of orbits $A \sim 1/B$ so Eq.(3.107) becomes

$$\frac{P}{n^2} \sim \frac{v_{T\perp}^2}{B} \quad (3.108)$$

which is again proportional to μ since $v_{T\perp}^2$ is proportional to the mean perpendicular thermal energy, i.e., the average of the gyrational energies of the individual particles making up the fluid.

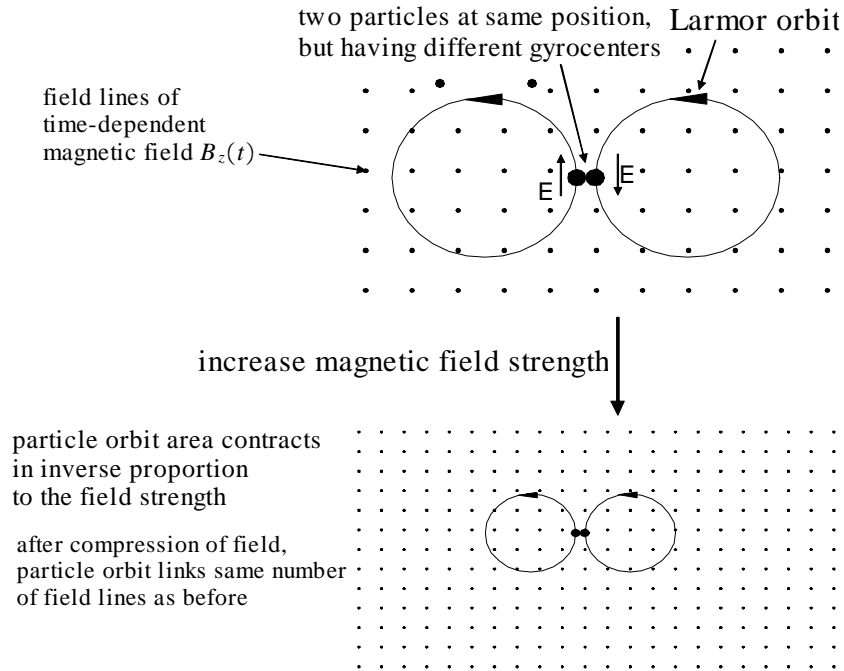


Figure 3.6: Illustration showing how conservation of flux linked by an orbit is equivalent to frozen-in field; also increasing magnetic field results in magnetic compression.

3.5.5 Magnetic mirrors- a consequence of μ conservation

Consider a charged particle moving in a static, but spatially nonuniform magnetic field. The non-uniformity is such that the field strength varies in the direction of the field line so that $\partial B/\partial s \neq 0$ where s is the distance along a field line. Such a field cannot be straight because if it were and so had the form $\mathbf{B} = B_z(z)\hat{z}$, it would necessarily have a non-zero divergence, i.e., it would have $\nabla \cdot \mathbf{B} = \partial B_z/\partial z \neq 0$. Because magnetic fields must have zero divergence there must be another component besides B_z and this other component must be spatially non-uniform also in order to contribute to the divergence. Hence the field must be curved if the field strength varies along the direction of the field.

This curvature is easy to see by sketching field lines, as shown in Fig.3.7. The density of field lines is proportional to the strength of the magnetic field and so a gradient of field strength along the field means that the field lines squeeze together as the field becomes stronger. Because magnetic field lines have zero divergence they are endless and so must bend as they squeeze together. This means that if $\partial B_z/\partial z \neq 0$ there must also be a field

transverse to the initial direction of the magnetic field, i.e., a field in the x or y directions. In a cylindrically symmetric system, this transverse field must be a radial field as indicated by the vector decomposition $\mathbf{B} = B_z \hat{z} + B_r \hat{r}$ in Fig.3.7.

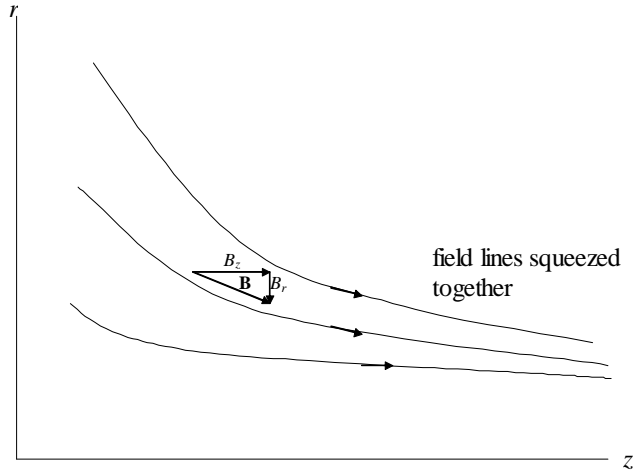


Figure 3.7: Field lines squeezing together when \mathbf{B} has a gradient. B field is stronger on the right than on the left because density of field lines is larger on the right.

The magnetic field is assumed to be static so that $\nabla \times \mathbf{E} = 0$ in which case $\mathbf{E} = -\nabla\phi$ and Eq.(3.92) can be written as

$$m \frac{dv_{\parallel}}{dt} = -q \frac{\partial \phi}{\partial s} - \mu \frac{\partial B}{\partial s}. \quad (3.109)$$

Multiplying Eq.(3.109) by v_{\parallel} gives

$$\frac{d}{dt} \left[\frac{mv_{\parallel}^2}{2} + q\phi + \mu B \right] = 0, \quad (3.110)$$

assuming that the electrostatic potential is also constant in time. Time integration gives

$$\frac{mv_{\parallel}^2}{2} + q\phi(s) + \mu B(s) = \text{const}. \quad (3.111)$$

Thus, $\mu B(s)$ acts as an effective potential energy since it adds to the electrostatic potential energy $q\phi(s)$. This property has the consequence that if $B(s)$ has a minimum with respect to s as shown in Fig.3.8, then μB acts as an effective potential well which can trap particles. A magnetic trap of this sort can be produced by two axially separated coaxial coils. On each field line $B(s)$ has at locations s_1 and s_2 maxima near the coils, a minimum at location s_0

between the coils, and $B(s)$ tends to zero as $s \rightarrow \pm\infty$. To focus attention on magnetic trapping, suppose now that no electrostatic potential exists so Eq.(3.111) reduces to

$$\frac{mv_{\parallel}^2}{2} + \mu B(s) = \text{const.} \quad (3.112)$$

Now consider a particle with parallel velocity $v_{\parallel 0}$ located at the well minimum s_0 at time $t = 0$. Evaluating Eq.(3.112) at $s = 0, t = 0$ and then again when the particle is at some arbitrary position s gives

$$\frac{mv_{\parallel}^2(s)}{2} + \mu B(s) = \frac{mv_{\parallel 0}^2}{2} + \mu B(s_0) = \frac{m(v_{\parallel 0}^2 + v_{\perp 0}^2)}{2} = W_0 \quad (3.113)$$

where W_0 is the particle's total kinetic energy at $t = 0$. Solving Eq.(3.113) for $v_{\parallel}(s)$ gives

$$v_{\parallel}(s) = \pm \sqrt{\frac{2}{m} [W_0 - \mu B(s)]}. \quad (3.114)$$

If $\mu B(s) = W_0$ at some position s , then $v_{\parallel}(s)$ must vanish at this position in which case the particle must reverse its direction of motion just like a pendulum reversing direction when its velocity goes through zero. This velocity reversal corresponds to a reflection of the particle and so this configuration is called a magnetic *mirror*. A particle can be trapped between two magnetic mirrors; such a configuration is called a magnetic trap or a magnetic well.

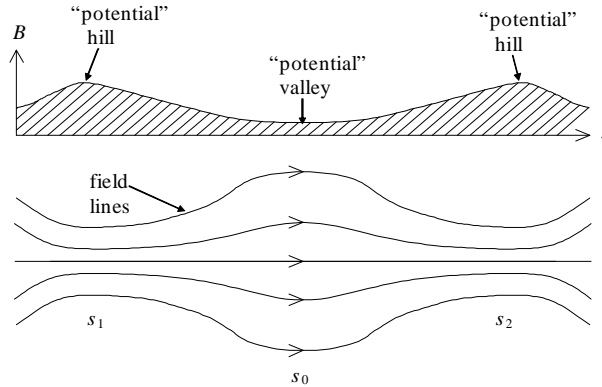


Figure 3.8: Magnetic mirror

If $W_0 > \mu B_{\max}$ where B_{\max} is the magnitude at $s_{1,2}$ then the velocity does not go to zero at the maximum amplitude of the mirror field. In this case the particle does not reflect, but instead escapes over the peak of the $\mu B(s)$ potential hill and travels out to infinity. Thus, there are two classes of particles:

1. trapped particles – these have $W_0 < \mu B_{\max}$ and bounce back and forth between the mirrors of the magnetic well,
2. untrapped (or passing) particles – these have $W_0 > \mu B_{\max}$ and are retarded at the potential hills but not reflected.

Since $\mu = mv_{\perp 0}^2/2B_{\min}$ and $W_0 = mv_0^2/2$, the criterion for trapping can be written as

$$\frac{B_{\min}}{B_{\max}} < \frac{v_{\perp 0}^2}{v_0^2}. \quad (3.115)$$

Let us define θ as the angle the velocity vector makes with respect to the magnetic field at s_0 , i.e., $\sin \theta = v_{\perp 0}/v_0$ and also define

$$\theta_{trap} = \sin^{-1} \sqrt{\frac{B_{\min}}{B_{\max}}}. \quad (3.116)$$

Thus, as shown in Fig.3.9 all particles with $\theta > \theta_{trap}$ are trapped, while all particles with $\theta < \theta_{trap}$ are untrapped. Suppose at $t = 0$ the particle velocity distribution at s_0 is isotropic. After a long time interval long enough for all untrapped particles to have escaped the trap, there will be no particles in the $\theta < \theta_{trap}$ region of velocity space. The velocity distribution will thus be zero for $\theta < \theta_{trap}$; such a distribution function is called a *loss-cone* distribution function.

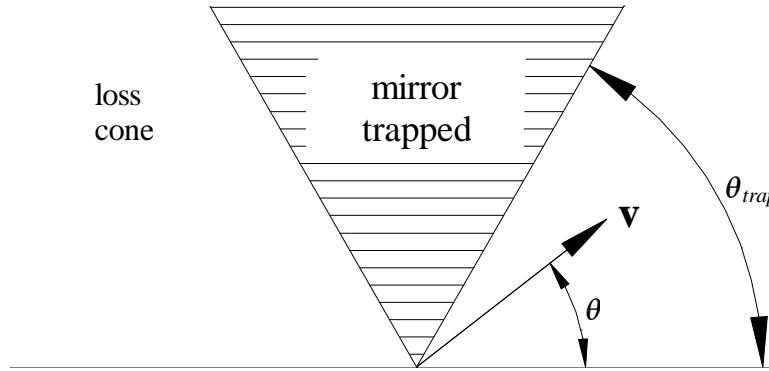


Figure 3.9: Loss-cone velocity distribution. Particles with velocity angle $\theta > \theta_{trap}$ are mirror trapped, others are lost.

3.5.6 \mathcal{J} , the Second Adiabatic Invariant

Trapped particles have periodic motion in the magnetic well, and so applying the concept

of adiabatic invariance presented in Sec.3.4.1, the quantity

$$\mathcal{J} = \oint P_{\parallel} ds = \oint (mv_{\parallel} + qA_{\parallel}) ds \quad (3.117)$$

will be an invariant if

1. any time dependence of the well shape is slow compared to the bounce frequency of the trapped particle,
2. any spatial inhomogeneities of the well magnetic field are so gradual that the particle's bounce trajectory changes by only a small amount from one bounce to the next.

To determine the circumstances where $A_{\parallel} \neq 0$, we use Coulomb gauge (i.e., assume $\nabla \cdot \mathbf{A} = 0$) and at any given location define a local Cartesian coordinate system with z axis parallel to the local field. From Ampere's law it is seen that

$$[\nabla \times (\nabla \times \mathbf{A})]_{\mathbf{z}} = -\nabla^2 A_z = \mu_0 J_z \quad (3.118)$$

so A_z is finite only if there is a *current parallel to the magnetic field*. Because J_z acts as the source term in a Poisson-like partial differential equation for A_z , the parallel current need not be at the same location as A_z . If there are no currents parallel to the magnetic field anywhere then $A_{\parallel} = 0$, and in this case the second adiabatic invariant reduces to

$$\mathcal{J} = m \oint v_{\parallel} ds. \quad (3.119)$$

Having a current flow along the magnetic field corresponds to a more complicated magnetic topology. The axial current produces an associated azimuthal magnetic field which links the axial magnetic field resulting in a helical twist. This more complicated situation of finite magnetic helicity will be discussed in a later chapter.

3.5.7 Consequences of \mathcal{J} -invariance

Just as μ invariance was related to the perpendicular CGL adiabatic invariant discussed in Sec.(2.101), \mathcal{J} -invariance is closely related to the parallel CGL adiabatic invariant also discussed in Sec.(2.101). To see this relation, recall that density in a one dimensional system has dimensions of particles per unit length, i.e., $n_{1D} \sim 1/L$, and pressure in a one dimensional system has dimensions of kinetic energy per unit length, i.e., $P_{1D} \sim v_{\parallel}^2/L$. For parallel motion the number of dimensions is $N = 1$ so that $\gamma = (N + 2)/N = 3$ and the fluid adiabatic relation is

$$const. \sim \frac{P_{1D}}{n_{1D}^3} \sim \frac{v_{\parallel}^2/L}{L^{-3}} \sim (v_{\parallel}L)^2 \quad (3.120)$$

which is a simplified form of Eq.(3.119) since Eq.(3.119) has the scaling $\mathcal{J} \sim v_{\parallel}L = const.$

\mathcal{J} -invariance combined with mirror trapping/detrapping is the basis of an acceleration mechanism proposed by Fermi (1954) as a means for accelerating cosmic ray particles to ultra-relativistic velocities. The Fermi mechanism works as follows: Consider a particle initially trapped in a magnetic mirror. This particle has an initial angle in velocity space $\theta > \theta_{trap}$; both θ and θ_{trap} are measured when the particle is at the mirror minimum. Now suppose the distance between the magnetic mirrors is slowly reduced so that the bounce

distance L of the mirror-trapped particle slowly decreases. This would typically occur by reducing the axial separation between the coils producing the magnetic mirror field. Because $\mathcal{J} \sim v_{\parallel} L$ is invariant, the particle's parallel velocity increases on each successive bounce as L slowly decreases. This steady increase in v_{\parallel} means that the velocity angle θ decreases. Eventually, θ becomes smaller than θ_{trap} whereupon the particle becomes detrapped and escapes from one end of the mirror with a large parallel velocity. This mechanism provides a slow pumping to very high energy, followed by a sudden and automatic ejection of the energetic particle.

3.5.8 The third adiabatic invariant

Consider a particle bouncing back and forth in either of the two geometries shown in Fig.3.10. In Fig.3.10(a), the magnetic field is produced by a single magnetic dipole and the field lines always have convex curvature, i.e. the radius of curvature is always on the inside of the field lines. The field decreases in magnitude with increasing distance from the dipole.

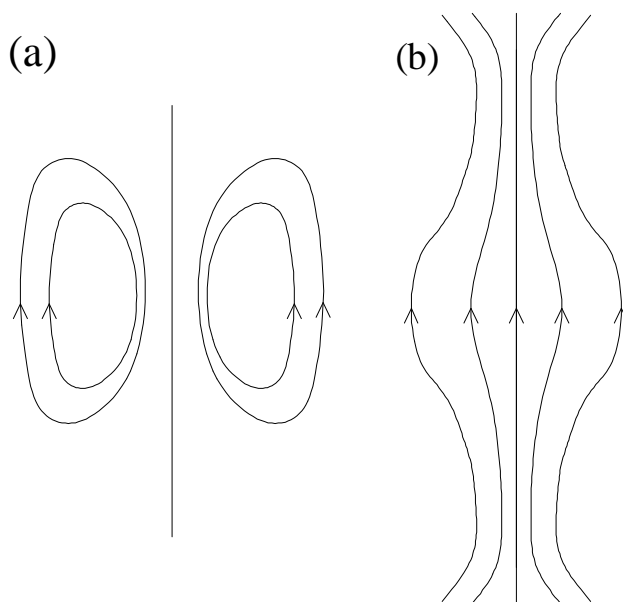


Figure 3.10: Magnetic field lines relevant to discussion of third adiabatic invariant: (a) field lines always have same curvature (dipole field), (b) field lines have both concave and convex curvature (mirror field).

In Fig.3.10(b) the field is produced by two coils and has convex curvature near the mirror minimum and concave curvature in the vicinity of the coils. On defining a cylindrical

coordinate system (r, θ, z) with z axis coaxial with the coils, it is seen that in the region between the two coils where the field bulges out, the field strength is a decreasing function of r , i.e. $\partial B/\partial r < 0$, whereas in the plane of each coil the opposite is true. Thus, in the mirror minimum, both the centrifugal and grad B forces are radially outward, whereas the opposite is true near the coils.

In both Figs. 3.10(a) and (b) a particle moving along the field line can be mirror-trapped because in both cases the field has a minimum flanked by two maxima. However, for Fig.3.10(a), the particle will have grad B and curvature drifts always in the same azimuthal sense, whereas for Fig.3.10(b) the azimuthal direction of these drifts will depend on whether the particle is in a region of concave or convex curvature. Thus, in addition to the mirror bouncing motion, much slower curvature and grad B drifts also exist, directed along the field binormal (i.e. the direction orthogonal to both the field and its radius of curvature). These higher-order drifts may alternate sign during the mirror bouncing. The binormally directed displacement made by a particle during its i^{th} complete period τ of mirror bouncing is

$$\delta \mathbf{r}_j = \int_0^\tau \mathbf{v} dt \quad (3.121)$$

where τ is the mirror bounce period and \mathbf{v} is the sum of the curvature and grad B drifts experienced in the course of a mirror bounce. This displacement is due to the cumulative effect of the curvature and grad B drifts experienced during one complete period of bouncing between the magnetic mirrors. The average velocity associated with this slow drifting may be defined as

$$\langle \mathbf{v} \rangle = \frac{1}{\tau} \int_0^\tau \mathbf{v} dt. \quad (3.122)$$

Let us calculate the action associated with a sequence of $\delta \mathbf{r}_j$. This action is

$$S = \sum_j [m \langle \mathbf{v} \rangle + q \mathbf{A}]_j \cdot \delta \mathbf{r}_j \quad (3.123)$$

where the quantity in square brackets is evaluated on the line segment $\delta \mathbf{r}_j$. If the $\delta \mathbf{r}_j$ are small then this can be converted into an action 'integral' for the path traced out by the $\delta \mathbf{r}_j$. If the $\delta \mathbf{r}_j$ are sufficiently small to behave as differentials, then we may write them as $d\mathbf{r}_{\text{bounce}}$ and express the summation as an action integral

$$S = \int [m \langle \mathbf{v} \rangle + q \mathbf{A}] \cdot d\mathbf{r}_{\text{bounce}} \quad (3.124)$$

where it must be remembered that $\langle \mathbf{v} \rangle$ is the *bounce-averaged* velocity. The quantity $m \langle \mathbf{v} \rangle + q \mathbf{A}$ is just the canonical momentum associated with the effective motion along the sequence of line segments $\delta \mathbf{r}_j$. The vector $\mathbf{r}_{\text{bounce}}$ is a vector pointing from the origin to the particle's location at successive bounces and so is the generalized coordinate associated with the bounce averaged velocity. If the motion resulting from $\langle \mathbf{v} \rangle$ is periodic, we expect S to be an adiabatic invariant. The first term in Eq.(3.124) will be of the order of $mv_{\text{drift}} 2\pi r$ where r is the radius of the trajectory described by the $\delta \mathbf{r}_j$. The second term is just $q\Phi$ where Φ is the magnetic flux enclosed by the trajectory. Let us compare the ratio of these two terms

$$\frac{\int m \langle \mathbf{v} \rangle \cdot d\mathbf{r}}{\int q \mathbf{A} \cdot d\mathbf{r}} \sim \frac{mv_{\text{drift}} 2\pi r}{qB\pi r^2} \sim \frac{v_{\text{drift}}}{\omega_c r} \sim \frac{r_L^2}{r^2} \quad (3.125)$$

where we have used $v_{\nabla B} \sim v_c \sim v_{\perp}^2 / \omega_c r \sim \omega_c r_L^2 / r$. Thus, if the Larmor radius is much smaller than the characteristic scale length of the field, the magnetic flux term dominates the action integral and adiabatic invariance corresponds to the particle *staying on a constant flux surface* as its orbit evolves following the various curvature and grad B drifts. This third adiabatic invariant is much more fragile than \mathcal{J} , which in turn was more fragile than μ , because the analysis here is based on the rather strong assumption that the curvature and grad B drifts are small enough for the $\delta \mathbf{r}_j$ to trace out a nearly periodic orbit.

3.6 Relation of Drift Equations to the Double Adiabatic MHD Equations

The derivation of the MHD Ohm's law involved dropping the Hall term (see p. 48) and the basis for dropping this term was assuming that $\omega \ll \omega_{ci}$ where ω is the characteristic rate of change of the electromagnetic field. The derivation of the single particle drift equations involved essentially the same assumption (i.e., the motion was slow compared to $\omega_{c\sigma}$). Thus, if the characteristic rate of change of the electromagnetic field is slow compared to ω_{ci} both the MHD and the single particle drift equations ought to be equally valid descriptions of the plasma dynamics. If so, then there also ought to be some sort of a correspondence relation between these two points of view. Some evidence supporting this hypothesis was the observation that the single particle adiabatic invariants μ and \mathcal{J} were respectively related to the perpendicular and parallel double adiabatic MHD equations. It thus seems reasonable to expect additional connections between the drift equations and the double adiabatic MHD equations.

In fact, an approximate derivation of the double adiabatic MHD equations can be obtained by summing the currents associated with the various particle drifts — providing one additional effect, *diamagnetic current*, is added to this sum. Diamagnetic current is a peculiar concept because it is a consequence of the macroscopic phenomenon of pressure gradients and so has no meaning in the context of a single particle description.

In order to establish this microscopic-macroscopic relationship we begin by recalling from electromagnetic theory² that a magnetic material with density \mathbf{M} of magnetic dipole moments per unit volume has an associated magnetization current

$$\mathbf{J}_M = \nabla \times \mathbf{M}. \quad (3.126)$$

The magnitude of the magnetic moment of a charged particle in a magnetic field was shown in Sec.3.5.4 to be μ . The magnetic moment of a magnetic dipole is a vector pointing in the direction of the magnetic field produced by the dipole. The vector magnetic moment of a charged particle gyrating in a magnetic field is $\mathbf{m} = -\mu \hat{B}$ where the minus sign corresponds to cyclotron motion being diamagnetic, i.e., the magnetic field resulting from cyclotron rotation opposes the original field in which the particle is rotating. For example, an individual ion placed in a magnetic field $\mathbf{B} = B \hat{z}$ rotates in the negative θ direction, and so the current associated with the ion motion creates a magnetic field pointing in the $-\hat{z}$ direction inside the ion orbit.

²For example, see p. 192 of (Jackson 1998).

Suppose there exists a large number or ensemble of particles with density n_σ and mean magnetic moment $\bar{\mu}_\sigma$. The density of magnetic moments, or magnetization density, of this ensemble is

$$\mathbf{M} = - \sum_{\sigma} n_{\sigma} \bar{\mu}_{\sigma} \hat{B} = - \sum_{\sigma} n_{\sigma} \left\langle \frac{m_{\sigma} v_{\perp}^2}{2B} \right\rangle \hat{B} = - \frac{P_{\perp} \hat{B}}{B} \quad (3.127)$$

where $\langle \rangle$ denotes averaging over the velocity distribution and Eq.(2.26) has been used. Inserting Eq.(3.127) into Eq.(3.126) shows that this ensemble of charged particles in a magnetic field has a *diamagnetic current*

$$\mathbf{J}_M = -\nabla \times \left(\frac{P_{\perp} \hat{B}}{B} \right). \quad (3.128)$$

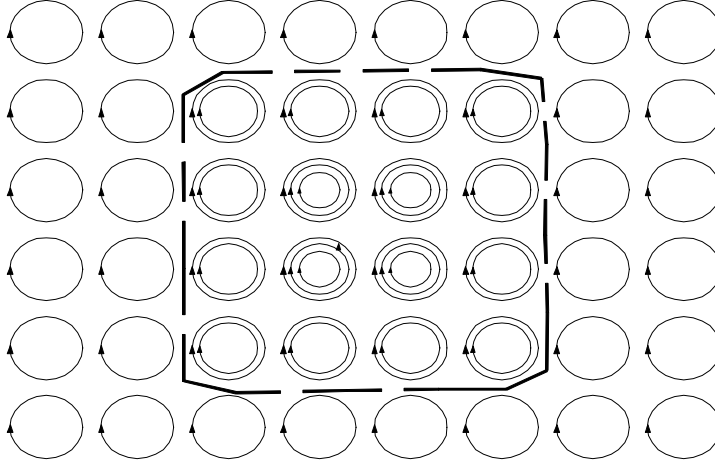


Figure 3.11: Gradient of magnetized particles gives apparent current as observed on dashed line.

Figure 3.11 shows the physical origin of \mathbf{J}_M . Here, a collection of ions all rotate clockwise in a magnetic field pointing out of the page. The azimuthally directed current on the dashed curve is the sum of contributions from (i) particles with guiding centers located one Larmor radius *inside* the dashed curve and (ii) particles with guiding centers located one Larmor radius *outside* the dashed curve. From the point of view of an observer located on the dashed curve, the inside particles [group (i)] constitute a clockwise current, whereas the outside [group (ii)] particles constitute a counterclockwise current. If there are unequal numbers of inside and outside particles (indicated here by concentric circles inside

the dashed curve), then the two opposing currents do not cancel and a net macroscopic current appears to flow around the dashed curve, even though *no* actual particles flow around the dashed curve. Inequality of the numbers of inside and outside particles corresponds to a density gradient and so we see that a radial density gradient of gyrating particles gives a net macroscopic azimuthal current. Similarly, if there is a radial temperature gradient, the velocities of the inner and outer groups differ, resulting again in an apparent macroscopic azimuthal current. The combination of density and temperature gradients is such that the net macroscopic current depends on the pressure gradient as given by Eq.(3.128).

Taking diamagnetic current into account is critical for establishing a correspondence between the single particle drifts and the MHD equations, and having recognized this, we are now in a position to derive this correspondence. In order for the derivation to be tractable yet non-trivial, it will be assumed that the magnetic field is time-independent, but the electric field will be allowed to depend on time. It is also assumed that the *dominant* cross-field particle motion is the $\mathbf{v}_E = \mathbf{E} \times \mathbf{B}/B^2$ drift; this assumption is consistent with the hierarchy of particle drifts (i.e., polarization drift is a higher-order correction to \mathbf{v}_E).

Because both species have the same \mathbf{v}_E , no macroscopic current results from \mathbf{v}_E , and so all cross-field currents must result from the other, smaller drifts, namely $\mathbf{v}_{\nabla B}$, \mathbf{v}_c , and \mathbf{v}_p . Let us now add the magnetization current to the currents associated with $\mathbf{v}_{\nabla B}$, \mathbf{v}_c , and \mathbf{v}_p to obtain the total macroscopic current

$$\mathbf{J}_{\text{total}} = \mathbf{J}_M + \mathbf{J}_{\nabla B} + \mathbf{J}_c + \mathbf{J}_p = \mathbf{J}_M + \sum_{\sigma} n_{\sigma} q_{\sigma} (\mathbf{u}_{\nabla B, \sigma} + \mathbf{u}_{c, \sigma} + \mathbf{u}_{p, \sigma}) \quad (3.129)$$

where $\mathbf{J}_{\nabla B}$, \mathbf{J}_c , \mathbf{J}_p are currents due to grad B , curvature, and polarization drifts respectively and $\mathbf{u}_{\nabla B, \sigma}$, $\mathbf{u}_{c, \sigma}$ and $\mathbf{u}_{p, \sigma}$ are the mean (i.e., fluid) velocities associated with these drifts. These currents are explicitly:

1. grad B current

$$\begin{aligned} \mathbf{J}_{\nabla B} &= \sum_{\sigma} n_{\sigma} q_{\sigma} \mathbf{u}_{\nabla B, \sigma} \\ &= - \sum_{\sigma} \frac{m_{\sigma} n_{\sigma} q_{\sigma} \langle v_{\perp \sigma}^2 \rangle}{2B} \frac{\nabla B \times \mathbf{B}}{q_{\sigma} B^2} = -P_{\perp} \frac{\nabla B \times \mathbf{B}}{B^3} \end{aligned} \quad (3.130)$$

2. curvature current

$$\begin{aligned} \mathbf{J}_c &= \sum_{\sigma} n_{\sigma} q_{\sigma} \mathbf{u}_{c, \sigma} \\ &= - \sum_{\sigma} n_{\sigma} q_{\sigma} m_{\sigma} \langle v_{\parallel \sigma}^2 \rangle \frac{\hat{B} \cdot \nabla \hat{B} \times \mathbf{B}}{q_{\sigma} B^2} = -P_{\parallel} \frac{\hat{B} \cdot \nabla \hat{B} \times \mathbf{B}}{B^2} \end{aligned} \quad (3.131)$$

3. polarization current

$$\mathbf{J}_p = \sum_{\sigma} n_{\sigma} q_{\sigma} \mathbf{u}_{p, \sigma} = \sum_{\sigma} n_{\sigma} q_{\sigma} \left(\frac{m_{\sigma}}{q_{\sigma} B^2} \frac{d\mathbf{E}_{\perp}}{dt} \right) = \frac{\rho}{B^2} \frac{d\mathbf{E}_{\perp}}{dt}. \quad (3.132)$$

Because the magnetic field was assumed to be constant, the time derivative of \mathbf{v}_E is the only contributor to the polarization drift current.

The total magnetic force is

$$\begin{aligned} \mathbf{J}_{total} \times \mathbf{B} &= (\mathbf{J}_M + \mathbf{J}_{\nabla B} + \mathbf{J}_c + \mathbf{J}_P) \times \mathbf{B} \\ &= \left[\begin{array}{l} -\nabla \times \left(\frac{P_{\perp} \hat{B}}{B} \right) - P_{\perp} \frac{\nabla B \times \mathbf{B}}{B^3} \\ -P_{\parallel} \frac{\hat{B} \cdot \nabla \hat{B} \times \mathbf{B}}{B^2} + \frac{\rho}{B^2} \frac{d\mathbf{E}}{dt} \end{array} \right] \times \mathbf{B}. \end{aligned} \quad (3.133)$$

The grad B current cancels part of the magnetization current as follows:

$$\begin{aligned} \nabla \times \left(\frac{P_{\perp} \hat{B}}{B} \right) + P_{\perp} \frac{\nabla B \times \mathbf{B}}{B^3} &= \left[\nabla \left(\frac{1}{B} \right) \times P_{\perp} \hat{B} + \frac{1}{B} \nabla \times (P_{\perp} \hat{B}) \right] \\ &\quad + P_{\perp} \frac{\nabla B \times \mathbf{B}}{B^3} \\ &= \frac{1}{B} \nabla \times (P_{\perp} \hat{B}) = \frac{P_{\perp}}{B} \nabla \times \hat{B} + \frac{\nabla P_{\perp} \times \hat{B}}{B} \end{aligned} \quad (3.134)$$

so that

$$\mathbf{J}_{total} \times \mathbf{B} = - \left[P_{\perp} \nabla \times \hat{B} + \nabla P_{\perp} \times \hat{B} + P_{\parallel} \hat{B} \cdot \nabla \hat{B} \times \hat{B} - \frac{\rho}{B} \frac{d\mathbf{E}}{dt} \right] \times \hat{B}. \quad (3.135)$$

The first term can be recast using the vector identity

$$\nabla \left(\frac{\hat{B} \cdot \hat{B}}{2} \right) = \mathbf{0} = \hat{B} \cdot \nabla \hat{B} + \hat{B} \times \nabla \times \hat{B} \quad (3.136)$$

while the electric field can be replaced using $\mathbf{E} = -\mathbf{U} \times \mathbf{B}$ to give

$$\mathbf{J}_{total} \times \mathbf{B} = - (P_{\perp} - P_{\parallel}) \hat{B} \cdot \nabla \hat{B} + \nabla_{\perp} P_{\perp} - \frac{\rho}{B} \frac{d(\mathbf{U} \times \mathbf{B})}{dt} \times \hat{B}. \quad (3.137)$$

Here the relation $[\hat{B} \cdot \nabla \hat{B}]_{\perp} = \hat{B} \cdot \nabla \hat{B}$ has been used; this relation follows from Eq. (3.136). Finally, it is observed that

$$[\nabla \cdot (\hat{B} \hat{B})]_{\perp} = [(\nabla \cdot \hat{B}) \hat{B} + \hat{B} \cdot \nabla \hat{B}]_{\perp} = \hat{B} \cdot \nabla \hat{B} \quad (3.138)$$

so

$$(P_{\perp} - P_{\parallel}) \hat{B} \cdot \nabla \hat{B} = (P_{\perp} - P_{\parallel}) [\nabla \cdot (\hat{B} \hat{B})]_{\perp} = [\nabla \cdot \{(P_{\perp} - P_{\parallel}) \hat{B} \hat{B}\}]_{\perp}. \quad (3.139)$$

Furthermore,

$$\frac{\rho}{B} \frac{d(\mathbf{U} \times \mathbf{B})}{dt} \times \hat{B} \simeq - \left[\rho \frac{d\mathbf{U}}{dt} \right]_{\perp} \quad (3.140)$$

since it has been assumed that the magnetic field is time-independent. Inserting these last two results in Eq.(3.137) gives

$$\mathbf{J}_{total} \times \mathbf{B} = [\nabla \cdot \{(P_{\perp} - P_{\parallel}) \hat{B} \hat{B}\}]_{\perp} + \nabla_{\perp} P_{\perp} + \left[\rho \frac{d\mathbf{U}}{dt} \right]_{\perp} \quad (3.141)$$

or

$$\left[\rho \frac{d\mathbf{U}}{dt} \right]_{\perp} = \left[\mathbf{J}_{total} \times \mathbf{B} - \nabla \cdot \left\{ P_{\perp} \overleftarrow{\mathbf{I}} + (P_{\perp} - P_{\parallel}) \hat{B}\hat{B} \right\} \right]_{\perp} \quad (3.142)$$

which is just the perpendicular component of the double adiabatic MHD equation of motion. This demonstrates that if diamagnetic current is taken into account, the drift equations for phenomena with characteristic frequencies ω much smaller than ω_{ci} and the double adiabatic MHD equations are equivalent descriptions of plasma dynamics. This analysis also shows that one has to be extremely careful when invoking single particle concepts to explain macroscopic behavior, because if diamagnetic effects are omitted, erroneous conclusions can result.

The reason for the name polarization current can now be addressed by comparing this current to the current flowing through a parallel plate capacitor with dielectric ε . The capacitance of the parallel plate capacitor is $C = \varepsilon A/d$ where A is the cross-sectional area of the capacitor plates and w is the gap between the plates. The charge on the capacitor is $Q = CV$ where V is the voltage across the capacitor plates. The current through the capacitor is $I = dQ/dt$ so

$$I = C \frac{dV}{dt} = \frac{\varepsilon A}{d} \frac{dV}{dt}. \quad (3.143)$$

However the electric field between the plates is $E = V/d$ and the current density is $J = I/A$ so this can be expressed as

$$J = \varepsilon \frac{dE}{dt} \quad (3.144)$$

which gives the alternating current density in a medium with dielectric ε . If this is compared to the polarization current

$$\mathbf{J}_p = \frac{\rho}{B^2} \frac{d\mathbf{E}_{\perp}}{dt} \quad (3.145)$$

it is seen that the plasma acts like a dielectric medium in the direction perpendicular to the magnetic field and has an effective dielectric constant given by ρ/B^2 .

3.7 Non-adiabatic motion in symmetric geometry

Adiabatic behavior occurs when temporal or spatial changes in the electromagnetic field from one cyclical orbit to the next are sufficiently gradual to be effectively continuous and differentiable (i.e., analytic). Thus, adiabatic behavior corresponds to situations where variations of the electromagnetic field are sufficiently gradual to be characterized by the techniques of calculus (differentials, limits, Taylor expansions, etc.).

Non-adiabatic particle motion occurs when this is not so. It is therefore no surprise that it is usually not possible to construct analytic descriptions of non-adiabatic particle motion. However, there exist certain special situations where non-adiabatic motion can be described analytically. Using these special cases as a guide, it is possible to develop an understanding for what happens when motion is non-adiabatic.

One special situation is where the electromagnetic field is *geometrically symmetric* with respect to some coordinate Q_j in which case the symmetry makes it possible to develop analytic descriptions of non-adiabatic motion. This is because symmetry in Q_j causes the canonical momentum P_j to be an exact constant of the motion. The critical feature is that P_j remains constant no matter how drastically the field changes in time or space because

Lagrange's equation $\dot{P}_j = -\partial L/\partial Q_j$ has no limitations on the rate at which changes can occur. In effect, being geometrically symmetric trumps being non-analytic. The absolute invariance of P_j when $\partial L/\partial Q_j = 0$ reduces the number of equations and allows a partial or sometimes even a complete solution of the motion. Solutions to symmetric problems give valuable insight regarding the more general situation of being both non-adiabatic and asymmetric.

Two closed related examples of non-adiabatic particle motion will now be analyzed: (i) sudden temporal and (ii) sudden spatial reversal of the polarity of an azimuthally symmetric magnetic field having no azimuthal component. The most general form of such a field can be written in cylindrical coordinates (r, θ, z) as

$$\mathbf{B} = \frac{1}{2\pi} \nabla\psi(r, z, t) \times \nabla\theta; \quad (3.146)$$

a field of this form is called poloidal. Rather than using $\hat{\theta}$ explicitly, the form $\nabla\theta$ has been used because $\nabla\theta$ is better suited for use with the various identities of vector calculus (e.g., $\nabla \times \nabla\theta = 0$) and leads to greater algebraic clarity. The relationship between $\nabla\theta$ and $\hat{\theta}$ is seen by simply taking the gradient:

$$\nabla\theta = \left(\hat{r} \frac{\partial}{\partial r} + \frac{\hat{\theta}}{r} \frac{\partial}{\partial \theta} + \hat{z} \frac{\partial}{\partial z} \right) \theta = \frac{\hat{\theta}}{r}. \quad (3.147)$$

Equation(3.146) automatically satisfies $\nabla \cdot \mathbf{B} = 0$ [by virtue of the vector identity $\nabla \cdot (\mathbf{G} \times \mathbf{H}) = \mathbf{H} \cdot \nabla \times \mathbf{G} - \mathbf{G} \cdot \nabla \times \mathbf{H}$], has no θ component, and is otherwise arbitrary since ψ is arbitrary. As shown in Fig.3.12, the magnetic flux linking a circle of radius r with center at axial position z is

$$\begin{aligned} \int \mathbf{B} \cdot d\mathbf{s} &= \int_0^r 2\pi r dr \hat{z} \cdot \left[\frac{1}{2\pi} \nabla\psi(r, z, t) \times \nabla\theta \right] \\ &= \int_0^r dr \frac{\partial\psi(r, z, t)}{\partial r} = \psi(r, z, t) - \psi(0, z, t). \end{aligned} \quad (3.148)$$

However,

$$B_r(r, z, t) = -\frac{1}{2\pi r} \frac{\partial\psi}{\partial z} \quad (3.149)$$

and since $\nabla \cdot \mathbf{B} = 0$, B_r must vanish at $r = 0$, and so $\partial\psi/\partial z = 0$ on the symmetry axis $r = 0$.

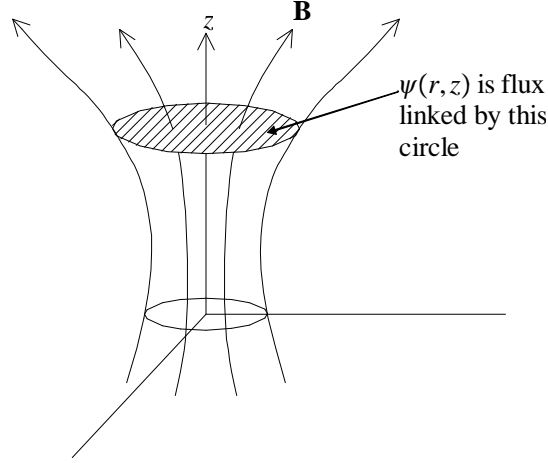


Figure 3.12: Azimuthally symmetric flux surface

Thus ψ is constant along the symmetry axis $r = 0$; for convenience we choose this constant to be zero. Hence, $\psi(r, z, t)$ is precisely the magnetic flux enclosed by a circle of radius r at axial location z . We can also use the vector potential \mathbf{A} to calculate the magnetic flux through the same circle and obtain

$$\int \mathbf{B} \cdot d\mathbf{s} = \int \nabla \times \mathbf{A} \cdot d\mathbf{s} = \oint \mathbf{A} \cdot d\mathbf{l} = \int_0^{2\pi} A_\theta r d\theta = 2\pi r A_\theta. \quad (3.150)$$

This shows that the flux ψ and the vector potential A_θ are related by

$$\psi(r, z, t) = 2\pi r A_\theta. \quad (3.151)$$

No other component of vector potential is required to determine the magnetic field and so we may set $\mathbf{A} = A_\theta(r, z, t)\hat{\theta}$.

The current $\mathbf{J} = \mu_0^{-1} \nabla \times \mathbf{B}$ producing this magnetic field is purely azimuthal as can be seen by considering the r and z components of $\nabla \times \mathbf{B}$. The actual current density is

$$\begin{aligned} J_\theta &= \mu_0^{-1} r \nabla \theta \cdot \nabla \times \mathbf{B} \\ &= \mu_0^{-1} r \nabla \cdot (\mathbf{B} \times \nabla \theta) \\ &= -\frac{r}{2\pi\mu_0} \nabla \cdot \left(\frac{1}{r^2} \nabla \psi \right) \\ &= -\frac{r}{2\pi\mu_0} \left[\frac{\partial}{\partial r} \left(\frac{1}{r^2} \frac{\partial \psi}{\partial r} \right) + \frac{1}{r^2} \frac{\partial^2 \psi}{\partial z^2} \right] \end{aligned} \quad (3.152)$$

a Poisson-like equation. Since no current loops can exist at infinity, the field prescribed by Eq.(3.146) must be produced by a set of coaxial coils having various finite radii r and various finite axial positions z .

The axial magnetic field is

$$B_z = \frac{1}{2\pi r} \frac{\partial \psi}{\partial r}. \quad (3.153)$$

Near $r = 0$, ψ can always be Taylor expanded as

$$\psi(r, z) = 0 + r \frac{\partial \psi(r=0, z)}{\partial r} + \frac{r^2}{2} \frac{\partial^2 \psi(r=0, z)}{\partial r^2} + \dots \quad (3.154)$$

Suppose that $\partial \psi / \partial r$ is non-zero at $r = 0$, i.e., $\psi \sim r$ near $r = 0$. If this were the case, then the first term in the right hand side of the last line of Eq.(3.152) would become infinite and so lead to an infinite current density at $r = 0$. Such a result is non-physical and so we require that the first non-zero term in the Taylor expansion of ψ about $r = 0$ to be the r^2 term.

Every field line that loops through the inside of a current loop also loops back in the reverse direction on the outside, so there is no net magnetic flux at infinity. This means that ψ must vanish at infinity and so as r increases, ψ increases from its value of zero at $r = 0$ to some maximum value ψ_{\max} at $r = r_{\max}$, and then slowly decreases back to zero as $r \rightarrow \infty$. As seen from Eq.(3.153) this behavior corresponds to B_z being positive for $r < r_{\max}$ and negative for $r > r_{\max}$. A contour plot of the $\psi(r, z)$ flux surfaces and a plot of $\psi(r, z = 0)$ versus r is shown in Fig.3.13.

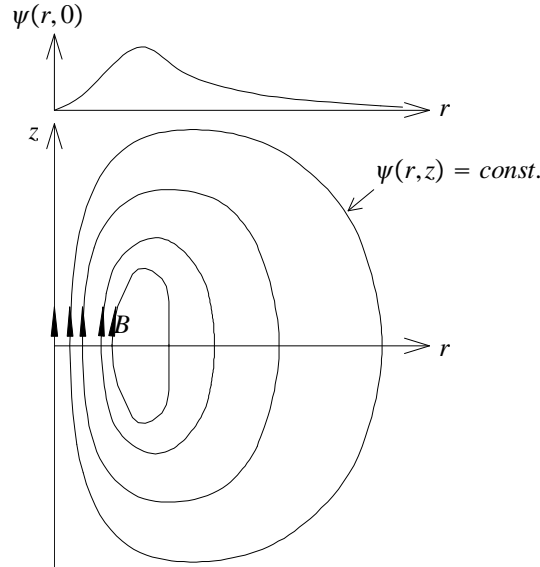


Figure 3.13: Contour plot of flux surfaces

In this cylindrical coordinate system the Lagrangian, Eq.(3.12), has the form

$$L = \frac{m}{2} (\dot{r}^2 + r^2\dot{\theta}^2 + \dot{z}^2) + qr\dot{\theta}A_\theta - q\phi(r, z, t). \quad (3.155)$$

Since θ is an ignorable coordinate, the canonical angular momentum is a constant of the motion, i.e.

$$P_\theta = \frac{\partial L}{\partial \dot{\theta}} = mr^2\dot{\theta} + qrA_\theta = \text{const.} \quad (3.156)$$

or, in terms of flux,

$$P_\theta = mr^2\dot{\theta} + \frac{q}{2\pi}\psi(r, z, t) = \text{const.} \quad (3.157)$$

Thus, the Hamiltonian is

$$\begin{aligned} H &= \frac{m}{2} (\dot{r}^2 + r^2\dot{\theta}^2 + \dot{z}^2) + \phi(r, z, t) \\ &= \frac{m}{2} (\dot{r}^2 + \dot{z}^2) + \frac{(P_\theta - q\psi(r, z, t)/2\pi)^2}{2mr^2} + \phi(r, z, t) \\ &= \frac{m}{2} (\dot{r}^2 + \dot{z}^2) + \chi(r, z, t) \end{aligned} \quad (3.158)$$

where

$$\chi(r, z, t) = \frac{1}{2m} \left[\frac{P_\theta - q\psi(r, z, t)/2\pi}{r} \right]^2 \quad (3.159)$$

is an *effective* potential. For purposes of plotting, the effective potential can be written in a dimensionless form as

$$\frac{\chi(r, z, t)}{\chi_0} = \left(\frac{\frac{2\pi P_\theta}{q\psi_0} - \frac{\psi(r, z, t)}{\psi_0}}{r/L} \right)^2 \quad (3.160)$$

where L is some reference scale length, ψ_0 is some arbitrary reference value for the flux, and $\chi_0 = q\psi_0^2/8\pi^2L^2m$. For simplicity we have set $\phi(r, z, t) = 0$, since this term gives the motion of a particle in a readily understood, two-dimensional electrostatic potential.

Suppose that for times $t < t_1$ the coil currents are constant in which case the associated magnetic field and flux are also constant. Since the Lagrangian does not explicitly depend on time, the energy H is a constant of the motion. Hence there are two constants of the motion, H and P_θ . Consider now a particle located initially on the midplane $z = 0$ with $r < r_{\max}$. The particle motion depends on the sign of $q\psi/P_\theta$ and so we consider each polarity separately.

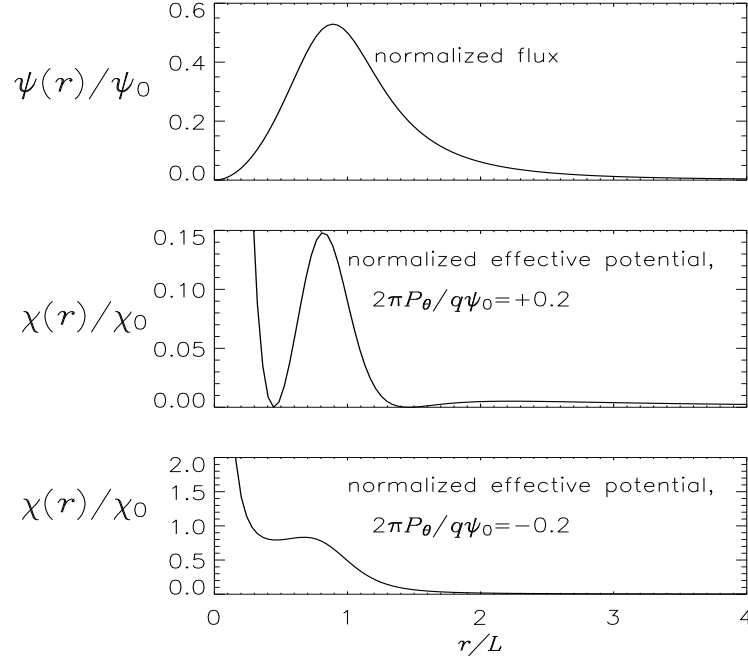


Figure 3.14: Specific example (with z dependence suppressed) showing ψ and χ relationship: top is plot of function $\psi(r)/\psi_0 = (r/L)^2 / (1 + (r/L)^6)$, middle and bottom plots show corresponding normalized effective potential for $2\pi P_\theta/q\psi_0 = +0.2$ and $2\pi P_\theta/q\psi_0 = -0.2$. Both middle and bottom plots have a minimum at $r/L \simeq 0.45$; middle plot also has a minimum at $r/L \simeq 1.4$. The two minima in the middle plot occur when $\chi(r)/\chi_0 = 0$ but the single minimum in the bottom plot occurs at a finite value of $\chi(r)/\chi_0$ indicating that an axis-encircling particle must have finite energy.

1. $q\psi/P_\theta$ is positive. If $2\pi|P_\theta| < |q\psi_{\max}|$ there exists a location inside r_{\max} where

$$P_\theta = \frac{q}{2\pi} \psi \quad (3.161)$$

and there exists a location outside r_{\max} where this equality holds as well. χ vanishes at these two points which are also local minima of χ because χ is positive-definite. The top plot in Fig.3.14 shows a nominal $\psi(r)/\psi_0$ flux profile and the middle plot shows the corresponding $\chi(r)/\chi_0$; the z and t dependence are suppressed from the arguments for clarity. There exists a maximum of χ between the two minima. We consider a particle initially located in one of the two minima of χ . If $H < \chi_{\max}$ the particle will be confined to an effective potential well centered about the flux surface

defined by Eq.(3.161). From Eq.(3.157) the angular velocity is

$$\dot{\theta} = \frac{1}{mr^2} \left(P_\theta - \frac{q\psi}{2\pi} \right). \quad (3.162)$$

The sign of $\dot{\theta}$ reverses periodically as the particle bounces back and forth in the χ potential well. This corresponds to localized gyromotion as shown in Fig.3.15.

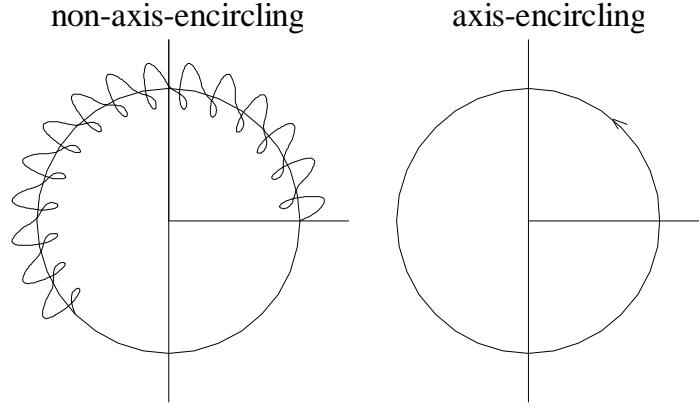


Figure 3.15: Localized gyro motion associated with particle bouncing in effective potential well.

2. $q\psi/P_\theta$ is *negative*. In this case χ can never vanish, because $P_\theta - q\psi/2\pi$ never vanishes. Nevertheless, it is still possible for χ to have a minimum and hence a potential well. This possibility can be seen by setting $\partial\chi/\partial r = 0$ which occurs when

$$\left(P_\theta - \frac{q}{2\pi} \psi \right) \frac{\partial}{\partial r} \left(\frac{P_\theta - q\psi/2\pi}{r} \right) = 0. \quad (3.163)$$

Equation (3.163) can be satisfied by having

$$\frac{\partial}{\partial r} \left(\frac{P_\theta - \frac{q}{2\pi} \psi}{r} \right) = 0 \quad (3.164)$$

which implies

$$P_\theta = -\frac{qr^2}{2\pi} \frac{\partial}{\partial r} \left(\frac{\psi}{r} \right). \quad (3.165)$$

Recall that ψ had a maximum, that $\psi \sim r^2$ near $r = 0$, and also that $\psi \rightarrow 0$ as $r \rightarrow \infty$. Thus $\psi/r \sim r$ for small r and $\psi/r \rightarrow 0$ for $r \rightarrow \infty$ so that ψ/r also has a maximum; this maximum is located at an r somewhat inside of the maximum of ψ . Thus Eq.(3.165) can only be valid at points inside of this maximum; otherwise the assumption of opposite signs for P_θ and ψ would be incorrect. Furthermore

Eq.(3.165) can only be satisfied if $|P_\theta|$ is not too large, because the right hand side of Eq.(3.165) has a maximum value. If all these conditions are satisfied, then χ will have a non-zero minimum as shown in the bottom plot of Fig.3.14.

A particularly simple example of this behavior occurs if Eq.(3.165) is satisfied near the $r = 0$ axis (i.e., where $\psi \sim r^2$) so that this equation becomes simply

$$P_\theta = -\frac{q}{2\pi}\psi \quad (3.166)$$

which is just the opposite of Eq.(3.161). Substituting in Eq.(3.162) we see that $\dot{\theta}$ now *never* changes sign; i.e., the particle is *axis-encircling*. The Larmor radius of this axis-encircling particle is just the radius of the minimum of the potential well, the radius where Eq.(3.165) holds. The azimuthal kinetic energy of the particle corresponds to the height of the minimum of χ in the bottom plot of Fig.3.14.

3.7.1 Temporal Reversal of Magnetic Field - Energy Gain

Armed with this information about axis-encircling and non-axis encircling particles, we now examine the strongly non-adiabatic situation where a coil current starts at $I = I_0$, is reduced to zero, and then becomes $I = -I_0$, so that all fields and fluxes reverse sign. The particle energy will not stay constant for this situation because the Lagrangian depends explicitly on time. However, since symmetry is maintained, P_θ *must* remain constant. Thus, a non-axis encircling particle (with radial location determined by Eq. (3.161)) will change to an axis-encircling particle if a minimum exists for χ when the sign of ψ is reversed. If such a minimum does exist and if the initial radius was near the axis where $\psi \sim r^2$, then comparison of Eqs.(3.161) and (3.166) shows that the particle will have the same radius after the change of sign as before. The particle will gain energy during the field reversal by an amount corresponding to the finite value of the minimum of χ for the axis-encircling case.

This process can also be considered from the point of view of particle drifts: Initially, the non-axis-encircling particle is frozen to a constant ψ surface (flux surface). When the coil current starts to decrease, the maximum value of the flux correspondingly decreases. The constant ψ contours on the *inside* of ψ_{\max} move outwards towards the location of ψ_{\max} where they are annihilated. Likewise, the contours outside of ψ_{\max} move inwards to ψ_{\max} where they are also annihilated.

To the extent that the $\mathbf{E} \times \mathbf{B}$ drift is a valid approximation, its effect is to keep the particle attached to a surface of constant flux. This can be seen by integrating Faraday's law over the area of a circle of radius r to obtain $\int ds \cdot \nabla \times \mathbf{E} = -\int ds \cdot \partial \mathbf{B} / \partial t$ and then invoking Stoke's theorem to give

$$E_\theta 2\pi r = -\frac{\partial \psi}{\partial t}. \quad (3.167)$$

The theta component of $\mathbf{E} + \mathbf{v} \times \mathbf{B} = 0$ is

$$E_\theta + v_z B_r - v_r B_z = 0 \quad (3.168)$$

and from (3.146), $B_r = -(2\pi r)^{-1} \partial \psi / \partial z$ and $B_z = -(2\pi r)^{-1} \partial \psi / \partial r$. Combination of Eqs.(3.167) and (3.168) thus gives

$$\frac{\partial \psi}{\partial t} + v_r \frac{\partial \psi}{\partial r} + v_z \frac{\partial \psi}{\partial z} = 0. \quad (3.169)$$

Because $\psi(r(t), z(t), t)$ is the flux measured in the frame of a particle moving with trajectory $r(t)$ and $z(t)$, Eq.(3.169) shows that the $\mathbf{E} \times \mathbf{B}$ drift maintains the particle on a surface of constant ψ , i.e., the $\mathbf{E} \times \mathbf{B}$ drift is such as to maintain $d\psi/dt = 0$ where d/dt means time derivative as measured in the particle frame.

The implication of this attachment of the particle to a surface of constant ψ can be appreciated by making an analogy to the motion of people initially located on the beach of a volcanic island which is slowly sinking into the sea. In order to avoid being drowned as the island sinks, the people will move towards the mountain top to stay at a constant height above the sea. The location of ψ_{\max} here corresponds to the mountain top and the particles trying to stay on surfaces of constant ψ correspond to people trying to stay at constant altitude. A particle initially located at some location away from the “mountain top” ψ_{\max} moves towards ψ_{\max} if the overall level of all the ψ surfaces is sinking. The reduction of ψ as measured at a fixed position will create the azimuthal electric field given by Eq.(3.167) and this electric field will, as shown by Eqs.(3.168) and (3.169), cause an $\mathbf{E} \times \mathbf{B}$ drift which convects each particle in just such a way as to stay on a constant ψ contour.

The $\mathbf{E} \times \mathbf{B}$ drift approximation breaks down when \mathbf{B} becomes zero, i.e., when ψ changes polarity. This breakdown corresponds to a breakdown of the adiabatic approximation. If ψ changes polarity before a particle reaches ψ_{\max} , the particle becomes axis-encircling. The extra energy associated with being axis-encircling is obtained when $\psi \simeq 0$ but $\partial\psi/\partial t \neq 0$ so that there is an electric field E_θ , but no magnetic field. Finite E_θ and no magnetic field results in a simple theta acceleration of the particle. Thus, when ψ reverses polarity the particle is accelerated azimuthally and develops finite kinetic energy. After ψ has changed polarity the magnitude of ψ increases and the adiabatic approximation again becomes valid. Because the polarity is reversed, increase of the magnitude of ψ is now analogous to creating an ever deepening crater. Particles again try to stay on constant flux surfaces as dictated by Eq.(3.169) and as the crater deepens, the particles have to move away from ψ_{\min} to stay at the same altitude. When the reversed flux attains the same magnitude as the original flux, the flux surfaces have the same shape as before. However, the particles are now axis-encircling and have the extra kinetic energy obtained at field reversal.

3.7.2 Spatial reversal of field - cusps

Suppose two solenoids with constant currents are arranged coaxially with their magnetic fields opposing each other as shown in Fig.3.16(a). Since the solenoid currents are constant, the Lagrangian does not depend explicitly on time in which case energy is a constant of the motion. Because of the geometrical arrangement, the flux function is anti-symmetric in z where $z = 0$ defines the midplane between the two solenoids.

Consider a particle injected with initial velocity $\mathbf{v} = v_{z0}\hat{z}$ at $z = -L, r = a$. Since this particle has no initial v_\perp , it simply streams along a magnetic field line. However, when the particle approaches the cusp region, the magnetic field lines start to curve causing the particle to develop both curvature and grad B drifts perpendicular to the magnetic field. When the particle approaches the $z = 0$ plane, the drift approximation breaks down because $B \rightarrow 0$ and so the particle’s motion becomes non-adiabatic [cf. Fig.3.16(a)].

Although the particle trajectory is very complex in the vicinity of the cusp, it is still possible to determine whether the particle will cross into the positive z half-plane, i.e.,

cross the cusp. Such an analysis is possible because two constants of the motion exist, namely P_θ and H . The energy

$$H = \frac{P_r^2}{2m} + \frac{P_z^2}{2m} + \frac{\left(P_\theta - \frac{q}{2\pi}\psi(r, z)\right)^2}{2mr^2} = \text{const.} \quad (3.170)$$

can be evaluated using

$$P_\theta = \left[mr^2\dot{\theta} + \frac{q}{2\pi}\psi\right]_{\text{initial}} = \frac{q}{2\pi}\psi_0 \quad (3.171)$$

since initially $\dot{\theta} = 0$. Here

$$\psi_0 = \psi(r = a, z = -L) \quad (3.172)$$

is the flux at the particle's initial position. Inserting initial values of all quantities in Eq.(3.170) gives

$$H = \frac{mv_{z0}^2}{2} \quad (3.173)$$

and so Eq.(3.170) becomes

$$\begin{aligned} \frac{mv_{z0}^2}{2} &= \frac{mv_r^2}{2} + \frac{mv_z^2}{2} + \frac{\left(\frac{q}{2\pi}\right)^2 (\psi_0 - \psi(r, z))^2}{2mr^2} \\ &= \frac{mv_r^2}{2} + \frac{mv_z^2}{2} + \frac{mv_\theta^2}{2} . \end{aligned} \quad (3.174)$$

The extent to which a particle penetrates the cusp can be easily determined if the particle starts close enough to $r = 0$ so that the flux may be approximated as $\psi \sim r^2$. Specifically, the flux will be $\psi = B_{z0}\pi r^2$ where B_{z0} is the on-axis magnetic field in the $z \ll 0$ region. The canonical momentum is simply $P_\theta = q\psi/2\pi = qB_{z0}a^2/2$ since the particle started as non-axis encircling.

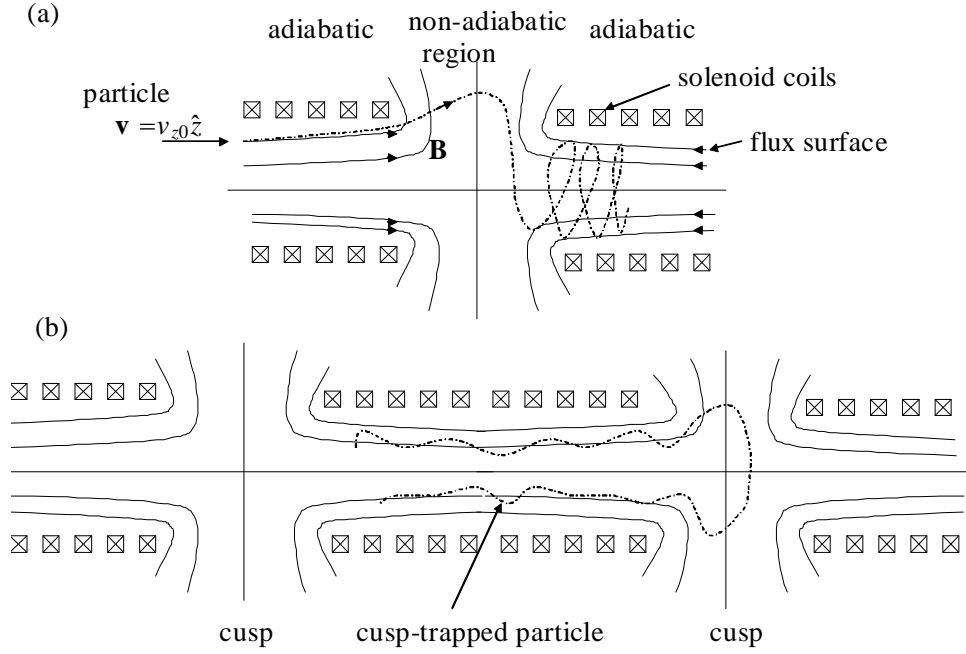


Figure 3.16: (a) Cusp field showing trajectory for particle with sufficient initial energy to penetrate the cusp; (b) two cusps used as magnetic trap to confine particles.

Suppose the particle penetrates the cusp and arrives at some region where again $\psi \sim r^2$. Since the particle is now axis-encircling, the relation between canonical momentum and flux is $P_\theta = -q\psi/2\pi = -q(-B_{z0}\pi r^2)/2\pi = qB_{z0}r^2/2$ from which it is concluded that $r = a$. Thus, if the particle is able to move across the cusp, it becomes an axis-encircling particle with the *same* radius $r = a$ it originally had when it was non-axis-encircling. The minimum energy an axis-encircling particle can have is when it is purely axis encircling, i.e., has $v_r = 0$ and $v_z = 0$. Thus, for the particle to cross the cusp and reach a location where it becomes purely axis-encircling, the particle's initial energy must satisfy

$$\frac{mv_{z0}^2}{2} \geq \frac{m(\omega_c a)^2}{2} \quad (3.175)$$

or simply

$$v_{z0} \geq \omega_c a. \quad (3.176)$$

If v_{z0} is too small to satisfy this relation, the particle reflects from the cusp and returns back to the negative z half-plane. Plasma confinement schemes have been designed based on particles reflecting from cusps as shown in Fig.3.16(b). Here a particle is trapped between two cusps and so long as its parallel energy is insufficient to violate Eq.(3.176), the

particle is confined between the two cusps.

Cusps have also been used to trap relativistic electron beams in mirror fields (Hudgings, Meger, Striffler, Destler, Kim, Reiser and Rhee 1978, Kribel, Shinsky, Phelps and Fleischmann 1974). In this scheme an additional opposing solenoid is added to one end of a magnetic mirror so as to form a cusp outside the mirror region. A relativistic electron beam is injected through the cusp into the mirror. The beam changes from non-axis-encircling into axis-encircling on passing through the cusp as in Fig.3.16(a). If energy is conserved, the beam is not trapped because the beam will reverse its trajectory and bounce back out of the mirror. However, if axial energy is removed from the beam once it is in the mirror, then the motion will not be reversible and the beam will be trapped. Removal of beam axial energy has been achieved by having the beam collide with neutral particles or by having the beam induce currents in a resistive wall.

3.7.3 Stochastic motion in large amplitude, low frequency waves

The particle drifts ($\mathbf{E} \times \mathbf{B}$, polarization, etc.) were derived using an iteration scheme which was based on the assumption that spatial changes in the electric and magnetic fields are sufficiently gradual to allow Taylor expansions of the fields about their values at the gyrocenter.

We now examine a situation where the fields change gradually in space relative to the initial gyro-orbit dimensions, but the fields also pump energy into the particle motion so that eventually the size of the gyro-orbit increases to the point that the smallness assumption fails. To see how this might occur consider motion of a particle in an electrostatic wave

$$\mathbf{E} = \hat{\mathbf{y}} k \phi \sin(ky - \omega t) \quad (3.177)$$

which propagates in a plasma immersed in a uniform magnetic field $\mathbf{B} = B\hat{\mathbf{z}}$. The wave frequency is much lower than the cyclotron frequency of the particle in question. This $\omega \ll \omega_c$ condition indicates that the drift equations in principle can be used and so according to these equations, the charged particle will have both an $\mathbf{E} \times \mathbf{B}$ drift

$$\mathbf{v}_E = \frac{\mathbf{E} \times \mathbf{B}}{B^2} = \hat{\mathbf{x}} \frac{k\phi}{B^2} \sin(ky - \omega t). \quad (3.178)$$

and a polarization drift

$$\mathbf{v}_p = \frac{m}{qB^2} \frac{d\mathbf{E}_\perp}{dt} = \hat{\mathbf{y}} \frac{mk\phi}{qB^2} \frac{d}{dt} \sin(ky - \omega t). \quad (3.179)$$

If the wave amplitude is infinitesimal, the spatial displacements associated with \mathbf{v}_E and \mathbf{v}_p are negligible and so the guiding center value of y may be used in the right hand side of Eq.(3.179) to obtain

$$\mathbf{v}_p = -\hat{\mathbf{y}} \frac{\omega mk\phi}{qB^2} \cos(ky - \omega t). \quad (3.180)$$

Equations (3.178) and (3.180) show that the combined \mathbf{v}_E and \mathbf{v}_p particle drift motion results in an elliptical trajectory.

Now suppose that the wave amplitude becomes so large that the particle is displaced significantly from its initial position. Since the polarization drift is in the y direction, there will be a substantial displacement in the y direction. Thus, the right side of Eq.(3.179)

should be construed as $\sin[ky(t) - \omega t]$ so that, taking into account the time dependence of y on the right hand sided, Eq.(3.179) becomes

$$\mathbf{v}_p = \hat{\mathbf{y}} \frac{mk\phi}{qB^2} \frac{d}{dt} \sin(ky - \omega t) = \hat{\mathbf{y}} \frac{mk\phi}{qB^2} \left(k \frac{dy}{dt} - \omega \right) \cos(ky - \omega t). \quad (3.181)$$

However, $dy/dt = v_p$ since \mathbf{v}_p is the motion in the y direction. Equation (3.181) becomes an implicit equation for \mathbf{v}_p and may be solved to give

$$\mathbf{v}_p = -\hat{\mathbf{y}} \frac{\omega mk\phi}{qB^2} \frac{\cos(ky - \omega t)}{[1 - \alpha \cos(ky - \omega t)]} \quad (3.182)$$

where

$$\alpha = \frac{mk^2\phi}{qB^2} \quad (3.183)$$

is a non-dimensional measure of the wave amplitude (McChesney, Stern and Bellan 1987, White, Chen and Lin 2002).

If $\alpha > 1$, the denominator in Eq.(3.182) vanishes when $ky - \omega t = \cos^{-1} \alpha^{-1}$ and this vanishing denominator would result in an infinite polarization drift. However, the derivation of the polarization drift was based on the assumption that the time derivative of the polarization drift was negligible compared to the time derivative of \mathbf{v}_E , i.e., it was explicitly assumed $d\mathbf{v}_p/dt \ll d\mathbf{v}_E/dt$. Clearly, this assumption fails when \mathbf{v}_p becomes infinite and so the iteration scheme used to derive the particle drifts fails. What is happening is that when $\alpha \sim 1$, the particle displacement due to polarization drift becomes $\sim k^{-1}$. Thus the displacement of the particle from its gyrocenter is of the order of a wavelength. In such a situation it is incorrect to represent its actual location by its gyrocenter because the particle experiences the wave field at the particle's actual location, not at its gyrocenter. Because the wave field is significantly different at two locations separated by $\sim k^{-1}$, it is essential to evaluate the wave field evaluated at the actual particle location rather than at the gyrocenter.

Direct numerical integration of the Lorentz equation in this large-amplitude limit shows that when α exceeds unity, particle motion becomes chaotic and cannot be described by analytic formulae. Onset of chaotic motion resembles heating of the particles since chaos and heating both broaden the velocity distribution function. However, chaotic heating is not a true heating because entropy is not increased — the motion is deterministic and not random. Nevertheless, this chaotic (or stochastic) heating is indistinguishable for practical purposes from ordinary collisional thermalization of directed motion.

An alternate way of looking at this issue is to consider the Lorentz equations for two initially adjacent particles, denoted by subscripts 1 and 2 which are in a wave electric field and a uniform, steady-state magnetic field (Stasiewicz, Lundin and Marklund 2000). The respective Lorentz equations of the two particles are

$$\begin{aligned} \frac{d\mathbf{v}_1}{dt} &= \frac{q}{m} [\mathbf{E}(\mathbf{x}_1, t) + \mathbf{v}_1 \times \mathbf{B}] \\ \frac{d\mathbf{v}_2}{dt} &= \frac{q}{m} [\mathbf{E}(\mathbf{x}_2, t) + \mathbf{v}_2 \times \mathbf{B}]. \end{aligned} \quad (3.184)$$

Subtracting these two equations gives an equation for the difference between the velocities of the two particles, $\delta\mathbf{v} = \mathbf{v}_1 - \mathbf{v}_2$ in terms of the difference $\delta\mathbf{x} = \mathbf{x}_1 - \mathbf{x}_2$ in their positions,

i.e.,

$$\frac{d\delta\mathbf{v}}{dt} = \frac{q}{m} [\delta\mathbf{x} \cdot \nabla\mathbf{E} + \delta\mathbf{v} \times \mathbf{B}] . \quad (3.185)$$

The difference velocity is related to the difference in positions by $d\delta\mathbf{x}/dt = \delta\mathbf{v}$. Let y be the direction in which the electric field is non-uniform, i.e., with this choice of coordinate system \mathbf{E} depends only on the y direction. To simplify the algebra, define $\mathcal{E}_x = qE_x/m$ and $\mathcal{E}_y = qE_y/m$ so the components of Eq.(3.185) transverse to the magnetic field are

$$\begin{aligned} \delta\ddot{x} &= \delta y \frac{\partial \mathcal{E}_x}{\partial y} + \omega_c \delta \dot{y} \\ \delta\ddot{y} &= \delta y \frac{\partial \mathcal{E}_y}{\partial y} - \omega_c \delta \dot{x}. \end{aligned} \quad (3.186)$$

Now take the time derivative of the lower equation to obtain

$$\delta\dddot{y} = \delta\dot{y} \frac{\partial \mathcal{E}_y}{\partial y} + \delta y \frac{\partial}{\partial y} \left(\frac{d\mathcal{E}_y}{dt} \right) - \omega_c \delta\ddot{x} \quad (3.187)$$

and then substitute for $\delta\ddot{x}$ giving

$$\delta\ddot{y} = \delta\dot{y} \frac{\partial \mathcal{E}_y}{\partial y} + \delta y \frac{\partial}{\partial y} \left(\frac{d\mathcal{E}_y}{dt} \right) - \omega_c \left(\delta y \frac{\partial \mathcal{E}_x}{\partial y} + \omega_c \delta \dot{y} \right). \quad (3.188)$$

This can be re-arranged as

$$\delta\ddot{y} + \omega_c^2 \left(1 - \frac{1}{\omega_c} \frac{\partial \mathcal{E}_y}{\partial y} \right) \delta \dot{y} = \omega_c \delta y \frac{\partial \mathcal{E}_x}{\partial y} - \delta y \frac{\partial}{\partial y} \left(\frac{d\mathcal{E}_y}{dt} \right). \quad (3.189)$$

Consider the right hand side of the equation as being a forcing term for the left hand side. If $\omega_c^{-1} \partial \mathcal{E}_y / \partial y < 1$, then the left hand side is a simple harmonic oscillator equation in the variable $\delta \dot{y}$. However, if $\omega_c^{-1} \partial \mathcal{E}_y / \partial y$ exceeds unity, then the left hand side becomes an equation with solutions that grow exponentially in time. If two particles are initially separated by the infinitesimal distance δy and if $\omega_c^{-1} \partial \mathcal{E}_y / \partial y < 1$ the separation distance between the two particles will undergo harmonic oscillations, but if $\omega_c^{-1} \partial \mathcal{E}_y / \partial y > 1$ the separation distance will exponentially diverge with time. It is seen that α corresponds to $\omega_c^{-1} \partial \mathcal{E}_y / \partial y$ for a sinusoidal wave. Exponential growth of the separation distance between two particles that are initially arbitrarily close together is called stochastic behavior.

3.8 Motion in small-amplitude oscillatory fields

Suppose a small-amplitude electromagnetic field exists in a plasma which in addition has a large uniform, steady-state magnetic field and no steady-state electric field. The fields can thus be written as

$$\begin{aligned} \mathbf{E} &= \mathbf{E}_1(\mathbf{x}, t) \\ \mathbf{B} &= \mathbf{B}_0 + \mathbf{B}_1(\mathbf{x}, t) \end{aligned} \quad (3.190)$$

where the subscript 1 denotes the small amplitude oscillatory quantities and the subscript 0 denotes large, uniform equilibrium quantities. A typical particle in this plasma will develop an oscillatory motion

$$\mathbf{x}(t) = \langle \mathbf{x}(t) \rangle + \delta \mathbf{x}(t) \quad (3.191)$$

where $\langle \mathbf{x}(t) \rangle$ is the particle's time-averaged position and $\delta \mathbf{x}(t)$ is the instantaneous deviation from this average position. If the amplitudes of $\mathbf{E}_1(\mathbf{x}, t)$ and $\mathbf{B}_1(\mathbf{x}, t)$ are sufficiently small, then the fields at the particle position can be approximated as

$$\begin{aligned} \mathbf{E}(\langle \mathbf{x}(t) \rangle + \delta \mathbf{x}(t), t) &\simeq \mathbf{E}_1(\langle \mathbf{x}(t) \rangle, t) \\ \mathbf{B}(\langle \mathbf{x}(t) \rangle + \delta \mathbf{x}(t), t) &\simeq \mathbf{B}_0 + \mathbf{B}_1(\langle \mathbf{x}(t) \rangle, t) \end{aligned} \quad (3.192)$$

This is the opposite limit from what was considered in Section 3.7.3. The Lorentz equation reduces in this small-amplitude limit to

$$m \frac{d\mathbf{v}}{dt} = q [\mathbf{E}_1(\langle \mathbf{x} \rangle, t) + \mathbf{v} \times (\mathbf{B}_0 + \mathbf{B}_1(\langle \mathbf{x}(t) \rangle, t))]. \quad (3.193)$$

Since the oscillatory fields are small, the resulting particle velocity will also be small (unless there is a resonant response as would happen at the cyclotron frequency). If the particle velocity is small, then the term $\mathbf{v} \times \mathbf{B}_1(\mathbf{x}, t)$ is of second order smallness, whereas \mathbf{E}_1 and $\mathbf{v} \times \mathbf{B}_0$ are of first-order smallness. The $\mathbf{v} \times \mathbf{B}_1(\mathbf{x}, t)$ is thus insignificant compared to the other two terms on the right hand side and therefore can be discarded so that the Lorentz equation reduces to

$$m \frac{d\mathbf{v}}{dt} = q [\mathbf{E}_1(\langle \mathbf{x} \rangle, t) + \mathbf{v} \times \mathbf{B}_0], \quad (3.194)$$

a linear differential equation for \mathbf{v} . Since $\delta \mathbf{x}$ is assumed to be so small that it can be ignored, the average brackets will be omitted from now on and the first order electric field will simply be written as $\mathbf{E}_1(\mathbf{x}, t)$ where \mathbf{x} can be interpreted as being either the actual or the average position of the particle.

The oscillatory electric field can be decomposed into Fourier modes, each having time dependence $\sim \exp(-i\omega t)$ and since Eq.(3.194) is linear, the particle response to a field $\mathbf{E}_1(\mathbf{x}, t)$ is just the linear superposition of its response to each Fourier mode. Thus it is appropriate to consider motion in a single Fourier mode of the electric field, say

$$\mathbf{E}_1(\mathbf{x}, t) = \bar{\mathbf{E}}(\mathbf{x}, \omega) \exp(-i\omega t). \quad (3.195)$$

If initial conditions are ignored for now, the particle motion can be found by simply assuming that the particle velocity also has the time dependence $\exp(-i\omega t)$ in which case the Lorentz equation becomes

$$-i\omega m \mathbf{v} = q [\bar{\mathbf{E}}(\mathbf{x}) + \mathbf{v} \times \mathbf{B}_0] \quad (3.196)$$

where a factor $\exp(-i\omega t)$ is implicitly assumed for all terms and also an ω argument is implicitly assumed for $\bar{\mathbf{E}}$. Equation (3.196) is a vector equation of the form

$$\mathbf{v} + \mathbf{v} \times \mathbf{A} = \mathbf{C} \quad (3.197)$$

where

$$\begin{aligned} \mathbf{A} &= \frac{\omega_c}{i\omega} \hat{z} \\ \omega_c &= \frac{qB_0}{m} \\ \mathbf{C} &= \frac{iq}{\omega m} \bar{\mathbf{E}}(\mathbf{x}) \end{aligned} \quad (3.198)$$

and the z axis has been chosen to be in the direction of \mathbf{B}_0 . Equation (3.197) can be solved for \mathbf{v} by first dotting with \mathbf{A} to obtain

$$\mathbf{A} \cdot \mathbf{v} = \mathbf{C} \cdot \mathbf{A} \quad (3.199)$$

and then crossing with \mathbf{A} to obtain

$$\mathbf{v} \times \mathbf{A} + \mathbf{A}\mathbf{A} \cdot \mathbf{v} - \mathbf{v}A^2 = \mathbf{C} \times \mathbf{A}. \quad (3.200)$$

Substituting for $\mathbf{A} \cdot \mathbf{v}$ using Eq.(3.199) and for $\mathbf{v} \times \mathbf{A}$ using Eq.(3.197) gives

$$\mathbf{v} = \frac{\mathbf{C} + \mathbf{A}\mathbf{A} \cdot \mathbf{C} - \mathbf{C} \times \mathbf{A}}{1 + A^2} = C_{\parallel} \hat{z} + \frac{\mathbf{C}_{\perp}}{1 + A^2} + \frac{\mathbf{A} \times \mathbf{C}}{1 + A^2} \quad (3.201)$$

where \mathbf{C} has been split into parallel and perpendicular parts relative to \mathbf{B}_0 and $\mathbf{A}\mathbf{A} \cdot \mathbf{C} = A^2 C_{\parallel} \hat{z}$ has been used. On substituting for \mathbf{A} and \mathbf{C} this becomes

$$\mathbf{v} = \frac{iq}{\omega m} \left[\tilde{E}_{\parallel}(\mathbf{x}) \hat{z} + \frac{\bar{\mathbf{E}}_{\perp}(\mathbf{x})}{1 - \omega_c^2/\omega^2} - \frac{i\omega_c}{\omega} \frac{\hat{z} \times \bar{\mathbf{E}}(\mathbf{x})}{1 - \omega_c^2/\omega^2} \right] e^{-i\omega t}. \quad (3.202)$$

The third term on the right hand side is a generalization of the $\mathbf{E} \times \mathbf{B}$ drift, since for $\omega \ll \omega_c$ this term reduces to the $\mathbf{E} \times \mathbf{B}$ drift. Similarly, the middle term on the right hand side is a generalization of the polarization drift, since for $\omega \ll \omega_c$ this term reduces to the polarization drift. The first term on the right hand side, the parallel quiver velocity, does not involve the magnetic field B_0 . This non-dependence on magnetic field is to be expected because no magnetic force results from motion parallel to a magnetic field. In fact, if the magnetic field were zero, then the second term would add to the first and the third term would vanish, giving a three dimensional unmagnetized quiver velocity $\mathbf{v} = iq\bar{\mathbf{E}}(\mathbf{x})/\omega m$.

If the electric field is in addition decomposed into spatial Fourier modes with dependence $\sim \exp(i\mathbf{k} \cdot \mathbf{x})$, then the velocity for a typical mode will be

$$\mathbf{v}(\mathbf{x}, t) = \frac{iq}{\omega m} \left[\tilde{E}_{\parallel} \hat{z} + \frac{\bar{\mathbf{E}}_{\perp}}{1 - \omega_c^2/\omega^2} - \frac{i\omega_c}{\omega} \frac{\hat{z} \times \bar{\mathbf{E}}}{1 - \omega_c^2/\omega^2} \right] e^{i\mathbf{k} \cdot \mathbf{x} - i\omega t}. \quad (3.203)$$

The convention of a negative coefficient for ω and a positive coefficient for \mathbf{k} has been adopted to give waves propagating in the positive x direction. Equation (3.203) will later be used as the starting point for calculating wave-generated plasma currents.

3.9 Wave-particle energy transfer

3.9.1 'Average velocity'

Anyone who has experienced delay in a traffic jam knows that it is usually impossible to make up for the delay by going faster after escaping from the traffic jam. To see why, define α as the fraction of the total trip length in the traffic jam, v_s as the slow (traffic jam)

speed, and v_f as the fast speed (out of traffic jam). It is tempting, but wrong, to say that the average velocity is $(1 - \alpha)v_f + \alpha v_s$ because

$$\text{average velocity of a trip} = \frac{\text{total distance}}{\text{total time}}. \quad (3.204)$$

Since the fast-portion duration is $t_f = (1 - \alpha)L/v_f$ while the the slow-portion duration is $t_s = \alpha L/v_s$, the average velocity of the complete trip is

$$v_{avg} = \frac{L}{(1 - \alpha)L/v_f + \alpha L/v_s} = \frac{1}{(1 - \alpha)/v_f + \alpha/v_s}. \quad (3.205)$$

Thus, if $v_s \ll v_f$ then $v_{avg} \simeq v_s/\alpha$ which (i) is not the weighted average of the fast and slow velocities and (ii) is almost entirely determined by the slow velocity.

3.9.2 Motion of particles in a sawtooth potential

The exact motion of a particle in a sinusoidal potential can be solved using elliptic integrals, but the obtained solution is implicit, i.e., the solution is expressed in the form of time as a function of position. While exact, the implicit nature of this solution obscures the essential physics. In order to shed some light on the underlying physics, we will first consider particle motion in the contrived, but analytically tractable, situation of the periodic sawtooth-shaped potential shown in Fig.3.17 and then later will consider particle motion in a more natural, but harder to analyze, sinusoidal potential.

When in the downward-sloping portion of the sawtooth potential, a particle experiences a constant acceleration $+a$ and when in the upward portion it experiences a constant acceleration $-a$. Our goal is to determine the average velocity of a group of particles injected with an initial velocity v_0 into the system. Care is required when using the word ‘average’ because this word has two meanings depending on whether one is referring to the average velocity of a single particle or the average velocity of a group of particles. The average velocity of a single particle is defined by Eq.(3.204) whereas the average velocity of a group of particles is defined as the sum of the velocities of all the particles in the group divided by the number of particles in the group.

The average velocity of any given individual particle depends on where the particle was injected. Consider the four particles denoted as $A, B, C,$ and D in Fig.3.17 as representatives of the various possibilities for injection location. Particle A is injected at a potential maximum, particle C at a potential minimum, particle B is injected half way on the downslope, and particle D is injected half way on the upslope.

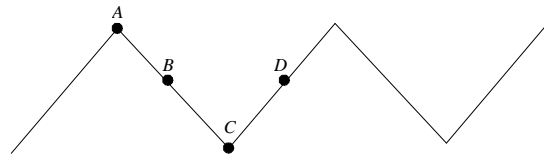


Figure 3.17: Initial positions of particles $A, B, C,$ and D . All are injected with same initial velocity v_0 , moving to the right.

The average velocity for each of these four representative particles will now be evaluated:

Particle *A* – Let the distance between maximum and minimum potential be d . Let $x = 0$ be the location of the minimum so the injection point is at $x = -d$. Thus the trajectory on the downslope is

$$x(t) = -d + v_0 t + at^2/2 \quad (3.206)$$

and the time for particle *A* to go from its injection point to the potential minimum is found by setting $x(t) = 0$ giving

$$t_{down}^A = \frac{v_0}{a} \left(-1 + \sqrt{1 + 2\delta} \right) \quad (3.207)$$

where $\delta = ad/v_0^2$ is the normalized acceleration. When particle *A* reaches the next potential peak, it again has velocity v_0 and if the time and space origins are re-set to be at the new peak, the trajectory will be

$$x(t) = v_0 t - at^2/2. \quad (3.208)$$

The negative time when the particle is at the preceding potential minimum is found from

$$-d = v_0 t - at^2/2. \quad (3.209)$$

Solving for this negative time and then calculating the time increment to go from the minimum to the maximum shows that this time is the same as going from the maximum to the minimum, i.e., $t_{down}^A = t_{up}^A$. Thus the average velocity for particle *A* is

$$v_{avg}^A = \frac{da/v_0}{-1 + \sqrt{1 + 2\delta}}. \quad (3.210)$$

The average velocity of particle *A* is thus always *faster* than its injection velocity.

Particle *C* – Now let $x = 0$ be the location of maximum potential and $x = -d$ be the point of injection so the particle trajectory is

$$x(t) = -d + v_0 t - at^2/2 \quad (3.211)$$

and the time to get to $x = 0$ is

$$t_{up}^C = \frac{v_0}{a} \left(1 - \sqrt{1 - 2\delta} \right). \quad (3.212)$$

From symmetry it is seen that the time to go from the maximum to the minimum will be the same so the average velocity will be

$$v_{avg}^C = \frac{ad/v_0}{1 - \sqrt{1 - 2\delta}}. \quad (3.213)$$

Because particle *B* is always on a potential hill relative to its injection position, its average velocity is always *slower* than its injection velocity.

Particles *B* and *D*- Particle *B* can be considered as first traveling in a potential well and then in a potential hill, while the reverse is the case for particle *D*. For the potential well

portion, the forces are the same, but the distances are half as much, so the time to traverse the potential well portion is

$$t_{well} = \frac{2v_0}{a} \left(-1 + \sqrt{1 + \delta} \right). \quad (3.214)$$

Similarly, the time required to traverse the potential hill portion will be

$$t_{hill} = \frac{2v_0}{a} \left(1 - \sqrt{1 - \delta} \right) \quad (3.215)$$

so the average velocity for particles B and D will be

$$v_{avg}^{B,D} = \frac{ad/v_0}{\sqrt{1 + \delta} - \sqrt{1 - \delta}}. \quad (3.216)$$

These particles move *slower* than the injection velocity, but the effect is second order in δ .

The average velocity of the four particles will be

$$\begin{aligned} v_{avg} &= \frac{1}{4} (v_{avg}^A + v_{avg}^B + v_{avg}^C + v_{avg}^D) \\ &= \frac{ad}{4v_0} \left[\frac{1}{-1 + \sqrt{1 + 2\delta}} + \frac{1}{1 - \sqrt{1 - 2\delta}} + \frac{2}{\sqrt{1 + \delta} - \sqrt{1 - \delta}} \right]. \end{aligned} \quad (3.217)$$

If δ is small this expression can be approximated as

$$\begin{aligned} v_{avg} &\simeq \frac{ad}{4\delta v_0} \left[\frac{1}{1 - \delta/2 + \delta^2/2} + \frac{1}{1 + \delta/2 + \delta^2/2} + \frac{2}{1 + \delta^2/8} \right] \\ &= \frac{ad}{2\delta v_0} \left[\frac{1 + \delta^2/2}{1 + 3\delta^2/4} + \frac{1}{1 + \delta^2/8} \right] \\ &\simeq v_0 [1 - 3\delta^2/16] \end{aligned} \quad (3.218)$$

so that the average velocity of the four representative particles is *smaller* than the injection velocity. This effect is second order in δ and shows that a group of particles injected at random locations with identical velocities into a sawtooth periodic potential will, on average, be slowed down.

3.9.3 Slowing down, energy conservation, and average velocity

The sawtooth potential analysis above shows that is necessary to be very careful about what is meant by energy and average velocity. Each particle individually conserves energy and regains its injection velocity when it returns to the phase at which it was injected. However, the average velocities of the particles are not the same as the injection velocities. Particle A has an average velocity higher than its injection velocity whereas particles B , C and D have average velocities smaller than their respective injection velocities. The average velocity of all the particles is less than the injection velocity so that the average kinetic energy of the particles is reduced relative to the injection kinetic energy. Thus the average velocity of a group of particles slows down in a periodic potential, yet paradoxically individual particles do not lose energy. The energy that appears to be missing is contained in the instantaneous potential energy of the individual particles.

3.9.4 Wave-particle energy transfer in a sinusoidal wave

The calculation will now redone for the physically more relevant situation where a group of particles interact with a sinusoidal wave. As a prerequisite for doing this calculation it must first be recognized that two distinct classes of particles exist, namely those which are trapped in the wave and those which are not. The trajectories of trapped particles differs in a substantive way from untrapped particles, but for low amplitude waves the number of trapped particles is so small as to be of no consequence. It therefore will be assumed that the wave amplitude is sufficiently small that the trapped particles can be ignored.

Particle energy is conserved in the wave frame but not in the lab frame because the particle Hamiltonian is time-independent in the wave frame but not in the lab frame. Since each additional conserved quantity reduces the number of equations to be solved, it is advantageous to calculate the particle dynamics in the wave frame, and then transform back to the lab frame.

The analysis in Sec.3.9.2 of particle motion in a sawtooth potential showed that randomly phased groups of particles have their average velocity slow down, i.e., the average velocity of the group tends towards zero as observed in the frame of the sawtooth potential. If the sawtooth potential were moving with respect to the lab frame, the sawtooth potential would appear as a propagating wave in the lab frame. A lab-frame observer would see the particle velocities tending to come to rest in the sawtooth frame, i.e., the lab-frame average of the particle velocities would tend to converge towards the velocity with which the sawtooth frame moves in the lab frame.

The quantitative motion of a particle in a one-dimensional wave potential $\phi(x, t) = \phi_0 \cos(kx - \omega t)$ will now be analyzed in some detail. This situation corresponds to a particle being acted on by a wave traveling in the positive x direction with phase velocity ω/k . It is assumed that there is no magnetic field so the equation of motion is simply

$$\frac{dv}{dt} = \frac{qk\phi_0}{m} \sin(kx - \omega t). \quad (3.219)$$

At $t = 0$ the particle's position is $x = x_0$ and its velocity is $v = v_0$. The wave phase at the particle location is defined to be $\psi = kx - \omega t$. This is a more convenient variable than x and so the differential equations for x will be transformed into a corresponding differential equation for ψ . Using ψ as the dependent variable corresponds to transforming to the wave frame, i.e., the frame moving with the phase velocity ω/k , and makes it possible to take advantage of the wave-frame energy being a constant of the motion. The equations are less cluttered with minus signs if a slightly modified phase variable $\theta = kx - \omega t - \pi$ is used.

The first and second derivatives of θ are

$$\frac{d\theta}{dt} = kv - \omega \quad (3.220)$$

and

$$\frac{d^2\theta}{dt^2} = k \frac{dv}{dt}. \quad (3.221)$$

Substitution of Eq.(3.221) into Eq.(3.219) gives

$$\frac{d^2\theta}{dt^2} + \frac{k^2 q \phi_0}{m} \sin \theta = 0. \quad (3.222)$$

By defining the *bounce* frequency

$$\omega_b^2 = \frac{k^2 q \phi_0}{m} \quad (3.223)$$

and the dimensionless bounce-normalized time

$$\tau = \omega_b t, \quad (3.224)$$

Eq. (3.222) reduces to the pendulum-like equation

$$\frac{d^2\theta}{d\tau^2} + \sin\theta = 0. \quad (3.225)$$

Upon multiplying by the integrating factor $2d\theta/d\tau$, Eq.(3.225) becomes

$$\frac{d}{d\tau} \left[\left(\frac{d\theta}{d\tau} \right)^2 - 2 \cos\theta \right] = 0. \quad (3.226)$$

This integrates to give

$$\left(\frac{d\theta}{d\tau} \right)^2 - 2 \cos\theta = \lambda = \text{const.} \quad (3.227)$$

which indicates the expected energy conservation in the wave frame. The value of λ is determined by two initial conditions, namely the wave-frame injection velocity

$$\left(\frac{d\theta}{d\tau} \right)_{\tau=0} = \frac{1}{\omega_b} \left(\frac{d\theta}{dt} \right)_{t=0} = \frac{kv_0 - \omega}{\omega_b} \equiv \alpha \quad (3.228)$$

and the wave-frame injection phase

$$\theta_{\tau=0} = kx_0 - \pi \equiv \theta_0. \quad (3.229)$$

Inserting these initial values in the left hand side of Eq. (3.227) gives

$$\lambda = \alpha^2 - 2 \cos\theta_0. \quad (3.230)$$

Except for a constant factor,

- λ is the total wave-frame energy
- $(d\theta/d\tau)^2$ is the wave-frame kinetic energy
- $-2 \cos\theta$ is the wave-frame potential energy.

If $-2 < \lambda < 2$, then the particle is trapped in a specific wave trough and oscillates back and forth in this trough. However, if $\lambda > 2$, the particle is untrapped and travels continuously in the same direction, speeding up when traversing a potential valley and slowing down when traversing a potential hill.

Attention will now be restricted to untrapped particles with kinetic energy greatly exceeding potential energy. For these particles

$$\alpha^2 \gg 2 \quad (3.231)$$

which corresponds to considering small amplitude waves since $\alpha \sim \omega_b^{-1}$ and $\omega_b \sim \sqrt{\phi_0}$.

We wish to determine how these untrapped particles exchange energy with the wave. To accomplish this the lab-frame kinetic energy must be expressed in terms of wave-frame quantities. From Eqs.(3.220) and (3.224) the lab-frame velocity is

$$v = \frac{1}{k} \left(\omega + \frac{d\theta}{dt} \right) = \frac{\omega_b}{k} \left(\frac{\omega}{\omega_b} + \frac{d\theta}{d\tau} \right) \quad (3.232)$$

so that the lab-frame kinetic energy can be expressed as

$$W = \frac{1}{2}mv^2 = \frac{m\omega_b^2}{2k^2} \left[\left(\frac{\omega}{\omega_b} \right)^2 + 2\frac{\omega}{\omega_b} \frac{d\theta}{d\tau} + \left(\frac{d\theta}{d\tau} \right)^2 \right]. \quad (3.233)$$

Substituting for $(d\theta/d\tau)^2$ using Eq.(3.227) gives

$$W = \frac{m\omega_b^2}{2k^2} \left[\left(\frac{\omega}{\omega_b} \right)^2 + 2\frac{\omega}{\omega_b} \frac{d\theta}{d\tau} + \lambda + 2\cos\theta \right]. \quad (3.234)$$

Since wave-particle energy transfer is of interest, attention is now focused on the *changes* in the lab-frame particle kinetic energy and so we consider

$$\begin{aligned} \frac{dW}{dt} &= \frac{m\omega_b^3}{k^2} \left[\frac{\omega}{\omega_b} \frac{d^2\theta}{d\tau^2} - \frac{d\theta}{d\tau} \sin\theta \right] \\ &= -\frac{m\omega_b^3}{k^2} \sin\theta \left[\frac{\omega}{\omega_b} + \frac{d\theta}{d\tau} \right] \end{aligned} \quad (3.235)$$

where Eq.(3.225) has been used. To proceed further, it is necessary to obtain the time dependence of both $\sin\theta$ and $d\theta/dt$.

Solving Eq.(3.227) for $d\theta/d\tau$ and assuming $\alpha \gg 1$ (corresponding to untrapped particles) gives

$$\begin{aligned} \frac{d\theta}{d\tau} &= \pm\sqrt{\lambda + 2\cos\theta} \\ &= \pm\sqrt{\alpha^2 + 2(\cos\theta - \cos\theta_0)} \\ &= \alpha \left(1 + \frac{2(\cos\theta - \cos\theta_0)}{\alpha^2} \right)^{1/2} \\ &\simeq \alpha + \frac{\cos\theta - \cos\theta_0}{\alpha}. \end{aligned} \quad (3.236)$$

This expression is valid for both positive and negative α , i.e. for particles going in either direction in the wave frame. The first term in the last line of Eq. (3.236) gives the velocity the particle would have if there were *no* wave (unperturbed orbit) while the second term gives the *perturbation* due to the small amplitude wave. The particle orbit $\theta(\tau)$ is now solved for iteratively. To lowest order (i.e., dropping terms of order α^{-2}) the particle velocity is

$$\frac{d\theta}{d\tau} = \alpha \quad (3.237)$$

and so the rate at which energy is transferred from the wave to the particles is

$$\begin{aligned}\frac{dW}{dt} &= -\frac{m\omega_b^3}{k^2} \sin \theta \left[\frac{\omega}{\omega_b} + \alpha \right] \\ &\simeq -\frac{m\omega_b^2 v_0}{k} \sin \theta\end{aligned}\quad (3.238)$$

Integration of Eq.(3.237) gives the unperturbed orbit solution

$$\theta(\tau) = \theta_0 + \alpha\tau. \quad (3.239)$$

This first approximation is then substituted back into Eq.(3.236) to get the corrected form

$$\frac{d\theta}{d\tau} = \alpha + \frac{\cos(\theta_0 + \alpha\tau) - \cos \theta_0}{\alpha} \quad (3.240)$$

which may be integrated to give the corrected phase

$$\theta(\tau) = \theta_0 + \alpha\tau + \frac{\sin(\theta_0 + \alpha\tau) - \sin \theta_0}{\alpha^2} - \frac{\tau}{\alpha} \cos \theta_0. \quad (3.241)$$

From Eq.(3.241) we may write

$$\sin \theta = \sin[(\theta_0 + \alpha\tau) + \Delta(\tau)] \quad (3.242)$$

where

$$\Delta(\tau) = \frac{\sin(\theta_0 + \alpha\tau) - \sin \theta_0}{\alpha^2} - \frac{\tau}{\alpha} \cos \theta_0 \quad (3.243)$$

is the ‘perturbed-orbit’ correction to the phase. If consideration is restricted to times where $\tau \ll |\alpha|$, the phase correction $\Delta(\tau)$ will be small. This restriction corresponds to

$$(\omega_b t)^2 \ll |k v_0 - \omega| t \quad (3.244)$$

which means that the number of wave peaks the particle passes greatly exceeds the number of bounce times. Since bounce frequency is proportional to wave amplitude, this condition will be satisfied for all finite times for an infinitesimal amplitude wave. Because Δ is assumed to be small, Eq.(3.242) may be expanded as

$$\sin \theta = \sin(\theta_0 + \alpha\tau) \cos \Delta + \sin \Delta \cos(\theta_0 + \alpha\tau) \simeq \sin(\theta_0 + \alpha\tau) + \Delta \cos(\theta_0 + \alpha\tau) \quad (3.245)$$

so that Eq. (3.238) becomes

$$\frac{dW}{dt} = -\frac{m\omega_b^2 v_0}{k} [\sin(\theta_0 + \alpha\tau) + \Delta \cos(\theta_0 + \alpha\tau)]. \quad (3.246)$$

The wave-to-particle energy transfer rate depends on the particle initial position. This is analogous to the earlier sawtooth potential analysis where it was shown that whether particles gain or lose average velocity depends on their injection phase. It is now assumed that there exist many particles with *evenly spaced* initial positions and then an averaging will be performed over all these particles which corresponds to averaging over all initial injection phases. Denoting such averaging by $\langle \rangle$ gives

$$\begin{aligned}\left\langle \frac{dW}{dt} \right\rangle &= -\frac{m\omega_b^2 v_0}{k} \langle \Delta \cos(\theta_0 + \alpha\tau) \rangle \\ &= -\frac{m\omega_b^2 v_0}{k} \left\langle \left[\frac{\sin(\theta_0 + \alpha\tau) - \sin \theta_0}{\alpha^2} - \frac{\tau}{\alpha} \cos \theta_0 \right] \cos(\theta_0 + \alpha\tau) \right\rangle\end{aligned}\quad (3.247)$$

Using the identities

$$\begin{aligned}\langle \sin(\theta_0 + \alpha\tau) \cos(\theta_0 + \alpha\tau) \rangle &= 0 \\ \langle \sin \theta_0 \cos(\theta_0 + \alpha\tau) \rangle &= -\frac{1}{2} \sin \alpha\tau \\ \langle \cos \theta_0 \cos(\theta_0 + \alpha\tau) \rangle &= \frac{1}{2} \cos \alpha\tau\end{aligned}\quad (3.248)$$

the wave-to-particle energy transfer rate becomes

$$\left\langle \frac{dW}{dt} \right\rangle = -\frac{m\omega_b^2 v_0}{2k} \left(\frac{\sin \alpha\tau}{\alpha^2} - \frac{\tau}{\alpha} \cos \alpha\tau \right) = \frac{m\omega_b^2 v_0}{2k} \frac{d}{d\alpha} \left(\frac{\sin \alpha\tau}{\alpha} \right). \quad (3.249)$$

At this point it is recalled that one representation for a delta function is

$$\delta(z) = \lim_{N \rightarrow \infty} \frac{\sin(Nz)}{\pi z} \quad (3.250)$$

so that for $|\alpha\tau| \gg 1$ Eq.(3.249) becomes

$$\left\langle \frac{dW}{dt} \right\rangle = \frac{\pi m \omega_b^2 v_0}{2k} \frac{d}{d\alpha} \delta(\alpha). \quad (3.251)$$

Since $\delta(z)$ has an infinite positive slope just to the left of $z = 0$ and an infinite negative slope just to the right of $z = 0$, the derivative of the delta function consists of a positive spike just to the left of $z = 0$ and a negative spike just to the right of $z = 0$. Furthermore $\alpha = (kv_0 - \omega)/\omega_b$ is slightly positive for particles moving a little faster than the wave phase velocity and slightly negative for particles moving a little slower. Thus $\langle dW/dt \rangle$ is large and positive for particles moving slightly slower than the wave, while it is large and negative for particles moving slightly faster. If the number of particles moving slightly slower than the wave equals the number moving slightly faster, the energy gained by the slightly slower particles is equal and opposite to that gained by the slightly faster particles.

However, if the number of slightly slower particles *differs* from the number of slightly faster particles, there will be a net transfer of energy from wave to particles or vice versa. Specifically, if there are more slow particles than fast particles, there will be a transfer of energy to the particles. This energy must come from the wave and a more complete analysis (cf. Chapter 5) will show that the wave *damps*. The direction of energy transfer depends critically on the slope of the distribution function in the vicinity of $v = \omega/k$, since this slope determines the ratio of slightly faster to slightly slower particles.

We now consider a large number of particles with an initial one-dimensional distribution function $f(v_0)$ and calculate the net wave-to-particle energy transfer rate averaged over all particles. Since $f(v_0)dv_0$ is the probability that a particle had its initial velocity between v_0 and $v_0 + dv_0$, the energy transfer rate averaged over all particles is

$$\begin{aligned}\left\langle \frac{dW_{\text{total}}}{dt} \right\rangle &= \int dv_0 f(v_0) \frac{\pi m \omega_b^2 v_0}{2k} \frac{d}{d\alpha} \delta(\alpha) \\ &= \frac{\pi m \omega_b^3}{2k^2} \int dv_0 f(v_0) v_0 \frac{d}{dv_0} \delta\left(\frac{kv_0 - \omega}{\omega_b}\right) \\ &= \frac{\pi m \omega_b^4}{2k^3} \int dv_0 f(v_0) v_0 \frac{d}{dv_0} \delta\left(v_0 - \frac{\omega}{k}\right) \\ &= -\frac{\pi m \omega_b^4}{2k^3} \left[\frac{d}{dv_0} (f(v_0)v_0) \right]_{v_0=\omega/k}.\end{aligned}\quad (3.252)$$

If the distribution function has the Maxwellian form $f \sim \exp(-v_0^2/2v_T^2)$ where v_T is the thermal velocity, and if $\omega/k \gg v_T$ then

$$\begin{aligned} \left[\frac{d}{dv_0} (f(v_0)v_0) \right]_{v_0=\omega/k} &= \left[v_0 \frac{d}{dv_0} (f(v_0)) + f(v_0) \right]_{v_0=\omega/k} \\ &= \left[-2 \frac{v_0^2}{v_T^2} f(v_0) + f(v_0) \right]_{v_0=\omega/k} \end{aligned} \quad (3.253)$$

showing that the derivative of f is the dominant term. Hence, Eq.(3.252) becomes

$$\left\langle \frac{dW_{\text{total}}}{dt} \right\rangle = -\frac{\pi m \omega_b^4 \omega}{2k^4} \left[\frac{d}{dv_0} (f(v_0)) \right]_{v_0=\omega/k}. \quad (3.254)$$

Substituting for the bounce frequency using Eq.(3.223) this becomes

$$\left\langle \frac{dW_{\text{total}}}{dt} \right\rangle = -\frac{\pi m \omega}{2k^2} \left(\frac{qk\phi_0}{m} \right)^2 \left[\frac{d}{dv_0} (f(v_0)) \right]_{v_0=\omega/k}. \quad (3.255)$$

Thus particles *gain* kinetic energy at the expense of the wave if the distribution function has negative slope in the range $v \sim \omega/k$. This process is called Landau damping and will be examined in the Chapter 5 from the wave viewpoint.

3.10 Assignments

1. A charged particle starts from *rest* in combined static fields $\mathbf{E} = E\hat{y}$ and $\mathbf{B} = B\hat{z}$ where $E/B \ll c$ and c is the speed of light. Calculate and plot its exact trajectory (do this both analytically and numerically).
2. Calculate (qualitatively and numerically) the trajectory of a particle starting from rest at $x = 0$, $y = 5a$ in combined E and B fields where $\mathbf{E} = E_0\hat{x}$ and $\mathbf{B} = \hat{z}B_0y/a$. What happens to μ conservation on the line $y = 0$? Sketch the motion showing both the Larmor motion and the guiding center motion.
3. Calculate the motion of a particle in the steady state electric field produced by a line charge λ along the z axis and a steady state magnetic field $\mathbf{B} = B_0\hat{z}$. Obtain an approximate solution using drift theory and also obtain a solution using Hamilton-Lagrange theory. Hint -for the drift theory show that the electric field has the form $\mathbf{E} = \hat{r}\lambda/2\pi r$. Assume that λ is small for approximate solutions.
4. Consider the magnetic field produced by a toroidal coil system; this coil consists of a single wire threading the hole of a torus (donut) N times with the N turns evenly arranged around the circumference of the torus. Use Ampere's law to show that the magnetic field is in the toroidal direction and has the form $B = \mu NI/2\pi r$ where N is the total number of turns in the coil and I is the current through the turn. What are the drifts for a particle having finite initial velocities both parallel and perpendicular to this toroidal field.

5. Show that of all the standard drifts ($\mathbf{E} \times \mathbf{B}$, ∇B , curvature, polarization) only the polarization drift causes a change in the particle energy. Hint: consider what happens when the following equation is dotted with \mathbf{v} :

$$m \frac{d\mathbf{v}}{dt} = \mathbf{F} + \mathbf{v} \times \mathbf{B}$$

6. Use the numerical Lorentz solver to calculate the motion of a charged particle in a uniform magnetic field $\mathbf{B} = B\hat{z}$ and an electric field given by Eq.(3.177). Compare the motion to the predictions of drift theory ($E \times B$, polarization). Describe the motion for cases where $\alpha \ll 1$, $\alpha \simeq 1$, and $\alpha \gg 1$ where $\alpha = mk^2\phi/qB^2$. Describe what happens when α becomes of order unity.
7. A “magnetic mirror” field in cylindrical coordinates r, θ, z can be expressed as $\mathbf{B} = (2\pi)^{-1} \nabla\psi \times \nabla\theta$ where $\psi = B_0\pi r^2(1 + (z/L)^2)$ where L is a characteristic length. Sketch by hand the field line pattern in the r, z plane and write out the components of \mathbf{B} . What are appropriate characteristic lengths, times, and velocities for an electron in this configuration? Use $r = (x^2 + y^2)^{1/2}$ and numerically integrate the orbit of an electron starting at $x = 0, y = L, z = 0$ with initial velocity $v_x = 0$ and initial v_y, v_z of the order of the characteristic velocity (try different values). Simultaneously plot the motion in the z, y plane and in the x, y plane. What interesting phenomena can be observed (e.g., reflection)? Does the electron stay on a constant ψ contour?
8. Consider the motion of a charged particle in the magnetic field

$$\mathbf{B} = \frac{1}{2\pi} \nabla\psi(r, z, t) \times \nabla\theta$$

where

$$\psi(r, z, t) = B_{\min}\pi r^2 \left[1 + 2\lambda \frac{\zeta^2}{\zeta^4 + 1} \right]$$

and

$$\zeta = \frac{z}{L(t)}.$$

Show by explicit evaluation of the flux derivatives and also by plotting contours of constant flux that this is an example of a magnetic mirror field with minimum axial field B_{\min} when $z = 0$ and maximum axial field λB_{\min} at $z = L(t)$. By making $L(t)$ a slowly decreasing function of time show that the magnetic mirrors slowly move together. Using numerical techniques to integrate the equation of motion, demonstrate Fermi acceleration of a particle when the mirrors move slowly together. Do not forget the electric field associated with the time-changing magnetic field (this electric field is closely related to the time derivative of $\psi(r, z, t)$; use Faraday’s law). Plot the velocity space angle at $z = 0$ for each bounce between mirrors and show that the particle becomes detrapped when this angle decreases below $\theta_{trap} = \sin^{-1}(\lambda^{-1})$.

9. Consider a point particle bouncing with nominal velocity v between a stationary wall and a second wall which is approaching the first wall with speed u . Calculate the change in speed of the particle after it bounces from the moving wall (hint: do this first in the frame of the moving wall, and then translate back to the lab frame). Calculate τ_b

the time for the particle to make one complete bounce between the walls if the nominal distance between walls is L . Calculate ΔL , the change in L during one complete bounce and show that if $u \ll v$, then Lv is a conserved quantity. By considering collisionless particles bouncing in a cube which is slowly shrinking self-similarly in three dimensions show that $PV^{5/3}$ is constant where $P = n\kappa T$, n is the density of the particles and T is the average kinetic energy of the particles. What happens if the shrinking is not self-similar (hint: consider the effect of collisions and see discussion in Bellan (2004a)).

10. Using numerical techniques to integrate the equation of motion illustrate how a charged particle changes from being non-axis-encircling to axis-encircling when a magnetic field $\mathbf{B} = (2\pi)^{-1} \nabla\psi(r, z, t) \times \nabla\theta$ reverses polarity at $t = 0$. For simplicity use $\psi = B(t)\pi r^2$, i.e., a uniform magnetic field. To make the solution as general as possible, normalize time to the cyclotron frequency by defining $\tau = \omega_c t$, and set $B(\tau) = \tanh \tau$ to represent a polarity reversing field. Normalize lengths to some reference length L and normalize velocities to $\omega_c L$. Show that the canonical angular momentum is conserved. Hint - do not forget about the inductive electric field associated with a time-dependent magnetic field.

11. Consider a cusp magnetic field given by $\mathbf{B} = (2\pi)^{-1} \nabla\psi(r, z) \times \nabla\theta$ where the flux function

$$\psi(r, z) = B\pi r^2 \frac{z}{\sqrt{1 + z^2/a^2}}.$$

is antisymmetric in z . Plot the surfaces of constant flux. Using numerical techniques to integrate the equation of motion demonstrate that a particle incident at $z \ll -a$ and $r = r_0$ with incident velocity $\mathbf{v} = v_{z0}\hat{z}$ will reflect from the cusp if $v_{z0} < r_0\omega_c$ where $\omega_c = qB/m$.

12. Consider the motion of a charged particle starting from rest in a simple one dimensional electrostatic wave field:

$$m \frac{d^2x}{dt^2} = -q \nabla \phi(x, t)$$

where $\phi(x, t) = \bar{\phi} \cos(kx - \omega t)$. How large does $\bar{\phi}$ have to be to give trapping of particles that start from rest. Demonstrate this trapping threshold numerically.

13. Prove Equation (3.218).

14. Prove that

$$\delta(z) = \lim_{N \rightarrow \infty} \frac{\sin(Nz)}{\pi z}$$

is a valid representation for the delta function.

15. As sketched in Fig.3.18, a current loop (radius r , current I) is located in the $x - y$ plane; the loop's axis defines the z axis of the coordinate system, so that the center of the loop is at the origin. The loop is immersed in a non-uniform magnetic field \mathbf{B} produced by external coils and oriented so that the magnetic field lines converge symmetrically about the z -axis. The current I is small and does not significantly modify \mathbf{B} . Consider the following three circles: the current loop, a circle of radius b coaxial with the loop but with center at $z = -L/2$ and a circle of radius a with

center at $z = +L/2$. The radii a and b are chosen so as to intercept the field lines that intercept the current loop (see figure). Assume the figure is somewhat exaggerated so that B_z is approximately uniform over each of the three circular surfaces and so one may ignore the radial dependence of B_z and therefore express $B_z = B_z(z)$.

(a) Note that $r = (a + b)/2$. What is the force (magnitude and direction) on the current loop expressed in terms of I , $B_z(0)$, a , b and L only? [Hint- use the field line slope to give a relationship between B_r and B_z at the loop radius.]

(b) For each of the circles and the current loop, express the magnetic flux enclosed in terms of B_z at the respective entity and the radius of the entity. What is the relationship between the B_z 's at these three entities?

(c) By combining the results of parts (a) and (b) above and taking the limit $L \rightarrow 0$, show that the force on the loop can be expressed in terms of a derivative of B_z .

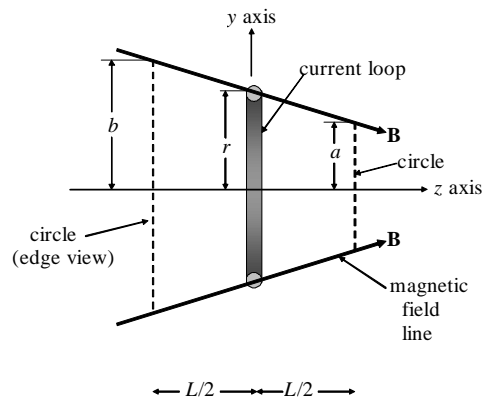


Figure 3.18: Non-uniform magnetic field acting on a current loop.

Elementary plasma waves

4.1 General method for analyzing small amplitude waves

All plasma phenomena can be described by combining Maxwell's equations with the Lorentz equation where the Lorentz equation is represented by the Vlasov, two-fluid or MHD approximations. The subject of linear plasma waves provides a good introduction to the study of plasma phenomena because linear waves are relatively simple to analyze and yet demonstrate many of the essential features of plasma behavior.

Linear analysis, a straightforward method applicable to any set of partial differential equations describing a physical system, reveals the physical system's simplest non-trivial, self-consistent dynamical behavior. In the context of plasma dynamics, the method is as follows:

1. By making appropriate physical assumptions, the general Maxwell-Lorentz system of equations is reduced to the simplest set of equations characterizing the phenomena under consideration.
2. An equilibrium solution is determined for this set of equations. The equilibrium might be trivial such that densities are uniform, the plasma is neutral, and all velocities are zero. However, less trivial equilibria could also be invoked where there are density gradients or flow velocities. Equilibrium quantities are designated by the subscript 0, indicating 'zero-order' in smallness.
3. If f, g, h , etc. represent the dependent variables and it is assumed that a specific perturbation is prescribed for one of these variables, then solving the system of differential equations will give the responses of all the other dependent variables to this prescribed perturbation. For example, suppose that a perturbation ϵf_1 is prescribed for the dependent variable f so that f becomes

$$f = f_0 + \epsilon f_1. \quad (4.1)$$

The system of differential equations gives the functional dependence of the other variables on f , and for example, would give $g = g(f) = g(f_0 + \epsilon f_1)$. Since the functional dependence of g on f is in general nonlinear, Taylor expansion gives $g = g_0 + \epsilon g_1 + \epsilon^2 g_2 + \epsilon^3 g_3 + \dots$. The ϵ 's are, from now on, considered implicit and

so the variables are written as

$$\begin{aligned} f &= f_0 + f_1 \\ g &= g_0 + g_1 + g_2 + \dots \\ h &= h_0 + h_1 + h_2 + \dots \end{aligned} \quad (4.2)$$

and it is assumed that the order of magnitude of f_1 is smaller than the magnitude of f_0 by a factor ϵ , etc. The smallness of the perturbation is an assumption which obviously must be satisfied in the real situation being modeled. Note that there is no f_2 or higher f terms because the perturbation to f was prescribed as being f_1 .

4. Each partial differential equation is re-written with all dependent quantities expanded to first order as in Eq.(4.2). For example, the two fluid continuity equation becomes

$$\frac{\partial(n_0 + n_1)}{\partial t} + \nabla \cdot [(n_0 + n_1)(\mathbf{u}_0 + \mathbf{u}_1)] = 0. \quad (4.3)$$

By assumption, equilibrium quantities satisfy

$$\frac{\partial n_0}{\partial t} + \nabla \cdot (n_0 \mathbf{u}_0) = 0. \quad (4.4)$$

The essence of linearization consists of subtracting the equilibrium equation (e.g., Eq.(4.4)) from the expanded equation (e.g., Eq.(4.3)). For this example such a subtraction yields

$$\frac{\partial n_1}{\partial t} + \nabla \cdot [n_1 \mathbf{u}_0 + n_0 \mathbf{u}_1 + n_1 \mathbf{u}_1] = 0. \quad (4.5)$$

The nonlinear term $n_1 \mathbf{u}_1$ which is a product of *two* first order quantities is discarded because it is of order ϵ^2 whereas all the other terms are of order ϵ . What remains is called the linearized equation, i.e., the equation which consists of only first-order terms. For the example here, the linearized equation would be

$$\frac{\partial n_1}{\partial t} + \nabla \cdot [n_1 \mathbf{u}_0 + n_0 \mathbf{u}_1] = 0.$$

The linearized equation is in a sense the differential of the original equation.

Before engaging in a methodical study of the large variety of waves that can propagate in a plasma, a few special cases of fundamental importance will first be examined.

4.2 Two-fluid theory of unmagnetized plasma waves

The simplest plasma waves are those described by two-fluid theory in an unmagnetized plasma, i.e., a plasma which has no equilibrium magnetic field. The theory for these waves also applies to magnetized plasmas in the special situation where all fluid motions are strictly parallel to the equilibrium magnetic field because fluid flowing along a magnetic field experience no $\mathbf{u} \times \mathbf{B}$ force and so behaves as if there were no magnetic field.

The two-fluid equation of motion corresponding to an unmagnetized plasma is

$$m_\sigma n_\sigma \frac{d\mathbf{u}_\sigma}{dt} = q_\sigma n_\sigma \mathbf{E} - \nabla P_\sigma \quad (4.6)$$

and these simple plasma waves are found by linearizing about an equilibrium where $\mathbf{u}_{\sigma 0} = 0$, $\mathbf{E}_0 = 0$, and $P_{\sigma 0}$ are all constant in time and uniform in space. The linearized form of

Eq. (4.6) is then

$$m_\sigma n_{\sigma 0} \frac{\partial \mathbf{u}_{\sigma 1}}{\partial t} = q_\sigma n_{\sigma 0} \mathbf{E}_1 - \nabla P_{\sigma 1}. \quad (4.7)$$

The electric field can be expressed as

$$\mathbf{E} = -\nabla\phi - \frac{\partial \mathbf{A}}{\partial t}, \quad (4.8)$$

a form that automatically satisfies Faraday's law. The vector potential \mathbf{A} is undefined with respect to a gauge since $\mathbf{B} = \nabla \times (\mathbf{A} + \nabla\psi) = \nabla \times \mathbf{A}$. It is convenient to choose ψ so as to have $\nabla \cdot \mathbf{A} = 0$. This is called Coulomb gauge and causes the divergence of Eq.(4.8) to give Poisson's equation so that charge density provides the only source term for the electrostatic potential ϕ . Since Eq. (4.8) is linear to begin with, its linearized form is just

$$\mathbf{E}_1 = -\nabla\phi_1 - \frac{\partial \mathbf{A}_1}{\partial t}. \quad (4.9)$$

4.2.1 Electrostatic (compressional waves)

These waves are characterized by having finite $\nabla \cdot \mathbf{u}_1$ and are variously called compressional, electrostatic, or longitudinal waves. The first step in the analysis is to take the divergence of Eq.(4.7) to obtain

$$m_\sigma n_{\sigma 0} \frac{\partial \nabla \cdot \mathbf{u}_{\sigma 1}}{\partial t} = -q_\sigma n_{\sigma 0} \nabla^2 \phi_1 - \nabla^2 P_{\sigma 1}. \quad (4.10)$$

Because Eq.(4.10) involves three variables (i.e., $\mathbf{u}_{\sigma 1}, \phi_1, P_{\sigma 1}$) two more equations are required to provide a complete description. One of these additional equations is the linearized continuity equation

$$\frac{\partial n_{\sigma 1}}{\partial t} + n_0 \nabla \cdot \mathbf{u}_{\sigma 1} = 0 \quad (4.11)$$

which, after substitution into Eq.(4.10), gives

$$m_\sigma \frac{\partial^2 n_{\sigma 1}}{\partial t^2} = q_\sigma n_{\sigma 0} \nabla^2 \phi_1 + \nabla^2 P_{\sigma 1}. \quad (4.12)$$

For adiabatic processes the pressure and density are related by

$$\frac{P_\sigma}{n_\sigma^\gamma} = \text{const}. \quad (4.13)$$

where $\gamma = (N + 2)/N$ and N is the dimensionality of the system, whereas for isothermal processes

$$\frac{P_\sigma}{n_\sigma} = \text{const}. \quad (4.14)$$

The same formalism can therefore be used for both isothermal and adiabatic processes by using Eq. (4.13) for both and then simply setting $\gamma = 1$ if the process is isothermal. Linearization of Eq.(4.13) gives

$$\frac{P_{\sigma 1}}{P_{\sigma 0}} = \gamma \frac{n_{\sigma 1}}{n_{\sigma 0}} \quad (4.15)$$

so Eq. (4.12) becomes

$$m_\sigma \frac{\partial^2 n_{\sigma 1}}{\partial t^2} = q_\sigma n_{\sigma 0} \nabla^2 \phi_1 + \gamma \kappa T_{\sigma 0} \nabla^2 n_{\sigma 1} \quad (4.16)$$

where $P_{\sigma 0} = n_{\sigma 0} \kappa T_{\sigma 0}$ has been used.

Although this system of linear equations could be solved by the formal method of Fourier transforms, we instead take the shortcut of making the simplifying assumption that the linear perturbation happens to be a single Fourier mode. Thus, it is assumed that *all* linearized dependent variables have the wave-like dependence

$$n_{\sigma 1} \sim \exp(\mathbf{i}\mathbf{k} \cdot \mathbf{x} - i\omega t), \quad \phi_1 \sim \exp(\mathbf{i}\mathbf{k} \cdot \mathbf{x} - i\omega t), \quad \text{etc.} \quad (4.17)$$

so that $\nabla \rightarrow \mathbf{i}\mathbf{k}$ and $\partial/\partial t \rightarrow -i\omega$. Equation (4.16) therefore reduces to the algebraic equation

$$m_\sigma \omega^2 n_{\sigma 1} = q_\sigma n_{\sigma 0} k^2 \phi_1 + \gamma \kappa T_{\sigma 0} k^2 n_{\sigma 1} \quad (4.18)$$

which may be solved for $n_{\sigma 1}$ to give

$$n_{\sigma 1} = \frac{q_\sigma n_{\sigma 0}}{m_\sigma} \frac{k^2 \phi_1}{(\omega^2 - \gamma k^2 \kappa T_{\sigma 0} / m_\sigma)}. \quad (4.19)$$

Poisson's equation provides another relation between ϕ_1 and $n_{\sigma 1}$, namely

$$-k^2 \phi_1 = \frac{1}{\epsilon_0} \sum_\sigma n_{\sigma 1} q_\sigma. \quad (4.20)$$

Equation (4.19) is substituted into Poisson's equation to give

$$k^2 \phi_1 = \sum_\sigma \frac{n_{\sigma 0} q_\sigma^2}{\epsilon_0 m_\sigma} \frac{k^2 \phi_1}{(\omega^2 - \gamma k^2 \kappa T_{\sigma 0} / m_\sigma)} \quad (4.21)$$

which may be re-arranged as

$$\left[1 - \sum_\sigma \frac{\omega_{p\sigma}^2}{(\omega^2 - \gamma k^2 \kappa T_{\sigma 0} / m_\sigma)} \right] \phi_1 = 0 \quad (4.22)$$

where

$$\omega_{p\sigma}^2 \equiv \frac{n_{\sigma 0} q_\sigma^2}{\epsilon_0 m_\sigma} \quad (4.23)$$

is the square of the *plasma frequency* of species σ . A useful way to recast Eq.(4.22) is

$$(1 + \chi_e + \chi_i) \phi_1 = 0 \quad (4.24)$$

where

$$\chi_\sigma = - \frac{\omega_{p\sigma}^2}{(\omega^2 - \gamma k^2 \kappa T_{\sigma 0} / m_\sigma)} \quad (4.25)$$

is called the susceptibility of species σ . In Eq.(4.24) the "1" comes from the "vacuum" part of Poisson's equation (i.e., the LHS term $\nabla^2 \phi$) while the susceptibilities give the respective contributions of each species to the right hand side of Poisson's equation. This formalism follows that of dielectrics where the displacement vector is $\mathbf{D} = \epsilon \mathbf{E}$ and the dielectric constant is $\epsilon = 1 + \chi$ where χ is a susceptibility.

Equation (4.24) shows that if $\phi_1 \neq 0$, the quantity $1 + \chi_e + \chi_i$ must vanish. In other words, in order to have a non-trivial normal mode it is necessary to have

$$1 + \chi_e + \chi_i = 0. \quad (4.26)$$

This is called a dispersion relation and prescribes a functional relation between ω and k . The dispersion relation can be considered as the determinant-like equation for the eigenvalues $\omega(k)$ of the system of equations.

The normal modes can be identified by noting that Eq.(4.25) has two limiting behaviors depending on how the wave phase velocity compares to $\sqrt{\kappa T_{\sigma 0}/m_\sigma}$, a quantity which is of the order of the thermal velocity. These limiting behaviors are

1. Adiabatic regime: $\omega/k \gg \sqrt{\kappa T_{\sigma 0}/m_\sigma}$ and $\gamma = (N + 2)/N$. Because plane waves are one-dimensional perturbations (i.e., the plasma is compressed in the $\hat{\mathbf{k}}$ direction only), $N = 1$ so that $\gamma = 3$. Hence the susceptibility has the limiting form

$$\begin{aligned} \chi_\sigma &= -\frac{\omega_{p\sigma}^2}{\omega^2(1 - \gamma k^2 \kappa T_{\sigma 0}/m_\sigma \omega^2)} \\ &\simeq -\frac{\omega_{p\sigma}^2}{\omega^2} \left(1 + 3 \frac{k^2 \kappa T_{\sigma 0}}{\omega^2 m_\sigma} \right) \\ &= -\frac{1}{k^2 \lambda_{D\sigma}^2} \frac{k^2 \kappa T_{\sigma 0}}{\omega^2 m_\sigma} \left(1 + 3 \frac{k^2 \kappa T_{\sigma 0}}{\omega^2 m_\sigma} \right). \end{aligned} \quad (4.27)$$

2. Isothermal regime: $\omega/k \ll \sqrt{\kappa T_{\sigma 0}/m_\sigma}$ and $\gamma = 1$. Here the susceptibility has the limiting form

$$\chi_\sigma = \frac{\omega_{p\sigma}^2}{k^2 \kappa T_{\sigma 0}/m_\sigma} = \frac{1}{k^2 \lambda_{D\sigma}^2}. \quad (4.28)$$

Figure 4.1 shows a plot of $\chi_\sigma k^2 \lambda_{D\sigma}^2$ versus $\omega/k \sqrt{\kappa T_{\sigma 0}/m_\sigma}$. The isothermal and adiabatic susceptibilities are seen to be substantially different and, in particular, do not coalesce when $\omega/k \sqrt{\kappa T_{\sigma 0}/m_\sigma} \rightarrow 1$. This non-coalescence as $\omega/k \sqrt{\kappa T_{\sigma 0}/m_\sigma} \rightarrow 1$ indicates that the fluid description, while valid in both the adiabatic and isothermal limits, fails in the vicinity of $\omega/k \sim \sqrt{\kappa T_{\sigma 0}/m_\sigma}$. As will be seen later, the more accurate Vlasov description must be used in the $\omega/k \sim \sqrt{\kappa T_{\sigma 0}/m_\sigma}$ regime.

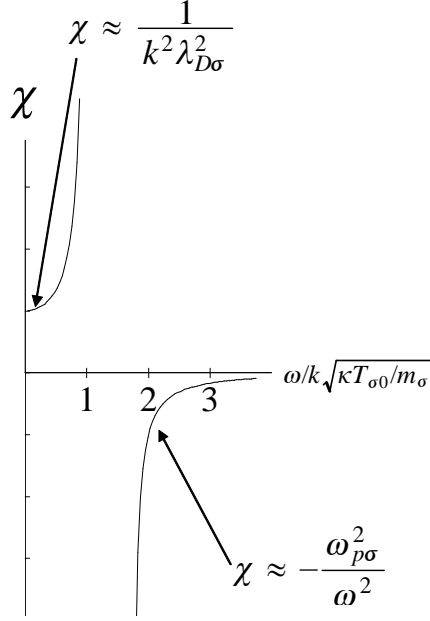


Figure 4.1: Susceptibility χ as a function of $\omega/k\sqrt{\kappa T_{\sigma 0}/m_{\sigma}}$.

Since the ion-to-electron mass ratio is large, ions and electrons typically have thermal velocities differing by at least one and sometimes two orders of magnitude. Furthermore, ion and electron temperatures often differ, again allowing substantially different electron and ion thermal velocities. Three different situations can occur in a typical plasma depending on how the wave phase velocity compares to thermal velocities. These situations are:

1. Case where $\omega/k \gg \sqrt{\kappa T_{e0}/m_e}, \sqrt{\kappa T_{i0}/m_i}$

Here both electrons and ions are adiabatic and the dispersion relation becomes

$$1 - \frac{\omega_{pe}^2}{\omega^2} \left(1 + 3 \frac{k^2 \kappa T_{e0}}{\omega^2 m_e} \right) - \frac{\omega_{pi}^2}{\omega^2} \left(1 + 3 \frac{k^2 \kappa T_{i0}}{\omega^2 m_i} \right) = 0. \quad (4.29)$$

Since $\omega_{pe}^2/\omega_{pi}^2 = m_i/m_e$ the ion contribution can be dropped, and the dispersion becomes

$$1 - \frac{\omega_{pe}^2}{\omega^2} \left(1 + 3 \frac{k^2 \kappa T_{e0}}{\omega^2 m_e} \right) = 0. \quad (4.30)$$

To lowest order, the solution of this equation is simply $\omega^2 = \omega_{pe}^2$. An iterative solution may be obtained by substituting this lowest order solution into the thermal term which, by assumption, is a small correction because $\omega/k \gg \sqrt{\kappa T_{e0}/m_e}$. This gives the

standard form for the high-frequency, electrostatic, unmagnetized plasma wave

$$\omega^2 = \omega_{pe}^2 + 3k^2 \frac{\kappa T_{e0}}{m_e}. \quad (4.31)$$

This most basic of plasma waves is called the electron plasma wave, the Langmuir wave (Langmuir 1928), or the Bohm-Gross wave (Bohm and Gross 1949).

2. Case where $\omega/k \ll \sqrt{\kappa T_{e0}/m_e}, \sqrt{\kappa T_{i0}/m_i}$

Here both electrons and ions are isothermal and the dispersion becomes

$$1 + \sum_{\sigma} \frac{1}{k^2 \lambda_{D\sigma}^2} = 0. \quad (4.32)$$

This has no frequency dependence, and is just the Debye shielding derived in Chapter 1. Thus, when $\omega/k \ll \sqrt{\kappa T_{e0}/m_e}, \sqrt{\kappa T_{i0}/m_i}$ the plasma approaches the steady-state limit and screens out any applied perturbation. This limit shows why ions cannot provide Debye shielding for electrons, because if the test particle were chosen to be an electron then its nominal speed would be the electron thermal velocity and from the point of view of an ion the test particle motion would constitute a disturbance with phase velocity $\omega/k \sim v_{Te}$ which would then violate the assumption $\omega/k \ll \sqrt{\kappa T_{i0}/m_i}$.

3. Case where $\sqrt{\kappa T_{i0}/m_i} \ll \omega/k \ll \sqrt{\kappa T_{e0}/m_e}$

Here the ions act adiabatically whereas the electrons act isothermally so that the dispersion becomes

$$1 + \frac{1}{k^2 \lambda_{De}^2} - \frac{\omega_{pi}^2}{\omega^2} \left(1 + 3 \frac{k^2}{\omega^2} \frac{\kappa T_{i0}}{m_i} \right) = 0. \quad (4.33)$$

It is conventional to define the ‘ion acoustic’ velocity

$$c_s^2 = \omega_{pi}^2 \lambda_{De}^2 = \kappa T_e / m_i \quad (4.34)$$

so that Eq.(4.33) can be recast as

$$\omega^2 = \frac{k^2 c_s^2}{1 + k^2 \lambda_{De}^2} \left(1 + 3 \frac{k^2}{\omega^2} \frac{\kappa T_{i0}}{m_i} \right). \quad (4.35)$$

Since $\omega/k \gg \sqrt{\kappa T_{i0}/m_i}$, this may be solved iteratively by first assuming $T_{i0} = 0$ giving

$$\omega^2 = \frac{k^2 c_s^2}{1 + k^2 \lambda_{De}^2}. \quad (4.36)$$

This is the most basic form for the *ion acoustic wave* dispersion and in the limit $k^2 \lambda_{De}^2 \gg 1$, becomes simply $\omega^2 = c_s^2 / \lambda_{De}^2 = \omega_{pi}^2$. To obtain the next higher order of precision for the ion acoustic dispersion, Eq.(4.36) may be used to eliminate k^2 / ω^2 from the ion thermal term of Eq.(4.35) giving

$$\omega^2 = \frac{k^2 c_s^2}{1 + k^2 \lambda_{De}^2} + 3k^2 \frac{\kappa T_{i0}}{m_i}. \quad (4.37)$$

For self-consistency, it is necessary to have $c_s^2 \gg \kappa T_{i0}/m_i$; if this were not true, the ion acoustic wave would become $\omega^2 = 3k^2 \kappa T_{i0}/m_i$ which would violate the assumption that $\omega/k \gg \sqrt{\kappa T_{i0}/m_i}$. The condition $c_s^2 \gg \kappa T_{i0}/m_i$ is the same as $T_e \gg T_i$ so ion acoustic waves can only propagate when the electrons are much hotter than the ions. This issue will be further explored when ion acoustic waves are re-examined from the Vlasov point of view.

4.2.2 Electromagnetic (incompressible) waves

The compressional waves discussed in the previous section were obtained by taking the divergence of Eq. (4.7). An arbitrary vector field \mathbf{V} can always be decomposed into a gradient of a potential and a solenoidal part, i.e., it can always be written as $\mathbf{V} = \nabla\psi + \nabla \times \mathbf{Q}$ where ψ and \mathbf{Q} can be determined from \mathbf{V} . The potential gradient $\nabla\psi$ has zero curl and so describes a conservative field whereas the solenoidal term $\nabla \times \mathbf{Q}$ has zero divergence and describes a non-conservative field. Because Coulomb gauge is being used, the $-\nabla\phi$ term on the right hand side of Eq.(4.8) is the only conservative field; the $-\partial\mathbf{A}/\partial t$ term is the solenoidal or non-conservative field.

Waves involving finite \mathbf{A} have coupled electric and magnetic fields and are a generalization of vacuum electromagnetic waves such as light or radio waves. These finite \mathbf{A} waves are variously called electromagnetic, transverse, or incompressible waves. Since no electrostatic potential is involved, $\nabla \cdot \mathbf{E} = 0$ and the plasma remains neutral. Because $\mathbf{A} \neq 0$, these waves involve electric currents.

Since the electromagnetic waves are solenoidal, the $-\nabla\phi$ term in Eq. (4.7) is superfluous and can be eliminated by taking the curl of Eq. (4.7) giving

$$\frac{\partial}{\partial t} \nabla \times (m_\sigma n_\sigma \mathbf{u}_{\sigma 1}) = -q_\sigma n_\sigma \frac{\partial \mathbf{B}_1}{\partial t}. \quad (4.38)$$

To obtain an equation involving currents, Eq.(4.38) is integrated with respect to time, multiplied by q_σ/m_σ , and then summed over species to give

$$\nabla \times \mathbf{J}_1 = -\varepsilon_0 \omega_p^2 \mathbf{B}_1 \quad (4.39)$$

where

$$\omega_p^2 = \sum_\sigma \omega_{p\sigma}^2. \quad (4.40)$$

However, Ampere's law can be written in the form

$$\mathbf{J}_1 = \frac{1}{\mu_0} \nabla \times \mathbf{B}_1 - \varepsilon_0 \frac{\partial \mathbf{E}_1}{\partial t} \quad (4.41)$$

which, after substitution into Eq. (4.39), gives

$$\nabla \times \left(\nabla \times \mathbf{B}_1 - \frac{1}{c^2} \frac{\partial \mathbf{E}_1}{\partial t} \right) = -\frac{\omega_p^2}{c^2} \mathbf{B}_1. \quad (4.42)$$

Using the vector identity $\nabla \times (\nabla \times \mathbf{Q}) = \nabla(\nabla \cdot \mathbf{Q}) - \nabla^2 \mathbf{Q}$ and Faraday's law this becomes

$$\nabla^2 \mathbf{B}_1 = \frac{1}{c^2} \frac{\partial^2 \mathbf{B}_1}{\partial t^2} + \frac{\omega_p^2}{c^2} \mathbf{B}_1. \quad (4.43)$$

In the limit of no plasma so that $\omega_p^2 \rightarrow 0$, Eq.(4.43) reduces to the standard vacuum electromagnetic wave. If it is assumed that $\mathbf{B}_1 \sim \exp(i\mathbf{k} \cdot \mathbf{x} - i\omega t)$, Eq.(4.43) becomes the electromagnetic, unmagnetized plasma wave dispersion

$$\omega^2 = \omega_p^2 + k^2 c^2. \quad (4.44)$$

Waves satisfying Eq. (4.44) are often used to measure plasma density. Such a measurement can be accomplished two ways:

1. Cutoff method

If $\omega^2 < \omega_p^2$ then k^2 becomes negative, the wave does not propagate, and only exponentially growing or decaying spatial behavior occurs (such behavior is called evanescent). If the wave is excited by an antenna driven by a fixed-frequency oscillator, the boundary condition that the wave field does not diverge at infinity means that only waves that decay away from the antenna exist. Thus, the field is localized near the antenna and there is no wave-like behavior. This is called *cutoff*. When the oscillator frequency is raised above ω_p , the wave starts to propagate so that a receiver located some distance away will abruptly start to pick up the wave. By scanning the transmitter frequency and noting the frequency at which the wave starts to propagate ω_p^2 is determined, giving a direct, unambiguous measurement of the plasma density.

2. Phase shift method

Here the oscillator frequency is set to be well above cutoff so that the wave is always propagating. The dispersion relation is solved for k and the phase delay $\Delta\phi$ of the wave through the plasma is measured by interferometric fringe-counting. The total phase delay through a length L of plasma is

$$\phi = \int_0^L k dx = \frac{1}{c} \int_0^L [\omega^2 - \omega_p^2]^{1/2} dx \simeq \frac{\omega}{c} \int_0^L \left[1 - \frac{\omega_p^2}{2\omega^2} \right] dx \quad (4.45)$$

so that the phase delay due to the presence of plasma is

$$\Delta\phi = -\frac{1}{2\omega c} \int_0^L \omega_{pe}^2 dx = -\frac{e^2}{2\omega c m_e \epsilon_0} \int_0^L n dx. \quad (4.46)$$

Thus, measurement of the phase shift $\Delta\phi$ due to the presence of plasma can be used to measure the average density along L ; this density is called the *line-averaged density*.

4.3 Low frequency magnetized plasma: Alfvén waves

4.3.1 Overview of Alfvén waves

We now consider low frequency waves propagating in a *magnetized* plasma, i.e. a plasma immersed in a uniform, constant magnetic field $\mathbf{B} = B_0 \hat{z}$. By low frequency, it is meant that the wave frequency ω is much smaller than the ion cyclotron frequency ω_{ci} . Several types of waves exist in this frequency range; certain of these involve electric fields having a purely electrostatic character (i.e., $\nabla \times \mathbf{E} = 0$), whereas others involve electric fields having

an inductive character (i.e., $\nabla \times \mathbf{E} \neq \mathbf{0}$). Faraday's law $\nabla \times \mathbf{E} = -\partial \mathbf{B} / \partial t$ shows that if the electric field is electrostatic the magnetic field must be constant, whereas inductive electric fields must have an associated time-dependent magnetic field.

We now further restrict attention to a specific category of these $\omega \ll \omega_{ci}$ modes. This category, called Alfvén waves are the normal modes of MHD, involve magnetic perturbations and have characteristic velocities of the order of the Alfvén velocity $v_A = B / \sqrt{\mu_0 \rho}$. The existence of such modes is not surprising if one considers that ordinary sound waves have a velocity $c_s = \sqrt{\gamma P / \rho}$ and the magnetic stress tensor scales as $\sim B^2 / \mu_0 \rho$ so that Alfvén-type velocities will result if P is replaced by $B^2 / 2\mu_0$. Two distinct kinds of Alfvén modes exist and to complicate matters these are called a variety of names by different authors. One mode, variously called the fast mode, the compressional mode, or the magnetosonic mode resembles a sound wave and involves compression and rarefaction of magnetic field lines; this mode has a finite B_{z1} . The other mode, variously called the Alfvén mode, the shear mode, the torsional mode, or the slow mode, involves twisting, shearing, or plucking motions; this mode has $B_{z1} = 0$. This latter mode appears in two distinct versions when modeled using two-fluid or Vlasov theory depending on the plasma β ; these are respectively called the inertial Alfvén wave and the kinetic Alfvén wave.

4.3.2 Zero-pressure MHD model

In order to understand the basic structure of these modes, the pressure will temporarily assumed to be zero so that all MHD forces are magnetic. The fundamental dynamics of both MHD modes comes from the polarization drift associated with a time-dependent perpendicular electric field, namely

$$\mathbf{u}_{\sigma, polarization} = \frac{m_{\sigma}}{q_{\sigma} B^2} \frac{d\mathbf{E}_{\perp}}{dt}; \quad (4.47)$$

this was discussed in the derivation of Eq.(3.77). The polarization drift results in a polarization current

$$\begin{aligned} \mathbf{J}_{\perp} &= \sum n_{\sigma} q_{\sigma} \mathbf{u}_{\sigma, polarization} \\ &= \frac{\rho}{B^2} \frac{d\mathbf{E}_{\perp}}{dt} \end{aligned} \quad (4.48)$$

where $\rho = \sum n_{\sigma} m_{\sigma}$ is the mass density. This can be recast as

$$\begin{aligned} \frac{d\mathbf{E}_{\perp}}{dt} &= \frac{B^2}{\mu_0 \rho} \mu_0 \mathbf{J} \\ &= v_A^2 (\nabla \times \mathbf{B}_1)_{\perp} \end{aligned} \quad (4.49)$$

where

$$v_A^2 = \frac{B^2}{\mu_0 \rho} \quad (4.50)$$

is the Alfvén velocity. Linearization and combining with Faraday's law gives the two basic coupled equations underlying these modes,

$$\begin{aligned} \frac{\partial \mathbf{E}_{\perp 1}}{\partial t} &= v_A^2 (\nabla \times \mathbf{B}_1)_{\perp} \\ \frac{\partial \mathbf{B}_1}{\partial t} &= -\nabla \times \mathbf{E}_1. \end{aligned} \quad (4.51)$$

The fields and gradient operator can be written as

$$\begin{aligned}\mathbf{E}_1 &= \mathbf{E}_{\perp 1} \\ \mathbf{B}_1 &= \mathbf{B}_{\perp 1} + B_{z1}\hat{z} \\ \nabla &= \hat{z}\frac{\partial}{\partial z} + \nabla_{\perp}\end{aligned}\quad (4.52)$$

since $E_{z1} = 0$ in the MHD limit as obtained from the linearized ideal Ohm's law

$$\mathbf{E}_1 + \mathbf{U}_1 \times \mathbf{B} = 0. \quad (4.53)$$

The curl operators can be expanded as

$$\begin{aligned}\nabla \times \mathbf{E}_1 &= \left(\hat{z}\frac{\partial}{\partial z} + \nabla_{\perp} \right) \times \mathbf{E}_{\perp 1} \\ &= \hat{z} \times \frac{\partial \mathbf{E}_{\perp 1}}{\partial z} + \nabla_{\perp} \times \mathbf{E}_{\perp 1}\end{aligned}\quad (4.54)$$

and

$$\begin{aligned}(\nabla \times \mathbf{B}_1)_{\perp} &= \left(\left(\hat{z}\frac{\partial}{\partial z} + \nabla_{\perp} \right) \times (\mathbf{B}_{\perp 1} + B_{z1}\hat{z}) \right)_{\perp} \\ &= \hat{z} \times \frac{\partial \mathbf{B}_{\perp 1}}{\partial z} + \nabla_{\perp} B_{z1} \times \hat{z}\end{aligned}\quad (4.55)$$

where it should be noted that both $\nabla_{\perp} \times \mathbf{E}_{\perp 1}$ and $\nabla_{\perp} \times \mathbf{B}_{\perp 1}$ are in the z direction.

Slow or Alfvén mode (mode where $B_{z1} = 0$) In this case $\mathbf{B}_1 = \mathbf{B}_{\perp 1}$ and Eqs.(4.51) become

$$\begin{aligned}\frac{\partial \mathbf{E}_{\perp 1}}{\partial t} &= v_A^2 \hat{z} \times \frac{\partial \mathbf{B}_{\perp 1}}{\partial z} \\ \frac{\partial \mathbf{B}_{\perp 1}}{\partial t} &= -\hat{z} \times \frac{\partial \mathbf{E}_{\perp 1}}{\partial z}.\end{aligned}\quad (4.56)$$

This can be re-written as

$$\begin{aligned}\frac{\partial}{\partial t} (\hat{z} \times \mathbf{E}_{\perp 1}) &= -v_A^2 \frac{\partial \mathbf{B}_{\perp 1}}{\partial z} \\ \frac{\partial \mathbf{B}_{\perp 1}}{\partial t} &= -\frac{\partial}{\partial z} (\hat{z} \times \mathbf{E}_{\perp 1})\end{aligned}\quad (4.57)$$

which gives a wave equation in the coupled variables $\hat{z} \times \mathbf{E}_{\perp 1}$ and $\mathbf{B}_{\perp 1}$. Taking a second time derivative of the bottom equation and then substituting the top equation gives the wave equation for the slow mode (Alfvén mode),

$$\frac{\partial^2 \mathbf{B}_{\perp 1}}{\partial t^2} = v_A^2 \frac{\partial^2 \mathbf{B}_{\perp 1}}{\partial z^2}. \quad (4.58)$$

This is the mode originally derived by Alfvén (1943).

4.3.3 Fast mode (mode where $B_{z1} \neq 0$)

In this case only the z component of Faraday's law is used and after crossing the top equation with \hat{z} , Eqs.(4.51) become

$$\begin{aligned} \frac{\partial}{\partial t} \mathbf{E}_{\perp 1} \times \hat{z} &= v_A^2 \left(\hat{z} \times \frac{\partial \mathbf{B}_{\perp 1}}{\partial z} + \nabla_{\perp} B_{z1} \times \hat{z} \right) \times \hat{z} = v_A^2 \left(\frac{\partial \mathbf{B}_{\perp 1}}{\partial z} - \nabla_{\perp} B_{z1} \right) \\ \frac{\partial B_{1z}}{\partial t} &= -\hat{z} \cdot \nabla_{\perp} \times \mathbf{E}_{\perp 1} = -\nabla \cdot (\mathbf{E}_{\perp 1} \times \hat{z}). \end{aligned} \quad (4.59)$$

Taking a time derivative of the bottom equation and then substituting for $\mathbf{E}_{\perp 1} \times \hat{z}$ gives

$$\frac{\partial^2 B_{1z}}{\partial t^2} = -v_A^2 \nabla \cdot \left(\frac{\partial \mathbf{B}_{\perp 1}}{\partial z} - \nabla_{\perp} B_{z1} \right). \quad (4.60)$$

However, using $\nabla \cdot \mathbf{B}_1 = 0$ it is seen that

$$\nabla \cdot \mathbf{B}_{\perp 1} = -\frac{\partial B_{z1}}{\partial z} \quad (4.61)$$

and so the fast wave equation becomes

$$\begin{aligned} \frac{\partial^2 B_{1z}}{\partial t^2} &= -v_A^2 \left(\frac{\partial \nabla \cdot \mathbf{B}_{\perp 1}}{\partial z} - \nabla_{\perp}^2 B_{z1} \right) \\ &= -v_A^2 \left(-\frac{\partial^2 B_{z1}}{\partial z^2} - \nabla_{\perp}^2 B_{z1} \right) \\ &= v_A^2 \nabla^2 B_{z1}. \end{aligned} \quad (4.62)$$

4.3.4 Comparison of the two modes

The slow mode Eq.(4.58) involves z only derivatives and so has a dispersion relation

$$\omega^2 = k_z^2 v_A^2 \quad (4.63)$$

whereas the fast mode involves the ∇^2 operator and so has the dispersion relation

$$\omega^2 = k^2 v_A^2. \quad (4.64)$$

The slow mode has $B_{z1} = 0$ and so its perturbed magnetic field is entirely orthogonal to the equilibrium field. Thus the slow mode magnetic perturbation is entirely perpendicular to the equilibrium field and corresponds to a twisting or plucking of the equilibrium field. The fast mode has $B_{z1} \neq 0$ which corresponds to a compression of the equilibrium field as shown in Fig.4.2.

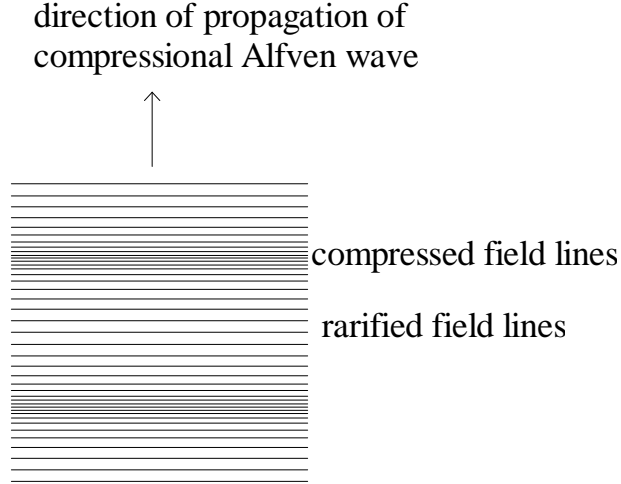


Figure 4.2: Compressional Alfvén waves

4.3.5 Finite-pressure analysis of MHD waves

If the pressure is allowed to be finite, then the two modes become coupled and an acoustic mode appears. Using the vector identity $\nabla B^2 = 2(\mathbf{B} \cdot \nabla \mathbf{B} + \mathbf{B} \times \nabla \times \mathbf{B})$ the $\mathbf{J} \times \mathbf{B}$ force in the MHD equation of motion can be written as

$$\mathbf{J} \times \mathbf{B} = -\nabla \left(\frac{B^2}{2\mu_0} \right) + \frac{1}{\mu_0} \mathbf{B} \cdot \nabla \mathbf{B}. \quad (4.65)$$

The MHD equation of motion thus becomes

$$\rho \frac{D\mathbf{U}}{Dt} = -\nabla \left(P + \frac{B^2}{2\mu_0} \right) + \frac{1}{\mu_0} \mathbf{B} \cdot \nabla \mathbf{B}. \quad (4.66)$$

Linearizing this equation about a stationary equilibrium where the pressure and the density are uniform and constant, gives

$$\rho \frac{\partial \mathbf{U}_1}{\partial t} = -\nabla \left(P_1 + \frac{\mathbf{B} \cdot \mathbf{B}_1}{\mu_0} \right) + \frac{1}{\mu_0} \mathbf{B} \cdot \nabla \mathbf{B}_1. \quad (4.67)$$

The curl of the linearized ideal MHD Ohm's law,

$$\mathbf{E}_1 + \mathbf{U}_1 \times \mathbf{B} = 0, \quad (4.68)$$

gives the induction equation

$$\frac{\partial \mathbf{B}_1}{\partial t} = \nabla \times (\mathbf{U}_1 \times \mathbf{B}), \quad (4.69)$$

while the linearized continuity equation

$$\frac{\partial \rho_1}{\partial t} + \rho \nabla \cdot \mathbf{U}_1 = 0 \quad (4.70)$$

together with the equation of state

$$\frac{P_1}{P} = \gamma \frac{\rho_1}{\rho} \quad (4.71)$$

give

$$\frac{\partial P_1}{\partial t} = -\gamma P \nabla \cdot \mathbf{U}_1. \quad (4.72)$$

To obtain an equation involving \mathbf{U}_1 only, we take the time derivative of Eq.(4.67) and use Eqs.(4.69) and (4.72) to eliminate the time derivatives of P_1 and \mathbf{B}_1 . This gives

$$\begin{aligned} \rho \frac{\partial^2 \mathbf{U}_1}{\partial t^2} = & -\nabla \left(-\gamma P \nabla \cdot \mathbf{U}_1 + \frac{1}{\mu_0} \mathbf{B} \cdot \nabla \times (\mathbf{U}_1 \times \mathbf{B}) \right) \\ & + \frac{1}{\mu_0} (\mathbf{B} \cdot \nabla) \nabla \times (\mathbf{U}_1 \times \mathbf{B}). \end{aligned} \quad (4.73)$$

This can be simplified using the identity $\nabla \cdot (\mathbf{a} \times \mathbf{b}) = \mathbf{b} \cdot \nabla \times \mathbf{a} - \mathbf{a} \cdot \nabla \times \mathbf{b}$ so that

$$\mathbf{B} \cdot \nabla \times (\mathbf{U}_1 \times \mathbf{B}) = \nabla \cdot [(\mathbf{U}_1 \times \mathbf{B}) \times \mathbf{B}] = -B^2 \nabla \cdot \mathbf{U}_{1\perp}. \quad (4.74)$$

Furthermore,

$$\mathbf{B} \cdot \nabla = B \frac{\partial}{\partial z} = ik_z B. \quad (4.75)$$

Using these relations Eq. (4.73) becomes

$$\frac{\partial^2 \mathbf{U}_1}{\partial t^2} = \nabla (c_s^2 \nabla \cdot \mathbf{U}_1 + v_A^2 \nabla \cdot \mathbf{U}_{1\perp}) + ik_z v_A^2 \nabla \times (\mathbf{U}_1 \times \hat{z}). \quad (4.76)$$

To proceed further we take either the divergence or the curl of this equation to obtain expressions for compressional or incompressible motions.

4.3.6 MHD compressional (fast) mode

Here we take the divergence of Eq. (4.76) to obtain

$$\frac{\partial^2 \nabla \cdot \mathbf{U}_1}{\partial t^2} = \nabla^2 (c_s^2 \nabla \cdot \mathbf{U}_1 + v_A^2 \nabla \cdot \mathbf{U}_{1\perp}) \quad (4.77)$$

or

$$\omega^2 \nabla \cdot \mathbf{U}_1 = (k_\perp^2 + k_z^2) (c_s^2 \nabla \cdot \mathbf{U}_1 + v_A^2 \nabla \cdot \mathbf{U}_{1\perp}). \quad (4.78)$$

On the other hand if Eq.(4.76) is operated on with $\nabla_\perp = \nabla - ik_z \hat{z}$ we obtain

$$\frac{\partial^2 \nabla_\perp \cdot \mathbf{U}_1}{\partial t^2} = \nabla_\perp^2 (c_s^2 \nabla \cdot \mathbf{U}_1 + v_A^2 \nabla \cdot \mathbf{U}_{1\perp}) + k_z^2 v_A^2 \hat{z} \cdot \nabla \times (\mathbf{U}_{1\perp} \times \hat{z}). \quad (4.79)$$

Using

$$\nabla \times (\mathbf{U}_1 \times \hat{z}) = \hat{z} \cdot \nabla \mathbf{U}_{1\perp} - \hat{z} \nabla \cdot \mathbf{U}_1 = ik_z \mathbf{U}_{1\perp} - \hat{z} \nabla \cdot \mathbf{U}_1 \quad (4.80)$$

Eq.(4.79) becomes

$$\omega^2 \nabla_\perp \cdot \mathbf{U}_1 = k_\perp^2 (c_s^2 \nabla \cdot \mathbf{U}_1 + v_A^2 \nabla \cdot \mathbf{U}_{1\perp}) + k_z^2 v_A^2 \nabla \cdot \mathbf{U}_{1\perp}. \quad (4.81)$$

Equations (4.78) and (4.81) constitute two coupled equations in the variables $\nabla \cdot \mathbf{U}_1$ and $\nabla_{\perp} \cdot \mathbf{U}_{1\perp}$, namely

$$\begin{aligned} (\omega^2 - k^2 c_s^2) \nabla \cdot \mathbf{U}_1 - k^2 v_A^2 \nabla_{\perp} \cdot \mathbf{U}_{1\perp} &= 0 \\ k_{\perp}^2 c_s^2 \nabla \cdot \mathbf{U}_1 + (k^2 v_A^2 - \omega^2) \nabla_{\perp} \cdot \mathbf{U}_{1\perp} &= 0. \end{aligned} \quad (4.82)$$

These coupled equations have the determinant

$$(\omega^2 - k^2 c_s^2) (k^2 v_A^2 - \omega^2) + k^2 v_A^2 k_{\perp}^2 c_s^2 = 0 \quad (4.83)$$

which can be re-arranged as a fourth order polynomial in ω ,

$$\omega^4 - \omega^2 k^2 (v_A^2 + c_s^2) + k^2 k_z^2 v_A^2 c_s^2 = 0 \quad (4.84)$$

having roots

$$\omega^2 = \frac{k^2 (v_A^2 + c_s^2) \pm \sqrt{k^4 (v_A^2 + c_s^2)^2 - 4k^2 k_z^2 v_A^2 c_s^2}}{2}. \quad (4.85)$$

Thus, according to the MHD model, the compressional mode dispersion relation has the following limiting forms

$$\omega^2 = k_{\perp}^2 (v_A^2 + c_s^2) \quad \text{if } k_z = 0 \quad (4.86)$$

$$\left. \begin{aligned} \omega^2 &= k_z^2 v_A^2 \\ \text{or} \\ \omega^2 &= k_z^2 c_s^2 \end{aligned} \right\} \text{if } k_{\perp}^2 = 0. \quad (4.87)$$

4.3.7 MHD shear (slow) mode

It is now assumed that $\nabla \cdot \mathbf{U}_1 = 0$ and taking the curl of Eq.(4.76) gives

$$\begin{aligned} \frac{\partial^2 \nabla \times \mathbf{U}_1}{\partial t^2} &= v_A^2 \nabla \times \nabla \times \left(\frac{\partial \mathbf{U}_1}{\partial z} \times \hat{z} \right) \\ &= v_A^2 \nabla \times \left(\underbrace{\frac{\partial \mathbf{U}_1}{\partial z} \cdot \nabla \cdot \hat{z}}_{\text{zero}} + \hat{z} \cdot \nabla \frac{\partial \mathbf{U}_1}{\partial z} - \underbrace{\hat{z} \nabla \cdot \frac{\partial \mathbf{U}_1}{\partial z}}_{\text{zero}} - \frac{\partial \mathbf{U}_1}{\partial z} \cdot \underbrace{\nabla \hat{z}}_{\text{zero}} \right) \\ &= v_A^2 \frac{\partial^2}{\partial z^2} \nabla \times \mathbf{U}_1 \end{aligned} \quad (4.88)$$

where the vector identity $\nabla \times (\mathbf{F} \times \mathbf{G}) = \mathbf{F} \nabla \cdot \mathbf{G} + \mathbf{G} \cdot \nabla \mathbf{F} - \mathbf{G} \nabla \cdot \mathbf{F} - \mathbf{F} \cdot \nabla \mathbf{G}$ has been used.

Equation (4.88) reduces to the slow wave dispersion relation Eq.(4.63). The associated spatial behavior is such that $\nabla \times \mathbf{U}_1 \neq 0$, and the mode is unaffected by existence of finite pressure. The perturbed magnetic field is orthogonal to the equilibrium field, i.e., $\mathbf{B}_1 \cdot \mathbf{B} = 0$, since it has been assumed that $\nabla \cdot \mathbf{U}_1 = 0$ and since finite $\mathbf{B}_1 \cdot \mathbf{B}$ corresponds to finite $\nabla \cdot \mathbf{U}_1$.

4.3.8 Limitations of the MHD model

The MHD model ignores parallel electron dynamics and so has a shear mode dispersion $\omega^2 = k_z^2 v_A^2$ that has no dependence on k_\perp . Some authors interpret this as a license to allow arbitrarily large k_\perp in which case a shear mode could be localized to a single field line. However, the two-fluid model of the shear mode does have a dependence on k_\perp which becomes important when either $k_\perp c/\omega_{pe}$ or $k_\perp \rho_s$ become of order unity (whether to use c/ω_{pe} or ρ_s depends on whether $\beta m_i/m_e$ is small or large compared to unity). Since c/ω_{pe} and ρ_s are typically small lengths, the MHD point of view is acceptable provided the characteristic length of perpendicular localization is much larger than c/ω_{pe} or ρ_s .

MHD also predicts a sound wave which is identical to the ordinary hydrodynamic sound wave of an unmagnetized gas. The perpendicular behavior of this sound wave is consistent with the two-fluid model because both two-fluid and MHD perpendicular motions involve compressional behavior associated with having finite B_{z1} . However, the parallel behavior of the MHD sound wave is problematical because E_{z1} is assumed to be identically zero in MHD. According to the two-fluid model, any parallel acceleration requires a parallel electric field. The two-fluid B_{z1} mode is decoupled from the two-fluid E_{z1} mode so that the two-fluid B_{z1} mode is both compressional and has no parallel motion associated with it.

The MHD analysis makes no restriction on the electron to ion temperature ratio and predicts that a sound wave would exist for $T_e = T_i$. In contrast, the two-fluid model shows that sound waves can only exist when $T_e \gg T_i$ because only in this regime is it possible to have $\kappa T_i/m_i \ll \omega^2/k_z^2 \ll \kappa T_e/m_e$ and so have inertial behavior for ions and kinetic behavior for electrons.

Various paradoxes develop in the MHD treatment of the shear mode but not in the two-fluid description. These paradoxes illustrate the limitations of the MHD description of a plasma and shows that MHD results must be treated with caution for the shear (slow) mode. MHD provides an adequate description of the fast (compressional) mode.

4.4 Two-fluid model of Alfvén modes

We now examine these modes from a two-fluid point of view. The two-fluid point of view shows that the shear mode occurs as one of two distinct modes, only one of which can exist for given plasma parameters. Which of these shear modes occurs depends upon the ratio of hydrodynamic pressure to magnetic pressure. This ratio is defined for each species σ as

$$\beta_\sigma = \frac{n\kappa T_\sigma}{B^2/\mu_0}; \quad (4.89)$$

the subscript σ is not used if electrons and ions have the same temperature. β_i measures the ratio of ion thermal velocity to the Alfvén velocity since

$$\frac{v_{Ti}^2}{v_A^2} = \frac{\kappa T_i/m_i}{B^2/nm_i\mu_0} = \beta_i. \quad (4.90)$$

Thus, $v_{Ti} \ll v_A$ corresponds to $\beta_i \ll 1$. Magnetic forces dominate hydrodynamic forces in a low β plasma, whereas in a high β plasma the opposite is true.

The ratio of electron thermal velocity to Alfvén velocity is also of interest and is

$$\frac{v_{Te}^2}{v_A^2} = \frac{\kappa T_e/m_e}{B^2/nm_i\mu_0} = \frac{m_i}{m_e}\beta_e. \quad (4.91)$$

Thus, $v_{Te}^2 \gg v_A^2$ when $\beta_e \gg m_e/m_i$ and $v_{Te}^2 \ll v_A^2$ when $\beta_e \ll m_e/m_i$. Shear Alfvén wave physics is different in the $\beta_e \gg m_e/m_i$ and $\beta_e \ll m_e/m_i$ regimes which therefore must be investigated separately. MHD ignores this β_e dependence, an oversimplification which leads to the paradoxes.

Both Faraday's law and the pre-Maxwell Ampere's law are fundamental to Alfvén wave dynamics. The system of linearized equations thus is

$$\nabla \times \mathbf{E}_1 = -\frac{\partial \mathbf{B}_1}{\partial t} \quad (4.92)$$

$$\nabla \times \mathbf{B}_1 = \mu_0 \mathbf{J}_1. \quad (4.93)$$

If the dependence of \mathbf{J}_1 on \mathbf{E}_1 can be determined, then the combination of Ampere's law and Faraday's law provides a complete self-consistent description of the coupled fields \mathbf{E}_1 , \mathbf{B}_1 and hence describes the normal modes. From a mathematical point of view, specifying $\mathbf{J}_1(\mathbf{E}_1)$ means that there are as many equations as dependent variables in the pair of Eqs.(4.92),(4.93). The relationship between \mathbf{J}_1 and \mathbf{E}_1 is determined by the Lorentz equation or some generalization thereof (e.g., drift equations, Vlasov equation, fluid equation of motion). The MHD derivation used the polarization drift to give a relationship between $\mathbf{J}_{1\perp}$ and $\mathbf{E}_{1\perp}$ but leaves ambiguous the relationship between $\mathbf{J}_{1\parallel}$ and $\mathbf{E}_{1\parallel}$.

The two-fluid equations provide a definite description of the relationship between $\mathbf{J}_{1\parallel}$ and $\mathbf{E}_{1\parallel}$. At frequencies well below the cyclotron frequency, decoupling of modes also occurs in the two-fluid description, and this decoupling is more clearly defined and more symmetric than in MHD. The decoupling in a uniform plasma results because the dependence of \mathbf{J}_1 on \mathbf{E}_1 has the property that $J_{1z} \sim E_{1z}$ and $\mathbf{J}_{1\perp} \sim \mathbf{E}_{1\perp}$. Thus, for $\omega \ll \omega_{ci}$ there is a simple linear relation between parallel electric field and parallel current and another distinct simple linear relation between perpendicular electric field and perpendicular current; these two linear relations mean that the tensor relating \mathbf{J}_1 to \mathbf{E}_1 is diagonal (at higher frequencies this is not the case). The decoupling can be seen by supposing that all first order quantities have the dependence $\exp(i\mathbf{k}_\perp \cdot \mathbf{x} + ik_z z)$ where $\mathbf{k}_\perp = k_x \hat{x} + k_y \hat{y}$. Here \hat{k}_\perp is the unit vector in the direction of \mathbf{k}_\perp and $\hat{z} \times \hat{k}_\perp$ is the binormal unit vector so that the set $\hat{k}_\perp, \hat{z} \times \hat{k}_\perp, \hat{z}$ form a right-handed coordinate system. Mode decoupling can be seen by examining the table below which lists the electric and magnetic field components in this coordinate system:

E components	B components
$\hat{k}_\perp \cdot \mathbf{E}_1$	$\hat{k}_\perp \cdot \mathbf{B}_1$
$\hat{z} \times \hat{k}_\perp \cdot \mathbf{E}_1$	$\hat{z} \times \hat{k}_\perp \cdot \mathbf{B}_1$
$\hat{z} \cdot \mathbf{E}_1$	$\hat{z} \cdot \mathbf{B}_1$

Because of the property that $J_{1z} \sim E_{1z}$ and $\mathbf{J}_{1\perp} \sim \mathbf{E}_{1\perp}$ the terms in boxes are decoupled from the terms not in boxes. Hence, one mode consists solely of interrelationships between

the boxed terms (this mode is called the E_z mode since it has finite E_z) and the other distinct mode consists solely of interrelationships between the unboxed terms (this mode is called the B_z mode since it has finite B_z). Since the modes are decoupled, it is possible to “turn off” the E_z mode when considering the B_z mode and vice versa. If the plasma is non-uniform, the E_z and B_z modes can become coupled.

The ideal MHD formalism sidesteps discussion of the E_z mode. Instead, two disconnected assumptions are invoked in ideal MHD, namely (i) it is assumed that $E_{z1} = 0$ and (ii) the parallel current J_{z1} is assumed to arrange itself spontaneously in such a way as to always satisfy $\nabla \cdot \mathbf{J}_1 = 0$. This pair of assumptions completes the system of equations, but omits the parallel dynamics associated with the E_z mode and instead replaces this dynamics with an assumption that J_{z1} is determined by some unspecified automatic feedback mechanism. In contrast, the two-fluid equations describe how particle dynamics determines the relationship between J_{z1} and E_{z1} . Thus, while MHD is both simpler and self-consistent, it omits some vital physics.

The two-fluid model is based on the linearized equations of motion

$$m_\sigma n \frac{\partial \mathbf{u}_{\sigma 1}}{\partial t} = n q_\sigma (\mathbf{E}_1 + \mathbf{u}_{\sigma 1} \times \mathbf{B}) - \nabla \cdot \mathbf{P}_{\sigma 1}. \quad (4.94)$$

Charge neutrality is assumed so that $n_i = n_e = n$. Also, the pressure term is

$$\nabla \cdot \mathbf{P}_{\sigma 1} = \nabla \cdot \begin{bmatrix} P_{\sigma \perp 1} & 0 & 0 \\ 0 & P_{\sigma \perp 1} & 0 \\ 0 & 0 & P_{\sigma z 1} \end{bmatrix} = \nabla_\perp P_{\sigma \perp 1} + \hat{z} \frac{\partial P_{\sigma z 1}}{\partial z}. \quad (4.95)$$

Assuming $\omega \ll \omega_{ci}$ implies $\omega \ll \omega_{ce}$ also and so perpendicular motion can be described by drift theory for both ions and electrons. However, here the drift approximation is used for the fluid equations, rather than for a single particle. Following the drift method of analysis, the left hand side of Eq.(4.94) is neglected to first approximation, resulting in

$$\mathbf{u}_{\sigma 1} \times \mathbf{B} \simeq -\mathbf{E}_{1\perp} + \nabla_\perp P_{\sigma \perp 1} / n q_\sigma \quad (4.96)$$

which may be solved for $\mathbf{u}_{\sigma \perp 1}$ to give

$$\mathbf{u}_{\sigma \perp 1} = \frac{\mathbf{E}_1 \times \mathbf{B}}{B^2} - \frac{\nabla P_{\sigma \perp 1} \times \mathbf{B}}{n q_\sigma B^2}. \quad (4.97)$$

The first term is the single-particle $E \times B$ drift and the second term is called the diamagnetic drift, a fluid effect that does not exist for single-particle motion. Because $\mathbf{u}_{\sigma \perp 1}$ is time-dependent there is also a polarization drift. Recalling that the form of the single-particle polarization drift for electric field only is $\mathbf{v}_p = m \dot{\mathbf{E}}_{1\perp} / q B^2$ and using $\mathbf{E}_{1\perp} - \nabla_\perp P_{\sigma \perp 1} / n q_\sigma$ for the fluid model instead of just $\mathbf{E}_{1\perp}$ for single particles (cf. right hand side of Eq.(4.96)) the fluid polarization drift is obtained. With the inclusion of this higher order correction, the perpendicular fluid motion becomes

$$\mathbf{u}_{\sigma \perp 1} = \frac{\mathbf{E}_1 \times \mathbf{B}}{B^2} - \frac{\nabla P_{\sigma \perp 1} \times \mathbf{B}}{n q_\sigma B^2} + \frac{m_\sigma}{q_\sigma B^2} \dot{\mathbf{E}}_{1\perp} - \frac{m_\sigma}{n q_\sigma^2 B^2} \nabla_\perp \dot{P}_{\sigma \perp 1}. \quad (4.98)$$

The last two terms are smaller than the first two terms by the ratio $\omega / \omega_{c\sigma}$ and so may be ignored when the electron and ion fluid velocities are considered separately. However,

when the perpendicular current, i.e., $\mathbf{J}_{\perp 1} = \sum nq_{\sigma} \mathbf{u}_{\sigma \perp 1}$ is considered, the electron and ion $E \times B$ drift terms cancel so that the polarization terms become the leading terms involving the electric field. Because of the mass in the numerator, the ion polarization drift is much larger than the electron polarization drift. Thus, the perpendicular current comes from ion polarization drift and diamagnetic current

$$\mu_0 \mathbf{J}_{\perp 1} = \frac{\mu_0 n m_i \dot{\mathbf{E}}_{\perp}}{B^2} - \sum_{\sigma} \frac{\nabla P_{\sigma \perp 1} \times \mathbf{B}}{B^2} = \frac{1}{v_A^2} \dot{\mathbf{E}}_{\perp 1} - \frac{\mu_0 \nabla P_{\perp 1} \times \mathbf{B}}{B^2} \quad (4.99)$$

where $P_{\perp 1} = \sum P_{\sigma \perp 1}$. The term involving $\dot{P}_{\perp 1}$ has been dropped because it is small by ω/ω_c compared to the $P_{\perp 1}$ term.

The center of mass perpendicular motion is

$$\mathbf{U}_{\perp 1} = \frac{\sum m_{\sigma} n \mathbf{u}_{\sigma \perp 1}}{\sum m_{\sigma} n} \approx \mathbf{u}_{i \perp 1} \quad (4.100)$$

An important issue for the perpendicular motion is whether $\mathbf{u}_{\sigma \perp 1}$ is compressible or incompressible. Let us temporarily ignore parallel motion and consider the continuity equation

$$\frac{\partial n_1}{\partial t} + n \nabla \cdot \mathbf{u}_{\sigma \perp 1} = 0. \quad (4.101)$$

If $\nabla \cdot \mathbf{u}_{\sigma \perp 1} = 0$, the mode does not involve any density perturbation, i.e., $n_1 = 0$, and is said to be an incompressible mode. On the other hand, if $\nabla \cdot \mathbf{u}_{\sigma \perp 1} \neq 0$ then there are fluctuations in density and the mode is said to be compressible.

To proceed further, consider the vector identity

$$\nabla \cdot (\mathbf{F} \times \mathbf{G}) = \mathbf{G} \cdot \nabla \times \mathbf{F} - \mathbf{F} \cdot \nabla \times \mathbf{G}.$$

If \mathbf{G} is spatially uniform, this identity reduces to $\nabla \cdot (\mathbf{F} \times \mathbf{G}) = \mathbf{G} \cdot \nabla \times \mathbf{F}$ which in turn vanishes if \mathbf{F} is the gradient of a scalar (since the curl of a gradient is always zero). Taking the divergence of Eq.(4.98) and ignoring the polarization terms (they are of order ω/ω_{ci} and are only important when calculating the current which we are not interested in right now) gives

$$\nabla \cdot \mathbf{u}_{\sigma \perp 1} = \frac{1}{B^2} \mathbf{B} \cdot \nabla \times \mathbf{E}_1 = \frac{1}{B} \hat{z} \cdot \nabla \times \mathbf{E}_1 \quad (4.102)$$

to lowest order. Setting $\mathbf{E}_1 = -\nabla \phi$ (i.e., assuming that the electric field is electrostatic) would cause the right hand side of Eq.(4.102) to vanish, but such an assumption is overly restrictive because all that matters here is the z -component of $\nabla \times \mathbf{E}_1$. The z -component of $\nabla \times \mathbf{E}_1$ involves only the perpendicular component of the electric field (i.e., only the x and y components of the electric field) and so the least restrictive assumption for the right hand side of Eq.(4.102) to vanish is to have $\mathbf{E}_{1\perp} = -\nabla_{\perp} \phi$. Thus, one possibility is to have $\mathbf{E}_{1\perp} = -\nabla_{\perp} \phi$ in which case the perpendicular electric field is electrostatic in nature and the mode is incompressible.

The other possibility is to have $\hat{z} \cdot \nabla \times \mathbf{E}_1 \neq 0$. In this case, invoking Faraday's law reduces Eq.(4.102) to

$$\begin{aligned} \nabla \cdot \mathbf{u}_{\sigma \perp 1} &= -\frac{1}{B} \hat{z} \cdot \frac{\partial \mathbf{B}_1}{\partial t} \\ &= -\frac{1}{B} \frac{\partial B_{z1}}{\partial t}. \end{aligned} \quad (4.103)$$

Combining Eqs.(4.103) and (4.101) and then integrating in time gives

$$\frac{n_1}{n} = \frac{B_{z1}}{B} \quad (4.104)$$

which shows that compression/rarefaction is associated with having finite B_{z1} .

In summary, there are two general kinds of behavior:

1. Modes with incompressible behavior; these are the *shear modes* and have $n_1 = 0$, $\nabla \cdot \mathbf{u}_{\sigma\perp 1} = 0$, $\mathbf{E}_{1\perp} = -\nabla_{\perp}\phi$ and $B_{z1} = 0$,
2. Modes with compressible behavior; these are the *compressible modes* and have $n_1 \neq 0$, $\nabla \cdot \mathbf{u}_{\sigma\perp 1} \neq 0$, $\nabla \times \mathbf{E}_{1\perp} \neq 0$, and $B_{z1} \neq 0$.

Equation (4.99) provides a relationship between the perpendicular electric field and the perpendicular current. A relationship between the parallel electric field and the parallel current is now required. To obtain this, all vectors are decomposed into components parallel and perpendicular to the equilibrium magnetic field, i.e., $\mathbf{E}_1 = \mathbf{E}_{1\perp} + E_{z1}\hat{z}$ etc. The ∇ operator is similarly decomposed into components parallel to and perpendicular to the equilibrium magnetic field, i.e., $\nabla = \nabla_{\perp} + \hat{z}\partial/\partial z$ and all quantities are assumed to be proportional to $f(x, y) \exp(ik_z z - i\omega t)$. Thus, Faraday's law can be written as

$$\nabla_{\perp} \times \mathbf{E}_{1\perp} + \nabla_{\perp} \times E_{z1}\hat{z} + \hat{z}\frac{\partial}{\partial z} \times \mathbf{E}_{1\perp} = -\frac{\partial}{\partial t} (\mathbf{B}_{1\perp} + B_{z1}\hat{z}) \quad (4.105)$$

which has a parallel component

$$\hat{z} \cdot \nabla_{\perp} \times \mathbf{E}_{1\perp} = i\omega B_{z1} \quad (4.106)$$

and a perpendicular component

$$(\nabla_{\perp} E_{z1} - ik_z \mathbf{E}_{1\perp}) \times \hat{z} = i\omega \mathbf{B}_{1\perp}. \quad (4.107)$$

Similarly Ampere's law can be decomposed into

$$\hat{z} \cdot \nabla_{\perp} \times \mathbf{B}_{1\perp} = \mu_0 J_{z1} \quad (4.108)$$

and

$$(\nabla_{\perp} B_{z1} - ik_z \mathbf{B}_{1\perp}) \times \hat{z} = \mu_0 \mathbf{J}_{1\perp}. \quad (4.109)$$

Substituting Eq.(4.99) into Eq.(4.109) gives

$$(\nabla_{\perp} B_{z1} - ik_z \mathbf{B}_{1\perp}) \times \hat{z} = -\frac{i\omega}{v_A^2} \mathbf{E}_{1\perp} - \frac{\mu_0 \nabla P_1 \times \hat{z}}{B} \quad (4.110)$$

or, after re-arrangement,

$$\nabla_{\perp} \left(B_{z1} + \frac{\mu_0 P_{1\perp}}{B} \right) \times \hat{z} - ik_z \mathbf{B}_{1\perp} \times \hat{z} = -\frac{i\omega}{v_A^2} \mathbf{E}_{1\perp}. \quad (4.111)$$

The slow (shear) and fast (compressional modes) are now considered separately.

4.4.1 Two-fluid slow (shear) modes

As discussed above these modes have $B_{z1} = 0$, $\mathbf{E}_{\perp 1} = -\nabla\phi_1$, and $\nabla \cdot \mathbf{u}_{\sigma\perp 1} = 0$. We first consider the parallel component of the linearized equation of motion, namely

$$nm_{\sigma} \frac{\partial u_{\sigma z1}}{\partial t} = nq_{\sigma} E_{z1} - \frac{\partial P_{\sigma 1}}{\partial z} \quad (4.112)$$

where $P_{\sigma 1} = \gamma_{\sigma} n_{\sigma 1} \kappa T_{\sigma}$ and $\gamma = 1$ if the motion is isothermal and $\gamma_{\sigma} = 3$ if the motion is adiabatic and the compression is one-dimensional. The isothermal case corresponds to $\omega^2/k_z^2 \ll \kappa T_{\sigma}/m_{\sigma}$ and vice versa for the adiabatic case.

The continuity equation is

$$\frac{\partial n_1}{\partial t} + \nabla \cdot (n\mathbf{u}_{\sigma 1}) = 0. \quad (4.113)$$

Because the shear mode is incompressible in the perpendicular direction, the continuity equation reduces to

$$\frac{\partial n_1}{\partial t} + \frac{\partial}{\partial z} (n_0 u_{\sigma z1}) = 0. \quad (4.114)$$

Taking the time derivative of Eq.(4.112) gives

$$\frac{\partial^2 u_{\sigma z1}}{\partial t^2} - \gamma_{\sigma} \frac{\kappa T_{\sigma}}{m_{\sigma}} \frac{\partial^2 u_{\sigma z1}}{\partial z^2} = \frac{q_{\sigma}}{m_{\sigma}} \frac{\partial E_{z1}}{\partial t} \quad (4.115)$$

which is similar to electron plasma wave and ion acoustic wave dynamics except it has *not* been assumed that E_{z1} is electrostatic.

Invoking the assumption that all quantities are of the form $f(x, y) \exp(ik_z z - i\omega t)$ Eq.(4.115) can be solved to give

$$u_{\sigma z1} = \frac{i\omega q_{\sigma}}{m_{\sigma}} \frac{E_{z1}}{\omega^2 - \gamma_{\sigma} k_z^2 \kappa T_{\sigma}/m_{\sigma}} \quad (4.116)$$

and so the relation between parallel current and parallel electric field is

$$\mu_0 J_{z1} = \frac{i\omega}{c^2} E_{z1} \sum_{\sigma} \frac{\omega_{p\sigma}^2}{\omega^2 - \gamma_{\sigma} k_z^2 \kappa T_{\sigma}/m_{\sigma}}. \quad (4.117)$$

Using $\hat{z} \cdot \nabla \times \mathbf{B}_1 = \nabla \cdot (\mathbf{B}_1 \times \hat{z}) = \nabla \cdot (\mathbf{B}_{\perp 1} \times \hat{z})$ the parallel component of Ampere's law becomes for the shear wave

$$\nabla_{\perp} \cdot (\mathbf{B}_{\perp 1} \times \hat{z}) = \frac{i\omega}{c^2} E_{z1} \sum_{\sigma} \frac{\omega_{p\sigma}^2}{\omega^2 - \gamma_{\sigma} k_z^2 \kappa T_{\sigma}/m_{\sigma}}. \quad (4.118)$$

Ion acoustic wave physics is embedded in Eq.(4.118) as well as shear Alfvén physics. The ion acoustic mode can be retrieved by assuming that the electric field is electrostatic in which case $\mathbf{B}_{\perp 1}$ vanishes. For the special case where the electric field is just in the z direction, and assuming that $\kappa T_i/m_i \ll \omega^2/k_z^2 \ll \kappa T_e/m_e$ the right hand side of Eq.(4.118) becomes

$$\left(\frac{\omega_{pi}^2}{\omega^2} - \frac{1}{k_z^2 \lambda_{De}^2} \right) E_{z1} = 0 \quad (4.119)$$

which gives the ion acoustic wave $\omega^2 = k_z^2 \kappa T_e / m_i$ discussed in Sec.4.2.1. This shows that the acoustic wave is associated with having finite E_{z1} and also requires $T_e \gg T_i$ in order to exist.

Returning to shear waves, we now assume that the electric field is not electrostatic so $\mathbf{B}_{\perp 1}$ does not vanish and Eq.(4.118) has to be considered in its entirety. For shear waves the character of the parallel current changes depending on whether the wave parallel phase velocity is faster or slower than the electron thermal velocity. The $\omega^2/k_z^2 \gg \kappa T_e/m_e$ case is called the inertial limit while the $\omega^2/k_z^2 \ll \kappa T_e/m_e$ case is called the kinetic limit. The perpendicular component of Faraday's law is

$$\nabla_{\perp} E_{z1} \times \hat{z} - ik_z \mathbf{E}_{\perp 1} \times \hat{z} = i\omega \mathbf{B}_{\perp 1}. \quad (4.120)$$

Substitution of $\mathbf{E}_{\perp 1}$ as determined from Eq.(4.111) into Eq.(4.120) gives

$$-\frac{i\omega}{v_A^2} \nabla_{\perp} E_{z1} \times \hat{z} - ik_z \left(\frac{\mu_0 \nabla P_{\perp 1}}{B} \times \hat{z} - ik_z \mathbf{B}_{\perp 1} \times \hat{z} \right) \times \hat{z} = \frac{\omega^2}{v_A^2} \mathbf{B}_{\perp 1} \quad (4.121)$$

which may be solved for $\mathbf{B}_{\perp 1}$ to give

$$\mathbf{B}_{\perp 1} = \frac{1}{\omega^2 - k_z^2 v_A^2} \left(-i\omega \nabla_{\perp} E_{z1} \times \hat{z} + ik_z v_A^2 \frac{\mu_0 \nabla_{\perp} P_{\perp 1}}{B} \right) \quad (4.122)$$

and

$$\mathbf{B}_{\perp 1} \times \hat{z} = \frac{1}{\omega^2 - k_z^2 v_A^2} \left(i\omega \nabla_{\perp} E_{z1} + ik_z v_A^2 \frac{\mu_0 \nabla_{\perp} P_{\perp 1}}{B} \times \hat{z} \right). \quad (4.123)$$

Substitution of $\mathbf{B}_{\perp 1} \times \hat{z}$ into Eq.(4.118) gives

$$\nabla_{\perp} \cdot \left(\frac{1}{\omega^2 - k_z^2 v_A^2} \left(\nabla_{\perp} E_{z1} + k_z v_A^2 \frac{\mu_0 \nabla_{\perp} P_{\perp 1}}{\omega B} \times \hat{z} \right) \right) = E_{z1} \sum_{\sigma} \frac{\omega_{p\sigma}^2 / c^2}{\omega^2 - \gamma_{\sigma} k_z^2 \kappa T_{\sigma} / m_{\sigma}}. \quad (4.124)$$

However, because $\nabla_{\perp} \cdot (\nabla_{\perp} P_{\perp 1} \times \hat{z}) = \nabla \cdot (\nabla P_{\perp 1} \times \hat{z}) = 0$ the term involving pressure vanishes, leaving an equation involving E_{z1} only, namely

$$\nabla_{\perp} \cdot \left(\frac{1}{(\omega^2 - k_z^2 v_A^2)} \nabla_{\perp} E_{z1} \right) - E_{z1} \sum_{\sigma} \frac{\omega_{p\sigma}^2 / c^2}{\omega^2 - \gamma_{\sigma} k_z^2 \kappa T_{\sigma} / m_{\sigma}} = 0. \quad (4.125)$$

This is the fundamental equation for shear waves. On replacing $\nabla_{\perp} \rightarrow i\mathbf{k}_{\perp}$, Eq.(4.125) becomes

$$\frac{k_{\perp}^2}{\omega^2 - k_z^2 v_A^2} + \frac{\omega_{pe}^2}{c^2} \frac{1}{\omega^2 - \gamma_e k_z^2 \kappa T_e / m_e} + \frac{\omega_{pi}^2}{c^2} \frac{1}{\omega^2 - \gamma_i k_z^2 \kappa T_i / m_i} = 0. \quad (4.126)$$

In the situation where $\omega^2/k_z^2 \gg \kappa T_e/m_e$, the second term dominates the third term since $\omega_{pe}^2 \gg \omega_{pi}^2$ and so Eq.(4.126) can be recast as

$$\omega^2 = \frac{k_z^2 v_A^2}{1 + k_{\perp}^2 c^2 / \omega_{pe}^2} \quad (4.127)$$

which is called the inertial Alfvén wave (IAW). If $k_{\perp}^2 c^2 / \omega_{pe}^2$ is not too large, then ω/k_z is of the order of the Alfvén velocity and the condition $\omega^2 \gg k_z^2 \kappa T_e / m_e$ corresponds to $v_A^2 \gg \kappa T_e / m_e$ or

$$\beta_e = \frac{n \kappa T_e}{B^2 / \mu_0} \ll \frac{m_e}{m_i}. \quad (4.128)$$

Thus, inertial Alfvén wave shear modes exist only in the ultra-low β regime where $\beta_e \ll m_e / m_i$.

In the situation where $\kappa T_i / m_i \ll \omega^2 / k_z^2 \ll \kappa T_e / m_e$, Eq.(4.126) can be recast as

$$\frac{k_{\perp}^2}{(\omega^2 - k_z^2 v_A^2)} - \frac{\omega_{pe}^2}{c^2} \frac{1}{k_z^2 \kappa T_e / m_e} + \frac{\omega_{pi}^2}{c^2} \frac{1}{\omega^2} = 0. \quad (4.129)$$

Because ω^2 appears in the respective denominators of two distinct terms, Eq.(4.129) is fourth order in ω^2 and so describes two distinct modes. Let us suppose that the mode in question is much faster than the acoustic velocity, i.e., $\omega^2 / k_z^2 \gg \kappa T_e / m_e$. In this case the ion term can be dropped and the remaining terms can be re-arranged to give

$$\omega^2 = k_z^2 v_A^2 \left(1 + \frac{k_{\perp}^2}{v_A^2} \frac{\kappa T_e}{m_e} \frac{c^2}{\omega_{pe}^2} \right); \quad (4.130)$$

this is called the kinetic Alfvén wave (KAW).

$$\rho_s^2 = \frac{1}{v_A^2} \frac{\kappa T_e}{m_e} \frac{c^2}{\omega_{pe}^2} = \frac{1}{\omega_{ci}^2} \frac{\kappa T_e}{m_i} \quad (4.131)$$

as a fictitious ion Larmor radius calculated using the electron temperature instead of the ion temperature, the kinetic Alfvén wave (KAW) dispersion relation can be expressed more succinctly as

$$\omega^2 = k_z^2 v_A^2 (1 + k_{\perp}^2 \rho_s^2). \quad (4.132)$$

If $k_{\perp}^2 \rho_s^2$ is not too large, then ω/k_z is again of the order of v_A and so the condition $\omega^2 \ll k_z^2 \kappa T_e / m_e$ corresponds to having $\beta_e \gg m_e / m_i$. The condition $\omega^2 / k_z^2 \gg \kappa T_e / m_e$ which was also assumed corresponds to assuming that $\beta_e \ll 1$. Thus, the KAW dispersion relation Eq.(4.132) is valid in the regime $m_e / m_i \ll \beta_e \ll 1$.

Let us now consider the situation where $\omega^2 / k_z^2 \ll \kappa T_i / m_i, \kappa T_e / m_e$. In this case Eq.(4.126) again reduces to

$$\omega^2 = k_z^2 v_A^2 (1 + k_{\perp}^2 \rho_s^2) \quad (4.133)$$

but this time

$$\rho_s^2 = \frac{\kappa (T_e + T_i)}{m_i \omega_{ci}^2}. \quad (4.134)$$

This situation would describe shear modes in a high β plasma (ion thermal velocity faster than Alfvén velocity).

To summarize: the shear mode has $B_{z1} = 0$, $E_{z1} \neq 0$, $J_{z1} \neq 0$, $\mathbf{E}_{\perp 1} = -\nabla \phi_1$ and exists in the form of the inertial Alfvén wave for $\beta_e \ll m_e / m_i$ and in the form of the kinetic Alfvén wave for $\beta_e \gg m_e / m_i$. The shear mode involves incompressible perpendicular motion, i.e., $\nabla \cdot \mathbf{u}_{\sigma \perp 1} = \mathbf{i} \mathbf{k}_{\perp} \cdot \mathbf{u}_{\sigma \perp 1} = 0$, which means that \mathbf{k}_{\perp} is orthogonal to $\mathbf{u}_{\sigma \perp 1}$. For example, in Cartesian geometry, this means that if $\mathbf{u}_{\sigma \perp 1}$ is in the x direction,

then \mathbf{k}_\perp must be in the y direction while in cylindrical geometry, this means that if $\mathbf{u}_{\sigma\perp 1}$ is in the θ direction, then \mathbf{k}_\perp must be in the r direction. The inertial Alfvén wave is known as a cold plasma wave because its dispersion relation does not depend on temperature (such a mode would exist even in the limit of a cold plasma). The kinetic Alfvén wave depends on the plasma having finite temperature and is therefore called a warm plasma wave. The shear mode can be coupled to ion acoustic modes since both shear and ion acoustic modes involve finite E_{z1} .

4.4.2 Two-fluid compressional modes

The compressional mode involves assuming that B_{z1} is finite and that $E_{z1} = 0$. Having $E_{z1} = 0$ means that there is no parallel motion and, in particular, implies that $J_{z1} = 0$. Thus, for the compressional mode Faraday's law has the form

$$\nabla_\perp \cdot (\mathbf{E}_{\perp 1} \times \hat{z}) = i\omega B_{z1} \quad (4.135)$$

$$-ik_z \mathbf{E}_{\perp 1} \times \hat{z} = i\omega \mathbf{B}_{\perp 1}. \quad (4.136)$$

Using Eq.(4.136) to substitute for $\mathbf{B}_{\perp 1}$ in Eq.(4.111) and then solving for $\mathbf{E}_{\perp 1}$ gives

$$\mathbf{E}_{\perp 1} = \frac{i\omega v_A^2}{\omega^2 - k_z^2 v_A^2} \nabla_\perp \left(B_{z1} + \frac{\mu_0 P_{\perp 1}}{B} \right) \times \hat{z}. \quad (4.137)$$

Since

$$\mathbf{E}_{\perp 1} \times \hat{z} = -\frac{i\omega v_A^2}{\omega^2 - k_z^2 v_A^2} \nabla_\perp \left(B_{z1} + \frac{\mu_0 P_{\perp 1}}{B} \right) \quad (4.138)$$

Eq.(4.135) becomes

$$\nabla_\perp \cdot \left(\frac{v_A^2}{\omega^2 - k_z^2 v_A^2} \nabla_\perp \left(B_{z1} + \frac{\mu_0 P_{\perp 1}}{B} \right) \right) + B_{z1} = 0. \quad (4.139)$$

If we assume that the perpendicular motion is adiabatic, then

$$\frac{P_{\perp 1}}{P} = \gamma \frac{n_1}{n} = \gamma \frac{B_{z1}}{B}. \quad (4.140)$$

Substitution for $P_{\perp 1}$ in Eq.(4.139) gives

$$\nabla_\perp \cdot \left(\frac{(v_A^2 + c_s^2)}{\omega^2 - k_z^2 v_A^2} \nabla_\perp B_{z1} \right) + B_{z1} = 0 \quad (4.141)$$

where

$$c_s^2 = \gamma \kappa \frac{T_e + T_i}{m_i}. \quad (4.142)$$

On replacing $\nabla_\perp \rightarrow i\mathbf{k}_\perp$, Eq.(4.141) becomes the dispersion relation

$$\frac{-k_\perp^2 (v_A^2 + c_s^2)}{\omega^2 - k_z^2 v_A^2} + 1 = 0 \quad (4.143)$$

or

$$\omega^2 = k^2 v_A^2 + k_\perp^2 c_s^2 \quad (4.144)$$

where $k^2 = k_z^2 + k_\perp^2$. Since $\nabla \cdot \mathbf{u}_{\sigma\perp 1} = i\mathbf{k}_\perp \cdot \mathbf{u}_{\sigma\perp 1} \neq 0$, the perpendicular wave vector \mathbf{k}_\perp is at least partially co-aligned with the perpendicular velocity.

4.4.3 Differences between the two-fluid and MHD descriptions

The two-fluid description shows that the slow mode (finite E_z) appears as either an inertial or a kinetic Alfvén wave depending on the plasma β ; the MHD description assumes that $E_z = 0$ for this mode and does not distinguish between inertial and kinetic modes. The two-fluid description also shows that finite E_z will give ion acoustic modes in the parallel direction which are decoupled. The MHD description predicts a so-called sound wave which differs from the ion acoustic wave because the MHD sound wave does not have the requirement that $T_e \gg T_i$; the MHD sound wave is an artifact for parallel propagation in a plasma with low collisionality (if the collisions are sufficiently large, then the plasma would behave like a neutral gas). Then MHD description predicts a coupling between oblique sound waves via a square root relation (see Eq.(4.85)) which does not exist in the two-fluid model.

4.5 Assignments

1. Plot frequency versus wavenumber for the electron plasma wave and the ion acoustic wave in an unmagnetized Argon plasma which has $n = 10^{18} \text{ m}^{-3}$, $T_e = 10 \text{ eV}$, and $T_i = 1 \text{ eV}$.
2. Let $\Delta\phi$ be the difference between the phase shift a Helium-Neon laser beam experiences on traversing a given length of vacuum and on traversing the same length of plasma. What is $\Delta\phi$ when the laser beam passes through 10 cm of plasma having a density of $n = 10^{22} \text{ m}^{-3}$? How could this be used as a density diagnostic?
3. Prove that the electrostatic plasma wave $\omega^2 = \omega_{pe}^2 + 3k^2\kappa T_e/m_e$ can also be written as

$$\omega^2 = \omega_{pe}^2 (1 + 3k^2\lambda_{De}^2)$$

and show over what range of $k^2\lambda_{De}^2$ the dispersion is valid. Plot the dispersion $\omega(k)$ versus k for both negative and positive k . Next plot on the same graph the electromagnetic dispersion $\omega^2 = \omega_{pe}^2 + k^2c^2$ and show the limits of validity. Plot the ion acoustic dispersion $\omega^2 = k^2c_s^2/(1 + k^2\lambda_{De}^2)$ on this graph showing its region of validity. Finally plot the ion acoustic dispersion with a finite ion temperature. Show the limits of validity of the ion acoustic dispersion.

4. Physical picture of plasma oscillations: Suppose that a plasma is cold and initially neutral. Consider a spherical volume of this plasma and imagine that a thin shell of electrons at spherical radius r having thickness δr moves radially outward by a distance equal to its thickness. Suppose further that the ions are infinitely massive and cannot move. What is the total ion charge acting on the electrons (consider the charge density and volume of the ions left behind when the electron shell is moved out)? What is the electric field due to these ions. By considering the force due to this electric field on an individual electron in the shell, show that the entire electron shell will execute simple harmonic motion at the frequency ω_{pe} . If the ions had finite mass how would you expect the problem to be modified (hint-consider the reduced mass)?
5. Suppose that an MHD plasma immersed in a uniform magnetic field $\mathbf{B} = B_0\hat{z}$ has

an oscillating electric field $\bar{\mathbf{E}}_{\perp}$ where \perp means in the direction perpendicular to \hat{z} . What is the polarization current associated with $\bar{\mathbf{E}}_{\perp}$? By substituting this polarization current into the MHD approximation of Ampere's law, find a relationship between $\partial\bar{\mathbf{E}}_{\perp}/\partial t$ and a spatial operator on $\bar{\mathbf{B}}$. Use Faraday's law to obtain a similar relationship between $\partial\bar{\mathbf{B}}_{\perp}/\partial t$ and a spatial operator on $\bar{\mathbf{E}}$. Consider a mode where $\tilde{E}_x(z, t)$ and $\tilde{B}_y(z, t)$ are the only finite components and derive a wave equation. Do the same for the pair $\tilde{E}_y(z, t)$ and $\tilde{B}_z(z, t)$. Which mode is the compressional mode and which is the shear mode?

Streaming instabilities and the Landau problem

5.1 Streaming instabilities

The electrostatic dispersion relation for a zero-temperature plasma is simply

$$1 - \sum_{\sigma} \frac{\omega_{p\sigma}^2}{\omega^2} = 0 \quad (5.1)$$

indicating that a *spatially-independent* oscillation at the plasma frequency

$$\omega_p = \sqrt{\omega_{pe}^2 + \omega_{pi}^2} \quad (5.2)$$

is a normal mode of a cold plasma. Once started, such an oscillation would persist indefinitely because no dissipative mechanism exists to quench it. On the other hand, the oscillation would have to be initiated by some source, because no available free energy exists from which the oscillation could draw to start spontaneously.

We now consider a slightly different situation where instead of being at rest in equilibrium, cold electrons or ions stream at some spatially-uniform initial velocity. In the special situation where electrons and ions have the same initial velocity, the center of mass would also move at this initial velocity and one could simply move to the center of mass frame where both species are stationary and so, as argued in the previous paragraph, an oscillation would not start spontaneously. However, in the more general situation where the electrons and ions stream at *different* velocities, then both species have kinetic energy in the center of mass frame. This free energy could drive an instability.

In order to determine the conditions where such an instability could occur, the situation where each species has the equilibrium streaming velocity $\mathbf{u}_{\sigma 0}$ will now be examined. The linearized equation of motion, the linearized continuity equation, and Poisson's equation become respectively

$$\frac{\partial \mathbf{u}_{\sigma 1}}{\partial t} + \mathbf{u}_{\sigma 0} \cdot \nabla \mathbf{u}_{\sigma 1} = -\frac{q_{\sigma}}{m_{\sigma}} \nabla \phi_1, \quad (5.3)$$

$$\frac{\partial n_{\sigma 1}}{\partial t} + \mathbf{u}_{\sigma 0} \cdot \nabla n_{\sigma 1} = -n_{\sigma 0} \nabla \cdot \mathbf{u}_{\sigma 1}, \quad (5.4)$$

and

$$\nabla^2 \phi_1 = -\frac{1}{\varepsilon_0} \sum_{\sigma} q_{\sigma} n_{\sigma 1}. \quad (5.5)$$

As before, all first-order dependent variables are assumed to vary as $\exp(i\mathbf{k} \cdot \mathbf{x} - i\omega t)$. Combining the equation of motion and the continuity equation gives

$$n_{\sigma 1} = n_{\sigma 0} \frac{k^2}{(\omega - \mathbf{k} \cdot \mathbf{u}_{\sigma 0})^2} \frac{q_{\sigma}}{m_{\sigma}} \phi_1. \quad (5.6)$$

Substituting this into Eq.(5.5) gives the dispersion relation

$$1 - \sum_{\sigma} \frac{\omega_{p\sigma}^2}{(\omega - \mathbf{k} \cdot \mathbf{u}_{\sigma 0})^2} = 0 \quad (5.7)$$

which is just like the susceptibility for stationary cold species except that here ω is replaced by the Doppler-shifted frequency $\omega_{Doppler} = \omega - \mathbf{k} \cdot \mathbf{u}_{\sigma 0}$.

Two examples of streaming instability will now be considered: (i) equal densities of positrons and electrons streaming past each other with equal and opposite velocities, and (ii) electrons streaming past stationary ions.

Positron-electron streaming instability

The positron/electron example, while difficult to realize in practice, is worth analyzing because it reveals the essential features of the instability with a minimum of mathematical complexity. The equilibrium positron and electron densities are assumed equal so as to have charge neutrality. Since electrons and positrons have identical mass, the positron plasma frequency ω_{pp} is the same as the electron plasma frequency ω_{pe} . Let \mathbf{u}_0 be the electron stream velocity and $-\mathbf{u}_0$ be the positron stream velocity. Defining $z = \omega/\omega_{pe}$ and $\lambda = \mathbf{k} \cdot \mathbf{u}_0/\omega_{pe}$, Eq. (5.7) reduces to

$$1 = \frac{1}{(z - \lambda)^2} + \frac{1}{(z + \lambda)^2}, \quad (5.8)$$

a quartic equation in z . Because of the symmetry, no odd powers of z appear and Eq.(5.8) becomes

$$z^4 - 2z^2(\lambda^2 + 1) + \lambda^4 - 2\lambda^2 = 0 \quad (5.9)$$

which may be solved for z^2 to give

$$z^2 = (\lambda^2 + 1) \pm \sqrt{4\lambda^2 + 1}. \quad (5.10)$$

Each choice of the \pm sign gives two roots for z . If $z^2 > 0$ then the two roots are real, equal in magnitude, and opposite in sign. On the other hand, if $z^2 < 0$, then the two roots are *pure imaginary*, equal in magnitude, and opposite in sign. Recalling that $\omega = \omega_{pe}z$ and that the perturbation varies as $\exp(i\mathbf{k} \cdot \mathbf{x} - i\omega t)$, it is seen that the positive imaginary root $z = +i|z|$ corresponds to instability; i.e., to a perturbation which *grows* exponentially in time.

Hence the condition for instability is $z^2 < 0$. Only the choice of minus sign in Eq.(5.10) allows this possibility, so choosing this sign, the condition for instability is

$$\sqrt{4\lambda^2 + 1} > \lambda^2 + 1 \quad (5.11)$$

which corresponds to

$$0 < \lambda < \sqrt{2}. \quad (5.12)$$

The maximum growth rate is found by maximizing the right hand side of Eq.(5.10) with the minus sign chosen. Taking the derivative with respect to λ and setting $dz/d\lambda = 0$ to find the maximum, gives

$$2z \frac{dz}{d\lambda} = 2\lambda - \frac{4\lambda}{\sqrt{4\lambda^2 + 1}} = 0$$

or $\lambda = \sqrt{3}/2$. Substituting this most unstable λ back into Eq.(5.10) (with the minus sign, since this is the potentially unstable root) gives the maximum growth rate to be $y = 1/2$ where $z = x + iy$.

Changing back to physical variables, it is seen that onset of instability occurs when

$$ku_0 < \sqrt{2}\omega_{pe},$$

and the maximum growth rate occurs when

$$ku_0 = \frac{\sqrt{3}}{2}\omega_{pe}$$

in which case

$$\omega = i\frac{\omega_{pe}}{2}.$$

Figure 5.1 plots the normalized instability growth rate $\text{Im } z$ as a function of λ ; both onset and maximum growth rate are indicated. Since the instability has a pure imaginary frequency it is called a purely growing mode. Because the growth rate is of the order of magnitude of the plasma frequency, the instability grows extremely quickly.

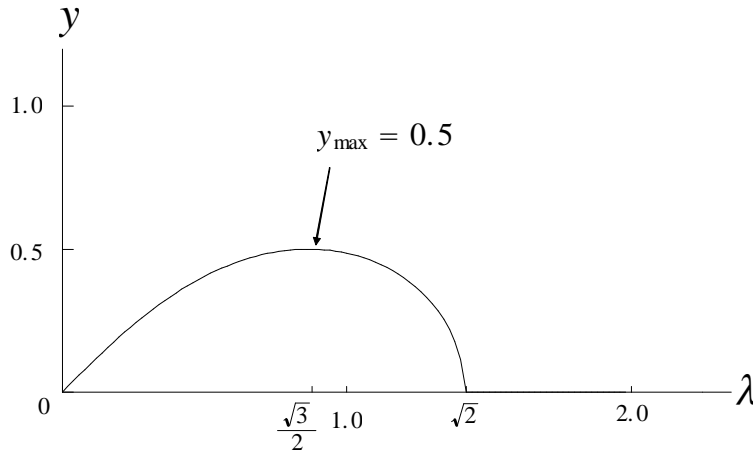


Figure 5.1: Normalized growth rate v. normalized wavenumber

Electron-ion streaming instability

Now consider the more realistic situation where electrons stream with velocity \mathbf{v}_0 through a background of stationary neutralizing ions. The dispersion relation here is

$$1 - \frac{\omega_{pi}^2}{\omega^2} - \frac{\omega_{pe}^2}{(\omega - \mathbf{k} \cdot \mathbf{u}_0)^2} = 0 \quad (5.13)$$

which can be recast in non-dimensional form by defining $z = \omega/\omega_{pe}$, $\epsilon = m_e/m_i$, and $\lambda = \mathbf{k} \cdot \mathbf{u}_0/\omega_{pe}$, giving

$$1 = \frac{\epsilon}{z^2} + \frac{1}{(z - \lambda)^2}. \quad (5.14)$$

The value of λ at which onset of instability occurs can be seen by plotting the right hand side of Eq.(5.14) versus z . The first term ϵ/z^2 diverges at $z = 0$, while the second term diverges at $z = \lambda$. Between $z = 0$ and $z = \lambda$, the right hand side of Eq.(5.14) has a minimum. If the value of the right hand side at this minimum is below unity, there will be two places between $z = 0$ and $z = \lambda$ where the right hand side of Eq.(5.14) equals unity. For $z > \lambda$, there is always one and only one place where the right hand side equals unity and similarly for $z < 0$ there is one and only one place where the right hand side equals unity. If the minimum of the right hand side drops below unity, then Eq.(5.14) has four real roots, but if the minimum of the right hand side is above unity there are only two real roots (those in the regions $z > \lambda$ and $z < 0$). In this latter case the other two roots of this quartic equation must be complex.

Because a quartic equation must be expressible in the form

$$(z - z_1)(z - z_2)(z - z_3)(z - z_4) = 0 \quad (5.15)$$

and because the coefficients of Eq.(5.14) are real, the two complex roots must be complex conjugates of each other. To see this, suppose the complex roots are z_1 and z_2 and the real roots are z_3 and z_4 . The product of the first two factors in Eq.(5.15) is $z^2 - (z_1 + z_2)z + z_1 z_2$; if the complex roots are not complex conjugates of each other then this product will contain complex coefficients and, when multiplied with the product of the terms involving the real roots, will result in an equation that contains complex coefficients. However, Eq.(5.14) has only real coefficients so the two complex roots must be complex conjugates of each other. The complex root with positive imaginary part will give rise to instability.

Thus, when the minimum of the right hand side of Eq.(5.14) is greater than unity, two of the roots become complex, and one of these complex roots gives instability. The onset of instability occurs when the minimum of the right hand side Eq.(5.14) equals unity. Straightforward analysis (cf. assignments) shows this occurs when

$$\lambda = (1 + \epsilon^{1/3})^{3/2}, \quad (5.16)$$

i.e., instability starts when

$$\mathbf{k} \cdot \mathbf{u}_0 = \omega_{pe} \left[1 + \left(\frac{m_e}{m_i} \right)^{1/3} \right]^{3/2}. \quad (5.17)$$

The maximum growth rate of the instability may be found by solving Eq.(5.14) for λ and then simplifying the resulting expression using ϵ as a small parameter. The details of this

are worked out in the assignments showing that the maximum growth rate is

$$\max \omega_i \simeq \frac{\sqrt{3}}{2} \left(\frac{m_e}{2m_i} \right)^{1/3} \omega_{pe} \quad (5.18)$$

which occurs when

$$\mathbf{k} \cdot \mathbf{u}_0 \simeq \omega_{pe}. \quad (5.19)$$

Again this is a very fast growing instability, about one order of magnitude smaller than the electron plasma frequency.

Streaming instabilities are a reason why certain simple proposed methods for attaining thermonuclear fusion will not work. These methods involve shooting an energetic deuterium beam at an oppositely directed energetic tritium beam with the expectation that collisions between the two beams would produce fusion reactions. However, such a system is extremely unstable with respect to the two-stream instability. This instability typically has a growth rate much faster than the fusion reaction rate and so will destroy the beams before significant fusion reactions can occur.

5.2 The Landau problem

A plasma wave behavior that is both of great philosophical interest and great practical importance can now be investigated. Before doing so, three seemingly disconnected results obtained thus far should be mentioned, namely:

1. When the exchange of energy between charged particles and a simple one-dimensional wave having dependence $\sim \exp(ikx - i\omega t)$ was considered, the particles were categorized into two general classes, trapped and untrapped, and it was found that untrapped particles tended to be dragged toward the wave phase velocity. Thus, untrapped particles moving slower than the wave gain kinetic energy, whereas those moving faster lose kinetic energy. This has the consequence that if there are more slow than fast particles, the particles gain net kinetic energy overall and this gain presumably comes at the expense of the wave. Conversely if there are more fast than slow particles, net energy flows from the particles to the wave.
2. When electrostatic plasma waves in an unmagnetized, uniform, stationary plasma were considered it was found that wave behavior is characterized by a dispersion relation $1 + \chi_e(\omega, k) + \chi_i(\omega, k) = 0$, where $\chi_\sigma(\omega, k)$ is the susceptibility of each species σ . These susceptibilities had simple limiting forms when $\omega/k \ll \sqrt{\kappa T_{\sigma 0}/m_\sigma}$ (isothermal limit) and when $\omega/k \gg \sqrt{\kappa T_{\sigma 0}/m_\sigma}$ (adiabatic limit), but the fluid analysis failed when $\omega/k \sim \sqrt{\kappa T_{\sigma 0}/m_\sigma}$ and the susceptibilities became undefined.
3. When the behavior of interacting beams of particles was considered, it was found that under certain conditions a fast growing instability would develop.

These three results will be tied together by the analysis of the Landau problem.

5.2.1 Attempt to solve the linearized Vlasov-Poisson system of equations using Fourier analysis

The method for manipulating fluid equations to find wave solutions was as follows: (i)

the relevant fluid equations were linearized, (ii) a perturbation $\sim \exp(\mathbf{ik} \cdot \mathbf{x} - i\omega t)$ was assumed, (iii) the system of partial differential equations was transformed into a system of algebraic equations, and then finally (iv) the roots of the determinant of the system of algebraic equations provided the dispersion relations which characterized the various wave solutions.

It seems reasonable to use this method again in order to investigate waves from the Vlasov point of view. However, it will be seen that this approach *fails* and that instead, a more complicated Laplace transform technique must be used in the Vlasov context. However, once the underlying difference between the Laplace and Fourier transform techniques has been identified, it is possible to go back and “patch up” the Fourier technique. Although perhaps not entirely elegant, this patching approach turns out to be a reasonable compromise that incorporates both the simplicity of the Fourier method and the correct mathematics/physics of the Laplace method.

The Fourier method will now be presented and, to highlight how this method fails, the simplest relevant example will be considered, namely a one dimensional, unmagnetized plasma with a stationary Maxwellian equilibrium. The ions are assumed to be so massive as to be immobile and the ion density is assumed to equal the electron equilibrium density. The electrostatic electric field $E = -\partial\phi/\partial x$ is therefore zero in equilibrium because there is charge neutrality in equilibrium. Since ions do not move there is no need to track ion dynamics. Thus, all perturbed quantities refer to electrons and so it is redundant to label these with a subscript “e”. In order to have a well-defined, physically meaningful problem, the equilibrium electron velocity distribution is assumed to be Maxwellian, i.e.,

$$f_0(v) = n_0 \frac{1}{\pi^{1/2} v_T} e^{-v^2/v_T^2} \quad (5.20)$$

where $v_T \equiv \sqrt{2\kappa T/m}$.

The one dimensional, unmagnetized Vlasov equation is

$$\frac{\partial f}{\partial t} + v \frac{\partial f}{\partial x} - \frac{q}{m} \frac{\partial \phi}{\partial x} \frac{\partial f}{\partial v} = 0 \quad (5.21)$$

and linearization of this equation gives

$$\frac{\partial f_1}{\partial t} + v \frac{\partial f_1}{\partial x} - \frac{q}{m} \frac{\partial \phi_1}{\partial x} \frac{\partial f_0}{\partial v} = 0. \quad (5.22)$$

Because the Vlasov equation describes evolution in phase-space, v is an *independent* variable just like x and t . Assuming a normal mode dependence $\sim \exp(ikx - i\omega t)$, Eq.(5.22) becomes

$$-i(\omega - kv)f_1 - ik\phi_1 \frac{q}{m} \frac{\partial f_0}{\partial v} = 0 \quad (5.23)$$

which gives

$$f_1 = -\frac{k}{(\omega - kv)} \frac{q}{m} \frac{\partial f_0}{\partial v} \phi_1. \quad (5.24)$$

The electron density perturbation is

$$n_1 = \int_{-\infty}^{\infty} f_1 dv = -\frac{q}{m} \phi_1 \int_{-\infty}^{\infty} \frac{k}{(\omega - kv)} \frac{\partial f_0}{\partial v} dv, \quad (5.25)$$

a relationship between n_1 and ϕ_1 . Another relationship between n_1 and ϕ_1 is Poisson's equation

$$\frac{\partial^2 \phi_1}{\partial x^2} = -\frac{n_1 q}{\varepsilon_0}. \quad (5.26)$$

Replacing $\partial/\partial x$ by ik , Eq.(5.26) becomes

$$k^2 \phi_1 = \frac{n_1 q}{\varepsilon_0}. \quad (5.27)$$

Combining Eqs.(5.25) and (5.27) gives the dispersion relation

$$1 + \frac{q^2}{k^2 m \varepsilon_0} \int_{-\infty}^{\infty} \frac{k}{(\omega - kv)} \frac{\partial f_0}{\partial v} dv = 0. \quad (5.28)$$

This can be written more elegantly by substituting for f_0 using Eq.(5.20), defining the non-dimensional particle velocity $\xi = v/v_T$, and the non-dimensional phase velocity $\alpha = \omega/kv_T$ to give

$$1 - \frac{1}{2k^2 \lambda_D^2} \frac{1}{\pi^{1/2}} \int_{-\infty}^{\infty} d\xi \frac{1}{(\xi - \alpha)} \frac{\partial}{\partial \xi} e^{-\xi^2} = 0. \quad (5.29)$$

or

$$1 + \chi = 0 \quad (5.30)$$

where the electron susceptibility is

$$\chi = -\frac{1}{2k^2 \lambda_D^2} \frac{1}{\pi^{1/2}} \int_{-\infty}^{\infty} d\xi \frac{1}{(\xi - \alpha)} \frac{\partial}{\partial \xi} e^{-\xi^2}. \quad (5.31)$$

In contrast to the earlier two-fluid wave analysis where in effect the zeroth, first, and second moments of the Vlasov equation were combined (continuity equation, equation of motion, and equation of state), here only the Vlasov equation is involved. Thus the Vlasov equation contains all the information of the moment equations and more. The Vlasov method therefore seems a simpler and more direct way for calculating the susceptibilities than the fluid method, except for a serious difficulty: the integral in Eq.(5.31) is mathematically ill-defined because the denominator vanishes when $\xi = \alpha$ (i.e., when $\omega = kv_T$). Because it is not clear how to deal with this singularity, the ζ integral cannot be evaluated and the Fourier method fails. This is essentially the same as the problem encountered in fluid analysis when ω/k became comparable to $\sqrt{\kappa T/m}$.

5.2.2 Landau method: Laplace transforms

Landau (1946) argued that the Fourier problem as presented above is ill-posed and showed that the linearized Vlasov-Poisson problem should be treated as an *initial value* problem, rather than as a normal mode problem. The initial value point of view is conceptually related to the analysis of single particle motion in sawtooth or sine waves. Before presenting the Landau analysis of the linearized Vlasov-Poisson problem, certain important features of Laplace transforms will now be reviewed.

The Laplace transform of a function $\psi(t)$ is defined as

$$\tilde{\psi}(p) = \int_0^{\infty} \psi(t) e^{-pt} dt \quad (5.32)$$

and can be considered as a “half of a Fourier transform” since the time integration starts at $t = 0$ rather than $t = -\infty$. Caution is required regarding the convergence of this integral for situations where $\psi(t)$ contains exponentially growing terms.

Suppose such exponentially growing terms exist. As $t \rightarrow \infty$, the fastest growing term, say $\exp(\gamma t)$, will dominate all other terms contributing to $\psi(t)$. The integral in Eq.(5.32) will then diverge as $t \rightarrow \infty$, unless a *restriction* is imposed on the real part of p . In particular, if it is *required* that $\text{Re } p > \gamma$, then the decaying $\exp(-pt)$ factor will always overwhelm the growing $\exp(\gamma t)$ factor so that the integral in Eq.(5.32) will converge. These issues of convergence are ignored in Fourier transforms where it is implicitly assumed that the function being transformed has neither exponentially growing terms (which diverge at $t = \infty$) nor exponentially decaying terms (which diverge at $t = -\infty$).

Thus, the integral transform in Eq.(5.32) is defined *only* for $\text{Re } p > \gamma$. To emphasize this restriction, Eq.(5.32) is re-written as

$$\tilde{\psi}(p) = \int_0^{\infty} \psi(t) e^{-pt} dt, \quad \text{Re } p > \gamma \quad (5.33)$$

where γ is the fastest growing exponential term contained in $\psi(t)$. Since p is typically complex, Eq.(5.33) means that $\tilde{\psi}(p)$ is *only* defined in that part of the complex p plane lying to the *right* of γ as sketched in Fig.5.2(a). Whenever $\tilde{\psi}(p)$ is used, one must be very careful to avoid venturing outside the region in p -space where $\tilde{\psi}(p)$ is defined (this restriction will later become an important issue).

To construct an inverse transform, consider the integral

$$g(t) = \int_C dp \tilde{\psi}(p) e^{pt}. \quad (5.34)$$

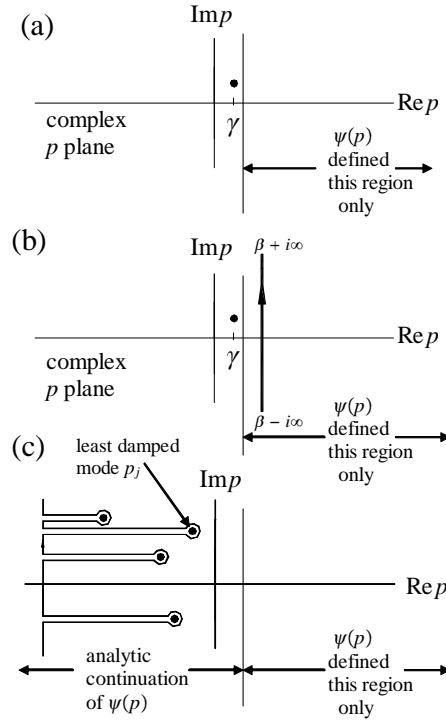
This integral is ambiguously defined for now because the integration contour C is unspecified. However, whatever integration contour is ultimately selected must not venture into regions where $\tilde{\psi}(p)$ is undefined. Thus, an allowed integration path must have $\text{Re } p > \gamma$. Substitution of Eq.(5.33) into Eq.(5.34) and interchanging the order of integration gives

$$g(t) = \int_0^{\infty} dt' \int_C dp \psi(t') e^{p(t-t')}, \quad \text{Re } p > \gamma. \quad (5.35)$$

A useful integration path C for the p integral will now be determined. Recall from the theory of Fourier transforms that the Dirac delta function can be expressed as

$$\delta(t) = \frac{1}{2\pi} \int_{-\infty}^{\infty} d\omega e^{i\omega t} \quad (5.36)$$

which is an integral along the real ω axis so that ω is always real. The integration path for Eq.(5.35) will now be chosen such that the real part of p stays constant, say at a value β which is larger than γ , while the imaginary part of p goes from $-\infty$ to ∞ . This path is shown in Fig.5.2(b), and is called the Bromwich contour.

Figure 5.2: Contours in complex p -plane

For this choice of path, Eq.(5.35) becomes

$$\begin{aligned}
 g(t) &= \int_0^{\infty} dt' \int_{\beta-i\infty}^{\beta+i\infty} d(p_r + ip_i) \psi(t') e^{(p_r + ip_i)(t-t')} \\
 &= i \int_0^{\infty} dt' e^{\beta(t-t')} \psi(t') \int_{-\infty}^{\infty} dp_i e^{ip_i(t-t')} \\
 &= 2\pi i \int_0^{\infty} dt' e^{\beta(t-t')} \psi(t') \delta(t-t') \\
 &= 2\pi i \psi(t)
 \end{aligned} \tag{5.37}$$

where Eq.(5.36) has been used. Thus, $\psi(t) = (2\pi i)^{-1}g(t)$ and so the inverse of the Laplace transform is

$$\psi(t) = \frac{1}{2\pi i} \int_{\beta-i\infty}^{\beta+i\infty} dp \psi(p) e^{pt}, \quad \beta > \gamma. \tag{5.38}$$

Before returning to physics, recall another peculiarity of Laplace transforms, namely the transformation procedure for derivatives. The Laplace transform of $d\psi/dt$; may be simplified by integrating by parts to give

$$\int_0^\infty dt \frac{d\psi}{dt} e^{-pt} = [\psi(t)e^{-pt}]_0^\infty + p \int_0^\infty dt \psi(t)e^{-pt} = p\tilde{\psi}(p) - \psi(0). \quad (5.39)$$

Unlike Fourier transforms, here the *initial value* forms part of the transform. Thus, Laplace transforms contain information about the initial value and so should be better suited than Fourier transforms for investigating initial value problems. The importance of initial value was also evident in the Chapter 3 analysis of particle motion in sawtooth or sine wave potentials.

The requisite mathematical tools are now in hand for investigating the Vlasov-Poisson system and its dependence on initial value. To obtain extra insights with little additional effort the analysis is extended to the more general situation of a three dimensional plasma where ions are allowed to move. Again electrostatic waves are considered and it is assumed that the equilibrium plasma is stationary, spatially uniform, neutral, and unmagnetized.

The equilibrium velocity distribution of each species is assumed to be a three dimensional Maxwellian distribution function

$$f_{\sigma 0}(\mathbf{v}) = n_{\sigma 0} \left(\frac{m_\sigma}{2\pi\kappa T_\sigma} \right)^{3/2} \exp(-m_\sigma v^2/2\kappa T_\sigma). \quad (5.40)$$

The equilibrium electric field is assumed to be zero so that the equilibrium potential is a constant chosen to be zero. It is further assumed that at $t = 0$ there exists a small perturbation of the distribution function and that this perturbation evolves in time so that at later times

$$f_\sigma(\mathbf{x}, \mathbf{v}, t) = f_{\sigma 0}(\mathbf{v}) + f_{\sigma 1}(\mathbf{x}, \mathbf{v}, t). \quad (5.41)$$

The linearized Vlasov equation for each species is therefore

$$\frac{\partial f_{\sigma 1}}{\partial t} + \mathbf{v} \cdot \nabla f_{\sigma 1} - \frac{q_\sigma}{m_\sigma} \nabla \phi_1 \cdot \frac{\partial f_{\sigma 0}}{\partial \mathbf{v}} = 0. \quad (5.42)$$

All perturbed quantities are assumed to have the spatial dependence $\sim \exp(i\mathbf{k} \cdot \mathbf{x})$; this is equivalent to Fourier transforming in space. Equation (5.42) becomes

$$\frac{\partial f_{\sigma 1}}{\partial t} + i\mathbf{k} \cdot \mathbf{v} f_{\sigma 1} - \frac{q_\sigma}{m_\sigma} \phi_1 i\mathbf{k} \cdot \frac{\partial f_{\sigma 0}}{\partial \mathbf{v}} = 0. \quad (5.43)$$

Laplace transforming in time gives

$$(p + i\mathbf{k} \cdot \mathbf{v}) \tilde{f}_{\sigma 1}(\mathbf{v}, p) - f_{\sigma 1}(\mathbf{v}, 0) - \frac{q_\sigma}{m_\sigma} \tilde{\phi}_1(p) i\mathbf{k} \cdot \frac{\partial f_{\sigma 0}}{\partial \mathbf{v}} = 0 \quad (5.44)$$

which may be solved for $\tilde{f}_{\sigma 1}(\mathbf{v}, p)$ to give

$$\tilde{f}_{\sigma 1}(\mathbf{v}, p) = \frac{1}{(p + i\mathbf{k} \cdot \mathbf{v})} \left[f_{\sigma 1}(\mathbf{v}, 0) + \frac{q_\sigma}{m_\sigma} \tilde{\phi}_1(p) i\mathbf{k} \cdot \frac{\partial f_{\sigma 0}}{\partial \mathbf{v}} \right]. \quad (5.45)$$

This is similar to Eq.(5.24), except that now the Laplace variable p occurs instead of the Fourier variable $-i\omega$ and also the initial value $f_{\sigma 1}(\mathbf{v}, 0)$ appears. As before, Poisson's equation can be written as

$$\nabla^2 \phi_1 = -\frac{1}{\varepsilon_0} \sum_{\sigma} q_{\sigma} n_{\sigma 1} = -\frac{1}{\varepsilon_0} \sum_{\sigma} q_{\sigma} \int d^3v f_{\sigma 1}(\mathbf{x}, \mathbf{v}, t). \quad (5.46)$$

Replacing $\nabla \rightarrow i\mathbf{k}$ and Laplace transforming with respect to time, Poisson's equation becomes

$$k^2 \tilde{\phi}_1(p) = \frac{1}{\varepsilon_0} \sum_{\sigma} q_{\sigma} \int d^3v \tilde{f}_{\sigma 1}(\mathbf{v}, p). \quad (5.47)$$

Substitution of Eq.(5.45) into the right hand side of Eq. (5.47) gives

$$k^2 \tilde{\phi}_1(p) = \frac{1}{\varepsilon_0} \sum_{\sigma} q_{\sigma} \int d^3v \left\{ \frac{f_{\sigma 1}(\mathbf{v}, 0) + \frac{q_{\sigma}}{m_{\sigma}} \tilde{\phi}_1(p) i\mathbf{k} \cdot \frac{\partial f_{\sigma 0}}{\partial \mathbf{v}}}{(p + i\mathbf{k} \cdot \mathbf{v})} \right\} \quad (5.48)$$

which is similar to Eq.(5.28) except that $-i\omega \rightarrow p$ and the initial value appears. Equation (5.48) may be solved for $\tilde{\phi}_1(p)$ to give

$$\tilde{\phi}_1(p) = \frac{N(p)}{D(p)} \quad (5.49)$$

where the numerator is

$$N(p) = \frac{1}{k^2 \varepsilon_0} \sum_{\sigma} q_{\sigma} \int d^3v \frac{f_{\sigma 1}(\mathbf{v}, 0)}{(p + i\mathbf{k} \cdot \mathbf{v})} \quad (5.50)$$

and the denominator is

$$D(p) = 1 - \frac{1}{k^2} \sum_{\sigma} \frac{q_{\sigma}^2}{\varepsilon_0 m_{\sigma}} \int d^3v \frac{i\mathbf{k} \cdot \frac{\partial f_{\sigma 0}}{\partial \mathbf{v}}}{(p + i\mathbf{k} \cdot \mathbf{v})}. \quad (5.51)$$

Note that the denominator is similar to Eq.(5.28). All that has to be done now is take the inverse Laplace transform of Eq.(5.49) to obtain

$$\phi_1(t) = \frac{1}{2\pi i} \int_{\beta - i\infty}^{\beta + i\infty} dp \frac{N(p)}{D(p)} e^{pt} \quad (5.52)$$

where β is chosen to be larger than the fastest growing exponential term in $N(p)/D(p)$.

This is an exact formal solution to the problem. However, because of the complexity of $N(p)$ and $D(p)$ it is impossible to evaluate the integral in Eq.(5.52). Nevertheless, it turns out to be feasible to evaluate the long-time asymptotic limit of this integral and for practical purposes, this is a sufficient answer to the problem.

5.2.3 The relationship between poles, exponential functions, and analytic continuation

Before evaluating Eq.(5.52), it is useful to examine the relationship between exponentially growing/decaying functions, Laplace transforms, poles, residues, and analytic continuation. This relationship is demonstrated by considering the exponential function

$$f(t) = e^{qt} \quad (5.53)$$

where q is a complex constant. If the real part of q is positive, then the amplitude of $f(t)$ is exponentially growing, whereas if the real part of q is negative, the amplitude of $f(t)$ is exponentially decaying. Now, calculate the Laplace transform of $f(t)$; it is

$$\tilde{f}(p) = \int_0^{\infty} e^{(q-p)t} dt = \frac{1}{p-q}, \quad \text{defined only for } \operatorname{Re} p > \operatorname{Re} q. \quad (5.54)$$

Let us examine the Bromwich contour integral for $\tilde{f}(p)$ and temporarily call this integral $F(t)$; evaluation of $F(t)$ ought to yield $F(t) = f(t)$. Thus, we define

$$F(t) = \frac{1}{2\pi i} \int_{\beta-i\infty}^{\beta+i\infty} dp \tilde{f}(p) e^{pt}, \quad \beta > \operatorname{Re} q. \quad (5.55)$$

If the Bromwich contour could be closed in the left hand p plane, the integral could easily be evaluated using the method of residues but closure of the contour to the left is forbidden because of the restriction that $\beta > \operatorname{Re} q$. This annoyance may be overcome by constructing a new function $\hat{f}(p)$ which

1. equals $\tilde{f}(p)$ in the region $\beta > \operatorname{Re} q$,
2. is *also* defined in the region $\beta < \operatorname{Re} q$, and
3. is analytic.

Integration of $\hat{f}(p)$ along the Bromwich contour gives the same result as does integration of $\tilde{f}(p)$ along the same contour because the two functions are *identical* along this contour [cf. stipulation (1) above]. Thus, it is seen that

$$F(t) = \frac{1}{2\pi i} \int_{\beta-i\infty}^{\beta+i\infty} dp \hat{f}(p) e^{pt}, \quad (5.56)$$

but now there is no restriction on which part of the p plane may be used. So long as the end points are kept fixed and no poles are crossed, the path of integration of an analytic function can be arbitrarily deformed. This is because the difference between the original path and a deformed path is a closed contour which integrates to zero if it does not enclose any poles. Because $\hat{f}(p) \rightarrow 0$ at the endpoints $\beta \pm \infty$, the integration path of $\hat{f}(p)$ can be deformed into the left hand plane as long as $\hat{f}(p)$ remains analytic (i.e., does not jump over any poles or branch cuts). How can this magic function $\hat{f}(p)$ be constructed?

The answer is simple; we *define* a function $\hat{f}(p)$ having the identical functional form as $\tilde{f}(p)$, but *without* the restriction that $\operatorname{Re} p > \operatorname{Re} q$. Thus, the analytic continuation of

$$\tilde{f}(p) = \frac{1}{p-q}, \quad \text{defined only for } \operatorname{Re} p > \operatorname{Re} q \quad (5.57)$$

is simply

$$\hat{f}(p) = \frac{1}{p - q}, \quad \text{defined for all } p \text{ provided } \hat{f}(p) \text{ remains analytic.} \quad (5.58)$$

The Bromwich contour can now be deformed into the left hand plane as shown in Fig. 5.3. Because $\exp(pt) \rightarrow 0$ for positive t and negative $\text{Re } p$, the integration contour can be closed by an arc that goes to the left (cf. Fig.5.3) into the region where $\text{Re } p \rightarrow -\infty$. The resulting contour encircles the pole at $p = q$ and so the integral can be evaluated using the method of residues as follows:

$$F(t) = \frac{1}{2\pi i} \oint \frac{1}{p - q} e^{pt} dp = \lim_{p \rightarrow q} 2\pi i (p - q) \left[\frac{1}{2\pi i (p - q)} e^{pt} \right] = e^{qt}. \quad (5.59)$$

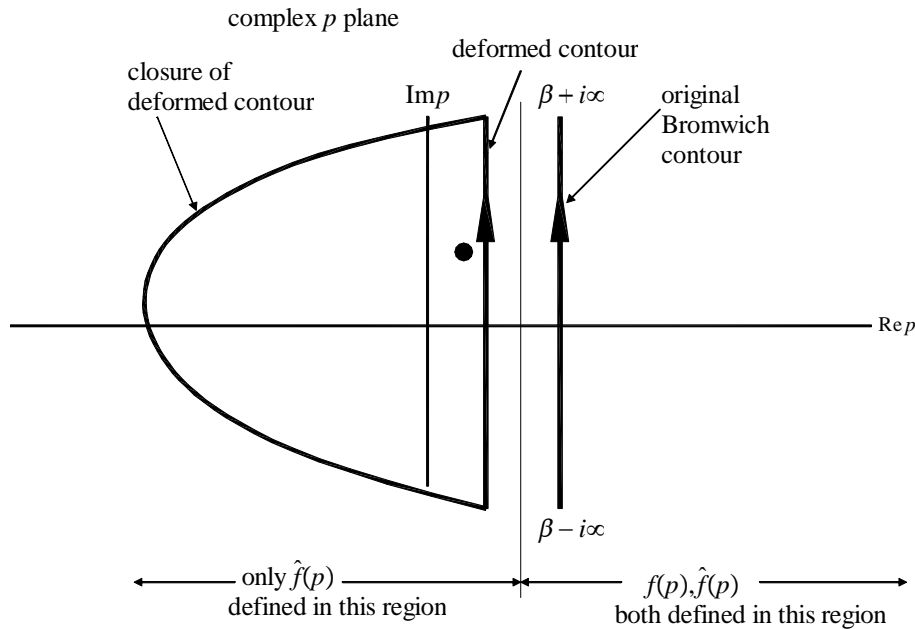


Figure 5.3: Bromwich contour

This simple example shows that while the Bromwich contour formally gives the inverse Laplace inverse transform of $\tilde{f}(p)$, the Bromwich contour by itself does not allow use of the method of residues, since the poles of interest are located precisely in the left hand complex p plane where $\tilde{f}(p)$ is undefined. However, analytic continuation of $f(p)$ allows deformation of the Bromwich contour into the formerly forbidden area, and then the inverse transform may be easily evaluated using the method of residues.

5.2.4 Asymptotic long time behavior of the potential oscillation

We now return to the more daunting problem of evaluating Eq.(5.52). As in the simple example above, the goal is to close the contour to the left, but because the functions $N(p)$ and $D(p)$ are not defined for $\text{Re } p < \gamma$, this is not immediately possible. It is first necessary to construct analytic continuations of $N(p)$ and $D(p)$ that extend the definition of these functions into regions of negative $\text{Re } p$. As in the simple example, the desired analytic continuations may be constructed by taking the same formal expressions as obtained before, but now extending the definition to the entire p plane with the proviso that *the functions remain analytic* as the region of definition is pushed leftwards in the p plane.

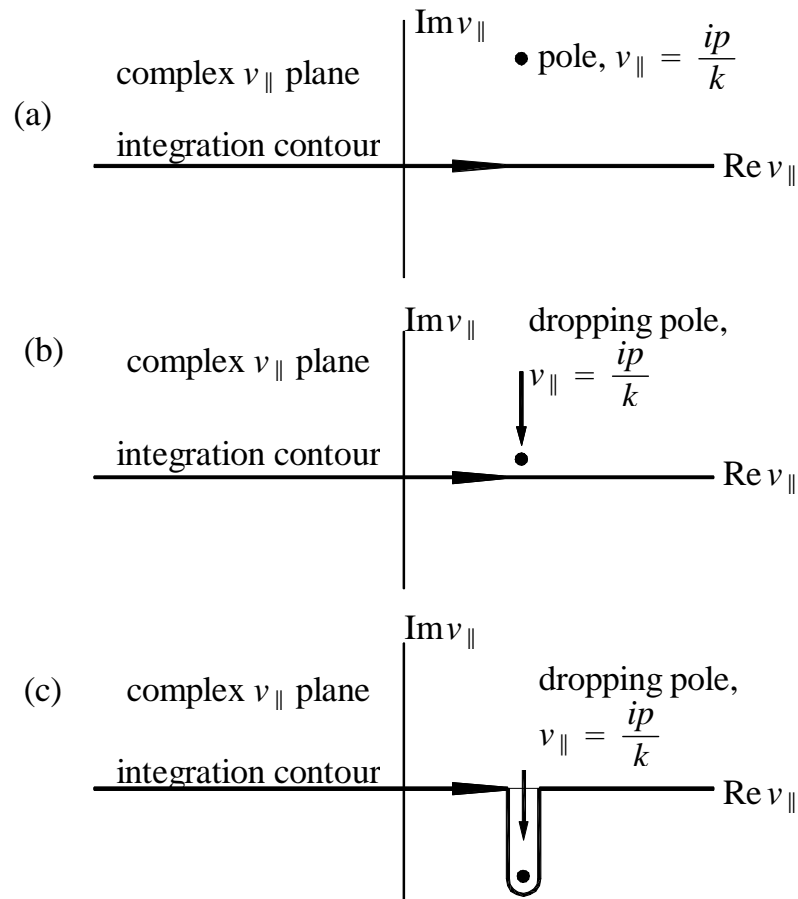
Consider first construction of an analytic continuation for the function $N(p)$. This function can be written as

$$N(p) = \frac{1}{k^2 \varepsilon_0} \sum_{\sigma} q_{\sigma} \int_{-\infty}^{\infty} dv_{\parallel} \frac{F_{\sigma 1}(v_{\parallel}, 0)}{(p + ikv_{\parallel})} = \frac{1}{ik^3 \varepsilon_0} \sum_{\sigma} q_{\sigma} \int_{-\infty}^{\infty} dv_{\parallel} \frac{F_{\sigma 1}(v_{\parallel}, 0)}{(v_{\parallel} - ip/k)}. \quad (5.60)$$

Here, \parallel means in the \mathbf{k} direction, and the parallel component of the initial value of the perturbed distribution function has been defined as

$$F_{\sigma 1}(v_{\parallel}, 0) = \int d^2 \mathbf{v}_{\perp} f_{\sigma 1}(\mathbf{v}, 0). \quad (5.61)$$

The integrand in Eq.(5.50) has a pole at $v_{\parallel} = ip/k$. Let us assume that $k > 0$ (the general case where k can be of either sign will be left as an assignment). Before we construct an analytic continuation, $\text{Re } p$ is restricted to be greater than γ so that the pole $v_{\parallel} = ip/k$ is in the *upper half* of the complex v_{\parallel} plane as shown in Fig.5.4(a). When $N(p)$ is analytically continued to the left hand region, the definition of $N(p)$ is extended to allow $\text{Re } p$ to become less than γ and even negative. As shown in Figs. 5.4(b), decreasing $\text{Re } p$ means that the pole at $v_{\parallel} = ip/k$ in Eq.(5.50) drops from its initial location in the upper half v_{\parallel} plane toward the lower half v_{\parallel} plane. A critical question now arises: how should we arrange this construction when $\text{Re } p$ passes through zero? If the pole is allowed to jump from being above the path of v_{\parallel} integration (which is along the real v_{\parallel} axis) to being below, the function $N(p)$ will *not* be analytic because it will have a discontinuous jump of $2\pi i$ times the residue associated with the pole. Since it was stipulated that $N(p)$ must be analytic, the pole cannot be allowed to jump over the v_{\parallel} contour of integration. Instead, the prescription proposed by Landau will be used which is to *deform* the v_{\parallel} contour as $\text{Re } p$ becomes negative so that the contour *always* lies below the pole; this deformation is shown in Figs.5.4(c).

Figure 5.4: Complex v plane

$D(p)$ involves a similar integration along the real v_{\parallel} axis. It also has a pole that is initially in the upper half plane when $\text{Re } p > 0$, but then drops to being below the axis as $\text{Re } p$ is allowed to become negative. Thus analytic continuation of $D(p)$ is also constructed by deforming the path of the v_{\parallel} integration so that the contour always lies below the pole.

Equipped with these suitably constructed analytic continuations of $N(p)$ and $D(p)$ into the left-hand p plane, evaluation of Eq.(5.52) can now be undertaken. As shown in the simple example, it is computationally advantageous to deform the Bromwich contour into the left hand p -plane. The deformed contour evaluates to the same result as the original Bromwich contour (provided the deformation does not jump over any poles) and this evaluation may be accomplished via the method of residues. In the general case where $N(p)/D(p)$ has several poles in the left hand p plane, then as shown in Fig.5.2(c), the

contour may be deformed so that the vertical portion is pushed to the far left, except where there is a pole p_j ; the contour “snags” around each pole p_j as shown in Fig.5.2(c). For $\text{Re } p \rightarrow -\infty$, the numerator $N(p) \rightarrow 0$, while the denominator $D(p) \rightarrow 1$. Since $\exp(pt) \rightarrow 0$ for $\text{Re } p \rightarrow -\infty$ and positive t , the left hand vertical line does not contribute to the integral and Eq.(5.52) simply consists of the sum of the residues of all the poles, i.e.

$$\phi_1(t) = \sum_j \lim_{p \rightarrow p_j} \left[(p - p_j) \frac{N(p)}{D(p)} e^{pt} \right]. \quad (5.62)$$

Where do the poles p_j come from? Upon examining Eq.(5.62), it is clear that poles could come either from (i) $N(p)$ having an explicit pole, i.e. $N(p)$ contains a term $\sim 1/(p - p_j)$, or (ii) from $D(p)$ containing a factor $\sim (p - p_j)$, i.e., p_j is a root of the equation $D(p) = 0$. The integrand in Eq. (5.60) has a pole in the v_{\parallel} plane; this pole is “used up” as a residue upon performing the v_{\parallel} integration, and so does not contribute a pole to $N(p)$. The only other possibility is that the initial value $F_{\sigma 1}(v_{\parallel}, 0)$ somehow provides a pole, but $F_{\sigma 1}(v_{\parallel}, 0)$ is a physical quantity with a bounded integral [i.e., $\int F_{\sigma 1}(v_{\parallel}, 0) dv_{\parallel}$ is finite] and so cannot contribute a pole in $N(p)$. It is therefore concluded that all poles in $N(p)/D(p)$ must come from the roots (also called zeros) of $D(p)$.

The problem can be simplified by deciding to be content with a *less* than complete solution. Instead of attempting to calculate $\phi_1(t)$ for all positive times (i.e., all the poles p_j contribute to the solution), we restrict ourselves to the less burdensome problem of finding the long time asymptotic behavior of $\phi_1(t)$. Because each term in Eq.(5.62) has a factor $\exp(ip_j t)$, the least damped term [i.e., the term with pole furthest to the right in Fig.5.2(c)], will dominate all the other terms at large t . Hence, in order to find the long-term asymptotic behavior, all that is required is to find the root p_j having the largest real part.

The problem is thus reduced to finding the roots of $D(p)$; this requires performing the v_{\parallel} integration sketched in Fig.5.4. Before doing this, it is convenient to integrate out the perpendicular velocity dependence from $D(p)$ so that

$$\begin{aligned} D(p) &= 1 - \frac{1}{k^2} \sum_{\sigma} \frac{q_{\sigma}^2}{\varepsilon_0 m_{\sigma}} \int d^3 v \frac{\mathbf{ik} \cdot \frac{\partial f_{\sigma 0}}{\partial \mathbf{v}}}{(p + \mathbf{ik} \cdot \mathbf{v})} \\ &= 1 - \frac{1}{k^2} \sum_{\sigma} \frac{q_{\sigma}^2}{\varepsilon_0 m_{\sigma}} \int_{-\infty}^{\infty} dv_{\parallel} \frac{\frac{\partial F_{\sigma 0}}{\partial v_{\parallel}}}{(v_{\parallel} - ip/k)}. \end{aligned} \quad (5.63)$$

Thus, the relation $D(p) = 0$ can be written in terms of susceptibilities as

$$D(p) = 1 + \chi_i + \chi_e = 0 \quad (5.64)$$

since the quantities being summed in Eq.(5.63) are essentially the electron and ion perturbations associated with the oscillation, and $D(p)$ is the Laplace transform analog of the the Fourier transform of Poisson’s equation. In the special case where the equilibrium distribution function is Maxwellian, the susceptibilities can be written in a standardized form

as

$$\begin{aligned}
\chi_\sigma &= -\frac{1}{2k^2\lambda_{D\sigma}^2} \frac{1}{\pi^{1/2}} \int_{-\infty}^{\infty} d\xi \frac{1}{(\xi - ip/kv_{T\sigma})} \frac{\partial}{\partial \xi} \exp(-\xi^2) \\
&= \frac{1}{k^2\lambda_{D\sigma}^2} \left[\frac{1}{\pi^{1/2}} \int_{-\infty}^{\infty} d\xi \frac{(\xi - ip/kv_{T\sigma} + ip/kv_{T\sigma})}{(\xi - ip/kv_{T\sigma})} \exp(-\xi^2) \right] \\
&= \frac{1}{k^2\lambda_{D\sigma}^2} \left[1 + \frac{1}{\pi^{1/2}} \alpha \int_{-\infty}^{\infty} d\xi \frac{\exp(-\xi^2)}{(\xi - \alpha)} \right] \\
&= \frac{1}{k^2\lambda_{D\sigma}^2} [1 + \alpha Z(\alpha)] \tag{5.65}
\end{aligned}$$

where $\alpha = ip/kv_{T\sigma}$, and the last line introduces the *plasma dispersion function* $Z(\alpha)$ defined as

$$Z(\alpha) \equiv \frac{1}{\pi^{1/2}} \int_{-\infty}^{\infty} d\xi \frac{\exp(-\xi^2)}{(\xi - \alpha)} \tag{5.66}$$

where the ξ integration path is under the dropped pole.

5.2.5 Evaluation of the plasma dispersion function

If the pole corresponding to the fastest growing (i.e., least damped) mode turns out to have dropped well below the real axis (corresponding to $\text{Re } p$ being large and negative), the fastest growing mode would be highly damped. We argue that this does not happen because there ought to be a correspondence between the Vlasov and fluid models in regimes where both are valid. Since the fluid model indicated the existence of undamped plasma waves when ω/k was much larger than the thermal velocity, the Vlasov model should predict nearly the same wave in this regime. The fluid wave model had no damping and so any damping introduced by the Vlasov model should be weak in order to maintain an approximate correspondence between fluid and Vlasov models. The Vlasov solution corresponding to the fluid mode can therefore have a pole only slightly below the real axis, i.e., only slightly negative. In this case, it is only necessary to analytically continue the definition of $N(p)/D(p)$ *slightly* into the negative p plane. Thus, the pole in Eq.(5.66) drops only slightly below the real axis as shown in Fig.5.5.

The ξ integration contour can therefore be divided into three portions, namely (i) from $\xi = -\infty$ to $\xi = \alpha - \delta$, just to the left of the pole; (ii) a counterclockwise semicircle of radius δ half way around and *under* the pole [cf. Fig.5.5]; and (iii) a straight line from $\alpha + \delta$ to $+\infty$. The sum of the straight line segments (i) and (iii) in the limit $\delta \rightarrow 0$ is called the *principle part* of the integral and is denoted by a ‘P’ in front of the integral sign. The semicircle portion is *half* a residue and so makes a contribution that is just πi times the residue (rather than the standard $2\pi i$ for a complete residue). Hence, the plasma dispersion function for a pole slightly below the real axis is

$$Z(\alpha) = \frac{1}{\pi^{1/2}} \left[\text{P} \int_{-\infty}^{\infty} d\xi \frac{\exp(-\xi^2)}{(\xi - \alpha)} \right] + i\pi^{1/2} \exp(-\alpha^2) \quad (5.67)$$

where P means principle part of the integral. Equation (5.67) prescribes how to evaluate ill-defined integrals of the type we first noted in Eq.(5.28).

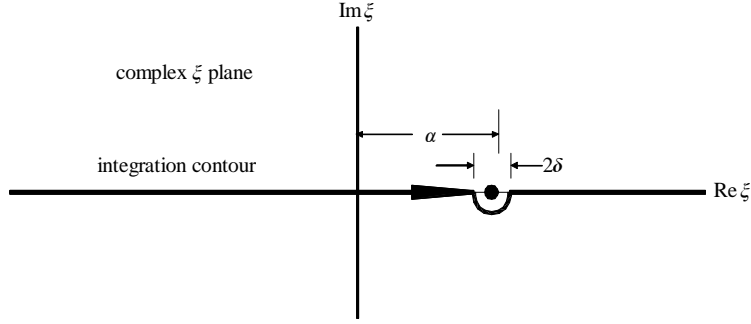


Figure 5.5: Contour for evaluating plasma dispersion function

There are two important limiting situations for $Z(\alpha)$, namely $|\alpha| \gg 1$ (corresponding to the adiabatic fluid limit since $\omega/k \gg v_{T\sigma}$) and $|\alpha| \ll 1$ (corresponding to the isothermal fluid limit since $\omega/k \ll v_{T\sigma}$). Asymptotic evaluations of $Z(\alpha)$ are possible in both cases and are found as follows:

1. $\alpha \gg 1$ case.

Here, it is noted that the factor $\exp(-\xi^2)$ contributes significantly to the integral only when ξ is of order unity or smaller. In the important part of the integral where this exponential term is finite, $|\alpha| \gg \xi$. In this region of ξ the other factor in the integrand can be expanded as

$$\frac{1}{(\xi - \alpha)} = -\frac{1}{\alpha} \left(1 - \frac{\xi}{\alpha} \right)^{-1} = -\frac{1}{\alpha} \left[1 + \frac{\xi}{\alpha} + \left(\frac{\xi}{\alpha} \right)^2 + \left(\frac{\xi}{\alpha} \right)^3 + \left(\frac{\xi}{\alpha} \right)^4 + \dots \right]. \quad (5.68)$$

The expansion is carried to fourth order because of numerous cancellations that eliminate several of the lower order terms. Substitution of Eq.(5.68) into the integral in Eq.(5.67) and noting that all odd terms in Eq.(5.68) do not contribute to the integral because the rest of the integrand is even gives

$$\text{P} \frac{1}{\pi^{1/2}} \int_{-\infty}^{\infty} d\xi \frac{\exp(-\xi^2)}{(\xi - \alpha)} = -\frac{1}{\alpha} \frac{1}{\pi^{1/2}} \int_{-\infty}^{\infty} d\xi \exp(-\xi^2) \left[1 + \left(\frac{\xi}{\alpha} \right)^2 + \left(\frac{\xi}{\alpha} \right)^4 + \dots \right]. \quad (5.69)$$

The 'P' has been dropped from the right hand side of Eq.(5.69) because there is no longer any problem with a singularity. These Gaussian-type integrals may be evaluated by taking successive derivatives with respect to a of the Gaussian

$$\frac{1}{\pi^{1/2}} \int d\xi \exp(-a\xi^2) = \frac{1}{a^{1/2}} \quad (5.70)$$

and then setting $a = 1$. Thus,

$$\frac{1}{\pi^{1/2}} \int d\xi \xi^2 \exp(-\xi^2) = \frac{1}{2}, \quad \frac{1}{\pi^{1/2}} \int d\xi \xi^4 \exp(-\xi^2) = \frac{3}{4} \quad (5.71)$$

so Eq.(5.69) becomes

$$P \frac{1}{\pi^{1/2}} \int_{-\infty}^{\infty} d\xi \frac{\exp(-\xi^2)}{(\xi - \alpha)} = -\frac{1}{\alpha} \left[1 + \frac{1}{2\alpha^2} + \frac{3}{4\alpha^4} + \dots \right]. \quad (5.72)$$

In summary, for $|\alpha| \gg 1$, the plasma dispersion function has the asymptotic form

$$Z(\alpha) = -\frac{1}{\alpha} \left[1 + \frac{1}{2\alpha^2} + \frac{3}{4\alpha^4} + \dots \right] + i\pi^{1/2} \exp(-\alpha^2). \quad (5.73)$$

2. $|\alpha| \ll 1$ case.

In order to evaluate the principle part integral in this regime the variable $\eta = \xi - \alpha$ is introduced so that $d\eta = d\xi$. The integral may be evaluated as follows:

$$\begin{aligned} P \frac{1}{\pi^{1/2}} \int_{-\infty}^{\infty} d\xi \frac{\exp(-\xi^2)}{(\xi - \alpha)} &= \frac{1}{\pi^{1/2}} \int_{-\infty}^{\infty} d\eta \frac{e^{-\eta^2 - 2\alpha\eta - \alpha^2}}{\eta} \\ &= \frac{e^{-\alpha^2}}{\pi^{1/2}} \int_{-\infty}^{\infty} d\eta \frac{e^{-\eta^2}}{\eta} \left[1 - 2\alpha\eta + \frac{(-2\alpha)^2}{2!} \right. \\ &\quad \left. + \frac{(-2\alpha)^3}{3!} + \dots \right] \\ &= -2\alpha \frac{e^{-\alpha^2}}{\pi^{1/2}} \int_{-\infty}^{\infty} d\eta e^{-\eta^2} \left[1 + \frac{2\eta^2\alpha^2}{3} + \dots \right] \\ &= -2\alpha (1 - \alpha^2 + \dots) \left(1 + \frac{\alpha^2}{3} + \dots \right) \\ &= -2\alpha \left(1 - \frac{2\alpha^2}{3} + \dots \right) \end{aligned} \quad (5.74)$$

where in the third line all odd terms from the second line integrated to zero due to their symmetry. Thus, for $\alpha \ll 1$, the plasma dispersion function has the asymptotic limit

$$Z(\alpha) = -2\alpha \left(1 - \frac{2\alpha^2}{3} + \dots \right) + i\pi^{1/2} \exp(-\alpha^2). \quad (5.75)$$

5.2.6 Landau damping of electron plasma waves

The plasma susceptibilities given by Eq.(5.65) can now be evaluated. For $|\alpha| \gg 1$, using Eq.(5.73), and introducing the “frequency” $\omega = ip$ so that $\alpha = \omega/kv_{T\sigma}$ and $\alpha_i = \omega_i/kv_{T\sigma}$ the susceptibility is seen to be

$$\begin{aligned}\chi_\sigma &= \frac{1}{k^2\lambda_{D\sigma}^2} \left\{ 1 + \alpha \left[-\frac{1}{\alpha} \left(1 + \frac{1}{2\alpha^2} + \frac{3}{4\alpha^4} + \dots \right) + i\pi^{1/2} \exp(-\alpha^2) \right] \right\} \\ &= \frac{1}{k^2\lambda_{D\sigma}^2} \left\{ -\left(\frac{1}{2\alpha^2} + \frac{3}{4\alpha^4} + \dots \right) + i\alpha\pi^{1/2} \exp(-\alpha^2) \right\} \\ &= -\frac{\omega_{p\sigma}^2}{\omega^2} \left(1 + 3\frac{k^2}{\omega^2} \frac{\kappa T_\sigma}{m_\sigma} + \dots \right) + i\frac{\omega}{kv_{T\sigma}} \frac{\pi^{1/2}}{k^2\lambda_{D\sigma}^2} \exp(-\omega^2/k^2v_{T\sigma}^2) .\end{aligned}\quad (5.76)$$

Thus, if the root is such that $|\alpha| \gg 1$, the equation for the poles $D(p) = 1 + \chi_i + \chi_e = 0$ becomes

$$\begin{aligned}1 - \frac{\omega_{pe}^2}{\omega^2} \left(1 + 3\frac{k^2}{\omega^2} \frac{\kappa T_e}{m_e} + \dots \right) + i\frac{\omega}{kv_{Te}} \frac{\pi^{1/2}}{k^2\lambda_{De}^2} \exp(-\omega^2/k^2v_{Te}^2) \\ - \frac{\omega_{pi}^2}{\omega^2} \left(1 + 3\frac{k^2}{\omega^2} \frac{\kappa T_i}{m_i} + \dots \right) + i\frac{\omega}{kv_{Ti}} \frac{\pi^{1/2}}{k^2\lambda_{Di}^2} \exp(-\omega^2/k^2v_{Ti}^2) = 0.\end{aligned}\quad (5.77)$$

This expression is similar to the previously obtained fluid dispersion relation, Eq. (4.31), but contains additional imaginary terms that did not exist in the fluid dispersion. Furthermore, Eq.(5.77) is not actually a dispersion relation. Instead, it is to be understood as the equation for the roots of $D(p)$. These roots determine the poles in $N(p)/D(p)$ producing the least damped oscillations resulting from some prescribed initial perturbation of the distribution function. Since $\omega_{pe}^2/\omega_{pi}^2 = m_i/m_e$ and in general $v_{Ti} \ll v_{Te}$, both the real and imaginary parts of the ion terms are much smaller than the corresponding electron terms. On dropping the ion terms, the expression becomes

$$1 - \frac{\omega_{pe}^2}{\omega^2} \left(1 + 3\frac{k^2}{\omega^2} \frac{\kappa T_e}{m_e} + \dots \right) + i\frac{\omega}{kv_{Te}} \frac{\pi^{1/2}}{k^2\lambda_{De}^2} \exp(-\omega^2/k^2v_{Te}^2) = 0.\quad (5.78)$$

Recalling that $\omega = ip$ is complex, we write $\omega = \omega_r + i\omega_i$ and then proceed to find the complex ω that is the root of Eq.(5.78). Although it would not be particularly difficult to simply substitute $\omega = \omega_r + i\omega_i$ into Eq.(5.78) and then manipulate the coupled real and imaginary parts of this equation to solve for ω_r and ω_i , it is better to take this analysis as an opportunity to introduce a more general way for solving equations of this sort.

Equation (5.78) can be written as

$$D(\omega_r + i\omega_i) = D_r(\omega_r + i\omega_i) + iD_i(\omega_r + i\omega_i) = 0\quad (5.79)$$

where D_r is the part of D that does not explicitly contain i and D_i is the part that does explicitly contain i . Thus

$$D_r = 1 - \frac{\omega_{pe}^2}{\omega^2} \left(1 + 3\frac{k^2}{\omega^2} \frac{\kappa T_e}{m_e} + \dots \right), \quad D_i = \frac{\omega}{kv_{Te}} \frac{\pi^{1/2}}{k^2\lambda_{De}^2} \exp(-\omega^2/k^2v_{Te}^2).\quad (5.80)$$

Since the oscillation has been assumed to be weakly damped, $\omega_i \ll \omega_r$ and so Eq.(5.79) can be Taylor expanded in the small quantity ω_i ,

$$D_r(\omega_r) + i\omega_i \left(\frac{dD_r}{d\omega} \right)_{\omega=\omega_r} + i \left[D_i(\omega_r) + i\omega_i \left(\frac{dD_i}{d\omega} \right)_{\omega=\omega_r} \right] = 0. \quad (5.81)$$

Since $\omega_i \ll \omega_r$, the real part of Eq.(5.81) is

$$D_r(\omega_r) \simeq 0. \quad (5.82)$$

Balancing the two imaginary terms in Eq.(5.81) gives

$$\omega_i = -\frac{D_i(\omega_r)}{\frac{dD_r}{d\omega}}. \quad (5.83)$$

Thus, Eqs.(5.82) and (5.80) give the real part of the frequency as

$$\omega_r^2 = \omega_{pe}^2 \left(1 + 3 \frac{k^2}{\omega_r^2} \frac{\kappa T_e}{m_e} \right) \simeq \omega_{pe}^2 (1 + 3k^2 \lambda_{De}^2) \quad (5.84)$$

while Eqs.(5.83) and (5.80) give the imaginary part of the frequency which is called the *Landau damping* as

$$\begin{aligned} \omega_i &= -\sqrt{\frac{\pi}{8}} \frac{\omega_{pe}}{k^3 \lambda_{De}^3} \exp(-\omega^2/k^2 v_{T\sigma}^2) \\ &= -\sqrt{\frac{\pi}{8}} \frac{\omega_{pe}}{k^3 \lambda_{De}^3} \exp[-(1 + 3k^2 \lambda_{De}^2)/2k^2 \lambda_{De}^2]. \end{aligned} \quad (5.85)$$

Since the least damped oscillation goes as $\exp(pt) = \exp(-i\omega t) = \exp(-i(\omega_r + i\omega_i)t) = \exp(-i\omega_r t + \omega_i t)$ and Eq.(5.85) gives a negative ω_i , this is indeed a damping. It is interesting to note that while Landau damping was proposed theoretically by Landau in 1949, it took sixteen years before Landau damping was verified experimentally (Malmberg and Wharton 1964).

What is meant by weak damping v. strong damping? In order to calculate ω_i it was assumed that ω_i is small compared to ω_r suggesting perhaps that ω_i is unimportant. However, even though small, ω_i can be important, because the factor 2π affects the real and imaginary parts of the wave phase differently. Suppose for example that the imaginary part of the frequency is $1/2\pi \sim 1/6$ the magnitude of the real part. This ratio is surely small enough to justify the Taylor expansion used in Eq.(5.81) and also to justify the assumption that the pole p_j corresponding to this mode is only slightly to the left of the imaginary p axis. Let us calculate how much the wave is attenuated in one period $\tau = 2\pi/\omega_r$. This attenuation will be $\exp(-|\omega_i|\tau) = \exp(-2\pi/6) \sim \exp(-1) \sim 0.3$. Thus, the wave amplitude decays to one third its original value in just one period, which is certainly important.

5.2.7 Power relationships

It is premature to calculate the power associated with wave damping, because we do not yet know how to add up all the energy in the wave. Nevertheless, if we are willing to assume temporarily that the wave energy is entirely in the wave electric field (it turns out there is

also energy in coherent particle motion - to be discussed in Chapter 14), it is seen that the power being lost from the wave electric field is

$$\begin{aligned} P_{wavelost} &\sim \frac{d}{dt} \left\langle \frac{\varepsilon_0 E_{wave}^2}{2} \right\rangle \sim \frac{d}{dt} \left[\frac{\varepsilon_0 |E_{wave}^2|}{4} \exp(-2|\omega_i|t) \right] = -\frac{|\omega_i| \varepsilon_0 E_{wave}^2}{2} \\ &= \sqrt{\frac{\pi}{8}} \frac{\omega_{pe}}{2k^3 \lambda_{De}^3} \exp(-\omega^2/k^2 v_{T\sigma}^2) \varepsilon_0 E_{wave}^2 \end{aligned} \quad (5.86)$$

where $\langle E_{wave}^2 \rangle = |E_{wave}|^2 \langle \cos(kx - \omega t) \rangle = |E_{wave}|^2/2$ has been used. However, in Sec.3.8, it was shown that the energy gained by untrapped resonant particles in a wave is

$$\begin{aligned} P_{partgain} &= \frac{-\pi m \omega}{2k^2} \left(\frac{q E_{wave}}{m} \right)^2 \left[\frac{d}{dv_0} f(v_0) \right]_{v_0=\omega/k} \\ &= \frac{-\pi m \omega}{2k^2} \left(\frac{q E_{wave}}{m} \right)^2 \left[\frac{d}{dv_0} \left\{ \left(\frac{m}{2\pi \kappa T} \right)^{1/2} n_0 \exp\left(-\frac{mv^2}{2\kappa T}\right) \right\} \right]_{v_0=\omega/k} \\ &= \frac{\pi m \omega}{2k^2} \left(\frac{q E_{wave}}{m} \right)^2 \left(\frac{m}{2\pi \kappa T} \right)^{1/2} \left(\frac{m \omega}{\kappa T k} \right) n_0 \exp\left(-\frac{\omega^2}{k^2 v_{T\sigma}^2}\right); \end{aligned} \quad (5.87)$$

using $\omega \sim \omega_{pe}$ this is seen to be the same as Eq.(5.86) except for a factor of two. We shall see later that this factor of two comes from the fact that the wave electric field actually contains *half* the energy of the electron plasma wave, with the other half in coherent particle motion, so the true power loss rate is really twice that given in Eq.(5.86).

5.2.8 Landau damping for ion acoustic waves

Ion acoustic waves resulted from a two-fluid analysis in the regime where the wave phase velocity was intermediate between the electron and ion thermal velocities. In this situation the electrons behave isothermally and the ions behave adiabatically. This suggests there might be another root of $D(p)$ if $|\alpha_e| \ll 1$ and $|\alpha_i| \gg 1$ or equivalently $v_{Ti} \ll \omega/k \ll v_{Te}$. From Eqs.(5.65) and (5.75), the susceptibility for $|\alpha| \ll 1$ is found to be

$$\begin{aligned} \chi_\sigma &= \frac{1}{k^2 \lambda_{D\sigma}^2} [1 + \alpha Z(\alpha)] \\ &= \frac{1}{k^2 \lambda_{D\sigma}^2} \left\{ 1 - 2\alpha^2 \left(1 - \frac{2\alpha^2}{3} + \dots \right) + i\alpha \pi^{1/2} \exp(-\alpha^2) \right\} \\ &\simeq \frac{1}{k^2 \lambda_{D\sigma}^2} + i \frac{\alpha}{k^2 \lambda_{D\sigma}^2} \pi^{1/2} \exp(-\alpha^2). \end{aligned} \quad (5.88)$$

Using Eq.(5.88) for the electron susceptibility and Eq.(5.76) for the ion susceptibility gives

$$\begin{aligned} D(\omega) &= 1 + \frac{1}{k^2 \lambda_{De}^2} + i \frac{\omega}{k v_{Te}} \frac{\pi^{1/2}}{k^2 \lambda_{De}^2} \exp(-\omega^2/k^2 v_{Te}^2) \\ &\quad - \frac{\omega_{pi}^2}{\omega^2} \left(1 + 3 \frac{k^2 \kappa T_i}{\omega^2 m_i} + \dots \right) + i \frac{\omega}{k v_{Ti}} \frac{\pi^{1/2}}{k^2 \lambda_{Di}^2} \exp(-\omega^2/k^2 v_{Ti}^2). \end{aligned} \quad (5.89)$$

On applying the Taylor expansion technique discussed in conjunction with Eqs.(5.82) and (5.83) we find that ω_r is the root of

$$D_r(\omega_r) = 1 + \frac{1}{k^2 \lambda_{De}^2} - \frac{\omega_{pi}^2}{\omega_r^2} \left(1 + 3 \frac{k^2 \kappa T_i}{\omega^2 m_i} \right) = 0, \quad (5.90)$$

i.e.,

$$\omega_r^2 = \frac{k^2 c_s^2}{1 + k^2 \lambda_{De}^2} \left(1 + 3 \frac{k^2 \kappa T_i}{\omega_r^2 m_i} \right) \simeq \frac{k^2 c_s^2}{1 + k^2 \lambda_{De}^2} + 3k^2 \frac{\kappa T_i}{m_i}. \quad (5.91)$$

Here, as in the two-fluid analysis of ion acoustic waves, $c_s^2 = \omega_{pi}^2 \lambda_{De}^2 = \kappa T_e / m_i$ has been defined. The imaginary part of the frequency is found to be

$$\begin{aligned} \omega_i &\simeq -\frac{D_i(\omega_r)}{dD_r/d\omega} \\ &= -\frac{\omega \pi^{1/2}}{k^3} \left[\frac{\frac{1}{\lambda_{De}^2 v_{Te}} \exp(-\omega^2/k^2 v_{Te}^2) + \frac{1}{\lambda_{Di}^2 v_{Ti}} \exp(-\omega^2/k^2 v_{Ti}^2)}{2\omega_{pi}^2/\omega^3} \right] \\ &= -\frac{\omega^4}{k^3 c_s^3} \sqrt{\frac{\pi}{8}} \left[\sqrt{\frac{m_e}{m_i}} + \left(\frac{T_e}{T_i} \right)^{3/2} \exp(-\omega^2/k^2 v_{Ti}^2) \right] \\ &= -\frac{|\omega_r|}{(1 + k^2 \lambda_{De}^2)^{3/2}} \sqrt{\frac{\pi}{8}} \left[\sqrt{\frac{m_e}{m_i}} + \left(\frac{T_e}{T_i} \right)^{3/2} \exp\left(-\frac{T_e/2T_i}{1 + k^2 \lambda_{De}^2} - \frac{3}{2} \right) \right]. \end{aligned} \quad (5.92)$$

The dominant Landau damping comes from the ions, since the electron Landau damping term has the small factor $\sqrt{m_e/m_i}$. If $T_e \gg T_i$ the ion term also becomes small because $x^{3/2} \exp(-x) \rightarrow 0$ as x becomes large. Hence, strong ion Landau damping occurs when T_i approaches T_e and so ion acoustic waves can only propagate without extreme attenuation if the plasma has $T_e \gg T_i$. Landau damping of ion acoustic waves was observed experimentally by Wong, Motley and D'Angelo (1964).

5.2.9 The Plemelj formula

The Landau method showed that the correct way to analyze problems that lead to ill-defined integrals such as Eq.(5.31) is to pose the problem as an initial value problem rather than as a steady-state situation. The essential result of the Landau method can be summarized by the Plemelj formula

$$\lim_{\varepsilon \rightarrow 0} \frac{1}{\xi - a \mp i|\varepsilon|} = \text{P} \frac{1}{\xi - a} \pm i\pi \delta(\xi - a) \quad (5.93)$$

which is a prescription showing how to deal with singular integrands of the form appearing in the plasma dispersion function. From now on, instead of repeating the lengthy Laplace transform analysis, we instead will use the less cumbersome, but formally incorrect Fourier method and then invoke Eq.(5.93) as a 'patch' to resolve any ambiguities regarding integration contours.

5.3 The Penrose criterion

The analysis so far showed that electrostatic plasma waves are subject to Landau damping, a collisionless attenuation proportional to $[\partial f/\partial v]_{v=\omega/k}$, and that this damping is consistent with the calculation of power input to particles by an electrostatic wave. Since a Maxwellian distribution function has a negative slope, its associated Landau damping is always a true wave damping. This is consistent with the physical picture developed in the single particle analysis which showed that energy is transferred from wave to particles if there are more slow than fast particles in the vicinity of the wave phase velocity. What happens if there is a non-Maxwellian distribution function, in particular one where there are more fast particles than slow particles in the vicinity of the wave phase velocity, i.e., $[\partial f/\partial v]_{v=\omega/k} > 0$? Because $f(v) \rightarrow 0$ as $v \rightarrow \infty$, f can only have a positive slope for a finite range of velocity; i.e., positive slopes of the distribution function must always be located to the left of a localized maximum in $f(v)$. A localized maximum in $f(v)$ corresponds to a beam of fast particles superimposed on a (possible) background of particles having a monotonically decreasing $f(v)$. Can the Landau damping process be run in reverse and so provide Landau growth, i.e., wave instability? The answer is yes. We will now discuss a criterion due to Penrose (1960) that shows how strong a beam must be to give Landau instability.

The procedure used to derive Eq.(5.28) is repeated, giving

$$1 + \frac{q^2}{k^2 m \epsilon_0} \int_{-\infty}^{\infty} \frac{k}{(\omega - kv)} \frac{\partial f_0}{\partial v} dv = 0 \quad (5.94)$$

which may be recast as

$$k^2 = Q(z) \quad (5.95)$$

where

$$Q(z) = \frac{q^2}{m \epsilon_0} \int_{-\infty}^{\infty} \frac{1}{(v - z)} \frac{\partial f_0}{\partial v} dv \quad (5.96)$$

is a complex function of the complex variable $z = \omega/k$. The wavenumber k is assumed to be a positive real quantity and the Plemelj formula will be used to resolve the ambiguity due to the singularity in the integrand.

The left hand side of Eq.(5.95) is, by assumption, always real and positive for any choice of k . A solution of this equation can therefore always be found if $Q(z)$ is simultaneously pure real and positive. The actual magnitude of $Q(z)$ does not matter, since the magnitude of k^2 can be adjusted to match the magnitude of $Q(z)$.

The function $Q(z)$ may be interpreted as a mapping from the complex z plane to the complex Q plane. Because solutions of Eq.(5.95) giving instability are those for which $\text{Im } \omega > 0$, the upper half of the complex z plane corresponds to instability and the real z axis represents the dividing line between stability and instability. Let us consider a straight-line contour C_z parallel to the real z axis, and slightly above. As shown in Fig.5.6(a) this contour can be prescribed as $z = z_r + i\delta$ where δ is a small constant and z_r ranges from $-\infty$ to $+\infty$.

The function $Q(z) \rightarrow 0$ when $z \rightarrow \pm\infty$ and so, as z is moved along the C_z contour, the corresponding path C_Q traced in the Q plane must start at the origin and end at the origin. Furthermore, since Q can be evaluated using the Plemelj formula, it is seen that Q is finite for all z on the path C_z . Thus, C_Q is a continuous finite curve starting at the

Q -plane origin and ending at this same origin as shown by the various possible mappings sketched in Figs.5.6(b), (c) and (d).

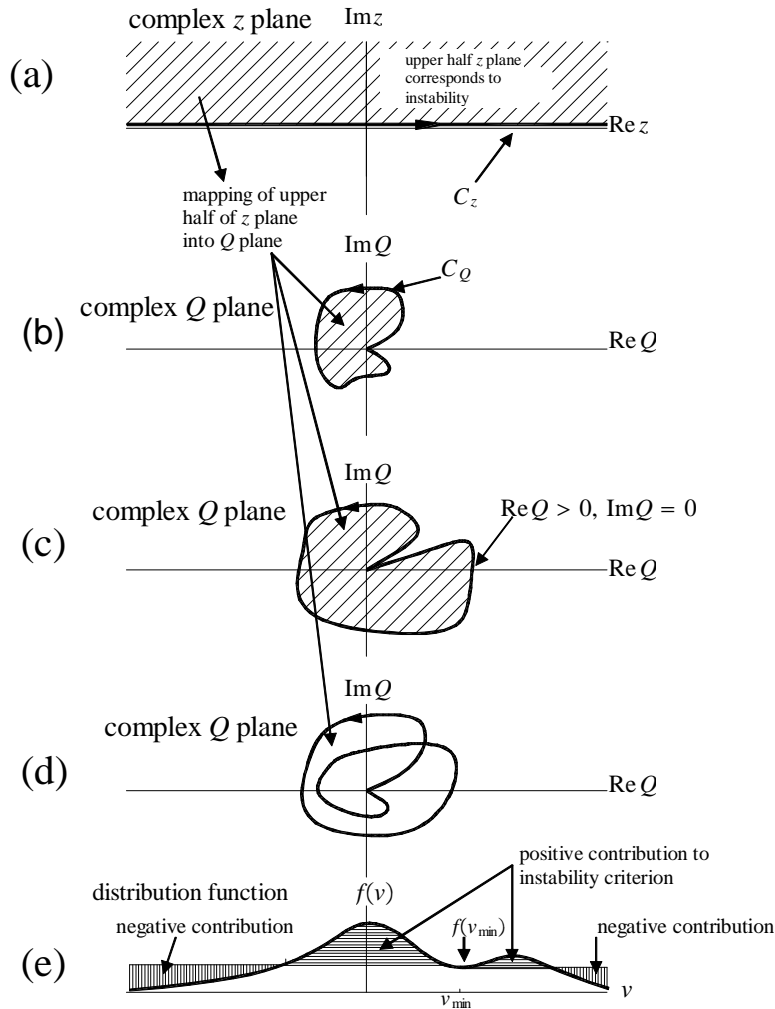


Figure 5.6: Penrose criterion: (a)-(d) mappings, (e) instability criterion.

The upper half z plane maps to the area inside the curve C_Q . If C_Q is of the form shown in Fig.5.6(b), then $Q(z)$ never takes on a positive real value for z being in the upper half z plane; thus a curve of this form cannot give a solution to Eq.(5.95) corresponding

to an instability. However, curves of the form sketched in Figs.5.6 (c) and (d) do have $Q(z)$ taking on positive real values and so do correspond to unstable solutions. Marginally unstable situations correspond to where C_Q crosses the positive real Q axis, since C_Q is a mapping of C_z which was the set of marginally unstable frequencies.

Let us therefore focus attention on what happens when C_Q crosses the positive real Q axis. Using the Plemelj formula on Eq.(5.96) it is seen that

$$\text{Im}Q = \frac{q^2}{m\varepsilon_0} \pi \left[\frac{\partial f_0}{\partial v} \right]_{v=\omega_r/k} \quad (5.97)$$

and, on moving along C_Q from a point just below the real Q axis to just above the real Q axis, $\text{Im}Q$ goes from being negative to positive. Thus, $[\partial f_0/\partial v]_{v=\omega_r/k}$ changes from being negative to positive, so that on the positive real Q axis f_0 is a *minimum* at some value $v = v_{\min}$ (here the subscript “min” means the value of v for which f_0 is at a minimum and not v itself is at a minimum). A Taylor expansion about this minimum gives

$$f(v) = f[v_{\min} + (v - v_{\min})] = f(v_{\min}) + 0 + \frac{(v - v_{\min})^2}{2} f''(v_{\min}) + \dots \quad (5.98)$$

Since $f(v_{\min})$ is a constant, it is permissible to write

$$\frac{\partial f_0}{\partial v} = \frac{\partial}{\partial v} [f_0(v) - f_0(v_{\min})]. \quad (5.99)$$

This innocuous insertion of $f(v_{\min})$ makes it easy to integrate Eq. (5.96) by parts

$$\begin{aligned} Q(z = v_{\min}) &= \frac{q^2}{m\varepsilon_0} \left\{ \text{P} \int_{-\infty}^{\infty} dv \frac{\frac{\partial}{\partial v} [f(v) - f(v_{\min})]}{(v - v_{\min})} + i\pi \left[\frac{\partial}{\partial v} f(v) \right]_{v=v_{\min}} \right\} \\ &= \frac{q^2}{m\varepsilon_0} \text{P} \int_{-\infty}^{\infty} dv \frac{1}{(v - v_{\min})^2} [f(v) - f(v_{\min})] \\ &= \frac{q^2}{m\varepsilon_0} \int_{-\infty}^{\infty} dv \frac{1}{(v - v_{\min})^2} \left[0 + \frac{(v - v_{\min})^2}{2} f''(v_{\min}) + \dots \right]; \end{aligned} \quad (5.100)$$

in the second line advantage has been taken of the fact that the imaginary part is zero by assumption, and in the third line the ‘P’ for principle part has been dropped because there is no longer a singularity at $v = v_{\min}$. In fact, since the leading term of $f(v) - f(v_{\min})$ is proportional to $(v - v_{\min})^2$, this qualifying ‘P’ can also be dropped from the second line. The requirement for marginal instability can be summarized as: $f(v)$ has a minimum at $v = v_{\min}$, and the value of Q is positive, i.e.,

$$Q(v_{\min}) = \frac{q^2}{m\varepsilon_0} \int_{-\infty}^{\infty} dv \left[\frac{f(v) - f(v_{\min})}{(v - v_{\min})^2} \right] > 0. \quad (5.101)$$

This is just a weighted measure of the strength of the bump in f located to the right of the minimum as shown in Fig.5.6(e). The hatched areas with horizontal lines make positive contributions to Q , while the hatched areas with vertical lines make negative contributions.

These contributions are weighted according to how far they are from v_{\min} by the factor $(v - v_{\min})^{-2}$.

The Penrose criterion extends the 2-stream instability analysis to an arbitrary distribution function containing finite temperature beams.

5.4 Assignments

1. Show that the electrostatic dispersion relation for electrons streaming through ions with velocity \mathbf{v}_0 through stationary ions is

$$1 - \frac{\omega_{pi}^2}{\omega^2} - \frac{\omega_{pe}^2}{(\omega - \mathbf{k} \cdot \mathbf{v}_0)^2} = 0.$$

- (a) Show that instability begins when

$$\left(\frac{\mathbf{k} \cdot \mathbf{v}_0}{\omega_{pe}} \right)^2 < \left[1 + \left(\frac{m_e}{m_i} \right)^{1/3} \right]^3$$

- (b) Split the frequency into its real and imaginary parts so that $\omega = \omega_r + i\omega_i$. Show that the instability has maximum growth rate

$$\frac{\omega_i}{\omega_{pe}} = \frac{\sqrt{3}}{2} \left(\frac{m_e}{2m_i} \right)^{1/3}.$$

What is the value of kv_0/ω_{pe} when the instability has maximum growth rate. Sketch the dependence of ω_i/ω_{pe} on kv_0/ω_{pe} . (Hint- define non-dimensional variables $\epsilon = m_e/m_i$, $z = \omega/\omega_{pe}$, and $\lambda = kv_0/\omega_{pe}$. Let $z = x + iy$ and look for the maximum y satisfying the dispersion. A particularly neat way to solve the dispersion is to solve the dispersion for the imaginary part of λ which of course is zero, since by assumption k is real. Take advantage of the fact that $\epsilon \ll 1$ to find a relatively simple expression involving y . Maximize y with respect to x and then find the respective values of x, y , and λ at this point of maximum y .

2. Prove the Plemelj formula.
3. Suppose that

$$\mathbf{E}(\mathbf{x}, t) = \int \bar{\mathbf{E}}(\mathbf{k}) e^{i\mathbf{k} \cdot \mathbf{x} - i\omega(\mathbf{k})t} d\mathbf{k} \quad (5.102)$$

where

$$\omega = \omega_r(\mathbf{k}) + i\omega_i(\mathbf{k})$$

is determined by an appropriate dispersion relation. Assuming that $\mathbf{E}(\mathbf{x}, t)$ is a real quantity, show by comparing Eq.(5.102) to its complex conjugate, that $\omega_r(\mathbf{k})$ must always be an odd function of \mathbf{k} while ω_i must always be an even function of \mathbf{k} . (Hint- Note that the left hand side of Eq.(5.102) is real by assumption, and so the right hand side must also be real. Take the complex conjugate of both sides and replace

the dummy variable of integration \mathbf{k} by $-\mathbf{k}$ so that $d\mathbf{k} \rightarrow -d\mathbf{k}$ and the $\pm\infty$ limits of integration are also interchanged).

4. Plot the real and imaginary parts of the plasma dispersion function. Plot the real and imaginary parts of the susceptibilities.
5. Is it possible to have electrostatic plasma waves with $k\lambda_{De} \gg 1$. Hint, consider Landau damping.
6. Plot the potential versus time in units of the real period of an electron plasma wave for various values of $\omega/k\sqrt{\kappa T_e/m_e}$ showing the onset of Landau damping.
7. Plot ω_i/ω_r for ion acoustic waves for various values of T_e/T_i and show that these waves have strong Landau damping when the ion temperature approaches the electron temperature.
8. Landau instability for ion acoustic waves- Plasmas with $T_e > T_i$ support propagation of ion acoustic waves; these waves are Landau damped by both electrons and ions. However, if there is a sufficiently strong current J flowing in the plasma giving a relative streaming velocity $u_0 = J/ne$ between the ions and electrons, the Landau damping can operate in reverse, and give a Landau growth. This can be seen by moving to the ion frame in which case the electrons appear as an offset Gaussian. If the offset is large enough it will be possible to have $[\partial f_e/\partial v]_{v \sim c_s} > 0$, giving more fast than slow particles at the wave phase velocity. Now, since f_e is a Gaussian with its center shifted to be at u_0 , show that if $u_0 > \omega/k$ the portion of f_e immediately to the left of u_0 will have positive slope and so lead to instability. These qualitative ideas can easily be made quantitative, by considering a 1-D equilibrium where the ion distribution is

$$f_{i0} = \frac{n_0}{\pi^{1/2}v_{Ti}} e^{-v^2/v_{Ti}^2}$$

and the drifting electron distribution is

$$f_{e0} = \frac{n_0}{\pi^{1/2}v_{Te}} e^{-(v-u_0)^2/v_{Te}^2}.$$

The ion susceptibility will be the same as before, but to determine the electron susceptibility we must reconsider the linearized Vlasov equation

$$\frac{\partial f_{e1}}{\partial t} + v \frac{\partial f_{e1}}{\partial x} - \frac{q_e}{m_e} \frac{\partial \phi_1}{\partial x} \frac{\partial}{\partial v} \left[\frac{n_0}{\pi^{1/2}v_{Te}} e^{-(v-u_0)^2/v_{Te}^2} \right] = 0.$$

This equation can be simplified by defining $v' = v - u_0$. Show that the electron susceptibility becomes

$$\chi_e = \frac{1}{k^2 \lambda_{De}^2} [1 + \alpha Z(\alpha)]$$

where now $\alpha = (\omega - ku_0)/kv_{Te}$. Suppose $T_e \gg T_i$ so that the electron Landau damping term dominates. Show that if $u_0 > \omega_r/k$ the electron imaginary term will reverse sign and give instability.

9. Suppose a current I flows in a long cylindrical plasma of radius a , density n , ion mass m_i for which $T_e \gg T_i$. Write a criterion for ion acoustic instability in terms of an

appropriate subset of these parameters. Suppose a cylindrical mercury plasma with $T_e = 1 - 2$ eV, $T_i = 0.1$ eV, diameter 2.5 cm, carries a current of $I = 0.35$ amps. At what density would an ion acoustic instability be expected to develop. Does this configuration remind you of an everyday object? Hint: there are several hanging from the ceiling of virtually every classroom.

Cold plasma waves in a magnetized plasma

Chapter 4 showed that finite temperature is responsible for the lowest order dispersive terms in both electron plasma waves [dispersion $\omega^2 = \omega_p^2 + 3k^2 \kappa T_e / m_e$] and ion acoustic waves [dispersion $\omega^2 = k^2 c_s^2 / (1 + k^2 \lambda_{De}^2)$]. Furthermore, finite temperature was shown in Chapter 5 to be essential to Landau damping and instability.

Chapter 4 also contained a derivation of the electromagnetic plasma wave [dispersion $\omega^2 = \omega_{pe}^2 + k^2 c^2$] and of the inertial Alfvén wave [dispersion $\omega^2 = k_z^2 v_A^2 / (1 + k_x^2 c^2 / \omega_{pe}^2)$], both of which had no dependence on temperature. To distinguish waves which depend on temperature from waves which do not, the terminology “cold plasma wave” and “hot plasma wave” is used. A cold plasma wave is a wave having a temperature-independent dispersion relation so that the temperature could be set to zero without changing the wave, whereas a hot plasma wave has a temperature-dependent dispersion relation. Thus hot and cold do not refer to a ‘temperature’ of the wave, but rather to the wave’s dependence or lack thereof on plasma temperature. Generally speaking, cold plasma waves are just the consequence of a large number of particles having identical Hamiltonian-Lagrangian dynamics whereas hot plasma waves involve different groups of particles having different dynamics because they have different initial velocities. Thus hot plasma waves involve statistical mechanical or thermodynamic considerations. The general theory of cold plasma waves in a uniformly magnetized plasma is presented in this chapter and hot plasma waves will be discussed in later chapters.

6.1 Redundancy of Poisson’s equation in electromagnetic mode analysis

When electrostatic waves were examined in Chapter 4 it was seen that the plasma response to the wave electric field could be expressed as a sum of susceptibilities where the susceptibility of each species was proportional to the density perturbation of that species. Combining the susceptibilities with Poisson’s equation gave a dispersion relation. However, because electric fields can also be generated inductively, electrostatic waves are not the only type of wave. Inductive electric fields result from time-dependent currents, i.e., from charged particle acceleration, and do not involve density perturbations. As an example, the electromagnetic plasma wave involved inductive rather than electrostatic electric fields. The inertial Alfvén wave involved inductive electric fields in the parallel direction and electrostatic electric fields in the perpendicular direction.

One might expect that a procedure analogous to the previous derivation of electrostatic susceptibilities could be used to derive inductive “susceptibilities” which would then be used to construct dispersion relations for inductive modes. It turns out that such a procedure not only gives dispersion relations for inductive modes, but also includes the electrostatic modes. Thus, it turns out to be unnecessary to analyze electrostatic modes separately. The main reason for investigating electrostatic modes separately as done earlier is pedagogical – it is easier to understand a simpler system. To see why electrostatic modes are automatically included in an electromagnetic analysis, consider the interrelationship between Poisson’s equation, Ampere’s law, and a charge-weighted summation of the two-fluid continuity equation,

$$\nabla \cdot \mathbf{E} = -\frac{1}{\varepsilon_0} \sum_{\sigma} n_{\sigma} q_{\sigma}, \quad (6.1)$$

$$\nabla \times \mathbf{B} = \mu_0 \mathbf{J} + \varepsilon_0 \mu_0 \frac{\partial \mathbf{E}}{\partial t}, \quad (6.2)$$

$$\sum_{\sigma} q_{\sigma} \left[\frac{\partial n_{\sigma}}{\partial t} + \nabla \cdot (n_{\sigma} \mathbf{v}_{\sigma}) \right] = \left[\frac{\partial}{\partial t} \sum_{\sigma} n_{\sigma} q_{\sigma} \right] + \nabla \cdot \mathbf{J} = 0. \quad (6.3)$$

The divergence of Eq.(6.2) gives

$$\nabla \cdot \mathbf{J} + \varepsilon_0 \frac{\partial}{\partial t} \nabla \cdot \mathbf{E} = 0 \quad (6.4)$$

and substituting Eq.(6.3) gives

$$\frac{\partial}{\partial t} \left[-\sum_{\sigma} n_{\sigma} q_{\sigma} + \varepsilon_0 \nabla \cdot \mathbf{E} \right] = 0 \quad (6.5)$$

which is just the time derivative of Poisson’s equation. Integrating Eq.(6.5) shows that

$$-\sum_{\sigma} n_{\sigma} q_{\sigma} + \varepsilon_0 \nabla \cdot \mathbf{E} = \text{const.} \quad (6.6)$$

Poisson’s equation, Eq.(6.1), thus provides an *initial condition* which fixes the value of the constant in Eq.(6.6). Since all small-amplitude perturbations are assumed to have the phase dependence $\exp(\mathbf{i}\mathbf{k} \cdot \mathbf{x} - i\omega t)$ and therefore behave as a single Fourier mode, the $\partial/\partial t$ operator in Eq. (6.5) is replaced by $-i\omega$ in which case the constant in Eq.(6.6) is automatically set to zero, making a separate consideration of Poisson’s equation redundant. In summary, the Fourier-transformed Ampere’s law effectively embeds Poisson’s equation and so a discussion of waves based solely on currents describes inductive, electrostatic modes and also contains modes involving a mixture of inductive and electrostatic electric fields such as the inertial Alfvén wave.

6.2 Dielectric tensor

Section 3.8 showed that a single particle immersed in a constant, uniform equilibrium magnetic field $\mathbf{B} = B_0 \hat{z}$ and subject to a *small-amplitude* wave with electric field $\sim \exp(\mathbf{i}\mathbf{k} \cdot \mathbf{x} - i\omega t)$ has the velocity

$$\bar{\mathbf{v}}_{\sigma} = \frac{iq_{\sigma}}{\omega m_{\sigma}} \left[\tilde{E}_z \hat{z} + \frac{\bar{\mathbf{E}}_{\perp}}{1 - \omega_{c\sigma}^2/\omega^2} - \frac{i\omega_{c\sigma}}{\omega} \frac{\hat{z} \times \bar{\mathbf{E}}}{1 - \omega_{c\sigma}^2/\omega^2} \right] e^{i\mathbf{k} \cdot \mathbf{x} - i\omega t}. \quad (6.7)$$

The tilde $\tilde{}$ denotes a small-amplitude oscillatory quantity with space-time dependence $\exp(i\mathbf{k} \cdot \mathbf{x} - i\omega t)$; this phase factor may or may not be explicitly written, but should always be understood to exist for a tilde-denoted quantity.

The three terms in Eq.(6.7) are respectively:

1. *The parallel quiver velocity*- this quiver velocity is the same as the quiver velocity of an unmagnetized particle, but is restricted to parallel motion. Because the magnetic force $q(\mathbf{v} \times \mathbf{B})$ vanishes for motion along the magnetic field, motion parallel to \mathbf{B} in a magnetized plasma is identical to motion in an unmagnetized plasma .
2. *The generalized polarization drift*- this motion has a resonance at the cyclotron frequency but at low frequencies such that $\omega \ll \omega_{c\sigma}$, it reduces to the polarization drift $\mathbf{v}_{p\sigma} = m_\sigma \tilde{\mathbf{E}}_\perp / q_\sigma B^2$ derived in Chapter 3.
3. *The generalized $E \times B$ drift*- this also has a resonance at the cyclotron frequency and for $\omega \ll \omega_{c\sigma}$ reduces to the drift $\mathbf{v}_E = \mathbf{E} \times \mathbf{B} / B^2$ derived in Chapter 3.

The particle velocities given by Eq.(6.7) produce a plasma current density

$$\begin{aligned} \bar{\mathbf{J}} &= \sum_\sigma n_{0\sigma} q_\sigma \bar{\mathbf{v}}_\sigma \\ &= i\varepsilon_0 \sum_\sigma \frac{\omega_{p\sigma}^2}{\omega} \left[\tilde{E}_z \hat{z} + \frac{\tilde{\mathbf{E}}_\perp}{1 - \omega_{c\sigma}^2/\omega^2} - \frac{i\omega_{c\sigma}}{\omega} \frac{\hat{z} \times \tilde{\mathbf{E}}}{1 - \omega_{c\sigma}^2/\omega^2} \right] e^{i\mathbf{k} \cdot \mathbf{x} - i\omega t}. \end{aligned} \quad (6.8)$$

If these plasma currents are written out explicitly, then Ampere's law has the form

$$\begin{aligned} \nabla \times \bar{\mathbf{B}} &= \mu_0 \bar{\mathbf{J}} + \mu_0 \varepsilon_0 \frac{\partial \tilde{\mathbf{E}}}{\partial t} \\ &= \mu_0 \left(i\varepsilon_0 \sum_\sigma \frac{\omega_{p\sigma}^2}{\omega} \left[\tilde{E}_z \hat{z} + \frac{\tilde{\mathbf{E}}_\perp}{1 - \omega_{c\sigma}^2/\omega^2} - \frac{i\omega_{c\sigma}}{\omega} \frac{\hat{z} \times \tilde{\mathbf{E}}}{1 - \omega_{c\sigma}^2/\omega^2} \right] - i\omega \varepsilon_0 \tilde{\mathbf{E}} \right) \end{aligned} \quad (6.9)$$

where a factor $\exp(i\mathbf{k} \cdot \mathbf{x} - i\omega t)$ is implicit.

The cold plasma wave equation is established by combining Ampere's and Faraday's law in a manner similar to the method used for vacuum electromagnetic waves. However, before doing so, it is useful to define the dielectric tensor $\overleftrightarrow{\mathbf{K}}$. This tensor contains the information in the right hand side of Eq.(6.9) so that this equation is written as

$$\nabla \times \mathbf{B} = \mu_0 \varepsilon_0 \frac{\partial}{\partial t} \left(\overleftrightarrow{\mathbf{K}} \cdot \mathbf{E} \right) \quad (6.10)$$

where

$$\begin{aligned} \overleftrightarrow{\mathbf{K}} \cdot \mathbf{E} &= \mathbf{E} - \sum_{\sigma=i,e} \frac{\omega_{p\sigma}^2}{\omega^2} \left[\tilde{E}_z \hat{z} + \frac{\tilde{\mathbf{E}}_\perp}{1 - \omega_{c\sigma}^2/\omega^2} - \frac{i\omega_{c\sigma}}{\omega} \frac{\hat{z} \times \tilde{\mathbf{E}}}{1 - \omega_{c\sigma}^2/\omega^2} \right] \\ &= \begin{bmatrix} S & -iD & 0 \\ iD & S & 0 \\ 0 & 0 & P \end{bmatrix} \cdot \mathbf{E} \end{aligned} \quad (6.11)$$

and the elements of the dielectric tensor are

$$S = 1 - \sum_{\sigma=i,e} \frac{\omega_{p\sigma}^2}{\omega^2 - \omega_{c\sigma}^2}, \quad D = \sum_{\sigma=i,e} \frac{\omega_{c\sigma}}{\omega} \frac{\omega_{p\sigma}^2}{\omega^2 - \omega_{c\sigma}^2}, \quad P = 1 - \sum_{\sigma=i,e} \frac{\omega_{p\sigma}^2}{\omega^2}. \quad (6.12)$$

The nomenclature S, D, P for the matrix elements was introduced by Stix (1962) and is a mnemonic for “Sum”, “Difference”, and “Parallel”. The reasoning behind “Sum” and “Difference” will become apparent later, but for now it is clear that the P element corresponds to the cold-plasma limit of the parallel dielectric, i.e., $P = 1 + \chi_i + \chi_e$ where $\chi_\sigma = -\omega_{p\sigma}^2/\omega^2$. This is just the cold limit of the unmagnetized dielectric because behavior involving parallel motions in a magnetized plasma is identical to that in an unmagnetized plasma. In the limit of no plasma, $\overleftrightarrow{\mathbf{K}}$ becomes the unit tensor and describes the effect of the vacuum displacement current only.

This definition of the dielectric tensor means that Maxwell’s equations, the Lorentz equation, and the plasma currents can now be summarized in just two coupled equations, namely

$$\nabla \times \mathbf{B} = \frac{1}{c^2} \frac{\partial}{\partial t} (\overleftrightarrow{\mathbf{K}} \cdot \mathbf{E}) \quad (6.13)$$

$$\nabla \times \mathbf{E} = -\frac{\partial \mathbf{B}}{\partial t}. \quad (6.14)$$

The cold plasma wave equation is obtained by taking the curl of Eq.(6.14) and then substituting for $\nabla \times \mathbf{B}$ using (6.13) to obtain

$$\nabla \times (\nabla \times \mathbf{E}) = -\frac{1}{c^2} \frac{\partial^2}{\partial t^2} (\overleftrightarrow{\mathbf{K}} \cdot \mathbf{E}). \quad (6.15)$$

Since a phase dependence $\exp(i\mathbf{k} \cdot \mathbf{x} - i\omega t)$ is assumed, this can be written in algebraic form as

$$\mathbf{k} \times (\mathbf{k} \times \mathbf{E}) = -\frac{\omega^2}{c^2} \overleftrightarrow{\mathbf{K}} \cdot \mathbf{E}. \quad (6.16)$$

It is now convenient to define the refractive index $\mathbf{n} = c\mathbf{k}/\omega$, a renormalization of the wavevector \mathbf{k} arranged so that light waves have a refractive index of unity. Using this definition Eq.(6.16) becomes

$$\mathbf{n}\mathbf{n} \cdot \mathbf{E} - n^2 \mathbf{E} + \overleftrightarrow{\mathbf{K}} \cdot \mathbf{E} = 0, \quad (6.17)$$

which is essentially a set of three homogeneous equations in the three components of \mathbf{E} .

The refractive index $\mathbf{n} = c\mathbf{k}/\omega$ can be decomposed into parallel and perpendicular components relative to the equilibrium magnetic field $\mathbf{B} = B_0 \hat{z}$. For convenience, the x axis of the coordinate system is defined to lie along the perpendicular component of \mathbf{n} so that $n_y = 0$ by assumption. This simplification is possible for a spatially uniform equilibrium only; if the plasma is non-uniform in the $x-y$ plane, there can be a real distinction between x and y direction propagation and the refractive index in the y -direction cannot be simply defined away by choice of coordinate system.

To set the stage for obtaining a dispersion relation, Eq.(6.17) is written in matrix form as

$$\begin{bmatrix} S - n_z^2 & -iD & n_x n_z \\ iD & S - n^2 & 0 \\ n_x n_z & 0 & P - n_x^2 \end{bmatrix} \cdot \begin{bmatrix} E_x \\ E_y \\ E_z \end{bmatrix} = 0 \quad (6.18)$$

where, for clarity, the tildes have been dropped. It is now useful to introduce a spherical coordinate system in k -space (or equivalently refractive index space) with \hat{z} defining the axis and θ the polar angle. Thus, the Cartesian components of the refractive index are related to the spherical components by

$$\begin{aligned} n_x &= n \sin \theta \\ n_z &= n \cos \theta \\ n^2 &= n_x^2 + n_z^2 \end{aligned} \quad (6.19)$$

and so Eq.(6.18) becomes

$$\begin{bmatrix} S - n^2 \cos^2 \theta & -iD & n^2 \sin \theta \cos \theta \\ iD & S - n^2 & 0 \\ n^2 \sin \theta \cos \theta & 0 & P - n^2 \sin^2 \theta \end{bmatrix} \cdot \begin{bmatrix} E_x \\ E_y \\ E_z \end{bmatrix} = 0. \quad (6.20)$$

6.2.1 Mode behavior at $\theta = 0$

Non-trivial solutions to the set of three coupled equations for E_x, E_y, E_z prescribed by Eq.(6.20) exist only if the determinant of the matrix vanishes. For arbitrary values of θ , this determinant is complicated. Rather than examining the arbitrary- θ determinant immediately, two simpler limiting cases will first be considered, namely the situations where $\theta = 0$ (i.e., $\mathbf{k} \parallel \mathbf{B}_0$) and $\theta = \pi/2$ (i.e., $\mathbf{k} \perp \mathbf{B}_0$). These special cases are simpler than the general case because the off-diagonal matrix elements $n^2 \sin \theta \cos \theta$ vanish for both $\theta = 0$ and $\theta = \pi/2$.

When $\theta = 0$ Eq.(6.20) becomes

$$\begin{bmatrix} S - n^2 & -iD & 0 \\ iD & S - n^2 & 0 \\ 0 & 0 & P \end{bmatrix} \cdot \begin{bmatrix} E_x \\ E_y \\ E_z \end{bmatrix} = 0 \quad (6.21)$$

The determinant of this system is

$$\left[(S - n^2)^2 - D^2 \right] P = 0 \quad (6.22)$$

which has roots

$$P = 0 \quad (6.23)$$

and

$$n^2 - S = \pm D. \quad (6.24)$$

Equation (6.24) may be rearranged in the form

$$n^2 = R, \quad n^2 = L \quad (6.25)$$

where

$$R = S + D, \quad L = S - D \quad (6.26)$$

have the mnemonics “right” and “left”. The rationale behind the nomenclature “S(um)” and “D(ifference)” now becomes apparent since

$$S = \frac{R + L}{2}, \quad D = \frac{R - L}{2}. \quad (6.27)$$

What does all this algebra mean? Equation (6.25) states that for $\theta = 0$ the dispersion relation has two distinct roots, each corresponding to a natural mode (or characteristic wave) constituting a self-consistent solution to the Maxwell-Lorentz system. The definitions in Eqs.(6.12) and (6.26) show that

$$R = 1 - \sum_{\sigma} \frac{\omega_{p\sigma}^2}{\omega(\omega + \omega_{c\sigma})}, \quad L = 1 - \sum_{\sigma} \frac{\omega_{p\sigma}^2}{\omega(\omega - \omega_{c\sigma})} \quad (6.28)$$

so that R diverges when $\omega = -\omega_{c\sigma}$ whereas L diverges when $\omega = \omega_{c\sigma}$. Since $\omega_{c\sigma} = q_{\sigma}B/m_{\sigma}$, the ion cyclotron frequency is positive and the electron cyclotron frequency is negative. Hence, R diverges at the electron cyclotron frequency, whereas L diverges at the ion cyclotron frequency. When $\omega \rightarrow \infty$, both $R, L \rightarrow 1$. In the limit $\omega \rightarrow 0$, evaluation of R, L must be done very carefully, since

$$\begin{aligned} \frac{\omega_{p\sigma}^2}{\omega_{c\sigma}} &= \frac{n_{\sigma}q_{\sigma}^2}{\varepsilon_0 m_{\sigma}} \frac{m_{\sigma}}{q_{\sigma}B} \\ &= \frac{n_{\sigma}q_{\sigma}}{\varepsilon_0 B} \end{aligned} \quad (6.29)$$

so that

$$\frac{\omega_{pi}^2}{\omega_{ci}} = -\frac{\omega_{pe}^2}{\omega_{ce}}. \quad (6.30)$$

Thus

$$\begin{aligned} \lim_{\omega \rightarrow 0} R, L &= 1 - \frac{1}{\omega} \left[\frac{\omega_{pi}^2}{(\omega \pm \omega_{ci})} + \frac{\omega_{pe}^2}{(\omega \pm \omega_{ce})} \right] \\ &= 1 - \frac{\omega_{pi}^2 + \omega_{pe}^2}{\omega_{ci}\omega_{ce}} \\ &\simeq 1 - \frac{n_e q_e^2}{\varepsilon_0 m_e} \frac{m_i}{q_i B} \frac{m_e}{q_e B} \\ &= 1 + \frac{\omega_{pi}^2}{\omega_{ci}^2} \\ &= 1 + \frac{c^2}{v_A^2} \end{aligned} \quad (6.31)$$

where $v_A^2 = B^2/\mu_0\rho$ is the Alfvén velocity. Thus, at low frequency, both R and L are related to Alfvén modes. The $n^2 = L$ mode is the slow mode (larger k) and the $n^2 = R$ mode is the fast mode (smaller k). Figure 6.1 shows the frequency dependence of the $n^2 = R, L$ modes.

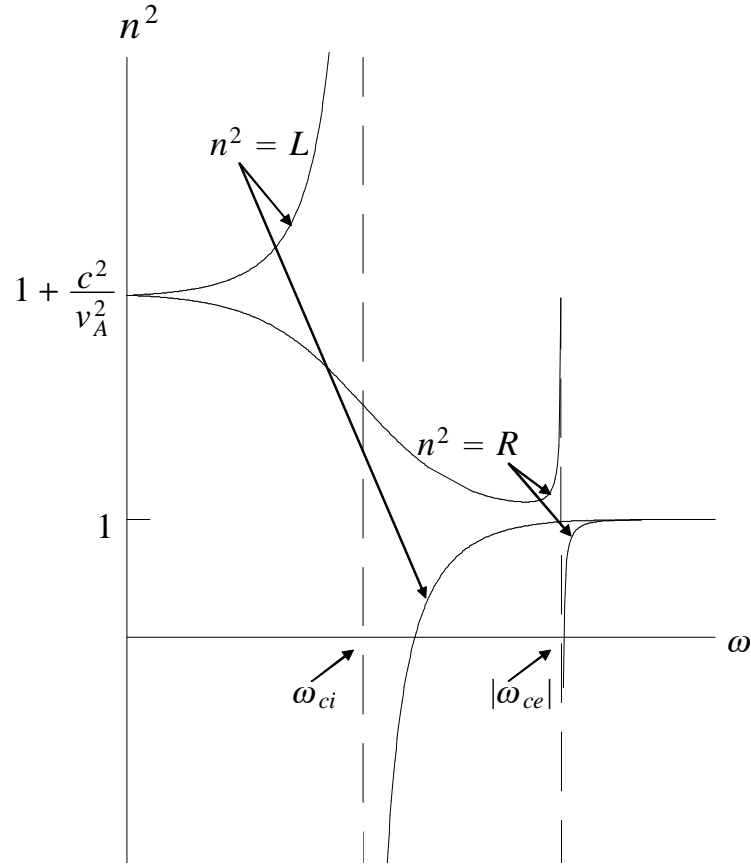


Figure 6.1: Propagation parallel to the magnetic field.

Having determined the eigenvalues for $\theta = 0$, the associated eigenvectors can now be found. These are obtained by substituting the eigenvalue back into the original set of equations; for example, substitution of $n^2 = R$ into Eq.(6.21) gives

$$\begin{bmatrix} -D & -iD & 0 \\ iD & -D & 0 \\ 0 & 0 & P \end{bmatrix} \cdot \begin{bmatrix} E_x \\ E_y \\ E_z \end{bmatrix} = 0, \quad (6.32)$$

so that the eigenvector associated with $n^2 = R$ is

$$\frac{E_x}{E_y} = -i, \quad \text{for eigenvalue } n^2 = R. \quad (6.33)$$

The implication of this eigenvector can be seen by considering the root $n = +\sqrt{R}$ so that

the electric field in the plane orthogonal to \hat{z} has the form

$$\begin{aligned}\mathbf{E}_\perp &= \text{Re} \{ E_\perp (\hat{x} + i\hat{y}) \exp(ik_z z - i\omega t) \} \\ &= |E_\perp| \{ \hat{x} \cos(k_z z - \omega t + \delta) - \hat{y} \sin(k_z z - \omega t + \delta) \}\end{aligned}\quad (6.34)$$

where $E_\perp = |E_\perp|e^{i\delta}$. This is a *right-hand* circularly polarized wave propagating in the positive z direction; hence the nomenclature R . Similarly, the $n^2 = L$ root gives a left-hand circularly polarized wave. Linearly polarized waves may be constructed from appropriate sums and differences of these left- and right-hand circularly polarized waves.

In summary, two distinct modes exist when the wavevector happens to be exactly parallel to the magnetic field ($\theta = 0$): a right-hand circularly polarized wave with dispersion $n^2 = R$ with $n \rightarrow \infty$ at the electron cyclotron resonance and a left-hand circularly polarized mode with dispersion $n^2 = L$ with $n \rightarrow \infty$ at the ion cyclotron resonance. Since ion cyclotron motion is left-handed (mnemonic ‘Lion’) it is reasonable that a left-hand circularly polarized wave resonates with ions, and vice versa for electrons. At low frequencies, these modes become Alfvén modes with dispersion $n_z^2 = 1 + c^2/v_A^2$ for $\theta = 0$. In the Chapter 4 discussion of Alfvén modes the dispersions of both compressional and shear modes were found to reduce to $c^2 k_z^2 / \omega^2 = n_z^2 = c^2 / v_A^2$ for $\theta = 0$. One may ask why a ‘1’ term did not appear in the Chapter 4 dispersion relations? The answer is that the ‘1’ term comes from displacement current, a quantity neglected in the Chapter 4 derivations. The displacement current term shows that if the plasma density is so low (or the magnetic field is so high) that v_A becomes larger than c , then Alfvén modes become ordinary vacuum electromagnetic waves propagating at nearly the speed of light. In order for a plasma to demonstrate significant Alfvénic (i.e., MHD behavior) it must satisfy $B / \sqrt{\mu_0 \rho} \ll c$ or equivalently have $\omega_{ci} \ll \omega_{pi}$.

6.2.2 Cutoffs and resonances

The general situation where $n^2 \rightarrow \infty$ is called a *resonance* and corresponds to the wavelength going to zero. Any slight dissipative effect in this situation will cause large wave damping. This is because if wavelength becomes infinitesimal and the fractional attenuation per wavelength is constant, there will be a near-infinite number of wavelengths and the wave amplitude is reduced by the same fraction for each of these. Figure 6.1 also shows that it is possible to have a situation where $n^2 = 0$. The general situation where $n^2 = 0$ is called a *cutoff* and corresponds to wave reflection, since n changes from being pure real to pure imaginary. If the plasma is non-uniform, it is possible for layers to exist in the plasma where either $n^2 \rightarrow \infty$ or $n^2 = 0$; these are called resonance or cutoff layers. Typically, if a wave intercepts a resonance layer, it is absorbed whereas if it intercepts a cutoff layer it is reflected.

6.2.3 Mode behavior at $\theta = \pi/2$

When $\theta = \pi/2$ Eq.(6.20) becomes

$$\begin{bmatrix} S & -iD & 0 \\ iD & S - n^2 & 0 \\ 0 & 0 & P - n^2 \end{bmatrix} \cdot \begin{bmatrix} E_x \\ E_y \\ E_z \end{bmatrix} = 0 \quad (6.35)$$

and again two distinct modes appear. The first mode has as its eigenvector the condition that $E_z \neq 0$. The associated eigenvalue equation is $P - n^2 = 0$ or

$$\omega^2 = k^2 c^2 + \sum_{\sigma} \omega_{p\sigma}^2 \quad (6.36)$$

which is just the dispersion for an electromagnetic plasma wave in an unmagnetized plasma. This is in accordance with the prediction that modes involving particle motion strictly parallel to the magnetic field are unaffected by the magnetic field. This mode is called the *ordinary* mode because it is unaffected by the magnetic field.

The second mode involves both E_x and E_y and has the eigenvalue equation $S(S - n^2) - D^2 = 0$ which gives the dispersion relation

$$n^2 = \frac{S^2 - D^2}{S} = 2 \frac{RL}{R + L}. \quad (6.37)$$

Cutoffs occur here when either $R = 0$ or $L = 0$ and a resonance occurs when $S = 0$. Since this mode depends on the magnetic field, it is called the *extraordinary* mode. The $S = 0$ resonance is called a hybrid resonance because it depends on a hybrid of $\omega_{c\sigma}^2$ and $\omega_{p\sigma}^2$ terms (note that $\omega_{c\sigma}^2$ terms depend on single-particle physics whereas $\omega_{p\sigma}^2$ terms depend on collective motion physics). Because S is quadratic in ω^2 , the equation $S = 0$ has two distinct roots and these are found by explicitly writing

$$S = 1 - \frac{\omega_{pi}^2}{\omega^2 - \omega_{ci}^2} - \frac{\omega_{pe}^2}{\omega^2 - \omega_{ce}^2} = 0. \quad (6.38)$$

A plot of this expression shows that the two roots are well separated. The large root may be found by assuming that $\omega \sim \mathcal{O}(\omega_{ce})$ in which case the ion term becomes insignificant. Dropping the ion term shows that the large root of S is simply

$$\omega_{uh}^2 = \omega_{pe}^2 + \omega_{ce}^2 \quad (6.39)$$

which is called the *upper hybrid frequency*. The small root may be found by assuming that $\omega^2 \ll \omega_{ce}^2$ which gives the *lower hybrid frequency*

$$\omega_{lh}^2 = \omega_{ci}^2 + \frac{\omega_{pi}^2}{1 + \frac{\omega_{pe}^2}{\omega_{ce}^2}}. \quad (6.40)$$

6.2.4 Very low frequency modes where θ is arbitrary

Equation (6.31) shows that for $\omega \ll \omega_{ci}$

$$\begin{aligned} S &\simeq R \simeq L \simeq 1 + c^2/v_A^2 \\ D &\simeq 0 \end{aligned} \quad (6.41)$$

so the cold plasma dispersion simplifies to

$$\begin{bmatrix} S - n_z^2 & 0 & n_x n_z \\ 0 & S - n^2 & 0 \\ n_x n_z & 0 & P - n_x^2 \end{bmatrix} \cdot \begin{bmatrix} E_x \\ E_y \\ E_z \end{bmatrix} = 0. \quad (6.42)$$

Because $D = 0$ the determinant factors into two modes, one where

$$(S - n^2) E_y = 0 \quad (6.43)$$

and the other where

$$\begin{bmatrix} S - n_z^2 & n_x n_z \\ n_x n_z & P - n_x^2 \end{bmatrix} \cdot \begin{bmatrix} E_x \\ E_z \end{bmatrix} = 0. \quad (6.44)$$

The former gives the dispersion relation

$$n^2 = S \quad (6.45)$$

with $E_y \neq 0$ as the eigenvector. This mode is the fast or compressional mode, since in the limit where the displacement current can be neglected, Eq.(6.45) becomes $\omega^2 = k^2 v_A^2$. The latter mode involves finite E_x and E_y and has the dispersion

$$n_x^2 = \frac{P}{S} (S - n_z^2) \quad (6.46)$$

which is the inertial Alfvén wave $\omega^2 = k_z^2 v_A^2 / (1 + k_x^2 c^2 / \omega_{pe}^2)$ in the limit that the displacement current can be neglected.

6.2.5 Modes where ω and θ are arbitrary

The respective behaviors at $\theta = 0$ and at $\theta = \pi/2$ and the low frequency Alfvén modes gave a useful introduction to the cold plasma modes and, in particular, showed how modes can be subject to cutoffs or resonances. We now evaluate the determinant of the matrix in Eq.(6.20) for arbitrary θ and arbitrary ω ; after some algebra this determinant can be written as

$$An^4 - Bn^2 + C = 0 \quad (6.47)$$

where

$$\begin{aligned} A &= S \sin^2 \theta + P \cos^2 \theta \\ B &= (S^2 - D^2) \sin^2 \theta + PS(1 + \cos^2 \theta) \\ C &= P(S^2 - D^2) = PRL. \end{aligned} \quad (6.48)$$

Equation (6.47) is quadratic in n^2 and has the two roots

$$n^2 = \frac{B \pm \sqrt{B^2 - 4AC}}{2A}. \quad (6.49)$$

Thus, the two distinct modes in the special cases of (i) $\theta = 0, \pi/2$ or (ii) $\omega \ll \omega_{ci}$ were just particular examples of the more general property that a cold plasma supports two distinct types of modes. Using a modest amount of algebraic manipulation (cf. assignments) it is straightforward to show that for real θ the quantity $B^2 - 4AC$ is positive definite, since

$$B^2 - 4AC = (S^2 - D^2 - SP)^2 \sin^4 \theta + 4P^2 D^2 \cos^2 \theta. \quad (6.50)$$

Thus n is either pure real (corresponding to a propagating wave) or pure imaginary (corresponding to an evanescent wave).

From Eqs.(6.47) and (6.48) it is seen that cutoffs occur when $C = 0$ which happens if $P = 0, L = 0$, or $R = 0$. Also, resonances correspond to having $A \rightarrow 0$ in which case

$$S \sin^2 \theta + P \cos^2 \theta \simeq 0. \quad (6.51)$$

6.2.6 Wave normal surfaces

The information contained in a dispersion relation can be summarized in a qualitative, visual manner by a *wave normal surface* which is a polar plot of the phase velocity of the wave normalized to c . Since $n = ck/\omega$, a wave normal surface is just a plot of $1/n(\theta)$ v. θ . The most basic wave normal surface is obtained by considering the equation for a light wave in vacuum,

$$\left(\frac{\partial^2}{\partial t^2} - c^2 \nabla^2 \right) \mathbf{E} = 0, \quad (6.52)$$

which has the simple dispersion relation

$$\frac{1}{n^2} = \frac{\omega^2}{k^2 c^2} = 1. \quad (6.53)$$

Thus the wave normal surface of a light wave in vacuum is just a sphere of radius unity because $\omega/k = 1/nc$ is independent of direction. Wave normal surfaces of plasma waves are typically more complicated because n usually depends on θ . The radius of the wave normal surface goes to zero at a resonance and goes to infinity at a cutoff (since $1/n \rightarrow 0$ at a resonance, $1/n \rightarrow \infty$ at a cutoff).

6.2.7 Taxonomy of modes – the CMA diagram

Equation (6.49) gives the general dispersion relation for arbitrary θ . While formally correct, this expression is of little practical value because of the complicated chain of dependence of n^2 on several variables. The CMA diagram (Clemmow and Mullaly (1955), Allis (1955)) provides an elegant method for revealing and classifying the large number of qualitatively different modes embedded in Eq.(6.49).

In principle, Eq. (6.49) gives the dependence of n^2 on the six parameters θ , ω , ω_{pe} , ω_{pi} , ω_{ce} , and ω_{ci} . However, ω_{pi} and ω_{pe} are not really independent parameters and neither are ω_{ci} and ω_{ce} because $\omega_{ce}^2/\omega_{ci}^2 = (m_i/m_e)^2$ and $\omega_{pe}^2/\omega_{pi}^2 = m_i/m_e$ for singly charged ions. Thus, once the ion species has been specified, the only free parameters are the density and the magnetic field. Once these have been specified, the plasma frequencies and the cyclotron frequencies are determined. It is reasonable to normalize these frequencies to the wave frequency in question since the quantities S , P , D depend only on the normalized frequencies. Thus, n^2 is effectively just a function of θ , ω_{pe}^2/ω^2 and ω_{ce}^2/ω^2 . Pushing this simplification even further, we can say that for fixed ω_{pe}^2/ω^2 and ω_{ce}^2/ω^2 , the refractive index n is just a function of θ . Then, once $n = n(\theta)$ is known, it can be used to plot a *wave normal surface*, i.e., ω/kc plotted v. θ .

The CMA diagram is developed by first constructing a chart where the horizontal axis is $\ln(\omega_{pe}^2/\omega^2 + \omega_{pi}^2/\omega^2)$ and the vertical axis is $\ln(\omega_{ce}^2/\omega^2)$. For a given ω any point on this chart corresponds to a unique density and a unique magnetic field. If we were ambitious, we could plot the wave normal surfaces $1/n$ v. θ for a very large number of points on this chart, and so have plots of dispersions for a large set of cold plasmas. While conceivable, such a thorough examination of all possible combinations of density and magnetic field would require plotting an inconveniently large number of wave normal surfaces.

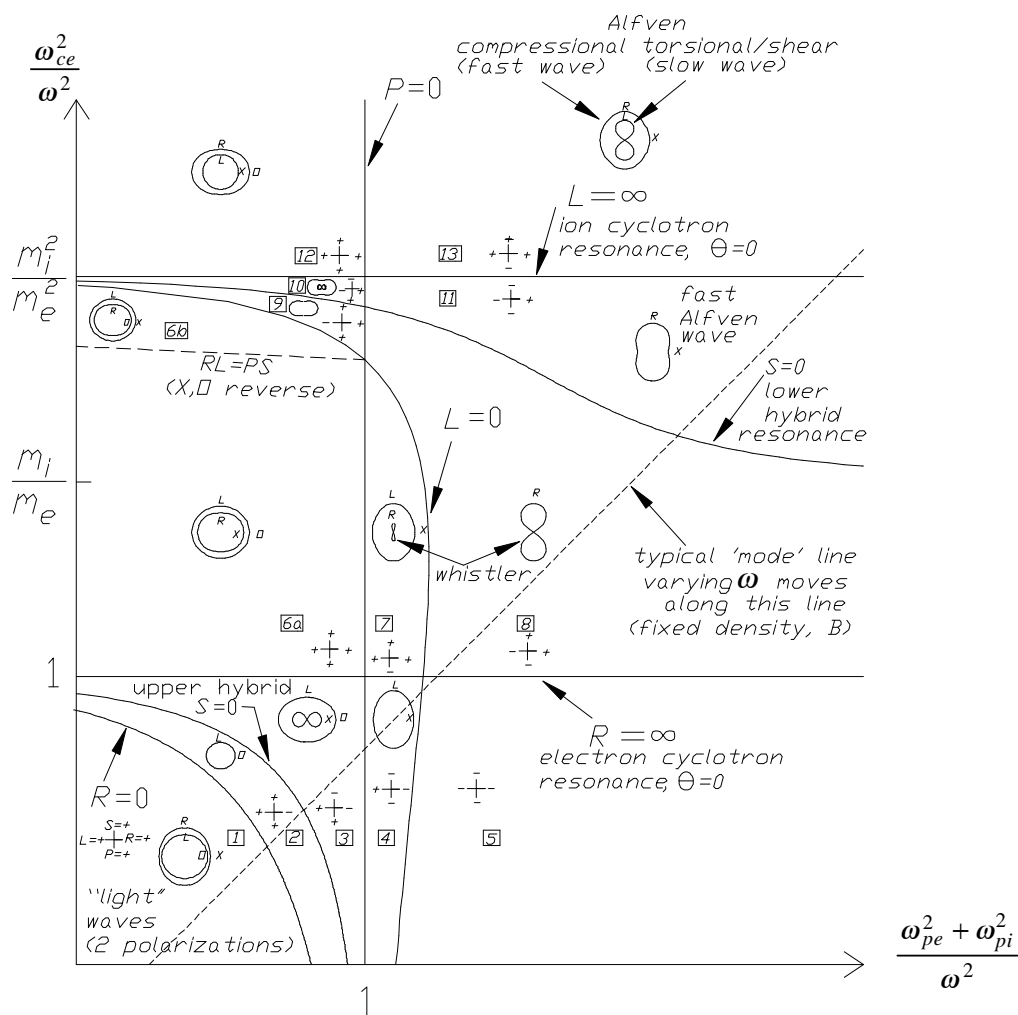


Figure 6.2: CMA diagram.

It is actually unnecessary to plot this very large set of wave normal surfaces because it turns out that the qualitative shape (i.e., topology) of the wave normal surfaces changes only at specific boundaries in parameter space and away from these boundaries the wave normal surface deforms, but does not change its topology. Thus, the parameter space boundaries enclose regions of parameter space where the qualitative shape (topology) of wave normal surfaces does not change. The CMA diagram, shown in Fig.6.2 charts these parameter space boundaries and so provides a powerful method for classifying cold plasma

modes. Parameter space is divided up into a finite number of regions, called bounded volumes, separated by curves in parameter space, called bounding surfaces, across which the modes change *qualitatively*. Thus, within a bounded volume, modes change quantitatively but not qualitatively. For example, if Alfvén waves exist at one point in a particular bounded volume, they must exist everywhere in that bounded volume, although the dispersion may not be quantitatively the same at different locations in the volume.

The appropriate choice of bounding surfaces consists of:

1. The *principle resonances* which are the curves in parameter space where n^2 has a resonance at either $\theta = 0$ or $\theta = \pi/2$. Thus, the principle resonances are the curves $R = \infty$ (i.e., electron cyclotron resonance), $L = \infty$ (i.e., ion cyclotron resonance), and $S = 0$ (i.e., the upper and lower hybrid resonances).
2. The cutoffs $R = 0$, $L = 0$, and $P = 0$.

The behavior of wave normal surfaces inside a bounded volume and when crossing a bounded surface can be summarized in five theorems (Stix 1962), each a simple consequence of the results derived so far:

1. Inside a bounded volume n cannot vanish. Proof: n vanishes only when $PRL = 0$, but $P = 0$, $R = 0$ and $L = 0$ have been defined to be bounding surfaces.
2. If n^2 has a resonance (i.e., goes to infinity) at *any* point in a bounded volume, then for *every* other point in the same bounded volume, there exists a resonance at some unique angle θ_{res} and its associated mirror angles, namely $-\theta_{res}$, $\pi - \theta_{res}$, and $-(\pi - \theta_{res})$ but at *no* other angles. Proof: If $n^2 \rightarrow \infty$ then $A \rightarrow 0$ in which case $\tan^2 \theta_{res} = -P/S$ determines the unique θ_{res} . Now $\tan^2(\pi - \theta_{res}) = \tan^2 \theta_{res}$ so there is also a resonance at the supplement $\theta = \pi - \theta_{res}$. Also, since the square of the tangent is involved, both θ_{res} and $\pi - \theta_{res}$ may be replaced by their negatives. Neither P nor S can change sign inside a bounded volume and both are single valued functions of their location in parameter space. Thus, $-P/S$ can only change sign at a bounding surface. In summary, if a resonance occurs at any point in a bounding surface, then a resonance exists at some unique angle θ_{res} and its associated mirror angles at every point in the bounding surface. Resonances only occur when P and S have opposite signs. Since $1/n$ goes to zero at a resonance, the radius of a wave normal surface goes to zero at a resonance.
3. At any point in parameter space, for a given interval in θ in which n is finite, n is either pure real or pure imaginary throughout that interval. Proof: n^2 is always real and is a continuous function of θ . The only situation where n can change from being pure real to being pure imaginary is when n^2 changes sign. This occurs when n^2 passes through zero, but because of the definition for bounding surfaces, n^2 does not vanish inside a bounded volume. Although n^2 may change sign when going through infinity, this situation is not relevant because the theorem was restricted to finite n .
4. n is symmetric about $\theta = 0$ and $\theta = \pi/2$. Proof: n is a function of $\sin^2 \theta$ and of $\cos^2 \theta$, both of which are symmetric about $\theta = 0$ and $\theta = \pi/2$.
5. Except for the special case where the surfaces $PD = 0$ and $RL = PS$ intersect, the two modes may coincide only at $\theta = 0$ or at $\theta = \pi/2$. Proof: For $0 < \theta < \pi/2$ the

square root in Eq.(6.49) is

$$\sqrt{B^2 - 4AC} = \sqrt{(RL - SP)^2 \sin^4 \theta + 4P^2 D^2 \cos^2 \theta} \quad (6.54)$$

and can only vanish if $PD = 0$ and $RL = PS$ simultaneously.

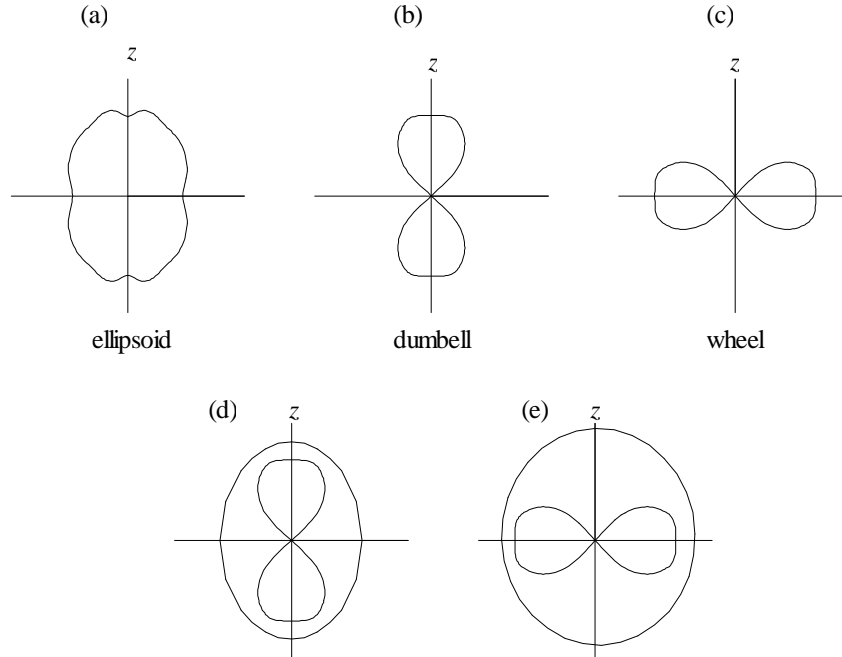


Figure 6.3: (a), (b), (c) show types of wave normal surfaces; (d) and (e) show permissible overlays of wave normal surfaces.

These theorems provide sufficient information to characterize the morphology of wave normal surfaces throughout all of parameter space. In particular, the theorems show that only three types of wave normal surfaces exist. These are ellipsoid, dumbbell, and wheel as shown in Fig.6.3(a,b,c) and each is a three-dimensional surface symmetric about the z axis.

We now discuss the features and interrelationships of these three types of wave normal surfaces. In this discussion, each of the two modes in Eq.(6.49) is considered separately; i.e., either the plus or the minus sign is chosen. The convention is used that a mode is considered to exist (i.e., has a wave normal surface) only if $n^2 > 0$ for at least some range of θ ; if $n^2 < 0$ for all angles, then the mode is evanescent (i.e., non-propagating) for all angles and is not plotted. The three types of wave normal surfaces are:

1. Bounded volume with no resonance and $n^2 > 0$ at some point in the bounded volume. Since $n^2 = 0$ occurs only at the bounding surfaces and $n^2 \rightarrow \infty$ only at resonances, n^2 must be positive and finite at every θ for each location in the bounded volume. The wave normal surface is thus ellipsoidal with symmetry about both $\theta = 0$ and $\theta = \pi/2$. The ellipse may deform as one moves inside the bounded volume, but will always have the morphology of an ellipse. This type of wave normal surface is shown in Fig.6.3(a). The wave normal surface is three dimensional and is azimuthally symmetric about the z axis.
2. Bounded volume having a resonance at some angle θ_{res} where $0 < \theta_{res} < \pi/2$ and $n^2(\theta)$ positive for $\theta < \theta_{res}$. At θ_{res} , $n \rightarrow \infty$ so the radius of the wave normal surface goes to zero. For $\theta < \theta_{res}$, the wave normal surface exists (n is pure real since $n^2 > 0$) and is plotted. At resonances $n^2(\theta)$ passes from $-\infty$ to $+\infty$ or vice versa. This type of wave normal surface is a dumbbell type as shown in Fig. 6.3(b).
3. Bounded volume having a resonance at some angle θ_{res} where $0 < \theta_{res} < \pi/2$ and $n^2(\theta)$ positive for $\theta > \theta_{res}$. This is similar to case 2 above, except that now the wave normal surface exists only for angles greater than θ_{res} resulting in the wheel type surface shown in Fig.6.3(c).

Consider now the relationship between the two modes (plus and minus sign) given by Eq.(6.49). Because the two modes cannot intersect (cf. theorem 5) at angles other than $\theta = 0, \pi/2$ and mirror angles, if one mode is an ellipsoid and the other has a resonance (i.e., is a dumbbell or wheel), the ellipsoid must be outside the other dumbbell or wheel; for if not, the two modes would intersect at an angle other than $\theta = 0$ or $\theta = \pi/2$). This is shown in Figs. 6.3(d) and (e).

Also, only one of the modes can have a resonance, so at most one mode in a bounded volume can be a dumbbell or wheel. This can be seen by noting that a resonance occurs when $A \rightarrow 0$. In this case $B^2 \gg |4AC|$ in Eq.(6.49) and the two roots are *well-separated*. This means that the binomial expansion can be used on the square root in Eq.(6.49) to obtain

$$\begin{aligned} n^2 &\simeq \frac{B \pm (B - 2AC/B)}{2A} \\ n_+^2 &\simeq \frac{B}{A}, \quad n_-^2 \simeq \frac{C}{B} \end{aligned} \quad (6.55)$$

where $|n_+^2| \gg |n_-^2|$ since $B^2 \gg |4AC|$. The root n_+^2 has the resonance and the root n_-^2 has no resonance. Since the wave normal surface of the minus root has no resonance, its wave normal surface must be ellipsoidal (if it exists). Because the ellipsoidal surface must always lie outside the wheel or dumbbell surface, the ellipsoidal surface will have a larger value of ω/kc than the dumbbell or wheel at every θ and so the ellipsoidal mode will always be the *fast* mode. The mode with the resonance will be a dumbbell or wheel, will lie inside the ellipsoidal surface, and so will always be the *slow* mode. This concept of well-separated roots is quite useful and, if the roots are well-separated, then Eq.(6.47) can be solved approximately for the large root (slow mode) by balancing the first two terms with each other, and for the small root (fast mode) by balancing the last two terms with each other.

Parameter space is subdivided into thirteen bounded volumes, each potentially con-

taining two normal modes corresponding to two qualitatively distinct propagating waves. However, since two modes do not exist in all bounded volumes, the actual number of modes is smaller than twenty-six. As an example of a bounded volume with two waves, the wave normal surfaces of the fast and slow Alfvén waves are in the upper right hand corner of the CMA diagram since this bounded volume corresponds to $\omega \ll \omega_{ci}$ and $\omega \ll \omega_{pe}$, i.e., above $L = 0$ and to the right of $P = 0$.

6.2.8 Use of the CMA diagram

The CMA diagram can be used in several ways. For example it can be used to (i) identify all allowed cold plasma modes in a given plasma for various values of ω or (ii) investigate how a given mode evolves as it propagates through a spatially inhomogeneous plasma and possibly intersects resonances or cutoffs due to spatial variation of density or magnetic field.

Let us consider the first example. Suppose the plasma is uniform and has a prescribed density and magnetic field. Since $\ln[(\omega_{pe}^2 + \omega_{pi}^2)/\omega^2]$ and $\ln[\omega_{ce}^2/\omega^2]$ are the coordinates of the CMA diagram, varying ω corresponds to tracing out a line having a slope of 45° and an offset determined by the prescribed density and magnetic field. High frequencies correspond to the lower left portion of this line and low frequencies to the upper right. Since the allowed modes lie along this line, if the line does not pass through a given bounded volume, then modes inside that bounded volume do not exist in the specified plasma.

Now consider the second example. Suppose the plasma is spatially non-uniform in such a way that both density and magnetic field are a function of position. To be specific, suppose that density increases as one moves in the x direction while magnetic field increases as one moves in the y direction. Thus, the CMA diagram becomes a map of the actual plasma. A wave with prescribed frequency ω is launched at some position x, y and then propagates along some trajectory in parameter space as determined by its local dispersion relation. The wave will continuously change its character as determined by the local wave normal surface. Thus a wave which is injected with a downward velocity as a fast Alfvén mode in the upper-right bounded volume will pass through the $L = \infty$ bounding surface and will undergo only a quantitative deformation. In contrast, a wave which is launched as a slow Alfvén mode (dumbbell shape) from the same position will disappear when it reaches the $L = \infty$ bounding surface, because the slow mode does not exist on the lower side (high frequency side) of the $L = \infty$ bounding surface. The slow Alfvén wave undergoes ion cyclotron resonance at the $L = \infty$ bounding surface and will be absorbed there.

6.3 Dispersion relation expressed as a relation between n_x^2 and n_z^2

The CMA diagram is very useful for classifying waves, but is often not so useful in practical situations where it is not obvious how to specify the angle θ . In a practical situation a wave is typically excited by an antenna that lies in a plane and the geometry of the antenna imposes the component of the wavevector in the antenna plane. The transmitter frequency determines ω .

For example, consider an antenna located in the $x = 0$ plane and having some specified z dependence. When Fourier analyzed in z , such an antenna would excite a characteristic k_z spectrum. In the extreme situation of the antenna extending to infinity in the $x = 0$ plane and having the periodic dependence $\exp(ik_z z)$, the antenna would excite just a single k_z . Thus, the antenna-transmitter combination in this situation would impose k_z and ω but leave k_x undetermined. The job of the dispersion relation would then be to determine k_x . It should be noted that antennas which are not both infinite and perfectly periodic will excite a spectrum of k_z modes rather than just a single k_z mode.

By writing $n_x^2 = n^2 \sin^2 \theta$ and $n_z^2 = n^2 \cos^2 \theta$, Eqs. (6.47) and (6.48) can be expressed as a quadratic equation for n_x^2 , namely

$$Sn_x^4 - [\bar{S}(S + P) - D^2]n_x^2 + P[\bar{S}^2 - D^2] = 0 \quad (6.56)$$

where

$$\bar{S} = S - n_z^2. \quad (6.57)$$

If the two roots of Eq.(6.56) are well-separated, the large root is found by balancing the first two terms to obtain

$$n_x^2 \simeq \frac{\bar{S}(S + P) - D^2}{S}, \quad (\text{large root}) \quad (6.58)$$

or in the limit of large P (i.e., low frequencies),

$$n_x^2 \simeq \frac{\bar{S}P}{S}, \quad (\text{large root}). \quad (6.59)$$

The small root is found by balancing the last two terms of Eq.(6.56) to obtain

$$n_x^2 \simeq \frac{P[\bar{S}^2 - D^2]}{[\bar{S}(S + P) - D^2]}, \quad (\text{small root}) \quad (6.60)$$

or in the limit of large P ,

$$n_x^2 \simeq \frac{(n_z^2 - R)(n_z^2 - L)}{S - n_z^2} \quad (\text{small root}). \quad (6.61)$$

Thus, any given n_z^2 always has an associated large n_x^2 mode and an associated small n_x^2 mode. Because the phase velocity is inversely proportion to the refractive index, the root with large n_x^2 is called the slow mode and the root with small n_x^2 is called the fast mode.

Using the quadratic formula it is seen that the exact form of these two roots of Eq.(6.56) is given by

$$n_x^2 = \frac{\bar{S}(S + P) - D^2 \pm \sqrt{[\bar{S}(S - P) - D^2]^2 + 4PD^2n_z^2}}{2S}. \quad (6.62)$$

It is clear that n_x^2 can become infinite only when $S = 0$. Situations where n_x^2 is complex (i.e., neither pure real or pure imaginary) can occur when P is large and negative in which case the argument of the square root can become negative. In these cases, θ also becomes complex and is no longer a physical angle. This shows that considering real angles between $0 < \theta < 2\pi$ does not account for all possible types of wave behavior. The regions where

n_x^2 becomes complex is called a region of inaccessibility and is a region where Eq.(6.56) does not have real roots. If a plasma is non-uniform in the x direction so that S, P , and D are functions of x and $\omega^2 < \omega_{pe}^2 + \omega_{pi}^2$, so that P is negative, the boundaries of a region of inaccessibility (if such a region exists) are the locations where the square root in Eq.(6.62) vanishes, i.e., where there is a solution for $\bar{S}(S - P) - D^2 = \pm \sqrt{-4PD^2n_z^2}$.

6.4 A journey through parameter space

Imagine an enormous plasma where the density increases in the x direction and the magnetic field points in the z direction but increases in the y direction. Suppose further that a radio transmitter operating at a frequency ω is connected to a hypothetical antenna which emits *plane waves*, i.e. waves with spatial dependence $\exp(i\mathbf{k} \cdot \mathbf{x})$. These assumptions are somewhat self-contradictory because, in order to excite plane waves, an antenna must be infinitely long in the direction normal to \mathbf{k} and if the antenna is infinitely long it cannot be localized. To circumvent this objection, it is assumed that the plasma is so enormous that the antenna at any location is sufficiently large compared to the wavelength in question to emit waves that are nearly plane waves.

The antenna is located at some point x, y in the plasma and the emitted plane waves are detected by a phase-sensitive receiver. The position x, y corresponds to a point in CMA space. The antenna is rotated through a sequence of angles θ and as the antenna is rotated, an observer walks in front of the antenna staying exactly one wavelength $\lambda = 2\pi/k$ from the face of the antenna. Since λ is proportional to $1/n = \omega/kc$ at fixed frequency, the locus of the observer's path will have the shape of a wave normal surface, i.e., a plot of $1/n$ versus θ .

Because of the way the CMA diagram was constructed, the topology of one of the two cold plasma modes always changes when a bounding surface is traversed. Which mode is affected and how its topology changes on crossing a bounding surface can be determined by monitoring the polarities of the four quantities S, P, R, L within each bounded volume. P changes polarity only at the $P = 0$ bounding surface, but R and L change polarity when they go through zero and also when they go through infinity. Furthermore, $S = (R + L)/2$ changes sign not only when $S = 0$ but also at $R = \infty$ and at $L = \infty$.

A straightforward way to establish how the polarities of S, P, R, L change as bounding surfaces are crossed is to start in the extreme lower left corner of parameter space, corresponding to $\omega^2 \gg \omega_{pe}^2, \omega_{ce}^2$. This is the limit of having no plasma and no magnetic field and so corresponds to unmagnetized vacuum. The cold plasma dispersion relation in this limit is simply $n^2 = 1$; i.e., vacuum electromagnetic waves such as ordinary light waves or radio waves. Here $S = P = R = L = 1$ because there are no plasma currents. Thus S, P, R, L are all *positive* in this bounded volume, denoted as Region 1 in Fig.6.2 (regions are labeled by boxed numbers). To keep track of the respective polarities, a small cross is sketched in each of the 13 bounded volumes. The signs of L and R are noted on the left and right of the cross respectively, while the sign of S is shown at the top and the sign of P is shown at the bottom.

In traversing from region 1 to region 2, R passes through zero and so reverses polarity but the polarities of L, S, P are unaffected. Going from region 2 to region 3, S passes through zero so the sign of S reverses. By continuing from region to region in this manner,

the plus or minus signs on the crosses in each bounded volume are established. It is important to remember that S changes sign at both $S = 0$ and the cyclotron resonances $L = \infty$ and $R = \infty$, but at all other bounding surfaces, only one quantity reverses sign.

Modes with resonances (i.e., dumbbells or wheels) only occur if S and P have opposite sign which occurs in regions 3, 7, 8, 10, and 13. The ordinary mode (i.e., $\theta = \pi/2$, $n^2 = P$) exists only if $P > 0$ and so exists only in those regions to the left of the $P = 0$ bounding surface. Thus, to the right of the $P = 0$ bounding surface only extraordinary modes exist (i.e., only modes where $n^2 = RL/S$ at $\theta = \pi/2$). Extraordinary modes exist only if $RL/S > 0$ which cannot occur if an odd subset of the three quantities R, L and S is negative. For example, in region 5 all three quantities are negative so extraordinary modes do not exist in region 5. The parallel modes $n^2 = R, L$ do not exist in region 5 because R and L are negative there. Thus, no modes exist in region 5, because if a mode were to exist there, it would need to have a limiting behavior of either ordinary or extraordinary at $\theta = \pi/2$ and of either right or left circularly polarized at $\theta = 0$.

When crossing a cutoff bounding surface ($R = 0, L = 0$, or $P = 0$), the outer (i.e., fast) mode has its wave normal surface become infinitely large, $\omega^2/k^2c^2 = 1/n^2 \rightarrow \infty$. Thus, immediately to the left of the $P = 0$ bounding surface, the fast mode (outer mode) is always the ordinary mode, because by definition this mode has the dispersion $n^2 = P$ at $\theta = \pi/2$ and so has a cutoff at $P = 0$. As one approaches the $P = 0$ bounding surface from the left, all the outer modes are ordinary modes and all disappear on crossing the $P = 0$ line so that to the right of the $P = 0$ line there are no ordinary modes.

In region 13 where the modes are Alfvén waves, the slow mode is the $n^2 = L$ mode since this is the mode which has the resonance at $L = \infty$. The slow Alfvén mode is the inertial Alfvén mode while the fast Alfvén mode is the compressional Alfvén mode. Going downwards from region 13 to region 11, the slow Alfvén wave undergoes ion cyclotron resonance and disappears, but the fast Alfvén wave remains. Similar arguments can be made to explain other boundary crossings in parameter space.

A subtle aspect of this taxonomy is the division of region 6 into two sub-regions 6a, and 6b. This subtlety arises because the dispersion at $\theta = \pi/2$ has the form

$$n^2 = \frac{RL + PS \pm |RL - PS|}{2S} = P, RL/S. \quad (6.63)$$

In region 6, both S and P are positive. If $RL - PS$ is also positive, then the plus sign gives the extraordinary mode which is the slow mode (bigger n , inner of the two wave normal surfaces). On the other hand, if $RL - PS$ is negative, then the absolute value operator inverts the sign of $RL - PS$ and the minus sign now gives the extraordinary mode which will be the fast mode (smaller n , outer of the two wave normal surfaces). Region 8 can also be divided into two regions (omitted here for clarity) separated by the $RL = PS$ line. In region 8 the ordinary mode does not exist, but the extraordinary mode will be given by either the plus or minus sign in Eq.(6.63) depending on which side of the $RL = PS$ line one is considering.

For a given plasma density and magnetic field, varying the frequency corresponds to moving along a ‘mode’ line which has a 45 degree slope on the log-log CMA diagram. If the plasma density is increased, the mode line moves to the right whereas if the magnetic field is increased, the mode line moves up. Since any single mode line cannot pass through all 13 regions of parameter space only a limited subset of the 13 regions of parameter space

can be accessed for any given plasma density and magnetic field. Plasmas with $\omega_{pe}^2 > \omega_{ce}^2$ are often labelled ‘overdense’ and plasmas with $\omega_{pe}^2 < \omega_{ce}^2$ are correspondingly labeled ‘underdense’. For overdense plasmas, the mode line passes to the right of the intersection of the $P = 0$, $R = \infty$ bounding surfaces while for underdense plasmas the mode line passes to the left of this intersection. Two different plasmas will be self-similar if they have similar mode lines. For example if a lab plasma has the same mode line as a space plasma it will support the same kind of modes, but do so in a scaled fashion. Because the CMA diagram is log-log the bounding surface curves extend infinitely to the left and right of the figure and also infinitely above and below it; however no new regions exist outside of what is sketched in Fig.6.2.

The weakly-magnetized case corresponds to the lower parts of regions 1-5, while the low-density case corresponds to the left parts of regions 1, 2, 3, 6, 9, 10, and 12. The CMA diagram provides a visual way for categorizing a great deal of useful information. In particular, it allows identification of isomorphisms between modes in different regions of parameter space so that understanding developed about the behavior for one kind of mode can be readily adapted to explain the behavior of a different, but isomorphic mode located in another region of parameter space.

6.5 High frequency waves: Altar-Appleton-Hartree dispersion relation

Examination of the dielectric tensor elements S , P , and D shows that while both ion and electron terms are of importance for low frequency waves, for high frequency waves ($\omega \gg \omega_{ci}, \omega_{pi}$) the ion terms are unimportant and may be dropped. Thus, for high frequency waves the dielectric tensor elements simplify to

$$\begin{aligned} S &= 1 - \frac{\omega_{pe}^2}{\omega^2 - \omega_{ce}^2} \\ P &= 1 - \frac{\omega_{pe}^2}{\omega^2} \\ D &= \frac{\omega_{ce}}{\omega} \frac{\omega_{pe}^2}{(\omega^2 - \omega_{ce}^2)} \end{aligned} \quad (6.64)$$

and the corresponding R and L terms are

$$\begin{aligned} R &= 1 - \frac{\omega_{pe}^2}{\omega(\omega + \omega_{ce})} \\ L &= 1 - \frac{\omega_{pe}^2}{\omega(\omega - \omega_{ce})}. \end{aligned} \quad (6.65)$$

The development of long distance short-wave radio communication in the 1930’s motivated investigations into how radio waves bounce from the ionosphere. Because the bouncing involves a $P = 0$ cutoff and because the ionosphere has ω_{pe}^2 of order ω_{ce}^2 but usually larger, the relevant frequencies must be of the order of the electron plasma frequency and so are much higher than both the ion cyclotron and ion plasma frequencies. Thus, ion effects are unimportant and so all ion terms may be dropped in order to simplify the analysis.

Perhaps the most important result of this era was a peculiar, but useful, reformulation by Appleton, Hartree, and Altar³ (Appleton 1932) of the $\omega \gg \omega_{pi}, \omega_{ci}$ limit of Eq.(6.49). The intent of this reformulation was to express n^2 in terms of its deviation from the vacuum limit, $n^2 = 1$. An obvious way to do this is to define $\xi = n^2 - 1$ and then re-write Eq.(6.47) as an equation for ξ , namely

$$A(\xi^2 + 2\xi + 1) - B(\xi + 1) + C = 0 \quad (6.66)$$

or, after regrouping,

$$A\xi^2 + \xi(2A - B) + A - B + C = 0. \quad (6.67)$$

Unfortunately, when this expression is solved for ξ , the leading term is -1 and so this attempt to find the deviation of n^2 from its vacuum limit fails. However, a slight rewriting of Eq.(6.67) as

$$\frac{A - B + C}{\xi^2} + \frac{2A - B}{\xi} + A = 0 \quad (6.68)$$

and then solving for $1/\xi$, gives

$$\xi = \frac{2(A - B + C)}{B - 2A \pm \sqrt{B^2 - 4AC}}. \quad (6.69)$$

This expression does not have a leading term of -1 and so allows the solution of Eq.(6.49) to be expressed as

$$n^2 = 1 + \frac{2(A - B + C)}{B - 2A \pm \sqrt{B^2 - 4AC}}. \quad (6.70)$$

In the $\omega \gg \omega_{ci}, \omega_{pi}$ limit where S, P, D are given by Eq.(6.64), algebraic manipulation of Eq.(6.70) (cf. assignments) shows that there exists a common factor in the numerator and denominator of the second term. After cancelling this common factor, Eq.(6.70) reduces to

$$n^2 = 1 - \left[\frac{2 \frac{\omega_{pe}^2}{\omega^2} \left(1 - \frac{\omega_{pe}^2}{\omega^2} \right)}{2 \left(1 - \frac{\omega_{pe}^2}{\omega^2} \right) - \frac{\omega_{ce}^2}{\omega^2} \sin^2 \theta \pm \Gamma} \right] \quad (6.71)$$

where

$$\Gamma = \sqrt{\frac{\omega_{ce}^4}{\omega^4} \sin^4 \theta + 4 \frac{\omega_{ce}^2}{\omega^2} \left(1 - \frac{\omega_{pe}^2}{\omega^2} \right)^2 \cos^2 \theta}. \quad (6.72)$$

Equation (6.71) is called the Altar-Appleton-Hartree dispersion relation (Appleton 1932) and has the desired property of showing the deviation of n^2 from the vacuum dispersion $n^2 = 1$.

We recall that the cold plasma dispersion relation simplified considerably when either $\theta = 0$ or $\theta = \pi/2$. A glance at Eq.(6.71) shows that this expression reduces indeed to $n^2 = R, L$ for $\theta = 0$. Somewhat more involved manipulation shows that Eq.(6.71) also reduces to $n_{\pm}^2 = P$ and $n_{\pm}^2 = RL/S$ for $\theta = \pi/2$.

³See discussion by Swanson (1989) regarding the recent addition of Altar to this citation

Equation (6.71) can be Taylor-expanded in the vicinity of the principle angles $\theta = 0$ and $\theta = \pi/2$ to give dispersion relations for quasi-parallel or quasi-perpendicular propagation. The terms quasi-longitudinal and quasi-transverse are commonly used to denote these situations. The nomenclature is somewhat unfortunate because of the possible confusion with the traditional convention that longitudinal and transverse refer to the orientation of \mathbf{k} relative to the wave electric field. Here, longitudinal means \mathbf{k} is nearly parallel to the static magnetic field while transverse means \mathbf{k} is nearly perpendicular to the static magnetic field.

6.5.1 Quasi-transverse modes ($\theta \simeq \pi/2$)

For quasi-transverse propagation, the first term in Γ dominates, that is

$$\frac{\omega_{ce}^4}{\omega^4} \sin^4 \theta \gg 4 \frac{\omega_{ce}^2}{\omega^2} \left(1 - \frac{\omega_{pe}^2}{\omega^2}\right)^2 \cos^2 \theta. \quad (6.73)$$

In this case a binomial expansion of Γ gives

$$\begin{aligned} \Gamma &= \frac{\omega_{ce}^2}{\omega^2} \sin^2 \theta \left[1 + 4 \frac{\omega^2}{\omega_{ce}^2} \left(1 - \frac{\omega_{pe}^2}{\omega^2}\right)^2 \frac{\cos^2 \theta}{\sin^4 \theta} \right]^{1/2} \\ &\simeq \frac{\omega_{ce}^2}{\omega^2} \sin^2 \theta + 2 \left(1 - \frac{\omega_{pe}^2}{\omega^2}\right)^2 \cot^2 \theta. \end{aligned} \quad (6.74)$$

Substitution of Γ into Eq.(6.71) shows that the generalization of the ordinary mode dispersion to angles in the vicinity of $\pi/2$ is

$$n_+^2 = \frac{1 - \frac{\omega_{pe}^2}{\omega^2}}{1 - \frac{\omega_{pe}^2}{\omega^2} \cos^2 \theta}. \quad (6.75)$$

The subscript + here means that the positive sign has been used in Eq.(6.71). This mode is called the QTO mode as an acronym for ‘quasi-transverse-ordinary’.

Choosing the – sign in Eq.(6.71) gives the quasi-transverse-extraordinary mode or QTX mode. After a modest amount of algebra (cf. assignments) the QTX dispersion is found to be

$$n_-^2 = \frac{\left(1 - \frac{\omega_{pe}^2}{\omega^2}\right)^2 - \frac{\omega_{ce}^2}{\omega^2} \sin^2 \theta}{1 - \frac{\omega_{pe}^2}{\omega^2} - \frac{\omega_{ce}^2}{\omega^2} \sin^2 \theta}. \quad (6.76)$$

Note that the QTX mode has a resonance near the upper hybrid frequency.

6.5.2 Quasi-longitudinal dispersion ($\theta \simeq 0$)

Here, the term containing $\cos^2 \theta$ dominates in Eq.(6.72). Because there are no cancellations of the leading terms in Γ with any remaining terms in the denominator of Eq.(6.71), it

suffices to keep only the leading term of Γ . Thus, in this limit

$$\Gamma \simeq 2 \left| \frac{\omega_{ce}}{\omega} \left(1 - \frac{\omega_{pe}^2}{\omega^2} \right) \cos \theta \right| = -2 \left(1 - \frac{\omega_{pe}^2}{\omega^2} \right) \left| \frac{\omega_{ce}}{\omega} \cos \theta \right| \quad (6.77)$$

since $P = 1 - \omega_{pe}^2/\omega^2$ is assumed to be negative. Upon substitution for Γ in Eq.(6.71) and then simplifying one obtains

$$n_+^2 = 1 - \frac{\omega_{pe}^2/\omega^2}{1 - \left| \frac{\omega_{ce}}{\omega} \cos \theta \right|}, \quad \text{QLR mode} \quad (6.78)$$

and

$$n_-^2 = 1 - \frac{\omega_{pe}^2/\omega^2}{1 + \left| \frac{\omega_{ce}}{\omega} \cos \theta \right|}, \quad \text{QLL mode.} \quad (6.79)$$

These simplified dispersions are based on the implicit assumption that $|P|$ is large, because if $P \rightarrow 0$ the presumption that Eq.(6.77) gives the leading term in Γ would be inappropriate. When $\omega < |\omega_{ce} \cos \theta|$ the QLR mode (quasi-longitudinal, right-hand circularly polarized) is called the whistler or helicon wave. This wave is distinguished by having a descending whistling tone which shows up at audio frequencies on sensitive amplifiers connected to long wire antennas. Whistlers may have been heard as early as the late 19th century by telephone linesmen installing long telephone lines. They become a subject of some interest in the trenches of the First World War when German scientist H. Barkhausen heard whistlers on a sensitive audio receiver while trying to eavesdrop on British military communications; the origin of these waves was a mystery at that time. After the war Barkhausen (1930) and Eckersley (1935) proposed that the descending tone was due to a dispersive propagation such that lower frequencies traveled more slowly, but did not explain the source location or propagation trajectory. The explanation had to wait over two more decades until Storey (1953) finally solved the mystery by showing that whistlers were caused by lightning bolts and identified two main types of propagation. The first type, called a short whistler resulted from a lightning bolt in the opposite hemisphere exciting a wave which propagated dispersively along the Earth's magnetic field to the observer. The second type, called a long whistler, resulted from a lightning bolt in the vicinity of the observer exciting a wave which propagated dispersively along field lines to the opposite hemisphere, then reflected, and traveled back along the same path to the observer. The dispersion would be greater in this round trip situation and also there would be a correlation with a click from the local lightning bolt. Whistlers are routinely observed by spacecraft flying through the Earth's magnetosphere and the magnetospheres of other planets.

The reason for the whistler's descending tone can be seen by representing each lightning bolt as a delta function in time

$$\delta(t) = \frac{1}{2\pi} \int e^{-i\omega t} d\omega. \quad (6.80)$$

A lightning bolt therefore launches a very broad frequency spectrum. Because the ionospheric electron plasma frequency is in the range 10-30 MHz, audio frequencies are much lower than the electron plasma frequency, i.e., $\omega_{pe} \gg \omega$ and so $|P| \gg 1$. The electron cyclotron frequency in the ionosphere is of the order of 1 MHz so $\omega_{ce} \gg \omega$ also. Thus, the

whistler dispersion for acoustic (a few kHz) waves in the ionosphere is

$$n_-^2 = \frac{\omega_{pe}^2}{\left| \frac{\omega_{ce}}{\omega} \cos \theta \right|} \quad (6.81)$$

or

$$k = \frac{\omega_{pe}}{c} \sqrt{\frac{\omega}{\left| \omega_{ce} \cos \theta \right|}}. \quad (6.82)$$

Each frequency ω in Eq.(6.80) has a corresponding k given by Eq.(6.82) so that the disturbance $g(x, t)$ excited by a lightning bolt has the form

$$g(x, t) = \frac{1}{2\pi} \int e^{ik(\omega)x - i\omega t} d\omega \quad (6.83)$$

where $x = 0$ is the location of the lightning bolt. Because of the strong dependence of k on ω , contributions to the phase integral in Eq.(6.83) at adjacent frequencies will in general have substantially different phases. The integral can then be considered as the sum of contributions having all possible phases. Since there will be approximately equal amounts of positive and negative contributions, the contributions will cancel each other out when summed; this cancelling is called phase mixing.

Suppose there exists some frequency ω at which the phase $k(\omega)x - \omega t$ has a local maximum or minimum with respect to variation of ω . In the vicinity of this extremum, the phase is independent of frequency and so the contributions from adjacent frequencies constructively interfere and produce a finite signal. Thus, an observer located at some position $x \neq 0$ will hear a signal only at the time when the phase in Eq.(6.83) is at an extrema. The phase extrema is found by setting to zero the derivative of the phase with respect to frequency, i.e. setting

$$\frac{\partial k}{\partial \omega} x - t = 0. \quad (6.84)$$

From Eq.(6.82) it is seen that

$$\frac{\partial k}{\partial \omega} = \frac{\omega_{pe}}{2c} \frac{1}{\sqrt{\omega \left| \omega_{ce} \cos \theta \right|}} \quad (6.85)$$

so that the time at which a frequency ω is heard by an observer at location x is

$$t = \frac{\omega_{pe}}{2c} \frac{x}{\sqrt{\omega \left| \omega_{ce} \cos \theta \right|}}. \quad (6.86)$$

This shows that lower frequencies are heard at later times, resulting in the descending tone characteristic of whistlers.

6.6 Group velocity

Suppose that at time $t = 0$ the electric field of a particular fast or slow mode is decomposed into spatial Fourier modes, each varying as $\exp(i\mathbf{k} \cdot \mathbf{x})$. The total wave field can then be written as

$$\mathbf{E}(\mathbf{x}) = \int d\mathbf{k} \bar{\mathbf{E}}(\mathbf{k}) \exp(i\mathbf{k} \cdot \mathbf{x}) \quad (6.87)$$

where $\bar{\mathbf{E}}(\mathbf{k})$ is the amplitude of the mode with wavenumber \mathbf{k} . The dispersion relation assigns an ω to each \mathbf{k} , so that at later times the field evolves as

$$\mathbf{E}(\mathbf{x}, t) = \int d\mathbf{k} \bar{\mathbf{E}}(\mathbf{k}) \exp(i\mathbf{k} \cdot \mathbf{x} - i\omega(\mathbf{k})t) \quad (6.88)$$

where $\omega(\mathbf{k})$ is given by the dispersion relation. The integration over \mathbf{k} may be viewed as a summation of rapidly oscillatory waves, each having different rates of phase variation. In general, this sum vanishes because the waves add destructively or “phase mix”. However, if the waves add constructively, a finite $\mathbf{E}(\mathbf{x}, t)$ will result. Denoting the phase by

$$\phi(\mathbf{k}) = \mathbf{k} \cdot \mathbf{x} - \omega(\mathbf{k})t \quad (6.89)$$

it is seen that the Fourier components add constructively at extrema (minima or maxima) of $\phi(\mathbf{k})$, because in the vicinity of an extrema, the phase is stationary with respect to \mathbf{k} , that is, the phase does not vary with \mathbf{k} . Thus, the trajectory $\mathbf{x} = \mathbf{x}(t)$ along which $\mathbf{E}(\mathbf{x}, t)$ is finite is the trajectory along which the phase is stationary. At time t the stationary phase is the place where $\partial\phi(\mathbf{k})/\partial\mathbf{k}$ vanishes which is where

$$\frac{\partial\phi}{\partial\mathbf{k}} = \mathbf{x} - \frac{\partial\omega}{\partial\mathbf{k}}t = 0. \quad (6.90)$$

The trajectory of the points of stationary phase is therefore

$$\mathbf{x}(t) = \mathbf{v}_g t \quad (6.91)$$

where $\mathbf{v}_g = \partial\omega/\partial\mathbf{k}$ is called the group velocity. The group velocity is the velocity at which a pulse propagates in a dispersive medium and is also the velocity at which energy propagates.

The phase velocity for a one-dimensional system is defined as $v_{ph} = \omega/k$. In three dimensions this definition can be extended to be $\mathbf{v}_{ph} = \hat{\mathbf{k}}\omega/k$, i.e. a vector in the direction of \mathbf{k} but with the magnitude ω/k .

Group and phase velocities are the same only for the special case where ω is linearly proportional to k , a situation which occurs only if there is no plasma. For example, the phase velocity of electromagnetic plasma waves (dispersion $\omega^2 = \omega_{pe}^2 + k^2c^2$) is

$$\mathbf{v}_{ph} = \hat{\mathbf{k}} \frac{\sqrt{\omega_{pe}^2 + k^2c^2}}{k} \quad (6.92)$$

which is faster than the speed of light. However, no paradox results because information and energy travel at the group velocity, not the phase velocity. The group velocity for this wave is evaluated by taking the derivative of the dispersion with respect to \mathbf{k} giving

$$2\omega \frac{\partial\omega}{\partial\mathbf{k}} = 2\mathbf{k}c \quad (6.93)$$

or

$$\frac{\partial\omega}{\partial\mathbf{k}} = \frac{\mathbf{k}c}{\sqrt{\omega_{pe}^2 + k^2c^2}} \quad (6.94)$$

which is less than the speed of light.

This illustrates an important property of the wave normal surface concept – a wave normal surface is a polar plot of the *phase velocity* and should not be confused with the group velocity.

6.7 Quasi-electrostatic cold plasma waves

Another useful way of categorizing waves is according to whether the wave electric field is:

1. electrostatic so that $\nabla \times \mathbf{E} = 0$ and $\mathbf{E} = -\nabla\phi$

or

2. inductive so that $\nabla \cdot \mathbf{E} = 0$ and in Coulomb gauge, $\mathbf{E} = -\partial\mathbf{A}/\partial t$, where \mathbf{A} is the vector potential.

An electrostatic electric field is produced by net charge density whereas an inductive field is produced by time-dependent currents. Inductive electric fields are always associated with time-dependent magnetic fields via Faraday's law.

Waves involving purely electrostatic electric fields are called electrostatic waves, whereas waves involving inductive electric fields are called electromagnetic waves because these waves involve both electric and magnetic wave fields. In actuality, electrostatic waves must always have some slight inductive component, because there must always be a small current which establishes the net charge density. Thus, strictly speaking, the condition for electrostatic modes is $\nabla \times \mathbf{E} \simeq 0$ rather than $\nabla \times \mathbf{E} = 0$.

In terms of Fourier modes where ∇ is replaced by $i\mathbf{k}$, electrostatic modes are those for which $\mathbf{k} \times \mathbf{E} = 0$ so that \mathbf{E} is parallel to \mathbf{k} ; this means that electrostatic waves are longitudinal waves. Electromagnetic waves have $\mathbf{k} \cdot \mathbf{E} = 0$ and so are transverse waves. Here, we are using the usual wave terminology where longitudinal and transverse refer to whether \mathbf{k} is parallel or perpendicular to \mathbf{E} .

The electron plasma waves and ion acoustic waves discussed in the previous chapter were electrostatic, the compressional Alfvén wave was inductive, and the inertial Alfvén wave was both electrostatic and inductive. We now wish to show that in a *magnetized* plasma, the wheel and dumbbell modes in the CMA diagram always have electrostatic behavior in the region where the wave normal surface comes close to the origin, i.e., near the cross-over in the figure-eight pattern of these wave normal surfaces. For these waves, when n becomes large (i.e., near the cross-over of the figure-eight pattern of the wheel or dumbbell), \mathbf{n} becomes nearly parallel to \mathbf{E} and the magnetic part of the wave becomes unimportant. We now prove this assertion and also take care to distinguish this situation from another situation where n becomes infinite, namely at cyclotron resonances.

When the two roots of the dispersion $An^4 - Bn^2 + C = 0$ are well-separated (i.e., $B^2 \gg 4AC$) the slow mode is found by assuming that n^2 is large. In this case the dispersion can be approximated as $An^4 - Bn^2 \simeq 0$ which gives the slow mode as $n^2 \simeq B/A$. Resonance (i.e., $n^2 \rightarrow \infty$) can thus occur either from

1. $A = S \sin^2\theta + P \cos^2\theta$ vanishing, or
2. $B = RL \sin^2\theta + PS(1 + \cos^2\theta)$ becoming infinite.

These two cases are different. In the first case S and P remain finite and the vanishing of A determines a critical angle $\theta_{res} = \tan^{-1} \sqrt{-P/S}$; this angle is the cross-over angle of the figure-eight pattern of the wheel or dumbbell. In the second case either R or L must become infinite, a situation occurring only at the R or L bounding surfaces.

The first case results in quasi-electrostatic cold plasma waves, whereas the second case does not. To see this, the electric field is first decomposed into its longitudinal and trans-

verse parts

$$\begin{aligned}\mathbf{E}^l &= \hat{n}\hat{n}\cdot\mathbf{E} \\ \mathbf{E}^t &= \mathbf{E} - \mathbf{E}^l\end{aligned}\quad (6.95)$$

where $\hat{n} = \hat{k} = \mathbf{n}/n$ is a unit vector in the direction of \mathbf{n} . The cold plasma wave equation, Eq. (6.17) can thus be written as

$$\mathbf{nn}\cdot(\mathbf{E}^t + \mathbf{E}^l) - n^2(\mathbf{E}^t + \mathbf{E}^l) + \overleftrightarrow{\mathbf{K}}\cdot(\mathbf{E}^t + \mathbf{E}^l) = 0. \quad (6.96)$$

Since $\mathbf{n}\cdot\mathbf{E}^t = 0$ and $\mathbf{nn}\cdot\mathbf{E}^l = n^2\mathbf{E}^l$ this expression can be recast as

$$\left(\overleftrightarrow{\mathbf{K}} - n^2\overleftrightarrow{\mathbf{I}}\right)\cdot\mathbf{E}^t + \overleftrightarrow{\mathbf{K}}\cdot\mathbf{E}^l = 0 \quad (6.97)$$

where $\overleftrightarrow{\mathbf{I}}$ is the unit tensor. If the resonance is such that

$$n^2 \gg K_{ij} \quad (6.98)$$

where K_{ij} are the elements of the dielectric tensor, then Eq.(6.97) may be approximated as

$$-n^2\mathbf{E}^t + \overleftrightarrow{\mathbf{K}}\cdot\mathbf{E}^l \simeq 0. \quad (6.99)$$

This shows that the transverse electric field is

$$\mathbf{E}^t = \frac{1}{n^2}\overleftrightarrow{\mathbf{K}}\cdot\mathbf{E}^l \quad (6.100)$$

which is much smaller in magnitude than the longitudinal electric field by virtue of Eq.(6.98).

An easy way to obtain the dispersion relation (determinant of this system) is to dot Eq.(6.100) with \mathbf{n} to obtain

$$\mathbf{n}\cdot\overleftrightarrow{\mathbf{K}}\cdot\mathbf{n} = n^2(S\sin^2\theta + P\cos^2\theta) \simeq 0 \quad (6.101)$$

which is just the first case discussed above. This argument is self-consistent because for the first case (i.e., $A \rightarrow 0$) the quantities S, P, D remain finite so the condition given by Eq.(6.98) is satisfied.

The second case, $B \rightarrow \infty$, occurs at the cyclotron resonances where S and D diverge so the condition given by Eq.(6.98) is not satisfied. Thus, for the second case the electric field is not quasi-electrostatic.

6.8 Resonance cones

The situation $A \rightarrow 0$ corresponds to Eq.(6.101) which is a dispersion relation having the surprising property of depending on θ , but *not* on the magnitude of n . This limiting form of dispersion has some bizarre aspects which will now be examined.

The group velocity in this situation can be evaluated by writing Eq.(6.101) as

$$k_x^2 S + k_z^2 P = 0 \quad (6.102)$$

and then taking the vector derivative with respect to \mathbf{k} to obtain

$$2k_x \hat{x} S + 2k_z \hat{z} P + \left(k_x^2 \frac{\partial S}{\partial \omega} + k_z^2 \frac{\partial P}{\partial \omega} \right) \frac{\partial \omega}{\partial \mathbf{k}} = 0 \quad (6.103)$$

which may be solved to give

$$\frac{\partial \omega}{\partial \mathbf{k}} = -2 \left(\frac{k_x \hat{x} S + k_z \hat{z} P}{k_x^2 \frac{\partial S}{\partial \omega} + k_z^2 \frac{\partial P}{\partial \omega}} \right). \quad (6.104)$$

If Eq.(6.104) is dotted with \mathbf{k} the surprising result

$$\mathbf{k} \cdot \frac{\partial \omega}{\partial \mathbf{k}} = 0, \quad (6.105)$$

is obtained which means that the group velocity is *orthogonal* to the phase velocity. The same result may also be obtained in a quicker but more abstract way by using spherical coordinates in k space in which case the group velocity is just

$$\frac{\partial \omega}{\partial \mathbf{k}} = \hat{\mathbf{k}} \frac{\partial \omega}{\partial k} + \frac{\hat{\theta}}{k} \frac{\partial \omega}{\partial \theta}. \quad (6.106)$$

Applying this to Eq.(6.101), it is seen that the first term on the right hand side vanishes because the dispersion relation is independent of the magnitude of \mathbf{k} . Thus, the group velocity is in the $\hat{\theta}$ direction, so the group and phase velocities are again *orthogonal*, since \mathbf{k} is orthogonal to $\hat{\theta}$. Thus, energy and information propagate at right angles to the phase velocity.

A more physically intuitive interpretation of this phenomenon may be developed by “un-Fourier” analyzing the cold plasma wave equation, Eq.(6.17) giving

$$\nabla \times \nabla \times \mathbf{E} - \frac{\omega^2}{c^2} \overleftrightarrow{\mathbf{K}} \cdot \mathbf{E} = 0. \quad (6.107)$$

The modes corresponding to $A \rightarrow 0$ were obtained by dotting the dispersion relation with \mathbf{n} , an operation equivalent to taking the divergence in real space, and then arguing that the wave is mainly longitudinal. Let us therefore assume that $\mathbf{E} \simeq -\nabla \phi$ and take the divergence of Eq.(6.107) to obtain

$$\nabla \cdot \left(\overleftrightarrow{\mathbf{K}} \cdot \nabla \phi \right) = 0 \quad (6.108)$$

which is essentially Poisson’s equation for a medium having dielectric tensor $\overleftrightarrow{\mathbf{K}}$. Equation (6.108) can be expanded to give

$$S \frac{\partial^2 \phi}{\partial x^2} + P \frac{\partial^2 \phi}{\partial z^2} = 0. \quad (6.109)$$

If S and P have the same sign, Eq.(6.109) is an elliptic partial differential equation and so is just a distorted form of Poisson’s equation. In fact, by defining the stretched coordinates $\xi = x/\sqrt{|S|}$ and $\eta = z/\sqrt{|P|}$, Eq.(6.109) becomes Poisson’s equation in $\xi - \eta$ space.

Suppose now that waves are being excited by a line source $q\delta(x)\delta(z)\exp(-i\omega t)$, i.e., a wire antenna lying along the y axis oscillating at the frequency ω . In this case Eq.(6.109) becomes

$$\frac{\partial^2\phi}{\partial\xi^2} + \frac{\partial^2\phi}{\partial\eta^2} = \frac{q}{|SP|^{3/2}\epsilon_0}\delta(\xi)\delta(\eta) \quad (6.110)$$

so that the equipotential contours excited by the line source are just static concentric circles in ξ, η or equivalently, static concentric ellipses in x, z .

However, if S and P have *opposite signs*, the situation is entirely different, because now the equation is hyperbolic and has the form

$$\frac{\partial^2\phi}{\partial x^2} = \left|\frac{P}{S}\right| \frac{\partial^2\phi}{\partial z^2}. \quad (6.111)$$

Equation (6.111) is formally analogous to the standard hyperbolic wave equation

$$\frac{\partial^2\psi}{\partial t^2} = c^2 \frac{\partial^2\psi}{\partial z^2} \quad (6.112)$$

which has solutions propagating along the characteristics $\psi = \psi(z \pm ct)$. Thus, the solutions of Eq.(6.111) also propagate along characteristics, i.e.,

$$\phi = \phi(z \pm \sqrt{-P/S}x) \quad (6.113)$$

which are characteristics in the $x - z$ plane rather than the $x - t$ plane. For a line source, the potential is infinite at the line, and this infinite potential propagates from the source following the characteristics

$$z = \pm \sqrt{-\frac{P}{S}}x. \quad (6.114)$$

If the source is a point source, then the potential has the form

$$\phi(r, z) \sim \frac{q}{4\pi\epsilon_0 \left(\frac{r^2}{S} + \frac{z^2}{P}\right)^{1/2}} \quad (6.115)$$

which diverges on the conical surface having cone angle $\tan\theta_{cone} = r/z = \pm\sqrt{-S/P}$ as shown in Fig.6.4. These singular surfaces are called resonance cones and were first observed by Fisher and Gould (1969). The singularity results because the cold plasma approximation allows k to be arbitrarily large (i.e., allows infinitesimally short wavelengths). However, when k is made larger than ω/v_T , the cold plasma assumption $\omega/k \gg v_T$ becomes violated and warm plasma effects need to be taken into account. Thus, instead of becoming infinite on the resonance cone, the potential is large and finite and has a fine structure determined by thermal effects (Fisher and Gould 1971).

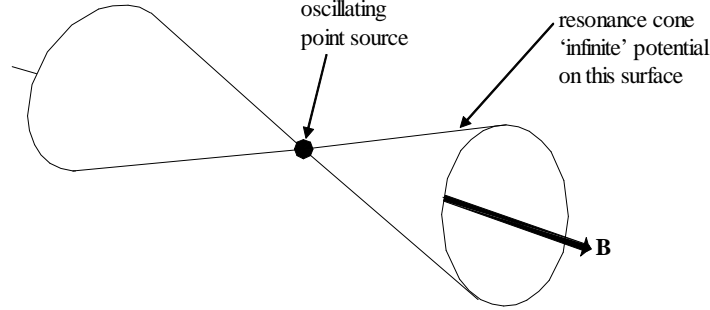


Figure 6.4: Resonance cone excited by oscillating point source in magnetized plasma.

Resonance cones exist in the following regions of parameter space

- (i) Region 3, where they are called upper hybrid resonance cones; here $S < 0, P > 0$,
- (ii) Regions 7 and 8, where they are a limiting form of the whistler wave and are also called lower hybrid resonance cones since they are affected by the lower hybrid resonance (Bellan and Porkolab 1975). For $\omega_{ci} \ll \omega \ll \omega_{pe}, \omega_{ce}$ the P and S dielectric tensor elements become

$$P \simeq -\frac{\omega_{pe}^2}{\omega^2}, \quad S \simeq 1 - \frac{\omega_{pi}^2}{\omega^2} + \frac{\omega_{pe}^2}{\omega_{ce}^2} \quad (6.116)$$

so that the cone angle $\theta_{cone} = \tan^{-1} r/z$ is

$$\theta_{cone} = \tan^{-1} \sqrt{-\frac{S}{P}} = \tan^{-1} \sqrt{(\omega^2 - \omega_{lh}^2)(\omega_{pe}^{-2} + \omega_{ce}^{-2})}. \quad (6.117)$$

If $\omega \gg \omega_{lh}$, the cone depends mainly on the smaller of ω_{pe}, ω_{ce} . For example, if $\omega_{ce} \ll \omega_{pe}$ then the cone angle is simply

$$\theta_{cone} \simeq \tan^{-1} \omega / \omega_{ce} \quad (6.118)$$

whereas if $\omega_{ce} \gg \omega_{pe}$ then

$$\theta_{cone} \simeq \tan^{-1} \omega / \omega_{pe}. \quad (6.119)$$

For low density plasmas this last expression can be used as the basis for a simple, accurate plasma density diagnostic.

- (iii) Regions 10 and 13. The Alfvén resonance cones in region 13 have a cone angle $\theta_{cone} = \omega / \sqrt{|\omega_{ce}\omega_{ci}|}$ and are associated with the electrostatic limit of inertial Alfvén waves (Stasiewicz, Bellan, Chaston, Kletzing, Lysak, Maggs, Pokhotelov, Seyler, Shukla, Stenflo, Streltsov and Wahlund 2000). To the best of the author's knowledge, cones have not been investigated in region 10 which corresponds to an unusual mix of parameters, namely ω_{pe} is the same order of magnitude as ω_{ci} .

6.9 Assignments

1. Prove that the cold plasma dispersion relation can be written as

$$An^4 - Bn^2 + C = 0$$

where

$$\begin{aligned} A &= S \sin^2 \theta + P \cos^2 \theta \\ B &= (S^2 - D^2) \sin^2 \theta + SP(1 + \cos^2 \theta) \\ C &= P(S^2 - D^2) \end{aligned}$$

so that the dispersion is

$$n^2 = \frac{B \pm \sqrt{B^2 - 4AC}}{2A}$$

Prove that

$$RL = S^2 - D^2.$$

2. Prove that n^2 is always real if θ is real, by showing that

$$B^2 - 4AC = [S^2 - D^2 - SP]^2 \sin^4 \theta + 4P^2 D^2 \cos^2 \theta.$$

3. Plot the bounding surfaces of the CMA diagram, by defining $m_e/m_i = \lambda$, $x = (\omega_{pe}^2 + \omega_{pi}^2)/\omega^2$, and $y = \omega_{ce}^2/\omega^2$. Show that

$$\frac{\omega_{pe}^2}{\omega^2} = \frac{x}{1 + \lambda}$$

so that

$$P = 1 - x$$

and S, R, L are functions of x and y with λ as a parameter. Hint– it is easier to plot x versus y for some of the functions.

4. Plot n^2 versus ω for $\theta = \pi/2$, showing the hybrid resonances.
5. Starting in region 1 of the CMA diagram, establish the signs of S, P, R, L in all the regions.
6. Plot the CMA mode lines for plasmas having $\omega_{pe}^2 \gg \omega_{ce}^2$ and vice versa.
7. Consider a plasma with two ion species. By plotting S versus ω show that there is an ion-ion hybrid resonance located between the two ion cyclotron frequencies. Give an approximate expression for the frequency of this resonance in terms of the ratios of the densities of the two ion species. Hint– compare the magnitude of the electron term to that of the two ion terms. Using quasineutrality, obtain an expression that depends only on the fractional density of each ion species.
8. Consider a two-dimensional plasma with an oscillatory delta function source at the origin. Suppose that slow waves are being excited which satisfy the electrostatic dispersion

$$k_x^2 S + k_z^2 P = 0$$

where $SP < 0$. By writing the source on the z axis as

$$f(z) = \frac{1}{2\pi} \int e^{ik_z z - i\omega t} dk_z$$

and by solving the dispersion to give $k_x = k_x(k_z)$ show that the potential excited in the plasma is singular along the resonance cone surfaces. Explain why this happens. Draw the group and phase velocity directions.

9. What is the polarization (i.e., relative magnitude of E_x, E_y, E_z) of the QTO, QTX, and the two QL modes? How should a microwave horn be oriented (i.e., in which way should the \mathbf{E} field of the horn point) when being used for (i) a QTO experiment, (ii) a QTX experiment. Which experiment would be best suited for heating the plasma and which best suited for measuring the density of the plasma?
10. Show that there is a simple factoring of the cold plasma dispersion relation in the low frequency limit $\omega \ll \omega_{ci}$. Hint - first find approximate forms of $S, P,$ and D in this limit and then show that the cold plasma dielectric tensor becomes diagonal. Consider a mode which has only E_y finite and a mode which only has E_x and E_z finite. What are the dispersion relations for these two modes, expressed in terms of ω as a function of k . Assume that the Alfvén velocity is much smaller than the speed of light.

Waves in inhomogeneous plasmas and wave energy relations

7.1 Wave propagation in inhomogeneous plasmas

Thus far in our discussion of wave propagation it has been assumed that the plasma is spatially uniform. While this assumption simplifies analysis, the real world is usually not so accommodating and it is plausible that spatial nonuniformity might modify wave propagation. The modification could be just a minor adjustment or it could be profound. Spatial nonuniformity might even produce entirely new kinds of waves. As will be seen, all these possibilities can occur.

To determine the effects of spatial nonuniformity, it is necessary to re-examine the original system of partial differential equations from which the wave dispersion relation was obtained. This is because the technique of substituting ik for ∇ is, in essence, a shortcut for spatial Fourier analysis, and so is mathematically valid *only* if the equilibrium is spatially uniform. This constraint on replacing ∇ by ik can be appreciated by considering the simple example of a high-frequency electromagnetic plasma wave propagating in an unmagnetized three-dimensional plasma having a gentle density gradient. The plasma frequency will be a function of position for this situation. To keep matters simple, the density non-uniformity is assumed to be in one direction only which will be labeled the x direction. The plasma is thus uniform in the y and z directions, but non-uniform in the x direction. Because the frequency is high, ion motion may be neglected and the electron motion is just

$$\mathbf{v}_1 = -\frac{q_e}{i\omega m_e} \mathbf{E}_1. \quad (7.1)$$

The current density associated with electron motion is therefore

$$\mathbf{J}_1 = -\frac{n_e(x)q_e^2}{i\omega m_e} \mathbf{E}_1 = -\varepsilon_0 \frac{\omega_{pe}^2(x)}{i\omega} \mathbf{E}_1. \quad (7.2)$$

Inserting this current density into Ampere's law gives

$$\nabla \times \mathbf{B}_1 = -\frac{\omega_{pe}^2(x)}{i\omega c^2} \mathbf{E}_1 - \frac{i\omega}{c^2} \mathbf{E}_1 = -\frac{i\omega}{c^2} \left(1 - \frac{\omega_{pe}^2(x)}{\omega^2} \right) \mathbf{E}_1. \quad (7.3)$$

Substituting Ampere's law into the curl of Faraday's law gives

$$\nabla \times \nabla \times \mathbf{E}_1 = \frac{\omega^2}{c^2} \left(1 - \frac{\omega_{pe}^2(x)}{\omega^2} \right) \mathbf{E}_1. \quad (7.4)$$

Attention is now restricted to waves for which $\nabla \cdot \mathbf{E}_1 = 0$; this is a generalization of the assumption that the waves are transverse (i.e., have $\mathbf{ik} \cdot \mathbf{E} = 0$) or equivalently are electromagnetic, and so involve no density perturbation. In this case, expansion of the left hand side of Eq.(7.4) yields

$$\left(\frac{\partial^2}{\partial x^2} + \frac{\partial^2}{\partial y^2} + \frac{\partial^2}{\partial z^2} \right) \mathbf{E}_1 + \frac{\omega^2}{c^2} \left(1 - \frac{\omega_{pe}^2(x)}{\omega^2} \right) \mathbf{E}_1 = 0. \quad (7.5)$$

It should be recalled that Fourier analysis is restricted to equations with constant coefficients, so Eq.(7.5) can only be Fourier transformed in the y and z directions. It cannot be Fourier transformed in the x direction because the coefficient $\omega_{pe}^2(x)$ depends on x . Thus, after performing only the allowed Fourier transforms, the wave equation becomes

$$\left(\frac{\partial^2}{\partial x^2} - k_y^2 - k_z^2 \right) \bar{\mathbf{E}}_1(x, k_y, k_z) + \frac{\omega^2}{c^2} \left(1 - \frac{\omega_{pe}^2(x)}{\omega^2} \right) \bar{\mathbf{E}}_1(x, k_y, k_z) = 0 \quad (7.6)$$

where $\bar{\mathbf{E}}_1(x, k_y, k_z)$ is the Fourier transform in the y and z directions. This may be rewritten as

$$\left(\frac{\partial^2}{\partial x^2} + \kappa^2(x) \right) \bar{\mathbf{E}}_1(x, k_y, k_z) = 0 \quad (7.7)$$

where

$$\kappa^2(x) = \frac{\omega^2}{c^2} \left(1 - \frac{\omega_{pe}^2(x)}{\omega^2} \right) - k_y^2 - k_z^2. \quad (7.8)$$

We now realize that Eq. (7.7) is just the spatial analog of the WKB equation for a pendulum with slowly varying frequency, namely Eq.(3.17); the only difference is that the independent variable t has been replaced by the independent variable x . Since changing the name of the independent variable is of no consequence, the solution here is formally the same as the previously derived WKB solution, Eq.(3.24). Thus the approximate solution to Eq.(7.8) is

$$\bar{\mathbf{E}}_1(x, k_y, k_z) \sim \frac{1}{\sqrt{\kappa(x)}} \exp(i \int^x \kappa(x') dx'). \quad (7.9)$$

Equation (7.9) shows that both the the wave amplitude and effective wavenumber change as the wave propagates in the x direction, i.e. in the direction of the inhomogeneity. It is clear that if the inhomogeneity is in the x direction, the wavenumbers k_y and k_z do not change as the wave propagates. This is because, unlike for the x direction, it was possible to Fourier transform in the y and z directions and so k_y and k_z are just coordinates in Fourier space. The effective wavenumber in the direction of the inhomogeneity, i.e., $\kappa(x)$, is not a coordinate in Fourier space because Fourier transformation was not allowed in the x direction. The spatial dependence of the effective wavenumber $\kappa(x)$ defined by Eq.(7.8) and the spatial dependence of the WKB amplitude together provide the means by which the system accommodates the spatial inhomogeneity. The invariance of the wavenumbers in the homogeneous directions is called Snell's law. An elementary example of Snell's law is the situation where light crosses an interface between two media having different dielectric constants and the refractive index parallel to the interface remains invariant.

One way of interpreting this result is to state that the WKB method gives qualified permission to Fourier analyze in the x direction. To the extent that such an x -direction Fourier analysis is allowed, $\kappa(x)$ can be considered as the effective wavenumber in the x direction, i.e., $\kappa(x) = k_x(x)$. The results in Chapter 3 imply that the WKB approximate solution, Eq.(7.9), is valid only when the criterion

$$\frac{1}{k_x} \frac{dk_x}{dx} \ll k_x \quad (7.10)$$

is satisfied. Inequality (7.10) is not satisfied when $k_x \rightarrow 0$, i.e., at a cutoff. At a resonance the situation is somewhat more complicated. According to cold plasma theory, k_x simply diverges at a resonance; however when hot plasma effects are taken into account, it is found that instead of having k_x going to infinity, the resonant cold plasma mode coalesces with a hot plasma mode as shown in Fig.7.1. At the point of coalescence $dk_x/dx \rightarrow \infty$ while all the other terms in Eq.(7.9) remain finite, and so the WKB method also breaks down at a resonance.

An interesting and important consequence of this discussion is the very real possibility that inequality (7.10) could be violated in a plasma having only the mildest of inhomogeneities. This breakdown of WKB in an apparently benign situation occurs because the critical issue is how $k_x(x)$ changes and not how plasma parameters change. For example, k_x could go through zero at some critical plasma density and, no matter how gentle the density gradient is, there will invariably be a cutoff at the critical density.

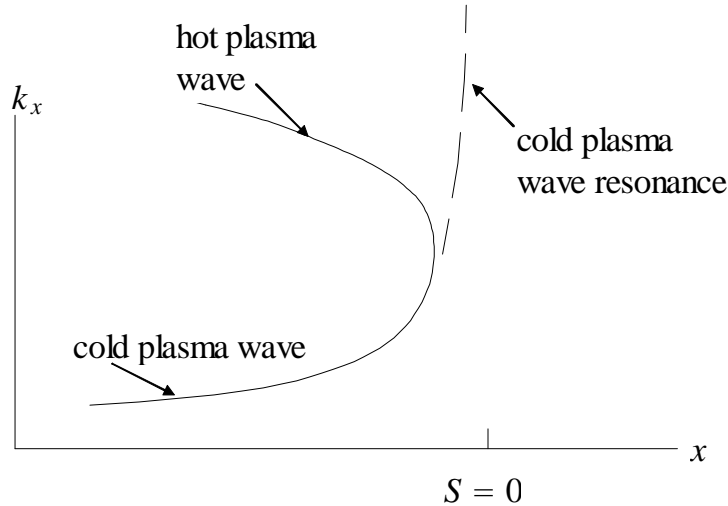


Figure 7.1: Example of coalescence of a cold plasma wave and a hot plasma wave near the resonance of the cold plasma wave. Here a hybrid resonance causes the cold resonance.

7.2 Geometric optics

The WKB method can be generalized to a plasma that is inhomogeneous in more than one dimension. In the general case of inhomogeneity in all three dimensions, the three components of the wavenumber will be functions of position, i.e., $\mathbf{k} = \mathbf{k}(\mathbf{x})$. How is the functional dependence determined? The answer is to write the dispersion relation as

$$D(\mathbf{k}, \mathbf{x}) = 0. \quad (7.11)$$

The \mathbf{x} -dependence of D denotes an explicit spatial dependence of the dispersion relation due to density or magnetic field gradients. This dispersion relation is now presumed to be satisfied at some initial point \mathbf{x} and then it is further assumed that all quantities evolve in such a way to keep the dispersion relation satisfied at other positions. Thus, at some arbitrary nearby position $\mathbf{x} + \delta\mathbf{x}$, the dispersion relation is also satisfied so

$$D(\mathbf{k} + \delta\mathbf{k}, \mathbf{x} + \delta\mathbf{x}) = 0 \quad (7.12)$$

or, on Taylor expanding,

$$\delta\mathbf{k} \cdot \frac{\partial D}{\partial \mathbf{k}} + \delta\mathbf{x} \cdot \frac{\partial D}{\partial \mathbf{x}} = 0. \quad (7.13)$$

The general condition for satisfying Eq.(7.13) can be established by assuming that both \mathbf{k} and \mathbf{x} depend on some parameter which increases monotonically along the trajectory of the wave, for example the distance s along the wave trajectory. The wave trajectory itself can also be parametrized as a function of s . Then using both $\mathbf{k} = \mathbf{k}(s)$ and $\mathbf{x} = \mathbf{x}(s)$, it is seen that moving a distance δs corresponds to respective increments $\delta\mathbf{k} = \delta s \, d\mathbf{k}/ds$ and $\delta\mathbf{x} = \delta s \, d\mathbf{x}/ds$. This means that Eq. (7.13) can be expressed as

$$\left[\frac{d\mathbf{k}}{ds} \cdot \frac{\partial D}{\partial \mathbf{k}} + \frac{d\mathbf{x}}{ds} \cdot \frac{\partial D}{\partial \mathbf{x}} \right] \delta s = 0. \quad (7.14)$$

The general solution to this equation are the two coupled equations

$$\frac{d\mathbf{k}}{ds} = - \frac{\partial D}{\partial \mathbf{x}}, \quad (7.15)$$

$$\frac{d\mathbf{x}}{ds} = \frac{\partial D}{\partial \mathbf{k}}. \quad (7.16)$$

These are just Hamilton's equations with the dispersion relation D acting as the Hamiltonian, the path length s acting like the time, \mathbf{x} acting as the position, and \mathbf{k} acting as the momentum. Thus, given the initial momentum at an initial position, the wavenumber evolution and wave trajectory can be calculated using Eqs.(7.15) and (7.16) respectively. The close relationship between wavenumber and momentum fundamental to quantum mechanics is plainly evident here. Snell's law states that the wavenumber in a particular direction remains invariant if the medium is uniform in that direction; this is clearly equivalent (cf. Eq.(7.15)) to the Hamilton-Lagrange result that the canonical momentum in a particular direction is invariant if the system is uniform in that direction.

This Hamiltonian point of view provides a useful way for interpreting cutoffs and resonances. Suppose that D is the dispersion relation for a particular mode and suppose that D can be written in the form

$$D(\mathbf{k}, \mathbf{x}) = \sum_{ij} \alpha_{ij} k_i k_j + g(\omega, n(\mathbf{x}), B(\mathbf{x})) = 0. \quad (7.17)$$

If D is construed to be the Hamiltonian, then the first term in Eq.(7.17) can be identified as the ‘kinetic energy’ while the second term can be identified as the ‘potential energy’. As an example, consider the simple case of an electromagnetic mode in an unmagnetized plasma which has nonuniform density, so that

$$D(\mathbf{k}, \mathbf{x}) = \frac{c^2 k^2}{\omega^2} - 1 + \frac{\omega_{pe}^2(x)}{\omega^2} = 0. \quad (7.18)$$

The wave propagation can be analyzed in analogy to the problem of a particle in a potential well. Here the kinetic energy is $c^2 k^2/\omega^2$, the potential energy is $-1 + \omega_{pe}^2(x)/\omega^2$, and the total energy is zero. This is a ‘wave-particle’ duality formally like that of quantum mechanics since there is a correspondence between wavenumber and momentum and between energy and frequency. Cutoffs give wave reflection in analogy to the reflection of a particle in a potential well at points where the potential energy equals the total energy. As shown in Fig.7.2(a), when the potential energy has a local minimum, waves will be trapped in the potential well associated with this minimum. Electrostatic plasma waves can also exhibit wave trapping between two reflection points; these trapped waves are called cavitons (the analysis is essentially the same; one simply replaces c^2 by $3\omega_{pe}^2 \lambda_{De}^2$). The bouncing of short wave radio waves from the ionospheric plasma can be analyzed using Eq.(7.18) together with Eqs.(7.15) and (7.16). As shown in Fig.7.2(b) a wave resonance (i.e., $k^2 \rightarrow \infty$) would correspond to a deep crevice in the potential energy. One must be careful to use geometric optics only when the plasma is weakly inhomogeneous, so that the waves change sufficiently gradually as to satisfy the WKB criterion.

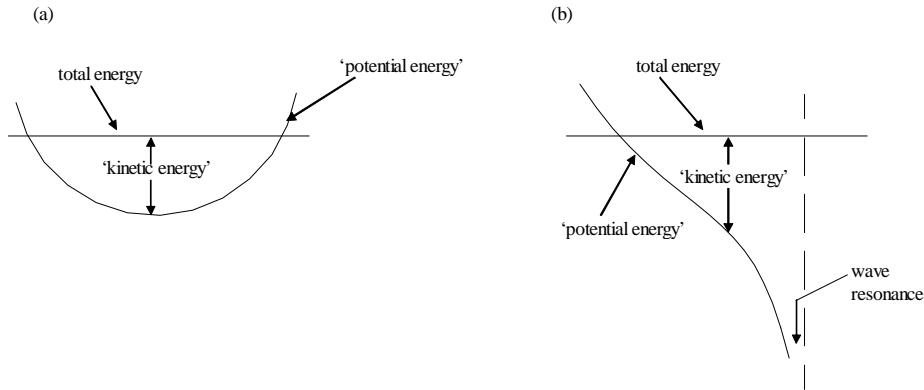


Figure 7.2: (a) Effective potential energy for trapped wave; (b) for wave resonance.

7.3 Surface waves - the plasma-filled waveguide

An extreme form of plasma inhomogeneity occurs when there is an abrupt transition from

plasma to vacuum – in other words, the plasma has an edge or surface. A qualitatively new mode, called a surface wave, appears in this circumstance. The physical basis of surface waves is closely related to the mechanism by which light waves propagate in an optical fiber.

Using the same analysis that led to Eq.(7.3), Maxwell's equations in an unmagnetized plasma may be expressed as

$$\nabla \times \mathbf{B} = -\frac{i\omega}{c^2} P \mathbf{E}, \quad \nabla \times \mathbf{E} = i\omega \mathbf{B} \quad (7.19)$$

where P is the unmagnetized plasma dielectric function

$$P = 1 - \frac{\omega_{pe}^2}{\omega^2}. \quad (7.20)$$

We consider a plasma which is uniform in the z direction but non-uniform in the directions perpendicular to z . The electromagnetic fields and gradient operator can be separated into axial components (i.e. z direction) and transverse components (i.e., perpendicular to z) as follows:

$$\mathbf{B} = \mathbf{B}_t + B_z \hat{z}, \quad \mathbf{E} = \mathbf{E}_t + E_z \hat{z}, \quad \nabla = \nabla_t + \hat{z} \frac{\partial}{\partial z}. \quad (7.21)$$

Using these definitions Eqs.(7.19) become

$$\begin{aligned} \left(\nabla_t + \hat{z} \frac{\partial}{\partial z} \right) \times (\mathbf{B}_t + B_z \hat{z}) &= -\frac{i\omega}{c^2} P (\mathbf{E}_t + E_z \hat{z}), \\ \left(\nabla_t + \hat{z} \frac{\partial}{\partial z} \right) \times (\mathbf{E}_t + E_z \hat{z}) &= i\omega (\mathbf{B}_t + B_z \hat{z}). \end{aligned} \quad (7.22)$$

Since the curl of a transverse vector is in the z direction, these equations can be separated into axial and transverse components,

$$\hat{z} \cdot \nabla_t \times \mathbf{B}_t = -\frac{i\omega}{c^2} P E_z, \quad (7.23)$$

$$\hat{z} \cdot \nabla_t \times \mathbf{E}_t = i\omega B_z, \quad (7.24)$$

$$\hat{z} \times \frac{\partial \mathbf{B}_t}{\partial z} + \nabla_t B_z \times \hat{z} = -\frac{i\omega}{c^2} P \mathbf{E}_t, \quad (7.25)$$

$$\hat{z} \times \frac{\partial \mathbf{E}_t}{\partial z} + \nabla_t E_z \times \hat{z} = i\omega \mathbf{B}_t. \quad (7.26)$$

The transverse electric field on the left hand side of Eq.(7.26) can be replaced using Eq.(7.25) to give

$$i\omega \mathbf{B}_t = \hat{z} \times \frac{\partial}{\partial z} \left[\frac{\hat{z} \times \frac{\partial \mathbf{B}_t}{\partial z} + \nabla_t B_z \times \hat{z}}{-\frac{i\omega}{c^2} P} \right] + \nabla_t E_z \times \hat{z}. \quad (7.27)$$

It is now assumed that all quantities have axial dependence $\sim \exp(ikz)$ so that Eq.(7.27) can be solved to give \mathbf{B}_t solely in terms of E_z and B_z , i.e.,

$$\mathbf{B}_t = \left(\frac{\omega^2}{c^2} P - k^2 \right)^{-1} \left[\nabla_t \frac{\partial B_z}{\partial z} - \frac{i\omega}{c^2} P \nabla_t E_z \times \hat{z} \right]. \quad (7.28)$$

This result can also be used to solve for the transverse electric field by interchanging $-\mathrm{i}\omega P/c^2 \longleftrightarrow \mathrm{i}\omega$ and $\mathbf{E} \longleftrightarrow \mathbf{B}$ to obtain

$$\mathbf{E}_t = \left(\frac{\omega^2}{c^2} P - k^2 \right)^{-1} \left[\nabla_t \frac{\partial E_z}{\partial z} + \mathrm{i}\omega \nabla_t B_z \times \hat{z} \right]. \quad (7.29)$$

Except for the plasma-dependent factor P , these are the standard waveguide equations. An important feature of these equations is that the transverse fields $\mathbf{E}_t, \mathbf{B}_t$ are functions of the axial fields E_z, B_z only and so all that is required is to construct wave equations characterizing the axial fields. This is an enormous simplification because, instead of having to derive and solve six wave equations in the six components of \mathbf{E}, \mathbf{B} as might be expected, it suffices to derive and solve wave equations for just E_z and B_z .

The sought-after wave equations are determined by eliminating \mathbf{E}_t and \mathbf{B}_t from Eqs.(7.23) and (7.24) to obtain

$$\hat{z} \cdot \nabla_t \times \left\{ \left(\frac{\omega^2}{c^2} P - k^2 \right)^{-1} \left[\mathrm{i}k \nabla_t B_z - \frac{\mathrm{i}\omega}{c^2} P \nabla_t E_z \times \hat{z} \right] \right\} = -\frac{\mathrm{i}\omega}{c^2} P E_z, \quad (7.30)$$

$$\hat{z} \cdot \nabla_t \times \left\{ \left(\frac{\omega^2}{c^2} P - k^2 \right)^{-1} \left[\mathrm{i}k \nabla_t E_z + \mathrm{i}\omega \nabla_t B_z \times \hat{z} \right] \right\} = \mathrm{i}\omega B_z. \quad (7.31)$$

In the special situation where $\nabla_t P \times \nabla_t B_z = \nabla_t P \times \nabla_t E_z = 0$, the first terms in the square brackets of the above equations vanish. This simplification would occur for example in an azimuthally symmetric plasma having an azimuthally symmetric perturbation so that $\nabla_t P, \nabla_t E_z$ and $\nabla_t B_z$ are all in the r direction. It is now assumed that both the plasma and the mode have this azimuthal symmetry so that Eqs.(7.30) and (7.31) reduce to

$$\hat{z} \cdot \nabla_t \times \left\{ \left(\frac{\omega^2}{c^2} P - k^2 \right)^{-1} (P \nabla_t E_z \times \hat{z}) \right\} = P E_z, \quad (7.32)$$

$$\hat{z} \cdot \nabla_t \times \left\{ \left(\frac{\omega^2}{c^2} P - k^2 \right)^{-1} (\nabla_t B_z \times \hat{z}) \right\} = B_z \quad (7.33)$$

or equivalently

$$\nabla_t \cdot \left\{ \frac{P}{P - k^2 c^2 / \omega^2} \nabla_t E_z \right\} + \frac{\omega^2}{c^2} P E_z = 0, \quad (7.34)$$

$$\nabla_t \cdot \left\{ \frac{1}{P - k^2 c^2 / \omega^2} \nabla_t B_z \right\} + \frac{\omega^2}{c^2} B_z = 0. \quad (7.35)$$

The assumption that both the plasma and the modes are azimuthally symmetric has the important consequence of decoupling the E_z and B_z modes so there are two distinct polarizations. These are (i) a mode where B_z is finite, but $E_z = 0$ and (ii) the reverse. Case (i) is called a transverse electric (TE) mode while case (ii) is called a transverse magnetic mode (TM) since in the first case the electric field is purely transverse while in the second case the magnetic field is purely transverse.

We now consider an azimuthally symmetric TM mode propagating in a uniform cylindrical plasma of radius a surrounded by vacuum. Since $B_z = 0$ for a TM mode, the transverse fields are the following functions of E_z :

$$\mathbf{B}_t = \left(\frac{\omega^2}{c^2} P - k^2 \right)^{-1} \left[-\frac{i\omega}{c^2} P \nabla_t E_z \times \hat{z} \right], \quad (7.36)$$

$$\mathbf{E}_t = \left(\frac{\omega^2}{c^2} P - k^2 \right)^{-1} \nabla_t \frac{\partial E_z}{\partial z}. \quad (7.37)$$

Additionally, because of the assumed symmetry, the TM mode Eq.(7.34) simplifies to

$$\frac{1}{r} \frac{\partial}{\partial r} \left(\frac{rP}{P - k^2 c^2 / \omega^2} \frac{\partial E_z}{\partial r} \right) + \frac{\omega^2}{c^2} P E_z = 0. \quad (7.38)$$

Since P is uniform within the plasma region and within the vacuum region, but has different values in these two regions, separate solutions to Eq.(7.38) must be obtained in the plasma and vacuum regions respectively and then matched at the interface. The jump in P is accommodated by defining distinct radial wave numbers

$$\kappa_p^2 = k^2 - \frac{\omega^2}{c^2} P, \quad (7.39)$$

$$\kappa_v^2 = k^2 - \frac{\omega^2}{c^2} \quad (7.40)$$

for the respective plasma and vacuum regions. The solutions to Eq.(7.38) in the respective plasma and vacuum regions are linear combinations of Bessel functions of order zero. If both of κ_p^2 and κ_v^2 are positive then the TM mode has the peculiar property of being radially evanescent in *both* the plasma and vacuum regions. In this case both the vacuum and plasma region solutions consist of modified Bessel functions I_0, K_0 . These solutions are constrained by physics considerations as follows:

1. Because the parallel electric field is a physical quantity it must be finite. In particular, E_z must be finite at $r = 0$ in which case only the $I_0(\kappa_p r)$ solution is allowed in the plasma region (the K_0 solution diverges at $r = 0$). Similarly, because E_z must be finite as $r \rightarrow \infty$, only the $K_0(\kappa_v r)$ solution is allowed in the vacuum region (the $I_0(\kappa_v r)$ solution diverges at $r = \infty$).
2. The parallel electric field E_z must be continuous across the vacuum-plasma interface. This constraint is imposed by Faraday's law and can be seen by integrating Faraday's law over an area in the $r - z$ plane of axial length L and infinitesimal radial width. The inner radius of this area is at r_- and the outer radius is at r_+ where $r_- < a < r_+$. Integrating Faraday's law over this area gives

$$\lim_{r_- \rightarrow r_+} \int ds \cdot \nabla \times \mathbf{E} = \oint \mathbf{E} \cdot d\mathbf{l} = - \lim_{r_- \rightarrow r_+} \int ds \cdot \frac{\partial \mathbf{B}}{\partial t}$$

or

$$E_z^{vac} L - E_z^{plasma} L = 0$$

showing that E_z must be continuous at the plasma-vacuum interface.

3. Integration of Eq.(7.38) across the interface shows that the quantity

$$P \left(P - k^2 c^2 / \omega^2 \right)^{-1} \partial E_z / \partial r$$

must be continuous across the interface.

In order to satisfy constraint #1 the parallel electric field in the plasma must be

$$E_z(r) = E_z(a) \frac{I_0(\kappa_p r)}{I_0(\kappa_p a)} \quad (7.41)$$

and the parallel electric field in the vacuum must be

$$E_z(r) = E_z(a) \frac{K_0(\kappa_v r)}{K_0(\kappa_v a)}. \quad (7.42)$$

The normalization has been set so that E_z is continuous across the interface as required by constraint #2.

Constraint #3 gives

$$\left[\left(\frac{\omega^2}{c^2} P - k^2 \right)^{-1} P \frac{\partial E_z}{\partial r} \right]_{r=a_-} = \left[\left(\frac{\omega^2}{c^2} - k^2 \right)^{-1} \frac{\partial E_z}{\partial r} \right]_{r=a_+}. \quad (7.43)$$

Inserting Eqs. (7.41) and (7.42) into the respective left and right hand sides of the above expression gives

$$\left(\frac{\omega^2}{c^2} P - k^2 \right)^{-1} P \frac{\kappa_p I_0'(\kappa_p a)}{I_0(\kappa_p a)} = \left(\frac{\omega^2}{c^2} - k^2 \right)^{-1} \frac{\kappa_v K_0'(\kappa_v a)}{K_0(\kappa_v a)} \quad (7.44)$$

where a prime means a derivative with respect to the argument of the function. This expression is effectively a dispersion relation since it prescribes a functional relationship between ω and k . It is qualitatively different from the previously discussed uniform plasma dispersion relations, because of the dependence on the plasma radius a , a physical dimension. This dependence indicates that this mode requires the existence of the plasma-vacuum interface. The mode amplitude is strongest in the vicinity of the interface because both the plasma and vacuum fields decay exponentially on moving away from the interface.

The surface wave dispersion depends on a combination of Bessel functions and the parallel dielectric P . However, a limit exists for which the dispersion relation reduces to a simpler form, and this limit illustrates important features of these surface waves. Specifically, if the axial wavelength is sufficiently short for k^2 to be much larger than both $\omega^2 P / c^2$ and ω^2 / c^2 then it is possible to approximate $k^2 \simeq \kappa_v^2 \simeq \kappa_p^2$ so that the dispersion simplifies to

$$P \frac{I_0'(ka)}{I_0(ka)} \simeq \frac{K_0'(ka)}{K_0(ka)}. \quad (7.45)$$

If, in addition, the axial wavelength is sufficiently long to satisfy $ka \ll 1$, then the small-argument limits of the modified Bessel functions can be used, namely,

$$\lim_{\xi \rightarrow 0} I_0(\xi) = 1 + \frac{\xi^2}{4}, \quad (7.46)$$

$$\lim_{\xi \rightarrow 0} K_0(\xi) = -\ln \xi. \quad (7.47)$$

Thus, in the limit $\omega^2 P/c^2, \omega^2/c^2 \ll k^2 \ll 1/a^2$, Eq.(7.45) simplifies to

$$\left(1 - \frac{\omega_{pe}^2}{\omega^2}\right) \frac{ka}{2} \simeq \frac{1}{ka \ln(ka)}. \quad (7.48)$$

Because $ka \ll 1$, the logarithmic term is negative. Hence, to satisfy Eq.(7.48) it is necessary to have $\omega \ll \omega_{pe}$ so that the dispersion further becomes

$$\frac{\omega}{\omega_{pe}} = ka \sqrt{\frac{1}{2} \ln\left(\frac{1}{ka}\right)}. \quad (7.49)$$

On the other hand, if $ka \gg 1$, then the large argument limit of the Bessel functions can be used, namely,

$$I_0(\xi) = e^\xi, \quad K_0(\xi) = e^{-\xi} \quad (7.50)$$

so that the dispersion relation becomes

$$1 - \frac{\omega_{pe}^2}{\omega^2} = -1 \quad (7.51)$$

or

$$\omega = \frac{\omega_{pe}}{\sqrt{2}}. \quad (7.52)$$

This provides the curious result that a finite-radius plasma cylinder resonates at a lower frequency than a uniform plasma if the axial wavelength is much shorter than the cylinder radius.

These surface waves are slow waves since $\omega/k \ll c$ has been assumed. They were first studied by Trivelpiece and Gould (1959) and are seen in cylindrical plasmas surrounded by vacuum. For $ka \ll 1$ the phase velocity is $\omega/k \sim \mathcal{O}(\omega_{pe}a)$ and for $ka \gg 1$ the phase velocity goes to zero since ω is a constant at large ka . More complicated variations of the surface wave dispersion are obtained if the vacuum region is of finite extent and is surrounded by a conducting wall, i.e., if there is plasma for $r < a$, vacuum for $a < r < b$ and a conducting wall at $r = b$. In this case the vacuum region solution consists of a linear combination of $I_0(\kappa_v r)$ and $K_0(\kappa_v r)$ terms with coefficients chosen to satisfy constraints #2 and #3 discussed earlier and also a new, additional constraint that E_z must vanish at the wall, i.e., at $r = b$.

7.4 Plasma wave-energy equation

The energy associated with a plasma wave is related in a subtle way to the dispersive properties of the wave. Quantifying this relation requires starting from first principles regarding the electromagnetic field energy density and taking into account specific features of dispersive waves. The basic equation characterizing electromagnetic energy density, called Poynting's theorem, is obtained by subtracting \mathbf{B} dotted with Faraday's law from \mathbf{E} dotted with Ampere's law,

$$\mathbf{E} \cdot \nabla \times \mathbf{B} - \mathbf{B} \cdot \nabla \times \mathbf{E} = \mathbf{E} \cdot \left(\mu_0 \mathbf{J} + \epsilon_0 \mu_0 \frac{\partial \mathbf{E}}{\partial t} \right) + \mathbf{B} \cdot \frac{\partial \mathbf{B}}{\partial t}$$

and expressing this result as

$$\frac{\partial w}{\partial t} + \nabla \cdot \mathbf{P} = 0 \quad (7.53)$$

where

$$\frac{\partial w}{\partial t} = \mathbf{E} \cdot \mathbf{J} + \varepsilon_0 \mathbf{E} \cdot \frac{\partial \mathbf{E}}{\partial t} + \frac{1}{\mu_0} \mathbf{B} \cdot \frac{\partial \mathbf{B}}{\partial t} \quad (7.54)$$

and

$$\mathbf{P} = \frac{\mathbf{E} \times \mathbf{B}}{\mu_0} \quad (7.55)$$

is called the Poynting flux. The quantities \mathbf{P} and $\partial w / \partial t$ are respectively interpreted as the electromagnetic energy flux into the system and the rate of change of energy density of the system. The energy density is obtained by time integration and is

$$\begin{aligned} w(t) &= w(t_0) + \int_{t_0}^t dt \left\{ \mathbf{E} \cdot \mathbf{J} + \varepsilon_0 \mathbf{E} \cdot \frac{\partial \mathbf{E}}{\partial t} + \frac{1}{\mu_0} \mathbf{B} \cdot \frac{\partial \mathbf{B}}{\partial t} \right\} \\ &= w(t_0) + \int_{t_0}^t dt \mathbf{E} \cdot \mathbf{J} + \left[\frac{\varepsilon_0}{2} E^2 + \frac{B^2}{2\mu_0} \right]_{t_0}^t \end{aligned} \quad (7.56)$$

where $w(t_0)$ is the energy density at some reference time t_0 .

The quantity $\mathbf{E} \cdot \mathbf{J}$ is the rate of change of kinetic energy density of the particles. This can be seen by first dotting the Lorentz equation with \mathbf{v} to obtain

$$m\mathbf{v} \cdot \frac{d\mathbf{v}}{dt} = q\mathbf{v} \cdot (\mathbf{E} + \mathbf{v} \times \mathbf{B}) \quad (7.57)$$

or

$$\frac{d}{dt} \left(\frac{1}{2} m v^2 \right) = q\mathbf{E} \cdot \mathbf{v}. \quad (7.58)$$

Since this is the rate of change of kinetic energy of a single particle, the rate of change of the kinetic energy density of all the particles, found by summing over all the particles, is

$$\begin{aligned} \frac{d}{dt} (\text{kinetic energy density}) &= \sum_{\sigma} \int d\mathbf{v} f_{\sigma} q_{\sigma} \mathbf{E} \cdot \mathbf{v} \\ &= \sum_{\sigma} n_{\sigma} q_{\sigma} \mathbf{E} \cdot \mathbf{u}_{\sigma} \\ &= \mathbf{E} \cdot \mathbf{J}. \end{aligned} \quad (7.59)$$

This shows that positive $\mathbf{E} \cdot \mathbf{J}$ corresponds to work going into the particles (increase of particle kinetic energy) whereas negative $\mathbf{E} \cdot \mathbf{J}$ corresponds to work coming out of the particles (decrease of the particle kinetic energy). The latter situation is obviously possible only if the particles start with a finite initial kinetic energy. Since $\mathbf{E} \cdot \mathbf{J}$ accounts for changes in the particle kinetic energy density, w must be the sum of the electromagnetic field density and the particle kinetic energy density.

The time integration of Eq.(7.59) must be done with great care if \mathbf{E} and \mathbf{J} are wave fields. This is because writing a wave field as $\psi = \tilde{\psi} \exp(i\mathbf{k} \cdot \mathbf{x} - i\omega t)$ must always be understood as a notational convenience which should never be taken to mean that the actual physical wave field is complex. The physical wave field is always real and so it is always understood that the physically meaningful variable is $\psi = \text{Re} \left[\tilde{\psi} \exp(i\mathbf{k} \cdot \mathbf{x} - i\omega t) \right]$. This

taking of the real part is often not explicitly stated in linear relationships where its omission does not affect the mathematical logic. However, taking the real part is a critical step in nonlinear relationships, because for nonlinear relationships omitting this step causes serious errors. In particular, when dealing with a product of two oscillating physical quantities, say $\psi(t) = \text{Re} [\tilde{\psi}e^{-i\omega t}]$ and $\chi(t) = \text{Re} [\tilde{\chi}e^{-i\omega t}]$, it is essential to write the product as

$$\psi(t)\chi(t) = \text{Re} [\tilde{\psi}e^{-i\omega t}] \times \text{Re} [\tilde{\chi}e^{-i\omega t}]; \quad (7.60)$$

that is the real part of the factors must always be established *before* calculating the product. If $\omega = \omega_r + i\omega_i$ is a complex frequency, then the product in Eq.(7.60) assumes the form

$$\begin{aligned} \psi(t)\chi(t) &= \left(\frac{\tilde{\psi}e^{-i\omega t} + \tilde{\psi}^*e^{i\omega^*t}}{2} \right) \left(\frac{\tilde{\chi}e^{-i\omega t} + \tilde{\chi}^*e^{i\omega^*t}}{2} \right) \\ &= \frac{1}{4} \left[\begin{aligned} &\tilde{\psi}\tilde{\chi}e^{-2i\omega t} + \tilde{\psi}^*\tilde{\chi}^*e^{2i\omega^*t} \\ &+ \tilde{\psi}\tilde{\chi}^*e^{-i(\omega-\omega^*)t} + \tilde{\psi}^*\tilde{\chi}e^{-i(\omega-\omega^*)t} \end{aligned} \right]. \end{aligned} \quad (7.61)$$

When considering the energy density of a wave, we are typically interested in time-average quantities, not rapidly fluctuating quantities. Thus the time average of the product $\psi(t)\chi(t)$ over one wave period will be considered. The $\tilde{\psi}\tilde{\chi}$ and $\tilde{\psi}^*\tilde{\chi}^*$ terms oscillate at the fast second harmonic of the frequency and vanish upon time-averaging. In contrast, the $\tilde{\psi}\tilde{\chi}^*$ and $\tilde{\psi}^*\tilde{\chi}$ terms survive time-averaging because these terms have no oscillatory factor since $\omega - \omega^* = 2i\omega_i$. Thus, the time average (denoted by $\langle \rangle$) of the product is

$$\begin{aligned} \langle \psi(t)\chi(t) \rangle &= \frac{1}{4} (\tilde{\psi}\tilde{\chi}^* + \tilde{\psi}^*\tilde{\chi}) e^{2\omega_i t}; \\ &= \frac{1}{2} \text{Re} (\tilde{\psi}\tilde{\chi}^*) e^{2\omega_i t}; \end{aligned} \quad (7.62)$$

this is the desired rule for time-averaging products of oscillating quantities.

7.5 Cold-plasma wave energy equation

The current density \mathbf{J} in Ampere's law consists of the explicit plasma currents which are frequency-dependent. This frequency dependence means that care is required when integrating $\mathbf{E} \cdot \mathbf{J}$. In order to arrange for this integration we express Eq.(6.9) and Eq.(6.10) as

$$\begin{aligned} \frac{1}{\mu_0} \nabla \times \bar{\mathbf{B}} &= \varepsilon_0 \frac{\partial}{\partial t} \left(\overleftrightarrow{\mathbf{K}}(\omega) \cdot \bar{\mathbf{E}}e^{-i\omega t} \right) \\ &= \bar{\mathbf{J}}e^{-i\omega t} + \varepsilon_0 \frac{\partial}{\partial t} \left(\bar{\mathbf{E}}e^{-i\omega t} \right) \end{aligned} \quad (7.63)$$

where $\bar{\mathbf{J}}$ consists of the plasma currents and the time dependence is shown explicitly.

Integration of Eq.(7.56) taking into account the prescription given by Eq.(7.60) has the form

$$\begin{aligned}
 w(t) &= w(-\infty) + \int_{-\infty}^t dt \left\langle \mathbf{E}(\mathbf{x},t) \cdot \left(\mathbf{J}(\mathbf{x},t) + \varepsilon_0 \frac{\partial \mathbf{E}(\mathbf{x},t)}{\partial t} \right) \right. \\
 &\quad \left. + \frac{1}{\mu_0} \mathbf{B}(\mathbf{x},t) \cdot \frac{\partial \mathbf{B}(\mathbf{x},t)}{\partial t} \right\rangle \\
 &= w(-\infty) + \frac{1}{4} \int_{-\infty}^t dt \left\langle \frac{\bar{\mathbf{E}} e^{-i\omega t} \cdot \varepsilon_0 \frac{\partial}{\partial t} \left(\overleftrightarrow{\mathbf{K}}(\omega) \cdot \bar{\mathbf{E}} e^{-i\omega t} \right)^*}{+ \frac{1}{\mu_0} \bar{\mathbf{B}} e^{-i\omega t} \cdot \frac{\partial}{\partial t} \left(\bar{\mathbf{B}} e^{-i\omega t} \right)^* + \text{c.c.}} \right\rangle \quad (7.64)
 \end{aligned}$$

where c.c. means complex conjugate. The term containing the rates of change of the electric field and the particle kinetic energy can be written as

$$\begin{aligned}
 \left\langle \mathbf{E} \cdot \left(\mathbf{J} + \varepsilon_0 \frac{\partial \mathbf{E}}{\partial t} \right) \right\rangle &= \frac{\varepsilon_0}{4} \left\{ \bar{\mathbf{E}} e^{-i\omega t} \cdot \left(i\omega^* \overleftrightarrow{\mathbf{K}}^* \cdot \bar{\mathbf{E}}^* e^{i\omega^* t} \right) + \text{c.c.} \right\} \\
 &= \frac{\varepsilon_0}{4} \left\{ \bar{\mathbf{E}} \cdot i\omega^* \overleftrightarrow{\mathbf{K}}^* \cdot \bar{\mathbf{E}}^* - \bar{\mathbf{E}}^* \cdot i\omega \overleftrightarrow{\mathbf{K}} \cdot \bar{\mathbf{E}} \right\} e^{2\omega_i t} \\
 &= \frac{\varepsilon_0}{4} \left\{ \begin{array}{l} i\omega_r \left[\bar{\mathbf{E}} \cdot \overleftrightarrow{\mathbf{K}}^* \cdot \bar{\mathbf{E}}^* - \bar{\mathbf{E}}^* \cdot \overleftrightarrow{\mathbf{K}} \cdot \bar{\mathbf{E}} \right] \\ + \omega_i \left[\bar{\mathbf{E}} \cdot \overleftrightarrow{\mathbf{K}}^* \cdot \bar{\mathbf{E}}^* + \bar{\mathbf{E}}^* \cdot \overleftrightarrow{\mathbf{K}} \cdot \bar{\mathbf{E}} \right] \end{array} \right\} e^{2\omega_i t}. \quad (7.65)
 \end{aligned}$$

To proceed further it is noted that

$$\bar{\mathbf{E}} \cdot \overleftrightarrow{\mathbf{K}}^* \bar{\mathbf{E}}^* = \sum_{pq} \tilde{E}_p K_{pq}^* \tilde{E}_q^* = \sum_{pq} \tilde{E}_p K_{qp}^{*t} \tilde{E}_q^* = \bar{\mathbf{E}}^* \cdot \overleftrightarrow{\mathbf{K}}^\dagger \cdot \bar{\mathbf{E}} \quad (7.66)$$

where the superscript t means transpose and the dagger superscript \dagger means Hermitian conjugate, i.e., the complex conjugate of the transpose. Thus, Eq.(7.65) can be re-written as

$$\left\langle \mathbf{E} \cdot \left(\mathbf{J} + \varepsilon_0 \frac{\partial \mathbf{E}}{\partial t} \right) \right\rangle = \frac{\varepsilon_0}{4} \left[i\omega_r \bar{\mathbf{E}}^* \cdot \left(\overleftrightarrow{\mathbf{K}}^\dagger - \overleftrightarrow{\mathbf{K}} \right) \cdot \bar{\mathbf{E}} + \omega_i \bar{\mathbf{E}}^* \cdot \left(\overleftrightarrow{\mathbf{K}}^\dagger + \overleftrightarrow{\mathbf{K}} \right) \cdot \bar{\mathbf{E}} \right] e^{2\omega_i t}. \quad (7.67)$$

Both the Hermitian part of the dielectric tensor,

$$\overleftrightarrow{\mathbf{K}}_h = \frac{1}{2} \left(\overleftrightarrow{\mathbf{K}} + \overleftrightarrow{\mathbf{K}}^\dagger \right), \quad (7.68)$$

and the anti-Hermitian part,

$$\overleftrightarrow{\mathbf{K}}_{ah} = \frac{1}{2} \left(\overleftrightarrow{\mathbf{K}} - \overleftrightarrow{\mathbf{K}}^\dagger \right), \quad (7.69)$$

occur in Eq. (7.67). The cold plasma dielectric tensor is a function of ω via the functions S , P , and D ,

$$\overleftrightarrow{\mathbf{K}}(\omega) = \begin{bmatrix} S(\omega) & -iD(\omega) & 0 \\ iD(\omega) & S(\omega) & 0 \\ 0 & 0 & P(\omega) \end{bmatrix}. \quad (7.70)$$

If $\omega_i = 0$ then S , P , and D are all pure real. In this case $\overleftrightarrow{\mathbf{K}}(\omega)$ is Hermitian so that $\overleftrightarrow{\mathbf{K}}_h = \overleftrightarrow{\mathbf{K}}$ and $\overleftrightarrow{\mathbf{K}}_{ah} = 0$. However, if ω_i is finite but small, then $\overleftrightarrow{\mathbf{K}}(\omega)$ will have a small non-Hermitian part. This non-Hermitian part is extracted using a Taylor expansion in terms of ω_i , i.e.,

$$\overleftrightarrow{\mathbf{K}}(\omega_r + i\omega_i) = \overleftrightarrow{\mathbf{K}}(\omega_r) + i\omega_i \left[\frac{\partial}{\partial \omega} \overleftrightarrow{\mathbf{K}}(\omega) \right]_{\omega=\omega_r}. \quad (7.71)$$

The transpose of the complex conjugate of this expansion is

$$\left[\overleftrightarrow{\mathbf{K}}(\omega_r + i\omega_i) \right]^\dagger = \overleftrightarrow{\mathbf{K}}(\omega_r) - i\omega_i \left[\frac{\partial}{\partial \omega} \overleftrightarrow{\mathbf{K}}(\omega) \right]_{\omega=\omega_r} \quad (7.72)$$

since $\overleftrightarrow{\mathbf{K}}$ is non-Hermitian only to the extent that ω_i is finite. Substituting Eqs.(7.71) and (7.72) into Eqs.(7.68) and (7.69) and assuming small ω_i gives

$$\overleftrightarrow{\mathbf{K}}_h = \overleftrightarrow{\mathbf{K}}(\omega_r) \quad (7.73)$$

and

$$\overleftrightarrow{\mathbf{K}}_{ah} = i\omega_i \left[\frac{\partial}{\partial \omega} \overleftrightarrow{\mathbf{K}}(\omega) \right]_{\omega=\omega_r}. \quad (7.74)$$

Inserting Eqs. (7.73) and (7.74) in Eq.(7.67) yields

$$\begin{aligned} \left\langle \mathbf{E} \cdot \left(\mathbf{J} + \varepsilon_0 \frac{\partial \mathbf{E}}{\partial t} \right) \right\rangle &= \frac{2\varepsilon_0 \omega_i}{4} \left[\omega_r \bar{\mathbf{E}}^* \cdot \left[\frac{\partial}{\partial \omega} \overleftrightarrow{\mathbf{K}}(\omega) \right]_{\omega=\omega_r} \cdot \bar{\mathbf{E}} + \bar{\mathbf{E}}^* \cdot \overleftrightarrow{\mathbf{K}}(\omega_r) \cdot \bar{\mathbf{E}} \right] e^{2\omega_i t} \\ &= \frac{2\varepsilon_0 \omega_i}{4} \bar{\mathbf{E}}^* \cdot \left[\frac{\partial}{\partial \omega} \omega \overleftrightarrow{\mathbf{K}}(\omega) \right]_{\omega=\omega_r} \cdot \bar{\mathbf{E}} e^{2\omega_i t}. \end{aligned} \quad (7.75)$$

Similarly, the rate of change of the magnetic energy density is

$$\left\langle \frac{1}{\mu_0} \mathbf{B} \cdot \frac{\partial \mathbf{B}}{\partial t} \right\rangle = \frac{1}{4\mu_0} \left[2\omega_i \bar{\mathbf{B}}^* \cdot \bar{\mathbf{B}} \right] e^{2\omega_i t}. \quad (7.76)$$

Using Eqs.(7.75) and (7.76) in Eq.(7.64) gives

$$w = w(-\infty) + \left\{ \frac{\varepsilon_0}{4} \bar{\mathbf{E}}^* \cdot \left[\frac{\partial}{\partial \omega} \left(\omega \overleftrightarrow{\mathbf{K}}(\omega) \right) \right]_{\omega=\omega_r} \cdot \bar{\mathbf{E}} + \frac{1}{4\mu_0} \left[\bar{\mathbf{B}}^* \cdot \bar{\mathbf{B}} \right] \right\} \int_{-\infty}^t dt 2\omega_i e^{2\omega_i t} \quad (7.77)$$

which now may be integrated in time to give the total energy density *associated with bringing the wave into existence*

$$\begin{aligned} \bar{w} &= w - w(-\infty) \\ &= \left\{ \frac{\varepsilon_0}{4} \bar{\mathbf{E}}^* \cdot \left[\frac{\partial}{\partial \omega} \left(\omega \overleftrightarrow{\mathbf{K}}(\omega) \right) \right]_{\omega=\omega_r} \cdot \bar{\mathbf{E}} + \frac{1}{4\mu_0} \left[\bar{\mathbf{B}}^* \cdot \bar{\mathbf{B}} \right] \right\} e^{2\omega_i t}. \end{aligned} \quad (7.78)$$

In the limit $\omega_i \rightarrow 0$ this reduces to

$$\bar{w} = \frac{\varepsilon_0}{4} \bar{\mathbf{E}}^* \cdot \frac{\partial}{\partial \omega} \left[\omega \overleftrightarrow{\mathbf{K}}(\omega) \right] \cdot \bar{\mathbf{E}} + \frac{|\bar{B}|^2}{4\mu_0}. \quad (7.79)$$

Since the energy density stored in the vacuum electric field is

$$w_E = \frac{\varepsilon_0 |\tilde{E}|^2}{4} \quad (7.80)$$

and the energy density stored in the vacuum magnetic field is

$$w_B = \frac{|\tilde{B}|^2}{4\mu_0} \quad (7.81)$$

the change in particle kinetic energy density associated with bringing the wave into existence is

$$\bar{w}_{part} = \frac{\varepsilon_0}{4} \tilde{\mathbf{E}}^* \cdot \left[\frac{\partial}{\partial \omega} \left(\omega \overleftrightarrow{\mathbf{K}}(\omega) \right) - \overleftrightarrow{\mathbf{I}} \right] \cdot \tilde{\mathbf{E}}. \quad (7.82)$$

Although this result has been established for the general case of the dielectric tensor $\overleftrightarrow{\mathbf{K}}(\omega)$ of a cold magnetized plasma, in order to appreciate its meaning it is useful to consider the simple example of high frequency electrostatic oscillations in an unmagnetized plasma. In this simplest case $S = P = 1 - \omega_{pe}^2/\omega^2$ and $D = 0$ so that $\overleftrightarrow{\mathbf{K}}(\omega) = (1 - \omega_{pe}^2/\omega^2) \overleftrightarrow{\mathbf{I}}$. Since the oscillations are electrostatic, $w_B = 0$. The energy density of the particles is therefore

$$\begin{aligned} \bar{w}_{part} &= \frac{\varepsilon_0 |\tilde{E}|^2}{4} \left[\frac{\partial}{\partial \omega} \left\{ \omega \left(1 - \frac{\omega_{pe}^2}{\omega^2} \right) \right\} - 1 \right] \\ &= \frac{\varepsilon_0 |\tilde{E}|^2}{4} \left[2 \frac{\omega_{pe}^2}{\omega^2} - 1 \right] \\ &= \frac{\varepsilon_0 |\tilde{E}|^2}{4} \end{aligned} \quad (7.83)$$

where the dispersion relation $1 - \omega_{pe}^2/\omega^2 = 0$ has been used. Thus, for this simple case, half of the average wave energy density is contained in the electric field while the other half is contained in the coherent particle motion associated with the wave.

7.6 Finite-temperature plasma wave energy equation

The dielectric tensor does not depend on the wavevector \mathbf{k} in a cold plasma, but does in a finite temperature plasma. For example, the electrostatic unmagnetized cold plasma dielectric $P(\omega) = 1 - \omega_{pe}^2/\omega^2$ becomes $P(\omega, k) = 1 - (1 + 3k^2 \lambda_{De}^2) \omega_{pe}^2/\omega^2$ in a warm plasma. The analysis of the previous section will now be generalized to allow for the possibility that the dielectric tensor depends on \mathbf{k} as well as on ω . In analogy to the method used in the previous section for treating complex ω , here \mathbf{k} will also be assumed to have a small imaginary part. In this case, Taylor expansion of the dielectric tensor and then extracting the anti-Hermitian part shows that the anti-Hermitian part is

$$\overleftrightarrow{\mathbf{K}}_{ah} = i\omega_i \left[\frac{\partial}{\partial \omega} \overleftrightarrow{\mathbf{K}}(\omega, \mathbf{k}) \right]_{\omega=\omega_r, \mathbf{k}=\mathbf{k}_r} + i\mathbf{k}_i \cdot \left[\frac{\partial}{\partial \mathbf{k}} \overleftrightarrow{\mathbf{K}}(\omega, \mathbf{k}) \right]_{\omega=\omega_r, \mathbf{k}=\mathbf{k}_r} \quad (7.84)$$

while the Hermitian part remains the same. There is now a new term involving \mathbf{k}_i . With the incorporation of this new term, Eq.(7.75) becomes

$$\left\langle \mathbf{E} \cdot \left(\mathbf{J} + \varepsilon_0 \frac{\partial \mathbf{E}}{\partial t} \right) \right\rangle = \left[\begin{array}{l} \frac{2\varepsilon_0\omega_i}{4} \bar{\mathbf{E}}^* \cdot \left[\frac{\partial}{\partial \omega} \omega \overleftrightarrow{\mathbf{K}}(\omega) \right]_{\omega=\omega_r} \cdot \bar{\mathbf{E}} + \\ \frac{\varepsilon_0}{4} \bar{\mathbf{E}}^* \cdot \left[2\omega \mathbf{k}_i \cdot \frac{\partial}{\partial \mathbf{k}} \overleftrightarrow{\mathbf{K}}(\omega, \mathbf{k}) \right]_{\substack{\omega=\omega_r, \\ \mathbf{k}=\mathbf{k}_r}} \cdot \bar{\mathbf{E}} \end{array} \right] e^{-2\mathbf{k}_i \cdot \mathbf{x} + 2\omega_i t} \quad (7.85)$$

where we have explicitly written the exponential space-dependent factor $\exp(-2\mathbf{k}_i \cdot \mathbf{x})$.

What is the meaning of this new term involving \mathbf{k}_i ? The answer to this question may be found by examining the Poynting flux for the situation where \mathbf{k}_i is finite. Using the product rule to allow for finite \mathbf{k}_i shows that

$$\begin{aligned} \langle \nabla \cdot \mathbf{P} \rangle &= \langle \nabla \cdot (\mathbf{E} \times \mathbf{H}) \rangle \\ &= \frac{1}{4} \nabla \cdot \left[(\bar{\mathbf{E}}^* \times \bar{\mathbf{H}} + \bar{\mathbf{E}} \times \bar{\mathbf{H}}^*) e^{-2\mathbf{k}_i \cdot \mathbf{x} + 2\omega_i t} \right] \\ &= \frac{1}{4} (-2\mathbf{k}_i \cdot (\bar{\mathbf{E}}^* \times \bar{\mathbf{H}} + \bar{\mathbf{E}} \times \bar{\mathbf{H}}^*)) e^{-2\mathbf{k}_i \cdot \mathbf{x} + 2\omega_i t}. \end{aligned} \quad (7.86)$$

Comparison of Eqs.(7.85) and (7.86) show that the factor $-2\mathbf{k}_i \cdot$ acts as a divergence and so the second term in Eq.(7.85) represents an *energy flux*. Since the Poynting vector \mathbf{P} is the energy flux associated with the electromagnetic field, this additional energy flux must be identified as the energy flux associated with particle motion due to the wave. Defining this flux as \mathbf{T} it is seen that

$$T_j = -\frac{\omega \varepsilon_0}{4} \bar{\mathbf{E}}^* \cdot \left[\frac{\partial}{\partial k_j} \overleftrightarrow{\mathbf{K}}(\omega, \mathbf{k}) \right] \cdot \bar{\mathbf{E}} \quad (7.87)$$

in the limit $\mathbf{k}_i \rightarrow 0$. For small but finite \mathbf{k}_i, ω_i the generalized Poynting theorem can be written as

$$-2\mathbf{k}_i \cdot (\mathbf{P} + \mathbf{T}) + 2\omega_i (w_E + w_B + \bar{w}_{part}) = 0. \quad (7.88)$$

We now define the generalized group velocity \mathbf{v}_g to be the velocity with which wave energy is transported. This velocity is the total energy flux divided by the total energy density, i.e.,

$$\mathbf{v}_g = \frac{\mathbf{P} + \mathbf{T}}{w_E + w_B + \bar{w}_{part}}. \quad (7.89)$$

The bar in the particle energy represents the fact that this is the difference between the particle energy with the wave and the particle energy without the wave and it should be recalled that this difference can be negative.

7.7 Negative energy waves

A curious consequence of this analysis is that a wave can have a *negative* energy density. While the field energy densities w_E and w_B are positive definite, the particle energy density \bar{w}_{part} can have either sign and in certain circumstances can be sufficiently negative to make the total wave energy density negative. This surprising possibility can occur because, as was shown in Eq.(7.78), the wave energy density is actually the *change* in the

total system energy density in going from a situation where there is no wave to a situation where there is a wave. Typically, negative energy waves occur when the equilibrium has a steady-state flow velocity and there exists a mode which causes the particles to develop a slower mean velocity than in steady state. Wave growth taps free energy from the flow.

As an example of a negative energy wave, we consider the situation where unmagnetized cold electrons stream with velocity v_0 through a background of infinitely massive ions. As shown earlier, the electrostatic dispersion for this simple 1D situation with flow involves a parallel dielectric involving a Doppler shifted frequency, i.e., the dispersion relation is

$$P(\omega, k) = 1 - \frac{\omega_{pe}^2}{(\omega - kv_0)^2} = 0. \quad (7.90)$$

Since the plasma is unmagnetized, its dielectric tensor is simply $\overleftrightarrow{\mathbf{K}}(\omega, \mathbf{k}) = P(\omega, k) \overleftrightarrow{\mathbf{I}}$. Using Eq.(7.79), the wave energy density is

$$w = \frac{\varepsilon_0 |E|^2}{4} \frac{\partial}{\partial \omega} (\omega P(\omega, k)) = \frac{\varepsilon_0 |E|^2}{2} \frac{\omega \omega_{pe}^2}{(\omega - kv_0)^3}. \quad (7.91)$$

However, the dispersion relation, Eq.(7.90), shows that

$$\omega = kv_0 \pm \omega_{pe} \quad (7.92)$$

so that Eq.(7.91) can be recast as

$$w = \frac{\varepsilon_0 |E|^2}{2} \left(1 \pm \frac{kv_0}{\omega_{pe}} \right). \quad (7.93)$$

Thus, if $kv_0 > \omega_{pe}$ and the minus sign is selected, the wave has *negative* energy density.

This result can be verified by direct calculation of the change in system energy density due to growth of the wave. When there is no wave, the electric field is zero and the system energy density w^{sys} is simply the beam kinetic energy density

$$w_0^{sys} = \frac{1}{2} n_0 m_e v_0^2. \quad (7.94)$$

Now consider a one dimensional electrostatic wave with electric field $E = \text{Re}(\tilde{E} e^{ikx - i\omega t})$. The system average energy density with this wave is

$$w_{wave}^{sys} = \frac{\varepsilon_0 |\tilde{E}|^2}{4} + \left\langle \frac{1}{2} n(x, t) m_e v(x, t)^2 \right\rangle \quad (7.95)$$

so that the change in system energy density due to the wave is

$$\bar{w}^{sys} = w_{wave}^{sys} - w_0^{sys} = \frac{\varepsilon_0 |\tilde{E}|^2}{4} + \left\langle \frac{1}{2} [n_0 + n_1(x, t)] m_e [v_0 + v_1(x, t)]^2 \right\rangle - \frac{1}{2} n_0 m_e v_0^2 \quad (7.96)$$

where

$$n_1(x, t) = \text{Re}(\tilde{n} e^{ikx - i\omega t}), \quad v_1(x, t) = \text{Re}(\tilde{v} e^{ikx - i\omega t}). \quad (7.97)$$

Since odd powers of oscillating quantities vanish upon time averaging, Eq.(7.96) becomes

$$\begin{aligned}\bar{w}^{sys} &= \frac{\varepsilon_0 |\tilde{E}|^2}{4} + n_0 m_e \left\langle \frac{1}{2} v_1^2 + \frac{n_1}{n_0} v_1 v_0 \right\rangle \\ &= \frac{\varepsilon_0 |\tilde{E}|^2}{4} + \frac{1}{2} n_0 m_e \langle v_1^2 \rangle + m_e v_0 \langle n_1 v_1 \rangle.\end{aligned}\quad (7.98)$$

The linearized continuity equation gives

$$-i(\omega - kv_0)\tilde{n} + n_0 ik\tilde{v} = 0 \quad (7.99)$$

or

$$\frac{\tilde{n}}{n_0} = \frac{k\tilde{v}}{\omega - kv_0}.\quad (7.100)$$

The fluid quiver velocity in the wave is

$$\tilde{v} = \frac{q\tilde{E}}{-i(\omega - kv_0)m_e} \quad (7.101)$$

so that

$$\langle v_1^2 \rangle = \frac{1}{2} \frac{q^2 E^2}{(\omega - kv_0)^2 m_e^2} \quad (7.102)$$

and

$$\langle n_1 v_1 \rangle = \frac{k}{2} \frac{n_0 q^2 E^2}{(\omega - kv_0)^3 m_e^2}.\quad (7.103)$$

We may now evaluate Eq.(7.98) to obtain

$$\begin{aligned}\bar{w}^{sys} &= \frac{\varepsilon_0 |\tilde{E}|^2}{4} + n_0 m_e \left[\frac{q^2 E^2}{4(\omega - kv_0)^2 m_e^2} + \frac{kv_0}{2} \frac{q^2 E^2}{(\omega - kv_0)^3 m_e^2} \right] \\ &= \frac{\varepsilon_0 |\tilde{E}|^2}{4} \left[1 + \frac{\omega_{pe}^2}{(\omega - kv_0)^2} + \frac{2\omega_{pe}^2 kv_0}{(\omega - kv_0)^3} \right] \\ &= \frac{\varepsilon_0 |\tilde{E}|^2}{2} \left[1 \pm \frac{kv_0}{\omega_{pe}} \right]\end{aligned}\quad (7.104)$$

where Eq.(7.92) has been invoked repeatedly. This is the same as Eq. (7.93). The energy flux associated with this wave shows is also negative (cf. assignments). However, the group velocity is positive (cf. assignments) because the group velocity is the ratio of a negative energy flux to a negative energy density.

Dissipation acts on negative energy waves in a manner opposite to the way it acts on positive energy waves. This can be seen by Taylor-expanding the dispersion relation $P(\omega, k) = 0$ as done in Eq.(5.83)

$$\omega_i = -\frac{P_i}{[\partial P_r / \partial \omega]_{\omega=\omega_r}}.\quad (7.105)$$

Expanding Eq.(7.91) gives

$$\bar{w} = \frac{\varepsilon_0 \omega |E|^2}{4} \frac{\partial P}{\partial \omega} \quad (7.106)$$

so a negative energy wave has $\omega \partial P / \partial \omega < 0$. If the dissipative term P_i is the same for both positive and negative waves, then for a given sign of ω , the critical difference between positive and negative waves is due to the sign of $\partial P / \partial \omega$. Equation (7.105) shows that ω_i will have opposite signs for positive and negative energy waves. Hence, dissipation tends to drive negative energy waves unstable. Since there is usually some dissipation in any real system, a negative energy wave will generally spontaneously develop if it is an allowable mode and will grow at the expense of the free energy in the system (e.g., the free energy in the streaming particles).

7.8 Assignments

1. Consider the problem of short wave radio transmission. Let x be the horizontal direction and z be the vertical direction. A short wave radio antenna is designed in such a way that it radiates most of the transmitter power into a specified k_x and k_z at the antenna. This is determined essentially by the Fourier transform of the antenna geometry.
 - (i) What is the frequency range of short wave radio communications?
 - (ii) For ionospheric parameters, and the majority of the short wave band should the ionospheric plasma be considered magnetized or unmagnetized?
 - (iii) What is the appropriate dispersion for short wave radio waves (hint-it is very simple)
 - (iv) Using Snell's law and geometric optics, sketch the trajectory of a radio wave showing what happens at the ionosphere.
2. Using geometric optics discuss qualitatively with sketches how a low frequency wave could act as a lens for a high frequency wave.
3. For the example of an electrostatic electron plasma wave [dispersion $\omega^2 = \omega_{pe}^2 (1 + 3k^2 \lambda_{de}^2)$] show that the generalized group velocity as defined in Eq.(7.89) gives the same group velocity as found using the previous definition based on $\partial \omega / \partial \mathbf{k}$.
4. Calculate the wave energy density, wave energy flux, and group velocity for the electrostatic wave that can exist when a beam of cold electrons having velocity \mathbf{v}_0 streams through a neutralizing background of infinitely massive ions. Discuss the signs of these three quantities.

Vlasov theory of warm electrostatic waves in a magnetized plasma

8.1 Uniform plasma

It has been tacitly assumed until now that the wave phase experienced by a particle is just what would have been experienced if the particle had not deviated from its initial position \mathbf{x}_0 . This means that the particle trajectory used when determining the wave phase experienced by the particle is $\mathbf{x} = \mathbf{x}_0$ instead of the actual trajectory $\mathbf{x} = \mathbf{x}(t)$. Thus the wave phase seen by the particle was approximated as

$$\mathbf{k} \cdot \mathbf{x}(t) - \omega t = \mathbf{k} \cdot \mathbf{x}_0 - \omega t. \quad (8.1)$$

This approximation is fine provided the deviation of the actual trajectory from the assumed trajectory satisfies the condition

$$|\mathbf{k} \cdot (\mathbf{x}(t) - \mathbf{x}_0)| \ll \pi/2 \quad (8.2)$$

so any phase error due to the deviation is insignificant. Two situations exist where this assumption fails:

1. the wave amplitude is so large that the particle displacement due to the wave is significant compared to a wavelength,
2. the wave amplitude is small, but the particle has a large initial velocity so that it moves substantially during one wave period.

The first case results in chaotic particle motion as discussed in Sec.3.7.3 while the second case, the subject of this chapter, occurs when the particles have significant thermal motion. If the motion is parallel to the magnetic field, significant thermal motion means that v_T is non-negligible compared to ω/k_{\parallel} , a regime already discussed in Sec.5.2 for unmagnetized plasmas. Thermal motion in the perpendicular direction becomes an issue when $k_{\perp} r_L \sim \pi/2$, i.e., when the Larmor orbit r_L becomes comparable to the wavelength. In this situation, the particle samples different phases of the wave as the particle traces out its Larmor orbit. The subscript \parallel is used here to denote the direction along the magnetic field. If the magnetic field is straight and given by $\mathbf{B} = B\hat{z}$, \parallel would simply be the z direction, but in a more general situation the \parallel component of a vector would be obtained by dotting the vector with \hat{B} .

Consider an electrostatic wave with potential

$$\phi_1(\mathbf{x}, t) = \tilde{\phi}_1 \exp(i\mathbf{k} \cdot \mathbf{x} - i\omega t). \quad (8.3)$$

As before the convention will be used that a tilde refers to the amplitude of a perturbed quantity; if there is no tilde, then the exponential phase factor is understood to be included. Because the wave is electrostatic, Poisson's equation is the relevant Maxwell's equation relating particle motion to fields, i.e.,

$$k^2 \phi_1 = \frac{1}{\varepsilon_0} \sum_{\sigma} n_{\sigma 1} q_{\sigma} \quad (8.4)$$

where $n_{\sigma 1}$ is the density perturbation for each species σ . Since the density perturbation is just the zeroth moment of the perturbed distribution function,

$$n_{\sigma 1} = \int f_{\sigma 1} d^3v, \quad (8.5)$$

the problem reduces to determining the perturbed distribution function $f_{\sigma 1}$.

In the presence of a uniform magnetic field the linearized Vlasov equation is

$$\frac{\partial f_{\sigma 1}}{\partial t} + \mathbf{v} \cdot \frac{\partial f_{\sigma 1}}{\partial \mathbf{x}} + \frac{q_{\sigma}}{m_{\sigma}} (\mathbf{v} \times \mathbf{B}) \cdot \frac{\partial f_{\sigma 1}}{\partial \mathbf{v}} = \frac{q_{\sigma}}{m_{\sigma}} \nabla \phi_1 \cdot \frac{\partial f_{\sigma 0}}{\partial \mathbf{v}} \quad (8.6)$$

where the subscript 0 refers to equilibrium quantities and the subscript 1 to first-order perturbations (no 0 has been used for the magnetic field, because the wave has been assumed to be electrostatic and so does not have any perturbed magnetic field, thus \mathbf{B} is the equilibrium magnetic field).

Consider an arbitrary point \mathbf{x}, \mathbf{v} in phase space at time t . All particles at this point \mathbf{x}, \mathbf{v} at time t have identical phase-space trajectories in both the future and the past because the particles are subject to the same forces and have the same temporal initial condition. By integrating the equation of motion starting from this point in phase space, the phase-space trajectory $\mathbf{x}(t'), \mathbf{v}(t')$ can be determined. The boundary conditions on such a phase-space trajectory are simply

$$\mathbf{x}(t) = \mathbf{x}, \quad \mathbf{v}(t) = \mathbf{v}. \quad (8.7)$$

Instead of treating \mathbf{x}, \mathbf{v} as independent variables denoting a point in phase space, let us think of these quantities as temporal boundary conditions for particles with phase-space trajectories $\mathbf{x}(t), \mathbf{v}(t)$ that happen to be at location \mathbf{x}, \mathbf{v} at time t . Thus, the velocity distribution function for all particles that happen to be at phase-space location \mathbf{x}, \mathbf{v} at time t is $f_{\sigma 1} = f_{\sigma 1}(\mathbf{x}(t), \mathbf{v}(t), t)$ and since \mathbf{x} and \mathbf{v} were arbitrary, this expression is valid for all particles. The time derivative of this function is

$$\frac{d}{dt} f_{\sigma 1}(\mathbf{x}(t), \mathbf{v}(t), t) = \frac{\partial f_{\sigma 1}}{\partial t} + \frac{\partial f_{\sigma 1}}{\partial \mathbf{x}} \cdot \frac{d\mathbf{x}}{dt} + \frac{\partial f_{\sigma 1}}{\partial \mathbf{v}} \cdot \frac{d\mathbf{v}}{dt}. \quad (8.8)$$

In principle, one ought to take into account the wave force on the particles when calculating their trajectories. However, if the wave amplitude is small enough, the particle trajectory will not be significantly affected by the wave and so will be essentially the same as the unperturbed trajectory, namely the trajectory the particle would have had if there were no wave. Since the unperturbed particle trajectory equations are

$$\frac{d\mathbf{x}}{dt} = \mathbf{v}, \quad \frac{d\mathbf{v}}{dt} = \frac{q_{\sigma}}{m_{\sigma}} (\mathbf{v} \times \mathbf{B}) \quad (8.9)$$

it is seen that Eq.(8.8) is identical to the left hand side of Eq.(8.6). Equation (8.6) can thus be rewritten as

$$\left(\frac{d}{dt} f_{\sigma 1}(\mathbf{x}(t), \mathbf{v}(t), t) \right)_{\text{unperturbed trajectory}} = \frac{q_{\sigma}}{m_{\sigma}} \nabla \phi_1 \cdot \frac{\partial f_{\sigma 0}}{\partial \mathbf{v}} \quad (8.10)$$

where the left hand side is the derivative of the distribution function that would be measured by an observer sitting on a particle having the *unperturbed* phase-space trajectory $\mathbf{x}(t), \mathbf{v}(t)$. Equation (8.10) may be integrated to give

$$f_{\sigma 1}(\mathbf{x}, \mathbf{v}, t) = \frac{q_{\sigma}}{m_{\sigma}} \int_{-\infty}^t dt' \left[\nabla \phi_1 \cdot \frac{\partial f_{\sigma 0}}{\partial \mathbf{v}} \right]_{\mathbf{x}=\mathbf{x}(t'), \mathbf{v}=\mathbf{v}(t')}. \quad (8.11)$$

If the right hand side of Eq.(8.10) is considered as a ‘force’ acting to change the perturbed distribution function, then Eq.(8.11) is effectively a statement that the perturbed distribution function at \mathbf{x}, \mathbf{v} for time t is a result of the sum of all the ‘forces’ acting over times prior to t calculated along the unperturbed trajectory of the particle. “Unperturbed trajectories” refers to the solution to Eqs.(8.9); these equations neglect any wave-induced changes to the particle trajectory and simply give the trajectory of a thermal particle. The ‘force’ in Eq.(8.11) must be evaluated along the *past* phase-space trajectory because *that* is where the particles at \mathbf{x}, \mathbf{v} were located at previous times and so that is where the particles ‘felt’ the ‘force’. This is called “integrating along the *unperturbed* orbits” and is only valid when the unperturbed orbits (trajectories) are a good approximation to the particles’ actual orbits. Mathematically speaking, these unperturbed orbits are the characteristics of the left hand side of Eq.(8.6), a homogeneous hyperbolic partial differential equation. The solutions of this homogeneous equation are constant along the characteristics. The right hand side is the inhomogeneous or forcing term and acts to modify the homogeneous solution; the cumulative effect of this force is found by integrating along the characteristics of the homogeneous part.

The problem is now formally solved; all that is required is an explicit evaluation of the integrals. The functional form of the equilibrium distribution function is determined by the specific physical problem under consideration. Often the plasma has a uniform Maxwellian distribution

$$f_{\sigma 0}(\mathbf{v}) = \frac{n_{\sigma 0}}{\pi^{3/2} v_{T\sigma}^3} e^{-v^2/v_{T\sigma}^2} \quad (8.12)$$

where

$$v_{T\sigma} = \sqrt{2\kappa T_{\sigma}/m_{\sigma}}. \quad (8.13)$$

It must be understood that Eq.(8.12) represents one of an infinity of possible choices for the equilibrium distribution function — *any* other function of the constants of the motion would also be valid. In fact, functions differing from Eq.(8.12) will later be used to model drifting plasmas and plasmas with density gradients.

Substitution of Eq.(8.12) into the orbit integral gives

$$f_{\sigma 1}(\mathbf{x}, \mathbf{v}, t) = -\frac{2n_{\sigma 0}q_{\sigma}\tilde{\phi}_1}{\pi^{3/2}m_{\sigma}v_{T\sigma}^3} \exp[-v^2/v_{T\sigma}^2] \times \int_{-\infty}^t dt' \left\{ \frac{\mathbf{ik} \cdot \mathbf{v}(t')}{v_{T\sigma}^2} \exp[\mathbf{ik} \cdot \mathbf{x}(t') - i\omega t'] \right\}. \quad (8.14)$$

Since the kinetic energy $mv^2/2$ of the unperturbed orbits is a constant of the motion, the quantity $\exp[-v^2/v_{T\sigma}^2]$ has been factored out of the time integral. This orbit integral may be simplified by noting

$$\frac{d}{dt'} \exp[\mathbf{ik} \cdot \mathbf{x}(t')] = \mathbf{ik} \cdot \mathbf{v}(t') \exp[\mathbf{ik} \cdot \mathbf{x}(t')] \quad (8.15)$$

so that Eq.(8.14) becomes

$$\begin{aligned} f_{\sigma 1}(\mathbf{x}, \mathbf{v}, t) &= -\frac{q_\sigma}{\kappa T_\sigma} \tilde{\phi}_1 f_{\sigma 0} \int_{-\infty}^t dt' \left\{ \exp[-i\omega t'] \frac{d}{dt'} \exp[\mathbf{ik} \cdot \mathbf{x}(t')] \right\} \\ &= -\frac{q_\sigma}{\kappa T_\sigma} \tilde{\phi}_1 f_{\sigma 0} \left\{ [\exp(\mathbf{ik} \cdot \mathbf{x}(t') - i\omega t')]_{-\infty}^t + i\omega I_{phase}(\mathbf{x}, t) \right\} \end{aligned} \quad (8.16)$$

where the phase-history integral is defined as

$$I_{phase}(\mathbf{x}, t) = \int_{-\infty}^t dt' \exp(\mathbf{ik} \cdot \mathbf{x}(t') - i\omega t').$$

Evaluation of I_{phase} requires knowledge of the unperturbed orbit trajectory $\mathbf{x}(t')$. This trajectory, determined by solving Eqs.(8.9) with boundary conditions specified by Eq.(8.7), has the velocity time-dependence

$$\mathbf{v}(t') = v_{\parallel} \hat{\mathbf{B}} + \mathbf{v}_{\perp} \cos[\omega_{c\sigma}(t' - t)] - \hat{\mathbf{B}} \times \mathbf{v}_{\perp} \sin[\omega_{c\sigma}(t' - t)]. \quad (8.17)$$

Equation (8.17) satisfies both the dynamics and the boundary condition $\mathbf{v}(t) = \mathbf{v}$ and so gives the correct helical ‘unwinding’ into the past for a particle at its present position in phase space. The position trajectory, found by integrating Eq.(8.17), is

$$\begin{aligned} \mathbf{x}(t') &= \mathbf{x} + v_{\parallel} (t' - t) \hat{\mathbf{B}} \\ &\quad + \frac{1}{\omega_{c\sigma}} \left\{ \mathbf{v}_{\perp} \sin[\omega_{c\sigma}(t' - t)] + \hat{\mathbf{B}} \times \mathbf{v}_{\perp} (\cos[\omega_{c\sigma}(t' - t)] - 1) \right\} \end{aligned} \quad (8.18)$$

which satisfies the related boundary condition $\mathbf{x}(t) = \mathbf{x}$.

To proceed further, we define φ to be the velocity-space angle between the fixed quantity \mathbf{k}_{\perp} and the dummy variable \mathbf{v}_{\perp} so that $\mathbf{k}_{\perp} \cdot \mathbf{v}_{\perp} = k_{\perp} v_{\perp} \cos \varphi$ and $\mathbf{k}_{\perp} \cdot \hat{\mathbf{B}} \times \mathbf{v}_{\perp} = k_{\perp} v_{\perp} \sin \varphi$. Using this definition, the time history of the spatial part of the phase can be written as

$$\mathbf{k} \cdot \mathbf{x}(t') = \mathbf{k} \cdot \mathbf{x} + k_{\parallel} v_{\parallel} (t' - t) + \frac{k_{\perp} v_{\perp}}{\omega_{c\sigma}} \{ \sin[\omega_{c\sigma}(t' - t) + \varphi] - \sin \varphi \}. \quad (8.19)$$

The phase integral can now be expanded

$$\begin{aligned} I_{phase}(\mathbf{x}, t) &= e^{-i\omega t} \int_{-\infty}^t dt' e^{i\mathbf{k} \cdot \mathbf{x}(t') - i\omega(t'-t)} \\ &= e^{i\mathbf{k} \cdot \mathbf{x} - i\omega t} \int_{-\infty}^0 d\tau \exp \left\{ i \left[\frac{k_{\perp} v_{\perp}}{\omega_{c\sigma}} \{ \sin[\omega_{c\sigma}\tau + \varphi] - \sin \varphi \} \right] \right\} \end{aligned} \quad (8.20)$$

where $\tau = t' - t$. Certain Bessel function relations are now of use. The first of these is the integral representation of the J_n Bessel function, namely

$$J_n(z) = \frac{1}{2\pi} \int_0^{2\pi} e^{iz \sin \theta - in\theta} d\theta. \quad (8.21)$$

The inverse of this relation is

$$e^{iz \sin \theta} = \sum_{n=-\infty}^{\infty} J_n(z) e^{in\theta} \quad (8.22)$$

which may be validated by taking the θ Fourier transform of both sides over the interval from 0 to 2π .

The phase integral can be evaluated using Eq.(8.22) in Eq.(8.20) to obtain

$$\begin{aligned} I_{phase}(\mathbf{x}, t) &= e^{i\mathbf{k} \cdot \mathbf{x} - i\omega t} \sum_{n=-\infty}^{\infty} J_n\left(\frac{k_{\perp} v_{\perp}}{\omega_{c\sigma}}\right) e^{-\frac{ik_{\perp} v_{\perp} \sin \varphi}{\omega_{c\sigma}}} \int_{-\infty}^0 d\tau e^{i(k_{\parallel} v_{\parallel} - \omega)\tau + in(\omega_{c\sigma}\tau + \varphi)} \\ &= e^{i\mathbf{k} \cdot \mathbf{x} - i\omega t} e^{-\frac{ik_{\perp} v_{\perp} \sin \varphi}{\omega_{c\sigma}}} \sum_{n=-\infty}^{\infty} J_n\left(\frac{k_{\perp} v_{\perp}}{\omega_{c\sigma}}\right) \frac{\left[e^{i(k_{\parallel} v_{\parallel} - \omega)\tau + in(\omega_{c\sigma}\tau + \varphi)} \right]_{-\infty}^0}{-i(\omega - k_{\parallel} v_{\parallel} - n\omega_{c\sigma})}. \end{aligned} \quad (8.23)$$

In Eqs. (8.16) and (8.23) there is a lower limit at $t = -\infty$; this limit corresponds to the phase in the distant past and is essentially the information regarding the initial condition of the system in the distant past. We saw in our previous discussion of the Landau problem that initial value problems are properly discussed using a Laplace transform approach and that Fourier transforms do not work properly when there is an initial value problem. However, if we ignore the initial conditions and use the Plemelj formula with Fourier transforms the same result as the Laplace method is obtained. This short-cut procedure will now be followed and so any reference to the initial conditions will be dropped and Fourier transforms will be used with invocation of the Plemelj formula whenever it is necessary to resolve any singularities in the integrations. Hence, terms evaluated at $t = -\infty$ in Eqs. (8.16) and (8.23) are dropped since these are initial values. After making these simplifications, the perturbed distribution function becomes

$$f_{\sigma 1}(\mathbf{x}, \mathbf{v}, t) = -\frac{q_{\sigma} \tilde{\phi}_1 f_{\sigma 0} e^{i\mathbf{k} \cdot \mathbf{x} - i\omega t}}{\kappa T_{\sigma}} \left\{ 1 - e^{-\frac{ik_{\perp} v_{\perp} \sin \varphi}{\omega_{c\sigma}}} \sum_n \frac{J_n\left(\frac{k_{\perp} v_{\perp}}{\omega_{c\sigma}}\right) \omega e^{in\varphi}}{(\omega - k_{\parallel} v_{\parallel} - n\omega_{c\sigma})} \right\}. \quad (8.24)$$

The next step is to evaluate the density perturbation Eq.(8.5), an operation which involves integrating the perturbed distribution function over velocity; the velocity integrals are evaluated using the Bessel identity (Watson 1922)

$$\int_0^{\infty} z J_n^2(\beta z) e^{-\alpha^2 z^2} dz = \frac{1}{2\alpha^2} e^{-\beta^2/2\alpha^2} I_n\left(\frac{\beta^2}{2\alpha^2}\right). \quad (8.25)$$

Using this identity, substitution of Eq.(8.24) into Eq.(8.5) gives

$$\begin{aligned}
n_{\sigma 1} &= -\frac{q_{\sigma}}{\kappa T_{\sigma}} \phi_1 n_{\sigma 0} \left[\frac{1 - \frac{\omega}{\pi^{3/2} v_{T\sigma}^3} \sum_n \int_{-\infty}^{\infty} dv_{\parallel} \int_0^{2\pi} d\varphi \int_0^{\infty} v_{\perp} dv_{\perp}}{e^{-i \frac{k_{\perp} v_{\perp}}{\omega_{c\sigma}} \sin \varphi + i n \varphi} J_n \left(\frac{k_{\perp} v_{\perp}}{\omega_{c\sigma}} \right) e^{-(v_{\parallel}^2 + v_{\perp}^2)/v_{T\sigma}^2}}}{(\omega - k_{\parallel} v_{\parallel} - n \omega_{c\sigma})} \right] \\
&= -\frac{q_{\sigma} \phi_1 n_{\sigma 0}}{\kappa T_{\sigma}} \left[1 - \frac{2\omega}{\sqrt{\pi} v_{T\sigma}^3} \sum_n \int_{-\infty}^{\infty} dv_{\parallel} \int_0^{\infty} v_{\perp} dv_{\perp} \frac{J_n^2 \left(\frac{k_{\perp} v_{\perp}}{\omega_{c\sigma}} \right) e^{-\frac{v_{\parallel}^2 + v_{\perp}^2}{v_{T\sigma}^2}}}{(\omega - k_{\parallel} v_{\parallel} - n \omega_{c\sigma})} \right] \\
&= -\frac{q_{\sigma}}{\kappa T_{\sigma}} \phi_1 n_{\sigma 0} \left[1 + \alpha_{0\sigma} e^{-k_{\perp}^2 r_{L\sigma}^2} \sum_n \frac{I_n(k_{\perp}^2 r_{L\sigma}^2)}{\pi^{1/2}} \int_{-\infty}^{\infty} d\xi \frac{e^{-\xi^2}}{\xi - \alpha_{n\sigma}} \right] \\
&= -\frac{q_{\sigma}}{\kappa T_{\sigma}} \phi_1 n_{\sigma 0} \left[1 + \alpha_{0\sigma} e^{-k_{\perp}^2 r_{L\sigma}^2} \sum_n I_n(k_{\perp}^2 r_{L\sigma}^2) Z(\alpha_{n\sigma}) \right]
\end{aligned} \tag{8.26}$$

where

$$\alpha_{n\sigma} = \frac{\omega - n \omega_{c\sigma}}{k_{\parallel} v_{T\sigma}}, \tag{8.27}$$

the Larmor radius is

$$r_{L\sigma} = \frac{\sqrt{\kappa T_{\sigma}/m_{\sigma}}}{\omega_{c\sigma}}, \tag{8.28}$$

and Z is the plasma dispersion function. Finally, Eq.(8.26) is substituted into Eq.(8.4) to obtain the warm magnetized plasma electrostatic dispersion relation

$$D(\omega, k) = 1 + \sum_{\sigma} \frac{1}{k^2 \lambda_{D\sigma}^2} \left[1 + \alpha_{0\sigma} e^{-k_{\perp}^2 r_{L\sigma}^2} \sum_{n=-\infty}^{\infty} I_n(k_{\perp}^2 r_{L\sigma}^2) Z(\alpha_{n\sigma}) \right] = 0. \tag{8.29}$$

Note that $D(\omega, k)$ refers to the dispersion relation and should not be confused with D the off-diagonal term of the cold-plasma dielectric tensor, nor with \mathbf{D} the displacement vector. A similar, but more involved calculation using unperturbed orbit phase integrals for the perturbed current density gives the hot plasma version of the full electromagnetic dispersion, i.e., the finite temperature generalization of the cold plasma dielectric tensor $\overleftrightarrow{\mathbf{K}}$. Although the calculation is essentially similar, it is considerably more tedious, and the interested reader is referred to specialized texts on plasma waves such as those by Stix (1992) or Swanson (2003).

8.2 Analysis of the warm plasma electrostatic dispersion relation

Equation (8.29) generalizes the unmagnetized warm plasma electrostatic dispersion rela-

tion Eq.(5.51) derived in Chapter 4 to the situation of a magnetized warm plasma. This means that Eq.(8.29) should revert to Eq.(5.51) in the limit that $B \rightarrow 0$. The Bessel identity

$$\sum_{n=-\infty}^{\infty} I_n(\lambda) = e^\lambda \quad (8.30)$$

together with the condition $\alpha_n \rightarrow \alpha_0$ if $B \rightarrow 0$ show that this is indeed the case.

Furthermore, Eq.(8.29) should also be the warm-plasma generalization of the cold, magnetized plasma, electrostatic dispersion

$$k_x^2 S + k_z^2 P = 0; \quad (8.31)$$

demonstration of this correspondence will be presented later. Equation (8.30) can be used to recast Eq.(8.29) as

$$\mathcal{D}(\omega, k) = 1 + \sum_{\sigma} \frac{e^{-k_{\perp}^2 r_{L\sigma}^2}}{k^2 \lambda_{D\sigma}^2} \sum_{n=-\infty}^{\infty} I_n(k_{\perp}^2 r_{L\sigma}^2) [1 + \alpha_{0\sigma} Z(\alpha_{n\sigma})] = 0. \quad (8.32)$$

Using $I_{-n}(z) = I_n(z)$, the summation over n can be rearranged to give

$$\mathcal{D}(\omega, k) = 1 + \sum_{\sigma} \frac{e^{-k_{\perp}^2 r_{L\sigma}^2}}{k^2 \lambda_{D\sigma}^2} \left\{ \begin{aligned} & I_0(k_{\perp}^2 r_{L\sigma}^2) (1 + \alpha_{0\sigma} Z(\alpha_{0\sigma})) \\ & + \sum_{n=1}^{\infty} I_n(k_{\perp}^2 r_{L\sigma}^2) [2 + \alpha_{0\sigma} \{Z(\alpha_{n\sigma}) + Z(\alpha_{-n\sigma})\}] \end{aligned} \right\}. \quad (8.33)$$

In order to obtain the lowest order thermal correction, it is assumed that $\alpha_0 = \omega/k_{\parallel} v_{T\sigma} \gg 1$ in which case the large argument expansion Eq.(5.73) can be used to evaluate $Z(\alpha_0)$. Invoking this expansion and keeping only lowest order terms, shows that

$$\begin{aligned} 1 + \alpha_0 Z(\alpha_0) &= 1 + \alpha_0 \left\{ -\frac{1}{\alpha_0} \left[1 + \frac{1}{2\alpha_0^2} + \dots \right] + i\pi^{1/2} \exp(-\alpha_0^2) \right\} \\ &= -\frac{1}{2\alpha_0^2} + i\alpha_0 \pi^{1/2} \exp(-\alpha_0^2). \end{aligned} \quad (8.34)$$

It is additionally assumed that $|\alpha_n| = |(\omega - n\omega_{c\sigma})/k_{\parallel} v_{T\sigma}| \gg 1$ for $n \neq 0$; this corresponds to assuming that the wave frequency is not too close to a cyclotron resonance. With this assumption the large argument expansion of the plasma dispersion function is also appropriate for the $n \neq 0$ terms, and so one can write

$$\begin{aligned} 2 + \alpha_0 [Z(\alpha_n) + Z(\alpha_{-n})] &= 2 + \alpha_0 \left[-\frac{1}{\alpha_n} - \frac{1}{\alpha_{-n}} + i\sqrt{\pi} (e^{-\alpha_n^2} + e^{-\alpha_{-n}^2}) \right] \\ &= 2 - \frac{\omega}{\omega - n\omega_{c\sigma}} - \frac{\omega}{\omega + n\omega_{c\sigma}} + i\alpha_0 \sqrt{\pi} (e^{-\alpha_n^2} + e^{-\alpha_{-n}^2}) \\ &= -\frac{2n^2 \omega_{c\sigma}^2}{\omega^2 - n^2 \omega_{c\sigma}^2} + i\alpha_0 \sqrt{\pi} (e^{-\alpha_n^2} + e^{-\alpha_{-n}^2}) \end{aligned} \quad (8.35)$$

where the subscript σ has been omitted from the α_n to keep the algebra uncluttered. Substitution of these expansions back into the dispersion relation gives

$$\begin{aligned} \mathcal{D}(\omega, k) &= 1 + \sum_{\sigma} \frac{e^{-k_{\perp}^2 r_{L\sigma}^2}}{k^2 \lambda_{D\sigma}^2} \left\{ \begin{array}{l} I_0(k_{\perp}^2 r_{L\sigma}^2) \left(-\frac{1}{2\alpha_{0\sigma}^2} + i\alpha_{0\sigma} \sqrt{\pi} \exp(-\alpha_{0\sigma}^2) \right) \\ + \sum_{n=1}^{\infty} I_n(k_{\perp}^2 r_{L\sigma}^2) \left(\begin{array}{l} -\frac{2n^2 \omega_{c\sigma}^2}{\omega^2 - n^2 \omega_{c\sigma}^2} \\ + i\alpha_{0\sigma} \sqrt{\pi} \begin{pmatrix} e^{-\alpha_n^2} \\ + e^{-\alpha_n^2} \end{pmatrix} \end{array} \right) \end{array} \right\} \\ &= 0. \end{aligned} \quad (8.36)$$

Equation (8.36) generalizes the magnetized cold plasma electrostatic dispersion to finite temperature and shows how Landau damping appears both at the wave frequency ω and also at cyclotron harmonics, i.e., in the vicinity of $n\omega_{c\sigma}$. Two important limits of Eq.(8.36) are discussed in the following sections.

8.3 Bernstein waves

Suppose the wave phase is uniform in the direction along the magnetic field. Such a situation would occur if the antenna exciting the wave is an infinitely long wire aligned parallel to a magnetic field line (in reality, the antenna would have to be sufficiently long to behave as if infinite). This situation corresponds to having $k_{\parallel} \rightarrow 0$ in which case the Landau damping terms and the $1/2\alpha_{0\sigma}^2$ term vanish. The dispersion relation Eq.(8.36) consequently reduces to

$$1 = \sum_{\sigma} \frac{e^{-\lambda_{\sigma}}}{\lambda_{\sigma}} \sum_{n=1}^{\infty} \frac{2n^2 \omega_{p\sigma}^2}{\omega^2 - n^2 \omega_{c\sigma}^2} I_n(\lambda_{\sigma}) \quad (8.37)$$

where

$$\lambda_{\sigma} = k_{\perp}^2 r_{L\sigma}^2 \quad (8.38)$$

and

$$r_{L\sigma}^2 = \frac{\omega_{p\sigma}^2 \lambda_{D\sigma}^2}{\omega_{c\sigma}^2} = \frac{\kappa T_{\sigma}}{m_{\sigma} \omega_{c\sigma}^2} \quad (8.39)$$

is the Larmor radius. The waves resulting from this dispersion were first derived by Bernstein (1958) and are called Bernstein waves or cyclotron harmonic waves; these waves are often called hot plasma waves because their existence depends on the plasma having a finite temperature. Both electron and ion Bernstein waves exist; early measurements of electron Bernstein waves in laboratory experiments were reported by Crawford (1965) and by Leuterer (1969) and of ion Bernstein waves were reported by Schmitt (1973). These waves have also been routinely observed by spacecraft and fitting of the measurements to the wave dispersion has been used, for example by Moncuquet, Meyervernet and Hoang (1995), to infer the electron temperature in the magnetized plasma of Jupiter's moon Io. Electron Bernstein waves involve ω being in the vicinity of an electron cyclotron harmonic, i.e., $\omega^2 \sim \mathcal{O}(n^2 \omega_{ce}^2)$, while for ion waves ω is in the vicinity of an ion cyclotron harmonic.

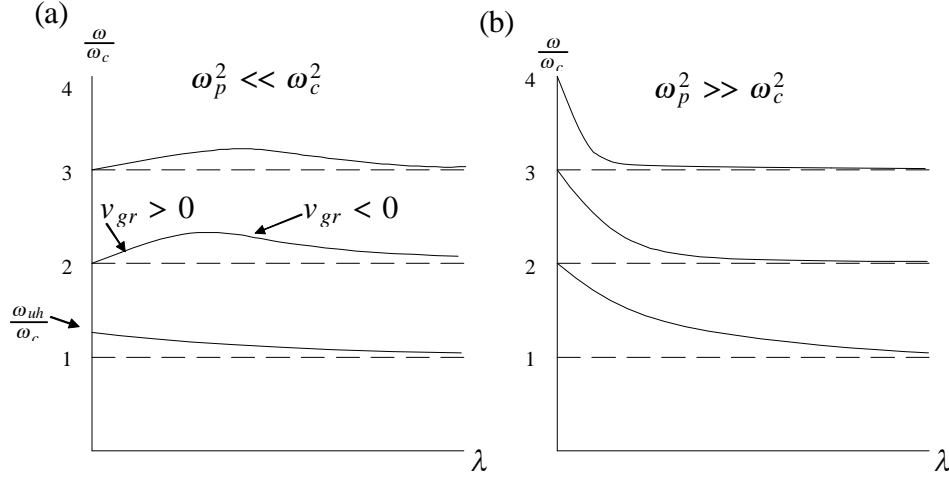


Figure 8.1: Electron Bernstein wave dispersion relations

The Bernstein wave dispersion relation, Eq. (8.37), provides a transcendental relation between ω and k_{\perp} and for any given k_{\perp} has an infinite number of roots ω . This is because as ω is varied, the factor $(\omega^2 - n^2\omega_{c\sigma}^2)^{-1}$ in each term of the summation takes on all values from $-\infty$ to ∞ so that there are an infinite number of ways for the right hand side to equal the left hand side. In particular, it should be noted that the right hand side becomes large and positive whenever ω is just slightly larger than $n\omega_{c\sigma}$ for any n .

We now consider electron Bernstein waves and so drop the ion terms from the summation (the analysis for ion Bernstein waves is similar). The subscript σ will now be dropped and it will be understood that all quantities refer to electrons. On keeping the electron terms only, Eq.(8.37) reduces to

$$1 = 2 \frac{e^{-\lambda}}{\lambda} \sum_{n=1}^{\infty} \frac{n^2 \omega_p^2}{\omega^2 - n^2 \omega_c^2} I_n(\lambda) \quad (8.40)$$

which has the following limiting forms when $\omega_p^2 \ll \omega_c^2$ and vice versa.

1. $\omega_p^2 \ll \omega_c^2$ case:

Here the term $2n^2\omega_p^2/(\omega^2 - n^2\omega_c^2)$ is negligible compared to unity except when $\omega^2 \sim \mathcal{O}(n^2\omega_c^2)$. Thus, for a given ω only one term in the summation is near resonance and the dispersion relation is satisfied by this one term on the right hand side of Eq.(8.40) balancing the left hand side. This results in a spectrum waves that are slightly above the cyclotron harmonics, namely

$$\omega^2 = n^2\omega_c^2 + 2 \frac{e^{-\lambda}}{\lambda} n^2\omega_p^2 I_n(\lambda), \quad \text{for } n = 1, 2, \dots, \infty. \quad (8.41)$$

The small and large λ limits of this expression are determined using the asymptotic values of the I_n Bessel function, namely for $n \geq 1$,

$$\begin{aligned} \lim_{\lambda \ll 1} I_n(\lambda) &= \frac{1}{n!} \left(\frac{\lambda}{2}\right)^n \\ \lim_{\lambda \gg 1} I_n(\lambda) &= e^\lambda \end{aligned} \quad (8.42)$$

to give

$$\begin{aligned} \omega^2 &= n^2 \omega_c^2 + (1 - \lambda) n^2 \omega_p^2 \frac{1}{n!} \left(\frac{\lambda}{2}\right)^{n-1} \quad \text{for } \lambda \ll 1, \\ \omega^2 &= n^2 \omega_c^2 \quad \text{for } \lambda \gg 1. \end{aligned} \quad (8.43)$$

The $n = 1$ mode differs slightly from the $n > 1$ modes because the $n = 1$ mode has the small λ dispersion

$$\omega^2 = \omega_{uh}^2 - \lambda \omega_p^2 \quad (8.44)$$

showing that this mode is the warm plasma generalization of the upper hybrid resonance. The modes for which $n > 1$ start at $\omega^2 = n^2 \omega_c^2$ when $\lambda = 0$, have a maximum frequency at some finite λ , and then revert to $\omega^2 = n^2 \omega_c^2$ as $\lambda \rightarrow \infty$. To the left of the frequency maximum the group velocity $\partial\omega/\partial k_\perp$ is positive and to the right of the maximum the group velocity is negative. This system of modes is sketched in Fig.8.1(a).

2. $\omega_p^2 \gg \omega_c^2$

For large λ , the product of the exponential factor and the modified Bessel function in Eq.(8.40) is unity, leaving one more factor of λ in the denominator, so again the dispersion reduces to cyclotron harmonics, $\omega^2 = n^2 \omega_c^2$ as $\lambda \rightarrow \infty$. For small λ the situation is more involved because to lowest order, the $n = 1$ term is independent of λ and so must always be retained when approximating Eq.(8.40). Let us suppose that some other term, say the $(n + 1)^{th}$ term is near resonance, i.e., $\omega^2 \sim (n + 1)^2 \omega_c^2$. Then, keeping the left hand side, the $n = 1$ term and the $(n + 1)^{th}$ term, expansion of Eq.(8.40) results in

$$1 \simeq \frac{\omega_p^2}{[(n + 1)^2 - 1] \omega_c^2} + \frac{(n + 1) \omega_p^2}{[\omega^2 - (n + 1)^2 \omega_c^2] n!} \left(\frac{\lambda}{2}\right)^n \quad (8.45)$$

which may be solved for ω to give

$$\omega = (n + 1) \omega_c \left\{ 1 - \frac{\omega_p^2 [(n + 1)^2 - 1]}{(\omega_p^2 - [(n + 1)^2 - 1] \omega_c^2) 2^{n+1} (n + 1)!} \lambda^n \right\}. \quad (8.46)$$

Thus, for small λ the n^{th} mode starts at $\omega \simeq (n + 1) \omega_c$ and then as $\lambda \rightarrow \infty$ the frequency decreases towards the asymptotic limit $n \omega_c$. This dispersion is sketched in Fig.8.1(b).

Excitation of Bernstein waves requires $k_\parallel = 0$ which is a quite stringent requirement. The antenna must be absolutely uniform in the direction along the magnetic field because otherwise a finite k_\parallel will be excited which will result in the waves being subject to strong Landau damping.

8.4 Warm, magnetized, electrostatic dispersion with small, but finite k_{\parallel}

An alternate limit for Eq.(8.36) would be to allow k_{\parallel} to be finite but also have $k_{\perp}^2 r_L^2 \ll 1$ so that only the lowest-order finite Larmor radius terms are retained. To keep matters simple and also to relate to cold plasma theory, k_{\parallel} will be assumed to be sufficiently small that $\omega/k_{\parallel} \gg v_{Te}, v_{Ti}$. Since $r_{L\sigma}^2/\lambda_{D\sigma}^2 = \omega_{p\sigma}^2/\omega_{c\sigma}^2$, the lowest-order perpendicular thermal terms will be $\mathcal{O}(k_{\perp}^4)$ and so perpendicular quantities up to fourth order must be retained. This means that both the $n = 1$ and the $n = 2$ terms must be retained in the summation over n . With these approximations and using $1/2\lambda_{D\sigma}^2\alpha_0^2 = \omega_p^2/\omega^2$, Eq.(8.36) becomes

$$k_{\parallel}^2 + k_{\perp}^2 + \sum_{\sigma} (1 - k_{\perp}^2 r_L^2) \left(\begin{array}{l} \left(1 + \frac{k_{\perp}^4 r_L^4}{4}\right) \left(-\frac{\omega_{p\sigma}^2}{\omega^2} + i\frac{\alpha_0\sqrt{\pi}}{\lambda_{D\sigma}} e^{-\alpha_0^2}\right) \\ + \frac{k_{\perp}^2 \omega_{p\sigma}^2}{2\omega_{c\sigma}^2} \left[\begin{array}{l} -\frac{2\omega_{c\sigma}^2}{\omega^2 - \omega_{c\sigma}^2} \\ + i\alpha_0\sqrt{\pi} \left(\begin{array}{l} e^{-\alpha_1^2} \\ + e^{-\alpha_{-1}^2} \end{array} \right) \end{array} \right] \\ + \frac{k_{\perp}^4 r_L^2 \omega_{p\sigma}^2}{8\omega_{c\sigma}^2} \left[\begin{array}{l} -\frac{8\omega_{c\sigma}^2}{\omega^2 - 4\omega_{c\sigma}^2} \\ + i\alpha_0\sqrt{\pi} \left(\begin{array}{l} e^{-\alpha_2^2} \\ + e^{-\alpha_{-2}^2} \end{array} \right) \end{array} \right] \end{array} \right) = 0. \quad (8.47)$$

The Landau damping terms will be assumed to be negligible to keep matters simple and the equation will now be grouped according to powers of k_{\perp}^2 . Retaining only the lowest-order finite-temperature perpendicular terms gives

$$k_{\parallel}^2 \left(1 - \sum_{\sigma} \frac{\omega_{p\sigma}^2}{\omega^2}\right) + k_{\perp}^2 \left(1 - \sum_{\sigma} \frac{\omega_{p\sigma}^2}{\omega^2 - \omega_{c\sigma}^2}\right) - k_{\perp}^4 \sum_{\sigma} \left(\frac{3\omega_{p\sigma}^4 \lambda_{D\sigma}^2}{(\omega^2 - \omega_{c\sigma}^2)(\omega^2 - 4\omega_{c\sigma}^2)}\right) = 0. \quad (8.48)$$

This is of the form

$$-k_{\perp}^4 \epsilon_{th} + k_{\perp}^2 S + k_{\parallel}^2 P = 0 \quad (8.49)$$

where the perpendicular fourth-order thermal coefficient is

$$\epsilon_{th} = \sum_{\sigma} \left(\frac{3\omega_{p\sigma}^4 \lambda_{D\sigma}^2}{(\omega^2 - \omega_{c\sigma}^2)(\omega^2 - 4\omega_{c\sigma}^2)}\right). \quad (8.50)$$

Equation (8.49) is a quadratic equation in k_{\perp}^2 . The cold-plasma model used earlier in effect set $\epsilon_{th} = 0$ so that a wave propagating through an inhomogeneous plasma towards a hybrid resonance where $S \rightarrow 0$ would have $k_{\perp}^2 \rightarrow \infty$. This non-physical prediction is resolved by the warm plasma theory because ϵ_{th} , while small, is finite and so prevents $k_{\perp}^2 \rightarrow \infty$ from occurring. What happens instead is that Eq. (8.49) has two qualitatively distinct roots,

namely

$$k_{\perp}^2 = \frac{S \pm \sqrt{S^2 + 4\epsilon_{th}k_{\parallel}^2 P}}{2\epsilon_{th}}. \quad (8.51)$$

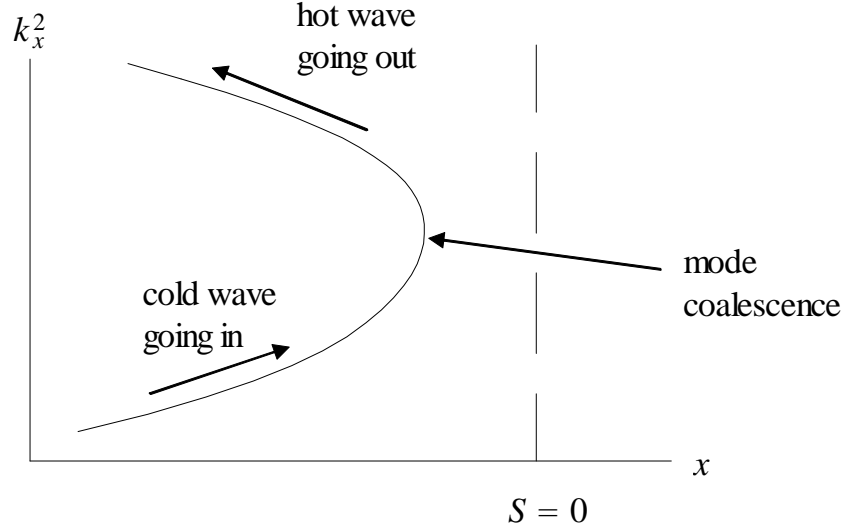


Figure 8.2: Linear mode conversion of cold mode into hot mode near hybrid resonance

Far from the hybrid resonance S is large so that the two modes are well separated and given by

$$\begin{aligned} k_{\perp}^2 &= -\frac{P}{S}k_{\parallel}^2, & \text{cold plasma wave} \\ k_{\perp}^2 &= \frac{S}{\epsilon_{th}}, & \text{hot plasma wave} \end{aligned} \quad (8.52)$$

but as $S \rightarrow 0$ these two modes coalesce. The hot plasma wave results from balancing the first and middle terms in Eq. (8.49) and the cold plasma wave results from balancing the middle and last terms. The actual mode coalescence occurs where the square root term in Eq.(8.51) vanishes, i.e., where

$$S^2 = -4\epsilon_{th}k_{\parallel}^2 P. \quad (8.53)$$

The WKB approximation fails at the mode coalescence, because here $dk_{\perp}/dx = \infty$ and so a more sophisticated analysis is required. This analysis, which will be discussed in the next section, shows that the hot and cold waves are strongly coupled at the coalescence region. In particular, it will be demonstrated that a cold wave propagating towards the hybrid resonance, as shown in Fig.8.2, will be linearly converted into a hot wave which then propagates back out from the resonance.

8.5 Analysis of linear mode conversion

8.5.1 Airy equation

The procedure for analyzing linear mode conversion was developed by Stix (1965) and is an extension of the standard method for connecting solutions of the Airy equation

$$y'' + xy = 0 \quad (8.54)$$

from the $x < 0$ region to the $x > 0$ region. The Airy problem involves a second order ordinary differential equation with a coefficient which goes through zero. The mode conversion problem involves a fourth order equation which also has a coefficient going through zero. The Airy connection method will first be examined to introduce the relevant concepts and then these will be applied to the actual mode conversion problem.

The sequence of steps for developing the solution to the Airy problem are as follows:

1. Laplace transform the equation: Equation (8.54) cannot be Fourier transformed because of the non-constant coefficient x in the second term; however it can be Laplace transformed by make use of the relation that the Laplace transform of $xy(x)$ is $-d\tilde{y}(p)/dp$. Thus, the Laplace transform of Eq.(8.54) is

$$p^2\tilde{y}(p) - \frac{d\tilde{y}(p)}{dp} = 0. \quad (8.55)$$

Strictly speaking, Laplace transform of y'' will also bring in terms involving initial conditions, but these will be ignored for now and this issue will be addressed later. Equation (8.55) is easily solved to give

$$\tilde{y}(p) = A \exp(p^3/3) \quad (8.56)$$

where A is a constant. The formal solution to Eq.(8.54) is the inverse transform

$$y(x) = (2\pi i)^{-1} \int_C \tilde{y}(p)e^{px} dp = a \int_C e^{f(p)} dp \quad (8.57)$$

where $a = A/2\pi i$, $f(p) = p^3/3 + px$, and C is some contour in the complex plane. By appropriate choice of this contour Eq.(8.57) is shown to be a valid solution to the original differential equation. In particular, if the endpoints p_1 and p_2 of the contour C are chosen to satisfy

$$\left[e^{f(p)} \right]_{p_1}^{p_2} = 0 \quad (8.58)$$

then Eq.(8.57) is a valid solution to Eq.(8.54). The reason for this may be seen by explicitly calculating y'' and xy using Eq.(8.57) to obtain

$$y'' = \frac{d^2}{dx^2} a \int_C e^{p^3/3+px} dp = a \int_C p^2 e^{p^3/3+px} dp \quad (8.59)$$

and

$$\begin{aligned}
 xy &= a \int_C e^{p^3/3} \left(\frac{d}{dp} e^{px} \right) dp \\
 &= a \left[e^{p^3/3+px} \right]_{p_1}^{p_2} - a \int_C \frac{d}{dp} \left(e^{p^3/3} \right) e^{px} dp \\
 &= -a \int_C p^2 e^{p^3/3+px} dp.
 \end{aligned} \tag{8.60}$$

Addition of these results corresponds to Eq.(8.54).

2. Suppose the integrand is analytic in some region and consider two different contours in this region having the *same* pair of endpoints. We can take one of these contours and deform it into the other. Thus, the two contours give the same result and so correspond to the same solution.
3. Independence of contours: Since Eq. (8.54) is a second order ordinary differential equation it must have two linearly independent solutions. This means there must be two linearly independent contours since a choice of contour corresponds to a solution. Linear independence of the contours means that one cannot be deformed into the other. One possible way for the two contours to be linearly independent is for them to have different pairs of end points. In this case, one contour can only be deformed into the other if the end points can be moved without changing the integral. If moving the end points changes the integral, then the two contours are independent. Another possibility is a situation where the two contours have the same pairs of endpoints, but the integrand is not analytic in the region between the two contours. For example there could be a pole or branch cut between the contours. Then, one contour could not be deformed into the other because of the non-analytic region separating the two contours. The two contours would then be linearly independent.

8.5.2 Steepest descent contour

The solution to the Airy equation is thus

$$y(x) = \int_C e^{f(p,x)} dp \tag{8.61}$$

where C satisfies the conditions listed above and the solution can be multiplied by an arbitrary constant. In order to evaluate the integral it is useful to first separate the complex function $f(p, x)$ into its real and imaginary parts,

$$f(p, x) = f_r(p, x) + i f_i(p, x). \tag{8.62}$$

Also, it should be remembered that for the purposes of the p integration, x can be considered as a fixed parameter. Thus, when performing the p integration, x need not be written explicitly and so we may simply write $f(p) = f_r(p) + i f_i(p)$ where $p = u + iv$ and u, v are the coordinates in the complex p plane. For an arbitrary contour in the p plane, both f_r and f_i will vary. The variation of phase means that there will be alternating positive and negative contributions to the integral in Eq.(8.61), making evaluation of this integral very delicate. However, evaluation of the integral can be made almost trivial if the contour is deformed to follow a certain optimum path.

To see this, it should first be recalled that the theory of complex variables shows that any function of a complex variable must satisfy the Cauchy-Riemann conditions, which means that f_r and f_i satisfy

$$\frac{\partial f_r}{\partial u} = \frac{\partial f_i}{\partial v}, \quad \frac{\partial f_r}{\partial v} = -\frac{\partial f_i}{\partial u}. \quad (8.63)$$

Also, on defining the gradient operator in the u, v plane $\nabla = \hat{u}\partial/\partial u + \hat{v}\partial/\partial v$ it is seen that

$$\nabla f_r \cdot \nabla f_i = \frac{\partial f_r}{\partial u} \frac{\partial f_i}{\partial u} + \frac{\partial f_r}{\partial v} \frac{\partial f_i}{\partial v} = 0. \quad (8.64)$$

This means that contours of constant f_r are everywhere orthogonal to contours of constant f_i .

Since f_i corresponds to the phase of $\exp(f_r(p) + if_i(p))$ and f_r corresponds to the amplitude, Eq.(8.64) shows that a path in the complex p plane which is arranged to follow the gradient of f_r will automatically be a contour of constant f_i , i.e., a contour of constant phase. Thus, the optimum path is to follow ∇f_r because on this path f_i will be constant and so there will not be any alternating positive and negative contributions as on any other path. In fact, because it is constant, the phase can be factored from the integral when using this optimum path, giving

$$y(x) = e^{if_i} \int_{C \parallel \nabla f_r} e^{f_r(p)} dp. \quad (8.65)$$

Clearly, the maximum contribution to this integral comes from the vicinity of where f_r assumes its maximum value. Since the maximum occurs where $\nabla f_r = 0$, most of the contribution to the integral comes from the vicinity of where $\nabla f_r = 0$. The extrema of f are always saddle points because the Cauchy-Reimann conditions imply $\partial^2 f_{r,i}/\partial u^2 + \partial^2 f_{r,i}/\partial v^2 = 0$. Thus, the vicinity of $\nabla f_r = 0$ must be a saddle point.

The discussion in the previous paragraph implies that once the endpoints of the contour have been chosen, for purposes of evaluation it is advantageous to deform the contour so that it follows the gradient of f_r ; this called the steepest ascent/descent path (usually just called steepest descent). This optimum choice of path ensures that (i) there is a localized region where f_r assumes a maximum value and (ii) the phase does not vary along the path. The contribution to the integral is concentrated into a small region of the complex p -plane in the vicinity of where f_r has its maximum value. Simple integration techniques may be used to evaluate the integral in this vicinity, and the contribution from this region dominates other contributions because $\exp(f_r(p))$ at the maximum of f_r is exponentially larger than at other places. Furthermore if the contour is chosen so that $f_r \rightarrow -\infty$ at the endpoints then Eq.(8.58) will be satisfied and the chosen contour will be a solution of the original differential equation.

The saddle points are located where $f'(p) = 0$. For the Airy function,

$$\begin{aligned} f(p) &= p^3/3 + px \\ f'(p) &= p^2 + x \\ f''(p) &= 2p \end{aligned} \quad (8.66)$$

so the saddle points (denoted by subscript s) are located at $p_s = \pm(-x)^{1/2}$. In the vicinity of the saddle point, f can be Taylor expanded as

$$f(p) \simeq f(p_s) + \frac{(p - p_s)^2}{2} f''(p_s). \quad (8.67)$$

It is now convenient to define the origin of the coordinate system to be at the saddle point and also use cylindrical coordinates, r, θ so that $p - p_s = r \exp(i\theta)$ and for fixed θ , $dp = dr e^{i\theta}$. Also, phasor notation is used for f'' so $f'' = |f''| \exp(i\psi)$ where ψ is the phase of f'' . Thus, in the vicinity of the saddle point we write

$$f(p) \simeq f(p_s) + r^2 \frac{|f''(p_s)|}{2} \exp(2i\theta + i\psi). \quad (8.68)$$

Choosing the contour to follow the path of steepest descent corresponds to choosing θ such that $2\theta + \psi = \pm\pi$ in which case

$$f(p) \simeq f(p_s) - r^2 \frac{|f''(p_s)|}{2} \quad (8.69)$$

and so Eq.(8.61) becomes

$$y(x) \simeq \int_{-\infty}^{\infty} e^{f(p_s) - \frac{1}{2} r^2 |f''(p_s)|} dr e^{i\theta} \quad (8.70)$$

where the approximation has been made that nearly all the contribution to the integral comes from small r ; it is not necessary to worry about errors in the Taylor expansion at large r , since the contributions from large r are negligible because of the exponential behavior. Thus f_r is maximum at the saddle point $r = 0$ and the main contribution to the integral comes from the contour going over the ridge of the saddle. The r integral is a Gaussian integral $\int \exp(-ar^2) dr = \sqrt{\pi/a}$ so

$$\begin{aligned} y(x) &\simeq \int_{-\infty}^{\infty} e^{f(p_s) - r^2 |f''(p_s)|/2} dr e^{i\theta} \\ &= e^{f(p_s) + i\theta} \int_{-\infty}^{\infty} e^{-r^2 |f''(p_s)|/2} dr \\ &= e^{f(p_s) + i\theta} \sqrt{\frac{2\pi}{|f''(p_s)|}} \\ &= e^{f(p_s)} \sqrt{\frac{2\pi e^{i2\theta}}{|f''(p_s)|}} \\ &= e^{f(p_s)} \sqrt{\frac{\pi e^{i(\pm\pi - \psi)}}{|f''(p_s)|}} \\ &= e^{f(p_s)} \sqrt{-\frac{2\pi}{f''(p_s)}}. \end{aligned} \quad (8.71)$$

Since $f(p_s) = p(p^2/3 + x) = \pm\sqrt{-x}(2x/3) = \mp 2(-x)^{3/2}/3$ and $f''(p_s) = \pm 2\sqrt{-x}$ it is seen that

$$\int_{\text{vicinity of saddle}} e^{f(p)} dp \simeq \sqrt{\frac{\mp\pi}{(-x)^{1/2}}} e^{\mp 2(-x)^{3/2}/3}. \quad (8.72)$$

Providing x is not too close to zero, the two saddle points determined by the \pm signs are well-separated and do not perturb each other; the integral will then be a summation over whichever saddle points the contour happens to pass over. The polarity of a saddle point is determined by the sense in which the contour passes through the saddle point.

8.5.3 Relationship between saddle point solutions and WKB modes

For large $|x|$ Eq. (8.54) can be solved approximately using the WKB method, in which case it is assumed that $y(x) = A(x) \exp(i \int^x k(x') dx')$. The wavevector $k(x)$ is determined from the dispersion relation associated with the original differential equation and $A(x)$ is a function of $k(x)$. At large $|x|$ the dispersion relation associated with Eq.(8.54) obtained by assuming $d/dx \rightarrow ik$ is

$$k^2 = x \quad (8.73)$$

so $k(x) = \pm x^{1/2}$ and $A(x) \sim (\pm x)^{-1/4}$. The WKB solution is thus

$$y_{WKB} \sim \frac{1}{(\pm x)^{1/4}} e^{\pm i \int^x x'^{1/2} dx'} = \frac{1}{(\pm x)^{1/4}} e^{\pm i 2x^{3/2}/3} \quad (8.74)$$

which is the same as the saddle point solution. Thus *each saddle point solution corresponds to a WKB mode*, and in particular to a propagating wave if $x > 0$ and to an evanescent mode if $x < 0$.

8.5.4 Using boundary conditions to choose contours

The choice of contour is determined by the boundary conditions which in turn are determined by the physical considerations. In this Airy equation problem, the boundary condition would typically be the physical constraint that no exponentially growing solutions are allowed for $x < 0$. This forces choice of a contour which does *not* pass through the saddle point having the plus sign in Eq.(8.74) when $x < 0$. This condition together with Eq.(8.58) uniquely determines the contour. Choosing a contour C is equivalent to specifying a particular solution to Eq.(8.57); this chosen solution can be evaluated for $x > 0$. For $x > 0$ the saddle points become reshuffled and different and so for purposes of evaluation along the steepest descent path, the chosen contour must be deformed to pass through the saddle points as they exist for $x > 0$. The sum of the contributions of these saddle points gives the form of the solution for $x > 0$. The important point here is that the *same* contour is used for both $x > 0$ and $x < 0$ because the linearly independent solution is determined by the contour. The contour is determined by its endpoints, but may be deformed provided analyticity is preserved. Thus, the endpoints are the same for both the $x > 0$ and $x < 0$ evaluations, but the deformations of the contour differ in order to pass through the respective $x > 0$ or $x < 0$ saddle points. The sign of x determines the character of the saddle points and so *for purposes of evaluation* the contour is deformed differently for $x > 0$ and $x < 0$.

This completes the discussion of the Airy problem and we now return to the linear mode conversion problem (Stix 1965). A comparison of Eqs.(6.108) and (8.49) shows that if Eq.(8.49) is “un-Fourier” analyzed in the x -direction, it becomes

$$\frac{d}{dx} \left(\epsilon_{th} \frac{d^3}{dx^3} + S \frac{d}{dx} \right) \phi - k_{\parallel}^2 P \phi = 0 \quad (8.75)$$

where it is assumed that ϵ_{th} is approximately constant. To prove this is the correct form, consider the following two statements: (i) if $\epsilon_{th} \rightarrow 0$, Eq.(8.75) reverts to Eq.(6.108) (Fourier-analyzed in the z direction, but not the x direction), (ii) if ϵ_{th} is finite and S and P are assumed uniform, then Fourier analysis in x restores Eq.(8.49).

We now suppose that the plasma is non-uniform such that $S(x) = 0$ at some particular value of x . The x origin is defined to be at this location and so corresponds to the location of the hybrid resonance. In order to be specific, we assume that we are dealing with a mode where $S > 0$ and $P < 0$, since S and P must have opposite signs for the cold plasma wave to propagate. Then, in the vicinity of $x = 0$ Taylor expansion of S gives $S = S'x$ so that Eq.(8.75) becomes

$$\epsilon_{th} \frac{d^4 \phi}{dx^4} + S' \frac{d\phi}{dx} + S' x \frac{d^2 \phi}{dx^2} - k_{\parallel}^2 P \phi = 0 \quad (8.76)$$

which has a coefficient which vanishes at $x = 0$ just like the Airy equation. Although Eq.(8.76) could be analyzed as it stands, it is better to clean it up somewhat by changing to a suitably chosen dimensionless coordinate. This is done by first defining

$$\xi = \frac{x}{\lambda} \quad (8.77)$$

where λ is a yet-undetermined characteristic length which will be chosen to provide maximum simplification of the coefficients. Replacing x by ξ in Eq.(8.76) gives

$$\frac{\epsilon_{th}}{\lambda^4} \frac{d^4 \phi}{d\xi^4} + \frac{S'}{\lambda} \frac{d\phi}{d\xi} + \frac{S'}{\lambda} \xi \frac{d^2 \phi}{d\xi^2} - k_{\parallel}^2 P \phi = 0. \quad (8.78)$$

This becomes

$$\frac{d^4 \phi}{d\xi^4} + \frac{d\phi}{d\xi} + \xi \frac{d^2 \phi}{d\xi^2} + \mu \phi = 0 \quad (8.79)$$

if λ is chosen to have $\epsilon_{th}/S'\lambda^3 = 1$ and we set $\mu = -k_{\parallel}^2 \lambda P/S'$. These choices imply

$$\lambda = \left(\frac{\epsilon_{th}}{S'} \right)^{1/3}, \quad \mu = -\frac{k_{\parallel}^2 P \epsilon_{th}^{1/3}}{(S')^{4/3}}. \quad (8.80)$$

Equation (8.79) describes a boundary layer problem having complicated behavior in the inner $|\xi| < 1$ region in the vicinity of the hybrid resonance and, presumably, simple WKB-like behavior in the outer $|\xi| \gg 1$ region away from the hybrid resonance. To solve this problem the technique discussed for the Airy equation will now be applied and generalized:

1. Laplace Transform: While Eq.(8.79) cannot be Fourier analyzed in the ξ direction, it can be Laplace transformed giving

$$p^4 \tilde{\phi}(p) + p \tilde{\phi}(p) - \frac{d}{dp} \left[p^2 \tilde{\phi}(p) \right] + \mu \tilde{\phi}(p) = 0 \quad (8.81)$$

or equivalently

$$\frac{1}{\left[p^2 \tilde{\phi}(p) \right]} \frac{d}{dp} \left[p^2 \tilde{\phi}(p) \right] = p^2 + \frac{1}{p} + \frac{\mu}{p^2}. \quad (8.82)$$

This has the solution

$$\tilde{\phi}(p) = A \exp(p^3/3 - \mu/p - \ln p) \quad (8.83)$$

where A is a constant. The inverse transform is

$$\phi(\xi) = A \int_C e^{f(p)} dp \quad (8.84)$$

where

$$f(p) = \frac{p^3}{3} - \frac{\mu}{p} - \ln(p) + p\xi. \quad (8.85)$$

2. Boundary conditions: Since Eq.(8.79) is a fourth-order ordinary differential equation, *four* independent solutions must exist with four associated independent choices for the contour C in Eq.(8.84). The appropriate contour is determined by the imposed physical boundary conditions which must be equal in number to the order of the equation. We consider a specific physical problem where an external antenna located at $\xi \gg 0$ generates a cold plasma wave propagating to the left. This physical prescription imposes the following four boundary conditions:

- (a) To the right of $\xi = 0$ there is a cold plasma wave with *energy* propagating to the left (i.e., towards the hybrid layer). It is important to take into account the fact that the group velocity is orthogonal to the phase velocity for these waves in which case the wave is backwards in either the x or the z direction. The dispersion of these waves is given in Eq.(6.102) and the group velocity in Eq.(6.104). A plot of $S(\omega)$ and $P(\omega)$ shows that $\partial S/\partial\omega > 0$ and $\partial P/\partial\omega > 0$. Thus, for the situation where $S > 0$ and $P < 0$ the x component of the wave phase and group velocities have opposite sign. Hence, the cold wave phase velocity must propagate to the *right* to be consistent with the boundary condition that cold wave energy is propagating to the *left*.
- (b) To the right of $\xi = 0$ there is *no* warm plasma wave propagating to the left (for the hot wave, energy and phase propagate in the same direction).
- (c) To the left of $\xi = 0$ the cold plasma evanescent mode vanishes as $\xi \rightarrow -\infty$.
- (d) To the left of $\xi = 0$ the hot plasma evanescent mode vanishes as $\xi \rightarrow -\infty$.

The question is: what happens at the hybrid layer? Possibilities include absorption of the incoming cold plasma wave (unlikely since there is no dissipation in this problem), reflection of the incoming cold plasma wave at the hybrid layer, or mode conversion.

3. Calculation of saddle points: The saddle points are the roots of

$$f'(p) = p^2 + \xi + \frac{\mu}{p^2} - \frac{1}{p} = 0. \quad (8.86)$$

For large ξ , these roots separate into two large roots (hot mode) given when the first two terms in Eq.(8.86) are balanced with each other and two small roots (cold mode) given by balancing the second and third terms. The large roots satisfy $p^2 = -\xi$ while the small roots satisfy $p^2 = -\mu/\xi$. For large ξ , the fourth term is small compared to the dominant terms for both large and small roots. The quantity f can be approximated

for large p as

$$\begin{aligned}
 f(p) &\simeq \frac{p^3}{3} + p\xi - \ln p \\
 &= p \left(\frac{p^2}{3} + \xi \right) - \ln p \\
 &= \frac{2}{3}p\xi - \ln p
 \end{aligned} \tag{8.87}$$

while for small p it can be approximated as

$$\begin{aligned}
 f(p) &\simeq p\xi - \frac{\mu}{p} - \ln p \\
 &= p \left(\xi - \frac{\mu}{p^2} \right) - \ln p \\
 &= p \left(\xi - \frac{\mu}{p^2} \right) - \ln p \\
 &= 2p\xi - \ln p.
 \end{aligned} \tag{8.88}$$

For $\xi > 0$ and large roots, the quantities p_l , $f(p_l)$ and $f''(p_l)$ are respectively

$$p_l = \pm(-\xi)^{1/2}, \quad f(p_l) = \mp \frac{2}{3}(-\xi)^{3/2} - \ln p_l, \quad f''(p_l) = \pm 2(-\xi)^{1/2}. \tag{8.89}$$

For $\xi > 0$ the corresponding quantities for the small roots are

$$p_s = \pm(-\mu/\xi)^{1/2}, \quad f(p_s) = \pm 2(-\xi\mu)^{1/2} - \ln p_s, \quad f''(p_s) = \mp 2 \frac{(-\xi)^{3/2}}{\mu^{1/2}}. \tag{8.90}$$

The Gaussian integrals corresponding to steepest descent paths over these $\xi > 0$ saddle points are

$$\text{large roots: } \int_{\text{vicinity of saddle}} e^{f(p)} dp = \sqrt{\frac{\mp\pi}{(-\xi)^{3/2}}} e^{\mp \frac{2}{3}(-\xi)^{3/2}} \tag{8.91}$$

$$\text{small roots: } \int_{\text{vicinity of saddle}} e^{f(p)} dp = \sqrt{\frac{\pm\pi}{(-\mu\xi)^{1/2}}} e^{\pm 2(-\xi\mu)^{1/2}} \tag{8.92}$$

where the logarithmic term in $f(p)$ has been taken into account. For $\xi < 0$, the large root quantities are

$$p_l = \pm|\xi|^{1/2}, \quad f(p_l) = \mp \frac{2}{3}|\xi|^{3/2} - \ln p_l, \quad f''(p_l) = \pm 2|\xi|^{1/2} \tag{8.93}$$

and the small root quantities are

$$p_s = \pm(\mu/|\xi|)^{1/2}, \quad f(p_s) = \mp 2(|\xi|\mu)^{1/2} - \ln p_s, \quad f''(p_s) = \mp 2 \frac{|\xi|^{3/2}}{\mu^{1/2}}. \tag{8.94}$$

4. Choice of contour path: For $\xi < 0$ and assuming $\mu > 0$ the saddle points giving solutions that vanish when $\xi \rightarrow -\infty$ are the saddle points with the upper (i.e., minus) sign chosen in the argument of the exponential. Hence, for $\xi < 0$ a contour must be chosen that passes through one or both of these saddle points. For $\xi > 0$ the upper sign corresponds to waves propagating to the left (i.e., towards the hybrid layer). Hence, we allow the upper sign (minus) for the small root (i.e., cold mode), but not for the large root since one of the boundary conditions was that there is no inward propagating hot plasma wave. To proceed further it is necessary to look at the topography of the real part of $f(p)$ for both signs of ξ ; see assignments.

From these plots it is seen that the correct joining is given by

$$\left\{ \begin{array}{l} i \frac{\exp(-\frac{2}{3}|\xi|^{3/2})}{|\xi|^{3/4}} \\ + \frac{\exp[-2\mu|\xi|^{1/2}]}{(|\xi|\mu)^{1/4}} \end{array} \right\} \iff \left\{ \begin{array}{l} \frac{\exp[\frac{2}{3}(i\xi)^{3/2}]}{i^{1/2}\xi^{3/4}} \\ + i^{1/2} \frac{\exp[2i(\mu\xi)^{1/2}]}{(\xi\mu)^{1/4}} \end{array} \right\} \quad (8.95)$$

evanescent side, $\xi < 0$

propagating side, $\xi > 0$

which shows that a cold wave with energy propagating into the $S = 0$ layer is converted into a hot wave that propagates back out.

5. WKB connection: The quantities in Eq.(8.95) can be expressed as integrals having the same form as WKB solutions. For example, the cold propagating term can be written as

$$\begin{aligned} \frac{\exp[2i(\mu\xi)^{1/2}]}{(\xi\mu)^{1/4}} &= \sqrt{2} \frac{\exp[i \int_0^\xi (\mu/\xi')^{1/2} d\xi']}{\sqrt{\int_0^\xi (\mu/\xi')^{1/2} d\xi'}} \\ &= \sqrt{2} \frac{\exp[i \int_0^x (-k_z^2 P/S)^{1/2} dx']}{\sqrt{\int_0^x (-k_z^2 P/S)^{1/2} dx'}} \end{aligned} \quad (8.96)$$

where the last form is clearly the WKB solution. A similar identification exists for the hot plasma mode, so that Eq. (8.95) can also be written in terms of the WKB solutions.

This is just one example of mode conversion; other forms also occur in different contexts but a similar analysis may be used and similar joining conditions are obtained. A curious feature of the mode conversion analysis is that the differential equation is never explicitly solved near $\xi = 0$; all that is done is match asymptotic solutions for the region where ξ is large and positive to the solutions for the region where ξ is large and negative.

8.6 Drift waves

Only textbook plasmas are uniform — real plasmas have both finite extent and pressure gradients. As an example, consider an azimuthally symmetric cylindrical plasma immersed in a strong axial magnetic field as sketched in Fig.8.3. Particles stream freely in the axial

direction but are constrained to make Larmor orbits in the perpendicular direction. Since the concept of pressure gradient has no meaning for an individual particle, consideration of the effect of pressure gradients requires a fluid or Vlasov point of view. This will be done first using a two-fluid analysis, then using a Vlasov analysis.

From the two-fluid point of view, the radial pressure gradient implies an equilibrium force balance

$$0 = q_\sigma \mathbf{u}_\sigma \times \mathbf{B} - n_\sigma^{-1} \nabla (n_\sigma \kappa T_\sigma). \quad (8.97)$$

Solving Eq.(8.97) for \mathbf{u}_σ shows that each species has a steady-state perpendicular motion at the *diamagnetic drift velocity*

$$\mathbf{u}_{d\sigma} = - \frac{\nabla (n_\sigma \kappa T_\sigma) \times \mathbf{B}}{q_\sigma n_\sigma B^2} \quad (8.98)$$

which is in the azimuthal direction. The corresponding diamagnetic drift current is

$$\begin{aligned} \mathbf{J}_d &= \sum_\sigma n_\sigma q_\sigma \mathbf{u}_{d\sigma} \\ &= - \frac{1}{B^2} \sum_\sigma \nabla (n_\sigma \kappa T_\sigma) \times \mathbf{B} \\ &= - \frac{1}{B^2} \nabla P \times \mathbf{B} \end{aligned} \quad (8.99)$$

which is just the azimuthal current associated with the MHD equilibrium equation $\mathbf{J} \times \mathbf{B} = \nabla P$ where $P = P_i + P_e$.

The electron and ion diamagnetic drift velocities thus provide the current needed to establish the magnetic force which balances the MHD pressure gradient. It turns out that magnetized plasmas with pressure gradients are unstable to a class of electrostatic modes called ‘drift’ waves. These modes exist in the same frequency regime as MHD but do not appear in standard MHD models, since standard MHD models do not provide enough detail on the difference between electron and ion dynamics.

From the particle point of view, the diamagnetic velocity is entirely fictitious because no particle actually moves at such a velocity. The diamagnetic drift velocity is nevertheless quite genuine from the fluid point of view and so a fluid-based wave analysis must linearize about an equilibrium that includes this equilibrium drift. As will be seen later, the Vlasov point of view confirms and extends the conclusions of the fluid theory, providing care is taken to start with an equilibrium velocity distribution function which is both valid and consistent with existence of a pressure gradient.

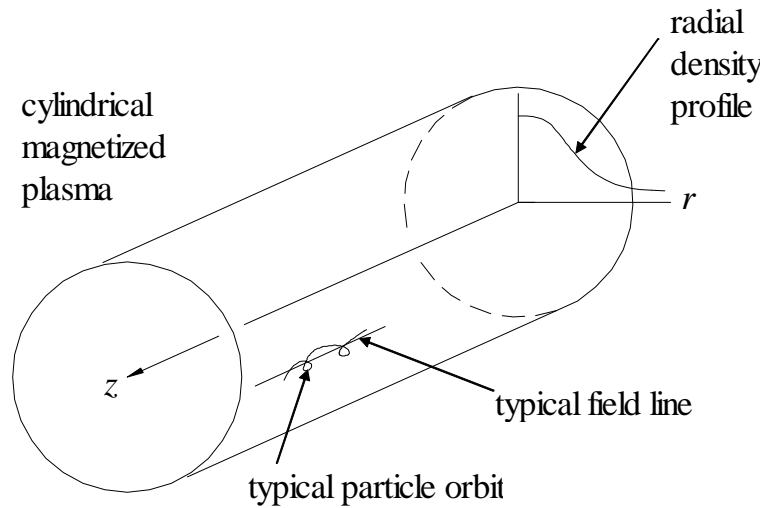


Figure 8.3: Cylindrical magnetized plasma with radial density gradient

Drift waves will be examined using three progressively more realistic points of view. These are:

1. A collisionless two-fluid model where ions are assumed to be cold and electrons are assumed to be hot. This model establishes existence of the mode and provides a derivation for the intrinsic frequency, but provides no information regarding stability.
2. A collisional two-fluid model which shows that *collisions* destabilize drift waves.
3. A Vlasov model including both finite ion temperature and net axial current. This model shows that both Landau damping and axial currents destabilize drift waves.

Drift waves involve physically distinctive ion and electron motions, three-dimensional geometry, magnetized warm plasma effects, pressure gradients, collisionality, and Landau damping/instability. Drift waves are often of practical importance because they are so easily driven unstable. While real plasmas have geometry resembling Fig.8.3, the cylindrical geometry will now be replaced by Cartesian geometry to make the analysis more straightforward.

Using Cartesian geometry, the equilibrium magnetic field is assumed to be in the z direction and the new feature, an exponential density gradient in the x direction, represents the pressure gradient. The x direction thus corresponds to the r direction of cylindrical geometry, and the y direction corresponds to the θ direction. The y and z directions, but not the x direction, are ignorable coordinates, and so the governing equations may be Fourier-transformed in the y and z directions, but not in the x direction.

8.6.1 Simple two-fluid model of drift waves

The plasma is assumed to have the exponential density gradient

$$n \sim \exp(-x/L) \quad (8.100)$$

where L is called the density-gradient scale length. We consider electrostatic, extremely low frequency ($\omega \ll \omega_{ci}$) waves having the potential perturbation

$$\phi_1 = \tilde{\phi} \exp(ik_y y + ik_z z - i\omega t). \quad (8.101)$$

The parallel phase velocity is assumed to lie in the range $v_{Ti} \ll \omega/k_z \ll v_{Te}$ so that ions are adiabatic and electrons are isothermal (this is the same regime as ion acoustic waves). The parallel and perpendicular wavelengths are both assumed to be much longer than the electron Debye length, so that the plasma may be considered quasi-neutral and so have $n_i \simeq n_e$. Since $\omega/k_z \ll v_{Te}$, the parallel component of the electron equation of motion is simply

$$0 \simeq -q_e \frac{\partial \phi_1}{\partial z} - \frac{1}{n_e} \frac{\partial}{\partial z} (n_e \kappa T_e) \quad (8.102)$$

which leads to a Boltzmann electron density,

$$n_e = n_{e0} \exp(-q_e \phi_1 / \kappa T_e). \quad (8.103)$$

Assuming ϕ_1 is small, linearization of this Boltzmann electron density gives the first-order electron density

$$\frac{n_{e1}}{n_{e0}} = -\frac{q_e \phi_1}{\kappa T_e}. \quad (8.104)$$

Since $\omega/k_z \gg v_{Ti}$, ions may be considered cold to first approximation and the zero-pressure limit of the ion equation of motion characterizes ion dynamics. Furthermore, since $\omega \ll \omega_{ci}$ the lowest-order perpendicular ion motion is just the $\mathbf{E} \times \mathbf{B}$ drift so

$$\mathbf{u}_{i1} = \frac{-\nabla \phi_1 \times \mathbf{B}}{B^2} = -\frac{ik_y \phi_1}{B} \hat{x}. \quad (8.105)$$

Since the $E \times B$ drift is in the x direction, it is *in the direction of the density gradient* and so this drift leads to an ion density perturbation because of a convective interaction with the equilibrium density gradient. The ion density perturbation is found by linearizing the ion continuity equation

$$\frac{\partial n_{i1}}{\partial t} + \mathbf{u}_{i1} \cdot \nabla n_{i0} + n_{i1} \nabla \cdot \mathbf{u}_{i1} = 0. \quad (8.106)$$

After noting that $\nabla \cdot \mathbf{u}_{i1} = 0$, substitution for \mathbf{u}_{i1} in the convective term gives

$$\frac{n_{i1}}{n_{i0}} = \frac{k_y \phi_1}{\omega L B}. \quad (8.107)$$

The density perturbation results from the ion $\mathbf{E} \times \mathbf{B}$ drift causing the ions with their density gradient to slosh back and forth in the x direction so that a stationary observer at a fixed point x sees oscillations of the ion density.

Quasi-neutrality means that the electron and ion density perturbations densities must be almost exactly equal although electrons and ions are governed by entirely different physics.

Equating the electron and ion perturbed densities, respectively given by Eqs.(8.104) and (8.107), provides the most basic form of the drift wave dispersion relation,

$$\omega = -\frac{k_y \kappa T_e}{q_e L B} = k_y u_{de}, \quad (8.108)$$

where

$$u_{de} = -\kappa T_e / q_e L B \quad (8.109)$$

is the electron diamagnetic drift velocity given by Eq.(8.97). Equation (8.108) describes a normal mode where Boltzmann electron density perturbations caused by isothermal electron motion along field lines neutralize ion density perturbations caused by ion $\mathbf{E} \times \mathbf{B}$ motion sloshing the x -dependent equilibrium density profile in the x direction. This basic dispersion relation provides no information about the mode stability because collisions and Landau damping have not yet been considered. The wave phase velocity ω/k_y is equal to the electron diamagnetic drift velocity given by Eq.(8.98). This dispersion relation has the interesting feature that it does not depend on the mass of either species; this is because neither the electron Boltzmann dependence nor the ion $E \times B$ drift depend on mass. This basic dispersion is the building block for the more complicated models to be considered later, and it is conventional to define the ‘drift frequency’

$$\omega^* = k_y u_{de} \quad (8.110)$$

which will appear repeatedly in the more complicated models. The basic dispersion is therefore simply $\omega = \omega^*$ (the asterisk should not be confused with complex conjugate).

8.6.2 Two-fluid drift wave model with collisions

The next level of sophistication involves assuming that the plasma is mildly collisional so that the electron equation of motion is now

$$m_e \frac{d\mathbf{u}_e}{dt} = q_e (-\nabla\phi + \mathbf{u}_e \times \mathbf{B}) - \frac{1}{n_e} \nabla (n_e \kappa T_e) - \nu_{ei} m_e (\mathbf{u}_e - \mathbf{u}_i). \quad (8.111)$$

The collision frequency is assumed to be small compared to the electron cyclotron frequency. Because $\omega/k_z \ll v_{Te}$, the electron inertia term on the left hand side is negligible compared to the electron pressure gradient term on the right hand side and so the parallel component of the electron equation reduces to

$$0 = -q_e \frac{\partial\phi}{\partial z} - \frac{\kappa T_e}{n_e} \frac{\partial n_e}{\partial z} - \nu_{ei} m_e u_{ez}; \quad (8.112)$$

the ion parallel velocity has been dropped since it is negligible compared to the electron parallel velocity. After linearization and assuming perturbed quantities have a space-time dependence given by Eq.(8.101), Eq.(8.112) can be solved to give the parallel electron velocity

$$u_{ez} = -\frac{ik_z \kappa T_e}{\nu_{ei} m_e} \left(\frac{q_e \phi_1}{\kappa T_e} + \frac{n_{e1}}{n_{e0}} \right). \quad (8.113)$$

It is seen that in the limit of no collisions, this reverts to the Boltzmann result, Eq.(8.104).

As in the previous section, quasi-neutrality is invoked so that the dispersion relation is obtained by equating the perturbed electron and ion densities. Equation (8.113) together

with the continuity equation gives the perturbed electron density, provided the electron perpendicular velocity is also known. Since it has been assumed that $\omega_{ce} \gg \nu_{ei}$, the magnetic force term in Eq.(8.111) is much greater than the perpendicular component of the collision term. The perpendicular component of the electron equation of motion is therefore

$$0 = q_e (-\nabla_{\perp} \phi + \mathbf{u}_e \times \mathbf{B}) - \frac{1}{n_e} \nabla_{\perp} (n_e \kappa T_e). \quad (8.114)$$

In previous derivations the continuity equation was typically linearized right away, but here it turns out to be computationally advantageous to postpone linearization and instead solve Eq.(8.114) as it stands for the perpendicular electron flux to obtain

$$\mathbf{\Gamma}_{e\perp} = n_e \mathbf{u}_{e\perp} = -\frac{n_e \nabla \phi \times \mathbf{B}}{B^2} - \frac{1}{q_e B^2} \nabla (n_e \kappa T_e) \times \mathbf{B}. \quad (8.115)$$

Using the vector identities $\nabla \cdot (\nabla \phi \times \mathbf{B}) = 0$ and $\nabla \cdot [\nabla (n_e \kappa T_e) \times \mathbf{B}] = 0$ it is seen that the divergence of the perpendicular electron flux is

$$\nabla \cdot \mathbf{\Gamma}_{e\perp} = -\nabla n_e \cdot \frac{\nabla \phi \times \mathbf{B}}{B^2}. \quad (8.116)$$

The electron continuity equation can be expressed as

$$\frac{\partial n_e}{\partial t} + \frac{\partial}{\partial z} (n_e u_{ez}) + \nabla \cdot \mathbf{\Gamma}_{e\perp} = 0, \quad (8.117)$$

and, after substitution for the perpendicular electron flux, this becomes

$$\frac{\partial n_e}{\partial t} + \frac{\partial}{\partial z} (n_e u_{ez}) - \nabla n_e \cdot \frac{\nabla \phi \times \mathbf{B}}{B^2} = 0. \quad (8.118)$$

At this stage of the derivation it is now appropriate to linearize the continuity equation which becomes

$$\frac{\partial n_e}{\partial t} + n_{e0} \frac{\partial u_{ez1}}{\partial z} - \frac{dn_{e0}}{dx} \hat{x} \cdot \frac{\nabla \phi_1 \times \mathbf{B}}{B^2} = 0. \quad (8.119)$$

Substituting for ϕ_1 using Eq.(8.101), and using Eq.(8.113) for u_{z1} gives

$$\frac{n_{e1}}{n_{e0}} \left(-i\omega + \frac{k_z^2 \kappa T_e}{\nu_{ei} m_e} \right) + \frac{q_e \phi_1}{T_e} \left(\frac{k_z^2 \kappa T_e}{\nu_{ei} m_e} + \frac{ik_y T_e}{q_e B L} \right) = 0 \quad (8.120)$$

which may be solved to give the sought-after electron density perturbation

$$\frac{n_{e1}}{n_{e0}} = -\frac{q_e \phi_1}{T_e} \frac{\left(-i\omega^* + \frac{1}{\tau_{\parallel}} \right)}{\left(-i\omega + \frac{1}{\tau_{\parallel}} \right)}. \quad (8.121)$$

Here

$$\tau_{\parallel} = \nu_{ei} m_e / k_z^2 T_e \quad (8.122)$$

is the nominal time required for electrons to diffuse a distance of the order of a parallel wavelength. This is because the parallel collisional diffusion coefficient scales as $D_{\parallel} \sim (\text{random step})^2 / (\text{collision period}) \sim T_e / \nu_{ei} m_e$ and according to the diffusion equation

the distance diffused in time t is given by $z^2 \sim 4D_{\parallel}t$. Equation (8.121) shows that in the limit $\tau_{\parallel} \rightarrow 0$, the electron density perturbation reverts to being Boltzmann, but for finite τ_{\parallel} , a phase lag occurs between n_{e1} and ϕ_1 .

The next step is to calculate the ion density perturbation. The ion equation of motion is

$$m_i \frac{d\mathbf{u}_i}{dt} = q_i (-\nabla\phi + \mathbf{u}_i \times \mathbf{B}) - \nu_{ie} m_i (\mathbf{u}_i - \mathbf{u}_e); \quad (8.123)$$

because the ions are heavy, the left hand side inertial term must now be retained. The ions are assumed to be cold and the ion inertial term is assumed to be much larger than the collisional term so that the parallel component of the linearized Eq.(8.123) is

$$u_{iz1} = \frac{k_z q_i \phi_1}{\omega m_i} = \frac{k_z c_s^2 q_i \phi_1}{\omega \kappa T_e}. \quad (8.124)$$

Again assuming that the inertial term is much larger than the collisional term, the linearized perpendicular ion equation becomes

$$m_i \frac{d\mathbf{u}_{i\perp}}{dt} = q_i (-\nabla\phi_{\perp} + \mathbf{u}_{i\perp} \times \mathbf{B}) \quad (8.125)$$

which can be solved to give the perpendicular velocity as a sum of an $\mathbf{E} \times \mathbf{B}$ drift and a polarization drift, i.e.,

$$\mathbf{u}_{i\perp} = \frac{-\nabla\phi \times \mathbf{B}}{B^2} + \frac{m_i}{q_i B^2} \frac{d}{dt} (-\nabla\phi). \quad (8.126)$$

The polarization drift is retained in the ion but not the electron equation, because polarization drift is proportional to mass. The perpendicular ion flux is

$$\mathbf{\Gamma}_{i\perp} = \frac{-n_i \nabla\phi \times \mathbf{B}}{B^2} + \frac{n_i m_i}{q_i B^2} \frac{d}{dt} (-\nabla_{\perp}\phi) \quad (8.127)$$

which has a divergence

$$\nabla \cdot \mathbf{\Gamma}_{i\perp} = -\nabla n_i \cdot \frac{\nabla\phi \times \mathbf{B}}{B^2} - \nabla \cdot \left(\frac{n_i m_i}{q_i B^2} \frac{d}{dt} (\nabla_{\perp}\phi) \right). \quad (8.128)$$

Substitution of Eq.(8.128) and (8.124) into the ion continuity equation, linearizing, and solving for the ion density perturbation gives

$$\begin{aligned} \frac{n_{i1}}{n_{i0}} &= \left[\frac{k_z^2 c_s^2}{\omega^2} + \frac{q_e}{q_i} \frac{k_y \kappa T_e}{\omega q_e L B} - \frac{m_i \kappa T_e}{q_i^2 B^2} k_y^2 \right] \frac{q_i \phi_1}{T_e} \\ &= \left[\frac{k_z^2 c_s^2}{\omega^2} - \frac{q_e}{q_i} \frac{\omega^*}{\omega} - k_y^2 \rho_s^2 \right] \frac{q_i \phi_1}{T_e} \end{aligned} \quad (8.129)$$

where $\rho_s^2 \equiv \kappa T_e / m_i \omega_{ci}^2$ is a fictitious ion Larmor orbit defined using the electron instead of ion temperature. The fictitious length ρ_s^2 is analogous to the fictitious velocity $c_s^2 = \kappa T_e / m_i$ that occurred in the analysis of ion acoustic waves.

Since the plasma is quasi-neutral, the normalized electron and ion density perturbations must be the same. Equating the normalized density perturbations obtained from Eq.(8.121) and (8.129) gives

$$\frac{\left(-i\omega^* + \frac{1}{\tau_{\parallel}}\right)}{\left(-i\omega + \frac{1}{\tau_{\parallel}}\right)} = \frac{\omega^*}{\omega} + \frac{k_z^2 c_s^2}{\omega^2} - k_y^2 \rho_s^2. \quad (8.130)$$

For simplicity it is assumed here that $q_i/q_e = -1$, which is the situation for low temperature plasmas where the ions are too cold to be multiply ionized ($q_i/q_e = -1$ is, of course, always true for hydrogen plasmas). It is also assumed that the collision frequency is sufficiently small to have $\omega\tau_{\parallel} = \omega\nu_{ei}m_e/k_z^2 T_e \ll 1$ and that ω is of the order of ω^* ; the self-consistency of these assumptions will be checked later. The left hand side of Eq.(8.130) can now be expanded using the binomial theorem to obtain the collisional drift wave dispersion relation

$$D(\omega, k_y, k_z) = 1 - \frac{\omega^*}{\omega} + k_y^2 \rho_s^2 - \frac{k_z^2 c_s^2}{\omega^2} + i(\omega - \omega^*)\tau_{\parallel} = 0. \quad (8.131)$$

This dispersion relation shows that drift waves have an association with ion acoustic waves since in the limit $k_y^2 \rho_s^2 \rightarrow 0$, the real part of the dispersion becomes

$$1 - \frac{\omega^*}{\omega} - \frac{k_z^2 c_s^2}{\omega^2} = 0 \quad (8.132)$$

which becomes an ion-acoustic wave in the limit of no equilibrium pressure gradient. Equation (8.132) has two roots

$$\omega = \frac{\omega^* \pm \sqrt{(\omega^*)^2 + 4k_z^2 c_s^2}}{2} \quad (8.133)$$

which for small $k_z c_s$ are

1. $\omega = \omega^*$ and $\omega = -|k_z c_s|$ if $\omega^* > 0$
2. $\omega = \omega^*$ and $\omega = |k_z c_s|$ if $\omega^* < 0$.

Thus, the drift mode is a distinct mode compared to the ion acoustic wave and its parallel phase velocity is much faster than the ion acoustic wave since the drift wave occurs in the limit $\omega/k_z \gg c_s$.

We now address the important question of the stability properties of Eq.(8.131). To do this, k_z is assumed to be sufficiently small to have $k_z c_s \ll \omega$ so that the dispersion describes the drift mode and not the ion acoustic mode. The real part of the dispersion is then set to zero to obtain the real part of the frequency

$$\omega_r = \frac{\omega^*}{1 + k_y^2 \rho_s^2} \quad (8.134)$$

showing that the actual frequency of the collisional drift wave is smaller than ω^* , but as assumed is of the same order, provided $k_y^2 \rho_s^2$ is not larger than order unity. The $k_y^2 \rho_s^2$ dependence results from ion polarization drift, an effect which was neglected in the initial simple model. The assumption $\omega\tau_{\parallel} = \omega\nu_{ei}m_e/k_z^2 T_e \ll 1$ implies $k_y \nu_{ei}/k_z^2 L\omega_{ce} \ll 1$

which is true provided the ratio ν_{ei}/ω_{ce} is sufficiently small for a given geometric factor $k_y/k_z^2 L$. The imaginary part of the frequency is

$$\omega_i = -\frac{D_i}{(\partial D_r/\partial \omega)_{\omega=\omega_r}} = -\frac{(\omega - \omega^*)\tau_{\parallel}}{\omega^*/\omega_r^2} = \omega^* \frac{k_y^2 \rho_s^2 \omega^* \tau_{\parallel}}{(1 + k_y^2 \rho_s^2)^3} \quad (8.135)$$

and has several important features:

1. ω_i is positive so collisional drift waves are *always unstable*.
2. ω_i is proportional to τ_{\parallel} so that modes with the smallest k_z and hence the fastest parallel phase velocities are the most unstable, subject to the proviso that $\omega\tau_{\parallel} \ll 1$ is maintained. This increase of growth rate with k_z^{-1} or equivalently parallel wavelength means that drift waves typically have the longest possible parallel wavelength consistent with boundary conditions. For example, a linear plasma of finite axial extent with grounded conducting end walls has the boundary condition that $\phi_1 = 0$ at both end walls; the longest allowed parallel wavenumber is π/h where h is the axial length of the plasma (i.e., half a wavelength is the minimum number of waves that can be fitted subject to the boundary condition).
3. Collisions make the wave unstable since $\tau_{\parallel} \sim \nu_{ei}$.
4. ω_i is proportional to the factor $k_y^2 \rho_s^2 / (1 + k_y^2 \rho_s^2)^3$ which has its maximum value when $k_y \rho_s$ is of order unity.
5. ω_i is proportional to L^{-2} ; for a realistic cylindrical plasma (cf. Fig.8.3) the density is uniform near the axis and has a gradient near the edge (e.g., a Gaussian density profile where $n(r) \sim \exp(-r^2/L^2)$). The density gradient is localized near the edge of the plasma and so drift waves should have the largest growth rate near the edge. Drift waves in real plasmas are typically observed to have maximum amplitude in the region of maximum density gradient.

The free energy driving drift waves is the pressure gradient and so the drift waves might be expected tend to deplete their energy source by flattening out the pressure gradient. This indeed happens and in particular, the nonlinear behavior of drift waves reduces the pressure gradient. Drift waves pump plasma from regions of high pressure to regions of low pressure. This pumping can be calculated by considering the time-averaged, nonlinear, x -directed particle flux associated with drift waves, namely

$$\Gamma_x = \langle \text{Re} n_1 \text{Re} u_{1x} \rangle = \frac{1}{2} \text{Re} (n_1 u_{1x}^*). \quad (8.136)$$

The species subscript σ has been omitted here, because to lowest order both species have the same u_{1x} given by the $E \times B$ drift, i.e.,

$$u_{1x} = \hat{x} \cdot \frac{-\nabla \phi_1 \times \mathbf{B}}{B^2} = -i k_y \phi_1 / B. \quad (8.137)$$

Being careful to remember that ω^* is a real quantity (this is a conventional, but confusing notation), Eqs.(8.121) and (8.137) are substituted into Eq.(8.136) to obtain the wave-induced particle flux

$$\begin{aligned}
\Gamma_x &= \frac{1}{2} \operatorname{Re} \left[-\frac{n_0 q_e}{T_e} (1 - i(\omega^* - \omega)\tau_{\parallel}) \frac{ik_y |\phi_1|^2}{B} \right] \\
&= -\frac{1}{2} \operatorname{Re} \left[\frac{n_0 q_e}{T_e} (\omega^* - \omega)\tau_{\parallel} \frac{k_y |\phi_1|^2}{B} \right] \\
&= \left(\frac{k_y^2 \rho_s^2}{1 + k_y^2 \rho_s^2} \right) \frac{k_y^2 |\phi_1|^2}{2LB^2} \frac{\nu_{ei} n_0 m_e}{k_z^2 T_e} \\
&= -D_{nl} \frac{dn_0}{dx}.
\end{aligned} \tag{8.138}$$

Thus, it is seen that collisional drift waves cause an outward diffusion of plasma with a nonlinear wave-induced diffusion coefficient

$$D_{nl} = \left(\frac{k_y^2 \rho_s^2}{1 + k_y^2 \rho_s^2} \right) \frac{k_y^2 |\phi_1|^2}{2B^2} \frac{\nu_{ei} m_e}{k_z^2 T_e}. \tag{8.139}$$

This diffusion coefficient has a proportionality similar to ω_i . The drift wave thus has the following properties: (i) the pressure gradient provides free energy and also an equilibrium where drift waves are a normal mode, (ii) collisions allow the drift wave to feed on the available free energy and grow, (iii) nonlinear diffusion flattens the pressure gradient thereby depleting the free energy and also undermining the confining effect of the magnetic field. A nonlinear saturated amplitude can result if some external source continuously replenishes the pressure gradient.

It was shown earlier that the most unstable drift waves are those having $k_y \rho_s$ of order unity. This property can be adapted to the more physically realistic situation of a cylindrical plasma by realizing that in a cylindrical plasma k_y is replaced by m/r where m is the azimuthal mode number. Periodicity in θ forces m to be an integer. If the most unstable m is a small integer, then the drift waves tend to be coherent, but if m is a large integer, many azimuthal wavelengths fit into the circumference of the cylinder. In this case, the periodicity condition is only a weak constraint and the waves typically become turbulent. Large m corresponds to small ρ_s which occurs when the magnetic field is strong. Thus, plasmas with strong magnetic fields tend to have turbulent, short perpendicular wavelength drift waves, whereas plasmas with weak magnetic fields have coherent, long perpendicular wavelength drift waves.

Drift wave turbulence has been found to be the main reason why the radial diffusion in tokamak magnetic plasma confinement devices is much worse than can be explained by simple random walks due to particle collisions.

8.6.3 Vlasov theory of drift waves: collisionless drift waves

Drift waves also exist when the plasma is so hot that the collision frequency becomes insignificant and the plasma can be considered collisionless. The previous section showed that a collision-induced phase lag between the density and potential fluctuations produces a destabilizing imaginary term in the dispersion relation. The analysis of collisionless plasma waves showed that Landau damping also causes a phase shift between the density

and potential fluctuations resulting in an imaginary term in the dispersion relation. Also, since Vlasov analysis showed that a relative motion between electrons and ions (i.e., a net current) destabilizes ion acoustic waves, it is reasonable to expect that current-driven destabilization could occur for drift waves.

The Vlasov analysis of drift waves is less intuitive than the fluid analysis, but the reward for abstraction is a more profound model. As in the fluid analysis, the plasma is assumed to have a uniform equilibrium magnetic field $\mathbf{B} = B\hat{z}$, an x -directed density gradient given by Eq.(8.100), and a perturbed potential given by Eq.(8.101). In a sense the Vlasov analysis is simpler than the fluid analysis, because the Vlasov analysis involves a modest extension of the warm plasma electrostatic Vlasov model discussed in Section 8.1. As before, the perturbed distribution function is evaluated by integrating along the unperturbed orbits, i.e.,

$$f_{\sigma 1}(\mathbf{x}, \mathbf{v}, t) = \int_{-\infty}^t dt' \left[\frac{q_{\sigma}}{m_{\sigma}} \nabla \phi_1 \cdot \frac{\partial f_{\sigma 0}}{\partial \mathbf{v}} \right]_{\mathbf{x}=\mathbf{x}(t'), \mathbf{v}=\mathbf{v}(t')}. \quad (8.140)$$

The new feature here is that the equilibrium distribution function must incorporate the assumed density gradient.

A first instinct would be to accomplish this by simply multiplying the Maxwellian distribution function of Section 8.1 by the factor $\exp(-x/L)$ so that the assumed equilibrium distribution function would be $f_{\sigma 0}(x, \mathbf{v}) = (\pi v_{T\sigma})^{-3/2} \exp(-v^2/v_{T\sigma}^2 - x/L)$. This approach turns out to be wrong because $f_{\sigma 0}(x, \mathbf{v}) = (\pi v_{T\sigma})^{-3/2} \exp(-v^2/v_{T\sigma}^2 - x/L)$ is *not* a function of the constants of the motion and so is not a solution of the equilibrium Vlasov equation.

What is needed is some constant of the motion which includes the parameter x . The equilibrium distribution function could then be constructed from this constant of the motion and arranged to have the desired x -dependence. The appropriate constant of the motion is the canonical momentum in the y direction, namely

$$P_y = m_{\sigma} v_y + q_{\sigma} A_y = m_{\sigma} v_y + q_{\sigma} B_z x = \left(\frac{v_y}{\omega_{c\sigma}} + x \right) q_{\sigma} B_z \quad (8.141)$$

since $B_z = \partial A_y / \partial x$. Multiplying the original Maxwellian by the factor $\exp[-(v_y/\omega_{c\sigma} + x)/L]$ produces the desired spatial dependence while simultaneously satisfying the requirement that the distribution function depends only on constants of the motion. Note that P_y is a constant of the motion because y is an ignorable coordinate.

It turns out that z -directed currents can also destabilize collisionless drift waves, much like currents provide free energy which can destabilize ion-acoustic waves. Since it takes little additional effort to include this possibility, a z -directed current will also be assumed so that electrons and ions are assumed to have distinct mean velocities $u_{\sigma z}$. In a frame moving with velocity $u_{\sigma z}$ the species σ is thus assumed to have a distribution function $\sim \exp[-mv'^2/2 - (v_y/\omega_{c\sigma} + x)/L]$ where $\mathbf{v}' = \mathbf{v} - u_{\sigma z} \hat{z}$ is the velocity in the moving frame. This is a valid solution to the equilibrium Vlasov equation, since both the energy $mv'^2/2$ and the y -direction canonical momentum $(v_y/\omega_{c\sigma} + x)/L$ are constants of the

motion. The appropriately normalized lab frame distribution function is

$$f_{\sigma 0}(x, \mathbf{v}) = \frac{n_{0\sigma}}{\pi^{3/2} v_{T\sigma}^3} \exp \left[-(\mathbf{v} - u_{\sigma z} \hat{z})^2 / v_{T\sigma}^2 - (v_y / \omega_{c\sigma} + x) / L - \left(\frac{v_T}{2\omega_c L} \right)^2 \right] \quad (8.142)$$

where the normalization factor $\exp \left(- (v_T / 2\omega_c L)^2 \right)$ has been inserted so that the zeroth moment of $f_{\sigma 0}$ gives the density. The necessity of this factor is made evident by completing the squares for the velocities and writing Eq.(8.142) in the equivalent form

$$f(x, \mathbf{v}) = \frac{n_0}{\pi^{3/2} v_T^3} \exp \left(- \left[\frac{v_x^2 + \left(v_y + \frac{v_T}{2\omega_c L} \right)^2 + (v_z - u_{\sigma z})^2}{v_T^2} \right] - \frac{x}{L} \right). \quad (8.143)$$

The term $v_y / \omega_{c\sigma}$ which crept into Eq.(8.142) because of the seemingly abstract requirement of having the distribution function depend on the constant of the motion P_y corresponds to the fluid theory equilibrium diamagnetic drift. This correspondence is easily seen by calculating the mean y -direction velocity (i.e. first moment of Eq.(8.142)) and finding that the $v_y / \omega_{c\sigma}$ term results in a fluid velocity u_y which is precisely the diamagnetic velocity given by Eq.(8.98).

We now insert Eq.(8.142) in Eq.(8.140) to calculate the perturbed distribution function. The unperturbed particle orbits are the same as in Section 8.1 because the concepts of both density gradient and axial current result from averaging over a distribution of many particles and so have no meaning for an individual particle. The integration over unperturbed orbits is thus identical to that of Section 8.1, except that a different equilibrium distribution function is used.

The essence of the calculation is in the term

$$\begin{aligned} \nabla \phi_1 \cdot \frac{\partial f_{\sigma 0}}{\partial \mathbf{v}} &= i\phi_1 \mathbf{k} \cdot \frac{\partial f_{\sigma 0}}{\partial \mathbf{v}} \\ &= -i\tilde{\phi} e^{i\mathbf{k} \cdot \mathbf{x}(t) - i\omega t} \left[\frac{2\mathbf{k} \cdot \mathbf{v}}{v_{T\sigma}^2} - \frac{2k_z u_{\sigma z}}{v_{T\sigma}^2} + \frac{k_y}{\omega_{c\sigma} L} \right] f_{\sigma 0} \end{aligned} \quad (8.144)$$

which causes Eq.(8.140) to become

$$\begin{aligned}
f_{\sigma 1}(\mathbf{x}, \mathbf{v}, t) &= -\frac{q_{\sigma} \tilde{\phi} f_{\sigma 0}}{m_{\sigma}} \int_{-\infty}^t dt' e^{i\mathbf{k} \cdot \mathbf{x}(t') - i\omega t'} \left[\frac{2i\mathbf{k} \cdot \mathbf{v}}{v_{T\sigma}^2} - \frac{2ik_z u_{\sigma z}}{v_{T\sigma}^2} + \frac{ik_y}{\omega_{c\sigma} L} \right] \\
&= -\frac{q_{\sigma} \tilde{\phi} f_{\sigma 0}}{m_{\sigma}} \int_{-\infty}^t dt' \left\{ \frac{2e^{-i\omega t'}}{v_{T\sigma}^2} \left[\frac{d}{dt'} e^{i\mathbf{k} \cdot \mathbf{x}(t')} \right] - \left(\frac{2ik_z u_{\sigma z}}{v_{T\sigma}^2} - \frac{ik_y}{\omega_{c\sigma} L} \right) e^{i\mathbf{k} \cdot \mathbf{x}(t') - i\omega t'} \right\} \\
&= -\frac{2q_{\sigma} \tilde{\phi} f_{\sigma 0}}{m_{\sigma} v_{T\sigma}^2} \left[e^{i\mathbf{k} \cdot \mathbf{x}(t) - i\omega t} + i(\omega - k_z u_{\sigma z} - \omega_{\sigma}^*) \int_{-\infty}^t dt' e^{i\mathbf{k} \cdot \mathbf{x}(t') - i\omega t'} \right];
\end{aligned} \tag{8.145}$$

here

$$\frac{k_y v_{T\sigma}^2}{2\omega_{c\sigma} L} = \frac{k_y k T}{qBL} = -\omega_{\sigma}^* \tag{8.146}$$

has been used as a generalization of Eq.(8.110). The rest of the analysis is as before and gives the dispersion relation

$$1 + \sum_{\sigma} \frac{1}{k^2 \lambda_{D\sigma}^2} \left[1 + \frac{(\omega - k_z u_{\sigma z} - \omega_{\sigma}^*)}{k_z v_{T\sigma}} \sum_{n=-\infty}^{\infty} I_n(\Lambda_{\sigma}) e^{-\Lambda_{\sigma}} Z(\alpha_{n\sigma}) \right] = 0 \tag{8.147}$$

where as before $\Lambda_{\sigma} = k_{\perp}^2 r_{L\sigma}^2$ and $\alpha_{n\sigma} = (\omega - n\omega_{c\sigma})/k_z v_{T\sigma}$. It is seen that the density gradient and the axial current both provide a Doppler shift in the $\alpha_{0\sigma}$ term. In both cases the Doppler shift is given by the wavenumber in the appropriate direction times the mean fluid velocity in that direction.

Because Eq.(8.147) contains so much detailed physics in addition to the sought-after collisionless drift wave⁴, some effort and guidance is required to disentangle the drift wave information from all the other information. This is done by taking appropriate asymptotic limits of Eq.(8.147) and guidance is obtained using the results from the two-fluid analysis. These results showed that drift waves exist in the regime where:

1. $v_{Ti} \ll \omega/k_z \ll v_{Te}$ so that the ions are adiabatic and the electrons are isothermal,
2. $\omega \sim \omega_e^* \ll \omega_{ci}, \omega_{ce}$,
3. $k_{\perp}^2 r_{Le}^2 \sim 0$ because the extremely small electron mass means that the electron Larmor orbit radius is negligible compared to the perpendicular wavelength even though the electrons are warm,
4. $k_{\perp}^2 r_{Li}^2 < 1$ since the ions were assumed cold,
5. $k_{\perp}^2 \rho_s^2 \sim 1$,
6. $k^2 \lambda_{De}^2 \ll 1$ so that the waves are quasi-neutral,

⁴Eq.(8.147) also describes Bernstein waves, the electrostatic limit of magnetized cold plasma waves, and mode conversion.

7. $|u_{zi}| \ll |u_{ze}|$ since the parallel equilibrium velocities satisfy $m_e u_{ez} + m_i u_{iz} = 0$; there is no parallel flow, just a parallel current.

Because $\Lambda_e \sim 0$, all electron terms in the summation over n vanish except for the $n = 0$ term. Since $\omega/k_z \ll v_{Te}$, the small-argument limit of the plasma dispersion function is used for electrons and it is seen that the imaginary term is the dominant term for the electrons. In contrast since $v_{Ti} \ll \omega/k_z$, the large-argument limit of the plasma dispersion function is used for the ions and also equilibrium parallel motion is neglected for ions because of the large ion mass. For the $n \neq 0$ harmonics the terms $Z(\alpha_1) + Z(\alpha_{-1}) \rightarrow -k_z v_{Ti} [1/(\omega - n\omega_{ci}) + 1/(\omega + n\omega_{ci})]$ and hence cancel each other since $\omega \ll \omega_{ci}$. On making these approximations, Eq.(8.147) reduces to

$$1 + \frac{T_e}{T_i} [1 - e^{-\Lambda_i} I_0(\Lambda_i)] - \frac{\omega_e^*}{\omega} e^{-\Lambda_i} I_0(\Lambda_i) + i\pi^{1/2} \frac{(\omega - k_z u_{ze} - \omega_e^*)}{k_z v_{Te}} = 0. \quad (8.148)$$

The real part of this dispersion gives

$$\omega_r = \omega_e^* \left\{ \frac{e^{-\Lambda_i} I_0(\Lambda_i)}{1 + \frac{T_e}{T_i} [1 - e^{-\Lambda_i} I_0(\Lambda_i)]} \right\} \quad (8.149)$$

or in the limit of small Λ_i

$$\omega_r = \omega_e^* \left\{ \frac{1 - \Lambda_i}{1 + k_\perp^2 \rho_s^2} \right\}; \quad (8.150)$$

this corresponds to the fluid dispersion and moreover shows how finite ion temperature affects the dispersion. Using the method of Eq.(8.135), the imaginary part of the frequency is obtained from Eq.(8.148) as

$$\begin{aligned} \omega_i &= -\frac{\omega^2 \pi^{1/2}}{\omega_e^* e^{-\Lambda_i} I_0(\Lambda_i)} \frac{(\omega_r - k_z u_{ze0} - \omega_e^*)}{k_z v_{Te}} \\ &= \frac{\pi^{1/2} (\omega_e^*)^2}{k_z v_{Te}} \left\{ \frac{(1 - \Upsilon)(1 + T_e/T_i) + k_z u_{ze0} \Upsilon / \omega_r}{[1 + (1 - \Upsilon) T_e/T_i]^3} \right\} \end{aligned} \quad (8.151)$$

where $\Upsilon = e^{-\Lambda_i} I_0(\Lambda_i)$. In the limit $\Lambda_i \rightarrow 0$, it is seen that $\Upsilon \rightarrow 1 - \Lambda_i$ so that the imaginary part of the frequency becomes

$$\omega_i = \frac{\pi^{1/2} (\omega_e^*)^2}{k_z v_{Te} [1 + k_\perp^2 \rho_s^2]^3} \{ k_\perp^2 (\rho_s^2 + r_{Li}^2) + k_z u_{ze0} / \omega \}. \quad (8.152)$$

The imaginary part of the frequency is therefore always positive so there is always instability. Two collisionless destabilization mechanisms are seen to exist, *normal Landau damping* represented by the term involving $k_\perp^2 (\rho_s^2 + r_{Li}^2)$ in the curly brackets, and *current*, represented by $k_z u_{ze0} / \omega$. Since collisions can also destabilize drift waves there are at least three mechanisms by which drift waves can be destabilized. Comparison of Eq.(8.152) with Eq.(8.135) shows which of these mechanisms will be dominant in a given plasma. Modes with long parallel wavelengths are the most unstable for drift waves driven unstable by Landau damping, just as for collisional drift waves.

There are many more varieties of drift waves besides the basic versions discussed here. The common feature is that the gradient of pressure perpendicular to the magnetic field provides a new mode and free energy from the pressure gradient or from parallel current can be tapped by this mode so that the mode is spontaneously unstable.

8.7 Assignments

1. Electrostatic ion cyclotron waves: Using the electrostatic hot plasma dispersion relation show that there exists a mode in the vicinity of the ion cyclotron frequency having the dispersion

$$\omega^2 = \omega_{ci}^2 + k_{\perp}^2 c_s^2 \quad (8.153)$$

Show that this mode can be driven unstable by an axial current.

2. Mode conversion: Work through the algebra of the linear mode conversion problem and plot the contours of $\text{Re}f(p)$ for both positive and negative ξ . Hint: It is easier to plot the contours of $f(p)$ if one uses polar coordinates in the complex p plane so that $p = re^{i\theta}$. Then the real part of the term p^3 is just $\text{Re}(r^3 e^{3i\theta}) = r^3 \cos(3\theta)$. Choose a set of contour paths for $\xi < 0$ which satisfy the boundary condition that there are no modes growing exponentially with increasing distance from $\xi = 0$. Then determine which combination of these contours does not give an inward propagating hot plasma wave when $\xi > 0$ (this was another boundary condition).
3. Prove that the distribution function

$$f_{\sigma 0}(x, \mathbf{v}) = \frac{n_{0\sigma}}{\pi^{3/2} v_{T\sigma}^3} \exp \left[-(\mathbf{v} - u_{\sigma z} \hat{z})^2 / v_{T\sigma}^2 - (v_y / \omega_{c\sigma} + x) / L - \left(\frac{v_T}{2\omega_c L} \right)^2 \right]$$

provides a mean drift in the y direction corresponding to the diamagnetic drift.

MHD equilibria

9.1 Why use MHD?

Of the three levels of plasma description – Vlasov, two-fluid, and MHD – Vlasov is the most accurate and MHD is the least accurate. So, why use MHD? The answer is that because MHD is a more macroscopic point of view, it is more efficient to use MHD in situations where the greater detail and accuracy of the Vlasov or two-fluid models are unnecessary. MHD is particularly suitable for situations having complex geometry because it is very difficult to model such situations using the microscopically oriented Vlasov or 2-fluid approaches and because geometrical complexities are often most important at the MHD level of description. The equilibrium and gross stability of three-dimensional, finite-extent plasma configurations are typically analyzed using MHD. Issues requiring a 2-fluid or a Vlasov point of view can exist and be important, but these more subtle questions can be addressed after an approximate understanding has first been achieved using MHD. The MHD point of view is especially relevant to situations where magnetic forces are used to confine or accelerate plasmas. Examples of such situations include magnetic fusion confinement plasmas, solar and astrophysical plasmas, planetary and stellar dynamos, arcs, and magnetoplasmadynamic thrusters. Although molten metals are not plasmas, they are described by MHD and in fact, the MHD description is actually more appropriate and more accurate for molten metals than it is for plasmas.

We begin our discussion by examining certain general properties of magnetic fields in order to develop an intuitive understanding of the various stresses governing MHD equilibrium and stability. The MHD equation of motion,

$$\rho \left[\frac{\partial \mathbf{U}}{\partial t} + \mathbf{U} \cdot \nabla \mathbf{U} \right] = \mathbf{J} \times \mathbf{B} - \nabla P, \quad (9.1)$$

is a generalization of the equation of motion for an ordinary fluid because it includes the $\mathbf{J} \times \mathbf{B}$ magnetic force. Plasma viscosity is normally very small and is usually omitted from the MHD equation of motion. However, when torques exist, a viscous damping term needs to be included if one wishes to consider equilibria. This is because such a damping is required to balance any torque; otherwise the plasma will spin up without limit. Such situations will be discussed in Section 9.9; until then, viscosity will be assumed to be negligible and will be omitted from Eq.(9.1).

9.2 Vacuum magnetic fields

The simplest non-trivial magnetic field results when the magnetic field is produced by electric currents located outside the volume of interest and there are no currents in the volume of interest. This type of magnetic field is called a vacuum field since it could exist in a vacuum. Because there are no local currents, a vacuum field satisfies

$$\nabla \times \mathbf{B}_{vac} = 0. \quad (9.2)$$

Since the curl of a gradient is always zero, a vacuum field must be the gradient of some scalar potential ψ , i.e., the vacuum field can always be expressed as $\mathbf{B}_{vac} = \nabla\psi$. For this reason vacuum magnetic fields are also called potential magnetic fields. Because all magnetic fields must satisfy $\nabla \cdot \mathbf{B} = 0$, the potential ψ satisfies Laplace's equation,

$$\nabla^2\psi = 0. \quad (9.3)$$

Hence the entire mathematical theory of vacuum electrostatic fields can be brought into play when studying vacuum magnetic fields. Vacuum electrostatic theory shows that if either ψ or its normal derivative is specified on the surface S bounding a volume V , then ψ is uniquely determined in V . Also, if an equilibrium configuration has symmetry in some direction so that the coefficients of the relevant linearized partial differential equations do not depend on this direction, the linearized equations may be Fourier transformed in this 'ignorable' direction. Vacuum is automatically symmetric in all directions and Poisson's equation reduces to Laplace's equation which is intrinsically linear. The linearity and symmetry causes Laplace's equation to reduce to one of the standard equations of mathematical physics. For example, consider a cylindrical configuration with coordinates r , θ , and z and suppose that this configuration is axially and azimuthally uniform so that both θ and z are ignorable coordinates; i.e., the coefficients of the partial differential equation do not depend on θ or on z . Fourier analysis of Eq.(9.3) implies that ψ can be expressed as the linear superposition of modes varying as $\exp(im\theta + ikz)$. For each choice of m and k , Eq. (9.3) becomes

$$\frac{\partial^2\psi}{\partial r^2} + \frac{1}{r} \frac{\partial\psi}{\partial r} - \left(\frac{m^2}{r^2} + k^2 \right) \psi = 0. \quad (9.4)$$

Defining $s = kr$, this can be recast as

$$\frac{\partial^2\psi}{\partial s^2} + \frac{1}{s} \frac{\partial\psi}{\partial s} - \left(1 + \frac{m^2}{s^2} \right) \psi = 0, \quad (9.5)$$

a modified Bessel's equation. The solutions of Eq.(9.5) are the modified Bessel functions $I_m(kr)$ and $K_m(kr)$. Thus, the general solution of Laplace's equation here is

$$\psi(r, \theta, z) = \sum_{m=-\infty}^{\infty} \int [a_m(k)I_m(kr) + b_m(k)K_m(kr)] e^{im\theta + ikz} dk \quad (9.6)$$

where the coefficients $a_m(k)$, $b_m(k)$ are determined by specifying either ψ or its normal derivative on the bounding surface. Analogous solutions can be found in geometries having other symmetries.

This behavior can be viewed in a more general way. Equation (9.3) states that the sum of partial second derivatives in two or three different directions is zero, so at least one of these terms must be negative and at least one term must be positive. Since negative ψ''/ψ corresponds to oscillatory (harmonic) behavior and positive ψ''/ψ corresponds to exponential (non-harmonic) behavior, any solution of Laplace's equation must be oscillatory in one

or two directions (the θ and z directions for the cylindrical example here), and exponentially growing or decaying in the remaining direction or directions (the r direction for the cylindrical example here).

Non-vacuum magnetic fields are more complicated than vacuum fields, and unlike vacuum fields, are not uniquely determined by the surface boundary conditions. This is because non-vacuum fields are determined by both the current distribution within the volume and the surface boundary conditions. Vacuum fields are distinguished from non-vacuum fields because vacuum fields are the lowest energy fields satisfying given boundary conditions on the surface S of a volume V . Let us now prove this statement.

Consider a volume V bounded by a surface S over which boundary conditions are specified. Let $\mathbf{B}_{\min}(\mathbf{r})$ be the magnetic field having the *lowest* stored magnetic energy of all possible magnetic fields satisfying the prescribed boundary conditions. We use methods of variational calculus to prove that this lowest energy field is the vacuum field.

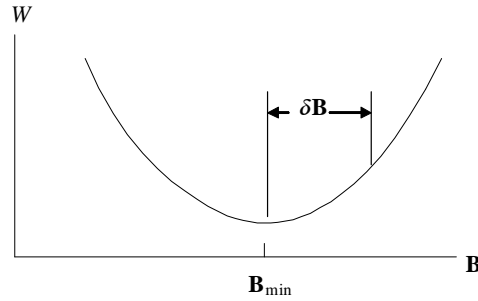


Figure 9.1: Magnetic field energy for different configurations, \mathbf{B}_{\min} is the configuration with minimum magnetic energy for a given boundary condition.

Consider some slightly different field denoted as $\mathbf{B}(\mathbf{r})$ which satisfies the same boundary conditions as \mathbf{B}_{\min} . This slightly different field can be expressed as $\mathbf{B}(\mathbf{r}) = \mathbf{B}_{\min}(\mathbf{r}) + \delta\mathbf{B}(\mathbf{r})$ where $\delta\mathbf{B}(\mathbf{r})$ is a small arbitrary variation about \mathbf{B}_{\min} . This situation is sketched in a qualitative fashion in Fig.9.1 where the horizontal axis represents a continuum of different allowed choices for the vector function $\mathbf{B}(\mathbf{r})$. Since $\mathbf{B}(\mathbf{r})$ satisfies the same boundary conditions as \mathbf{B}_{\min} , $\delta\mathbf{B}(\mathbf{r})$ must vanish on S . The magnetic energy W associated with $\mathbf{B}(\mathbf{r})$ can be evaluated as

$$\begin{aligned} 2\mu_0 W &= \int_V (\mathbf{B}_{\min} + \delta\mathbf{B})^2 d^3r \\ &= \int_V \mathbf{B}_{\min}^2 d^3r + 2 \int_V \delta\mathbf{B} \cdot \mathbf{B}_{\min} d^3r + \int_V (\delta\mathbf{B})^2 d^3r. \end{aligned} \quad (9.7)$$

If the middle term does not vanish, $\delta\mathbf{B}$ could always be chosen to be antiparallel to \mathbf{B}_{\min} inside V so that $\delta\mathbf{B} \cdot \mathbf{B}_{\min}$ would be negative. Since $\delta\mathbf{B}$ is assumed small, $\delta\mathbf{B} \cdot \mathbf{B}_{\min}$ would be larger in magnitude than $(\delta\mathbf{B})^2$. Such a choice for $\delta\mathbf{B}$ would make W lower than the energy of the assumed lowest energy field, thus contradicting the assumption that \mathbf{B}_{\min}

is in fact the lowest energy field. Thus, the only way to ensure that \mathbf{B}_{\min} is indeed the true minimum is to require

$$\int_V \delta \mathbf{B} \cdot \mathbf{B}_{\min} d^3r = 0 \quad (9.8)$$

no matter how $\delta \mathbf{B}$ is chosen. Using $\delta \mathbf{B} = \nabla \times \delta \mathbf{A}$ and the vector identity $\nabla \cdot (\mathbf{A} \times \mathbf{B}) = \mathbf{B} \cdot \nabla \times \mathbf{A} - \mathbf{A} \cdot \nabla \times \mathbf{B}$, Eq. (9.8) can be integrated by parts to obtain

$$\int_V [\nabla \cdot (\delta \mathbf{A} \times \mathbf{B}_{\min}) + \delta \mathbf{A} \cdot \nabla \times \mathbf{B}_{\min}] d^3r = 0. \quad (9.9)$$

The first term can be transformed into a surface integral over S using Gauss's theorem. This surface integral vanishes because $\delta \mathbf{A}$ must vanish on the bounding surface (recall that the variation satisfies the same boundary condition as the minimum energy field). Because $\delta \mathbf{B}$ is arbitrary within V , $\delta \mathbf{A}$ must also be arbitrary within V and so the only way for the second term in Eq. (9.9) to vanish is to have $\nabla \times \mathbf{B}_{\min} = 0$. Thus, \mathbf{B}_{\min} must be a vacuum field.

An important corollary is as follows: Suppose boundary conditions are specified on the surface enclosing some volume. These boundary conditions can be considered as “rules” which must be satisfied by any solution to the equations. All configurations satisfying the imposed boundary condition and having finite current within the volume are *not* in the lowest energy state. Thus, non-vacuum fields can, in principle, have free energy available for driving boundary-condition-preserving instabilities.

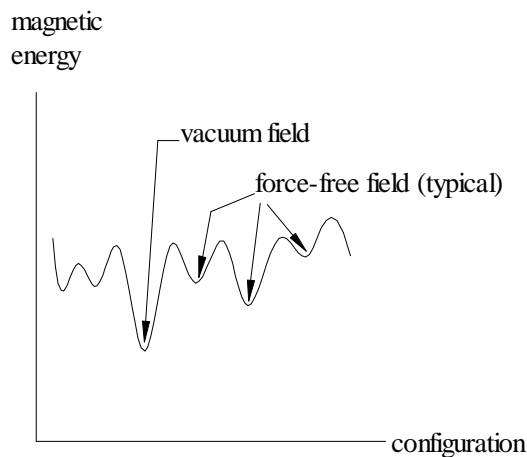


Figure 9.2: Sketch of magnetic energy dependence on configuration of a system with fixed, specified boundary conditions. The variation of the configuration would correspond to different internal current profiles. The force-free configurations are local energy minima while the vacuum configuration has the absolute lowest minimum.

9.3 Force-free fields

Although the vacuum field is the lowest energy configuration satisfying prescribed boundary conditions, non-vacuum configurations do not always ‘decay’ to this lowest energy state. This is because there also exists a family of higher energy configurations to which the system may decay; these are the so-called force-free states. The current is not zero in a force-free state but the magnetic force is zero because the current density is everywhere parallel to the magnetic field. Thus $\mathbf{J} \times \mathbf{B}$ vanishes even though both \mathbf{J} and \mathbf{B} are finite. If a plasma initially in a non-force-free state evolves toward a force-free state it becomes ‘stuck’ in the force-free state because there are no forces acting to change the equilibrium. The magnetic energy of a force-free field is not the absolute minimum energy for the specified boundary conditions, but it is a local minimum in configuration space as sketched in Fig.9.2. This hierarchy of states is somewhat analogous to the states of a quantum system – the vacuum field is the analog of the ground state and the force-free states are the analogs of higher energy quantum states.

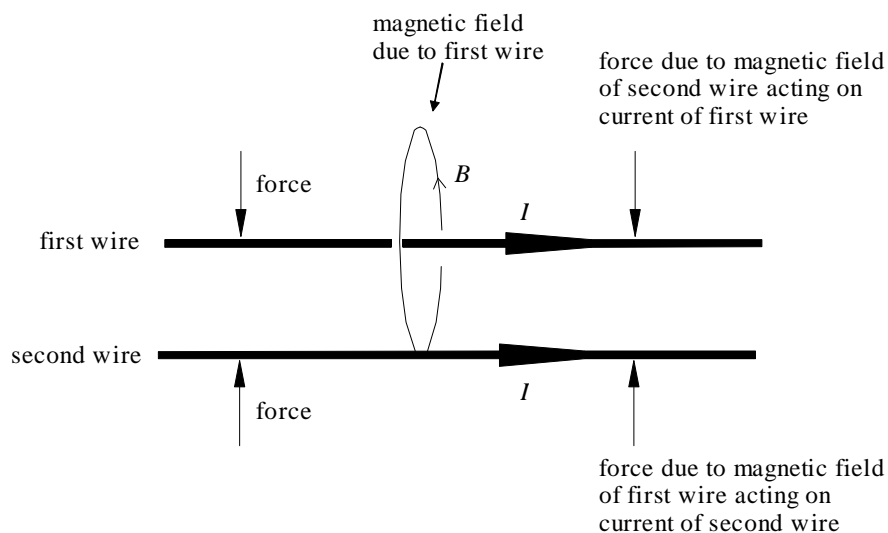


Figure 9.3: Parallel currents attract each other

9.4 Magnetic pressure and tension

Much useful insight can be obtained by considering the force between two parallel current-carrying wires as shown in Fig.9.3. Calculation of the field \mathbf{B} observed at one wire due to current in the other shows that the $\mathbf{J} \times \mathbf{B}$ force is such as to push the wires together; i.e.,

parallel currents attract each other. Conversely, anti-parallel currents repel each other.

A bundle of parallel wires as shown in Fig. 9.4 will therefore mutually attract each other resulting in an effective net force which acts to reduce the diameter of the bundle. The bundle could be replaced by a distributed current such as the current carried by a finite-radius, cylindrical plasma. This contracting, inward directed force is called the pinch force or the pinch effect.

The pinch force may be imagined as being due to a 'tension' in the azimuthal magnetic field which wraps around the distributed current. Extending this metaphor, the azimuthal magnetic field is visualized as acting like an 'elastic band' which encircles the distributed current and squeezes or pinches the current to a smaller diameter. This concept is consistent with the situation of two permanent magnets attracting each other when the respective north and south poles face each other. The magnetic field lines go from the north pole of one magnet to the south pole of the other and so one can pretend that the attraction of the two magnets is due to tension in the field lines spanning the gap between the two magnets.

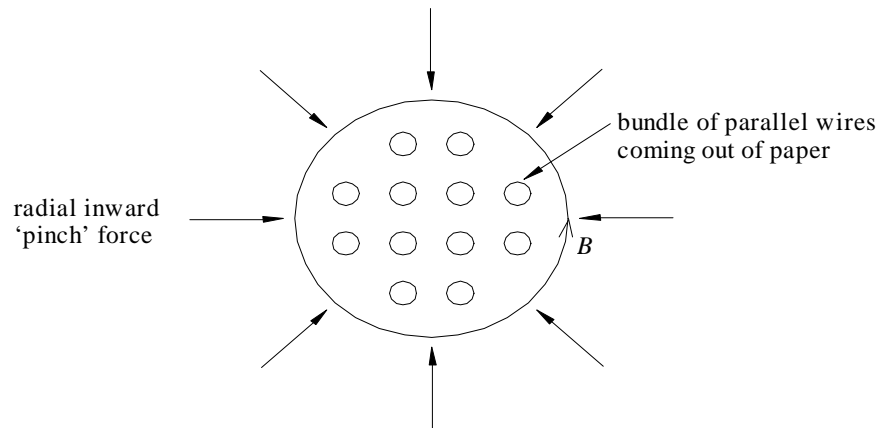


Figure 9.4: Bundle of currents attract each other, giving effective radial inward pinch force.

Now consider a current-carrying loop such as is shown in Fig.9.5. Because the currents on opposite sides of the loop flow in opposing directions, there will be a repulsive force between the current element at each point and the current element on the opposite side of the loop. The net result is a force directed to expand the diameter of the loop. This force is called the hoop force or hoop stress. Hoop force may also be interpreted metaphorically by introducing the concept of magnetic pressure. As shown in Fig.9.5, the magnetic field lines linking the current are more dense inside the loop than outside, a purely geometrical effect resulting from the curvature of the current path. Since magnetic field strength is proportional to field line density, the magnetic field is stronger on the inside of the loop than on the outside, i.e., B^2 is stronger on the inside than on the outside. The magnetic field in the plane of the loop is normal to the plane and so one can explain the hoop force

by assigning a magnetic ‘pressure’ proportional to B^2 acting in the direction perpendicular to \mathbf{B} . Because B^2 is stronger on the inside of the loop than on the outside, there is a larger magnetic pressure on the inside. The outward force due to this pressure imbalance is consistent with the hoop force.

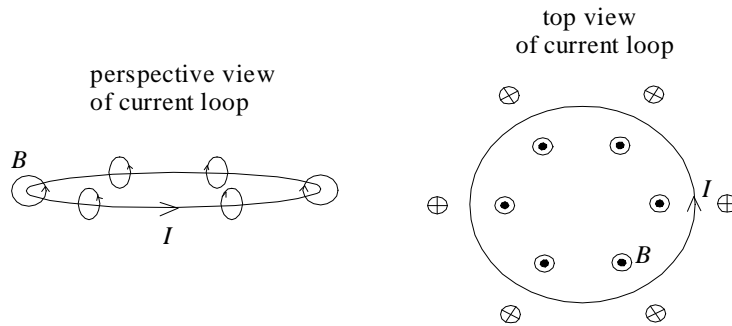


Figure 9.5: Perspective and top view of magnetic fields generated by a current loop.

The combined effects of magnetic pressure and tension can be visualized by imagining a current-carrying loop where the conductor has a finite diameter. Suppose that this loop initially has the relative proportions of an automobile tire, as shown in Fig.9.6. The hoop force will cause the diameter of the loop to increase, while the pinch force will cause the diameter of the conductor to decrease. The net result is that these combined forces will cause the automobile tire to evolve towards the relative proportions of a bicycle tire (large major radius, small minor radius).

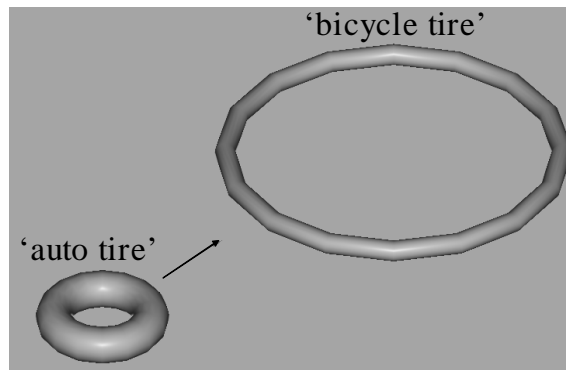


Figure 9.6: Magnetic forces act to transform a fat small current loop (auto tire) into a large skinny loop (bicycle tire)

9.5 Magnetic stress tensor

The existence of magnetic pressure and tension shows that the magnetic force is different in different directions, and so the magnetic force ought to be characterized by an anisotropic stress tensor. To establish this mathematically, the vector identity $\nabla B^2/2 = \mathbf{B} \cdot \nabla \mathbf{B} + \mathbf{B} \times \nabla \times \mathbf{B}$ is invoked so that the magnetic force can be expressed as

$$\begin{aligned} \mathbf{J} \times \mathbf{B} &= \frac{1}{\mu_0} (\nabla \times \mathbf{B}) \times \mathbf{B} \\ &= \frac{1}{\mu_0} \left[-\nabla \left(\frac{B^2}{2} \right) + \mathbf{B} \cdot \nabla \mathbf{B} \right] \\ &= -\frac{1}{\mu_0} \nabla \cdot \left[\frac{B^2}{2} \mathbf{I} - \mathbf{B}\mathbf{B} \right] \end{aligned} \quad (9.10)$$

where \mathbf{I} is the unit tensor and the relation $\nabla \cdot (\mathbf{B}\mathbf{B}) = (\nabla \cdot \mathbf{B}) \mathbf{B} + \mathbf{B} \cdot \nabla \mathbf{B} = \mathbf{B} \cdot \nabla \mathbf{B}$ has been used. At any point \mathbf{r} a local Cartesian coordinate system can be defined with z axis parallel to the local value of \mathbf{B} so that Eq.(9.1) can be written as

$$\rho \left[\frac{\partial \mathbf{U}}{\partial t} + \mathbf{U} \cdot \nabla \mathbf{U} \right] = -\nabla \cdot \begin{bmatrix} P + \frac{B^2}{2\mu_0} & & \\ & P + \frac{B^2}{2\mu_0} & \\ & & P - \frac{B^2}{2\mu_0} \end{bmatrix} \quad (9.11)$$

showing again that the magnetic field acts like a pressure in the directions transverse to \mathbf{B} (i.e., x, y directions in the local Cartesian system) and like a tension in the direction parallel to \mathbf{B} .

While the above interpretation is certainly useful, it can be somewhat misleading because it might be interpreted as implying the existence of a force in the direction of \mathbf{B} when in fact no such force exists because $\mathbf{J} \times \mathbf{B}$ clearly does not have a component in the \mathbf{B} direction. A more accurate way to visualize the relation between magnetic pressure and tension is to rearrange the second line of Eq.(9.10) as

$$\mathbf{J} \times \mathbf{B} = \frac{1}{\mu_0} \left[-\nabla \left(\frac{B^2}{2} \right) + B^2 \hat{B} \cdot \nabla \hat{B} + \hat{B} \hat{B} \cdot \nabla \left(\frac{B^2}{2} \right) \right] = \frac{1}{\mu_0} \left[-\nabla_{\perp} \left(\frac{B^2}{2} \right) + B^2 \boldsymbol{\kappa} \right] \quad (9.12)$$

or

$$\mathbf{J} \times \mathbf{B} = \frac{1}{\mu_0} \left[-\nabla_{\perp} \left(\frac{B^2}{2} \right) + B^2 \boldsymbol{\kappa} \right]. \quad (9.13)$$

Here

$$\boldsymbol{\kappa} = \hat{B} \cdot \nabla \hat{B} = -\frac{\hat{R}}{R} \quad (9.14)$$

is a measure of the curvature of the magnetic field at a selected point on a field line and, in particular, \mathbf{R} is the local radius of curvature vector. The vector \mathbf{R} goes from the center of curvature to the selected point on the field line. The $\boldsymbol{\kappa}$ term in Eq.(9.13) describes a force which tends to straighten out magnetic curvature and is a more precise way for characterizing field line tension (recall that tension similarly acts to straighten out curvature). The

term involving $\nabla_{\perp} B^2$ portrays a magnetic force due to pressure gradients perpendicular to the magnetic field and is a more precise expression of the hoop force.

In our earlier discussion it was shown that the vacuum magnetic field is the lowest energy state of all fields satisfying prescribed boundary conditions. A vacuum field might be curved for certain boundary conditions (e.g., a permanent magnet with finite dimensions) and, in such a case, the two terms in Eq.(9.13) are both finite but exactly cancel each other. We can think of the minimum-energy state for given boundary conditions as being analogous to the equilibrium state of a system of stiff rubber hoses which have been pre-formed into shapes having the morphology of the vacuum magnetic field and which have their ends fixed at the bounding surface. Currents will cause the morphology of this system to deviate from the equilibrium state, but since any deformation requires work to be done on the system, currents invariably cause the system to be in a higher energy state.

9.6 Flux preservation, energy minimization, and inductance

Another useful way of understanding magnetic field behavior relates to the concept of electric circuit inductance. The self-inductance L of a circuit component is defined as the magnetic flux Φ linking the component divided by the current I flowing through the component, i.e.

$$L = \frac{\Phi}{I}. \quad (9.15)$$

Consider an arbitrary short-circuited coil with current I located in an infinite volume V and let C denote the three-dimensional spatial contour traced out by the wire constituting the coil. The total magnetic flux linked by the turns of the coil can be expressed as

$$\Phi = \int \mathbf{B} \cdot d\mathbf{s} = \int \nabla \times \mathbf{A} \cdot d\mathbf{s} = \oint_C \mathbf{A} \cdot d\mathbf{l} \quad (9.16)$$

where the surface integral is over the area elements linked by the coil turns. The energy contained in the magnetic field produced by the coil is

$$\begin{aligned} W &= \int_V \frac{B^2}{2\mu_0} d^3r \\ &= \frac{1}{2\mu_0} \int_V \mathbf{B} \cdot \nabla \times \mathbf{A} d^3r. \end{aligned} \quad (9.17)$$

However, using the vector identity $\nabla \cdot (\mathbf{A} \times \mathbf{B}) = \mathbf{B} \cdot \nabla \times \mathbf{A} - \mathbf{A} \cdot \nabla \times \mathbf{B}$ this magnetic energy can be expressed as

$$W = \frac{1}{2\mu_0} \int_V \mathbf{A} \cdot \nabla \times \mathbf{B} d^3r + \frac{1}{2\mu_0} \int_{S_{\infty}} d\mathbf{s} \cdot \mathbf{A} \times \mathbf{B} \quad (9.18)$$

where Gauss's law has been invoked to obtain the second term, an integral over the surface at infinity S_{∞} . This surface integral vanishes because (i) at infinity the magnetic field must fall off at least as fast as a dipole, i.e., $B \sim R^{-3}$ where R is the distance to the origin, (ii) the vector potential magnitude A scales as the integral of B so $A \sim R^{-2}$, and (iii) the surface at infinity scales as R^2 .

Using Ampere's law, Eq.(9.18) can thus be rewritten as

$$W = \frac{1}{2} \int_V \mathbf{A} \cdot \mathbf{J} d^3r. \quad (9.19)$$

However, \mathbf{J} is only finite in the coil wire and so the integral reduces to an integral over the volume of the wire. A volume element of wire can be expressed as $d^3r = ds \cdot d\mathbf{l}$ where $d\mathbf{l}$ is an element of length along the wire, and ds is the cross-sectional area of the wire. Since \mathbf{J} and $d\mathbf{l}$ are parallel, they can be interchanged in Eq.(9.19) which becomes

$$\begin{aligned} W &= \frac{1}{2} \int_{V_{coil}} \mathbf{A} \cdot d\mathbf{l} \mathbf{J} \cdot ds \\ &= \frac{I}{2} \oint \mathbf{A} \cdot d\mathbf{l} \\ &= \frac{I\Phi}{2} \\ &= \frac{\Phi^2}{2L} \\ &= \frac{1}{2} LI^2 \end{aligned} \quad (9.20)$$

where $\mathbf{J} \cdot ds = I$ is the current flowing through the wire. Thus, the energy stored in the magnetic field produced by a coil is just the inductive energy of the coil.

If the coil is perfectly short-circuited, then it must be flux conserving, for if there were a change in flux, a voltage would appear across the ends of the coil. A closed current flowing in a perfectly conducting plasma is thus equivalent to a short-circuited current-carrying coil and so the perfectly conducting plasma can be considered as a flux-conserver. If flux is conserved, i.e. $\Phi = const.$, the second from last line in Eq.(9.20) shows that *the magnetic energy of the system will be lowered by any rearrangement of circuit topology that increases self-inductance.*

Hot plasmas are reasonably good flux conservers because of their high electrical conductivity. Thus, any inductance-increasing change in the topology of plasma currents will release free energy which could be used to drive an instability. Since forces act so as to reduce the potential energy of a system, magnetic forces due to current flowing in a plasma will always act so as to increase the self-inductance of the configuration. One can therefore write the force \mathbf{F} due to a flux-conserving change in inductance L as

$$\mathbf{F} = -\frac{\Phi^2}{2} \nabla \left(\frac{1}{L} \right). \quad (9.21)$$

The pinch force is consistent with this interpretation since the inductance of a conductor depends inversely on its radius. The hoop force is also consistent with this interpretation since inductance of a current loop increases with the major radius of the loop. More complicated behavior can also be explained, especially the kink instability to be discussed later. In the kink instability, current initially flowing in a straight line develops an instability that causes the current path to become helical. Since a coil (helix) has more inductance than a straight length of the same wire, the effect of the kink instability also acts so as to increase the circuit self-inductance.

9.7 Static versus dynamic equilibria

We define (i) a static equilibrium to be a time-independent solution to Eq.(9.1) having no flow velocity and (ii) a dynamic equilibrium as a solution with steady-state flow velocities. Thus $\mathbf{U} = 0$ for a static equilibrium whereas \mathbf{U} is finite and steady-state for a dynamic equilibrium. For a static equilibrium the MHD equation of motion reduces to

$$\nabla P = \mathbf{J} \times \mathbf{B}. \quad (9.22)$$

For a dynamic equilibrium the MHD equation of motion reduces to

$$\rho \mathbf{U} \cdot \nabla \mathbf{U} + \nabla P = \mathbf{J} \times \mathbf{B} + \nu \rho \nabla^2 \mathbf{U} \quad (9.23)$$

where the last term represents a viscous damping and ν is the kinematic viscosity. By taking the curl of these last two equations we see that for static equilibria the magnetic force must be conservative i.e., $\nabla \times (\mathbf{J} \times \mathbf{B}) = 0$ whereas for dynamic equilibria the magnetic force is typically not conservative since in general $\nabla \times (\mathbf{J} \times \mathbf{B}) \neq 0$. Thus, the character of the magnetic field is quite different for the two cases. Static equilibria are relevant to plasma confinement devices such as tokamaks, stellarators, reversed field pinches, spheromaks while dynamic equilibria are mainly relevant to arcs, jets, magnetoplasmadynamic thrusters, but can also be relevant to tokamaks, etc., if there are flows. Both static and dynamic equilibria occur in space plasmas.

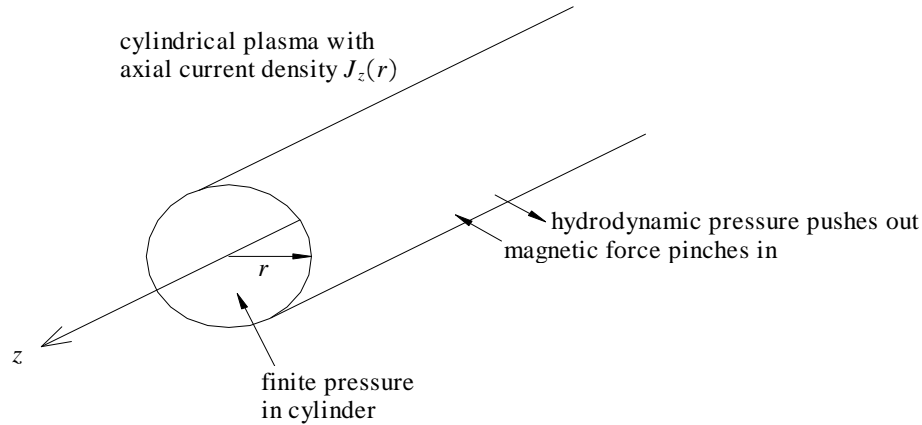


Figure 9.7: Geometry of Bennett pinch.

9.8 Static equilibria

9.8.1 Static equilibria in two dimensions: the Bennett pinch

The simplest static equilibrium was first investigated by Bennett (1934) and is called the Bennett pinch or z -pinch (here z refers to the direction of the current). This configuration, sketched in Fig.9.7, consists of an infinitely long axisymmetric cylindrical plasma with axial current density $J_z = J_z(r)$ and no other currents.

The axial current flowing within a circle of radius r is

$$I(r) = \int_0^r 2\pi r' J_z(r') dr' \quad (9.24)$$

and the axial current density is related to this integrated current by

$$J_z(r) = \frac{1}{2\pi r} \frac{\partial I}{\partial r}. \quad (9.25)$$

Since Ampere's law gives

$$B_\theta(r) = \frac{\mu_0 I(r)}{2\pi r}, \quad (9.26)$$

Eq.(9.22) can be written

$$r^2 \frac{\partial P}{\partial r} = -\frac{\mu_0}{8\pi^2} \frac{\partial I^2}{\partial r}. \quad (9.27)$$

Integrating Eq. (9.27) from $r = 0$ to $r = a$, where a is the outer radius of the cylindrical plasma, gives the relation

$$\int_0^a r^2 \frac{\partial P}{\partial r} dr = [r^2 P(r)]_0^a - 2 \int_0^a r P(r) dr = -\frac{\mu_0 I^2(a)}{8\pi^2}. \quad (9.28)$$

The integrated term vanishes at both $r = 0$ and $r = a$ since $P(a) = 0$ by definition. If the temperature is uniform, the pressure can be expressed as $P(r) = n(r)\kappa T$ and so Eq.(9.28) can be expressed as

$$I^2 = \frac{8\pi N \kappa T}{\mu_0} \quad (9.29)$$

where $N = \int_0^a n(r)2\pi r dr$ is the number of particles per axial length. Equation (9.29), called the Bennett relation, shows that the current required to confine a given N and T is independent of the details of the internal density profile. This relation describes the simplest non-trivial MHD equilibrium and suggests that quite modest currents could contain substantial plasma pressures. This relation motivated the design of early magnetic fusion confinement devices but, as will be seen, it is overly optimistic because simple z -pinch equilibria turn out to be highly unstable.

Confinement using currents that flow in the azimuthal direction is also possible, but this configuration, known as a θ -pinch, is fundamentally transient. In a θ -pinch a rapidly changing azimuthal current in a coil going around a cylindrical plasma creates a transient B_z field as shown in Fig. 9.8. Because the conducting plasma conserves magnetic flux, the transient B_z field cannot penetrate the plasma and so is confined to the vacuum region between the plasma and the coil. This exclusion of the B_z field by the plasma requires

the existence in the plasma surface of an induced azimuthal current which creates a magnetic field in the plasma interior that exactly cancels the coil-produced transient B_z field. The radial confining force results from a radially inward force $\mathbf{J} \times \mathbf{B} = J_\theta \hat{\theta} \times B_z \hat{z}$ where B_z is the magnetic field associated with the current in the coil and J_θ is the plasma surface current. An alternative but equivalent point of view is to invoke the concept that opposite currents repel and argue that the azimuthal current in the coil repels the oppositely directed azimuthal current in the plasma surface, thereby pushing the plasma inwards and so balancing the outwards force due to plasma pressure. The θ -pinch configuration is necessarily transient, because the induced surface current cannot be sustained in steady-state.

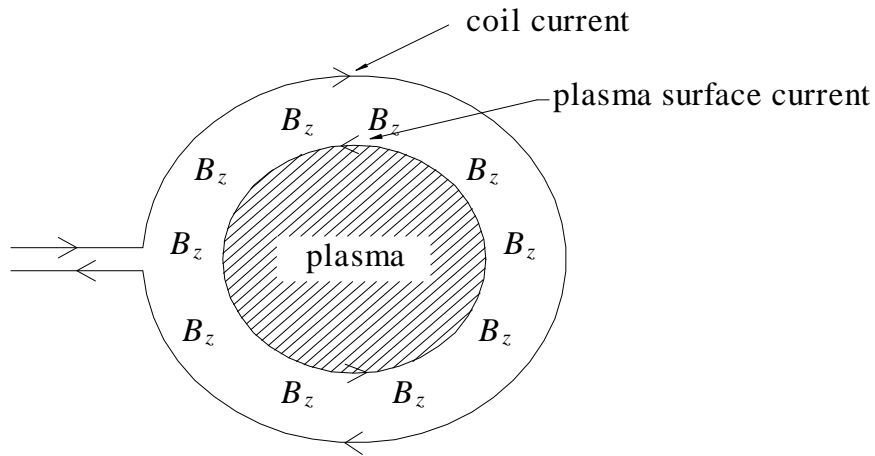


Figure 9.8: Theta pinch configuration. Rapidly changing azimuthal coil current induces equal and opposite azimuthal current in plasma surface. Pressure of B_z between these two currents pushes in on plasma and provides confinement.

9.8.2 Impossibility of self-confinement of current-carrying plasma in three dimensions: the virial theorem

The Bennett analysis showed that axial currents flowing in an infinitely long cylindrical plasma generate a pinch force which confines a finite pressure plasma. The inward pinch force balances the outward force associated with the pressure gradient. The question now is whether this two-dimensional result can be extended to three dimensions; i.e., is it possible to have a finite-pressure three-dimensional plasma, as shown in Fig.9.9, which is confined entirely by currents circulating within the plasma? To be more specific, is it possible to have a finite-radius plasma sphere surrounded by vacuum where the confinement of the finite plasma pressure is entirely provided by the magnetic force of currents circulating in the plasma; i.e., can the plasma hold itself together by its own ‘bootstraps’? The answer,

a resounding ‘no’, is provided by a virial theorem due to Shafranov (1966). A virial is a suitably weighted integral over the entirety of a system and contains information about how an extensive property such as energy is partitioned in the system. For example, in mechanics the virial can be the time average of the potential or of the kinetic energy.

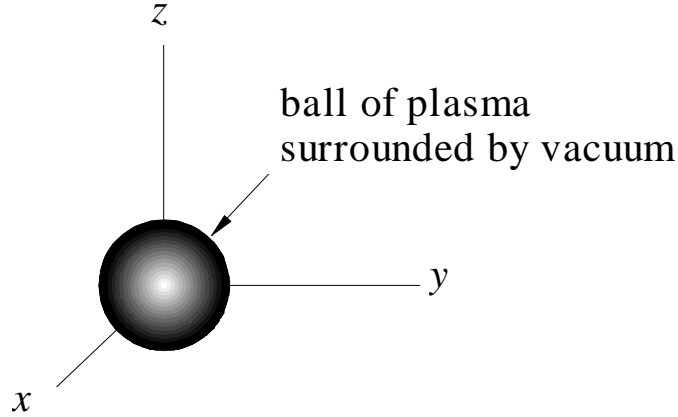


Figure 9.9: Plasma sphere with finite pressure surrounded by vacuum

The MHD virial theorem is obtained by supposing that a self-confining configuration exists and then showing this leads to a contradiction.

We therefore postulate the existence of a spherical plasma with the following properties:

1. the plasma has finite radius a and is surrounded by vacuum,
2. the plasma is in static MHD equilibrium,
3. the plasma has finite internal pressure and the pressure gradient is entirely balanced by magnetic forces due to currents circulating in the plasma; i.e. there are no currents in the surrounding vacuum region.

Using Eqs.(9.10) and (9.11) the static MHD equilibrium can be expressed as

$$\nabla \cdot \mathbf{T} = 0 \quad (9.30)$$

where the tensor \mathbf{T} is defined as

$$\mathbf{T} = \left(P + \frac{B^2}{2\mu_0} \right) \mathbf{I} - \frac{1}{\mu_0} \mathbf{B}\mathbf{B}. \quad (9.31)$$

Let $\mathbf{r} = x\hat{x} + y\hat{y} + z\hat{z}$ be the vector from the center of the plasma to the point of observation.

Consider the virial expression

$$\begin{aligned}
 \nabla \cdot (\mathbf{T} \cdot \mathbf{r}) &= \sum_{jk} \frac{\partial}{\partial x_j} (T_{jk} x_k) \\
 &= (\nabla \cdot \mathbf{T}) \cdot \mathbf{r} + \sum_{jk} T_{jk} \frac{\partial}{\partial x_j} x_k \\
 &= \text{Trace } \mathbf{T}
 \end{aligned} \tag{9.32}$$

where $\text{Trace } \mathbf{T} = \sum_{jk} T_{jk} \delta_{jk}$. From Eq.(9.31) (or, equivalently from the matrix form in Eq.(9.11)) it is seen that

$$\text{Trace } \mathbf{T} = 3P + B^2/2\mu_0$$

is *positive definite*.

We now integrate both sides of Eq.(9.32) over all space. Since the right hand side of Eq.(9.32) is positive definite, the integral of the right hand side over all space is finite and positive. The integral of the left hand side can be transformed to a surface integral at infinity using Gauss' theorem

$$\begin{aligned}
 \int d^3r \nabla \cdot (\mathbf{T} \cdot \mathbf{r}) &= \int_{S_\infty} d\mathbf{s} \cdot \mathbf{T} \cdot \mathbf{r} \\
 &= \int_{S_\infty} d\mathbf{s} \cdot \left[\left(P + \frac{B^2}{2\mu_0} \right) \mathbf{I} - \frac{1}{\mu_0} \mathbf{B}\mathbf{B} \right] \cdot \mathbf{r} .
 \end{aligned} \tag{9.33}$$

Since the plasma is assumed to have finite extent, P is zero on the surface at infinity. The magnetic field can be expanded in multipoles with the lowest order multipole being a dipole. The magnetic field of a dipole scales as r^{-3} for large r while the surface area $\int d\mathbf{s}$ scales as r^2 . Thus the left hand side term scales as $\int d\mathbf{s} B^2 r \sim r^{-3}$ and so vanishes as $r \rightarrow \infty$. This is in contradiction to the right hand side being positive definite and so the set of initial assumptions must be erroneous. Thus, any finite extent, three-dimensional, static plasma equilibrium must involve at least some currents external to the plasma. A finite extent, three-dimensional static plasma can therefore only be in equilibrium if at least some of the magnetic field is produced by currents in coils that are external to the plasma and that are held in place by some mechanical structure. If the coils were not supported by a mechanical structure, then the current in the coils could be considered as part of the MHD plasma and the virial theorem would be violated. In summary, a finite extent three-dimensional plasma in static equilibrium with a finite internal hydrodynamic pressure P must ultimately have some tangible exterior object to "push against". The buttressing is provided by magnetic forces acting between currents in external coils and currents in the plasma.

9.8.3 Three-dimensional static equilibria: the Grad-Shafranov equation

Despite the simple appearance of Eq.(9.22), its three-dimensional solution is far from trivial. Before even attempting to find a solution, it is important to decide the appropriate way to pose the problem, i.e., it must be decided which quantities are prescribed and which are to be solved for. For example, one might imagine prescribing a pressure profile $P(\mathbf{r})$ and

showing that the functional form of Eq.(9.34) is consistent with Ampere's law $\oint \mathbf{B} \cdot d\mathbf{l} = \mu_0 I$. The poloidal magnetic field is

$$\mathbf{B}_{pol} = \frac{1}{2\pi} (\nabla\psi \times \nabla\phi). \quad (9.36)$$

Integration of the poloidal magnetic field over the area of a circle of radius r with center at axial location z gives

$$\int_0^r \mathbf{B}_{pol} \cdot d\mathbf{s} = \int_0^r \frac{1}{2\pi} \nabla\psi \times \nabla\phi \cdot \hat{z} 2\pi r' dr' = \psi(r, z); \quad (9.37)$$

thus $\psi(r, z)$ is the poloidal flux at location r, z . The concept of poloidal flux depends on the existence of axisymmetry so that a circle of radius r can always be associated with a location r, z .

Axisymmetry also provides a useful relationship between toroidal and poloidal vectors. In particular, the curl of a toroidal vector is poloidal since

$$\nabla \times \mathbf{B}_{tor} = \frac{\mu_0}{2\pi} \nabla I \times \nabla\phi \quad (9.38)$$

and similarly the curl of a poloidal vector is toroidal since

$$\nabla \times \mathbf{B}_{pol} = \nabla \times (B_r \hat{r} + B_z \hat{z}) = \hat{\phi} \left(\frac{\partial B_r}{\partial z} - \frac{\partial B_z}{\partial r} \right). \quad (9.39)$$

The curl of the poloidal magnetic field is a Laplacian-like operator on ψ since

$$\nabla\phi \cdot \nabla \times \mathbf{B}_{pol} = \nabla \cdot (\mathbf{B}_{pol} \times \nabla\phi) = \nabla \cdot \left(\frac{1}{2\pi} [\nabla\psi \times \nabla\phi] \times \nabla\phi \right) = -\frac{1}{2\pi} \nabla \cdot \left(\frac{1}{r^2} \nabla\psi \right), \quad (9.40)$$

a relationship established using the vector identity $\nabla \cdot (\mathbf{F} \times \mathbf{G}) = \mathbf{G} \cdot \nabla \times \mathbf{F} - \mathbf{F} \cdot \nabla \times \mathbf{G}$. Because $\nabla \times \mathbf{B}_{pol}$ is purely toroidal and $\hat{\phi} = r\nabla\phi$, one can write

$$\nabla \times \mathbf{B}_{pol} = -\frac{r^2}{2\pi} \nabla \cdot \left(\frac{1}{r^2} \nabla\psi \right) \nabla\phi. \quad (9.41)$$

Ampere's law states that $\nabla \times \mathbf{B} = \mu_0 \mathbf{J}$. Thus, from Eqs. (9.38) and (9.41) the respective toroidal and poloidal currents are

$$\mathbf{J}_{tor} = -\frac{r^2}{2\pi\mu_0} \nabla \cdot \left(\frac{1}{r^2} \nabla\psi \right) \nabla\phi \quad (9.42)$$

and

$$\mathbf{J}_{pol} = \frac{1}{2\pi} \nabla I \times \nabla\phi. \quad (9.43)$$

We are now in a position to evaluate the magnetic force in Eq.(9.22). After decomposing the magnet field and current into toroidal and poloidal components, Eq.(9.22) becomes

$$\nabla P = \mathbf{J}_{pol} \times \mathbf{B}_{tor} + \mathbf{J}_{tor} \times \mathbf{B}_{pol} + \mathbf{J}_{pol} \times \mathbf{B}_{pol}. \quad (9.44)$$

The $\mathbf{J}_{pol} \times \mathbf{B}_{pol}$ term is in the toroidal direction and is the only toroidally directed term on the right hand side of the equation. However $\partial P / \partial \phi = 0$ because all physical quantities are independent of ϕ and so $\mathbf{J}_{pol} \times \mathbf{B}_{pol}$ must vanish. This implies

$$(\nabla I \times \nabla\phi) \times (\nabla\psi \times \nabla\phi) = 0 \quad (9.45)$$

which further implies that ∇I must be parallel to $\nabla\psi$. An arbitrary displacement $d\mathbf{r}$ results in respective changes in current and poloidal flux $dI = d\mathbf{r} \cdot \nabla I$ and $d\psi = d\mathbf{r} \cdot \nabla\psi$ so that

$$\frac{dI}{d\psi} = \frac{d\mathbf{r} \cdot \nabla I}{d\mathbf{r} \cdot \nabla\psi};$$

since ∇I is parallel to $\nabla\psi$, the derivative $dI/d\psi$ is always defined. Thus I must be a function of ψ and it is always possible to write

$$\nabla I(\psi) = I'(\psi)\nabla\psi \quad (9.46)$$

where prime means derivative with respect to the argument. The poloidal current can therefore be expressed in terms of the poloidal flux function as

$$\mathbf{J}_{pol} = \frac{I'}{2\pi} \nabla\psi \times \nabla\phi. \quad (9.47)$$

Substitution for the currents and magnetic fields in Eq.(9.44) gives the expression

$$\begin{aligned} \nabla P &= \frac{I'}{2\pi} (\nabla\psi \times \nabla\phi) \times \frac{\mu_0 I}{2\pi} \nabla\phi - \nabla\phi \frac{r^2}{2\pi\mu_0} \nabla \cdot \left(\frac{1}{r^2} \nabla\psi \right) \times \frac{1}{2\pi} [\nabla\psi \times \nabla\phi] \\ &= - \left[\frac{\mu_0 I I'}{(2\pi r)^2} + \frac{1}{(2\pi)^2 \mu_0} \nabla \cdot \left(\frac{1}{r^2} \nabla\psi \right) \right] \nabla\psi. \end{aligned} \quad (9.48)$$

This gives the important result that ∇P must also be parallel to $\nabla\psi$ which in turn implies that $P = P(\psi)$ so that $\nabla P = P'\nabla\psi$. Equation (9.48) now has a common vector factor $\nabla\psi$ which may be divided out, so that the original vector equation reduces to the *scalar* equation

$$\nabla \cdot \left(\frac{1}{r^2} \nabla\psi \right) + 4\pi^2 \mu_0 P' + \frac{\mu_0^2}{r^2} I I' = 0. \quad (9.49)$$

This equation, known as the Grad-Shafranov equation (Grad and Rubin 1958, Shafranov 1966), has the peculiarity that ψ shows up as both an independent variable and as a dependent variable, i.e., there are both derivatives of ψ and derivatives with respect to ψ . Axisymmetry has made it possible to transform a three-dimensional vector equation into a one-dimensional scalar equation. It is not surprising that axisymmetry would transform a three dimensional system into a two dimensional system, but the transformation of a three dimensional system into a one dimensional system suggests more profound physics is involved than just geometrical simplification.

The Grad-Shafranov equation can be substituted back into Eq.(9.42) to give

$$\mathbf{J}_{tor} = \left(2\pi r^2 P' + \frac{\mu_0}{2\pi} I I' \right) \nabla\phi \quad (9.50)$$

so that the total current can be expressed as

$$\mathbf{J} = \mathbf{J}_{pol} + \mathbf{J}_{tor} = \frac{I'}{2\pi} \nabla\psi \times \nabla\phi + \left(2\pi r^2 P' + \frac{\mu_0}{2\pi} I I' \right) \nabla\phi = 2\pi r^2 P' \nabla\phi + I' \mathbf{B}. \quad (9.51)$$

The last term is called the ‘force-free’ current because it is parallel to the magnetic field and so provides no force. The first term on the right hand side is the diamagnetic current.

The Grad-Shafranov equation is a non-linear equation in ψ and, in general, cannot be solved analytically. It does not in itself determine the equilibrium because it involves three independent quantities, ψ , $P(\psi)$, and $I(\psi)$. Thus, use of the Grad-Shafranov equation involves specifying two of these functions and then solving for the third. Typically $P(\psi)$ and $I(\psi)$ are specified (either determined from other equations or from experimental data) and then the Grad-Shafranov equation is used to determine ψ .

Although the Grad-Shafranov equation must in general be solved numerically, there exist a limited number of analytic solutions. These can be used as idealized examples that demonstrate typical properties of axisymmetric equilibria. We shall now examine one such analytic solution, the Solov'ev solution (Solov'ev 1976).

The Solov'ev solution is obtained by invoking two assumptions: first, the pressure is assumed to be a linear function of ψ ,

$$P = P_0 + \lambda\psi \quad (9.52)$$

and second, I is assumed to be constant within the plasma so

$$I' = 0. \quad (9.53)$$

The second assumption corresponds to having all the z -directed current flowing on the z -axis, so that away from the z -axis, the toroidal field is a vacuum field (cf. Eq.(9.35)). This arrangement is equivalent to having a zero-radius current-carrying wire going up the z axis acting as the sole source for the toroidal magnetic field. The region over which the Solov'ev solution applies excludes the z -axis and so the problem is analogous to a central force problem where the source of the central force is a singularity at the origin. The excluded region of the z -axis corresponds to the 'hole in the doughnut' of a tokamak. In the more general case where I' is finite, the plasma is either diamagnetic (toroidal field is weaker than the vacuum field) or paramagnetic (toroidal field is stronger than the vacuum field).

Using these two simplifying assumptions the Grad-Shafranov equation reduces to

$$r \frac{\partial}{\partial r} \left(\frac{1}{r} \frac{\partial \psi}{\partial r} \right) + \frac{\partial^2 \psi}{\partial z^2} + 4\pi^2 r^2 \mu_0 \lambda = 0 \quad (9.54)$$

which has the exact solution (Solov'ev solution)

$$\psi(r, z) = \psi_0 \frac{r^2}{r_0^4} (2r_0^2 - r^2 - 4\alpha^2 z^2) \quad (9.55)$$

where ψ_0 , r_0 , and α are constants. Figure 9.11 shows a contour plot of ψ as a function of r/r_0 and z/z_0 for the case $\alpha = 1$. Note that there are three distinct types of curves in Fig.9.11, namely (i) open curves going to $z = \pm\infty$, (ii) concentric closed curves, and (iii) a single curve called the separatrix which separates the first two types of curves.

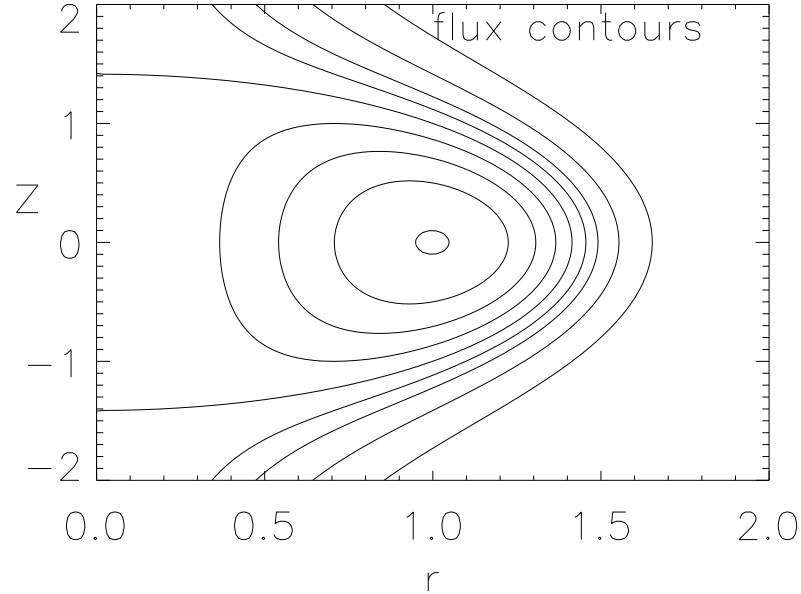


Figure 9.11: Contours of constant flux of Solov'ev solution to Grad-Shafranov equation.

Even though it is an idealization, the Solov'ev solution illustrates many important features of three-dimensional, static MHD equilibria. Let us now examine some of these features. The constants in Eq.(9.55) have been chosen so that $\psi = \psi_0$ at $r = r_0, z = 0$ (in the figure this point corresponds to $r = 1, z = 0$ since lengths in the figure have been normalized to r_0). The location $r = r_0, z = 0$ is called the *magnetic axis* because it is the axis linked by the closed contours of poloidal flux.

Let us temporarily assume that ψ_0 is positive. Examination of Eq.(9.55) shows that if ψ is positive, then the quantity $2r_0^2 - r^2 - 4\alpha^2 z^2$ is positive and vice versa. For any negative value of ψ , Eq.(9.55) can be satisfied by making r very small and z very large. In particular, if r is infinitesimal then z must become infinite. Thus, all contours for which ψ is negative go to $z = \pm\infty$; these contours are the open or type (i) contours.

On the other hand, if ψ is positive then it has a maximum value of ψ_0 which occurs on the magnetic axis and if $0 < \psi < \psi_0$ then ψ must be located at some point outside the magnetic axis, but inside the curve $2r_0^2 - r^2 - 4\alpha^2 z^2 = 0$. Hence all contours of positive ψ must lie inside the curve $2r_0^2 - r^2 - 4\alpha^2 z^2 = 0$ and correspond to field lines that do not go to infinity. These contours are the closed or type (ii) contours, since they form closed curves in the r, z plane.

The contour separating the closed contours from the contours going to infinity is the

separatrix and is given by the ellipse

$$r^2 + 4\alpha^2 z^2 = 2r_0^2. \quad (9.56)$$

On the magnetic axis ψ is a local maximum if ψ_0 is positive or a local minimum if ψ_0 is negative (the sign depends on the sense of the toroidal current). Thus, one can imagine that a hill (or valley) of poloidal flux exists with apex (or bottom) at the magnetic axis and in the vicinity of the apex (bottom) the contours of constant ψ are circles or ellipses enclosing the magnetic axis. The degree of ellipticity of these surfaces is determined by the value of α . These closed flux surfaces are a set of nested toroidal surfaces sharing the same magnetic axis. The projection of the total magnetic field lies in a flux surface since Eq.(9.34) shows

$$\mathbf{B} \cdot \nabla\psi = 0,$$

i.e., the magnetic field does not have a component in the direction normal to the flux surface.

Direct substitution of Eq.(9.55) into Eq.(9.54) gives

$$\lambda = \frac{2\psi_0}{\pi^2 r_0^4 \mu_0} (1 + \alpha^2) \quad (9.57)$$

so that the pressure is

$$P(\psi) = P_0 + \frac{2\psi_0}{\pi^2 r_0^4 \mu_0} (1 + \alpha^2) \psi. \quad (9.58)$$

Pressure vanishes at the plasma edge so if ψ_{edge} is the poloidal flux at the edge, then the constant P_0 is determined and Eq.(9.58) becomes

$$P(\psi) = \frac{2\psi_0}{\pi^2 r_0^4 \mu_0} (1 + \alpha^2) [\psi - \psi_{edge}]. \quad (9.59)$$

In the earlier discussion of single particle motion it was shown that particles were attached to flux surfaces. Particles that start on a particular flux surface always stay on that flux surface, although they may travel to any part of that flux surface. The equilibrium prescribed by Eq.(9.55) is essentially a three-dimensional vortex with pressure peaking on the magnetic axis and then falling monotonically to zero at the edge.

This is a particularly simple solution to the Grad-Shafranov equation, but nevertheless demonstrates several important features:

1. Three dimensional equilibria can incorporate closed nested poloidal flux surfaces which are concentric about a magnetic axis and correspond to local maxima or minima of the flux ψ .
2. There can also be open flux surfaces; i.e., flux surfaces which go to infinity.
3. The flux surface separating closed and open flux surfaces is called a separatrix.
4. The total magnetic field projects into the flux surfaces since $\mathbf{B} \cdot \nabla\psi = 0$.
5. Finite pressure corresponds to a depression (or elevation) of the poloidal flux. The pressure maximum and flux extrema are located at the magnetic axis.
6. The poloidal magnetic field and associated poloidal flux ψ are responsible for plasma confinement and result from the toroidal current. Thus *toroidal* current is essential for confinement in an axisymmetric geometry. For a given $P(\psi)$ the toroidal magnetic

field does not contribute to confinement if $I' = 0$. If I' is finite, plasma diamagnetism or paramagnetism will affect $P(\psi)$. Although the toroidal field does not directly provide confinement, it can affect the rate of cross-field particle and energy diffusion and hence the functional form of $P(\psi)$. For example, the frequency of drift waves will be a function of the toroidal field and drift waves can cause an outward diffusion of plasma across flux surfaces, thereby affecting $P(\psi)$.

7. The poloidal flux surfaces are related to the surfaces of constant canonical angular momentum since $\mathbf{B}_{pol} = \nabla \times (\psi \nabla \phi / 2\pi) = \nabla \times (\psi \hat{\phi} / 2\pi r) = \nabla \times A_\phi \hat{\phi}$ implies $A_\phi = \psi / 2\pi r$. Thus, the canonical angular momentum can be expressed as

$$\begin{aligned} p_\phi &= mr^2 \dot{\phi} + qr A_\phi \\ &= mrv_\phi + \frac{q\psi}{2\pi}. \end{aligned} \quad (9.60)$$

Surfaces of constant canonical angular momentum correspond to surfaces of constant poloidal flux in the limit $m \rightarrow 0$. Because the system is toroidally symmetric (axisymmetric) the canonical angular momentum of each particle is a constant of the motion and so, to the extent that the particles can be approximated as having zero mass, particle trajectories are constrained to lie on surfaces of constant ψ . Since p_ϕ is a conserved quantity, the maximum excursion a finite-mass particle can make from a poloidal flux surface can be estimated by writing

$$\delta p_\phi = \delta (mrv_\phi + qr A_\phi) = 0. \quad (9.61)$$

Thus,

$$\frac{v_\phi}{r} \delta r + \delta v_\phi + \frac{q}{m} \delta r \frac{1}{r} \frac{\partial}{\partial r} (r A_\phi) = 0 \quad (9.62)$$

or

$$\delta r = - \frac{r \delta v_\phi}{v_\phi + r \omega_{c,pol}} \quad (9.63)$$

where $\omega_{c,pol} = qB_{pol}/m$ is the cyclotron frequency measured using the poloidal magnetic field. Since v_ϕ is of the order of the thermal velocity or smaller, if the poloidal field is sufficiently strong that the poloidal Larmor radius $r_{lpol} \sim v_\phi / \omega_{c,pol}$ is much smaller than the radius r , then the first term in the denominator may be dropped. Since δv_ϕ is also of the order of the thermal velocity or smaller, the particle cannot deviate from its initial flux surface by more than a poloidal Larmor radius. Since poloidal field is produced by toroidal current, it is clear that particle confinement to axisymmetric flux surfaces requires the existence of a toroidal current.

Tokamaks, reverse field pinches, spheromaks, and field reversed configurations are all magnetic confinement configurations having three dimensional axisymmetric equilibria similar to this Solov'ev solution and all involve a toroidal current to produce a set of nested, closed poloidal flux surfaces which link a magnetic axis. Stellarators are non-axisymmetric configurations which have poloidal flux surfaces without toroidal currents; the advantage of current-free operation is offset by the complexity of non-axisymmetry.

9.9 Dynamic equilibria: flows

The basic mechanism driving MHD flows will first be discussed using the simplified assumptions of incompressibility and self-field only. This situation is relevant to simple arcs, basic concepts of magnetoplasmadynamic thrusters, and to currents driven in molten metals. The more general situation where the plasma is compressible and where there are external, applied magnetic fields in addition to the self-field will then be addressed.

9.9.1 Incompressible plasma with self-field only

MHD-driven flows involve situations where $\nabla \times (\mathbf{J} \times \mathbf{B})$ is non-zero. This means the MHD force $\mathbf{J} \times \mathbf{B}$ is non-conservative in which case its finite curl acts as torque or equivalently as a source for hydrodynamic vorticity. When the MHD force is non-conservative a closed line integral $\oint d\mathbf{l} \cdot \mathbf{J} \times \mathbf{B}$ will be finite, whereas in contrast a closed line integral of a pressure gradient $\oint d\mathbf{l} \cdot \nabla P$ is always zero. Since a pressure gradient cannot balance the torque produced by a non-conservative $\mathbf{J} \times \mathbf{B}$, it is necessary to include a vorticity-damping term (viscosity term) to allow for the possibility of balancing this torque. Plasma viscosity is mainly due to ion-ion collisions and is typically very small. With the addition of viscosity, the MHD equation of motion becomes

$$\rho \left(\frac{\partial \mathbf{U}}{\partial t} + \mathbf{U} \cdot \nabla \mathbf{U} \right) = \mathbf{J} \times \mathbf{B} - \nabla P + \rho \nu \nabla^2 \mathbf{U} \quad (9.64)$$

where ν is the kinematic viscosity. To focus attention on vorticity generation, transport, and decay the following simplifying assumptions are made:

1. The motion is incompressible so that $\rho = \text{const}$.

This is an excellent assumption for a molten metal, but is questionable for a plasma. However, this assumption could be at least locally reasonable for a plasma if the region of vorticity generation is smaller in scale than regions of compression or rarefaction or is spatially distinct from these regions. The consequences of compressibility will be discussed later.

2. The system is cylindrically symmetric.

A cylindrical coordinate system r, ϕ, z can then be used and ϕ is ignorable. This geometry corresponds to magnetohydrodynamic thrusters and arcs.

3. The flow velocities \mathbf{U} and the current density \mathbf{J} are in the poloidal direction (r and z plane). Restricting the current to be poloidal means that the magnetic field is purely toroidal (see Fig.9.10).

The most general poloidal velocity for a constant-density, incompressible fluid has the form

$$\mathbf{U} = \frac{1}{2\pi} \nabla \psi \times \nabla \phi \quad (9.65)$$

where $\psi(r, z)$ is the flux of fluid through a circle of radius r at location z . Note the analogy to the poloidal magnetic flux function used in Eqs.(3.146) and (9.34). Since \mathbf{U} lies entirely in the r, z plane and since the system is axisymmetric, the curl of \mathbf{U} will be in the ϕ direction. It is thus useful to define a scalar cylindrical ‘‘vorticity’’ $\chi = r \hat{\phi} \cdot \nabla \times \mathbf{U}$; this

definition differs slightly from the conventional definition of vorticity (curl of velocity) because it includes an extra factor of r . This slight change of definition is essentially a matter of semantics, but makes the algebra more transparent.

Since $\nabla\phi = \hat{\phi}/r$ it is seen that

$$\nabla \times \mathbf{U} = \frac{\hat{\phi}}{r} \hat{\phi} \cdot \nabla \times \mathbf{U} = \chi \nabla \phi \quad (9.66)$$

and so

$$\nabla \times \left(\frac{1}{2\pi} \nabla \psi \times \nabla \phi \right) = \chi \nabla \phi. \quad (9.67)$$

Dotting Eq.(9.67) with $\nabla\phi$ and using the vector identity $\nabla\phi \cdot \nabla \times \mathbf{Q} = \nabla \cdot (\mathbf{Q} \times \nabla\phi)$ gives

$$\nabla \cdot \left(\frac{1}{2\pi} (\nabla \psi \times \nabla \phi) \times \nabla \phi \right) = \frac{\chi}{r^2} \quad (9.68)$$

or

$$r^2 \nabla \cdot \left(\frac{1}{r^2} \nabla \psi \right) = -2\pi \chi \quad (9.69)$$

which is a Poisson-like relation between the vorticity and the stream function. The vorticity plays the role of the source (charge-density) and the stream function plays the role of the potential function (electrostatic potential). However, the elliptic operator is not exactly a Laplacian and when expanded has the form

$$r^2 \nabla \cdot \left(\frac{1}{r^2} \nabla \psi \right) = r \frac{\partial}{\partial r} \left(\frac{1}{r} \frac{\partial \psi}{\partial r} \right) + \frac{\partial^2 \psi}{\partial z^2} \quad (9.70)$$

which is just the operator in the Grad-Shafranov equation.

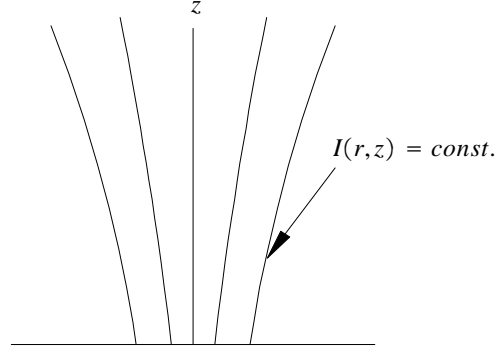
Since the current was assumed to be purely poloidal, the magnetic field must be purely toroidal and so can be written as

$$\mathbf{B} = \frac{\mu_0}{2\pi} I \nabla \phi \quad (9.71)$$

where I is the current through a circle of radius r at location z . This is consistent with the integral form of Ampere's law, $\oint \mathbf{B} \cdot d\mathbf{l} = \mu_0 I$. The curl of Eq.(9.71) gives

$$\nabla \times \mathbf{B} = \frac{\mu_0}{2\pi} \nabla I \times \nabla \phi \quad (9.72)$$

showing that I acts like a stream-function for the magnetic field.

Figure 9.12: Current channel $I(r, z)$.

The magnetic force is therefore

$$\mathbf{J} \times \mathbf{B} = \frac{1}{2\pi} (\nabla I \times \nabla \phi) \times \frac{\mu_0}{2\pi} I \nabla \phi = -\frac{\mu_0}{(2\pi r)^2} \nabla \left(\frac{I^2}{2} \right). \quad (9.73)$$

It is seen that there is an axial force if I^2 depends on z ; this is the essential condition that produces axial flows in MHD arcs (Maecker 1955) and plasma guns (Marshall 1960).

Using the identities $\nabla U^2/2 = \mathbf{U} \cdot \nabla \mathbf{U} + \mathbf{U} \times \nabla \times \mathbf{U}$ and $\nabla \times \nabla \times \mathbf{U} = -\nabla^2 \mathbf{U} = \nabla \chi \times \nabla \phi$ the equation of motion Eq.(9.64) becomes

$$\rho \left(\frac{\partial \mathbf{U}}{\partial t} + \nabla \frac{U^2}{2} - \mathbf{U} \times \chi \nabla \phi \right) = -\frac{\mu_0}{(2\pi r)^2} \nabla \left(\frac{I^2}{2} \right) - \nabla P - \rho \nu \nabla \chi \times \nabla \phi \quad (9.74)$$

or

$$\begin{aligned} \rho \left(\frac{\partial \mathbf{U}}{\partial t} + \nabla \frac{U^2}{2} - \mathbf{U} \times \chi \nabla \phi \right) = & - \frac{\mu_0}{(2\pi)^2} \nabla \left(\frac{I^2}{2r^2} \right) + \frac{\mu_0 I^2}{(2\pi)^2} \nabla \left(\frac{1}{2r^2} \right) \\ & - \nabla P - \rho \nu \nabla \chi \times \nabla \phi. \end{aligned} \quad (9.75)$$

Every term in this equation is either a gradient of a scalar or else can be expressed as a cross-product involving $\nabla \phi$. The equation can thus be regrouped as

$$\nabla \left(\frac{\rho U^2}{2} + \frac{\mu_0}{(2\pi)^2} \frac{I^2}{2r^2} + P \right) + \left(\frac{\rho}{2\pi} \nabla \frac{\partial \psi}{\partial t} - \rho \mathbf{U} \chi - \frac{\mu_0 I^2}{(2\pi r)^2} \hat{z} + \rho \nu \nabla \chi \right) \times \nabla \phi = 0. \quad (9.76)$$

Similarly, the MHD Ohm's law $\mathbf{E} + \mathbf{U} \times \mathbf{B} = \eta \mathbf{J}$ can be written as

$$-\frac{\partial \mathbf{A}}{\partial t} - \nabla V + \mathbf{U} \times \frac{\mu_0}{2\pi} I \nabla \phi = \frac{\eta}{2\pi} \nabla I \times \nabla \phi \quad (9.77)$$

where V is the electrostatic potential. Since \mathbf{B} is purely toroidal, \mathbf{A} is poloidal and so is orthogonal to $\nabla \phi$. Thus, both the equation of motion and Ohm's law are equations of the

form

$$\nabla g + \mathbf{Q} \times \nabla \phi = 0. \quad (9.78)$$

which is the most general form of an axisymmetric partial differential equation involving a potential. Two distinct scalar partial differential equations can be extracted from Eq.(9.78) by (i) operating with $\nabla \phi \cdot \nabla \times$ and (ii) taking the divergence. Doing the former it is seen that Eq.(9.78) becomes

$$\nabla \phi \cdot \nabla \times (\mathbf{Q} \times \nabla \phi) = 0 \quad (9.79)$$

or

$$\nabla \cdot \left(\frac{1}{r^2} \mathbf{Q}_{pol} \right) = 0. \quad (9.80)$$

Applying this procedure to Eq.(9.76) gives

$$\frac{\rho}{2\pi} \frac{\partial}{\partial t} \left(\nabla \cdot \frac{1}{r^2} \nabla \psi \right) - \rho \nabla \cdot \left(\frac{1}{r^2} \mathbf{U} \chi \right) - \nabla \cdot \left(\frac{\mu_0 I^2}{(2\pi r^2)^2} \hat{z} \right) + \rho v \nabla \cdot \left(\frac{1}{r^2} \nabla \chi \right) = 0 \quad (9.81)$$

or

$$\frac{\partial}{\partial t} \left(\frac{\chi}{r^2} \right) + \nabla \cdot \left(\mathbf{U} \frac{\chi}{r^2} \right) = - \frac{\mu_0}{4\pi^2 \rho r^4} \frac{\partial I^2}{\partial z} + v \nabla \cdot \left(\frac{1}{r^2} \nabla \chi \right). \quad (9.82)$$

Since $\nabla \cdot \mathbf{U} = 0$, this can also be written as

$$\frac{\partial}{\partial t} \left(\frac{\chi}{r^2} \right) + \mathbf{U} \cdot \nabla \left(\frac{\chi}{r^2} \right) = - \frac{\mu_0}{4\pi^2 \rho r^4} \frac{\partial I^2}{\partial z} + v \nabla \cdot \frac{1}{r^2} \nabla \chi \quad (9.83)$$

which shows that if there is no viscosity and if $\partial I^2 / \partial z = 0$, then the scaled vorticity χ/r^2 convects with the fluid; i.e., is frozen into the fluid. The viscous term on the right hand side describes a diffusive-like dissipation of vorticity. The remaining term $r^{-4} \partial I^2 / \partial z$ acts as a *vorticity source* and is finite only if I^2 is non-uniform in the z direction. The vorticity source has a strong r^{-4} weighting factor so that axial non-uniformities of I near $r = 0$ dominate. Positive χ corresponds to a clockwise rotation in the r, z plane. If I^2 is an increasing function of z then the source term is negative, implying that a counterclockwise vortex is generated and vice versa. Suppose as shown in Fig.9.12 that the current channel becomes wider with increasing z corresponding to a fanning out of the current with increasing z . In this case $\partial I^2 / \partial z$ will be negative and a clockwise vortex will be generated. Fluid will flow radially inwards at small z , then flow vertically upwards, and finally radially outwards at large z . The fluid flow produced by the vorticity source will convect the vorticity along with the flow until it is dissipated by viscosity.

Operating on Ohm's law, Eq.(9.77), with $\nabla \phi \cdot \nabla \times$ gives

$$\frac{\partial}{\partial t} \left(\frac{I}{r^2} \right) + \mathbf{U} \cdot \nabla \left(\frac{I}{r^2} \right) = \frac{\eta}{\mu_0} \nabla \cdot \left(\frac{1}{r^2} \nabla I \right) \quad (9.84)$$

showing that I/r^2 is similarly convected with the fluid and also has a diffusive-like term, this time with coefficient η/μ_0 .

Thus, the system of equations can be summarized as (Bellan 1992)

$$\frac{\partial}{\partial t} \left(\frac{\chi}{r^2} \right) + \mathbf{U} \cdot \nabla \left(\frac{\chi}{r^2} \right) = v \nabla \cdot \frac{1}{r^2} \nabla \chi - \frac{\mu_0}{4\pi^2 \rho r^4} \frac{\partial I^2}{\partial z} \quad (9.85)$$

$$\frac{\partial}{\partial t} \left(\frac{I}{r^2} \right) + \mathbf{U} \cdot \nabla \left(\frac{I}{r^2} \right) = \frac{\eta}{\mu_0} \nabla \cdot \left(\frac{1}{r^2} \nabla I \right) \quad (9.86)$$

$$r^2 \nabla \cdot \left(\frac{1}{r^2} \nabla \psi \right) = -2\pi \chi \quad (9.87)$$

$$\mathbf{U} = \frac{1}{2\pi} \nabla \psi \times \nabla \phi \quad . \quad (9.88)$$

This system cannot be solved analytically, but its general behavior can be described in a qualitative manner. The system involves three scalar variables, χ , ψ , and I all of which are functions of r and z . Boundary conditions must be specified in order to have a well-posed problem. If a recirculating flow is driven, the fluid flux ψ will be zero on the boundary whereas I will be finite on electrodes at the boundary. In particular, the current I will typically flow from the anode into the plasma and then from the plasma into the cathode. The vorticity χ will usually have the boundary condition of vanishing on the bounding surface.

Initially, there is no flow so ψ is zero everywhere. An initial solution of Eq.(9.86) in this no-flow situation will establish a current profile between the two electrodes. For any reasonable situation, this $I(r, z)$ profile will have $\partial I^2 / \partial z \neq 0$ so that a vorticity source will be created. The source will be quite localized because of the r^{-4} coefficient. Once vorticity χ is created as determined by Eq.(9.85), the vorticity acts as a source term for the fluid flux ψ in Eq.(9.87), and so a finite ψ will be developed. Thus a flow $\mathbf{U}(r, z)$ will be created as specified by Eq.(9.88), and this flow will convect both χ/r^2 and I/r^2 .

A good analogy is to think of the $r^{-4} \partial I^2 / \partial z$ term as constituting a toroidally symmetric centrifugal pump which accelerates fluid radially from large to small r . This radial acceleration takes place at z locations where the current channel radius is constricted. The pump then accelerates the ingested fluid up or down the z axis, in a direction away from the current constriction. This vortex generation can also be seen by drawing vectors showing the magnitude and orientation of the $\mathbf{J} \times \mathbf{B}$ force in the vicinity of a current constriction. It is seen that the $\mathbf{J} \times \mathbf{B}$ force is non-conservative and provides a centrifugal pumping as described above.

An arc or magnetoplasmadynamic thruster can thus be construed as a pump which sucks fluid radially inward towards the smaller radius electrode and then shoots the fluid axially away from the smaller electrode towards the larger radius electrode. The sign of the current does not matter, since the pumping action depends only on the z derivative of I^2 . If the equations are put in dimensionless form, it is seen that the characteristic flow velocity is of the order of the Alfvén velocity.

Once χ , ψ and I have been determined, it is possible to determine the pressure and electrostatic potential profiles. This is done by taking the divergence of Eq.(9.78) to obtain

$$\nabla^2 g = -\nabla\phi \cdot \nabla \times \mathbf{Q}. \quad (9.89)$$

The pressure and electrostatic potential are contained within the g term, whereas the \mathbf{Q} term involves only χ , ψ and I or functions of χ , ψ and I (e.g., the velocity). Thus, the right hand side of Eq.(9.89) is known and so can be considered as the source for a Poisson-like equation for the left hand side. For the equation of motion

$$g_{motion} = \frac{\rho U^2}{2} + \frac{\mu_0}{(2\pi)^2} \frac{I^2}{2r^2} + P \quad (9.90)$$

so that

$$P = g_{motion} - \frac{\rho U^2}{2} - \frac{\mu_0}{(2\pi)^2} \frac{I^2}{2r^2}. \quad (9.91)$$

Regions where g_{motion} is constant satisfy an extended form of the Bernoulli theorem, namely

$$\frac{\rho U^2}{2} + \frac{B^2}{2\mu_0} + P = const. \quad (9.92)$$

Similarly, taking the divergence of Eq.(9.77) gives an equation for the electrostatic potential (using Coulomb gauge so that $\nabla \cdot \mathbf{A} = 0$). Thus, a complete solution for incompressible flow is obtained by first solving for χ , ψ and I using prescribed boundary conditions, and then solving for the pressure and electrostatic potential.

9.9.2 Compressible plasma and applied poloidal field

The previous discussion assumed that the plasma was incompressible and the magnetic field was purely toroidal (i.e., generated by the prescribed poloidal current). The more general situation involves having a pre-existing poloidal magnetic field such as would be generated by external coils and also allowing for plasma compressibility. This situation will now be discussed qualitatively making reference to the sketch provided in Fig.9.13 (a more thorough discussion is provided in Bellan (2003)).

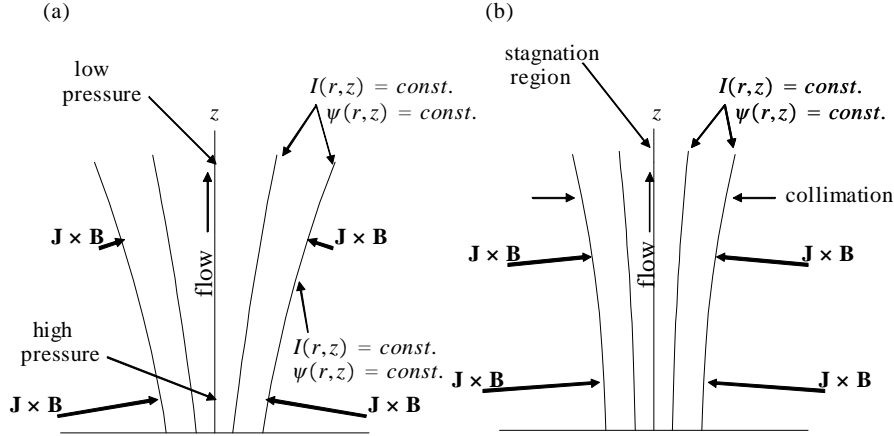


Figure 9.13: (a) Current channel $I(r, z)$ which has same contours as poloidal flux surfaces $\psi(r, z)$ so that ∇I is parallel to $\nabla \psi$ in order to have no toroidal acceleration. The $\mathbf{J} \times \mathbf{B}$ force shown by thick arrows is larger at the bottom and canted giving both a higher on-axis pressure at the bottom and an axial upwards flow. (b) If the flow stagnates (slows down) for some reason, then mass accumulates at the top. The frozen-in convected toroidal flux also accumulates which thus increases B_ϕ and so forces r to decrease since Ampere's law gives $2\pi B_\phi r = I(r, z)$ which is constant on a surface of constant $I(r, z)$. The upward-moving, stagnating plasma flow with embedded toroidal flux acts somewhat like a zipper for the surfaces of constant $I(r, z)$ and $\psi(r, z)$.

Consider the initial situation shown in Fig.9.13(a) in which a plasma is immersed in an axisymmetric vacuum poloidal field $\psi(r, z)$ with a poloidal current $I(r, z)$. Because ψ is assumed to correspond to a vacuum field it is produced by external coils with toroidal currents. There are thus no toroidal currents in the volume under consideration (i.e., in the region described by Fig.9.13(a)) and so using Eq.(9.42) it is seen that $\psi(r, z)$ satisfies $\nabla \cdot (r^{-2} \nabla \psi) = 0$. The poloidal current $I(r, z)$ has an associated poloidal current density

$$\mathbf{J}_{pol} = \frac{1}{2\pi} \nabla I \times \nabla \psi \quad (9.93)$$

and an associated toroidal magnetic field

$$B_\phi = \frac{\mu_0 I(r, z)}{2\pi}. \quad (9.94)$$

The poloidal flux $\psi(r, z)$ has an associated poloidal magnetic field

$$\mathbf{B}_{pol} = \frac{1}{2\pi} \nabla \psi \times \nabla \phi. \quad (9.95)$$

If \mathbf{J}_{pol} is parallel to \mathbf{B}_{pol} then ∇I would be parallel to $\nabla \psi$ so that constant $I(r, z)$ would be coincident with constant $\psi(r, z)$ surfaces as indicated in the figure. On the other

hand if \mathbf{J}_{pol} were not parallel to \mathbf{B}_{pol} , these surfaces would not be coincident and there would be a force $\mathbf{J}_{pol} \times \mathbf{B}_{pol}$ in the toroidal direction would tend to cause a change in the toroidal velocity, i.e., an acceleration or deceleration of U_ϕ . We argue that $\mathbf{J}_{pol} \times \mathbf{B}_{pol}$ must be a transient force with zero time average because any current which flows perpendicular to the poloidal flux surfaces must be the polarization current as given by Eq.(3.145). This polarization current results from the time derivative of the electric field perpendicular to the poloidal flux surfaces and this electric field in turn is proportional to the time rate of change of the poloidal current as determined from Faraday's law. Thus, once the current is in steady state, it is necessary to have $I = I(\psi)$ and so the surfaces of constant $I(r, z)$ in Fig.9.12 can also be considered as surfaces of constant $\psi(r, z)$. Another way to see this, is to realize that a steady current perpendicular to flux surfaces would cause a continuous electrostatic charging of the flux surfaces which would then violate the stipulation that the plasma is quasi-neutral.

The initial magnetic force is thus the same as for the situation of a purely toroidal magnetic field since

$$\mathbf{J} \times \mathbf{B} = \underbrace{\mathbf{J}_{tor}}_{\text{zero}} \times \mathbf{B}_{pol} + \mathbf{J}_{pol} \times \mathbf{B}_{tor}. \quad (9.96)$$

The remaining force $\mathbf{J}_{pol} \times \mathbf{B}_{tor} = (J_r \hat{r} + J_z \hat{z}) \times B_\phi \hat{\phi} = J_r B_\phi \hat{z} - J_z B_\phi \hat{r}$ has components in both the r and z directions. If the plasma axial length is much larger than its radius (i.e., it is long and skinny) then the plasma will develop a local radial pressure balance

$$(-\nabla P + \mathbf{J}_{pol} \times \mathbf{B}_{tor}) \cdot \hat{r} = 0. \quad (9.97)$$

However, this local radial pressure balance precludes the possibility of an axial pressure balance if $\partial\psi/\partial z \neq 0$ because, as discussed earlier, ∇P cannot balance $\mathbf{J} \times \mathbf{B}$ if the latter has a finite curl. Suppose that the radius of the current channel and the poloidal flux are both given by $a = a(z)$ and since $I = I(\psi)$ let us assume a simple linear dependence where $\mu_0 I(r, z) = \lambda \psi(r, z)$. Thus, ∇I is parallel to $\nabla \psi$ and I is just the current per flux. We assume a parabolic poloidal flux

$$\frac{\psi(r, z)}{\psi_0} = \left(\frac{r}{a(z)} \right)^2 \quad (9.98)$$

for $r \leq a(z)$ and ψ_0 is the flux at $r = a$; this is the simplest allowed form for the flux (if ψ depended linearly on r , there would be infinite fields at $r = 0$). The local radial pressure balance is essentially a local version of the Bennett pinch relation

$$\begin{aligned} \frac{\partial P}{\partial r} &= -J_z B_\phi \\ &= -\frac{\lambda^2}{8\pi^2 \mu_0 r^2} \frac{\partial \psi^2}{\partial r}. \end{aligned} \quad (9.99)$$

On substitution of Eq.(9.98) this becomes

$$\begin{aligned} \frac{\partial P}{\partial r} &= -\frac{\mu_0 \lambda^2 \psi_0^2}{8\pi^2 r^2} \frac{\partial}{\partial r} \left(\frac{r}{a(z)} \right)^4 \\ &= -\frac{\lambda^2 \psi_0^2}{2\pi^2 \mu_0} \frac{r}{a^4}. \end{aligned} \quad (9.100)$$

Integration and using the boundary condition that $P = 0$ at $r = a$ gives

$$P(r) = \frac{\lambda^2 \psi_0^2}{4\pi^2 \mu_0 a^2} \left(1 - \frac{r^2}{a^2}\right) \quad (9.101)$$

which shows that the on-axis pressure is larger where $a(z)$ is smaller as indicated in Fig.9.13(a). The axial component of the equation of motion is thus

$$\begin{aligned} F_z &= \hat{z} \cdot (-\nabla P + \mathbf{J}_{pol} \times \mathbf{B}_{tor}) \\ &= -\frac{\partial P}{\partial z} + J_r B_\phi \\ &= -\frac{\lambda^2 \psi_0^2}{4\pi^2 \mu_0} \frac{\partial}{\partial z} \left(\frac{1}{a^2} - \frac{r^2}{a^4}\right) - \frac{1}{\mu_0} B_\phi \frac{\partial B_\phi}{\partial z} \\ &= -\frac{\lambda^2 \psi_0^2}{\pi^2 \mu_0} \left(-\frac{1}{2a^3} + \frac{r^2}{a^5}\right) \frac{\partial a}{\partial z} - \frac{1}{2\mu_0} \frac{\partial}{\partial z} \left(\frac{\lambda \psi}{2\pi r}\right)^2 \\ &= \frac{\lambda^2 \psi_0^2}{\pi^2 a^3 \mu_0} \left(\frac{1}{2} - \frac{r^2}{a^2}\right) \frac{\partial a}{\partial z} - \frac{\lambda^2 \psi_0^2}{8\pi^2 r^2 \mu_0} \frac{\partial}{\partial z} \left(\frac{r}{a}\right)^4 \\ &= \frac{\mu_0 I_0^2}{2\pi^2 a^3} \left(1 - \frac{r^2}{a^2}\right) \frac{\partial a}{\partial z} \end{aligned} \quad (9.102)$$

which shows that there is an axial force which peaks on axis. This force is proportional to current flowing along the flux tube and to the axial non-uniformity of the flux tube, i.e., to $\partial a/\partial z$ and accelerates plasma away from regions where a is small to regions where a is large.

If the flow stagnates, i.e., is such that the axial velocity is non-uniform so that $\nabla \cdot \mathbf{U}$ is negative, then there will be a net inflow of matter into the stagnation region and hence an increase of mass density at the locations where $\nabla \cdot \mathbf{U}$ is negative. Because magnetic flux is frozen to the plasma, there will be a corresponding accumulation of toroidal magnetic flux at the locations where $\nabla \cdot \mathbf{U}$ is negative. If U_ϕ is zero (as assumed on the basis of there being no steady toroidal acceleration and zero initial toroidal velocity), then the accumulation of toroidal flux will increase the toroidal field. This can be seen by considering the toroidal component of the induction equation

$$\frac{\partial B_\phi}{\partial t} = r \mathbf{B}_{pol} \cdot \nabla \left(\frac{U_\phi}{r}\right) - r \mathbf{U}_{pol} \cdot \nabla \left(\frac{B_\phi}{r}\right) - B_\phi \nabla \cdot \mathbf{U}_{pol} \quad (9.103)$$

or

$$\frac{DB_\phi}{Dt} = -B_\phi \nabla \cdot \mathbf{U}_{pol} \quad (9.104)$$

where $D/DT = \partial/\partial t + \mathbf{U} \cdot \nabla$ and $U_\phi = 0$ has been assumed. Thus, it is seen that B_ϕ will increase in the frame of the plasma when $\nabla \cdot \mathbf{U}_{pol}$ is negative. However, Ampere's law gives $\mu_0 I = 2\pi r B_\phi$ and since $I = I_0$ at the outer radius of the current channel, it is seen that if B_ϕ increases, then the radius of the current channel has to decrease in order to keep rB_ϕ fixed. The result is that stagnation of the flow tends to collimate the flux tube, i.e., make it axially uniform as shown in Fig.9.13(b). The plasma accelerated upwards in Fig.9.12 will then squeeze together the ψ and thus I surfaces so that these surfaces will become vertical lines; very roughly stagnation of an upward moving plasma in Fig.9.12

can be imagined as a sort of “zipper” which collimates the flux surfaces. Collimation is often seen in current-carrying magnetic flux tubes (e.g., see Hansen and Bellan (2001) and is an important property of solar coronal loops (Klimchuk 2000) and of astrophysical jets (Livio 1999)).

9.10 Assignments

1. Show that if a Bennett pinch equilibrium has a J_z independent of r , then the azimuthal magnetic field is of the form $B_\theta(r) = B_\theta(a)r/a$. Then show that if the temperature is uniform, the pressure will be of the form $P = P_0(1 - r^2/a^2)$ where $P_0 = \mu_0 I^2 / 4\pi^2 a^2$. Show that this result is consistent with Eq.(9.29).
2. Show that it is impossible to confine a spherically symmetric pressure profile using magnetic forces alone and therefore show that three dimensional magnetostatic equilibria cannot be found for arbitrarily specified pressure profiles. To do this suppose there exists a magnetic field that satisfies $\mathbf{J} \times \mathbf{B} = \nabla P$ where $P = P(r)$ and r is the radius in spherical coordinates $\{r, \theta, \phi\}$.
 - (a) Show that neither \mathbf{J} nor \mathbf{B} can have a component in the \hat{r} direction. Hint: assume that B_r is finite and write out the three components of $\mathbf{J} \times \mathbf{B} = \nabla P$ in spherical coordinates. By eliminating either J_r or B_r from the equations resulting from the θ and ϕ components, obtain equations of the form $J_r \partial P / \partial r = 0$ and $B_r \partial P / \partial r = 0$. Then use the fact that $\partial P / \partial r$ is finite to develop a contradiction regarding the original assumption regarding J_r or B_r .
 - (b) By calculating J_θ and J_ϕ from Ampere’s law (use the curl in spherical coordinates as given on p.523), show that $\mathbf{J} \times \mathbf{B} = \nabla P$ implies $B_\theta^2 + B_\phi^2 = B^2(r)$. Argue that this means that the magnitude of $\mathbf{B} = B_\theta \hat{\theta} + B_\phi \hat{\phi}$ must be independent of θ and ϕ and therefore B_θ and B_ϕ must be of the form $B_\theta = B \sin [\eta(\theta, \phi, r)]$ and $B_\phi = B \cos [\eta(\theta, \phi, r)]$ where η is some arbitrary function.
 - (c) Using $J_r = 0$, $B_r = 0$ and $\nabla \cdot \mathbf{B} = 0$ (see p. 523 for the latter) derive a pair of coupled equations for $\partial \eta / \partial \theta$ and $\partial \eta / \partial \phi$. Solve these coupled equations for $\partial \eta / \partial \theta$ and $\partial \eta / \partial \phi$ using the method of determinants (the solutions for $\partial \eta / \partial \theta$ and $\partial \eta / \partial \phi$ should be very simple). Integrate the $\partial \eta / \partial \phi$ equation to obtain η and show that this solution for η is inconsistent with the requirements of the solution for $\partial \eta / \partial \theta$, thereby demonstrating that the original assumption of existence of a spherically symmetric equilibrium must be incorrect.
3. Using numerical methods solve for the motion of charged particles in the Solov’ev field, $\mathbf{B} = \nabla \psi \times \nabla \phi$ where $\psi = B_0 r^2 (2a^2 - r^2 - 4(\alpha z)^2) / a^4$ where B_0 , a and α are constants. Plot the surfaces of constant ψ and show there are open and closed surfaces. Select appropriate characteristic times, lengths, and velocities and choose appropriate time steps, initial conditions, and graph windows. Plot the x, y plane and the x, z plane. What interesting features are observed in the orbits. How do they relate to the flux surfaces $\psi = \text{const.}$ What can be said about flux conservation?
4. *Grad-Shafranov equation for a current-carrying flux tube:* The Grad-

Shafranov equation describes axisymmetric equilibria and so can be used to characterize an axisymmetric magnetic flux tube. Suppose that $\psi = \psi(r, z)$ and that ψ is a monotonically increasing function of r . Assume that both the current I and pressure P are linear functions of ψ so that

$$\begin{aligned}\mu_0 I &= \lambda \psi \\ P &= P_0(1 - \psi/\psi_0)\end{aligned}$$

where ψ_0 is the flux surface at which P vanishes and P_0 is the pressure on the z axis. Show that the Grad-Shafranov equation can be written in the form

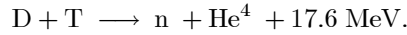
$$r^2 \nabla \cdot \left(\frac{1}{r^2} \nabla \bar{\psi} \right) + \mu_0^2 \lambda^2 \bar{\psi} = \frac{4\pi^2 r^2 \mu_0 P_0}{\psi_0^2}$$

where $\bar{\psi} = \psi(r, z)/\psi_0$. Show that if

$$P_0 = \frac{\mu_0^2 \lambda^2 \psi_0^2}{4\pi^2 \mu_0 a^2}$$

where a is the radius at which the pressure vanishes at $z = 0$, the flux tube must be axially uniform, i.e., ψ cannot have any z dependence. Express this condition in terms of the pitch angle of the magnetic field B_ϕ/B_z measured at $r = a$. Hint: note that the Grad-Shafranov equation has a both homogeneous part (left hand side) and inhomogeneous part (right hand side). Show that $\bar{\psi} = r^2/a^2$ is a particular solution and then consider the form of the general solution (homogenous plus inhomogeneous solution).

5. *Lawson Criterion:* Of the many possible thermonuclear reactions, the deuterium-tritium (DT) reaction stands out as being most attractive because it has the largest reaction cross-section at accessible temperatures. The DT reaction has the form



The output energy consists of 3.5 MeV neutron kinetic energy and 14.1 MeV alpha particle kinetic energy. Fusion reaction cross-sections have a very strong dependence on the impact energy of the reacting ions because of the Coulomb barrier. In order for a controlled fusion reaction to be economically useful, more energy must be generated than is invested. The break-even condition is determined by equating the energy input per volume to the energy output for the reaction duration. The time duration that this condition is maintained is called the *energy confinement* time τ_E of the configuration, a measure of the insulating capability of the plasma confinement device. Let all temperatures and energies be measured in kilovolts (keV) so that the Boltzmann constant is $\kappa = 1.6 \times 10^{-16}$ and consider a volume V of reacting deuterium, tritium and associated neutralizing electrons (the plasma needs to be overall neutral, otherwise there will be enormous electrostatic forces).

- (a) Show that if the electrons and ions have the same temperature T the energy required to heat this volume is $E_{in} \sim 3n_e V \kappa T$ where n_e is the electron density and equal densities of deuterium and tritium are assumed so that $n_D = n_T =$

$n_e/2$. (Hint: the mean energy per degree of freedom is $\kappa T/2$ so the mean energy of a particle moving in three dimensional space is $3\kappa T/2$).

- (b) What is the fusion reaction rate R for a single incident ion of velocity v passing through stationary target ions where $\sigma(v)$ is the fusion reaction rate cross-section and n_t is the density of the target ions (assumed stationary). If $\langle \sigma(v)v \rangle$ denotes the velocity average of $\sigma(v)v$ what is the velocity-averaged reaction rate?
- (c) Assume that the reaction of hot tritium with hot deuterium can be approximated as the sum of hot deuterium interacting with stationary tritium and hot tritium interacting with stationary deuterium. Show that the fusion output power in the volume is

$$P = n_D n_T \langle \sigma(v)v \rangle V E_{reaction}$$

where $E_{reaction} = 17.6 \times 10^3$ keV.

- (d) Show that the ratio Q of the fusion output energy to the input energy satisfies the relation

$$n_e \tau_E \sim \frac{6.8 \times 10^{-4} T_{keV}}{\langle \sigma(v)v \rangle} Q$$

At break-even $Q = 1$.

- (e) For a thermal ion distribution and the experimentally measured reaction cross-section $\sigma(v)$ the velocity averaged rate integral has the following values

Temperature in keV	$\langle \sigma(v)v \rangle$ in m^3/s	$n_e \tau_E$
1	5.5×10^{-27}	
2	2.6×10^{-25}	
5	1.3×10^{-23}	
10	1.1×10^{-22}	
20	4.2×10^{-22}	
50	8.7×10^{-22}	
100	8.5×10^{-22}	

Calculate the $n_e \tau_E$ required for break-even at the listed temperatures (i.e. fill in the last column).

- (f) The Joint European Tokamak (JET) located in Culham, UK (in operation during the latter 20th and early 21st century) has a plasma volume of approximately 80 cubic meters. Suppose JET has an energy confinement time of $\tau_E \sim 0.3$ s at $n_e \sim 10^{20} m^{-3}$ and $T \sim 10$ keV. If the plasma is a 50%-50% mixture of D-T how much fusion power would be produced in JET and what is Q ? What is the weight of the plasma? How much does the confinement time have to be scaled up to achieve break-even? How much does the volume have to be scaled up to achieve 2000 MWt power output at breakeven? In order to achieve this volume scale-up, how much does the linear dimension have to be scaled up?

Stability of static MHD equilibria

Solutions to Eq.(9.49), the Grad-Shafranov equation, (or to some more complicated counterpart in the case of non-axisymmetric geometry) provide a static MHD equilibrium. The question now arises whether the equilibrium is stable. This issue was forced upon early magnetic fusion researchers who found that plasma which was expected to be well-confined in a static MHD equilibrium configuration would instead become violently unstable and crash destructively into the wall in a few microseconds.

The difference between stable and unstable equilibria is shown schematically in Fig.10.1. Here a ball, representing the plasma, is located at either the bottom of a valley or the top of a hill. If the ball is at the bottom of a valley, i.e., a minimum in the potential energy, then a slight lateral displacement results in a restoring force which pushes the ball back. The ball then overshoots and oscillates about the minimum with a constant amplitude because energy is conserved. On the other hand, if the ball is initially located at the top of a hill, then a slight lateral displacement results in a force that pushes the ball further to the side so that there is an increase in the velocity. The perturbed force is not restoring, but rather the opposite. The velocity is always in the direction of the original displacement; i.e., there is no oscillation in velocity.

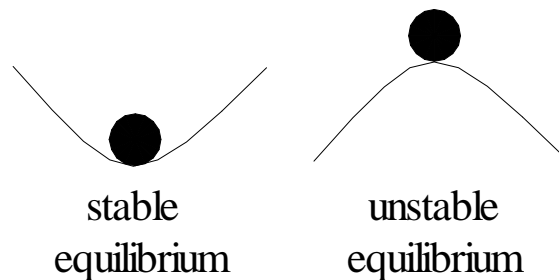


Figure 10.1: Stable and unstable equilibria

The equation of motion for this system is

$$m \frac{d^2 x}{dt^2} = \pm \kappa x \quad (10.1)$$

where κ is assumed positive, the plus sign is chosen for the ball on hill case, and the minus sign is chosen for the ball in valley case. This equation has a solution $x \sim \exp(-i\omega t)$ where $\omega = \pm \sqrt{\kappa/m}$ for the valley case and $\omega = \pm i \sqrt{\kappa/m}$ for the hill case. The hill solution $\omega = -i \sqrt{\kappa/m}$ is unstable and corresponds to the ball accelerating down the hill when perturbed from its initial equilibrium position.

If this configuration is extended to two dimensions, then stability would require an absolute minimum in both directions. However, a saddle point potential would suffice for instability, since the ball could always roll down from the saddle point. Thus, a multi-dimensional system can only be stable if the equilibrium potential energy corresponds to an absolute minimum with respect to all possible displacements.

The problem of determining MHD stability is analogous to having a ball on a multi-dimensional hill. If the potential energy of the system increases for any allowed perturbation of the system, then the system is stable. However, if there exists even a single allowed perturbation that decreases the system's potential energy, then the system is unstable.

10.1 The Rayleigh-Taylor instability of hydrodynamics

An important subset of MHD instabilities is formally similar to the Rayleigh-Taylor instability of hydrodynamics; it is therefore useful to put aside MHD for the moment and examine this classical problem. As any toddler learns from stacking building blocks, it is possible to construct an equilibrium whereby a heavy object is supported by a light object, but such an equilibrium is unstable. The corresponding hydrodynamic situation has a heavy fluid supported by a light fluid as shown in Fig.10.2(a); this situation is unstable with respect to the rippling shown in Fig.10.2(b). The ripples are unstable because they effectively interchange volume elements of heavy fluid with equivalent volume elements of light fluid. Each volume element of interchanged heavy fluid originally had its center of mass a distance Δ above the interface while each volume element of interchanged light fluid originally had its center of mass a distance Δ below the interface. Since the potential energy of a mass m at height h in a gravitational field g is mgh the respective changes in potential energy of the heavy and light fluids are,

$$\delta W_h = -2\rho_h V \Delta g, \quad \delta W_l = +2\rho_l V \Delta g \quad (10.2)$$

where V is the volume of the interchanged fluid elements and ρ_h and ρ_l are the mass densities of the heavy and light fluids. The net change in the total system potential energy is

$$\delta W = -2(\rho_h - \rho_l) V \Delta g \quad (10.3)$$

which is negative so that the system *lowers* its potential energy by forming ripples. This is analogous to the ball falling off the top of the hill.

A well-known example of this instability is the situation of an inverted glass of water. The heavy fluid in this case is the water and the light fluid is the air. The system is stable when a piece of cardboard is located at the interface between the water and the air, but when the cardboard is removed the system becomes unstable and the water falls out. The function of the cardboard is to prevent ripple interchange from occurring. The system is in stable equilibrium when ripples are prevented because atmospheric pressure is

adequate to support the inverted water. From a mathematical point of view, the cardboard places a constraint on the system by imposing a boundary condition which prevents ripple formation.

When the cardboard is removed so that there is no longer a constraint against ripple formation, the ripples grow from noise to large amplitude, and the water falls out. This is an example of an unstable equilibrium.

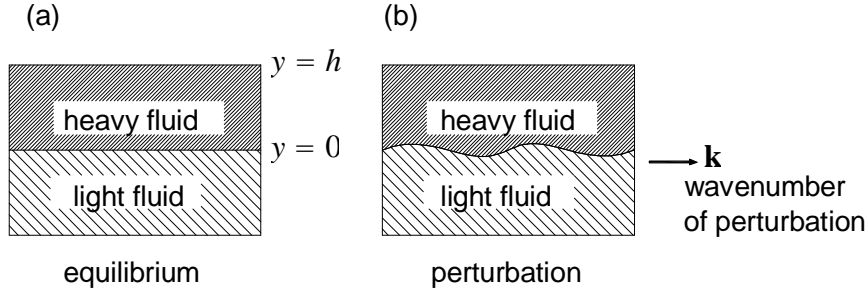


Figure 10.2: (a) Top-heavy fluid equilibrium, (b) rippling instability.

The geometry shown in Fig.10.2 is now used to analyze the stability of a heavy fluid supported by a light fluid in the situation where no constraint exists at the interface. Here y corresponds to the vertical direction so that gravity is in the negative y direction. To simplify the analysis, it is assumed that $\rho_l \ll \rho_h$ in which case the mass of the light fluid can be ignored. The water and air are assumed to be incompressible, i.e., $\rho = \text{const.}$, so that the continuity equation

$$\frac{\partial \rho}{\partial t} + \mathbf{v} \cdot \nabla \rho + \rho \nabla \cdot \mathbf{v} = 0 \quad (10.4)$$

reduces to

$$\nabla \cdot \mathbf{v} = 0. \quad (10.5)$$

The linearized continuity equation in the water therefore reduces to

$$\frac{\partial \rho_1}{\partial t} + \mathbf{v}_1 \cdot \nabla \rho_0 = 0 \quad (10.6)$$

and the linearized equation of motion in the water is

$$\rho_0 \frac{\partial \mathbf{v}_1}{\partial t} = -\nabla P_1 - \rho_1 g \hat{y}. \quad (10.7)$$

The location $y = 0$ is defined to be at the unperturbed air-water interface and the top of the glass is at $y = h$. The water fills the glass to the top and thus is constrained from moving at the top, giving the top boundary condition

$$v_y = 0 \text{ at } y = h. \quad (10.8)$$

The perturbation is assumed to have the form

$$\mathbf{v}_1 = \mathbf{v}_1(y)e^{\gamma t + i\mathbf{k} \cdot \mathbf{x}} \quad (10.9)$$

where \mathbf{k} lies in the $x - z$ plane and positive γ implies instability. The incompressibility condition, Eq.(10.5), can thus be written as

$$\frac{\partial v_{1y}}{\partial y} + i\mathbf{k} \cdot \mathbf{v}_{1\perp} = 0 \quad (10.10)$$

where \perp means perpendicular to the y direction. The y and \perp components of Eq.(10.7) become respectively

$$\gamma\rho_0 v_{1y} = -\frac{\partial P_1}{\partial y} - \rho_1 g \quad (10.11)$$

$$\gamma\rho_0 \mathbf{v}_{1\perp} = -i\mathbf{k} P_1. \quad (10.12)$$

The system is solved by dotting Eq.(10.12) with $i\mathbf{k}$ and then using Eq. (10.10) to eliminate $\mathbf{k} \cdot \mathbf{v}_{1\perp}$ and so obtain

$$-\gamma\rho_0 \frac{\partial v_{1y}}{\partial y} = k^2 P_1. \quad (10.13)$$

The perturbed density, as given by Eq.(10.6), is

$$\gamma\rho_1 = -v_{1y} \frac{\partial \rho_0}{\partial y}. \quad (10.14)$$

Next, ρ_1 and P_1 are substituted for in Eq. (10.11) to obtain the eigenvalue equation

$$\frac{\partial}{\partial y} \left[\gamma^2 \rho_0 \frac{\partial v_{1y}}{\partial y} \right] = \left[\gamma^2 \rho_0 - g \frac{\partial \rho_0}{\partial y} \right] k^2 v_{1y}. \quad (10.15)$$

This equation is solved by considering the interior and the interface separately:

1. Interior: Here $\partial \rho_0 / \partial y = 0$ and $\rho_0 = \text{const.}$ in which case Eq.(10.15) becomes

$$\frac{\partial^2 v_{1y}}{\partial y^2} = k^2 v_{1y}. \quad (10.16)$$

The solution satisfying the boundary condition given by Eq.(10.8) is

$$v_{1y} = A \sinh(k(y - h)). \quad (10.17)$$

2. Interface: To find the properties of this region, Eq.(10.15) is integrated across the interface from $y = 0_-$ to $y = 0_+$ to obtain

$$\left[\gamma^2 \rho_0 \frac{\partial v_{1y}}{\partial y} \right]_{0_-}^{0_+} = - [g \rho_0 k^2 v_{1y}]_{0_-}^{0_+} \quad (10.18)$$

or

$$\gamma^2 \frac{\partial v_{1y}}{\partial y} = -g k^2 v_{1y} \quad (10.19)$$

where all quantities refer to the upper (water) side of the interface, since by assumption $\rho_0(y = 0_-) \simeq 0$.

Substitution of Eq.(10.17) into Eq.(10.19) gives the dispersion relation

$$\gamma^2 = kg \tanh(k_{\perp} h) \quad (10.20)$$

which shows that the configuration is always unstable since $\gamma^2 > 0$. Equation (10.20) furthermore shows that short wavelengths are most unstable, but a more detailed analysis taking into account surface tension (which is stronger for shorter wavelengths) would show that γ^2 has a maximum at some wavelength. Above this most unstable wavelength, surface tension would decrease the growth rate.

10.2 MHD Rayleigh-Taylor instability

We define a ‘magnetofluid’ as a fluid which satisfies the MHD equations. A given plasma may or may not behave as a magnetofluid, depending on the validity of the MHD approximation for the circumstances of the given plasma. The magnetofluid concept provides a legalism which allows consideration of the implications of MHD without necessarily accepting that these implications are relevant to a specific actual plasma. In effect, the magnetofluid concept can be considered as a tentative model of plasma.

Let us now replace the water in the Rayleigh-Taylor instability by magnetofluid. We further suppose that instead of atmospheric pressure supporting the magnetofluid, a vertical magnetic field gradient balances the downwards gravitational force, i.e., at each y the upward force of $-\nabla B^2/2\mu_0$ supports the downward force of the weight of the plasma above. Although gravity is normally unimportant in actual plasmas, the gravitational model is nevertheless quite useful for characterizing situations of practical interest, because gravity can be considered as a proxy for the actual forces which typically have a more complex structure. An important example is the centrifugal force associated with thermal particle motion along curved magnetic field lines acting like a gravitational force in the direction of the radius of curvature of these field lines. The curved field with associated centrifugal force due to parallel thermal motion is replaced by a Cartesian geometry model having straight field lines and, perpendicular to the field lines, a gravitational force is invoked to represent the effect of the centrifugal force. The y direction corresponds to the direction of the radius of curvature.

In order for $-\nabla B^2$ to point upwards in the y direction, the magnetic field must depend on y such that its magnitude decreases with increasing y . Furthermore it is required that $B_y = 0$ so that ∇B^2 is perpendicular to the magnetic field and the field can be considered as locally straight (field line curvature has already been taken into account by introducing the fictitious gravity). Thus, the equilibrium magnetic field is assumed to be of the general form

$$\mathbf{B}_0 = B_{x0}(y)\hat{x} + B_{z0}(y)\hat{z}. \quad (10.21)$$

The unit vector associated with the equilibrium field is

$$\hat{B}_0 = \frac{B_{x0}(y)\hat{x} + B_{z0}(y)\hat{z}}{\sqrt{B_{x0}(y)^2 + B_{z0}(y)^2}}. \quad (10.22)$$

For the special case where $B_{x0}(y)$ and $B_{z0}(y)$ are proportional to each other, the field line direction is independent of y , but in the more general case where this is not so, \hat{B}_0 depends

on y and thus rotates as a function of y . In this latter case, the magnetic field lines are said to be sheared, since adjacent y -layers of field lines are not parallel to each other.

The magnetofluid is assumed incompressible and so using Eq.(9.10) the linearized equation of motion becomes

$$\rho_0 \frac{\partial \mathbf{v}_1}{\partial t} = -\nabla \bar{P}_1 + \frac{\mathbf{B}_0 \cdot \nabla \mathbf{B}_1 + \mathbf{B}_1 \cdot \nabla \mathbf{B}_0}{\mu_0} - \rho_1 g \hat{y} \quad (10.23)$$

where

$$\bar{P}_1 = P_1 + \frac{\mathbf{B}_0 \cdot \mathbf{B}_1}{\mu_0}$$

is the perturbation of the combined hydrodynamic and magnetic pressure, i.e., the perturbation of $P + B^2/2\mu_0$. It is again assumed that all quantities vary in the manner of Eq.(10.9) so Eq.(10.23) has the respective y and \perp components

$$\gamma \rho_0 v_{1y} = -\frac{\partial \bar{P}_1}{\partial y} + \frac{i(\mathbf{k} \cdot \mathbf{B}_0) B_{1y}}{\mu_0} - \rho_1 g \quad (10.24)$$

$$\gamma \rho_0 \mathbf{v}_{1\perp} = -i\mathbf{k} \bar{P}_1 + \frac{1}{\mu_0} \left[i(\mathbf{k} \cdot \mathbf{B}_0) \mathbf{B}_{1\perp} + B_{1y} \frac{\partial \mathbf{B}_0}{\partial y} \right]. \quad (10.25)$$

In analogy to the glass of water problem, Eq.(10.25) is dotted with $i\mathbf{k}$ and Eq.(10.10) is invoked to obtain

$$-\gamma \rho_0 \frac{\partial v_{1y}}{\partial y} = k^2 \bar{P}_1 + \frac{1}{\mu_0} \left[-(\mathbf{k} \cdot \mathbf{B}_0) \mathbf{k} \cdot \mathbf{B}_{1\perp} + i B_{1y} \frac{\partial (\mathbf{k} \cdot \mathbf{B}_0)}{\partial y} \right]. \quad (10.26)$$

Because $\nabla \cdot \mathbf{B}_1 = 0$, the perturbed perpendicular field is

$$i\mathbf{k} \cdot \mathbf{B}_{1\perp} = -\frac{\partial B_{1y}}{\partial y} \quad (10.27)$$

so that Eq.(10.26) can be recast as

$$k^2 \bar{P}_1 = -\gamma \rho_0 \frac{\partial v_{1y}}{\partial y} - \frac{1}{\mu_0} \left[-i(\mathbf{k} \cdot \mathbf{B}_0) \frac{\partial B_{1y}}{\partial y} + i B_{1y} \frac{\partial (\mathbf{k} \cdot \mathbf{B}_0)}{\partial y} \right]. \quad (10.28)$$

Following a procedure analogous to that used in the inverted glass of water problem, \bar{P}_1 is eliminated in Eq.(10.24) by substitution of Eq. (10.28) to obtain

$$\gamma \rho_0 v_{1y} = -\frac{1}{k^2} \frac{\partial}{\partial y} \left\{ -\gamma \rho_0 \frac{\partial v_{1y}}{\partial y} - \frac{1}{\mu_0} \left[-i(\mathbf{k} \cdot \mathbf{B}_0) \frac{\partial B_{1y}}{\partial y} + B_{1y} \frac{\partial (i\mathbf{k} \cdot \mathbf{B}_0)}{\partial y} \right] \right\} + \frac{i(\mathbf{k} \cdot \mathbf{B}_0) B_{1y}}{\mu_0} - \rho_1 g. \quad (10.29)$$

To proceed further, it is necessary to know B_{1y} . The complete vector \mathbf{B}_1 is found by first linearizing the MHD Ohm's law to obtain

$$\mathbf{E}_1 + \mathbf{v}_1 \times \mathbf{B}_0 = 0, \quad (10.30)$$

then taking the curl, and finally using Faraday's law to obtain

$$\gamma \mathbf{B}_1 = \nabla \times [\mathbf{v}_1 \times \mathbf{B}_0]. \quad (10.31)$$

The y component is found by dotting with \hat{y} and then using the vector identity $\nabla \cdot (\mathbf{F} \times \mathbf{G}) = \mathbf{G} \cdot \nabla \times \mathbf{F} - \mathbf{F} \cdot \nabla \times \mathbf{G}$ to obtain

$$\gamma B_{1y} = \hat{y} \cdot \nabla \times [\mathbf{v}_1 \times \mathbf{B}_0] = \nabla \cdot [(\mathbf{v}_1 \times \mathbf{B}_0) \times \hat{y}] = \nabla \cdot [v_{1y} \mathbf{B}_0] = \mathbf{i} \mathbf{k} \cdot \mathbf{B}_0 v_{1y}. \quad (10.32)$$

Substituting into Eq.(10.29) using Eq.(10.32) and Eq.(10.14) and rearranging the order gives

$$\frac{\partial}{\partial y} \left\{ \left[\gamma^2 \rho_0 + \frac{1}{\mu_0} (\mathbf{k} \cdot \mathbf{B}_0)^2 \right] \frac{\partial v_{1y}}{\partial y} \right\} = k^2 \left\{ \gamma^2 \rho_0 - g \frac{\partial \rho_0}{\partial y} + \frac{(\mathbf{k} \cdot \mathbf{B}_0)^2}{\mu_0} \right\} v_{1y} \quad (10.33)$$

which is identical to the inverted glass of water problem if $\mathbf{k} \cdot \mathbf{B}_0 = 0$.

Rather than have an abrupt interface between a heavy and light fluid as in the glass of water problem, it is assumed that the magnetofluid fills the container between $y = 0$ and $y = h$ and that there is a density gradient in the y direction. This situation is more appropriate for a plasma which would typically have a continuous density gradient. It is assumed that rigid boundaries exist at both $y = 0$ and $y = h$ so that $v_{1y} = 0$ at both $y = 0$ and $y = h$. These boundary conditions mean that rippling is not allowed at $y = 0, h$ but could occur in the interior, $0 < y < h$. Equation (10.33) is now impossible to solve analytically because all the coefficients are functions of y . However, an approximate understanding for the behavior predicted by this equation can be found by multiplying the equation by v_{1y} and integrating from $y = 0$ to $y = h$ to obtain

$$\begin{aligned} \left[\left\{ \gamma^2 \rho_0 + \frac{1}{\mu_0} (\mathbf{k} \cdot \mathbf{B}_0)^2 \right\} v_{1y} \frac{\partial v_{1y}}{\partial y} \right]_0^h - \int_0^h \left[\gamma^2 \rho_0 + \frac{1}{\mu_0} (\mathbf{k} \cdot \mathbf{B}_0)^2 \right] \left(\frac{\partial v_{1y}}{\partial y} \right)^2 dy \\ = k^2 \int_0^h \left\{ \gamma^2 \rho_0 - g \frac{\partial \rho_0}{\partial y} + \frac{(\mathbf{k} \cdot \mathbf{B}_0)^2}{\mu_0} \right\} v_{1y}^2 dy. \end{aligned} \quad (10.34)$$

The integrated term vanishes because of the boundary conditions (which could also have been $\partial v_{1y}/\partial y = 0$). Solving for γ^2 gives

$$\gamma^2 = \frac{\int_0^h dy \left[k^2 g \frac{\partial \rho_0}{\partial y} v_{1y}^2 - \frac{(\mathbf{k} \cdot \mathbf{B}_0)^2}{\mu_0} \left(k^2 v_{1y}^2 + \left(\frac{\partial v_{1y}}{\partial y} \right)^2 \right) \right]}{\int_0^h dy \rho_0 \left[k^2 v_{1y}^2 + \left(\frac{\partial v_{1y}}{\partial y} \right)^2 \right]}. \quad (10.35)$$

If $\mathbf{k} \cdot \mathbf{B}_0 = 0$ and the density gradient is positive everywhere then $\gamma^2 > 0$ so there is instability. If the density gradient is negative everywhere except at one stratum with thickness Δy , then the system will be unstable with respect to an interchange at that one 'top-heavy' stratum. The velocity will be concentrated at this unstable stratum and so the integrands will vanish everywhere except at the unstable stratum giving a growth rate $\gamma^2 \sim g \Delta y \rho_0^{-1} \partial \rho_0 / \partial y$ where $\partial \rho_0 / \partial y$ is the value in the unstable region. This MHD version of the Rayleigh-Taylor instability is called the Kruskal-Schwarzschild instability (Kruskal and Schwarzschild 1954).

Finite $\mathbf{k} \cdot \mathbf{B}_0$ opposes the effect of the destabilizing positive density gradient, reducing the growth rate to $\gamma^2 \sim g \Delta y \rho_0^{-1} \partial \rho_0 / \partial y - (\mathbf{k} \cdot \mathbf{B}_0)^2 / \mu_0$. A sufficiently strong field will stabilize the system. However, thermally excited noise excites modes with all possible values of \mathbf{k} and those modes aligned such that $\mathbf{k} \cdot \mathbf{B}_0 = 0$ will not be stabilized. A shear in the magnetic field has the effect of making it possible to have $\mathbf{k} \cdot \mathbf{B}_0(y) = 0$ at only a single value of y . The lack of any spatial dependence of \mathbf{k} results from the translational invariance of the plasma with respect to both x and z implying that $\mathbf{k} = k_x \hat{x} + k_z \hat{z}$ is independent of position. Thus, magnetic shear constrains the instability to a narrow y stratum.

The stabilizing effect of finite $\mathbf{k} \cdot \mathbf{B}_0$ can be understood by considering Eq.(10.32) which shows that the amount of B_{1y} associated with a given v_{1y} is proportional to $\mathbf{k} \cdot \mathbf{B}_0$. Since the original equilibrium field had no y component, introducing a finite B_{1y} corresponds to ‘plucking’ the equilibrium field. The plucking varies sinusoidally along the equilibrium field and stretches the equilibrium field like a plucked violin string. The plucked field has a restoring force which pulls the field back to its equilibrium position. If the energy associated with plucking the magnetic field exceeds the energy liberated by the interchange of heavy upper magnetofluid with light lower magnetofluid, the mode is stable.

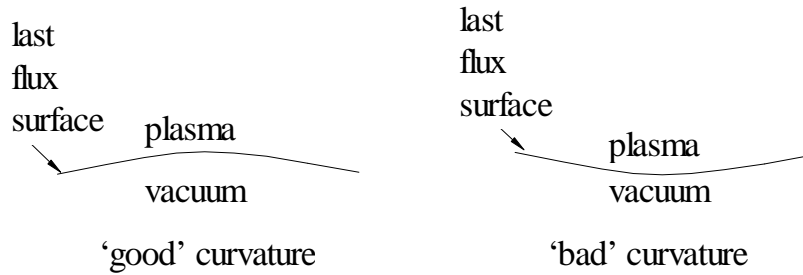


Figure 10.3: Good and bad curvature of the plasma-vacuum interface.

As discussed earlier, the gravitational force in the magnetofluid model represents the centrifugal force resulting from guiding center motion along curved field lines. This leads to the concept of ‘good’ and ‘bad’ curvature illustrated in Fig.10.3. A plasma has bad curvature if the field lines at the plasma-vacuum boundary have a convex shape as seen by an observer outside the plasma since in this case the centrifugal force is outwards from the plasma. Bad curvature gives a centrifugal force that can drive interchange instabilities whereas good curvature corresponds to a concave shape so that the centrifugal force is always inwards. Mirror magnetic fields as sketched in Fig.10.4 have good curvature in the vicinity of the mirrors and bad curvature in the vicinity of the mirror minimum so that a detailed analysis of interchange instabilities requires averaging the ‘goodness/badness’ along the portion of the flux tube experienced by the particle. Cusp magnetic fields (cf. Fig.10.4) have good curvature everywhere, but have singular behavior at the cusps. Plasmas with internal currents such as tokamaks have significant shear everywhere since $\partial B_x / \partial y \sim$

J_z and $\partial B_z/\partial y \sim J_x$; this shear inhibits interchange instabilities. However, as will be shown later this current can be the source for another class of instability called a current-driven instability.

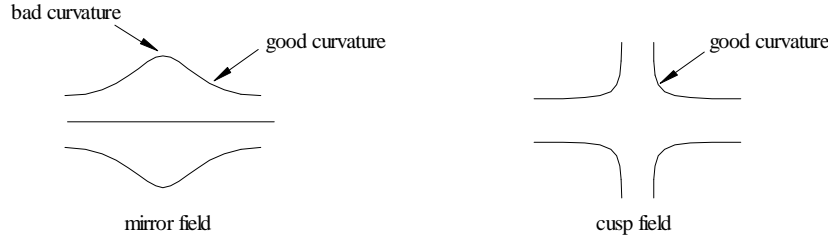


Figure 10.4: Mirror fields have bad curvature at the mirror minimum, good curvature near the maximum; cusp fields have good curvature everywhere.

10.3 The MHD energy principle

Suppose a system initially in equilibrium is subject to a small perturbation instigated by random thermal noise. The perturbation will affect all the various dependent variables in a way which must be consistent with all the relevant equations and boundary conditions. Thus, the perturbation may be considered as a low-level excitation of some allowed normal mode of the system. The mode will be unstable if it reduces the potential energy of the system and, if unstable, the mode growth rate will be proportional to the amount by which the potential energy is reduced. In order to investigate whether a given system is stable, it suffices to show that no modes exist which reduce the system potential energy. Demonstrating MHD stability this way was first done by Bernstein, Frieman, Kruskal and Kuslud (1958) and the method is called the MHD energy principle.

Each mode has its own specific pattern for displacing the magnetofluid volume elements from their equilibrium positions. The pattern of displacements can be represented by a vector function of position $\xi(\mathbf{x})$ that prescribes how a fluid volume element originally at location \mathbf{x} is displaced. Thus, the mode involves moving a fluid element initially at \mathbf{x} to the position $\mathbf{x} + \xi(\mathbf{x})$. The displacement of a magnetofluid element initially at the surface is shown in Fig. 10.5, a sketch of a two-dimensional cut of a three dimensional magnetofluid (plasma) surrounded by a vacuum region in turn bounded by a conducting wall. The wall could be brought right up to the magnetofluid to eliminate the vacuum region or, alternatively, the wall could be placed at infinity to represent a system having no wall and surrounded by vacuum.

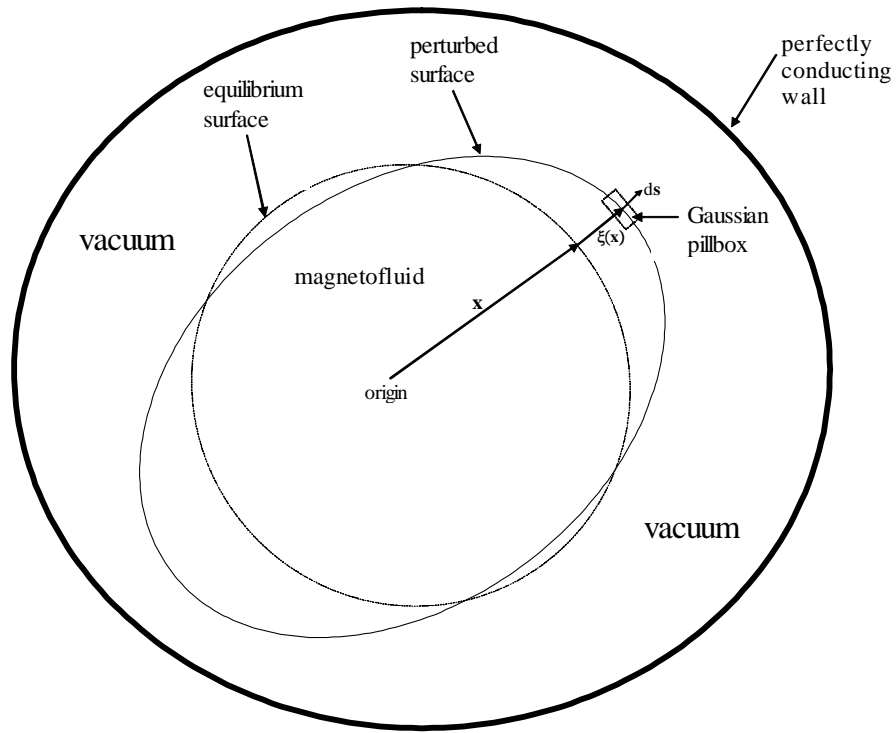


Figure 10.5: Two-dimensional cut of three-dimensional plasma equilibrium and perturbation; Gaussian pillbox is used to relate quantities in vacuum to quantities in plasma. Each volume element at a position \mathbf{x} is displaced by an amount $\boldsymbol{\xi}(\mathbf{x})$. The displacement of a volume element at the surface is illustrated.

10.3.1 Energy equation for a magnetofluid

The energy content of a magnetofluid can be obtained from the ideal MHD equations if it is assumed that all motions are sufficiently fast to be adiabatic but slow enough for collisions to keep the pressure isotropic. The ideal MHD equations are

$$\rho \left(\frac{\partial \mathbf{U}}{\partial t} + \mathbf{U} \cdot \nabla \mathbf{U} \right) = \mathbf{J} \times \mathbf{B} - \nabla P \quad (10.36)$$

$$\mathbf{E} + \mathbf{U} \times \mathbf{B} = 0 \quad (10.37)$$

$$\nabla \times \mathbf{E} = -\frac{\partial \mathbf{B}}{\partial t} \quad (10.38)$$

$$\nabla \times \mathbf{B} = \mu_o \mathbf{J} \quad (10.39)$$

$$\frac{\partial \rho}{\partial t} + \nabla \cdot (\rho \mathbf{U}) = 0 \quad (10.40)$$

$$P \sim \rho^\gamma. \quad (10.41)$$

Ohm's law, Eq.(10.37), and Faraday's law, Eq. (10.38), are combined to give the *induction equation*

$$\frac{\partial \mathbf{B}}{\partial t} = \nabla \times (\mathbf{U} \times \mathbf{B}) \quad (10.42)$$

which prescribes the magnetic field evolution and, as discussed in the context of Eq.(2.82), shows that the magnetic flux is frozen into the magnetofluid. Equation (10.41), the adiabatic relation, implies the following relationships for spatial and temporal derivatives of density and pressure

$$\frac{\nabla P}{P} = \gamma \frac{\nabla \rho}{\rho}, \quad \frac{1}{P} \frac{\partial P}{\partial t} = \frac{\gamma}{\rho} \frac{\partial \rho}{\partial t}. \quad (10.43)$$

Combining these relationships with the continuity equation, Eq.(10.40), gives the pressure evolution equation

$$\frac{\partial P}{\partial t} + \mathbf{U} \cdot \nabla P + \gamma P \nabla \cdot \mathbf{U} = 0 \quad (10.44)$$

which can also be written as

$$\frac{\partial P}{\partial t} + \nabla \cdot (P \mathbf{U}) + (\gamma - 1) P \nabla \cdot \mathbf{U} = 0. \quad (10.45)$$

An expression for the overall energy can be derived by first writing the equation of motion, Eq.(10.36), as

$$\rho \frac{\partial \mathbf{U}}{\partial t} + \rho \nabla \left(\frac{U^2}{2} \right) - \rho \mathbf{U} \times \nabla \times \mathbf{U} = \mathbf{J} \times \mathbf{B} - \nabla P \quad (10.46)$$

and then dotting Eq.(10.46) with \mathbf{U} to obtain

$$\rho \frac{\partial}{\partial t} \left(\frac{U^2}{2} \right) + \rho \mathbf{U} \cdot \nabla \left(\frac{U^2}{2} \right) = \mathbf{J} \times \mathbf{B} \cdot \mathbf{U} - \mathbf{U} \cdot \nabla P. \quad (10.47)$$

Multiplying the entire continuity equation by $U^2/2$ and adding the result gives

$$\frac{\partial}{\partial t} \left(\frac{\rho U^2}{2} \right) + \nabla \cdot \left(\frac{\rho U^2}{2} \mathbf{U} \right) = -\mathbf{J} \cdot \mathbf{U} \times \mathbf{B} - \nabla \cdot (P \mathbf{U}) + P \nabla \cdot \mathbf{U}. \quad (10.48)$$

Using Ampere's law, Eq.(10.39), to eliminate \mathbf{J} , then Ohm's law, Eq.(10.37), to eliminate $\mathbf{U} \times \mathbf{B}$, and the pressure evolution equation, Eq.(10.45), to eliminate $P \nabla \cdot \mathbf{U}$, this energy equation becomes

$$\frac{\partial}{\partial t} \left(\frac{\rho U^2}{2} \right) + \nabla \cdot \left(\frac{\rho U^2}{2} \mathbf{U} \right) = \frac{(\nabla \times \mathbf{B}) \cdot \mathbf{E}}{\mu_0} - \nabla \cdot (P \mathbf{U}) - \frac{1}{(\gamma - 1)} \left(\frac{\partial P}{\partial t} + \nabla \cdot (P \mathbf{U}) \right). \quad (10.49)$$

Finally, using the vector identity

$$\begin{aligned} \nabla \cdot (\mathbf{E} \times \mathbf{B}) &= \mathbf{B} \cdot \nabla \times \mathbf{E} - \mathbf{E} \cdot \nabla \times \mathbf{B} \\ &= -\mathbf{B} \cdot \frac{\partial \mathbf{B}}{\partial t} - \mathbf{E} \cdot \nabla \times \mathbf{B} \end{aligned} \quad (10.50)$$

Eq.(10.49) can be written as

$$\frac{\partial}{\partial t} \left(\frac{\rho U^2}{2} + \frac{P}{\gamma-1} + \frac{B^2}{2\mu_0} \right) + \nabla \cdot \left(\rho \frac{U^2}{2} \mathbf{U} + \frac{\mathbf{E} \times \mathbf{B}}{\mu_0} + \frac{\gamma}{\gamma-1} P \mathbf{U} \right) = 0. \quad (10.51)$$

This is a conservation equation relating energy density and energy flux. The time derivative operates on the magnetofluid energy density and the divergence operates on the energy flux. The energy density is comprised of kinetic energy density $\rho U^2/2$, thermal energy density $P/(\gamma-1)$, and magnetic energy $B^2/2\mu_0$. The energy flux is comprised of convection of kinetic energy $\rho U^2 \mathbf{U}/2$, the Poynting vector $\mathbf{E} \times \mathbf{B}/\mu_0$, and convection of thermal energy density $\gamma P \mathbf{U}/(\gamma-1)$.

The pressure and density both vanish at the magnetofluid surface, but the Poynting flux $\mathbf{E} \times \mathbf{B}$ can be finite. However, if the tangential electric field vanishes at the surface, then the Poynting flux normal to the surface will be zero. This situation occurs if the magnetofluid is bounded by a perfectly conducting wall with no vacuum region between the magnetofluid and the wall. On the other hand, if a vacuum region bounds the magnetofluid, then a tangential electric field can exist at the vacuum-magnetofluid interface and allow a Poynting flux normal to the surface. Energy could then flow back and forth between the magnetofluid and the vacuum region. For example, if the magnetofluid were to move towards the wall thereby reducing the volume of the vacuum region, any vacuum region magnetic field would be compressed and so raise the energy contained in this vacuum magnetic field. This flow of energy into the vacuum region would require a Poynting flux from the magnetofluid into the vacuum region.

Let us now consider the energy properties of the vacuum region between the magnetofluid and a perfectly conducting wall. The equations characterizing the vacuum region are Faraday's law

$$\nabla \times \mathbf{E} = -\frac{\partial \mathbf{B}}{\partial t} \quad (10.52)$$

and Ampere's law

$$\nabla \times \mathbf{B} = 0. \quad (10.53)$$

Dotting Faraday's law with \mathbf{B} , Ampere's law with \mathbf{E} and subtracting gives

$$\frac{\partial}{\partial t} \left(\frac{B^2}{2\mu_0} \right) + \nabla \cdot \left(\frac{\mathbf{E} \times \mathbf{B}}{\mu_0} \right) = 0 \quad (10.54)$$

which is just the limit of Eq.(10.51) for zero density and zero pressure. Thus, Eq. (10.51) characterizes not only the magnetofluid, but also the surrounding vacuum region. As mentioned earlier, the Poynting flux is the means by which electromagnetic energy flows between the magnetofluid and the vacuum region.

If the vacuum region is bounded by a conducting wall, then the tangential electric field must vanish on the wall. The integral of the energy equation over the volume of both the magnetofluid and the surrounding vacuum region then becomes

$$\frac{\partial}{\partial t} \int d^3r \left(\frac{\rho U^2}{2} + \frac{P}{\gamma-1} + \frac{B^2}{\mu_0} \right) = 0 \quad (10.55)$$

since on the wall $ds \cdot \mathbf{E} \times \mathbf{B} = 0$ where ds is a surface element of the wall. If the wall is brought right up to the magnetofluid so there is no vacuum region, then Eq.(10.55) will also

result with the additional stipulation that the normal component of the velocity vanishes at the wall (i.e., the wall is impermeable).

A system consisting of a magnetofluid surrounded by a vacuum region enclosed by an impermeable perfectly conducting wall will therefore have its total internal energy conserved, that is

$$\int_{V_{mf}} d^3r \left(\frac{\rho U^2}{2} + \frac{P}{\gamma - 1} + \frac{B^2}{\mu_0} \right) + \int_{V_{vac}} d^3r \frac{B^2}{\mu_0} = \text{const.} \quad (10.56)$$

where V_{mf} is the volume of the magnetofluid and V_{vac} is the volume of the vacuum region between the magnetofluid and the wall.

This total system energy can be split into a kinetic energy term

$$T = \int d^3r \frac{\rho U^2}{2} \quad (10.57)$$

and a potential energy term

$$W = \int_V d^3r \left(\frac{P}{\gamma - 1} + \frac{B^2}{\mu_0} \right) \quad (10.58)$$

so that

$$T + W = \mathcal{E} \quad (10.59)$$

where the total energy \mathcal{E} is a constant. Here V includes the volume of both the magnetofluid and any vacuum region between the magnetofluid and the wall.

We will now consider a static equilibrium (i.e., an equilibrium with $\mathbf{U}_0 = 0$) so that

$$0 = \mathbf{J}_0 \times \mathbf{B}_0 - \nabla P_0. \quad (10.60)$$

Dotting with either \mathbf{B}_0 or \mathbf{J}_0 shows that

$$\mathbf{B}_0 \cdot \nabla P_0 = 0, \quad \mathbf{J}_0 \cdot \nabla P_0 = 0 \quad (10.61)$$

so that ∇P_0 is normal to the surface defined by the \mathbf{J}_0 and \mathbf{B}_0 vectors.

10.3.2 Self-adjointness of potential energy as a consequence of energy integral

From Eq.(10.57) it is seen that in static equilibrium $T_0 = 0$. This means that all the internal energy must be in the form of stored potential energy, i.e.,

$$W_0 = \mathcal{E}. \quad (10.62)$$

It is now supposed that thermal noise causes a small motion of order ϵ to develop at each point in the magnetofluid. This means there is a first-order velocity

$$\mathbf{U}_1 \sim \epsilon. \quad (10.63)$$

The displacement of a fluid element is obtained by time integration to be

$$\boldsymbol{\xi} = \int_0^t \mathbf{U}_1 dt'; \quad (10.64)$$

because ϵ is small the spatial dependence of \mathbf{U}_1 can be ignored when evaluating the time integral, i.e., terms of order $\boldsymbol{\xi} \cdot \nabla \mathbf{U}_1$ are ignored since these are of order ϵ^2 .

The kinetic energy associated with the mode is

$$\delta T = \int d^3r \frac{\rho_0 U_1^2}{2} \quad (10.65)$$

which clearly is of order ϵ^2 . Since total energy is conserved it is necessary to have

$$\delta T + \delta W = 0 \quad (10.66)$$

leading to the important conclusion that the perturbed potential energy δW must also be of order ϵ^2 .

The perturbed pressure and magnetic field can be found to first-order in ϵ by integrating Eqs.(10.42) and (10.44) respectively to obtain

$$\mathbf{B}_1 = \nabla \times (\boldsymbol{\xi} \times \mathbf{B}_0) \quad (10.67)$$

and

$$P_1 = -\boldsymbol{\xi} \cdot \nabla P_0 - \gamma P_0 \nabla \cdot \boldsymbol{\xi} \quad (10.68)$$

showing that the first-order pressure and first-order magnetic fields are linear functions of $\boldsymbol{\xi}$. However, since it was shown above that δW scales as ϵ^2 , only terms second-order in $\boldsymbol{\xi}$ can contribute to δW , and so all first-order terms must average to zero when integrating over the volume. To specify that δW depends only to second-order in $\boldsymbol{\xi}$, we write

$$\delta W = \delta W(\boldsymbol{\xi}, \boldsymbol{\xi}) \quad (10.69)$$

where the double argument means that δW is a bilinear function, i.e., $\delta W(a\boldsymbol{\xi}, b\boldsymbol{\eta}) = ab\delta W(\boldsymbol{\xi}, \boldsymbol{\eta})$ for arbitrary $\boldsymbol{\xi}, \boldsymbol{\eta}$. The time derivative of δW is thus

$$\delta \dot{W} = \delta W(\dot{\boldsymbol{\xi}}, \boldsymbol{\xi}) + \delta W(\boldsymbol{\xi}, \dot{\boldsymbol{\xi}}). \quad (10.70)$$

Since $\dot{\boldsymbol{\xi}}$ is algebraically independent of $\boldsymbol{\xi}$, Eq.(10.70) means that $\delta \dot{W}$ is self-adjoint (i.e., $\delta \dot{W}$ is invariant when its two arguments are interchanged). Self-adjointness is a direct consequence of the existence of an energy integral.

10.3.3 Formal solution for perturbed potential energy

The self-adjointness property can be exploited by explicitly calculating the time derivative of the perturbed potential energy. This is done using the linearized equation of motion

$$\rho_0 \frac{\partial^2 \boldsymbol{\xi}}{\partial t^2} = \mathbf{F}_1 \quad (10.71)$$

where

$$\mathbf{F}_1 = \mathbf{J}_0 \times \mathbf{B}_1 + \mathbf{J}_1 \times \mathbf{B}_0 - \nabla P_1 \quad (10.72)$$

results from linear operations on $\boldsymbol{\xi}$ since $\mathbf{B}_1, \mu_0 \mathbf{J}_1 = \nabla \times \mathbf{B}_1$ and P_1 are all result from linear operations on $\boldsymbol{\xi}$.

Multiplying Eq.(10.71) by the perturbed velocity $\dot{\boldsymbol{\xi}}$ and integrating over the volume of the magnetofluid and vacuum region gives

$$\int d^3r \rho_0 \frac{\partial}{\partial t} \left(\frac{\dot{\boldsymbol{\xi}}^2}{2} \right) = \int d^3r \dot{\boldsymbol{\xi}} \cdot \mathbf{F}_1(\boldsymbol{\xi}). \quad (10.73)$$

Although the integration includes the vacuum region, both the right and left hand sides of this equation vanish in the vacuum region because no density, current, or pressure exist there.

The left hand side of Eq.(10.73) is just the time derivative of the kinetic energy $\delta\dot{T}$. Since $\delta\dot{T} + \delta\dot{W} = 0$, it is seen that

$$\delta\dot{W} = - \int d^3r \dot{\boldsymbol{\xi}} \cdot \mathbf{F}_1(\boldsymbol{\xi}). \quad (10.74)$$

However, since $\delta\dot{W}$ was shown to be self-adjoint, Eq.(10.74) can also be written as $\delta\dot{W} = - \int d^3r \boldsymbol{\xi} \cdot \mathbf{F}_1(\dot{\boldsymbol{\xi}})$. Combining these last two equations provides an integrable form for $\delta\dot{W}$, namely

$$\begin{aligned} \delta\dot{W} &= -\frac{1}{2} \left(\int d^3r \boldsymbol{\xi} \cdot \mathbf{F}_1(\dot{\boldsymbol{\xi}}) + \int d^3r \dot{\boldsymbol{\xi}} \cdot \mathbf{F}_1(\boldsymbol{\xi}) \right) \\ &= -\frac{1}{2} \frac{\partial}{\partial t} \left(\int d^3r \boldsymbol{\xi} \cdot \mathbf{F}_1(\boldsymbol{\xi}) \right). \end{aligned} \quad (10.75)$$

Performing the time integration gives the desired result, namely the change in system potential energy as a function of the fluid displacement is

$$\delta W = -\frac{1}{2} \int d^3r \boldsymbol{\xi} \cdot \mathbf{F}_1(\boldsymbol{\xi}). \quad (10.76)$$

Standard techniques of normal mode analysis can be invoked by assuming that the displacement has the form

$$\boldsymbol{\xi} = \text{Re} \left(\bar{\boldsymbol{\xi}} e^{-i\omega t} \right) \quad (10.77)$$

so the equation of motion can be written as

$$-\omega^2 \rho \bar{\boldsymbol{\xi}} = \mathbf{F}_1(\bar{\boldsymbol{\xi}}). \quad (10.78)$$

Multiplication by $\bar{\boldsymbol{\xi}}^*$ and integrating over the volume gives

$$-\omega^2 \int d^3r \rho |\bar{\boldsymbol{\xi}}|^2 = \int d^3r \bar{\boldsymbol{\xi}}^* \cdot \mathbf{F}_1(\bar{\boldsymbol{\xi}}). \quad (10.79)$$

In the earlier discussion of self-adjointness, it was noted that $\dot{\boldsymbol{\xi}}$ is essentially an arbitrary function for a given $\boldsymbol{\xi}$, i.e., any $\dot{\boldsymbol{\xi}}$ could be obtained by choosing a suitable time dependence for $\boldsymbol{\xi}$. Thus, $\dot{\boldsymbol{\xi}}$ could be chosen to be proportional to $\bar{\boldsymbol{\xi}}^*$ and so the right hand side of Eq.(10.79) is also self-adjoint. Equation (10.79) can therefore be recast as

$$-\omega^2 \int d^3r \rho |\bar{\boldsymbol{\xi}}|^2 = \frac{1}{2} \left[\int d^3r \bar{\boldsymbol{\xi}}^* \cdot \mathbf{F}_1(\bar{\boldsymbol{\xi}}) + \int d^3r \bar{\boldsymbol{\xi}} \cdot \mathbf{F}_1(\bar{\boldsymbol{\xi}}^*) \right] \quad (10.80)$$

which shows that ω^2 must be pure real. Negative ω^2 corresponds to instability.

Equation (10.78) can be considered as an eigenvalue problem where ω^2 is the eigenvalue and ξ is the eigenvector. As in the usual linear algebra sense, eigenvectors having different eigenvalues are orthogonal and so, in principle, a basis set of normalized orthogonal eigenvectors $\{\zeta_m\}$ can be constructed where

$$\mathbf{F}_1(\zeta_m) = -\omega_m^2 \rho \zeta_m. \quad (10.81)$$

Thus any arbitrary displacement can be expressed as a suitably weighted sum of eigenvectors,

$$\xi = \sum_m \alpha_m \zeta_m. \quad (10.82)$$

The orthogonality of the basis set gives the relation

$$\int d^3r \zeta_m \cdot \mathbf{F}(\zeta_n) = -\omega_m^2 \int d^3r \rho \zeta_m \cdot \zeta_n = 0 \text{ if } m \neq n. \quad (10.83)$$

Instability will result if there exists some perturbation that makes δW negative. Conversely, if all possible perturbations result in positive δW for a given equilibrium, then the equilibrium is MHD stable.

10.3.4 Evaluation of δW

Since \mathbf{F}_1 consists of three terms involving \mathbf{J}_0 , \mathbf{B}_1 and P_1 respectively, δW can be decomposed into three terms,

$$\delta W = \delta W_{J_0} + \delta W_{B_1} + \delta W_{P_1}. \quad (10.84)$$

Using Eqs. (10.72), (10.67), (10.68) in Eq.(10.76) shows that these terms are

$$\delta W_{J_0} = -\frac{1}{2} \int d^3r \xi \cdot \mathbf{J}_0 \times \mathbf{B}_1, \quad (10.85)$$

$$\delta W_{B_1} = -\frac{1}{2\mu_0} \int d^3r \xi \cdot (\nabla \times \mathbf{B}_1) \times \mathbf{B}_0, \quad (10.86)$$

$$\delta W_{P_1} = \frac{1}{2} \int d^3r \xi \cdot \nabla P_1. \quad (10.87)$$

Although the above three right hand sides are in principle integrated over the volumes of both the magnetofluid and the vacuum regions, in fact, the integrands vanish in the vacuum region for all three cases and so the integration is effectively over the magnetofluid volume only. The second two integrals can be simplified using the vector identities $\nabla \cdot (\mathbf{C} \times \mathbf{D}) = \mathbf{D} \cdot \nabla \times \mathbf{C} - \mathbf{C} \cdot \nabla \times \mathbf{D}$ and $\nabla \cdot (f \mathbf{a}) = \mathbf{a} \cdot \nabla f + f \nabla \cdot \mathbf{a}$ to obtain

$$\begin{aligned} \delta W_{B_1} &= \frac{1}{2\mu_0} \int_{V_{mf}} d^3r (\xi \times \mathbf{B}_0) \cdot \nabla \times \mathbf{B}_1 \\ &= \frac{1}{2\mu_0} \int_{V_{mf}} d^3r B_1^2 + \frac{1}{2\mu_0} \int_{S_{mf}} ds \cdot \mathbf{B}_1 \times (\xi \times \mathbf{B}_0) \end{aligned} \quad (10.88)$$

and

$$\begin{aligned}
\delta W_{P_1} &= -\frac{1}{2} \int_{V_{mf}} d^3r \boldsymbol{\xi} \cdot \nabla [\boldsymbol{\xi} \cdot \nabla P_0 + \gamma P_0 \nabla \cdot \boldsymbol{\xi}] \\
&= \frac{1}{2} \int_{V_{mf}} d^3r \left[-\boldsymbol{\xi} \cdot \nabla (\boldsymbol{\xi} \cdot \nabla P_0) + \gamma P_0 (\nabla \cdot \boldsymbol{\xi})^2 \right] - \frac{1}{2} \int_{S_{mf}} ds \cdot \boldsymbol{\xi} \gamma P_0 \nabla \cdot \boldsymbol{\xi}.
\end{aligned} \tag{10.89}$$

Since both $\mathbf{J} \times \mathbf{B}$ and ∇P are perpendicular to \mathbf{B} at the surface of the magnetofluid, the force acting on the magnetofluid at the surface is perpendicular to \mathbf{B} and so the displacement $\boldsymbol{\xi}$ of the magnetofluid at the surface is perpendicular to \mathbf{B} , i.e., at the surface $\boldsymbol{\xi} = \boldsymbol{\xi}_\perp$. The surface integral in Eq.(10.88) can be expanded

$$\frac{1}{2\mu_0} \int_{S_{mf}} ds \cdot \mathbf{B}_1 \times (\boldsymbol{\xi} \times \mathbf{B}_0) = \frac{1}{2\mu_0} \int_{S_{mf}} ds \cdot \boldsymbol{\xi}_\perp \mathbf{B}_0 \cdot \mathbf{B}_1 \tag{10.90}$$

since $ds \cdot \mathbf{B}_0 = 0$ on the magnetofluid surface. This latter condition is true because the magnetic field was initially tangential to the magnetofluid surface (i.e., $\mathbf{J}_0 \times \mathbf{B}_0 = \nabla P_0$ implies ∇P_0 is perpendicular to \mathbf{B}_0) and must remain so since the field is frozen into the magnetofluid.

Recombining and re-ordering these separate contributions gives

$$\begin{aligned}
\delta W &= \frac{1}{2} \int_{V_{mf}} d^3r \left\{ \gamma P_0 (\nabla \cdot \boldsymbol{\xi})^2 + \frac{B_1^2}{\mu_0} - \boldsymbol{\xi} \cdot [\mathbf{J}_0 \times \mathbf{B}_1 + \nabla (\boldsymbol{\xi} \cdot \nabla P_0)] \right\} \\
&\quad + \frac{1}{2\mu_0} \int_{S_{mf}} ds \cdot \boldsymbol{\xi}_\perp [\mathbf{B}_0 \cdot \mathbf{B}_1 - \mu_0 \gamma P_0 \nabla \cdot \boldsymbol{\xi}].
\end{aligned} \tag{10.91}$$

The substitution $ds \cdot \boldsymbol{\xi} = ds \cdot \boldsymbol{\xi}_\perp$ has been made for the pressure contribution to the surface term on the grounds that ds must be perpendicular to \mathbf{B}_0 . Further simplification is obtained by considering the dot product with \mathbf{B}_0 of the term in square brackets in Eq.(10.91), namely

$$\begin{aligned}
\mathbf{B}_0 \cdot [\mathbf{J}_0 \times \mathbf{B}_1 + \nabla (\boldsymbol{\xi} \cdot \nabla P_0)] &= -\nabla P_0 \cdot \mathbf{B}_1 + \mathbf{B}_0 \cdot \nabla (\boldsymbol{\xi} \cdot \nabla P_0) \\
&= -\nabla P_0 \cdot \nabla \times (\boldsymbol{\xi} \times \mathbf{B}_0) + \mathbf{B}_0 \cdot \nabla (\boldsymbol{\xi} \cdot \nabla P_0) \\
&= \nabla \cdot \{ \nabla P_0 \times (\boldsymbol{\xi} \times \mathbf{B}_0) + (\boldsymbol{\xi} \cdot \nabla P_0) \mathbf{B}_0 \} \\
&= \nabla \cdot [\boldsymbol{\xi} \mathbf{B}_0 \cdot \nabla P_0] \\
&= 0
\end{aligned} \tag{10.92}$$

where Eq.(10.61) has been used to obtain the last line. Thus, $\boldsymbol{\xi} \cdot [\mathbf{J}_0 \times \mathbf{B}_1 + \nabla (\boldsymbol{\xi} \cdot \nabla P_0)] = \boldsymbol{\xi}_\perp \cdot [\mathbf{J}_0 \times \mathbf{B}_1 + \nabla (\boldsymbol{\xi} \cdot \nabla P_0)]$ since Eq.(10.92) shows that the factor in square brackets has no component parallel to the equilibrium magnetic field.

The potential energy variation δW is now decomposed into its magnetofluid volume and surface components,

$$\delta W_{F'} = \frac{1}{2} \int_{V_{mf}} d^3r \left\{ \begin{array}{l} \gamma P_0 (\nabla \cdot \boldsymbol{\xi})^2 + \frac{B_{1\perp}^2}{\mu_0} + \frac{B_{1\parallel}^2}{\mu_0} \\ -\boldsymbol{\xi}_\perp \cdot \mathbf{J}_0 \times \mathbf{B}_1 - \boldsymbol{\xi}_\perp \cdot \nabla_\perp (\boldsymbol{\xi}_\perp \cdot \nabla P_0) \end{array} \right\} \tag{10.93}$$

and

$$\delta W_{S'} = \frac{1}{2\mu_0} \int_{S_{mf}} ds \cdot \boldsymbol{\xi}_\perp (\mathbf{B}_0 \cdot \mathbf{B}_1 - \mu_0 \gamma P_0 \nabla \cdot \boldsymbol{\xi}). \quad (10.94)$$

At this point it is useful to examine the parallel and perpendicular components of \mathbf{B}_1 . Finite $\mathbf{B}_{1\perp}$ corresponds to changing the curvature of field lines (twanging or plucking) whereas finite $\mathbf{B}_{1\parallel}$ corresponds to compressing or rarefying the density of field lines. The equilibrium force balance can be written as

$$\mu_0 \nabla P_0 = -\nabla_\perp \frac{B_0^2}{2} + \boldsymbol{\kappa} B_0^2 \quad (10.95)$$

where $\boldsymbol{\kappa} = \hat{B}_0 \cdot \nabla \hat{B}_0$ is related to the local curvature of the equilibrium magnetic field. Applying the vector identity $\nabla(\mathbf{C} \cdot \mathbf{D}) = \mathbf{C} \cdot \nabla \mathbf{D} + \mathbf{D} \cdot \nabla \mathbf{C} + \mathbf{D} \times \nabla \times \mathbf{C} + \mathbf{C} \times \nabla \times \mathbf{D}$ gives

$$\boldsymbol{\kappa} = -\hat{B}_0 \times \nabla \times \hat{B}_0, \quad (10.96)$$

a relation which will be used when evaluating $B_{1\parallel}$. From Eq.(10.67) it is seen that the parallel component of the perturbed magnetic field is

$$\begin{aligned} B_{1\parallel} &= \hat{B}_0 \cdot \nabla \times (\boldsymbol{\xi}_\perp \times \mathbf{B}_0) \\ &= (\boldsymbol{\xi}_\perp \times \mathbf{B}_0) \cdot \nabla \times \hat{B}_0 + \nabla \cdot [(\boldsymbol{\xi}_\perp \times \mathbf{B}_0) \times \hat{B}_0] \\ &= -B_0 \boldsymbol{\xi}_\perp \cdot \boldsymbol{\kappa} - \nabla \cdot (B_0 \boldsymbol{\xi}_\perp) \\ &= -B_0 \boldsymbol{\xi}_\perp \cdot \boldsymbol{\kappa} - B_0 (\nabla \cdot \boldsymbol{\xi}_\perp) - \frac{\boldsymbol{\xi}_\perp \cdot \nabla B_0^2}{B_0} \\ &= -B_0 [2\boldsymbol{\xi}_\perp \cdot \boldsymbol{\kappa} + \nabla \cdot \boldsymbol{\xi}_\perp] + \frac{\mu_0}{B_0} \boldsymbol{\xi}_\perp \cdot \nabla P_0. \end{aligned} \quad (10.97)$$

The term involving \mathbf{J}_0 in Eq.(10.93) can be expanded to give

$$\begin{aligned} \boldsymbol{\xi}_\perp \cdot \mathbf{J}_0 \times \mathbf{B}_1 &= \boldsymbol{\xi}_\perp \cdot \mathbf{J}_{0\perp} \times \hat{B}_0 B_{1\parallel} + \boldsymbol{\xi}_\perp \cdot J_{0\parallel} \hat{B}_0 \times \mathbf{B}_{1\perp} \\ &= (\boldsymbol{\xi}_\perp \cdot \nabla P_0) \frac{B_{1\parallel}}{B_0} + \boldsymbol{\xi}_\perp \cdot J_{0\parallel} \hat{B}_0 \times \mathbf{B}_{1\perp}. \end{aligned} \quad (10.98)$$

Substituting for this term in Eq.(10.93), factoring out one power of $B_{1\parallel}$, and then sub-

stituting Eq.(10.97) gives

$$\begin{aligned}
\delta W_{F'} &= \frac{1}{2} \int_{V_{mf}} d^3r \left\{ \begin{aligned} &\gamma P_0 (\nabla \cdot \boldsymbol{\xi})^2 + \frac{B_{1\perp}^2}{\mu_0} \\ &+ \frac{B_{1\parallel}^2}{\mu_0} - (\boldsymbol{\xi}_\perp \cdot \nabla P_0) \frac{B_{1\parallel}}{B_0} \\ &-\boldsymbol{\xi}_\perp \cdot J_{0\parallel} \hat{B}_0 \times \mathbf{B}_{1\perp} - \boldsymbol{\xi}_\perp \cdot \nabla_\perp (\boldsymbol{\xi}_\perp \cdot \nabla P_0) \end{aligned} \right\} \\
&= \frac{1}{2} \int_{V_{mf}} d^3r \left\{ \begin{aligned} &\gamma P_0 (\nabla \cdot \boldsymbol{\xi})^2 + \frac{B_{1\perp}^2}{\mu_0} \\ &+ \frac{B_{1\parallel}}{\mu_0} \left(B_{1\parallel} - \frac{\mu_0 \boldsymbol{\xi}_\perp \cdot \nabla P_0}{B_0} \right) \\ &-\boldsymbol{\xi}_\perp \cdot J_{0\parallel} \hat{B}_0 \times \mathbf{B}_{1\perp} - \boldsymbol{\xi}_\perp \cdot \nabla_\perp (\boldsymbol{\xi}_\perp \cdot \nabla P_0) \end{aligned} \right\} \\
&= \frac{1}{2} \int_{V_{mf}} d^3r \left\{ \begin{aligned} &\gamma P_0 (\nabla \cdot \boldsymbol{\xi})^2 + \frac{B_{1\perp}^2}{\mu_0} + \\ &\left(\frac{B_0^2}{\mu_0} [2\boldsymbol{\xi}_\perp \cdot \boldsymbol{\kappa} + \nabla \cdot \boldsymbol{\xi}_\perp] - \boldsymbol{\xi}_\perp \cdot \nabla P_0 \right) [2\boldsymbol{\xi}_\perp \cdot \boldsymbol{\kappa} + \nabla \cdot \boldsymbol{\xi}_\perp] \\ &-\boldsymbol{\xi}_\perp \cdot J_{0\parallel} \hat{B}_0 \times \mathbf{B}_{1\perp} + (\boldsymbol{\xi}_\perp \cdot \nabla P_0) \nabla \cdot \boldsymbol{\xi}_\perp \\ &\quad - \nabla \cdot [\boldsymbol{\xi}_\perp (\boldsymbol{\xi}_\perp \cdot \nabla P_0)] \end{aligned} \right\} \\
&= \frac{1}{2} \int_{V_{mf}} d^3r \left\{ \begin{aligned} &\gamma P_0 (\nabla \cdot \boldsymbol{\xi})^2 + \frac{B_{1\perp}^2}{\mu_0} + \frac{B_0^2}{\mu_0} [2\boldsymbol{\xi}_\perp \cdot \boldsymbol{\kappa} + \nabla \cdot \boldsymbol{\xi}_\perp]^2 \\ &-(\boldsymbol{\xi}_\perp \cdot \nabla P_0) (2\boldsymbol{\xi}_\perp \cdot \boldsymbol{\kappa}) - \boldsymbol{\xi}_\perp \cdot J_{0\parallel} \hat{B}_0 \times \mathbf{B}_{1\perp} \\ &\quad - \nabla \cdot [\boldsymbol{\xi}_\perp (\boldsymbol{\xi}_\perp \cdot \nabla P_0)] \end{aligned} \right\} \\
&= \frac{1}{2\mu_0} \int_{V_{mf}} d^3r \left\{ \begin{aligned} &\gamma \mu_0 P_0 (\nabla \cdot \boldsymbol{\xi})^2 + B_{1\perp}^2 + B_0^2 [2\boldsymbol{\xi}_\perp \cdot \boldsymbol{\kappa} + \nabla \cdot \boldsymbol{\xi}_\perp]^2 \\ &-2\mu_0 (\boldsymbol{\xi}_\perp \cdot \nabla P_0) (\boldsymbol{\xi}_\perp \cdot \boldsymbol{\kappa}) + \boldsymbol{\xi}_\perp \times \mathbf{B}_{1\perp} \cdot (\mu_0 J_{0\parallel} \hat{B}_0) \end{aligned} \right\} \\
&\quad - \frac{1}{2} \int_{S_{mf}} ds \cdot \boldsymbol{\xi}_\perp (\boldsymbol{\xi}_\perp \cdot \nabla P_0). \tag{10.99}
\end{aligned}$$

A new surface term has appeared because of an integration by parts; this new term is absorbed into the previous surface term and the fluid and surface terms are redefined by removing the primes; thus

$$\delta W_F = \frac{1}{2\mu_0} \int_{V_{mf}} d^3r \left\{ \begin{aligned} &\gamma \mu_0 P_0 (\nabla \cdot \boldsymbol{\xi})^2 + B_{1\perp}^2 + B_0^2 [2\boldsymbol{\xi}_\perp \cdot \boldsymbol{\kappa} + (\nabla \cdot \boldsymbol{\xi}_\perp)]^2 \\ &-2\mu_0 (\boldsymbol{\xi}_\perp \cdot \nabla P_0) (\boldsymbol{\xi}_\perp \cdot \boldsymbol{\kappa}) + \boldsymbol{\xi}_\perp \times \mathbf{B}_{1\perp} \cdot (\mu_0 J_{0\parallel} \hat{B}_0) \end{aligned} \right\} \tag{10.100}$$

and

$$\begin{aligned}
\delta W_S &= \frac{1}{2\mu_0} \int_{S_{mf}} ds \cdot \boldsymbol{\xi}_\perp \{ \mathbf{B}_0 \cdot \mathbf{B}_1 - \mu_0 (\gamma P_0 \nabla \cdot \boldsymbol{\xi} + \boldsymbol{\xi}_\perp \cdot \nabla P_0) \} \\
&= \frac{1}{2\mu_0} \int_{S_{mf}} ds \cdot \boldsymbol{\xi}_\perp \{ \mathbf{B}_0 \cdot \mathbf{B}_1 + \mu_0 P_1 \} \tag{10.101}
\end{aligned}$$

where $\mathbf{B}_0 \cdot ds = 0$ and Eq.(10.68) have been used to simplify the surface integral. The surface integral can be further re-arranged by considering the relationship between the vacuum

and magnetofluid fields at the perturbed surface. If the equilibrium force balance is integrated over the volume of the small Gaussian pillbox located at the perturbed magnetofluid surface in Fig.10.5, it is seen that

$$0 = \int_{V_{pillbox,ps}} d^3r \nabla \cdot \left[\left(P + \frac{B^2}{2\mu_0} \right) \mathbf{I} - \frac{1}{\mu_0} \mathbf{B}\mathbf{B} \right] = \int_{S,ps} ds \left[P + \frac{B^2}{2\mu_0} \right]_{magnetofluid}^{vac} \quad (10.102)$$

since $ds \cdot \mathbf{B} = 0$ at the perturbed surface. The subscripts *ps* indicate that the volume and surface integrals are at the perturbed surface.

Quantities evaluated at the perturbed surface are of the form

$$f_{pert\,sfc} = f_0 + f_1 + \boldsymbol{\xi} \cdot \nabla f_0; \quad (10.103)$$

i.e., both absolute and convective first-order terms must be included. Since the pillbox extent was arbitrary in Eq.(10.102), the integrand $\left[P + B^2/2\mu_0 \right]_{magnetofluid}^{vac}$ must vanish at each point on the perturbed surface, giving the relation

$$\left(P_1 + \frac{\mathbf{B}_0 \cdot \mathbf{B}_1}{\mu_0} \right)_{magnetofluid} + \boldsymbol{\xi} \cdot \nabla \left(P + \frac{B^2}{2\mu_0} \right)_{magnetofluid} = \left(\frac{\mathbf{B}_0 \cdot \mathbf{B}_1}{\mu_0} \right)_{vac} + \boldsymbol{\xi} \cdot \nabla \left(\frac{B^2}{2\mu_0} \right)_{vac} \quad (10.104)$$

which can be rewritten as

$$\left(P_1 + \frac{\mathbf{B}_0 \cdot \mathbf{B}_1}{\mu_0} \right)_{magnetofluid} = \boldsymbol{\xi} \cdot \nabla \left[P + \frac{B^2}{2\mu_0} \right]_{magnetofluid}^{vac} + \left(\frac{\mathbf{B}_0 \cdot \mathbf{B}_1}{\mu_0} \right)_{vac}. \quad (10.105)$$

Thus the surface integral Eq.(10.101) can be rewritten as

$$\delta W_S = \frac{1}{2} \int_{S_{mf}} ds \cdot \boldsymbol{\xi}_\perp \boldsymbol{\xi}_\perp \cdot \nabla \left[P + \frac{B^2}{2\mu_0} \right]_{magnetofluid}^{vac} + \frac{1}{2\mu_0} \int_{S_{mf}} ds \cdot \boldsymbol{\xi}_\perp (\mathbf{B}_0 \cdot \mathbf{B}_1)_{vac}. \quad (10.106)$$

The volume integral in Eq.(10.100) is over the magnetofluid volume and the direction of ds in Eq.(10.106) is outwards from the magnetofluid volume. The energy stored in the vacuum region between the magnetofluid and wall is

$$\begin{aligned} \delta W_{vac} &= \frac{1}{2\mu_0} \int_{V_{vac}} d^3r B_{1v}^2 \\ &= \frac{1}{2\mu_0} \int_{V_{vac}} d^3r \mathbf{B}_{1v} \cdot \nabla \times \mathbf{A}_{1v} \\ &= \frac{1}{2\mu_0} \int_{V_{vac}} d^3r \nabla \cdot (\mathbf{A}_{1v} \times \mathbf{B}_{1v}) \\ &= \frac{1}{2\mu_0} \int_{S_{vac}} ds \cdot (\mathbf{A}_{1v} \times \mathbf{B}_{1v}) \end{aligned} \quad (10.107)$$

where ds points *out* from the vacuum region and $\nabla \times \mathbf{B}_{1v} = 0$ has been used when integrating by parts. At the conducting wall (which might be at infinity) the integrand vanishes since it contains the factor $ds \times \mathbf{A}_{1v}$ which is proportional to the tangential electric field and the tangential electric field vanishes at a conductor. Thus, only the surface integral over

the magnetofluid-vacuum interface remains. Since an element of surface ds pointing out of the vacuum points into the magnetofluid, using ds to mean out of the magnetofluid (as before), this becomes

$$\delta W_{vac} = -\frac{1}{2\mu_0} \int_{S_{mf}} ds \cdot (\mathbf{A}_{1v} \times \mathbf{B}_{1v}) \quad (10.108)$$

where S_{mf} has been used instead of S_{vac} to indicate that ds points out of the magnetofluid.

The tangential component of the electric field must be continuous at the magnetofluid-vacuum interface. This field is not necessarily zero. The electric field inside the magnetofluid is determined by Ohm's law, Eq.(10.37). Thus the electric field on the magnetofluid side of the magnetofluid-vacuum interface is

$$\mathbf{E}_{1p} = -\mathbf{v}_1 \times \mathbf{B}_0 \quad (10.109)$$

while on the vacuum side of this interface the electric field is simply

$$\mathbf{E}_{1v} = -\frac{\partial \mathbf{A}_{1v}}{\partial t} \quad (10.110)$$

where \mathbf{A}_{1v} is the vacuum vector potential. Defining the surface normal unit vector \hat{n} and integrating both electric fields with respect to time, the condition that the tangential electric field is continuous is seen to be

$$\hat{n} \times \mathbf{A}_{1v} = \hat{n} \times (\boldsymbol{\xi} \times \mathbf{B}_0) = -\hat{n} \cdot \boldsymbol{\xi} \mathbf{B}_0 \quad (10.111)$$

where $\hat{n} \cdot \mathbf{B}_0 = 0$ has been used. Thus, the second surface integral in Eq.(10.106) can be written as

$$\frac{1}{2\mu_0} \int_S ds \hat{n} \cdot \boldsymbol{\xi}_\perp \mathbf{B}_0 \cdot \mathbf{B}_{1v} = -\frac{1}{2\mu_0} \int_S ds \hat{n} \times \mathbf{A}_{1v} \cdot \mathbf{B}_{1v} = \delta W_{vac}. \quad (10.112)$$

These results are now summarized. The perturbed potential energy can be expressed as

$$\delta W = \delta W_F + \delta W_{int} + \delta W_{vac} \quad (10.113)$$

where the contribution from the fluid volume interior is

$$\delta W_F = \frac{1}{2\mu_0} \int_{V_{mf}} d^3r \left\{ \begin{aligned} &\gamma \mu_0 P_0 (\nabla \cdot \boldsymbol{\xi})^2 + B_{1\perp}^2 + B_0^2 [2\boldsymbol{\xi}_\perp \cdot \boldsymbol{\kappa} + (\nabla \cdot \boldsymbol{\xi}_\perp)]^2 \\ &+ \boldsymbol{\xi}_\perp \times \mathbf{B}_{1\perp} \cdot \hat{B}_0 \mu_0 J_{0\parallel} - 2\mu_0 (\boldsymbol{\xi}_\perp \cdot \boldsymbol{\kappa}) (\boldsymbol{\xi}_\perp \cdot \nabla P_0) \end{aligned} \right\} \quad (10.114)$$

the contribution from the vacuum-magnetofluid interface is

$$\delta W_{int} = \frac{1}{2\mu_0} \int_{S_{mf}} ds \cdot \boldsymbol{\xi}_\perp \boldsymbol{\xi}_\perp \cdot \nabla \left[\mu_0 P + \frac{B^2}{2} \right]_{magnetofluid}^{vac} \quad (10.115)$$

and the contribution from the vacuum region is

$$\delta W_{vac} = \frac{1}{2\mu_0} \int_{vac} d^3r B_{1v}^2. \quad (10.116)$$

10.4 Discussion of the energy principle

The terms in the integrands of δW_F , δW_{int} , and δW_{vac} are of two types: those that are positive-definite and those that are not. Positive-definite terms always increase δW and are therefore stabilizing whereas terms that could be negative are potentially destabilizing. Consideration of δW_F in particular shows that magnetic perturbations interior to the magnetofluid and perpendicular to the equilibrium field are always stabilizing, since these perturbations appear in the form $B_{1\perp}^2$. It is also seen that a positive-definite term $\sim (\nabla \cdot \boldsymbol{\xi})^2$ exists indicating that a compressible magnetofluid is always more stable than an otherwise identical incompressible magnetofluid. Hence, incompressible instabilities are more violent than compressible ones. It is also seen that two types of destabilizing terms exist. One gives instability if

$$(\boldsymbol{\kappa} \cdot \boldsymbol{\xi}_\perp) (\boldsymbol{\xi}_\perp \cdot \nabla P_0) > 0; \quad (10.117)$$

this is a generalization of the good curvature/bad curvature result obtained in the earlier Rayleigh-Taylor analysis. In the vicinity of the magnetofluid surface all quantities in Eq.(10.117) point in the same direction and so Eq.(10.117) can be written as

$$\boldsymbol{\kappa} \cdot \nabla P_0 > 0 \implies \text{instability} \quad (10.118)$$

which gives instability for bad curvature ($\boldsymbol{\kappa}$ parallel to ∇P_0) and stability for good curvature ($\boldsymbol{\kappa}$ antiparallel to ∇P_0). A Bennett pinch has bad curvature and is therefore grossly unstable to Rayleigh-Taylor interchange modes. Instabilities associated with Eq.(10.117) are called pressure-driven instabilities, and are important in plasmas where there is significant energy stored in the pressure (high β where $\beta = 2\mu_0 P_0/B_0^2$).

The other type of destabilizing term depends on the existence of a force-free current (i.e., $J_{0\parallel} \neq 0$) and leads to internal kink instabilities. These sorts of instabilities are called current-driven instabilities (although strictly speaking, only the parallel component of the current is involved).

There also exist instabilities associated with the magnetofluid-vacuum interface. The energy δW_{int} can be thought of as the change in potential energy of a stretched membrane at the magnetofluid-vacuum interface where the stretching force is given by the difference between the vacuum and magnetofluid forces pushing on the membrane surface; instability will occur if $\delta W_{int} < 0$. When investigating these surface instabilities it is convenient to set δW_F to zero by idealizing the plasma to being incompressible, having uniform internal pressure, and no internal currents. Surface instabilities can exist only if the surface can move, and so require a vacuum region between the wall and the plasma. Thus, moving a conducting wall right up to the surface of a conducting plasma prevents surface instabilities. These surface instabilities will be investigated in detail later in this chapter.

10.5 Current-driven instabilities and helicity

We shall now discuss current driven instabilities and show that these are helical in nature and are driven by gradients in $J_{0\parallel}/B_0$. To simplify the analysis $P \rightarrow 0$ is assumed so that pressure-driven instabilities can be neglected since they have already been discussed. On making this simplification, Eq.(10.97) shows that the parallel component of the perturbed

magnetic field reduces to

$$B_{1\parallel} = -B_0 [2\boldsymbol{\xi}_\perp \cdot \boldsymbol{\kappa} + \nabla \cdot \boldsymbol{\xi}_\perp]. \quad (10.119)$$

Thus, we may identify

$$B_1^2 = B_{1\perp}^2 + B_{1\parallel}^2 = \mathbf{B}_{1\perp}^2 + B_0^2 [2\boldsymbol{\xi}_\perp \cdot \boldsymbol{\kappa} + \nabla \cdot \boldsymbol{\xi}_\perp]^2 \quad (10.120)$$

and so the perturbed potential energy of the magnetofluid volume reduces to

$$\delta W_F = \frac{1}{2\mu_0} \int d^3r \left\{ B_1^2 + \boldsymbol{\xi}_\perp \times \mathbf{B}_{1\perp} \cdot \mathbf{B}_0 \frac{\mu_0 J_{0\parallel}}{B_0} \right\}. \quad (10.121)$$

Equation (10.67) shows that the perturbed vector potential can be identified as

$$\mathbf{A}_1 = \boldsymbol{\xi} \times \mathbf{B}_0 \quad (10.122)$$

so that Eq.(10.121) can be recast as

$$\delta W_F = \frac{1}{2\mu_0} \int d^3r \left\{ B_1^2 - \mathbf{A}_1 \cdot \mathbf{B}_1 \frac{\mu_0 J_{0\parallel}}{B_0} \right\}. \quad (10.123)$$

We now show that finite $\mathbf{A}_1 \cdot \mathbf{B}_1$ corresponds to a helical perturbation. Consider the simplest situation where $\mathbf{A}_1 \cdot \mathbf{B}_1$ is simply a constant and define a local Cartesian coordinate system with z axis parallel to the local \mathbf{B}_0 . Equation (10.122) shows that $\mathbf{A}_1 = A_{1x} \hat{x} + A_{1y} \hat{y}$ so

$$\mathbf{A}_1 \cdot \mathbf{B}_1 = -A_{1x} \frac{\partial A_{1y}}{\partial z} + A_{1y} \frac{\partial A_{1x}}{\partial z}. \quad (10.124)$$

Suppose both components of \mathbf{A}_1 are non-trivial functions of z and, in particular, assume $A_{1x} = \text{Re } \mathcal{A}_{1x} \exp(ikz)$ and $A_{1y} = \text{Re } \mathcal{A}_{1y} \exp(ikz)$. In this case

$$\mathbf{A}_1 \cdot \mathbf{B}_1 = \frac{1}{2} \text{Re} \left[-\mathcal{A}_{1x}^* \frac{\partial \mathcal{A}_{1y}}{\partial z} + \mathcal{A}_{1y}^* \frac{\partial \mathcal{A}_{1x}}{\partial z} \right] = -\frac{k}{2} \text{Re} [i (\mathcal{A}_{1x}^* \mathcal{A}_{1y} - \mathcal{A}_{1y}^* \mathcal{A}_{1x})] \quad (10.125)$$

which can be finite only if $\mathcal{A}_{1x}^* \mathcal{A}_{1y}$ is not pure real. The simplest such case is where $\mathcal{A}_{1y} = i\mathcal{A}_{1x}$ so

$$\mathbf{A}_1 \cdot \mathbf{B}_1 = k |\mathcal{A}_{1x}|^2 \quad (10.126)$$

and

$$\mathbf{A}_1 = \text{Re} [\mathcal{A}_{1x} (\hat{x} + i\hat{y}) \exp(ikz)] \quad (10.127)$$

which is a helically polarized field since $A_{1x} \sim \cos kz$ and $A_{1y} \sim \sin kz$.

10.6 Magnetic helicity

Since finite $\mathbf{A}_1 \cdot \mathbf{B}_1$ corresponds to the local helical polarization of the perturbed fields, it is reasonable to define $\mathbf{A} \cdot \mathbf{B}$ as the density of magnetic helicity and to define the total magnetic helicity in a volume as

$$K = \int_V d^3r \mathbf{A} \cdot \mathbf{B}. \quad (10.128)$$

The question immediately arises whether this definition makes sense, i.e., is it reasonable to define $\mathbf{A} \cdot \mathbf{B}$ as an intensive property and K as an extensive property. An obvious problem is that \mathbf{A} is undefined with respect to a gauge, since \mathbf{A} can be redefined to be $\mathbf{A}' = \mathbf{A} + \nabla f$ where f is an arbitrary scalar function without affecting the magnetic field, because $\nabla \times \mathbf{A} = \nabla \times (\mathbf{A} + \nabla f)$. The above definition for magnetic helicity would be of little use if K depended on choice of gauge. However, if no magnetic field penetrates the surface S enclosing the volume V , the proposed definition of K is gauge-independent. This is because $\mathbf{B} \cdot d\mathbf{s} = 0$ everywhere on the surface if no magnetic field penetrates the surface. If this is so, then

$$\begin{aligned} \int_V d^3r (\mathbf{A} + \nabla f) \cdot \mathbf{B} &= \int_V d^3r \mathbf{A} \cdot \mathbf{B} + \int_V d^3r \nabla \cdot (f\mathbf{B}) \\ &= \int_V d^3r \mathbf{A} \cdot \mathbf{B} + \int_S d\mathbf{s} \cdot (f\mathbf{B}) \\ &= \int_V d^3r \mathbf{A} \cdot \mathbf{B} \end{aligned} \quad (10.129)$$

and so the helicity is gauge-independent even though the helicity density is gauge-dependent.

Let us consider the situation where there is no vacuum region between the plasma and an impermeable wall. Thus the normal fluid velocity $\mathbf{u}_{1\perp}$ must vanish at the wall. From Ohm's law the component of the perturbed electric field tangential to the wall \mathbf{E}_{1t} is just

$$\mathbf{E}_{1t} = -\mathbf{u}_{1\perp} \times \mathbf{B}_0 = 0 \quad (10.130)$$

since \mathbf{B}_0 lies in the plane of the wall. Thus, an impermeable wall is equivalent to a conducting wall. If the magnetic field initially does not penetrate the wall, i.e. $\mathbf{B} \cdot d\mathbf{s} = 0$ initially, then the field will always remain tangential to the wall and the helicity K in the volume enclosed by the wall will always be a well-defined quantity (i.e., will always be gauge-invariant).

The time derivative of the magnetic helicity density together with Faraday's law gives a conservation equation for helicity density. This is seen by direct calculation:

$$\begin{aligned} -\frac{\partial}{\partial t} (\mathbf{A} \cdot \mathbf{B}) &= -\frac{\partial \mathbf{A}}{\partial t} \cdot \mathbf{B} - \mathbf{A} \cdot \frac{\partial \mathbf{B}}{\partial t} \\ &= (\mathbf{E} + \nabla \varphi) \cdot \mathbf{B} + \mathbf{A} \cdot \nabla \times \mathbf{E} \\ &= 2\mathbf{E} \cdot \mathbf{B} + \nabla \cdot (\varphi \mathbf{B} + \mathbf{E} \times \mathbf{A}) \end{aligned} \quad (10.131)$$

where φ is the electrostatic potential. Since the ideal MHD Ohm's law gives $\mathbf{E} \cdot \mathbf{B} = 0$, Eq. (10.131) can be rearranged in the form of a helicity conservation equation

$$\frac{\partial}{\partial t} (\mathbf{A} \cdot \mathbf{B}) + \nabla \cdot (\varphi \mathbf{B} + \mathbf{E} \times \mathbf{A}) = 0. \quad (10.132)$$

Integration of Eq.(10.132) over the entire magnetofluid volume gives a global helicity conservation relation

$$\frac{\partial}{\partial t} \left[\int d^3r \mathbf{A} \cdot \mathbf{B} \right] + \int d\mathbf{s} \hat{n} \cdot (\varphi \mathbf{B} + \mathbf{E} \times \mathbf{A}) = 0. \quad (10.133)$$

Since both $\mathbf{B} \cdot \hat{n} = 0$ and $\mathbf{E}_t = 0$ at the wall, this reduces to

$$K = \int d^3r \mathbf{A} \cdot \mathbf{B} = \text{const.}; \quad (10.134)$$

i.e., the total helicity (integral of the helicity density) is conserved for an ideal plasma surrounded by a rigid or conducting wall.

Now recall that \mathbf{A}_1 is a linear function of $\boldsymbol{\xi}$ as given in Eq.(10.122) and that $\boldsymbol{\xi}$ was assumed to be of order ϵ . Consider the implications of this result for perturbed magnetic fields. We write $\mathbf{B} = \mathbf{B}_0 + \mathbf{B}_1$ and $\mathbf{A} = \mathbf{A}_0 + \mathbf{A}_1$ so that the total magnetic helicity, a constant, is

$$\begin{aligned} K = \int d^3r \mathbf{A}_0 \cdot \nabla \times \mathbf{A}_0 &= \int d^3r (\mathbf{A}_0 + \mathbf{A}_1) \cdot \nabla \times (\mathbf{A}_0 + \mathbf{A}_1) \\ &= \int d^3r \mathbf{A}_0 \cdot \nabla \times \mathbf{A}_0 + \int d^3r \mathbf{A}_1 \cdot \nabla \times \mathbf{A}_0 \\ &\quad + \int d^3r \mathbf{A}_0 \cdot \nabla \times \mathbf{A}_1 + \int d^3r \mathbf{A}_1 \cdot \nabla \times \mathbf{A}_1. \end{aligned} \quad (10.135)$$

Thus, to first-order in the perturbation (i.e., to order ϵ),

$$\int d^3r \mathbf{A}_1 \cdot \nabla \times \mathbf{A}_0 + \int d^3r \mathbf{A}_0 \cdot \nabla \times \mathbf{A}_1 = 0 \quad (10.136)$$

and to second-order (i.e., to order ϵ^2 which is what is relevant for the energy principle),

$$\int d^3r \mathbf{A}_1 \cdot \nabla \times \mathbf{A}_1 = \int d^3r \mathbf{A}_1 \cdot \mathbf{B}_1 = 0. \quad (10.137)$$

This can be compared to Eq.(10.123); the second term is almost the same as Eq.(10.137) except for a factor $-\mu_0 J_{0\parallel}/B_0$ which, in general, is some complicated function of position. However, in the special case where $\mu_0 J_{0\parallel}/B_0 = \text{const.}$, it is possible to factor $\mu_0 J_{0\parallel}/B_0$ out of the integral and obtain, using Eq.(10.137),

$$\delta W_F = \frac{1}{2\mu_0} \int d^3r B_1^2 \quad (10.138)$$

which is positive-definite and therefore gives absolute stability. Thus, equilibria which have $\mu_0 J_{0\parallel}/B_0 = \lambda$ where $\lambda = \text{const.}$ are stable against current-driven modes. Since these equilibria are helical or kinked, they may be considered as being the final relaxed state associated with a kink instability –once a system attains this state no free energy remains to drive further instability. Since pressure has been assumed to be negligible, Eq.(10.60) implies that the equilibrium current must be parallel to the equilibrium magnetic field, but does not specify the proportionality factor. What has been shown here is that if the proportionality factor is spatially uniform, i.e.,

$$\mu_0 \mathbf{J}_0 = \lambda \mathbf{B}_0 \quad (10.139)$$

where λ does not depend on position, then the system is stable against any further helical perturbations. This gives rise to the relation

$$\nabla \times \mathbf{B}_0 = \lambda \mathbf{B}_0 \quad (10.140)$$

where λ is spatially uniform. This equation is called the force-free equilibrium and its solutions are helical vector fields, namely fields where the curl of the field is parallel to the field itself. If a field is confined to a plane, then its curl will be normal to the plane and so a field confined to a plane cannot be a solution to Eq.(10.140). The field must be three-dimensional.

To summarize, it has been shown that current-driven instabilities are helical and drive the plasma towards a force-free equilibrium as prescribed by Eq.(10.140). Current-driven instabilities are energized by the gradient of $J_{0\parallel}/B_0$ and become stabilized when $J_{0\parallel}/B_0$ becomes spatially uniform. Gradients in $J_{0\parallel}/B_0$ can therefore be considered as the free energy for driving kink modes. When all the free energy is consumed, the kinks are stabilized and the plasma assumes a force-free equilibrium with spatially uniform $J_{0\parallel}/B_0$.

This tendency to coil up or kink is a means by which the plasma increases its inductance. However, when the plasma coils up into a state satisfying Eq.(10.140) it is in a stable equilibrium. This stable equilibrium represents a local minimum in potential energy. There might be several such local minima, each of which has a different value as sketched in Fig.9.2. As mentioned earlier this set of discrete energy levels is somewhat analogous to the ground and excited states of a quantum system. Here, the vacuum magnetic field is analogous to the ground state, while the various force-free equilibria (i.e., solutions of Eq.(10.140)) are analogous to higher energy states.

10.7 Qualitative description of free-boundary instabilities

The previous section considered internal instabilities of a magnetofluid bounded by a rigid wall so that no vacuum region existed between the magnetofluid and the wall. Let us now consider the other extreme, namely a situation where not only does a vacuum region exist external to the magnetofluid, but in addition, the location of the vacuum-magnetofluid interface is not fixed and can move around. To focus attention on the effect of surface motions, the simplest non-trivial configuration will be considered, namely a configuration where the interior pressure is both uniform and finite. This corresponds to having $\nabla P = 0$ in the interior so that the entire pressure gradient and therefore the entire $\mathbf{J} \times \mathbf{B}$ force is concentrated in an infinitesimally thin surface layer.

The MHD energy principle showed that compressibility, manifested by having finite $\nabla \cdot \boldsymbol{\xi}$, is stabilizing. Therefore, if a given system is stable with respect to incompressible modes, it will be even more stable with respect to compressible modes, or equivalently, with respect to modes having finite $\nabla \cdot \boldsymbol{\xi}$. Thus by assuming $\nabla \cdot \boldsymbol{\xi} = 0$, the worst-case scenario is considered and, in addition, the analysis is simplified. Finally, it is assumed that the plasma is cylindrical and uniform in the z direction (axially uniform). For example, the Bennett pinch would satisfy these assumptions if all the current were concentrated on the plasma surface. The physical basis of the two main types of current-driven instability, sausage and kink, will first be discussed before engaging in a detailed mathematical analysis.

10.7.1 Qualitative examination of the sausage instability

Consider a Bennett pinch (z -pinch), that is an axially uniform cylindrical plasma with an axial current and an associated azimuthal magnetic field. In addition, as discussed above

the pressure is assumed to be (i) uniform in the interior region $r < a$ where a is the plasma radius and (ii) zero in the exterior region $r > a$. In equilibrium, the radially inward $\mathbf{J} \times \mathbf{B}$ pinch force balances the radially outward force associated with the pressure gradient so that $-J_{z0}B_{\theta0} = \partial P_0/\partial r$ where both sides of this equation are finite only in an infinitesimal surface layer at $r = a$. We now suppose that thermal noise causes the incompressible plasma to develop axially periodic constrictions and bulges as shown in Fig.10.6. At the constrictions the azimuthal magnetic field $B_\theta = \mu_0 I/2\pi r$ becomes larger than in equilibrium because $r < a$ at a constriction whereas I is fixed. Thus, at the constriction the pinch force $\sim B_\theta^2/r$ is greater than its equilibrium value and so exceeds the outward force from the internally uniform pressure. The resulting net force will be inwards and will cause a radial inwards motion which will enhance the constriction. Because the configuration is assumed incompressible, any plasma squeezed inwards at constrictions must flow into the interspersed bulges shown in Fig.10.6. The azimuthal magnetic field at a bulge is weaker than its equilibrium value because $r > a$ at a bulge so the tables are now turned in the competition between outward pressure and inward pinch force — at a bulge the pressure exceeds the weakened pinch force and this force imbalance causes the bulge to increase. Hence any initial perturbed combination of constrictions and bulges will tend to grow and so the system is unstable. This behavior is called the ‘sausage’ instability because what results is a plasma resembling a string of sausages.

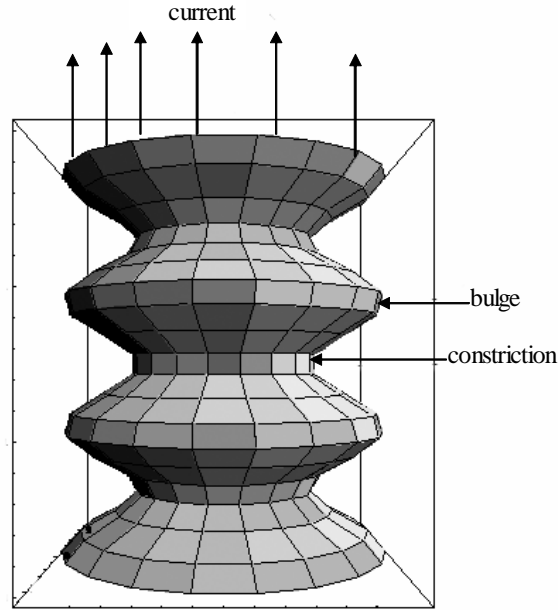


Figure 10.6: Sausage instability, current is axial, magnetic field is azimuthal

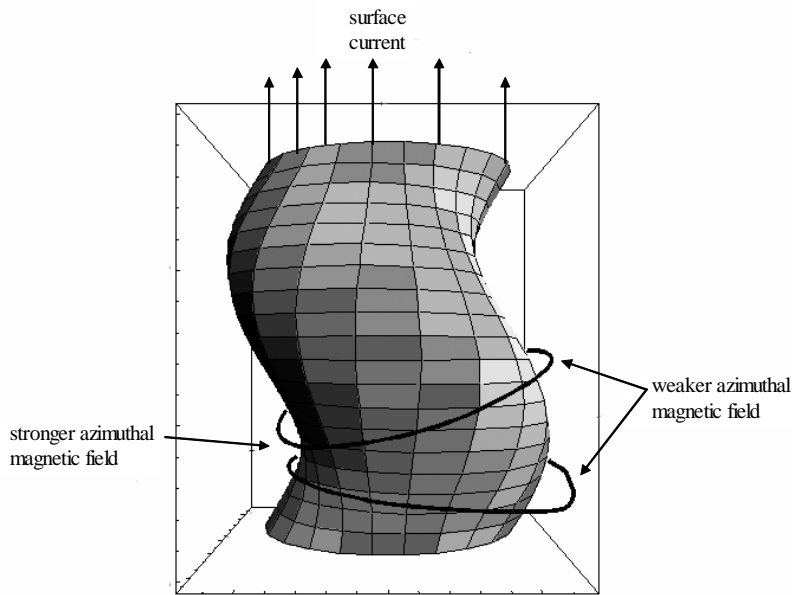


Figure 10.7: Kink instability can occur when the equilibrium magnetic field is helical

The sausage instability can be prevented by surrounding the plasma with a perfectly conducting wall or by immersing the plasma in a strong axial vacuum magnetic field generated by currents in external solenoid coils coaxial with the plasma. If a plasma with embedded axial field attempts to sausage, the axial rippling of the plasma would have to bend the embedded axial field since this axial field is frozen into the plasma. Any bending of a magnetic field requires work and so the free energy available to drive the sausage instability would also have to do work to bend the axial field. If bending the axial magnetic field absorbs more energy than liberated by the sausageing motion, the plasma is stabilized. The axial field stabilizes the plasma in a manner analogous to a steel reinforcing rod embedded in concrete. The other method for stabilization, a close-fitting conducting wall, works because image currents induced in the wall by the sausage motion produce a magnetic field which interacts with the plasma current in such a way as to repel the plasma away from the wall.

10.7.2 Qualitative examination of the kink instability

The axial magnetic field B_z combined with the azimuthal magnetic field B_θ produced by the plasma current results in a magnetic field that is helical. This helical magnetic field is susceptible to the helical kink instabilities sketched in Fig.10.7. At the concave parts of the plasma surface there is a concentration of the azimuthal field resulting in a magnetic pressure that increases the concavity. Similarly, at the convex portions of the surface, the

azimuthal field is weaker so that the convex bulge will tend to increase. This is just the hoop force trying to increase the major radius of a curved current. If the externally imposed axial magnetic field is sufficiently strong, the energy required to bend the external field will exceed the free energy available from the kinking and the instability will be prevented.

10.7.3 Qualitative examination of wall stabilization

Now consider a plasma with no externally produced B_z field but surrounded by a close-fitting perfectly conducting wall. The plasma axial current generates an azimuthal field in the vacuum region between the plasma and the wall. If an instability causes the plasma to move towards the wall, then the vacuum region becomes thinner and the magnetic field in the vacuum region becomes compressed since it cannot penetrate the wall or the plasma. The increased magnetic pressure acts a restoring force, pushing the plasma back away from the wall. Thus, a close-fitting perfectly conducting wall can stabilize both kinks and sausages.

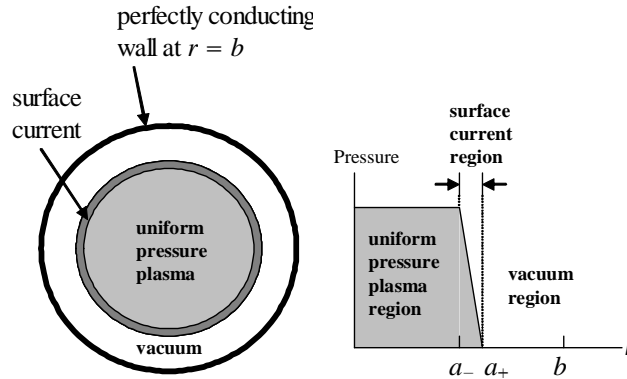


Figure 10.8: Equilibrium for free-boundary stability analysis: assumed cross-section (left) and assumed pressure profile (right).

10.8 Analysis of free-boundary instabilities

Consider the azimuthally symmetric, axially uniform cylindrical plasma of radius a shown in Fig.10.8. The plasma is subdivided into two concentric regions consisting of (i) the interior region $0 < r < a_-$ and (ii) a thin surface layer $a_- < r < a_+$. In the limit of infinitesimal surface thickness, a_- approaches a_+ . The interior pressure P_0 is uniform and the interior current density is zero so that both $\mathbf{J} \times \mathbf{B}$ and ∇P are zero in the interior. Thus, a finite current density exists *only* in the surface layer and everywhere else the magnetic field is a vacuum magnetic field. The plasma is also assumed to be surrounded by a perfectly conducting wall located at a radius b where b is larger than a . The MHD equilibrium

can be written as

$$0 = -\mu_0 \nabla P_0 - \nabla \left(\frac{B_0^2}{2} \right) + \mathbf{B}_0 \cdot \nabla \mathbf{B}_0. \quad (10.141)$$

Because $\nabla \cdot \mathbf{B}_0 = r^{-1} \partial / \partial r (r B_{0r}) = 0$ for an azimuthally symmetric, axially uniform system and because B_r cannot be singular, B_{0r} must be zero everywhere. Since all equilibrium quantities depend only on r , the third term in Eq.(10.141) can be expanded

$$\begin{aligned} \mathbf{B}_0 \cdot \nabla \mathbf{B}_0 &= (B_{0\theta}(r)\hat{\theta} + B_{0z}(r)\hat{z}) \cdot \nabla (B_{0\theta}(r)\hat{\theta} + B_{0z}(r)\hat{z}) \\ &= B_{0\theta}^2 \hat{\theta} \cdot \nabla \hat{\theta} = -\frac{B_{0\theta}^2}{r} \hat{r}. \end{aligned} \quad (10.142)$$

Thus, Eq.(10.141) has only r components and reduces to the relation

$$0 = -\mu_0 \frac{\partial P_0}{\partial r} - \frac{\partial}{\partial r} \left(\frac{B_0^2}{2} \right) - \frac{B_{0\theta}^2}{r}. \quad (10.143)$$

On integrating across the surface layer, this becomes

$$P_0 + \frac{B_{0pz}^2}{2\mu_0} = \frac{B_{0v\theta}^2 + B_{0vz}^2}{2\mu_0} \quad (10.144)$$

where the subscript p refers to being at the inner radius (plasma side) of the surface layer and the subscript v refers to the outer radius (vacuum side). The reason there is no $B_{0p\theta}^2$ term on the left hand side is that there are no interior plasma currents (from Ampere's law $2\pi a B_{0p\theta} = \mu_0 I_z = 0$).

The equilibrium surface can be described by the function $r = a$ or equivalently, the surface-defining equation

$$S_0(r) = r - a = 0. \quad (10.145)$$

The incompressible perturbation is characterized by a harmonic deformation of the plasma surface such that $r = a + \xi e^{im\theta + ikz}$. The surface equation for the perturbed surface is thus

$$S(r, \theta, z) = r - a - \xi e^{im\theta + ikz} = 0 \quad (10.146)$$

where without loss of generality it is assumed that $\xi > 0$. The equilibrium magnetic field had $B_{0r} = 0$, i.e., had no component normal to the surface, and so the equilibrium magnetic field lines at the surface lie in the surface. This is equivalent to stating that $\mathbf{B}_0 \cdot \nabla S_0 = 0$ which implies that the equilibrium magnetic field is tangential to the surface. Since the magnetic field is assumed frozen into the plasma, the magnetic field must *continue* to be tangential to the surface even when the surface becomes deformed from its equilibrium shape. Thus, the condition

$$\mathbf{B} \cdot \nabla S = 0 \quad (10.147)$$

must be satisfied at all times where ∇S is in the direction normal to the surface; this is essentially a statement that no magnetic field line penetrates the surface.

A quantity f at the perturbed surface (denoted by the subscript ps) can be expressed as

$$f_{ps} = f_0 + f_1 + \boldsymbol{\xi} \cdot \nabla f_0 \quad (10.148)$$

where the the middle term is the absolute first-order change and the last term is the convective term due to the motion of the surface.

If a configuration is to be stable, any perturbation must generate a restoring force which pushes the perturbed surface back to its equilibrium location. The competition between destabilizing and restoring forces is found by integrating Eq.(10.141) across the perturbed surface. This integration gives Eq.(10.144) evaluated at the perturbed surface, i.e., using Eq.(10.148) to take into account the effect of the perturbation of the surface. Since ξ was assumed positive (outward bulge at $\theta = 0, z = 0$) the perturbed system will be stable if the effective pressure on the outside of the perturbed surface exceeds the effective pressure on the inside, i.e., if

$$\left[\frac{B_{v\theta}^2 + B_{vz}^2}{2\mu_0} \right]_{\text{perturbed sfc}} > \left[P + \frac{B_{pz}^2}{2\mu_0} \right]_{\text{perturbed sfc}} \implies \text{stable.} \quad (10.149)$$

In this case, the restoring force pushes back the bulge and makes the system revert to its equilibrium condition. Subtracting the equilibrium pressure balance relation, Eq.(10.144), this becomes

$$\frac{B_{0v\theta}B_{1v\theta} + B_{0vz}B_{1vz}}{\mu_0} + \xi \frac{\partial}{\partial r} \left[\frac{B_{0v\theta}^2 + B_{0vz}^2}{2\mu_0} \right] > P_1 + \frac{B_{0pz}B_{1pz}}{\mu_0} + \xi \frac{\partial}{\partial r} \left[P_0 + \frac{B_{0pz}^2}{2\mu_0} \right] \quad (10.150)$$

where all quantities are evaluated at $r = a$.

Equation (10.150) can be simplified considerably because of the following relationships:

1. There are no currents in either the plasma interior or the external vacuum so

$$\frac{\partial B_{0pz}}{\partial r} = \frac{\partial B_{0vz}}{\partial r} = 0. \quad (10.151)$$

2. The adiabatic pressure equation gives

$$P_1 + \xi \cdot \nabla P_0 + \gamma P_0 \nabla \cdot \xi = 0. \quad (10.152)$$

Since incompressibility $\nabla \cdot \xi = 0$ has been assumed, the adiabatic relation reduces to

$$P_1 + \xi \partial P_0 / \partial r = 0. \quad (10.153)$$

3. From Ampere's law it is seen that $B_{0v\theta}^2 \sim r^{-2}$ so $[\partial B_{0v\theta}^2 / \partial r]_{r=a} = -2B_{0v\theta}^2/a$; thus Eq.(10.150) simplifies to

$$B_{0v\theta}B_{1v\theta} + B_{0vz}B_{1vz} - \frac{\xi}{a} B_{0v\theta}^2 > B_{0pz}B_{1pz} \implies \text{stable} \quad (10.154)$$

where again all fields are evaluated at $r = a$.

To simplify the algebra all fields are now normalized to $B_{0v\theta}(a)$. The normalized fields are denoted by a bar on top and are

$$\begin{aligned} \bar{B}_{0vz} &= \frac{B_{0vz}}{B_{0v\theta}(a)}, & \bar{B}_{0pz} &= \frac{B_{0pz}}{B_{0v\theta}(a)}, \\ \bar{B}_{1vz} &= \frac{B_{1vz}}{B_{0v\theta}(a)}, & \bar{B}_{1v\theta} &= \frac{B_{1v\theta}}{B_{0v\theta}(a)}, & \bar{B}_{1pz} &= \frac{B_{1pz}}{B_{0v\theta}(a)} \end{aligned} \quad (10.155)$$

so that, when expressed as a relationship between normalized fields, Eq.(10.154) becomes

$$\bar{B}_{1v\theta} + \bar{B}_{0vz}\bar{B}_{1vz} - \frac{\xi}{a} > \bar{B}_{0pz}\bar{B}_{1pz} \implies \text{stable.} \quad (10.156)$$

What remains to be done is express all first-order magnetic fields in terms of ξ . This is relatively easy because the current is confined to the surface layer so the magnetic field is a vacuum magnetic field everywhere but exactly on the surface.

Since \mathbf{B} is a vacuum magnetic field for both $0 < r < a$ and $a < r < b$, it must be of the form $\mathbf{B} = \nabla\chi$ where $\nabla^2\chi = 0$ in both regions, but there could be a jump discontinuity at $r = a$. Because the perturbed fields were assumed to have an $\exp(im\theta + ikz)$ dependence, the Laplacian becomes

$$\nabla^2\chi = \frac{d^2\chi(r)}{dr^2} + \frac{1}{r}\frac{d\chi(r)}{dr} - \left(\frac{m^2}{r^2} + k^2\right)\chi(r) = 0 \quad (10.157)$$

which is just the equation for modified Bessel functions, $I_{|m|}(|k|r)$ and $K_{|m|}(|k|r)$. Absolute value signs have been used to avoid possible confusion later for situations where m or k could be negative. The $I_{|m|}(|k|r)$ function is finite at $r = 0$ but diverges at $r = \infty$ while the opposite is true for $K_{|m|}(|k|r)$.

The surface current causes a discontinuity in the tangential components of the perturbed magnetic field. Hence, different solutions must be used in the respective plasma and vacuum regions and then these solutions must be related to each other in such a way as to satisfy the requirements of this discontinuity. The forms of the plasma and vacuum solutions are, in addition, constrained by the respective boundary conditions at $r = 0$ and at $r = b$. In particular, the $K_{|m|}(|k|r)$ solution is not allowed in the plasma because of the constraint that the magnetic field must be finite at $r = 0$; thus inside the plasma the solution is of the form

$$\chi = \alpha I_{|m|}(|k|r) \quad \text{in plasma region } 0 < r < a_- . \quad (10.158)$$

On the other hand, both the $I_{|m|}(|k|r)$ and $K_{|m|}(|k|r)$ solutions are permissible in the vacuum region and so the vacuum region solution is of the general form

$$\chi = \beta_1 I_{|m|}(|k|r) + \beta_2 K_{|m|}(|k|r) \quad \text{in vacuum region } a_+ < r < b . \quad (10.159)$$

The objective now is to express the coefficients α , β_1 , and β_2 in terms of ξ so that all components of the perturbed magnetic field can be expressed as a function of ξ , both in the plasma and in the vacuum.

The functional dependence of these coefficients is determined by considering boundary conditions at the wall and then at the plasma-vacuum interface:

1. Wall: Since the wall is perfectly conducting it is a flux conserver. There is no radial magnetic field initially and so there is no flux linking each small patch of the wall. Thus $\bar{B}_{1vr}(b)$ must vanish at the wall in order to maintain zero flux at each patch of the wall. Using Eq.(10.159) to calculate the perturbed radial magnetic field at the wall, this condition means that

$$\beta_1 I'_{|m|}(|k|b) + \beta_2 K'_{|m|}(|k|b) = 0 \quad (10.160)$$

which may be solved for β_2 to give

$$\beta_2 = -\beta_1 \frac{\hat{I}'_{|m|}}{\hat{K}'_{|m|}}; \quad (10.161)$$

here the circumflex means the modified Bessel function is evaluated at the wall, i.e., with its argument set to $|k|b$. Equation (10.159) can then be recast as

$$\chi = \beta \left[I_{|m|}(|k|r) \hat{K}'_{|m|} - \hat{I}'_{|m|} K_{|m|}(|k|r) \right] \quad (10.162)$$

where $\beta = \beta_1 / \hat{K}'_{|m|}$. The wall boundary condition has reduced the number of independent coefficients by one.

2. Vacuum side of plasma-vacuum interface: Here Eq.(10.147) is linearized to obtain

$$\mathbf{B}_1 \cdot \nabla S_0 + \mathbf{B}_0 \cdot \nabla S_1 = 0 \quad (10.163)$$

or using Eqs.(10.145) and (10.146)

$$\bar{B}_{1vr} - i \left(\frac{m}{a} + k \bar{B}_{0vz} \right) \xi = 0. \quad (10.164)$$

On the vacuum side Eq.(10.162) gives

$$\bar{B}_{1vr} = |k| \beta \left[I'_{|m|} \hat{K}'_{|m|} - \hat{I}'_{|m|} K'_{|m|} \right] \quad (10.165)$$

where omission of the argument means that the modified Bessel function is evaluated at $r = a$. Substitution of Eq.(10.165) into Eq.(10.164) gives

$$\beta = \frac{i \left(\frac{m}{a} + k \bar{B}_{0z} \right)}{|k| \left[I'_{|m|} \hat{K}'_{|m|} - \hat{I}'_{|m|} K'_{|m|} \right]} \xi \quad (10.166)$$

so the complete vacuum field can now be expressed in terms of ξ .

3. Plasma side of plasma-vacuum interface: The plasma-side version of Eq.(10.163) gives

$$\bar{B}_{1pr} - ik \bar{B}_{0pz} \xi = 0 \quad (10.167)$$

since $B_{0p\theta}$ vanishes inside the plasma. From Eq.(10.158) the perturbed radial magnetic field on the plasma side of the interface is

$$\bar{B}_{1pr} = |k| \alpha I'_{|m|}. \quad (10.168)$$

The plasma side version of Eq.(10.164) is thus

$$\alpha = \frac{ik \bar{B}_{0pz}}{|k| I'_{|m|}} \xi \quad (10.169)$$

and so the plasma fields can now also be expressed in terms of ξ .

The stability condition, Eq.(10.156), can be written in terms of α and β to obtain

$$\beta \left(\frac{im}{a} + ik \bar{B}_{0vz} \right) \left(I_{|m|} \hat{K}'_{|m|} - \hat{I}'_{|m|} K_{|m|} \right) - \frac{\xi}{a} > \alpha \bar{B}_{0pz} ik I_{|m|}. \quad (10.170)$$

Substituting for α and β and re-arranging the order gives

$$|k| a \bar{B}_{0pz}^2 \left[\frac{I_{|m|}}{I'_{|m|}} \right] - \frac{(m + ka \bar{B}_{0vz})^2}{|k| a} \left[\frac{I_{|m|} \hat{K}'_{|m|} - \hat{I}'_{|m|} K_{|m|}}{I'_{|m|} \hat{K}'_{|m|} - \hat{I}'_{|m|} K'_{|m|}} \right] > 1 \implies \text{stable.} \quad (10.171)$$

If we introduce the normalized pressure

$$\bar{P}_0 = \frac{2\mu_0 P_0}{B_{0v\theta}^2(a)} \quad (10.172)$$

the MHD equilibrium, Eq.(10.144), can be written in normalized form as

$$\bar{P}_0 + \bar{B}_{0pz}^2 = 1 + \bar{B}_{0vz}^2. \quad (10.173)$$

Substitution for \bar{B}_{0pz}^2 into Eq.(10.171) and rearranging the order of the second term gives

$$|k|a \left[1 + \bar{B}_{0vz}^2 - \bar{P}_0 \right] \left[\frac{I_{|m|}}{I'_{|m|}} \right] + \frac{(m + ka\bar{B}_{0vz})^2}{|k|a} \left[\frac{-I_{|m|}\hat{K}'_{|m|} + \hat{I}'_{|m|}K_{|m|}}{I'_{|m|}\hat{K}'_{|m|} - \hat{I}'_{|m|}K'_{|m|}} \right] > 1 \quad (10.174)$$

which is the general requirement for stability of a configuration having a specified internal pressure, vacuum axial field, plasma radius, and wall radius.

Conditions for sausage and kink instability Let us now examine the effect of the various factors in Eq.(10.174). For large argument, the modified Bessel functions have the asymptotic form

$$\lim_{s \rightarrow \infty} I_{|m|}(s) \rightarrow e^s; \quad \lim_{s \rightarrow \infty} K_{|m|}(s) \rightarrow e^{-s} \quad (10.175)$$

so if the wall radius goes to infinity, the factor

$$\left[\frac{-I_{|m|}\hat{K}'_{|m|} + \hat{I}'_{|m|}K_{|m|}}{I'_{|m|}\hat{K}'_{|m|} - \hat{I}'_{|m|}K'_{|m|}} \right] \rightarrow -\frac{K_{|m|}}{K'_{|m|}} = \text{positive definite.} \quad (10.176)$$

Since bringing the wall closer is stabilizing, the factor

$$\frac{-I_{|m|}\hat{K}'_{|m|} + \hat{I}'_{|m|}K_{|m|}}{I'_{|m|}\hat{K}'_{|m|} - \hat{I}'_{|m|}K'_{|m|}}$$

will always be positive-definite. In particular, if $b \rightarrow a$ then $I'_{|m|}\hat{K}'_{|m|} \rightarrow \hat{I}'_{|m|}K'_{|m|}$ so that the wall stabilization becomes arbitrarily large.

As $|k|a \rightarrow \infty$ the left hand side of Eq.(10.174) becomes infinite. Thus, the configuration is stable with respect to modes having short axial wavelengths. The reason for this is that short wavelength perturbations cause more bending of the magnetic field than a long wavelength perturbation and so require more energy.

We therefore focus attention on modes with a *long* axial wavelength (i.e., modes with a small k) since these offer the only possibility of instability. The analysis can be subdivided into specific cases, such as $m = 0$, $|m| = 1$, $|m| > 1$, close-fitting wall, no wall, low pressure, high pressure, etc. Before getting into the details let us take a broader look at the effect of the various terms in Eq. (10.174). Since $I_{|m|}/I'_{|m|} > 0$ we see that increasing \bar{P}_0 is destabilizing, while increasing \bar{B}_{0vz}^2 is stabilizing. Also, if $m + ka\bar{B}_{0vz} = 0$ the second term vanishes, leading to *reduced* stability; by defining the wavevector as $\mathbf{k} = (m/a)\hat{\theta} + k\hat{z}$ it is seen that $m + ka\bar{B}_{0vz} = 0$ corresponds to having $\mathbf{k} \cdot \mathbf{B}_0 = 0$ at the surface.

Sausage modes

The $m = 0$ modes are the sausage instabilities and here Eq. (10.174) reduces to

$$\left[1 + \bar{B}_{0vz}^2 - \bar{P}_0\right] \left[\frac{I_0}{I'_0}\right] + \bar{B}_{0vz}^2 \left[\frac{-I_0 \hat{K}'_0 + \hat{I}'_0 K_0}{I'_0 \hat{K}'_0 - \hat{I}'_0 K'_0}\right] > \frac{1}{|k|a} \implies \text{stable.} \quad (10.177)$$

For a given normalized plasma pressure and normalized wall radius b/a , this expression can be used to make a stability plot of \bar{B}_{0vz}^2 versus $|k|a$. Since the wall always provides stabilization if brought in close enough, let us consider situations where there is no wall (i.e., $b \rightarrow \infty$) in which case the stability condition reduces to

$$\left[1 + \bar{B}_{0vz}^2 - \bar{P}_0\right] \left[\frac{I_0}{I'_0}\right] + \bar{B}_{0vz}^2 \left[\frac{-K_0}{K'_0}\right] > \frac{1}{|k|a} \implies \text{stable.} \quad (10.178)$$

For small arguments, the modified Bessel functions of order zero have the asymptotic values

$$I_0(s) \simeq 1 + \frac{s^2}{4}; \quad K_0(s) \simeq -\ln s \quad (10.179)$$

so the stability criterion becomes

$$\bar{B}_{0vz}^2 \left[1 - k^2 a^2 \ln(|k|a)\right] > \bar{P}_0 \implies \text{stable.} \quad (10.180)$$

This gives a simple criterion for how much \bar{B}_{0vz}^2 is required to stabilize a given plasma pressure against sausage instabilities. The logarithmic term is stabilizing for $|k|a < 1$ but is destabilizing for $|k|a > 1$; however this region of instability is limited because we showed that very large $|k|a$ is stable.

Kink modes

The finite m modes are the kink modes. It was shown earlier that large $|k|a$ is stable so again we confine attention to small $|k|a$. In addition, we again let the wall location go to infinity to simplify the analysis. The stability condition now reduces to

$$|k|a \left[1 + \bar{B}_{0vz}^2 - \bar{P}_0\right] \left[\frac{I_{|m|}}{I'_{|m|}}\right] + \frac{(m + ka\bar{B}_{0vz})^2}{|k|a} \left[\frac{-K_{|m|}}{K'_{|m|}}\right] > 1 \implies \text{stable.} \quad (10.181)$$

For $m \neq 0$ the small argument asymptotic limits of the modified Bessel functions are

$$I_{|m|}(s) \simeq \frac{1}{|m|!} \left(\frac{s}{2}\right)^{|m|}; \quad K_{|m|}(s) \simeq \frac{|m-1|!}{2} \left(\frac{s}{2}\right)^{-|m|} \quad (10.182)$$

so the stability condition becomes

$$k^2 a^2 \left[1 + \bar{B}_{0vz}^2 - \bar{P}_0\right] + (m + ka\bar{B}_{0vz})^2 > |m| \implies \text{stable} \quad (10.183)$$

which is a quadratic equation in ka . Let us consider plasmas where $\bar{B}_{0vz}^2 \gg 1$ and $\bar{B}_{0vz}^2 \gg \bar{P}_0$; this corresponds to a low beta plasma where the externally imposed axial field is much stronger than the field generated by the internal plasma currents (tokamaks are in this category). Let us define

$$x = ka\bar{B}_{0vz} \quad (10.184)$$

so the stability condition becomes

$$x^2 + (m+x)^2 > |m| \implies \text{stable.} \quad (10.185)$$

Without loss of generality x can be assumed to be positive, in which case instability occurs only when m is negative. Thus, Eq.(10.185) can be written as

$$2x^2 - 2|m|x + m^2 - |m| > 0 \implies \text{stable.} \quad (10.186)$$

The threshold for instability occurs when the left hand side of Eq. (10.186) vanishes, i.e., at the roots of the left hand side. These roots are

$$x = \frac{|m| \pm \sqrt{2|m| - m^2}}{2}. \quad (10.187)$$

Since the left hand side of Eq.(10.186) goes to positive infinity for $|x| \rightarrow \infty$, the left hand side is negative only in the region between the two roots. Thus, the plasma is unstable only if $|x|$ lies between the two roots. The stability condition is that $|x|$ must lie outside the region between the two roots, i.e., for stability we must have

$$\begin{aligned} x &> \frac{|m| + \sqrt{2|m| - m^2}}{2} \quad \text{or} \\ x &< \frac{|m| - \sqrt{2|m| - m^2}}{2}. \end{aligned} \quad (10.188)$$

For $m = -1$ modes this gives the stability condition

$$x > 1. \quad (10.189)$$

In un-normalized quantities and using $k = 2\pi/L$ where L is the length of the system, the stability condition is

$$\frac{2\pi a}{L} \frac{B_{0z}}{B_{0\theta}} > 1;$$

this is known as the Kruskal-Shafranov stability criterion (Kruskal, Johnson, Gottlieb and Goldman 1958, Shafranov 1958).

For $m = -2$ modes, the two roots coalesce at $x = 1$ and so Eq.(10.189) also gives stability. For $m \geq 3$ the argument of the square root in Eq.(10.187) is negative so there is no region of instability.

In toroidal devices such as tokamaks, the axial wavenumber corresponds to the toroidal wavenumber since the dominant magnetic field is in the toroidal direction, i.e. $B_{0z} \rightarrow B_{0\phi}$ where ϕ is the toroidal angle. The axial wavenumber k becomes n/R where n is the toroidal mode number. Since we saw that long axial wavelengths are the most unstable we take $n = 1$. The Kruskal-Shafranov kink stability condition becomes

$$q = \frac{aB_{0\phi}}{RB_{0\theta}} > 1 \quad (10.190)$$

where q is called the safety factor. Typical tokamaks operate with $q \sim 3$ at the wall; this q condition is one of the most important design criteria for tokamaks since it dictates the magnitude of the large and expensive toroidal field system.

10.9 Assignments

1. Interchange instabilities and volume per unit flux- Another way to consider interchange instabilities is to calculate the consequence of interchanging two flux tubes having the same magnetic flux. Doing so will not change the magnetic energy since the magnetic field is unchanged by this interchange. However, if the flux tubes contain finite-pressure plasma and the volumes of the two flux tubes differ, then the interchange will result in compression of the plasma in the flux tube which initially had the larger volume and expansion of plasma in the flux tube which initially had the smaller volume. The former requires work on the plasma and the latter involves work by the plasma. If the net work must be done on the plasma to effect the interchange, then the interchange is stable and vice versa. In a magnetic confinement configuration, the high pressure is by assumption on the inside of the configuration and the low pressure is on the outside. Thus, the question is whether interchanging a high pressure, inner region flux tube with a low pressure out region flux tube requires positive or negative work.

- (a) Show that the volume per unit flux in a flux tube is given by

$$V' = \oint \frac{dl}{B}$$

where the contour is over the length of the flux tube. Hint: Consider that $BA = \text{const.}$ on a flux tube.

- (b) Show that instability corresponds to V' increasing on going outwards.
 - (c) Consider the magnetic field external to a current-carrying straight wire. How does V' scale with distance from the wire and would a plasma confined by such a magnetic field be stable or unstable to interchanges. Is this result consistent with the concepts of good and bad curvature?
2. Work through the algebra of the magnetic energy principle and verify Eqs.(10.113), (10.114), (10.115), and (10.116).
 3. Show that the force on a plasma in an *arched magnetic field* with fixed ends tends to push the plasma towards the shape of a vacuum magnetic field arch having the same boundary conditions. Under what circumstances will the force (i) increase the magnetic field arch major radius, (ii) decrease the magnetic field arch major radius, (iii) leave the magnetic field arch major radius unchanged. Show that, in contrast, the force on a plasma containing an *arched current* always tends to increase the major radius of the arched current.
 4. Show that if the wall radius $b \rightarrow \infty$, then Eq.(10.174) reduces to the condition

$$F(x, \bar{B}_{0vz}, \bar{P}_0) = x \bar{B}_{pvz}^2 \left[\frac{I_m(x)}{I'_m(x)} \right] - \frac{(m + x \bar{B}_{0vz})^2}{x} \frac{K_m(x)}{K'_m(x)} - 1 > 0 \text{ for stability}$$

where $x = ka$. Assume that $\bar{B}_{pvz} = \bar{B}_{0vz}$ and use a computer to evaluate the modified Bessel functions numerically. Make a plot of this expression in a parameter space where the vertical axis is x and the horizontal axis is $B_{0v\theta}/B_{0vz} = 1/\bar{B}_{0vz}$ and in

particular, indicate by shading regions where $F < 0$. Do this for both $m = 0$ and for $m = -1$ so as to show the regions of the parameter space where kinks and sausages are unstable. For a given k show on the plot how raising the axial current would lead to kink or sausage instability. Which happens first (kink or sausage)?

5. Are kink instabilities diamagnetic or paramagnetic with respect to the axial field? To find this, consider the kinked current as a solenoid and determine whether the orientation of the solenoid is such as to add or subtract from the initial B_z field.
6. According to Eq.(10.139) current driven instabilities cause the plasma to relax to a situation where $\mu_0 \mathbf{J} = \lambda \mathbf{B}$.

- (a) Show that a class of solutions to this can be found if it is assumed that \mathbf{B} has the form

$$\mathbf{B} = \lambda \nabla \psi \times \hat{z} + \nabla \times (\nabla \psi \times \hat{z})$$

provided $\nabla^2 \psi + \lambda^2 \psi = 0$.

- (b) Suppose that $\psi(x, z) = f(z) \cos(kx)$. What is the form of $f(z)$? Show that solutions which decay in z are only possible for a certain range of λ^2 .
- (c) Consider a two dimensional force-free solar coronal loop. Let the $z = 0$ plane denote the solar surface. Calculate the functional form of B_x and B_z using the solution in part (a) above.
- (d) Sketch the shape of the field line going from $x = -\pi/k$ to $x = +\pi/k$ in the $z = 0$ plane. Do this for a sequence of increasing values of λ^2 . What happens to the shape of the field line as λ^2 is increased? How is current related to λ ?

Magnetic helicity interpreted and Woltjer-Taylor relaxation

11.1 Introduction

The previous chapter introduced the concept of magnetic helicity by using arguments deriving from the energy principle and showed that global helicity $K = \int d^3r \mathbf{A} \cdot \mathbf{B}$ is a conserved quantity in an ideal plasma. We show in this chapter that magnetic helicity has an important topological interpretation and furthermore that the conservation property of global helicity is more robust than magnetic energy conservation. By robust, it is meant that when some dissipation exists and the plasma is no longer ideal, helicity conservation holds up much better than magnetic energy conservation, i.e., helicity is nearly conserved even though energy is not conserved. This difference in the relative loss rates of energy and helicity provides the basis for the Woltjer-Taylor theory which predicts a minimum-energy, conserved-helicity final state which any arbitrary initial state will always relax towards. Relaxation theory has been very successful for predicting the general behavior of many laboratory, space, and astrophysical plasmas. Finally, it will be shown that helicity can be manifested in more than one way and in particular that the kink instability can be considered as a conversion of helicity from one form (twist) to another form (writhe).

11.2 Topological interpretation of magnetic helicity

11.2.1 Linkage helicity

Consider the two thin linked untwisted flux tubes labeled as flux tube #1 and flux tube #2 shown in Fig. 11.1. The respective fluxes are Φ_1 and Φ_2 and the tube axes follow the contours C_1 and C_2 , and the tube volumes are V_1 and V_2 . The magnetic field is assumed to vanish outside of the flux tubes.

The helicity of the volume V containing the two linked flux tubes is

$$K = \int_V \mathbf{A} \cdot \mathbf{B} d^3r. \quad (11.1)$$

Because \mathbf{B} vanishes outside of the two flux tubes, the helicity integral is finite only in the volumes V_1 and V_2 of the two tubes and so the helicity can be expressed as (Moffatt 1978)

$$K = \int_{V_1} \mathbf{A} \cdot \mathbf{B} d^3r + \int_{V_2} \mathbf{A} \cdot \mathbf{B} d^3r. \quad (11.2)$$

The contribution to the helicity from integrating over the volume of flux tube #1 is

$$K_1 = \int_{V_1} \mathbf{A} \cdot \mathbf{B} d^3r. \quad (11.3)$$

In order to evaluate this integral it is recalled that the magnetic flux through a surface S with perimeter C can be expressed as

$$\Phi = \int_S \mathbf{B} \cdot d\mathbf{s} = \oint_C \mathbf{A} \cdot d\mathbf{l}. \quad (11.4)$$

In flux tube #1, $d^3r = d\mathbf{l} \cdot \hat{\mathbf{B}} \Delta S$, where ΔS is the cross-sectional area of flux tube #1 and $d\mathbf{l}$ is an element of length along C_1 . It is therefore possible to recast the integrand in Eq.(11.3) as

$$\begin{aligned} \mathbf{A} \cdot \mathbf{B} d^3r &= \mathbf{A} \cdot \mathbf{B} d\mathbf{l} \cdot \hat{\mathbf{B}} \Delta S \\ &= \mathbf{A} \cdot d\mathbf{l} \Phi_1 \end{aligned} \quad (11.5)$$

since $d\mathbf{l}$ is parallel to \mathbf{B} and $B \Delta S = \Phi_1$. Because Φ_1 is by definition constant along the length of flux tube #1, it may be factored from the K_1 integral, giving

$$K_1 = \Phi_1 \int_{C_1} \mathbf{A} \cdot d\mathbf{l}. \quad (11.6)$$

However, the flux linked by contour C_1 is precisely the flux in tube #2, i.e., $\int_{C_1} \mathbf{A} \cdot d\mathbf{l} = \Phi_2$ and so

$$K_1 = \Phi_1 \Phi_2. \quad (11.7)$$

The same analysis applied to flux tube #1 leads to $K_2 = \Phi_1 \Phi_2$ and so the helicity content of the linked flux tubes is therefore

$$K = K_1 + K_2 = 2\Phi_1 \Phi_2. \quad (11.8)$$

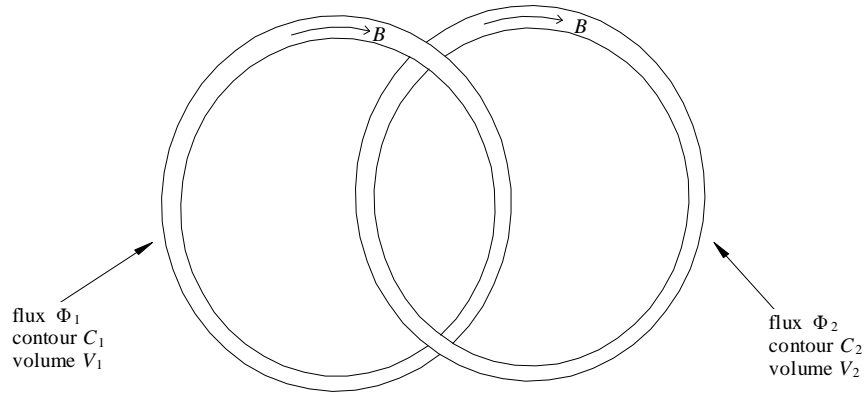


Figure 11.1: Two linked thin untwisted flux tubes. Magnetic field is zero outside the flux tubes.

The flux tubes did not actually have to be thin: a fat flux tube #2 could be decomposed into a number of adjacent thin flux tubes in which case K_1 would be Φ_1 times the sum of the flux in all of the thin #2 flux tubes. The helicity is thus just the sum of flux tube linkages since if the two flux tubes each had unit flux, there would be one linkage of flux tube #1 with flux tube #2 and one linkage of flux tube #2 with flux tube #1. As a generalization, if flux tube #2 wrapped around flux tube #1 twice, then the contributions would be $K_1 = 2\Phi_1\Phi_2$ and $K_2 = 2\Phi_1\Phi_2$ in which case the helicity would be $K = 4\Phi_1\Phi_2$. This would correspond to two linkages of flux tube #2 on flux tube #1 and two linkages of flux tube #1 on flux tube #2.

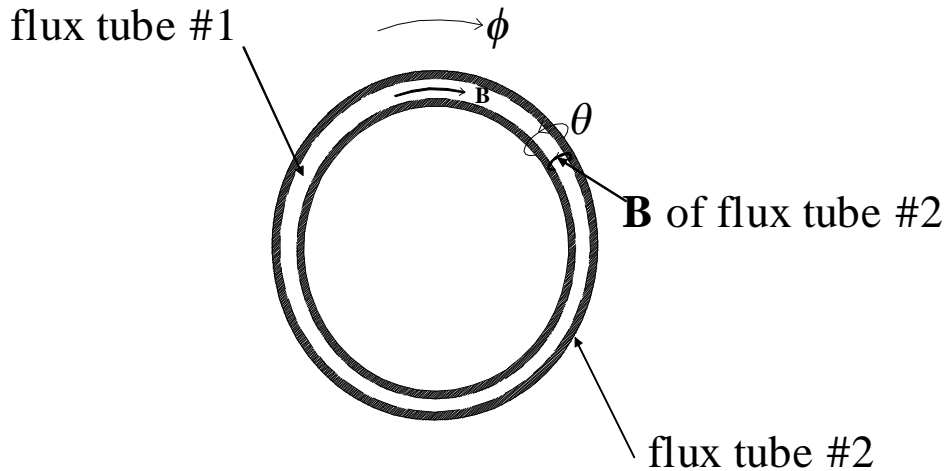


Figure 11.2: Flux tube #2 deformed so that it tightly encircles flux tube #1 and its cross-section is squeezed and stretched so as to uniformly cover flux tube #1 like a coat of paint (shaded area).

11.2.2 Twist helicity

Now suppose that the major radius of flux tube #2 is first shrunk until flux tube #2 tightly encircles flux tube #1 and then as sketched in Fig.11.2, the cross-section of flux tube #2 is both squeezed and stretched until its field lines are uniformly distributed over the length of flux tube #1; the field lines of flux tube #2 are shown shaded in Fig.11.2. The result is that the volume of flux tube #2 is like a thin coat of paint applied to flux tube #1 (shaded region in figure). Let Φ denote the flux in flux tube #1 and $d\psi$ denote the flux in flux tube #2 so, using Eq.(11.8), the helicity in this configuration is seen to be

$$dK = 2\Phi d\psi. \quad (11.9)$$

We next add another layer of ‘paint’ with more embedded ψ flux, and also with embedded Φ flux so that both ψ and Φ increase. The value of Φ can be used to label the layers of ‘paint’ so that Φ is the amount of flux in flux tube #1 up to the layer of ‘paint’ labeled by Φ . Furthermore, since ψ increases with added layers of ‘paint’, ψ must be a function of the layer of ‘paint’ and so $\psi = \psi(\Phi)$. It is therefore possible to write $d\psi = \psi' d\Phi$ where $\psi' = d\psi/d\Phi$. Thus, the amount of helicity added with each layer of ‘paint’ is

$$dK = 2\Phi \psi' d\Phi \quad (11.10)$$

and so the sum of the helicity contributions from all the layers of ‘paint’ is

$$K = 2 \int_0^\Phi \Phi \psi' d\Phi. \quad (11.11)$$

We now show that ψ' represents the twist of the embedded magnetic field. Let ϕ be the angle the long way around flux tube #1 and θ be the angle the long way around flux tube #2 as shown in Fig.11.2. Thus increasing ϕ is in the direction of contour C_1 and increasing θ is in the direction of contour C_2 . The perimeter of a cross-section of flux tube #1 is in the θ direction and the perimeter of a cross-section of flux tube #2 is in the ϕ direction. The magnetic field in flux tube #1 can be written as

$$\mathbf{B}_1 = \frac{1}{2\pi} \nabla\Phi \times \nabla\theta = \frac{1}{2\pi} \nabla \times \Phi \nabla\theta \quad (11.12)$$

which is in the ϕ direction since $\nabla\Phi$ is orthogonal to $\nabla\theta$. Here Φ is the flux linked by a contour going in the direction of $\nabla\theta$. To verify that this is the appropriate expression for \mathbf{B}_1 , the flux through the cross section S_1 of flux tube #1 is calculated as follows:

$$\begin{aligned} \text{flux through } S_1 &= \int_{S_1} d\mathbf{s} \cdot \mathbf{B}_1 \\ &= \frac{1}{2\pi} \int_{S_1} d\mathbf{s} \cdot \nabla \times \Phi \nabla\theta \\ &= \frac{1}{2\pi} \int_{C_2} d\mathbf{l} \cdot \Phi \nabla\theta \\ &= \frac{\Phi}{2\pi} \int_{C_2} d\mathbf{l} \cdot \nabla\theta \\ &= \frac{\Phi}{2\pi} \oint d\theta \\ &= \Phi. \end{aligned} \quad (11.13)$$

The flux Φ can be factored from the integral in the third line above, because Φ is the flux linked by contour C_2 which goes in the direction of $\nabla\theta$. Similarly, it is possible to write

$$\mathbf{B}_2 = \frac{1}{2\pi} \nabla\psi \times \nabla\phi = \frac{1}{2\pi} \nabla \times \psi \nabla\phi \quad (11.14)$$

which is in the θ direction since $\nabla\psi$ is orthogonal to $\nabla\phi$. Since \mathbf{B}_1 is in the ϕ direction and \mathbf{B}_2 is in the θ direction, the total magnetic field can be written as $\mathbf{B} = B_1 \hat{\phi} + B_2 \hat{\theta}$ which is helical.

The twist of the magnetic field is defined as the number of times a field line goes around in the θ direction for one circuit in the ϕ direction. If dl_ϕ is a displacement in the ϕ direction then

$$d\phi = |\nabla\phi| dl_\phi \quad (11.15)$$

and similarly

$$d\theta = |\nabla\theta| dl_\theta. \quad (11.16)$$

The trajectory of a magnetic field line is parallel to the magnetic field so if $d\mathbf{l}$ is an increment along a magnetic field line then $\mathbf{B} \times d\mathbf{l} = 0$ or

$$\frac{dl_\theta}{B_\theta} = \frac{dl_\phi}{B_\phi}. \quad (11.17)$$

This means that

$$\frac{d\theta}{|\nabla\theta| B_\theta} = \frac{d\phi}{|\nabla\phi| B_\phi}. \quad (11.18)$$

However $B_\theta = |\nabla\psi| |\nabla\phi| / 2\pi$ and $B_\phi = |\nabla\Phi| |\nabla\theta| / 2\pi$ so

$$\begin{aligned} \frac{d\theta}{d\phi} &= \frac{|\nabla\theta| B_\theta}{|\nabla\phi| B_\phi} \\ &= \frac{|\nabla\theta| |\nabla\psi| |\nabla\phi| / 2\pi}{|\nabla\phi| |\nabla\Phi| |\nabla\theta| / 2\pi} \\ &= \frac{|\nabla\psi|}{|\nabla\Phi|}. \end{aligned} \quad (11.19)$$

Finally, if $\psi = \psi(\Phi)$ then $\nabla\psi = \psi' \nabla\Phi$ where $\psi' = d\psi/d\Phi$ and so

$$\frac{d\theta}{d\phi} = \psi'. \quad (11.20)$$

Thus, θ increases ψ' times faster than does ϕ and so if ϕ makes one complete circuit (i.e., goes from 0 to 2π), then θ makes ψ' circuits (i.e., θ goes from 0 to $2\pi\psi'$). The number of times the field line goes around in the θ direction for each time it goes around in the ϕ direction is called the twist

$$T(\Phi) = \psi'. \quad (11.21)$$

Hence Eq. (11.11), which gave the helicity when the ψ flux is embedded in the Φ flux, can be expressed in terms of the twist as

$$K = 2 \int \Phi T(\Phi) d\Phi. \quad (11.22)$$

and if the twist is a constant (i.e., $T' = 0$) then

$$K = T\Phi^2. \quad (11.23)$$

11.2.3 Conservation of magnetic helicity during magnetic reconnection

Ideal MHD constrains magnetic flux to be frozen into the frame of the plasma. This means that the topology (connectedness) of magnetic field lines in a perfectly conducting plasma cannot change. As will be shown in Chapter 12, introduction of a small amount of resistivity allows the frozen-in condition to be violated at locations where the velocity must vanish due to symmetry. At these locations, the approximation of the resistive MHD Ohm's law $\mathbf{E} + \mathbf{U} \times \mathbf{B} = \eta \mathbf{J}$ to the ideal form $\mathbf{E} + \mathbf{U} \times \mathbf{B} = 0$ necessarily fails. Instead, Ohm's law has the form $\mathbf{E} = \eta \mathbf{J}$ so that magnetic field lines can diffuse across the plasma and reconnect with each other. Even though the reconnection is localized to a small region in the vicinity of where \mathbf{U} vanishes, it nevertheless changes the overall magnetic field topology. As will be shown below, reconnection destroys individual linkages between flux tubes, but creates a replacement linkage for every destroyed linkage so that the total system helicity is conserved. The result is that the ideal MHD constraint of having perfect flux conservation everywhere is replaced by the somewhat weaker constraint that total magnetic helicity is conserved. Reconnection necessarily involves energy dissipation since reconnection requires finite resistivity. Thus reconnection dissipates magnetic field energy while conserving magnetic helicity.

Conservation of helicity during reconnection is demonstrated in Fig. 11.3. Two linked untwisted ribbons of magnetic flux are shown in Fig. 11.3(a). If each ribbon is imagined to be a magnetic field line bundle having nominal flux Φ , then according to Eq.(11.8) this initial configuration has helicity $K = 2\Phi^2$. The ribbons are then cut at their line of overlap as in Fig. 11.3(b) and reconnected as in Fig. 11.3(c) to form one long ribbon. This long ribbon in Fig. 11.3(c) may then be continuously deformed until in the shape shown in Fig. 11.3(f), a long ribbon having *two* twists. Thus, the twist parameter for Fig. 11.3(f) is $T = 2$ and so according to Eq.(11.23) this two-twist ribbon has a helicity $K = T\Phi^2 = 2\Phi^2$. Hence, magnetic helicity is conserved by the reconnection. Since the magnetic equivalent of cutting ribbons with scissors involves the dissipative process of resistive diffusion of magnetic field across the plasma, it can be concluded that magnetic reconnection conserves helicity, but dissipates magnetic energy.

11.3 Woltjer-Taylor relaxation

Woltjer (1958) provided a mathematical proof that the lowest energy state of a magnetic system with a fixed amount of magnetic helicity was a certain kind of force-free state, but did not provide any detailed explanation on how the system would attain this state. Taylor (1974) argued that because reconnection conserves helicity while dissipating magnetic energy, reconnection events will provide the mechanism by which an isolated plasma relaxes towards a state having the lowest magnetic energy consistent with conservation of helicity. The discussion of Eq.(10.133) showed that the isolation requirement corresponds to having no field lines penetrate the surface bounding the plasma and also arranging for this surface to be an electrostatic equipotential. It will therefore be assumed that the plasma is bounded by a perfectly conducting wall and that no magnetic field lines penetrate this wall. The tangential electric field and hence the tangential component of the vector potential must therefore vanish at the wall.

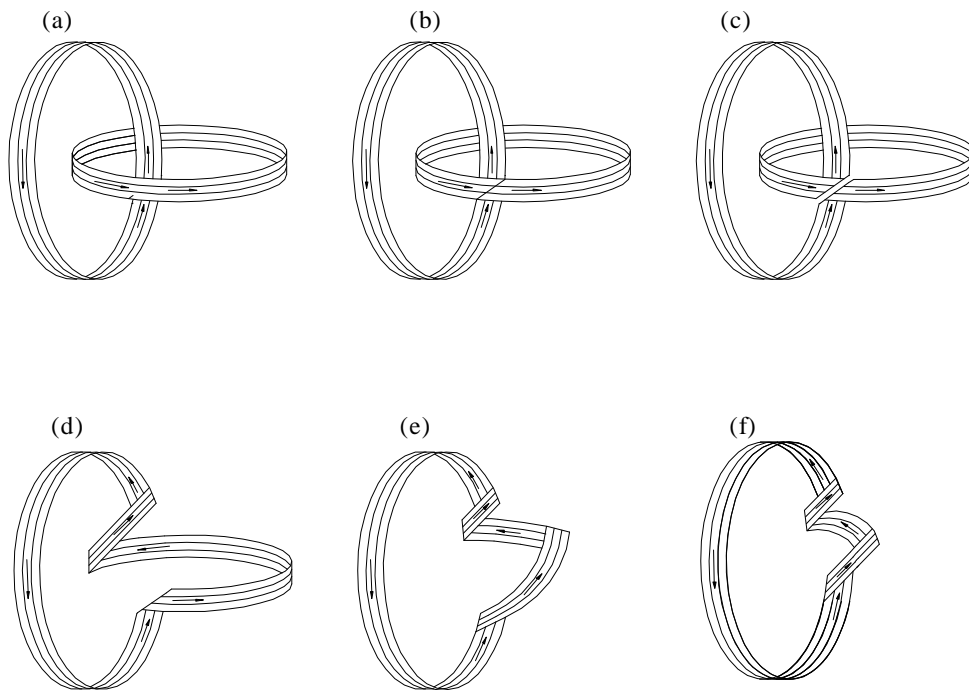


Figure 11.3: (a) Two linked, untwisted flux tube squeezed to be ribbons, magnetic field directions shown by arrows; (b) cut at overlay of two ribbons; (c) reconnection at cut; (d) deformation; (e) more deformation; (f) more deformation showing there are two complete twists of magnetic field.

The relaxation process involves minimizing the magnetic energy

$$W = \frac{1}{2\mu_0} \int B^2 d^3r \quad (11.24)$$

subject to the constraint that the magnetic helicity

$$K = \int \mathbf{A} \cdot \mathbf{B} d^3r \quad (11.25)$$

is conserved (Woltjer 1958, Taylor 1974). The minimum-energy magnetic field for the given helicity is called \mathbf{B}_{ME} and its associated magnetic energy is

$$W_{ME} = \frac{1}{2\mu_0} \int B_{ME}^2 d^3r. \quad (11.26)$$

In order to determine \mathbf{B}_{ME} , we consider an arbitrary variation $\mathbf{B} = \mathbf{B}_{ME} + \delta\mathbf{B}$ satisfying the same boundary conditions; by assumption, this variation has a higher associated magnetic energy than \mathbf{B}_{ME} . The magnetic field \mathbf{B} has an associated vector potential $\mathbf{A} = \mathbf{A}_{ME} + \delta\mathbf{A}$ and because the tangential electric field must vanish at the wall to prevent helicity flux across the wall, the tangential component of $\delta\mathbf{A}$ must also vanish at the wall. A naive solution for minimizing W_{ME} would be to set \mathbf{B}_{ME} to zero, but this is forbidden because it would make K vanish and violate the helicity conservation requirement. Thus W must be minimized subject to the constraint that K remains constant. The variation of the magnetic energy about the minimum energy state is

$$\begin{aligned} \delta W &= \frac{1}{2\mu_0} \int [(\mathbf{B}_{ME} + \delta\mathbf{B})^2 - B_{ME}^2] d^3r \\ &= \frac{1}{\mu_0} \int \mathbf{B}_{ME} \cdot \delta\mathbf{B} d^3r \\ &= \frac{1}{\mu_0} \int \mathbf{B}_{ME} \cdot \nabla \times \delta\mathbf{A} d^3r \\ &= \frac{1}{\mu_0} \int [\nabla \cdot (\mathbf{B}_{ME} \times \delta\mathbf{A}) + \delta\mathbf{A} \cdot \nabla \times \mathbf{B}_{ME}] d^3r \\ &= \frac{1}{\mu_0} \int ds \cdot \mathbf{B}_{ME} \times \delta\mathbf{A} + \int \delta\mathbf{A} \cdot \nabla \times \mathbf{B}_{ME} d^3r \\ &= \int \delta\mathbf{A} \cdot \nabla \times \mathbf{B}_{ME} d^3r \end{aligned} \quad (11.27)$$

since $ds \cdot \mathbf{B}_{ME} \times \delta\mathbf{A} = 0$ everywhere on the wall. The variation of the helicity is

$$\begin{aligned} \delta K &= \int (\delta\mathbf{A} \cdot \mathbf{B}_{ME} + \mathbf{A}_{ME} \cdot \delta\mathbf{B}) d^3r \\ &= \int (\delta\mathbf{A} \cdot \mathbf{B}_{ME} + \mathbf{A}_{ME} \cdot \nabla \times \delta\mathbf{A}) d^3r \\ &= \int (\delta\mathbf{A} \cdot \mathbf{B}_{ME} + \delta\mathbf{A} \cdot \nabla \times \mathbf{A}_{ME}) + \nabla \cdot (\delta\mathbf{A} \times \mathbf{A}_{ME}) d^3r \\ &= 2 \int \delta\mathbf{A} \cdot \mathbf{B}_{ME} d^3r. \end{aligned} \quad (11.28)$$

Minimization of δW subject to the constraint that K remains constant is characterized using a Lagrange multiplier λ so that the constrained variational equation is

$$\delta W = \lambda \delta K. \quad (11.29)$$

Substitution for δW and δK gives

$$\int \delta \mathbf{A} \cdot \nabla \times \mathbf{B}_{ME} d^3r = 2\lambda \int \delta \mathbf{A} \cdot \mathbf{B}_{ME} d^3r \quad (11.30)$$

or, after re-defining the arbitrary parameter λ ,

$$\int \delta \mathbf{A} \cdot (\nabla \times \mathbf{B}_{ME} - \lambda \mathbf{B}_{ME}) d^3r = 0. \quad (11.31)$$

Since $\delta \mathbf{A}$ is arbitrary, the quantity in parentheses must vanish and so

$$\nabla \times \mathbf{B}_{ME} = \lambda \mathbf{B}_{ME}. \quad (11.32)$$

It is clear that λ is a spatially uniform constant because the Lagrange multiplier is a constant. Thus, relaxation leads to the same force-free state as predicted by Eq.(10.140). These states are a good approximation to many solar and astrophysical plasmas as well as certain laboratory plasmas such as spheromaks and reversed field pinches.

The energy per helicity of a minimum energy state can be written as

$$\begin{aligned} \frac{W}{K} &= \frac{\int B_{ME}^2 d^3r}{2\mu_0 \int \mathbf{A}_{ME} \cdot \mathbf{B}_{ME} d^3r} \\ &= \frac{\int \mathbf{B}_{ME} \cdot \nabla \times \mathbf{A}_{ME} d^3r}{2\mu_0 \int \mathbf{A}_{ME} \cdot \mathbf{B}_{ME} d^3r} \\ &= \frac{\int [\mathbf{A}_{ME} \cdot \nabla \times \mathbf{B} + \nabla \cdot (\mathbf{A}_{ME} \times \mathbf{B}_{ME})] d^3r}{2\mu_0 \int \mathbf{A} \cdot \mathbf{B} d^3r}. \end{aligned} \quad (11.33)$$

However, Eq. (11.32) can be integrated to give

$$\mathbf{B}_{ME} = \lambda \mathbf{A}_{ME} + \nabla f \quad (11.34)$$

where f is an arbitrary scalar function of position. This can be used to show

$$\nabla \cdot (\mathbf{A}_{ME} \times \mathbf{B}_{ME}) = \nabla \cdot (\mathbf{A}_{ME} \times \nabla f) = \nabla f \cdot \nabla \times \mathbf{A}_{ME} = \mathbf{B}_{ME} \cdot \nabla f = \nabla \cdot (f \mathbf{B}_{ME}) \quad (11.35)$$

so that

$$\int \nabla \cdot (\mathbf{A}_{ME} \times \mathbf{B}_{ME}) d^3r = \int ds \cdot (f \mathbf{B}_{ME}) = 0 \quad (11.36)$$

since $\mathbf{B}_{ME} \cdot ds = 0$ by assumption. Thus, Eq.(11.33) reduces to

$$\frac{W}{K} = \frac{\lambda}{2\mu_0} \quad (11.37)$$

indicating that the minimum energy state must have the lowest value of λ consistent with the prescribed boundary conditions.

11.4 Kinking and magnetic helicity

Magnetic helicity can be manifested in various forms and plasma dynamics cause this form to be altered. We now discuss an important example of helicity-conserving, morphology-altering dynamics, namely the situation where kink instability causes the twist of a straight-axis flux tube to be transformed into the writhe of the axis of an untwisted flux tube (Berger and Field 1984, Moffatt and Ricca 1992).

Consider a volume V bounded by a surface S where no magnetic field lines penetrate the surface S so that $\mathbf{B} \cdot d\mathbf{s} = 0$ over all of S . It is assumed here that V extends to infinity, but the analysis would equally apply for a finite-extent volume V so long as no magnetic field lines penetrate its bounding surface S . The helicity contained in V is

$$K_V = \int_V \mathbf{A} \cdot \mathbf{B} d^3r. \quad (11.38)$$

Equation (10.129) showed that K_V is gauge-independent because no field lines penetrate S .

The volume V is now decomposed into two subvolumes which have $\mathbf{B} \cdot d\mathbf{s} = 0$ at all locations on their mutual interface. Thus, any specific field line in V is entirely in one or the other of the two subvolumes.

1. The first subvolume, called V_{tube} , is a closed flux tube of minor radius a with a possibly helical axis as shown in Fig. 11.4. The length of the axis of this flux tube is denoted l_{axis} and the variable ξ denotes the distance along this axis from some fixed reference point \mathbf{x}_0 on the axis. Incrementing ξ from 0 to l_{axis} thus corresponds to going once around the flux tube axis. A pseudo-angular coordinate ϕ is defined as

$$\phi = 2\pi \frac{\xi}{l_{axis}} \quad (11.39)$$

so that going once around the axis corresponds to incrementing ϕ from 0 to 2π and $\hat{\phi}$ defines the local direction of the axis. Because the axis of the flux tube has the complex curvature of a helix, everywhere along the axis there exists a radius of curvature vector $\boldsymbol{\kappa} = \hat{\phi} \cdot \nabla \hat{\phi}$ which is at right angles to $\hat{\phi}$. The local radius of curvature of the axis is $r_{curve} = |\hat{\phi} \cdot \nabla \hat{\phi}|^{-1}$ (see discussion of Eq.(3.85)). From the point of view of an observer inside the flux tube, the flux tube appears as a long curved tunnel that eventually closes upon itself. The flux tube minor radius a must always be smaller than r_{curve} which corresponds locally to the condition that by definition the major radius of a torus must exceed the minor radius. The flux tube interior volume is now imagined to be filled with fiduciary lines all of which are parallel to the flux tube axis; the lengths of these fiduciary lines will vary according to their location relative to the axis. We define ξ' as the distance along a fiduciary line of length l' from a plane perpendicular to the flux tube axis at the reference point \mathbf{x}_0 . The meaning of ϕ can then be extended to indicate the distance along any fiduciary line using the relation $\xi' = \phi l' / 2\pi$. Incrementing ϕ from 0 to 2π thus corresponds to going once around any or all of these fiduciary lines and so ϕ provides an unambiguous measure of fractional distance along the flux tube for any point within the flux tube even though the flux tube may be curved, twisted, or helical.

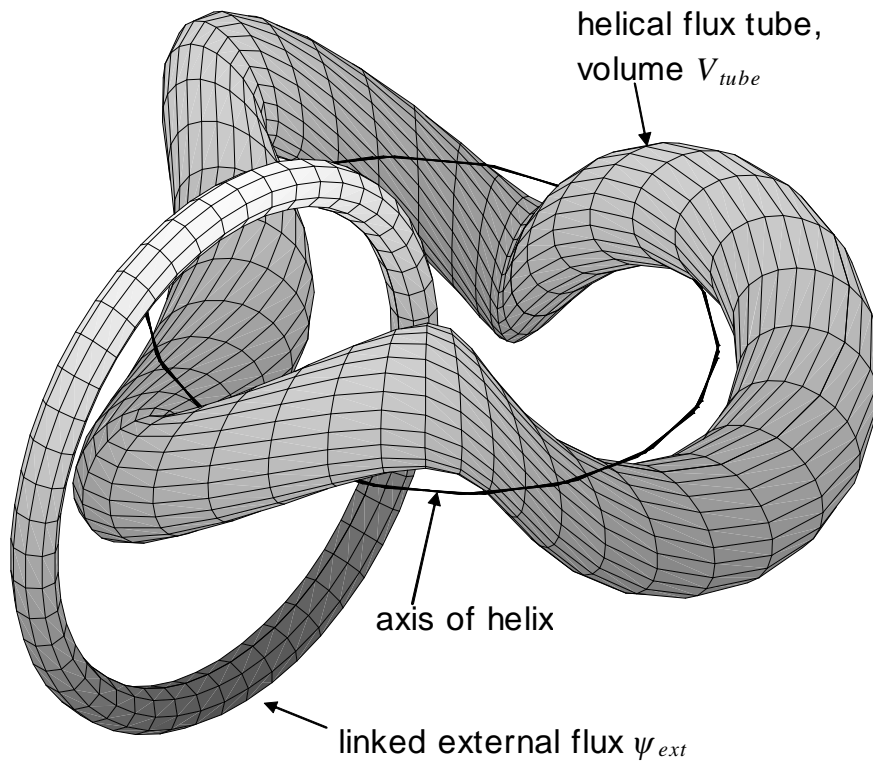


Figure 11.4: Subvolume #1 is a flux tube with a possibly helical axis and volume V_{tube} . Subvolume #2 is all space external to subvolume #1. All field lines in subvolume #2 which link subvolume #1 are represented by the vertical flux tube in figure labeled ψ_{ext} .

2. The second subvolume in this decomposition is the remaining volume of V and is labeled as V_{ext} . There might be field lines in this second subvolume which link the flux tube V_{tube} and the flux due to all these linkages is labeled ψ_{ext} . This external flux linkage is represented by the vertical flux tube labeled ψ_{ext} in Fig. 11.4.

If the dynamics within the volume V are governed by ideal MHD, then the helicity K_V in V must be conserved and, since K_V is a volume integral, the volume of integration can be subdivided into the flux tube volume and the volume external to the flux tube,

$$K_V = K_{V_{tube}} + K_{V_{ext}}.$$

11.4.1 $K_{V_{tube}}$, helicity content of the flux tube

We now consider the helicity content of the possibly helical flux tube,

$$K_{V_{tube}} = \int_{V_{tube}} \mathbf{A} \cdot \mathbf{B} d^3r. \quad (11.40)$$

The magnetic field in the flux tube is decomposed into a component \mathbf{B}_{axis} parallel to the flux tube axis and an orthogonal component $\mathbf{B}_{azimuthal}$ which goes the short way around the axis; thus the magnetic field inside the flux tube is

$$\mathbf{B} = \mathbf{B}_{axis} + \mathbf{B}_{azimuthal}. \quad (11.41)$$

The field lines in the flux tube are assumed to lie in successive layers (magnetic surfaces) wrapped around the flux tube axis. The axial and azimuthal magnetic fields are derived from respective vector potentials \mathbf{A}_{axis} and $\mathbf{A}_{azimuthal}$ such that

$$\begin{aligned} \mathbf{B}_{axis} &= \nabla \times \mathbf{A}_{axis} \\ \mathbf{B}_{azimuthal} &= \nabla \times \mathbf{A}_{azimuthal}. \end{aligned} \quad (11.42)$$

It should be emphasized that these definitions say nothing about the direction of \mathbf{A}_{axis} or $\mathbf{A}_{azimuthal}$ and so, unlike axisymmetric situations, here neither \mathbf{A}_{axis} nor $\mathbf{A}_{azimuthal}$ should be construed to be in a particular direction because of the possibility that the flux tube is helical. All that can be said is that the curl of \mathbf{A}_{axis} gives the flux tube axial magnetic field and the curl of $\mathbf{A}_{azimuthal}$ gives the azimuthal field.

The helicity content of the flux tube is thus

$$K_{V_{tube}} = \int_{V_{tube}} (\mathbf{A}_{axis} + \mathbf{A}_{azimuthal}) \cdot (\mathbf{B}_{axis} + \mathbf{B}_{azimuthal}) d^3r \quad (11.43)$$

and this is true even though the axis of the flux tube could be helical.

By definition, each layer of field lines constituting a magnetic surface encloses a flux Φ . An equivalent definition is to state that Φ is the magnetic flux linked by a contour in the magnetic surface going the short way around the flux tube axis. The magnetic surface is labeled by Φ and so Φ can be considered to be a coordinate having its gradient always normal to the flux surface. In effect Φ is a re-scaled minor radius, since Φ increases monotonically with minor radius.

These definitions are sufficiently general to allow for the axis of the flux tube to be a helix, a knot, or a simple closed curve lying in a plane. If the axis is just a simple closed curve lying in a plane, then $\nabla \times \hat{\phi}$ is normal to the plane and therefore normal to $\hat{\phi}$. In the slightly more general case where the axis is not in a plane but $\hat{\phi} \cdot \nabla \times \hat{\phi} = 0$, the path traced out by $\hat{\phi}$ can be considered to be the perimeter of a some bumpy surface. However, in the most general case where $\hat{\phi} \cdot \nabla \times \hat{\phi}$ is finite, the path traced out by $\hat{\phi}$ is not the perimeter of even a bumpy surface (Barnes 1977). There might also be situations where $\hat{\phi} \cdot \nabla \times \hat{\phi} \neq 0$ but the sign of $\hat{\phi} \cdot \nabla \times \hat{\phi}$ alternates. If the average of $\hat{\phi} \cdot \nabla \times \hat{\phi}$ over the length of the axis is zero, then the situation would be similar to the case where $\hat{\phi} \cdot \nabla \times \hat{\phi} = 0$ everywhere, because twists in the axis could be squeezed together axially until mutually cancelling out.

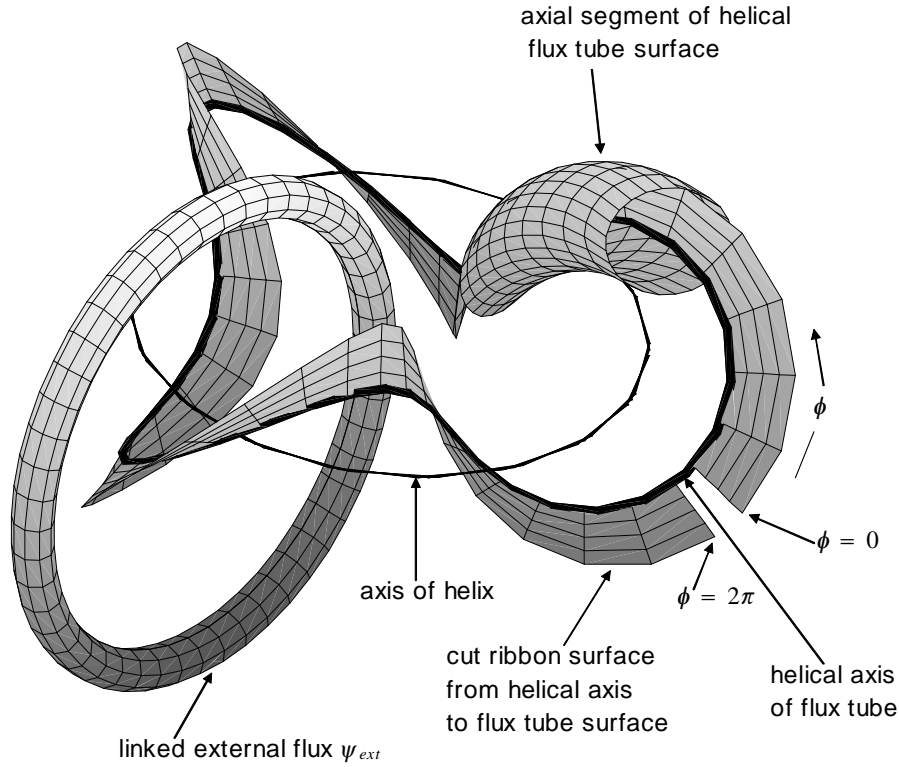


Figure 11.5: Ribbon surface extending from helical axis of helical flux tube to surface of flux tube with normal to $\hat{\phi} \times \hat{\kappa}$

Because any magnetic field line in the flux tube lies in some magnetic surface labeled by Φ , any field line in the flux tube has a component parallel to the axis and possibly also a component perpendicular to the axis, but never a component in the $\nabla\Phi$ direction. This suggests introduction of an azimuthal coordinate θ which is defined as the angular distance around the axis in the direction given by $\nabla\phi \times \nabla\Phi$, i.e., θ is defined such that

$$\frac{\nabla\theta}{|\nabla\theta|} = \frac{\nabla\phi \times \nabla\Phi}{|\nabla\phi \times \nabla\Phi|}. \quad (11.44)$$

The local direction of $\nabla\theta$ depends on both ϕ and θ ; furthermore, for θ to denote some definite position, θ must be measured with respect to some unambiguous origin. An unambiguous θ origin can be defined by using as a reference the negative of the direction of the local radius of curvature vector κ of the flux tube axis. The $\theta = 0$ surface is then a ribbon surface, as shown in Fig. 11.5, that extends from the flux tube axis to the flux tube outer surface so that $\hat{\phi} \times \hat{\kappa}$ is normal to the ribbon surface. The ribbon is considered to have a cut at $\phi = 0$ so that the ribbon ends at $\phi = 0$ and $\phi = 2\pi$ are distinct.

Figure 11.6 shows a cross-section of this system. The flux tube has minor radius a and the helical axis of the flux tube traces out a trajectory with minor radius b about an axis which has major radius R . Representative magnetic surfaces (surfaces of constant Φ), the ribbon surface, and the angle θ are also shown.

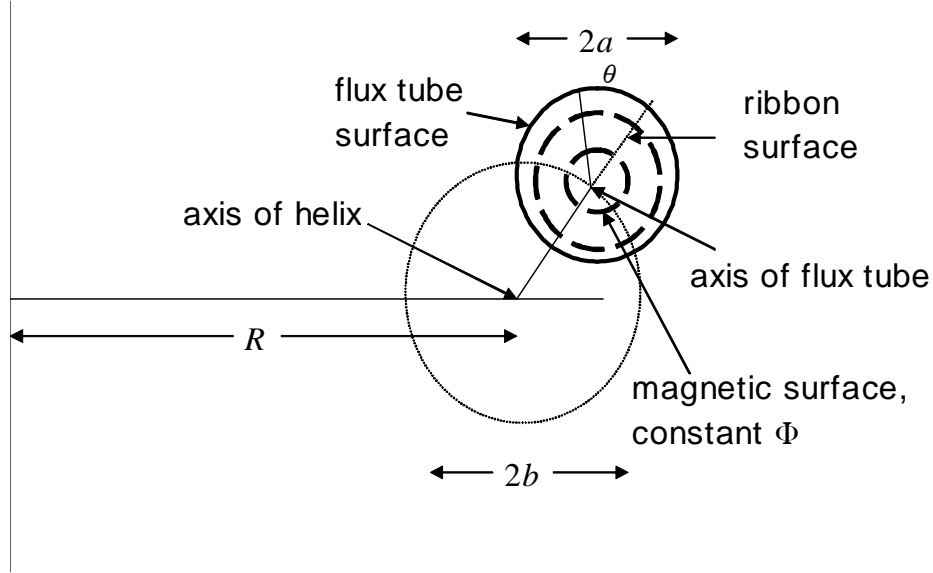


Figure 11.6: Cross-section showing flux tube of minor radius a , with its axis making a helix of radius b . Interior flux surfaces with $\Phi = \text{const.}$ and the ribbon surface defining $\theta = 0$ are also shown.

The flux Φ was a generalization of the toroidal flux of an axisymmetric system. We now define a corresponding generalization of the poloidal flux $\psi(\Phi)$ as the magnetic flux penetrating a sub-ribbon extending inwards from the outer surface of the possibly helical flux tube to some given interior magnetic surface Φ . This subribbon is shown in Fig.11.7 and the definition is such that

$$\begin{aligned}
 \psi &= \int_{\text{subribbon}} \mathbf{ds} \cdot \mathbf{B} \\
 &= \int_{\text{subribbon}} \mathbf{ds} \cdot \nabla \times \mathbf{A} \\
 &= \oint_C \mathbf{dl} \cdot \mathbf{A}
 \end{aligned} \tag{11.45}$$

where the contour C follows the perimeter of the subribbon and specifically follows the

two ends at $\phi = 0$ and $\phi = 2\pi$. This definition implies that $\psi = 0$ on the outer surface of the flux tube because the sub-ribbon area will be zero in this case.

We define the vector potential

$$\mathbf{A}_{azimuthal} = \frac{\psi(\Phi)}{2\pi} \nabla\phi \quad (11.46)$$

and note that this definition is valid only in the range $0 \leq \phi < 2\pi$. The appropriateness of this definition is established by integrating following the contour C around the subribbon to obtain

$$\begin{aligned} \oint_C \mathbf{dl} \cdot \mathbf{A}_{azimuthal} &= \oint_C \mathbf{dl} \cdot \frac{\psi(\Phi)}{2\pi} \nabla\phi \\ &= \frac{\psi(\Phi)}{2\pi} \int_{C_\Phi} \mathbf{dl} \cdot \nabla\phi \\ &= \psi(\Phi) \end{aligned} \quad (11.47)$$

where $\mathbf{dl} \cdot \nabla\phi = d\phi$. As seen in Fig.11.7, the contour C consists of four segments, namely a segment following the outside edge of the sub-ribbon (this segment lies in the outer surface of the flux tube where $\psi = 0$), the segment labeled C_Φ on the inside edge of the sub-ribbon, a segment at the $\phi = 0$ end, and an oppositely directed segment at the $\phi = 2\pi_-$ end. Only the C_Φ segment contributes to the integral because (i) $\mathbf{dl} \cdot \nabla\phi = 0$ on the ends $\phi = 0$ and $\phi = 2\pi_-$ since ϕ is constant on both these ends and (ii) $\psi = 0$ on the outside edge of the sub-ribbon.

The magnetic field inside the flux tube can thus be written as

$$\mathbf{B} = \mathbf{B}_{axis} + \nabla \times \frac{\psi(\Phi)}{2\pi} \nabla\phi \quad (11.48)$$

where \mathbf{B}_{axis} is the magnetic field component parallel to the flux tube axis. This decomposition of the magnetic field is valid even for a twisted or knotted axis provided it is used only for situations where $0 \leq \phi < 2\pi$.

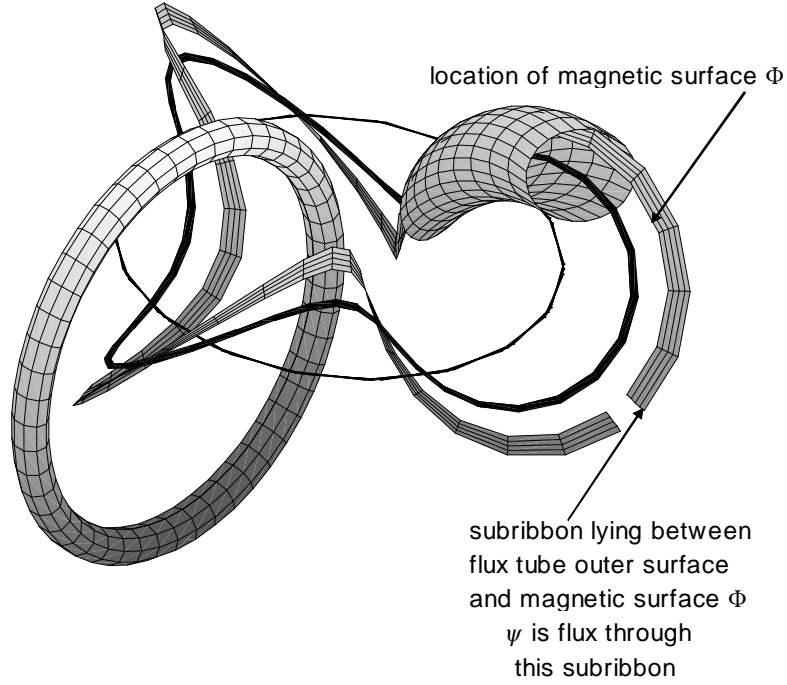


Figure 11.7: ψ is flux through cut subribbon located between magnetic surface Φ and outer surface of flux tube.

The vector potential for the entire field can be written as

$$\mathbf{A} = \mathbf{A}_{axis} + \frac{\psi(\Phi)}{2\pi} \nabla\phi. \quad (11.49)$$

These results can be used in Eq.(11.43) to give the helicity content of the flux tube as

$$\begin{aligned} K_{V_{tube}} &= \int_{V_{tube}} d^3r \left(\mathbf{A}_{axis} + \frac{\psi(\Phi)}{2\pi} \nabla\phi \right) \cdot \left(\mathbf{B}_{axis} + \frac{1}{2\pi} \nabla\psi \times \nabla\phi \right) \\ &= \int_{V_{tube}} d^3r \left(\mathbf{A}_{axis} \cdot \mathbf{B}_{axis} + \frac{\psi(\Phi)}{2\pi} \nabla\phi \cdot \mathbf{B}_{axis} + \mathbf{A}_{axis} \cdot \frac{1}{2\pi} \nabla\psi \times \nabla\phi \right) \end{aligned} \quad (11.50)$$

and this may be decomposed into writhe and twist terms,

$$K_{V_{tube}} = K_{writhe} + K_{twist}$$

respectively defined as

$$K_{writhe} = \int_{V_{tube}} d^3r \mathbf{A}_{axis} \cdot \mathbf{B}_{axis} \quad (11.51)$$

and

$$K_{twist} = \int_{V_{tube}} d^3r \left(\frac{\psi(\Phi)}{2\pi} \nabla\phi \cdot \mathbf{B}_{axis} + \mathbf{A}_{axis} \cdot \frac{1}{2\pi} \nabla\psi \times \nabla\phi \right). \quad (11.52)$$

As will be shown below, K_{twist} depends on ψ being finite whereas K_{writhe} depends on the extent to which the flux tube axis is helical. The flux tube helicity can thus be entirely due to K_{writhe} , entirely due to K_{twist} , or due to some combination of these types of helicity.

11.4.2 Evaluation of K_{twist}

Since the K_{twist} integral is a *volume* integral, the flux tube may be cut at $\phi = 0$ without affecting this integral. Making such a cut means that ϕ is restricted to the range $0 \leq \phi < 2\pi$ and therefore does not make a complete circuit around the axis of the flux tube. The evaluation of this integral is insensitive to the connectivity of the axis because connectivity is a concept which makes sense only after making a complete circuit of the axis. The axial magnetic field within the cut volume may be expressed as

$$\mathbf{B}_{axis} = \frac{1}{2\pi} \nabla \times \Phi \nabla \theta \quad (11.53)$$

where θ is the angular distance on a contour C_θ encircling the flux tube axis and lies in a magnetic surface. This representation for the axial magnetic field is appropriate here since at each ϕ for $0 \leq \phi < 2\pi$ we may write

$$\begin{aligned} \Phi &= \int ds \cdot \mathbf{B}_{axis} \\ &= \frac{1}{2\pi} \int ds \cdot \nabla \times \Phi \nabla \theta \\ &= \frac{1}{2\pi} \oint_{C_\theta} d\mathbf{l} \cdot \Phi \nabla \theta \\ &= \frac{\Phi}{2\pi} \oint_{C_\theta} d\mathbf{l} \cdot \nabla \theta \\ &= \frac{\Phi}{2\pi} \oint_{C_\theta} d\theta. \end{aligned} \quad (11.54)$$

By uncurling Eq.(11.53) it is seen that vector potential associated with the axial magnetic field may be represented in the cut flux tube as

$$\mathbf{A}_{axis} = \frac{\Phi}{2\pi} \nabla \theta, \quad 0 \leq \phi < 2\pi \quad (11.55)$$

so that

$$\begin{aligned} K_{twist} &= \frac{1}{4\pi^2} \int_{V_{tube}} d^3r (\psi \nabla\phi \cdot \nabla\Phi \times \nabla\theta + \Phi \nabla\theta \cdot \nabla\psi \times \nabla\phi) \\ &= \frac{1}{4\pi^2} \int_{V_{tube}} d^3r (\psi \nabla\phi \cdot \nabla\Phi \times \nabla\theta + \Phi \psi' \nabla\theta \cdot \nabla\Phi \times \nabla\phi) \\ &= \frac{1}{4\pi^2} \int_{V_{tube}} d^3r (-\psi + \Phi \psi') \nabla\theta \cdot \nabla\Phi \times \nabla\phi. \end{aligned} \quad (11.56)$$

The three direction gradients $\nabla\theta$, $\nabla\Phi$, and $\nabla\phi$ form an orthonormal coordinate system and an element of volume in this system is given by

$$d^3r = dl_\Phi dl_\theta dl_\phi = \frac{d\Phi d\theta d\phi}{\nabla\theta \cdot \nabla\Phi \times \nabla\phi} \quad (11.57)$$

since $d\theta = dl_\theta |\nabla\theta|$, $d\phi = dl_\phi |\nabla\phi|$, and $d\Phi = dl_\Phi |\nabla\Phi|$. Thus,

$$\begin{aligned} K_{twist} &= \frac{1}{4\pi^2} \int_0^\Phi d\Phi \int_{\theta=0}^{2\pi} d\theta \int_{\phi=0}^{(2\pi)_-} d\phi (-\psi + \Phi\psi') \\ &= - \int_0^\Phi \psi d\Phi + \int_0^\Phi \psi' \Phi d\Phi \\ &= 2 \int_0^\Phi \Phi \frac{d\psi}{d\Phi} d\Phi. \end{aligned} \quad (11.58)$$

where the integration limit $(2\pi)_-$ corresponds to being infinitesimally less than 2π . The last line has been obtained using the relationship $\int d(\psi\Phi) = [\psi\Phi]_{axis}^{surface} = \int \Phi d\psi + \int \psi d\Phi$ and noting that the integrated term vanishes since $\psi = 0$ in the flux tube surface and $\Phi = 0$ on the flux tube axis.

11.4.3 Evaluation of K_{writhe}

Connectivity of the flux tube is now the important issue. In order to evaluate the K_{writhe} integral the volume element is expressed as

$$d^3r = dl ds \quad (11.59)$$

where dl is an increment of length along the axis and ds is an element of surface in the plane perpendicular to the axis so that $\mathbf{B}_{axis} \cdot ds = d\Phi$. Because the line integral will involve a complete circuit of the flux tube axis, in contrast to the earlier evaluation of K_{twist} , we now avoid using the gradient of a scalar to denote distance along the axis. Using Eq.(11.59) the writhe helicity may therefore be expressed as

$$\begin{aligned} K_{writhe} &= \int_{C_{axis}} \mathbf{A}_{axis} \cdot d\mathbf{l}_{axis} \int d\Phi \\ &= \Phi \int_{C_{axis}} \mathbf{A}_{axis} \cdot d\mathbf{l}_{axis}. \end{aligned} \quad (11.60)$$

This integral differs topologically from the integrals of the previous section, because here the contour is a *complete circuit*, i.e., ϕ varies from 0 to 2π , and not from 0 to $2\pi_-$.

A contour path C of an integral $\int_C \mathbf{A} \cdot d\mathbf{l}$ may be continuously deformed into a new contour path C' without changing the value of the integral provided no magnetic flux is linked by the surface S bounded by C and C' ; this behavior is a three dimensional analog to the concept of analyticity for a contour integral in the complex plane. The validity of this assertion is established by the relation

$$0 = \int_S \mathbf{B} \cdot ds = \oint \mathbf{A} \cdot d\mathbf{l} = \int_C \mathbf{A} \cdot d\mathbf{l} - \int_{C'} \mathbf{A} \cdot d\mathbf{l}. \quad (11.61)$$

It should be noted that the ability for C to be continuously deformed into C' imposes the requirement that a surface S exists between C and C' ; this is only true if C does not link C' .

We now consider some limiting cases for K_{writhe} and to aid in visualization it should be recalled that the flux tube axis is assumed to have a helical trajectory with helix major radius R and helix minor radius b as shown in Fig.11.6.

Limiting case where flux tube axis not helical

This situation corresponds to having $b = 0$ in which case the flux tube axis lies in a plane. The contour C_{axis} in Eq.(11.60) can thus be slipped from its original position through the \mathbf{B}_{axis} field lines to the surface of the flux tube without crossing any \mathbf{B}_{axis} field lines. This is topologically possible because by definition, all \mathbf{B}_{axis} field lines in the flux tube are parallel to the flux tube axis. Thus, here

$$K_{writhe} = \Phi \int_{C'} \mathbf{A}_{axis} \cdot d\mathbf{l}_{axis} \tag{11.62}$$

where C' lies on the flux tube surface. The line integral C' encircles the external flux linked by the flux tube and so

$$K_{writhe} = \Phi \psi_{ext}, \text{ when the flux tube axis is not helical} \tag{11.63}$$

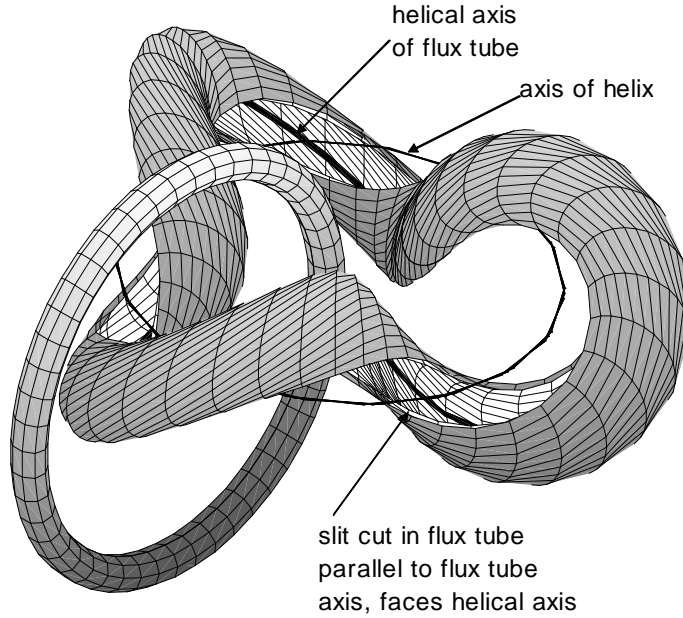


Figure 11.8: Helical axis of flux tube may be slipped through \mathbf{B}_{axis} field lines of flux tubes to coincide of axis of helix (note that open slit in flux tube always faces axis of helix).

Case where axis is helical and $b > a$

Because the helix minor radius b exceeds the flux tube minor radius a , the entire flux tube revolves around the axis of the helix as shown in Fig.11.8. Because the helical axis closes upon itself, it must have an integral number of periods and we let N be the number of helix periods. However, because \mathbf{B}_{axis} is everywhere parallel to the flux tube axis, the flux tube axis may again be slipped through the \mathbf{B}_{axis} field lines and in this case moved towards the helix axis until it coincides with the helix axis C_{helix} . The writhe helicity can thus be expressed as

$$K_{writhe} = \Phi \int_{C_{helix}} \mathbf{A}_{axis} \cdot d\mathbf{l}_{axis}. \quad (11.64)$$

However, the flux tube links the helix axis N times and so

$$\int_{C_{helix}} \mathbf{A}_{axis} \cdot d\mathbf{l}_{axis} = N\Phi + \psi_{ext}. \quad (11.65)$$

Thus,

$$K_{writhe} = N\Phi^2 + \Phi\psi_{ext} \text{ if } b > a. \quad (11.66)$$

Case where flux tube axis is helical but $a > b$

In this situation the flux tube may be subdivided into an inner core with minor radius $r < b$ and associated flux $\Phi b^2/a^2$ and an outer annular region with $b < r < a$ with the remainder of Φ . We again slip the flux tube axis through the parallel \mathbf{B}_{axis} field lines to be coincident with the helix axis. However, now only the inner core of the flux tube ($r < b_{axis}$) rotates around the helix axis. The outer annular region of the flux tube merely wobbles around the helix axis and does not link the helix axis. Thus, the linked flux is

$$\int_{C_{helix}} \mathbf{A}_{axis} \cdot d\mathbf{l}_{axis} = N\Phi b^2/a^2 + \psi_{ext} \quad (11.67)$$

and so the writhe helicity is

$$K_{writhe} = N\Phi^2 b^2/a^2 + \Phi\psi_{ext} \text{ if } a > b. \quad (11.68)$$

Hence, the helicity of the flux tube is

$$\begin{aligned} K_{V_{tube}} &= K_{twist} + K_{writhe} \\ &= 2 \int \Phi \frac{d\psi}{d\Phi} d\Phi + N\Phi^2 b^2/a^2 + \Phi\psi_{ext} \text{ if } a > b. \end{aligned} \quad (11.69)$$

The distinction between the $a < b$ and $a > b$ cases is sketched in Fig.11.9.

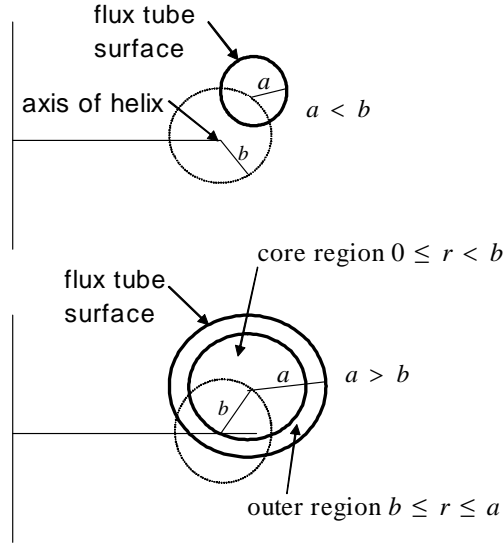


Figure 11.9: Top: case where flux tube radius a is less than radius b of helix traced out by flux tube axis. Bottom: Case where $a > b$; the core region $0 \leq r < b$ rotates around the axis of the helix whereas the outer region with $b < r < a$ wobbles about the axis of the helix.

11.4.4 Twist and writhe exchange in a kink instability

A kink instability is governed by ideal MHD and so must be helicity-conserving. The number of turns of the kink is defined by the initial twist condition $\mathbf{k} \cdot \mathbf{B} = k_\phi B_\phi + k_\theta B_\theta = 0$ so if $k_\theta = 1/a$ and $k_\phi = n/R$ then the kink will result in a helix with $N = n$. Since helicity is conserved, it is seen that as the amplitude of the kink increases (i.e., b increases), the flux tube twist $d\psi/d\Phi$ will have to decrease. In particular if the twist is uniform so that $\psi = T\Phi$ where twist T is independent of Φ , then as in Section 11.2.2 we may write

$$2 \int \Phi \frac{d\psi}{d\Phi} d\Phi = T\Phi^2 \quad (11.70)$$

and so from conservation of helicity we may conclude that

$$T + Nb^2/a^2 = \text{const. for } b < a; \quad (11.71)$$

this is an example of the Calugareanu theorem (Calugareanu 1959).

A kink instability which starts with $b = 0$ and an initial twist $T_{initial} = n$ will grow until at $b = a$ the twist vanishes and all helicity is contained by an N -turn writhe where $N = T_{initial}$. Thus, a kink will convert twist into writhe so that for $b > a$, $T = 0$ and $N = T_{initial}$. This property can be confirmed by taking a length of garden hose with a stripe running along the length and connecting the two ends together to form a closed flux tube with a stripe running along the axis. Initially, $N + T = 0$ because the stripe is not twisted and the hose axis is not helical. If the hose is deformed into a right-handed helix, then the stripe will make a left-handed helix about the hose axis to keep $N + T = 0$. If the stripe is initially a right-handed helix when the hose is not a helix, then deformation of the hose into a right handed helix will result in the stripe becoming parallel to the hose axis.

11.5 Assignments

1. Derive the helicity conservation equation for a resistive plasma

$$\frac{dK}{dt} + \int_S ds \cdot (\varphi \mathbf{B} + \mathbf{E} \times \mathbf{A}) = -2 \int d^3r \eta \mathbf{J} \cdot \mathbf{B} \quad (11.72)$$

and express it in the form

$$\frac{dK}{dt} + \int_S ds \cdot \left(2\varphi \mathbf{B} + \mathbf{A} \times \frac{\partial \mathbf{A}}{\partial t} \right) = -2 \int d^3r \eta \mathbf{J} \cdot \mathbf{B} \quad (11.73)$$

where φ is the electrostatic potential. What happens to the surface integral when the surface is a perfectly conducting wall? Hint: Start by evaluating $-\partial(\mathbf{A} \cdot \mathbf{B})/\partial t$ and make repeated use of Faraday's law $\nabla \times \mathbf{E} = -\partial \mathbf{B}/\partial t$, the electric field expressed as $\mathbf{E} = -\nabla\varphi - \partial \mathbf{B}/\partial t$ and the resistive MHD Ohm's law $\mathbf{E} + \mathbf{U} \times \mathbf{B} = \eta \mathbf{J}$.

2. Alternative explanation for why helicity is conserved better than magnetic energy:
 - (a) By subtracting \mathbf{E} dotted with Ampere's law from \mathbf{B} dotted with Faraday's law derive the MHD limit of Poynting's theorem:

$$\frac{\partial}{\partial t} \left(\frac{B^2}{2\mu_0} \right) + \nabla \cdot \left(\frac{\mathbf{E} \times \mathbf{B}}{\mu_0} \right) = -\mathbf{E} \cdot \mathbf{J} \quad (11.74)$$

- (b) Consider a plasma in a perfectly conducting chamber with no vacuum gap between the plasma and the chamber wall. Show that integration of Eq.(11.72) and Eq.(11.74) over the entire volume give respectively

$$\frac{dK}{dt} = -2 \int d^3r \eta \mathbf{J} \cdot \mathbf{B} \quad (11.75)$$

and

$$\frac{dW}{dt} = - \int d^3r \eta J^2. \quad (11.76)$$

where $W = \int d^3r B^2/2\mu_0$ is the magnetic energy.

- (c) Show that the right hand side of Eq. (11.76) is proportional to higher order spatial derivatives of \mathbf{B} than is the right hand side of Eq. (11.75). Use this

property to argue that the rate of dissipation of magnetic energy greatly exceeds that of magnetic helicity when the dynamics is spatially complex so that most of the spectral power is in short characteristic scale lengths.

- (d) Explain why this difference in dissipation rates could be approximated by assuming that magnetic helicity remains constant while magnetic energy decays in the presence of dynamics having fine scales. Argue that the decay of magnetic energy is thereby constrained by the requirement that helicity is conserved.
3. Show that the minimum energy state given by Eq.(11.32) is a force-free configuration. Is λ spatially uniform? Is this the same result as given in Eqs.(10.139) and (10.140)? Take the curl again to obtain

$$\nabla^2 \mathbf{B} + \lambda^2 \mathbf{B} = 0.$$

What are the components of this equation in axisymmetric cylindrical geometry? Be careful when evaluating the components of $\nabla^2 \mathbf{B}$ to take into account derivatives operating on unit vectors (e.g., $\nabla^2 (B_\phi \hat{\phi}) \neq \hat{\phi} \nabla^2 B_\phi$).

- (a) Show that for axisymmetric cylindrical geometry the minimum-energy states have the magnetic field components

$$B_z(r) = \bar{B} J_0(\lambda r)$$

$$B_\phi(r) = \bar{B} J_1(\lambda r).$$

Sketch $B_z(r)$ and $B_\phi(r)$. This is called the Bessel function model or Lundquist solution (Lundquist 1950) to the force-free equation and is often a good first guess representation for nearly force-free equilibria such as spheromaks, reversed field pinches, and solar coronal loops.

4. For a cylindrical system with coordinates $\{r, \phi, z\}$ show that if χ satisfies the Helmholtz equation

$$\nabla^2 \chi + \lambda^2 \chi = 0$$

then

$$\mathbf{B} = \lambda \nabla \chi \times \nabla z + \nabla \times (\nabla \chi \times \nabla z)$$

is a solution of the force-free equation $\mu_0 \mathbf{J} = \lambda \mathbf{B}$. By assuming that χ is independent of ϕ and is of the form $\chi \sim f(r) \cos kz$ find $f(r)$ and then determine the components of \mathbf{B} . Show that if λ satisfies an eigenvalue condition, it is possible to have a finite force-free field having no normal component on the walls of a cylinder of length h and radius a . Give the magnetic field components for this situation. Calculate the poloidal flux $\psi(r, z)$ by direct integration of $B_z(r, z)$. Hint: the answers will be in terms of Bessel functions J_0 and J_1 .

5. Obtain a ribbon such as is used in gift-wrapping, make one complete twist in this ribbon and tape the ends together. By manipulating the twisted ribbon show the following:
- (a) If the ribbon is manipulated to have no twists, then it has a figure-eight pattern with a cross-over. If the flux through the ribbon is Φ , show that the helicity of one full twist is Φ^2 , show that the helicity of one cross-over is also .

- (b) Cut the ribbon all the way along its length so that it becomes two interlinked ribbons of unequal width. Assuming that the original ribbon had a flux Φ , calculate the helicity of the configuration taking into account the helicity due to both twists and linkages and show that helicity is conserved.
- (c) Demonstrate that the sum of twist plus writhe is conserved using a bundle of flexible wires (or ropes) that are initially twisted about a straight axis and then manipulated into a kink where the wires are parallel to the locus of the kink. The ends of the bundle should be fixed. Similarly, start with a bundle of untwisted wires that are parallel to a straight axis and manipulate the wires into a helix. Show that the sense of the twist of the wires about their local axis is opposite to the sense of the helix so that a condition of zero helicity is maintained.

Magnetic reconnection

12.1 Introduction

Section 2.5.4 established the fundamental concept underlying ideal MHD, namely that magnetic flux is frozen into the plasma. Chapter 10 showed that ideal MHD plasmas are susceptible to two distinct types of instabilities, pressure-driven and current-driven. Pressure-driven modes draw on free energy associated with heavy fluids stacked on top of light fluids in an effective gravitational field whereas current-driven instabilities draw on free magnetic energy and involve the plasma attempting to increase its inductance in a flux-conserving manner. Both of these instabilities occur on the Alfvén time scale defined as some characteristic distance divided by v_A .

It is possible for an MHD equilibrium to be stable to all ideal MHD modes and yet not be in a lowest energy state. Free energy is therefore available to drive an instability but this energy cannot be tapped by ideal MHD modes. Magnetic tearing and associated reconnection is a non-ideal instability where the plasma is effectively ideal everywhere *except at a very thin boundary layer* where the ideal assumption breaks down and magnetic fields can diffuse across the plasma. Even though the boundary layer is thin, the tearing/reconnection causes the overall topology of the magnetic field to change. It is the changing of the topology (the local unfreezing of the magnetic field from the plasma) that allows the configuration to relax to a lower energy state. Because ideal MHD does not allow the topology to change, the lower energy state cannot be accessed via ideal MHD instabilities. The non-ideal resistive modes are much slower than ideal modes because the non-ideal mode relies on a diffusion or leakage of magnetic field across the plasma in some very limited spatial region where ideal MHD breaks down.

Magnetic tearing is an intrinsically complicated boundary layer phenomenon because two very different length scales mutually interact; the mathematical description has to reconcile behavior in a microscopic thin diffusion layer with behavior in a macroscopic outer ideal layer. We shall begin the discussion with an analogy drawn from everyday experience and use this analogy to show why it is energetically favorable for a sheet current to break up into filaments. The time scale for this process will be estimated and shown to be much slower than ideal MHD. Finally, the tearing and reconnection concept will be generalized to sheared magnetic fields and helical equilibria.

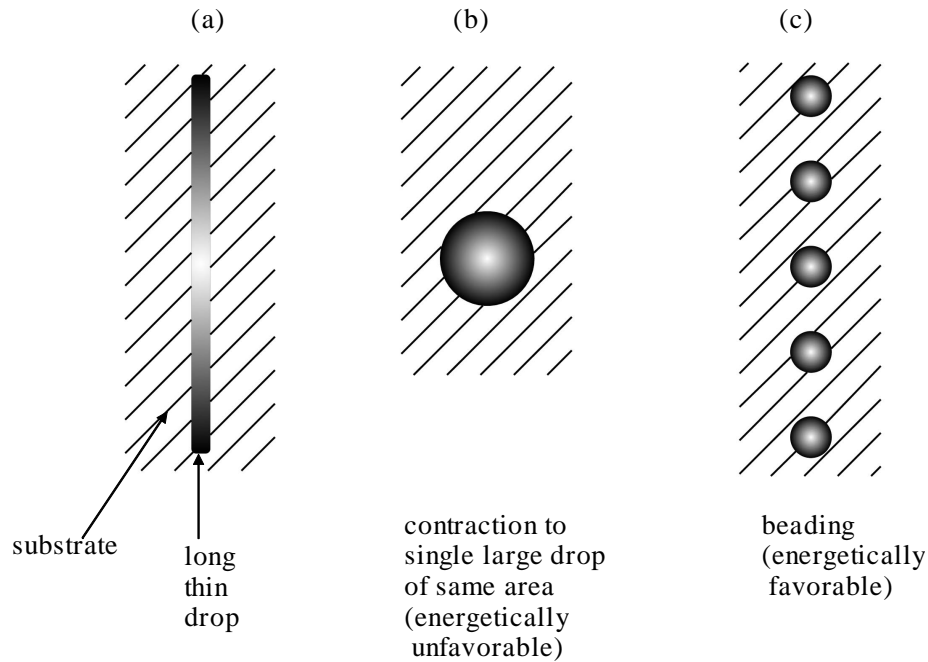


Figure 12.1: (a) Initial long thin drop, (b) contraction into big round drop (too much scraping on substrate), (c) beading into chain of little drops.

12.2 Water-beading: an analogy to magnetic tearing and reconnection

Since magnetic tearing and reconnection is not a simple process, it is helpful to start by considering the dynamics of a somewhat analogous instability known from everyday experience, namely the process of water beading. The initial condition in water beading is shown in Fig.12.1(a) and consists of a long, thin, two-dimensional, incompressible drop of water (approximate analog to the magnetic field) frictionally attached to a substrate (approximate analog to the plasma). The long thin drop has surface tension ‘trying’ to reduce the perimeter of the drop (this is analogous to the pinch force being interpreted as field line “tension” squeezing on a current channel). If the drop were not attached to the substrate, then as shown in Fig.12.1(b), the surface tension would simply collapse the long thin incompressible drop into a circular drop having area equal to that of the initial long thin drop. Because of the frictional work involved in dragging the water over the substrate, this wholesale collapse is not energetically favorable and does not occur. On the other hand, if as shown in Fig.12.1(c) the long thin drop breaks up into a line of discrete segments (which does not involve significant dragging of water across the substrate), the surface tension of each line segment causes each discrete segment to contract in length and bulge in

width until circular. Because only modest frictional dragging of water across the substrate is required to do this, the process can be energetically favorable, and so result in water beading.

12.3 Qualitative description of sheet current instability

Suppose an infinite-extent plasma has a thin sheet of current flowing in the z direction as shown in Fig.12.2(a). The sheet current is centered at $x = 0$ and extends from $y = -\infty$ to $y = +\infty$. The current is uniform in both the y and the z directions and roughly corresponds to the initial long thin water drop. This somewhat artificial situation can be considered as the Cartesian analog of a cylindrical shell current flowing in the z direction, localized at some radius $r = r_0$ and azimuthally symmetric. Thus, we identify r with x and y with θ .

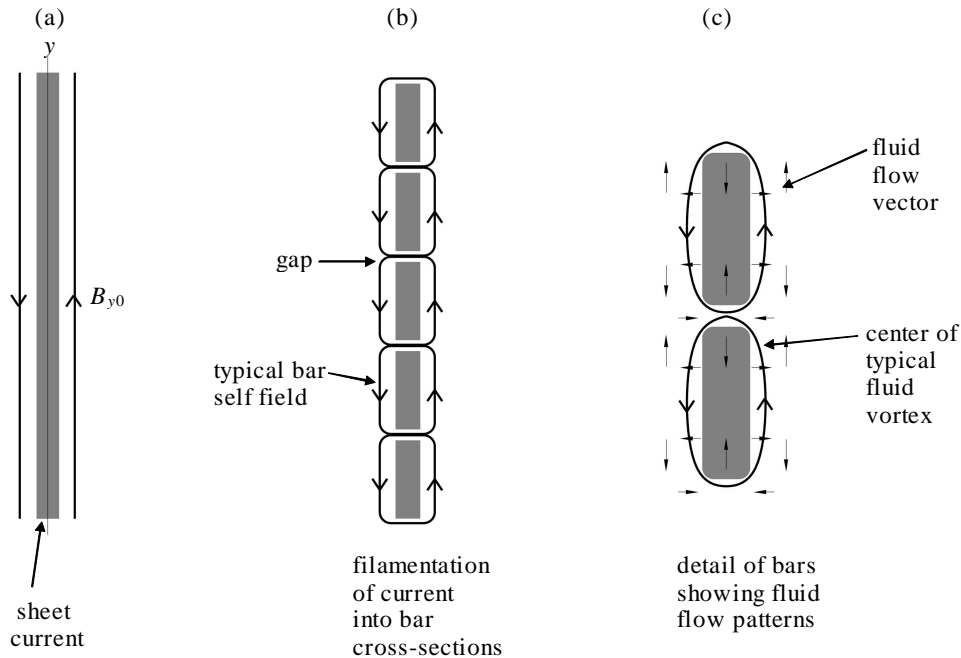


Figure 12.2: (a) Initial sheet current; (b) breaking up into bar cross-section filaments; (c) detail showing fluid flow consists of set of small vortices which are antisymmetric in x .

Since all quantities depend on x only, Ampere's law reduces to

$$\mu_0 J_z(x) = \frac{\partial B_y}{\partial x} \quad (12.1)$$

which integrates to give

$$B_y(x) = B_y(0) + \int_0^x \mu_0 J_z(x') dx'. \quad (12.2)$$

On the basis of symmetry the sheet current cannot generate a magnetic field at $x = 0$ so the field $B_y(0)$ must entirely be due to external currents. Let us assume for now that no external currents exist and set $B_y(0) = 0$; the situation of finite $B_y(0)$ will be treated later in Sec.12.5. Thus $B_y(x)$ is a sheared magnetic field which is positive for $x > 0$ and negative for $x < 0$. The magnitude of $B_y(x)$ changes rapidly inside the current layer and becomes constant for $|x| \rightarrow \infty$.

This situation can be characterized analytically by using a magnetic field

$$B_y(x) = B \tanh(x/L) \quad (12.3)$$

where L is the scale width of the current layer. Substituting in Eq.(12.1) gives

$$J_z(x) = \frac{B}{\mu_0 L} \operatorname{cosh}^{-2}(x/L) \quad (12.4)$$

which is sharply peaked in the neighborhood of $x = 0$.

Suppose that the perturbation shown in Fig.12.2(b) is introduced so that the current sheet cross-section is broken up into a number of bar-shaped structures each with current I_{bar} separated by small gaps in the y direction; these bars are roughly analogous to the water beads discussed above. Each bar's self magnetic field acts like an elastic band wrapped around the bar (analogous to the surface tension of a drop). This tension contracts the y dimension of the bar, and if the bar is incompressible, the x dimension will then have to grow, as shown in Fig.12.2(c). As the bar deforms from a rectangle into a circle having the same area, its perimeter becomes shorter giving rise to a stronger field (and effective surface tension) since

$$\int_{perimeter} \mathbf{B} \cdot d\mathbf{l} = \mu_0 I_{bar}. \quad (12.5)$$

Hence, this deformation feeds upon itself and is unstable. Note that the inductance of the system increases as the current breaks into filaments, consistent with the earlier observation that the plasma is always 'trying' to increase its inductance.

This energetically allowed filamentation instability is forbidden in ideal MHD because the topology of the magnetic field changes at the gaps between the bars. Before the gaps form, the magnetic field lines are open and straight, stretching from $y = -\infty$ to $y = +\infty$ whereas after the gaps form, some field lines circle the current filaments; these field lines are finite in length and curved. In order to go from the initial state to the filamented state, some magnetic field lines must move across plasma in violation of ideal MHD (this change in topology is approximately analogous to dragging the water drops across the substrate in the water beading problem). The field lines have an 'X' shape at the center of the gaps and the change in topology occurs at these X-points. The center of the bar is called an O-point since the field around this point has an O-shape.

If some mechanism exists that allows X-points to develop, instability can occur. Since finite resistivity allows magnetic field to diffuse across plasma, a resistive plasma will be susceptible to this instability at locations where the magnetic field attachment to the plasma

is weakest. The location of the weak spot can be deduced by examining Ohm's law for a nearly ideal plasma (i.e., small but finite resistivity),

$$\mathbf{E} + \mathbf{U} \times \mathbf{B} = \eta \mathbf{J}. \quad (12.6)$$

At most locations in the plasma, the two left hand side terms are both much larger than the right hand side resistive term and so plasma behavior is determined by these two left hand terms balancing each other. This balancing causes the electric field in the plasma frame to be zero, which corresponds to the magnetic field being frozen into the plasma. However, if there exists a point, line or plane of symmetry where either \mathbf{U} or \mathbf{B} vanishes, then in the vicinity of this special region, Eq.(12.6) reduces to

$$\mathbf{E} \approx \eta \mathbf{J}. \quad (12.7)$$

The curl of Eq.(12.7) gives

$$\frac{\partial \mathbf{B}}{\partial t} = \frac{\eta}{\mu_0} \nabla^2 \mathbf{B} \quad (12.8)$$

a *diffusion equation* for the magnetic field. Thus, in this *special region* the magnetic field is not frozen to the plasma and diffuses across the plasma.

Let us now examine the fluid flow pattern associated with the bars as they contract in the y direction and expand in the x direction. As shown in Fig. 12.2(c), each bar has y -directed velocities pointing from the gap toward the bar center and x -directed velocities pointing out from the center of the bar. To complete the incompressible flow there must also be oppositely directed x and y velocities just outside the bar with the net result that there is a set of small fluid vortices which are anti-symmetric in x and in addition have a y -dependence which is 90° out of phase with respect to the current bar y -direction periodicity. In particular, there is an outward x -directed velocity at the y location of the O-points and an inward x -directed at the y location of the X-points. The fluid motion in summary consists of a spatially periodic set of vortices that are antisymmetric with respect to $x = 0$. Each bar has a pair of opposite vortices for positive x and a mirror image pair of vortices for negative x so that there are four vortices for each bar.

12.4 Semi-quantitative estimate of the tearing process

An exact, self-consistent description of tearing and reconnection is beyond the capability of standard analytic methods because of the multi-scale nature of this process. However, the essential features (geometry, critical parameters, growth rate) and a reasonable physical understanding can be deduced using a semi-quantitative analysis which outlines the basic physics and determines the relevant orders of magnitude. The starting point for this analysis involves solving for the vector potential associated with the magnetic field in Eq.(12.3), obtaining

$$A_z(x) = - \int^x B_y(x') dx' = -BL \ln [\cosh(x/L)] + \text{const}. \quad (12.9)$$

The constant is chosen to give $A_z = 0$ at $x = 0$ so

$$A_z(x) = -BL \ln [\cosh(x/L)]. \quad (12.10)$$

For $|x| \ll L$, $\cosh(x/L) \simeq 1 + x^2/L^2$ while for $|x| \gg L$, $\cosh(x/L) \simeq \exp(|x|/L)/2$. Thus, the limiting forms of the vector potential are

$$\lim_{|x| \ll L} A_z(x) = -\frac{Bx^2}{L} \quad (12.11)$$

and

$$\lim_{|x| \gg L} A_z(x) = -BL(|x| - \ln 2). \quad (12.12)$$

Near $x = 0$, A_z is parabolic with a maximum value of zero, while far from $x = 0$, A_z is linear and becomes more negative with increasing displacement from $x = 0$. This behavior of the vector potential is consistent with the field being uniform far from $x = 0$, but reversing sign on going across $x = 0$. The behavior is also consistent with the relationship between the current density and the second derivative of the vector potential,

$$\mu_0 J_z = \frac{\partial B_y}{\partial x} = -\frac{\partial^2 A_z}{\partial x^2}. \quad (12.13)$$

Thus, current density is associated with curvature in $A_z(x)$ or, in more extreme form, with a discontinuity in the first derivative of $A_z(x)$. Specifying the vector potential is sufficient to characterize the problem since the magnetic field and currents are respectively the first and second derivatives of $A_z(x)$. This general idea can be extended to more complicated geometries if there is sufficient symmetry so that specification of an equilibrium flux profile uniquely gives both the equilibrium field and the current distribution.

The reconnection process is characterized by the MHD equation of motion

$$\rho \frac{d\mathbf{U}}{dt} = \mathbf{J} \times \mathbf{B} - \nabla P, \quad (12.14)$$

Faraday's law expressed as

$$\mathbf{E} = -\frac{\partial \mathbf{A}}{\partial t}, \quad (12.15)$$

Ampere's law

$$\nabla \times \mathbf{B} = \mu_0 \mathbf{J}, \quad (12.16)$$

and the resistive Ohm's law

$$\mathbf{E} + \mathbf{U} \times \mathbf{B} = \eta \mathbf{J}. \quad (12.17)$$

The analysis involves relating the velocity vortices to the linearized Ohm's law, and in particular to its z component

$$E_{1z} + U_{1x} B_{0y} = \eta J_{1z}. \quad (12.18)$$

The sense of the vortices sketched in Fig.12.2(c) indicate that the velocity perturbation is uniform in the z direction and U_{1x} is *antisymmetric* with respect to x . Also, since the motion consists of vortices, there is no net divergence of the fluid velocity and so it is reasonable and appropriate to stipulate that the flow is *incompressible* with $\nabla \cdot \mathbf{U} = 0$. Since the perturbed current density is in the z direction, and since for straight geometries the vector potential is parallel to the current density, the perturbed vector potential may also be assumed to be in the z direction. Hence, both equilibrium and perturbed vector potentials are in the z direction and so the total magnetic field is related to the total vector potential by

$$\mathbf{B} = \nabla \times A_z \hat{z} = \nabla A_z \times \hat{z}. \quad (12.19)$$

Equation (12.18) can be recast using Eqs.(12.15) and (12.19) as an *induction equation*,

$$-\frac{\partial A_{1z}}{\partial t} - U_{1x} \frac{\partial A_{0z}}{\partial x} = \eta J_{1z}. \quad (12.20)$$

The current has the form

$$\mu_0 J_z = \hat{z} \cdot \nabla \times \mathbf{B} = \hat{z} \cdot \nabla \times (\nabla \times A_z \hat{z}) = \hat{z} \cdot \nabla \times (\nabla A_z \times \hat{z}) = -\nabla_{\perp}^2 A_z \quad (12.21)$$

where the subscript \perp means perpendicular to \hat{z} . Thus, the induction equation becomes

$$\frac{\partial A_{1z}}{\partial t} + U_{1x} \frac{\partial A_{0z}}{\partial x} = \frac{\eta}{\mu_0} \nabla_{\perp}^2 A_{1z}. \quad (12.22)$$

To proceed, it is necessary to express the perturbed velocity U_{1x} in terms of A_{1z} ; this relation is obtained from the equation of motion.

While we could just plow ahead and manipulate the equation of motion to obtain U_{1x} in terms of A_{1z} , it is more efficient to exploit the incompressibility relation. In two-dimensional hydrodynamics, incompressibility simplifies flow dynamics so that flow is described by two related scalars, the stream-function f and the vorticity Ω . For two-dimensional motion in the $x - y$ plane of interest here, the general incompressible velocity can be expressed as

$$\mathbf{U} = \nabla f \times \hat{z} \quad (12.23)$$

since

$$\nabla \cdot \mathbf{U} = \nabla \cdot (\nabla f \times \hat{z}) = \hat{z} \cdot \nabla \times \nabla f = 0. \quad (12.24)$$

The vorticity is the curl of the velocity and because the velocity lies in the $x - y$ plane, the vorticity vector is in the z direction. The vorticity magnitude Ω is given by

$$\Omega = \hat{z} \cdot \nabla \times \mathbf{U} = \hat{z} \cdot \nabla \times (\nabla f \times \hat{z}) = \nabla \cdot [(\nabla f \times \hat{z}) \times \hat{z}] = -\nabla_{\perp}^2 f \quad (12.25)$$

where \perp means perpendicular with respect to z . Given the vorticity, f can be found by solving the Poisson-like Eq.(12.25), and then knowing f , the velocity can be evaluated using Eq.(12.23). Appropriate boundary conditions must be specified for both f and Ω ; these boundary conditions are that the vorticity is antisymmetric in x and is only large in the vicinity of $x = 0$ as indicated in Fig.12.2(c).

The curl of the equation of motion provides the vorticity evolution and also annihilates ∇P ; this elimination of P from consideration is why the vorticity/stream-line method is a more efficient approach rather than direct solution of the equation of motion.

Let us now solve for U_{1x} following this procedure. The linearized equation of motion is

$$\rho_0 \frac{\partial U_1}{\partial t} = (\mathbf{J} \times \mathbf{B})_1 - \nabla P_1; \quad (12.26)$$

taking the curl and dotting with \hat{z} gives

$$\begin{aligned} \rho_0 \frac{\partial \Omega_1}{\partial t} &= \hat{z} \cdot \nabla \times (\mathbf{J} \times \mathbf{B})_1 \\ &= \hat{z} \cdot \nabla \times [J_z \hat{z} \times (\nabla A_z \times \hat{z})]_1 \\ &= \hat{z} \cdot \nabla \times (J_z \nabla A_z)_1 \\ &= \hat{z} \cdot (\nabla J_z \times \nabla A_z)_1. \end{aligned} \quad (12.27)$$

Using Eq.(12.21) this can be written as

$$\frac{\partial \Omega_1}{\partial t} = \frac{1}{\mu_0 \rho_0} \hat{z} \cdot [\nabla A_z \times \nabla (\nabla_{\perp}^2 A_z)]_1. \quad (12.28)$$

From Fig.12.2(c) it is expected that the vortices have significant amplitude only in the vicinity of where the current bars are deforming and that at large $|x|$ there will be negligible vorticity. Thus, it is assumed that the vorticity evolution equation has the following behavior:

1. Inner (tearing/reconnection) region: Here it is assumed that the perturbation has much steeper gradients than the equilibrium so

$$\frac{|\nabla (\nabla_{\perp}^2 A_{z0})|}{|\nabla A_{z0}|} \ll \frac{|\nabla (\nabla_{\perp}^2 A_{z1})|}{|\nabla A_{z1}|}. \quad (12.29)$$

This allows Eq.(12.28) to be approximated as

$$\begin{aligned} \frac{\partial \Omega_1}{\partial t} &\simeq \frac{1}{\mu_0 \rho_0} \hat{z} \cdot [\nabla A_{z0} \times \nabla (\nabla_{\perp}^2 A_{z1})] \\ &= \frac{1}{\mu_0 \rho_0} \frac{dA_{z0}}{dx} \frac{\partial}{\partial y} (\nabla_{\perp}^2 A_{z1}) \end{aligned} \quad (12.30)$$

which shows that J_{1z} crossed with B_{y0} generates vorticity. Since B_{y0} is antisymmetric with respect to x , the vortices have the assumed antisymmetry. Furthermore, because J_{1z} is symmetric with respect to x and localized in the vicinity of $x = 0$ the vortices are localized to the vicinity of $x = 0$.

2. Outer (ideal) region: Here it is assumed that $\Omega_1 \simeq 0$, so Eq.(12.28) becomes

$$\frac{dA_{z0}}{dx} \frac{\partial}{\partial y} (\nabla_{\perp}^2 A_{z1}) - \frac{\partial A_{z1}}{\partial y} \frac{d^3 A_{z0}}{dx^3} = 0 \quad (12.31)$$

which is a specification for A_{z1} in the outer region for a given A_{z0} . Thus, it is effectively assumed that the outer perturbed field is force-free, i.e., $(\mathbf{J} \times \mathbf{B})_1 = 0$ so that no vorticity is generated in the outer region.

The perturbed quantities will now be assumed to have the space-time dependence

$$\begin{aligned} A_{z1} &= A_{z1}(x) e^{iky + \gamma t} \\ \Omega_1 &= \Omega_1(x) e^{iky + \gamma t} \end{aligned} \quad (12.32)$$

so that Eq.(12.30) gives the inner region vorticity as

$$\Omega_1 = \frac{1}{\mu_0 \gamma \rho_0} \frac{dA_{z0}}{dx} ik (\nabla_{\perp}^2 A_{z1}) = -\frac{1}{\gamma \rho_0} \frac{dA_{z0}}{dx} ik J_{z1}. \quad (12.33)$$

This satisfies all the geometric conditions noted earlier, namely the antisymmetric dependence on x , the localization near $x = 0$ and, consistent with Fig.12.2(c), a periodicity in y that is 90° out of phase with the periodicity of J_{1z} .

Using Eq. (12.23), it is seen that

$$U_{1x} = \frac{\partial f_1}{\partial y} = ik f_1. \quad (12.34)$$

The stream-function f_1 is a solution of the Poisson-like system Eq.(12.25) and Eq.(12.33),

$$\frac{\partial^2 f_1}{\partial x^2} - k^2 f_1 = \frac{1}{\gamma \rho_0} \frac{dA_{z0}}{dx} ikJ_{z1}. \quad (12.35)$$

Since the perturbed current peaks at $x = 0$ and has a width of the order of ϵ , it may be characterized by the Gaussian profile

$$J_{z1} \simeq \frac{\lambda}{\epsilon \sqrt{\pi}} e^{-x^2/\epsilon^2} \quad (12.36)$$

where

$$\lambda = \int_{layer} J_{z1} dx \quad (12.37)$$

is the total perturbed current in the tearing layer. The gradient of the vector potential can be written as

$$\frac{dA_{z0}}{dx} = -B_{y0}(x) \simeq -\frac{x}{L} B'_{y0}. \quad (12.38)$$

Assuming that the tearing layer is very narrow gives

$$\frac{\partial^2 f_1}{\partial x^2} \gg k^2 f_1 \quad (12.39)$$

so that Eq.(12.35) becomes

$$\frac{\partial^2 f_1}{\partial x^2} = -\frac{B'_{y0}}{\gamma L \rho_0} ik \frac{\lambda}{\epsilon \sqrt{\pi}} x e^{-x^2/\epsilon^2} = \frac{ikB'_{y0}}{2\gamma L \rho_0} \frac{\lambda \epsilon}{\sqrt{\pi}} \frac{d}{dx} e^{-x^2/\epsilon^2}. \quad (12.40)$$

The profiles of J_{z1} , $B_{y0}(x)$ and their product (right hand side of Eq.(12.40)) are shown in Fig.12.3.

Integrating Eq.(12.40) with respect to x gives

$$\frac{\partial f_1}{\partial x} = \frac{ikB'_{y0}}{2\gamma L \rho_0} \frac{\lambda \epsilon}{\sqrt{\pi}} e^{-x^2/\epsilon^2} \quad (12.41)$$

which incidentally gives $U_{1y} = -\partial f_1/\partial x$. Since it is desired to find the magnitude of U_{1x} in the region $x \sim \epsilon$, a rough 'order of magnitude' integration of Eq.(12.41) in this region gives

$$f_1 \sim \frac{ikB'_{y0}\lambda\epsilon^2}{2\gamma L\sqrt{\pi}\rho_0} \text{sign}(x) \text{ for } x \sim \epsilon \quad (12.42)$$

and so

$$U_{1x} \sim -\frac{k^2 B \lambda \epsilon^2}{2\gamma L \sqrt{\pi} \rho_0} \text{sign}(x) \text{ for } x \sim \epsilon. \quad (12.43)$$

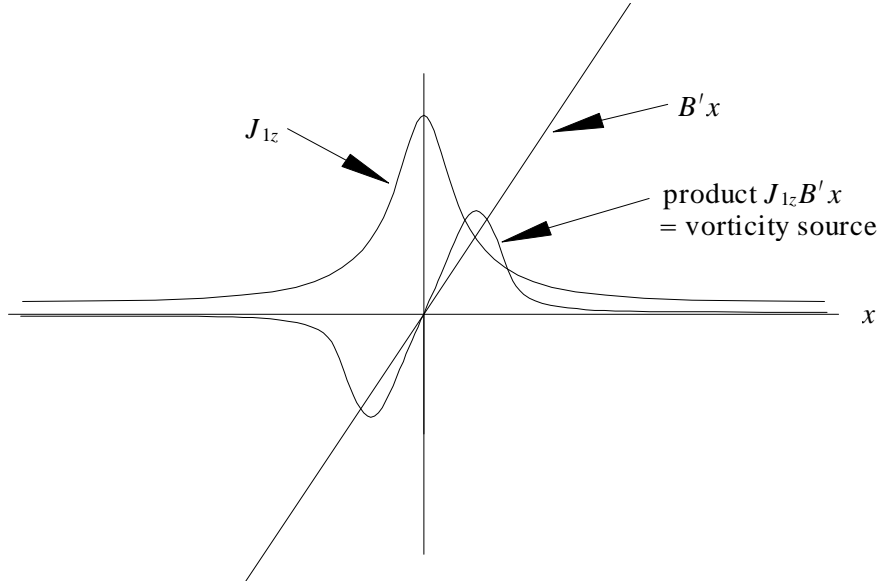


Figure 12.3: Product of symmetric perturbed current with antisymmetric equilibrium field results in antisymmetric vorticity source localized near $x = 0$.

The amplitude factor λ can be expressed using Eq. (12.21) as

$$\begin{aligned}
 \lambda &= -\frac{1}{\mu_0} \int_{\text{layer}} \nabla_{\perp}^2 A_{1z} dx \\
 &\simeq -\frac{1}{\mu_0} \int_{\text{layer}} \frac{\partial^2 A_{1z}}{\partial x^2} dx \\
 &= -\frac{1}{\mu_0} \left[\left(\frac{\partial A_{1z}}{\partial x} \right)_{+} - \left(\frac{\partial A_{1z}}{\partial x} \right)_{-} \right] \quad (12.44)
 \end{aligned}$$

where the subscripts \pm mean evaluated at $x = \pm\epsilon$. For purposes of joining to the outer ideal solution, the normalized jump derivative is defined as

$$\Delta' = \frac{\left(\frac{\partial A_{1z}}{\partial x} \right)_{+} - \left(\frac{\partial A_{1z}}{\partial x} \right)_{-}}{A_{1z}(0)} \quad (12.45)$$

so that

$$\lambda = -\frac{\Delta'}{\mu_0} A_{1z}(0). \quad (12.46)$$

The velocity becomes

$$U_{1x} \sim \frac{k^2 B \Delta' \epsilon^2}{2\gamma L \sqrt{\pi} \mu_0 \rho_0} A_{1z}(0) \text{sign}(x) \quad (12.47)$$

and using Eq.(12.36), the current density becomes

$$J_{1z} \sim -\frac{\Delta'}{\epsilon\mu_0\sqrt{\pi}}A_{1z}(0). \quad (12.48)$$

We now repeat the induction equation, Eq.(12.20),

$$-\frac{\partial A_{1z}}{\partial t} - U_{1x}\frac{\partial A_{0z}}{\partial x} = \eta J_{1z} \quad (12.49)$$

and substitute for U_{1x} , J_{1z} and assume that $\partial A_{0z}/\partial x = -B_{y0} \simeq -B\epsilon/L$ in the tearing layer. This gives

$$\underset{\#1}{\gamma} - \frac{k^2 B^2 \Delta' \epsilon^3}{2\gamma L^2 \sqrt{\pi} \mu_0 \rho_0} \underset{\#2}{=} \frac{\eta \Delta'}{\epsilon \mu_0 \sqrt{\pi}} \underset{\#3}{=} \quad (12.50)$$

where the terms have been numbered for reference in the following discussion.

In the ideal plasma limit, terms #1 and #2 balance each other while term #3 is small; this gives the frozen-in condition. At exactly $x = 0$, term #2 vanishes and so terms #1 and #3 must balance each other, resulting in diffusion of the magnetic field. At the edge of the tearing layer, which is the transition from the ideal limit to the diffusive limit *all three terms are of the same size*. Thus, the three terms may be equated; this gives two equations which may be solved for γ and ϵ with Δ' as a parameter. Equating terms #1 and #3 gives

$$\gamma = \frac{\eta \Delta'}{\epsilon \mu_0 \sqrt{\pi}} \quad (12.51)$$

while equating terms #2 and #3 gives

$$\gamma = \frac{(kB')^2 \epsilon^4}{2\eta \rho_0} \quad (12.52)$$

where $B' = B/L$ is the derivative of the equilibrium field at $x = 0$. Equating these last two equations to eliminate γ gives the width of the tearing layer to be

$$\epsilon \simeq \left[\frac{2\eta^2 \rho_0 \Delta'}{\mu_0 \sqrt{\pi} (kB')^2} \right]^{1/5}. \quad (12.53)$$

Substituting ϵ back into Eq.(12.51) gives

$$\gamma = 0.55 (\Delta')^{4/5} \left[\frac{\eta}{\mu_0} \right]^{3/5} \left[\frac{(kB')^2}{\rho_0 \mu_0} \right]^{1/5}. \quad (12.54)$$

This result can be put in a more transparent form by defining characteristic times for ideal processes and for resistive processes. The characteristic time for ideal processes is the Alfvén time τ_A , defined as the time to move the characteristic length L when traveling at the Alfvén velocity, i.e.,

$$\tau_A^{-1} = \frac{v_A}{L} = \frac{\sqrt{B^2/\rho_0 \mu_0}}{L} = \sqrt{\frac{(B')^2}{\rho_0 \mu_0}}. \quad (12.55)$$

The Alfvén time is the characteristic time of ideal MHD and is typically a very fast time. The characteristic time for resistive processes is the time τ_R , defined as the time to diffuse resistively a distance L ,

$$\tau_R^{-1} = \frac{\eta}{L^2 \mu_0}. \quad (12.56)$$

For nearly ideal plasmas the resistive time scale is very slow. Using these definitions, Eq.(12.54) can be written as (Furth, Killeen and Rosenbluth 1963)

$$\gamma = 0.55 (\Delta' L)^{4/5} (kL)^{2/5} \tau_R^{-3/5} \tau_A^{-2/5} \quad (12.57)$$

All that is needed now is Δ' . This jump condition is found from Eq.(12.31) which gives the form of A_{z1} in the ideal region outside the tearing layer. This can be expressed as

$$\nabla_{\perp}^2 A_{z1} + \left[B_{y0}^{-1} \frac{d^2 B_{y0}}{dx^2} \right] A_{z1} = 0 \quad (12.58)$$

which shows that the equilibrium magnetic field acts like a ‘potential’ for the perturbed vector potential ‘wavefunction’. If boundary conditions are specified at large $|x|$ for the perturbed vector potential, then in general, there will be a discontinuity in the first derivative of A_{z1} at $x = 0$; this discontinuity gives Δ' . The jump depends on the existence of a localized equilibrium current since

$$\frac{d^2 B_{y0}}{dx^2} = \mu_0 \frac{dJ_{z0}}{dx}. \quad (12.59)$$

In general the outer equation must be solved numerically.

The main result, as given by Eq.(12.57), is that if $\Delta' > 0$ an instability develops having a growth rate *intermediate* between the fast Alfvén time scale and the slow resistive time scale. Since a nearly ideal plasma is being considered, η is extremely small. The width of the tearing layer is therefore very narrow, since as shown by Eq.(12.53), this width is proportional to $\eta^{2/5}$.

12.5 Generalization of tearing to sheared magnetic fields

The sheet current discussed above can occur in real situations but is a special case of the more general situation where the equilibrium magnetic field does not have a null, but instead is simply sheared. This means that the equilibrium magnetic field is straight, has components in both the y and z directions, and has direction that is a varying function of x . The sheared situation thus has a uniform magnetic field in the z direction and instead of the current being concentrated in a sheet, there is simply a non-uniform $B_{y0}(x)$. In this more general situation the equilibrium magnetic field has the form

$$\mathbf{B}_0 = B_{y0}(x)\hat{y} + B_{z0}\hat{z}. \quad (12.60)$$

A nontrivial feature of this situation is that unlike the previously considered sheet current equilibrium, here $B_{y0}(x)$ does not vanish at any particular x . Instead, as will be seen later, what counts is the vanishing of $\mathbf{k} \cdot \mathbf{B}_0$. Equation (12.60) can be used as a slab representation of the straight cylindrical geometry equilibrium field

$$\mathbf{B}_0 = \nabla\psi_0(r) \times \nabla z + B_{z0}\hat{z}; \quad (12.61)$$

which in turn can be thought of as the straight cylindrical approximation of a toroid with z corresponding to the toroidal angle.

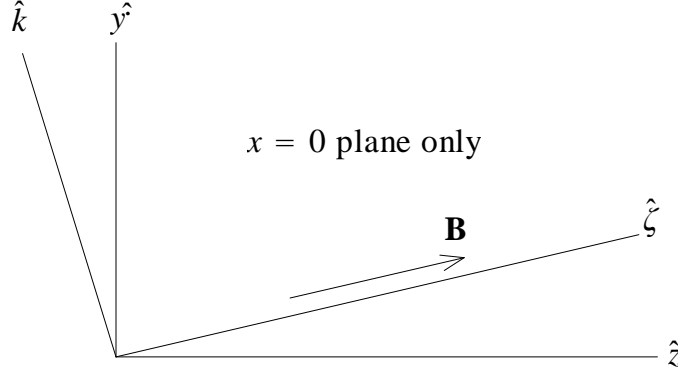


Figure 12.4: Tilted coordinate system for general sheared field.

Figure 12.4 shows the magnetic field given by Eq.(12.60) as viewed in the $x = 0$ plane. In the sheet current analysis discussed in the previous section, the perturbed vector potential pointed in the z direction and was periodic in the y direction. This corresponded to having $\mathbf{k} \cdot \mathbf{A}_1 = 0$ so that the wavevector was orthogonal to the vector potential and both were orthogonal to x . Other important properties were that $\mathbf{k} \cdot \mathbf{B}$ vanished at the reconnection layer, the fluid vorticity vector was pointed in the z direction, the perturbed currents and perturbed magnetic fields were such that $J_1/J_0 \gg B_1/B_0$ in the reconnection layer, and $J_1/J_0 \sim B_1/B_0$ in the exterior region.

These relationships and approximations are generalized here and, in particular, it is assumed that all perturbed quantities have functional dependence $\sim g(x) \exp(ik_y y + ik_z z + \gamma t)$. As before, the vorticity equation is the curl of the linearized equation of motion, i.e.

$$\rho \frac{\partial \Omega_1}{\partial t} = \nabla \times (\mathbf{J}_1 \times \mathbf{B}_0 + \mathbf{J}_0 \times \mathbf{B}_1) \quad (12.62)$$

and in the reconnection layer where $J_1/J_0 \gg B_1/B_0$ this becomes

$$\begin{aligned} \rho \frac{\partial \Omega_1}{\partial t} &= \nabla \times (\mathbf{J}_1 \times \mathbf{B}_0) \\ &= \mathbf{B}_0 \cdot \nabla \mathbf{J}_1 - \mathbf{J}_1 \cdot \nabla \mathbf{B}_0 \end{aligned} \quad (12.63)$$

since $\nabla \cdot \mathbf{B}_0 = 0$ and $\nabla \cdot \mathbf{J}_1 = 0$.

An essential feature of the reconnection topology is that the vorticity must be antisymmetric about the reconnection layer, as can be seen from examination of the fluid flow vectors in Fig.12.2(c). Since the vorticity is created by the torque (i.e., the curl of the force), it is clear that the torque must be antisymmetric about the reconnection layer. As will be seen in the next paragraphs, the condition that the torque is antisymmetric does not imply that either \mathbf{B}_0 or \mathbf{J}_1 are antisymmetric, but rather implies some more subtle conditions.

Thus, if $x = 0$ is defined to be the location of the reconnection layer, then Ω_1 must be an odd function of x and therefore must vanish at $x = 0$. Hence the right hand side of Eq.(12.63) must vanish at $x = 0$ and since there need be no particular functional relationship between \mathbf{B}_0 and its gradient, the two terms on the right hand side of Eq.(12.63) must separately vanish. Therefore one of the requirements is to choose the origin of the x axis such that $\mathbf{B}_0 \cdot \nabla \mathbf{J}_1 = 0$ at $x = 0$ or, equivalently,

$$\mathbf{k} \cdot \mathbf{B}_0 = 0 \text{ at } x = 0 \quad (12.64)$$

so that

$$k_y B_{y0}(0) + k_z B_{z0} = 0. \quad (12.65)$$

Having $\mathbf{k} \cdot \mathbf{B}$ vanish at the reconnection layer is physically reasonable, since finite $\mathbf{k} \cdot \mathbf{B}$ implies a periodic bending of the equilibrium field; such a bending absorbs energy and so is stabilizing. Having $\mathbf{k} \cdot \mathbf{B}$ vanish is like letting the instability cleave the system at a weak point so that the instability can develop without requiring much free energy.

The second requirement for the right hand side of Eq.(12.63) to vanish is to have $\mathbf{J}_1 \cdot \nabla \mathbf{B}_0 = 0$. If the flow is incompressible, then the perturbed magnetic field must be orthogonal to the equilibrium magnetic field and since the perturbed current is the curl of the perturbed magnetic field, the perturbed current must be parallel to the equilibrium magnetic field. Since \mathbf{B}_0 is assumed straight, $\mathbf{B}_0 \cdot \nabla \mathbf{B}_0 = 0$ and since \mathbf{J}_1 is parallel to \mathbf{B}_0 , it is seen that $\mathbf{J}_1 \cdot \nabla \mathbf{B}_0 = (J_1/B_0) \mathbf{B}_0 \cdot \nabla \mathbf{B}_0 = 0$. Because \mathbf{J}_1 is parallel to \mathbf{B}_0 , \mathbf{J}_1 must also be straight and so a Coulomb gauge vector potential will be parallel to \mathbf{J}_1 , since

$$\begin{aligned} \mu_0 \mathbf{J}_1 &= \nabla \times \nabla \times \mathbf{A}_1 \\ &= \nabla \nabla \cdot \mathbf{A}_1 - \nabla^2 \mathbf{A}_1 \\ &= -\nabla^2 \mathbf{A}_1 \end{aligned} \quad (12.66)$$

$$= -\hat{\zeta} \nabla^2 A_1 \quad (12.67)$$

can be satisfied by having both \mathbf{J}_1 and \mathbf{A}_1 in the direction of $\hat{\zeta}$ where $\hat{\zeta} = \mathbf{B}_0(0)/B_0(0)$ does not depend on position.

It is therefore assumed that \mathbf{A}_1 is parallel to $\mathbf{B}_0(0)$ and so

$$\mathbf{A}_1(x, y, z, t) = A_1 \hat{\zeta}(x) e^{ik_y y + ik_z z + \gamma t}. \quad (12.68)$$

Thus, $\mathbf{k} \cdot \mathbf{A}_1 = 0$ in this tilted coordinate system and also $\nabla \cdot \mathbf{A}_1 = 0$ so that the Coulomb gauge assumption is satisfied.

Reconsideration of the right hand side of Eq. (12.63) shows that although the two terms both vanish at $x = 0$ there is a difference in the geometrical dependence of these terms. In particular

$$\mathbf{J}_1 \cdot \nabla \mathbf{B}_0 = 0$$

is true for all x because \mathbf{J}_1 is in the $\hat{\zeta}$ direction and \mathbf{B}_0 is a function of x only. Thus, Eq. (12.63) reduces to

$$\begin{aligned} \rho \frac{\partial \Omega_1}{\partial t} &= \mathbf{B}_0 \cdot \nabla \mathbf{J}_1 \\ &= i(\mathbf{k} \cdot \mathbf{B}_0) \mathbf{J}_1 \end{aligned} \quad (12.69)$$

where, by assumption, $\mathbf{k} \cdot \mathbf{B}_0$ vanishes at $x = 0$.

Continuing this discussion of the ramifications of the antisymmetry of $\mathbf{k} \cdot \mathbf{B}_0$ about $x = 0$, we now define an artificial reference magnetic field $\bar{\mathbf{B}}$ that is parallel to the real field at $x = 0$, but has no shear (i.e. has no x dependence). The reference field therefore has the form

$$\bar{\mathbf{B}} = B_{y0}(0)\hat{y} + B_{z0}\hat{z} = B_0(0)\hat{\zeta} \text{ for all values of } x. \quad (12.70)$$

We now define \mathbf{b}_0 as the difference between the real field and $\bar{\mathbf{B}}$ so that

$$\mathbf{B}_0(x) = \bar{\mathbf{B}} + \mathbf{b}_0(x) \quad (12.71)$$

and $\mathbf{b}_0(x)$ has the same x -dependence as the B_{y0} field used for the sheet current instability in the previous section in that (i) it is antisymmetric about x and (ii) is in the y direction. One way of thinking about this is to realize that $\mathbf{b}_0(x)$ is the component of $\mathbf{B}_0(x)$ which is antisymmetric about $x = 0$. With this definition

$$\mathbf{k} \cdot \mathbf{B}_0 = \mathbf{k} \cdot \mathbf{b}_0(x) = k_y b_0 \quad (12.72)$$

and so Eq.(12.69) becomes

$$\gamma\rho\Omega_{1\zeta} = ik_y b_0 J_{1\zeta}. \quad (12.73)$$

This equation provides the essence of the dynamics. It shows how the component of the magnetic field that is antisymmetric about $x = 0$ creates fluid vortices that are antisymmetric with respect to x . In particular, since $\mathbf{b}_0(x)$ is an odd function of x and $J_{1\zeta}$ is an even function of x , $\Omega_{1\zeta}$ is an odd function of x .

The complete self-consistent description is obtained by in addition taking into account the induction equation which shows how fluid motion acts to create perturbations of the electromagnetic field.

Since we are working with vector potentials, Ohm's law provides the induction equation. In the sheet current case the component of Ohm's law in the direction of symmetry of the perturbation was considered, i.e., the component in the z direction. Here, the corresponding symmetry direction for the perturbation is the ζ direction and so the relevant component of Ohm's law is the ζ component,

$$\hat{\zeta} \cdot [\mathbf{E}_1 + \mathbf{U}_1 \times \mathbf{B}_0(x)] = \hat{\zeta} \cdot \eta \mathbf{J}_1 \quad (12.74)$$

which becomes

$$-\frac{\partial A_{1\zeta}}{\partial t} + (\hat{y} \times \hat{\zeta} \cdot \mathbf{U}_1) b_0(x) = \eta J_{1\zeta}. \quad (12.75)$$

Since the vorticity vector lies along $\hat{\zeta}$ the incompressible velocity must be orthogonal to $\hat{\zeta}$ and so has the form

$$\mathbf{U}_1 = \nabla f_1 \times \hat{\zeta}. \quad (12.76)$$

Thus

$$\hat{y} \times \hat{\zeta} \cdot \mathbf{U}_1 = (\hat{y} \times \hat{\zeta}) \cdot (\nabla f_1 \times \hat{\zeta}) = ik_y f_1. \quad (12.77)$$

Again, taking into account the fact that the vorticity points in the ζ direction it is seen that $\Omega_1 = \Omega_{1\zeta} \hat{\zeta}$ where

$$\Omega_{1\zeta} = \hat{\zeta} \cdot \nabla \times \mathbf{U}_1 = -\nabla_{\perp}^2 f_1 \quad (12.78)$$

and now \perp means perpendicular to $\hat{\zeta}$.

Substituting for $\Omega_{1\zeta}$ in Eq.(12.73) using Eq. (12.78) gives

$$\nabla_{\perp}^2 f_1 = -\frac{ik_y b_0(x) J_{1\zeta}}{\gamma\rho_0}; \quad (12.79)$$

this equation provides the essential dynamics of fluid vortices that are antisymmetric with respect to x and driven by the torque associated with the non-conservative nature, i.e., curl, of the $\mathbf{J} \times \mathbf{B}$ force. This is essentially the same as Eq.(12.35) and the rest of the analysis is the same as for the sheet current problem except that now k_y is used instead of k and b'_0 is used instead of B'_{0y} . Since $b_0(x)$ only differs from $B_{y0}(x)$ by a constant, $b'_0 = B'_{y0}$. Thus, using Eq.(12.54) the growth rate will be

$$\gamma = 0.55 (\Delta')^{4/5} \left[\frac{\eta}{\mu_0} \right]^{3/5} \left[\frac{(k_y B'_{y0})^2}{\rho_0 \mu_0} \right]^{1/5}. \quad (12.80)$$

The global system has to be periodic in both the y and z direction in order for well-defined k_y and k_z to exist. In particular, the physical arrangement and dimensions of the global system determine the quantized spectra of k_y and k_z and so determine the allowed planes where $\mathbf{k} \cdot \mathbf{B}_0$ can vanish. As suggested earlier, the allowed planes can be considered as 'cleavage' planes where the magnetic field can most easily become unglued from the plasma.

Let us express this result in the context of toroidal geometry such as that of a tokamak. This is done by letting B_{z0} correspond to the toroidal field B_ϕ and B_y correspond to B_θ the poloidal field. The Alfvén time is now defined in terms of B_ϕ as

$$\tau_A^{-1} = \frac{B_\phi}{a \sqrt{\rho_0 \mu_0}} \quad (12.81)$$

where a is the minor radius. The safety factor, a measure of the twist, is defined as

$$q = \frac{a B_\phi}{R B_\theta} \quad (12.82)$$

so that

$$B_\theta = \frac{a B_\phi}{R q} \quad (12.83)$$

and

$$B'_{y0} \rightarrow -\frac{a B_\phi}{R q^2} q'. \quad (12.84)$$

Thus it is possible to replace $k_y \rightarrow m/a$ and

$$\frac{(k_y B'_{y0})^2}{\rho_0 \mu_0} \rightarrow \left(\frac{m a}{R q^2} q' \right)^2 \frac{1}{\tau_A}. \quad (12.85)$$

At the tearing layer $\mathbf{k} \cdot \mathbf{B} = 0$ or

$$\frac{m}{a} B_\theta + \frac{n}{R} B_\phi = 0 \quad (12.86)$$

so

$$q = -\frac{m}{n} \quad (12.87)$$

and Eq.(12.85) becomes

$$\frac{(k_y B'_{y0})^2}{\rho_0 \mu_0} \rightarrow \left(\frac{n a}{R} \frac{q'}{q} \right)^2 \frac{1}{\tau_A}. \quad (12.88)$$

Thus, Eq.(12.80) becomes

$$\gamma = 0.55 (\Delta' a)^{4/5} \tau_R^{-3/5} \tau_A^{-2/5} \left(\frac{na^2 q'}{R q} \right)^{2/5} \quad (12.89)$$

where

$$\tau_R^{-1} = \frac{\eta}{a^2 \mu_0}. \quad (12.90)$$

In the form given by Eq.(12.89), it is seen that the essential source for the tearing instability is q' . From this point of view, the 'free energy' is in the gradient of q and so as the tearing mode uses up this free energy, the q profile will be flattened.

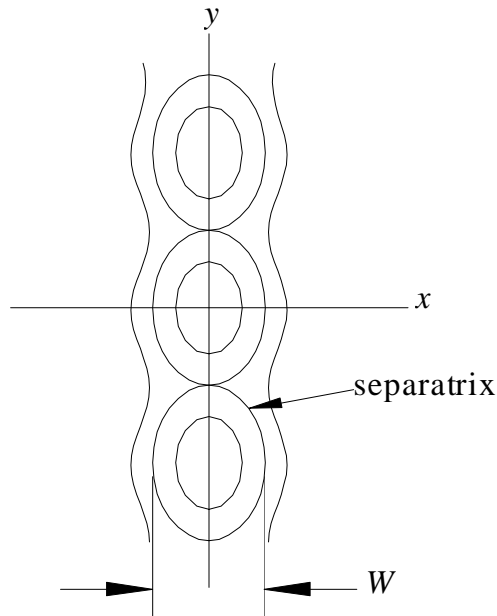


Figure 12.5: Surfaces of constant A_z showing magnetic islands and separatrix with width w .

12.6 Magnetic islands

The tearing instability changes the topology of the magnetic field and causes the formation of magnetic 'islands' (Bateman 1978). The equilibrium magnetic field has the form

$$\mathbf{B} = \bar{\mathbf{B}} + B_*(x)\hat{y} = \bar{\mathbf{B}} + xB'_*\hat{y} = \bar{\mathbf{B}} + \nabla A_{z0}(x) \times \hat{z} \quad (12.91)$$

where

$$A_{z0}(x) = \frac{x^2 B'_*}{2}. \quad (12.92)$$

It is seen that

$$\mathbf{B}_\perp \cdot \nabla A_{z0} = 0 \quad (12.93)$$

where \mathbf{B}_\perp is the component perpendicular to z . Thus, the surfaces $A_z = \text{const.}$ give the projection of the field lines in the plane perpendicular to z ; these projections correspond to the poloidal flux surfaces in toroidal geometry.

If it is assumed that $k_z \ll k_y$, so that ζ is very nearly parallel to z , then it is seen that the tearing instability adds a perturbation to A_z so that now

$$A_z(x, y) = \frac{x^2 B'_*}{2} + A_{z1} \cos k_y y. \quad (12.94)$$

A sketch of a set of surfaces of constant $A_z(x, y)$ is shown in Fig.12.5. These surfaces consist of (i) closed curves called islands, (ii) a separatrix which passes through the x point, and (iii) open outer surfaces. The width w of the separatrix can be calculated, by noting that at the x -point

$$A_{sep} = 0 + A_{z1} \quad (12.95)$$

while at the point of maximum width, $x = w/2$,

$$A_{sep} = \frac{(w/2)^2 B'_*}{2} - A_{z1}. \quad (12.96)$$

Equating these gives

$$w = 4 \sqrt{\frac{A_{z1}}{B'_*}} = 4 \sqrt{\left| \frac{B_{x1}}{k_y B'_*} \right|} \quad (12.97)$$

using $B_{x1} = ik_y A_z$. In tokamak terminology we identify $B_{x1} \rightarrow B_{r1}$ where r is the minor radius, and using Eq.(12.84), (12.87) and $k_y \rightarrow m/a$ this becomes

$$w = 4 \sqrt{\left| \frac{Rq}{nq'} \frac{B_{r1}}{B_\phi} \right|}. \quad (12.98)$$

It is important to realize that the width of the island is much larger than the width of the tearing layer. Since particles tend to be attached to magnetic flux surfaces, the formation of islands means that particles can circulate around the island, thereby causing a flattening of the pressure gradient because the pressure is constant along a magnetic field line.

12.7 Assignments

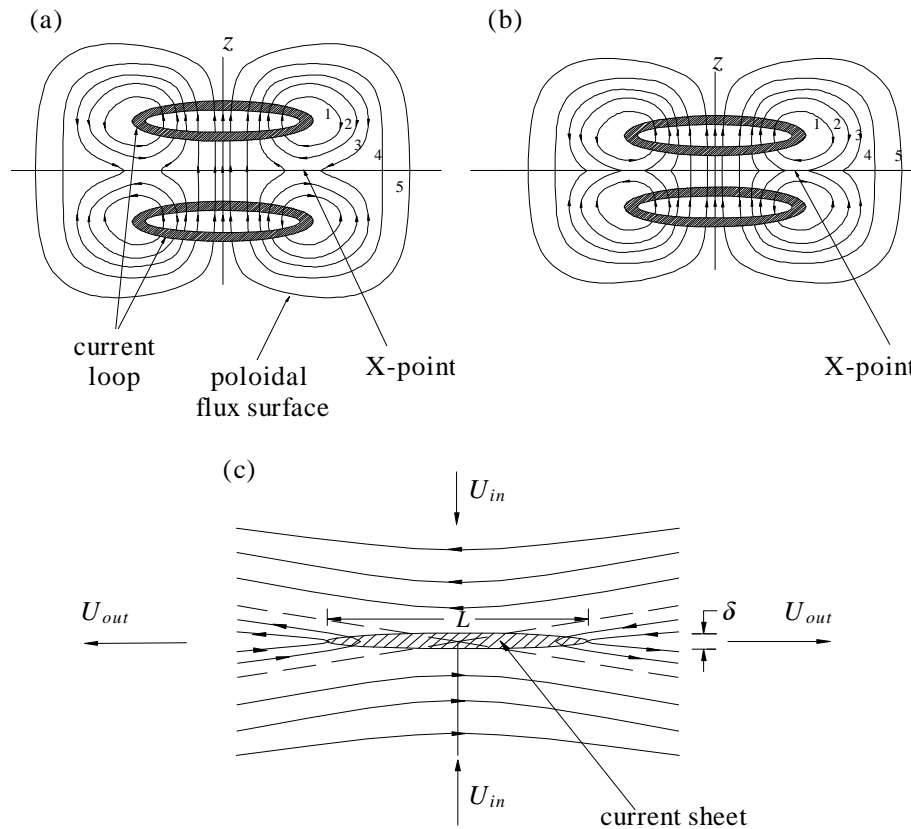


Figure 12.6: (a) Two identical coaxial current loops; (b) current loops approaching each other; (c) detail of X-point region of (b) showing inflows/outflows and current-sheet (shaded region) having nominal length L and thickness δ .

1. Sweet-Parker type reconnection (Sweet 1958, Parker 1957): Consider the two identical flux-conserving current loops shown in Fig. 12.6(a). Because the system is axisymmetric, the magnetic field can be expressed as

$$\mathbf{B} = \frac{1}{2\pi} \nabla\psi \times \nabla\phi.$$

- (a) Explain why there is an attractive force between the current loops (hint: consider the force between parallel currents or between north and south poles of two magnets).

- (b) Define private flux to be a flux surface that links only one of the current loops (examples are the flux surfaces labeled 1 and 2 in Fig.12.6(a)). Define public flux to be a flux surface that links both of the current loops (examples are flux surfaces 3,4,5 in Fig.12.6(a)). Define the X-point to be the location in the $z = 0$ plane where there is a field null as shown in Fig.12.6(a); let r_0 be the radius of the X-point. Show by sketching that as the two current loops approach each other in vacuum, a private flux surface above the midplane will merge with a private flux surface below to form a public flux surface.
- (c) Show that the flux linked by a circle in the $z = 0$ plane with radius r_0 (i.e., the circle follows the locus of the X-point) is the public flux. Argue that if the current loops approach each other, this public flux will increase at the rate that private flux is converted into public flux. By integrating Faraday's law over the surface of this circle in the z plane with radius r_0 , show that there exists a toroidal electric field at the X-point,

$$E_\phi = -\frac{1}{2\pi r_0} \frac{\partial \psi_{public}}{\partial t}$$

where $\partial \psi_{public} / \partial t$ is the rate of increase of public flux.

- (d) Now suppose that the vacuum is replaced by perfectly conducting plasma so that plasma is frozen to field lines. Show from symmetry that the plasma velocity at the x point must vanish. What is E_ϕ at the X-point if the two current loops are immersed in a plasma which satisfies the ideal Ohm's law,

$$\mathbf{E} + \mathbf{U} \times \mathbf{B} = 0.$$

Can there be any conversion of private flux into public flux in an ideal plasma? Sketch contours of private and public flux when two current loops approach each other in an ideal plasma.

- (e) Now suppose the two current loops are immersed in a non-ideal plasma which satisfies the resistive Ohm's law

$$\mathbf{E} + \mathbf{U} \times \mathbf{B} = \eta \mathbf{J}.$$

Can private flux be converted into public flux in this situation, and if so, what is the relationship between the rate of increase of public flux and the resistivity?

- (f) By writing E_ϕ , B_r , B_z , and J_ϕ in terms of the poloidal flux function show that the toroidal component of the resistive Ohm's law can be expressed as

$$\frac{\partial \psi}{\partial t} + \mathbf{U} \cdot \nabla \psi = r^2 \nabla \cdot \left(\frac{\eta}{\mu_0 r^2} \nabla \psi \right).$$

Show that this equation implies that flux convects with the plasma if $\eta = 0$, but diffuses across the plasma if $\mathbf{U} = 0$. Show that the diffusion increases if ψ develops a steep gradient at the location where $\mathbf{U} = 0$. By considering your response to (d) above, discuss how the flux gradient in the z direction might steepen in the vicinity of the X-point. Taking into account the relationship between \mathbf{J} and ψ , show that this corresponds to developing a thin sheet of current in the midplane

(current-sheet) as shown in Fig.12.6(c). Show that in order to have an X-point geometry and also satisfy Faraday's law, the flux function must have the form

$$\psi(r, z, t) = \left(1 + \frac{z^2}{2\delta^2} - \frac{(r - r_0)^2}{2L^2} \right) \psi_0 - 2\pi r E_\phi t$$

in the vicinity of the X-point; here ψ_0 is the flux at the X-point at $t = 0$ and r_0 is the radial location of the X-point. What is the relationship between δ and L in vacuum and in a resistive plasma? Is δ larger or smaller than L if the two current loops are approaching each other? If $\delta < L$ is there a current in the vicinity of the X-point? What is the direction of this current with respect to the currents in the two current loops? Will the force on the current loops from the current in the current sheet accelerate or retard the motion of the two current loops towards each other? What is the direction of E_ϕ ? Is ψ increasing or decreasing at the X-point?

- (g) Suppose that the current sheet has a nominal thickness of δ in the z direction and a nominal width of L in the r direction as shown in Fig.12.6(c). Let U_{in} be the nominal vertical velocity with which the plasma approaches the x point and let U_{out} be the nominal horizontal velocity with which the plasma leaves the x point region as shown in Fig.12.6(c). If the plasma motion is incompressible show that

$$U_{in}L \simeq U_{out}\delta. \quad (12.99)$$

- (h) Consider the transition from the ideal MHD form of Ohm's law to the form at the X-point. Argue that in the region of this transition the terms $\mathbf{U} \times \mathbf{B}$ and $\eta \mathbf{J}$ should have the same order of magnitude (this is essentially the same argument that was used to analyze Eq.(12.49)). Use this result and Ampere's law to find a relationship between ηJ , B_{in} and δ . Use this to show

$$U_{in} \sim \eta / \mu_0 \delta \quad (12.100)$$

and explain this result in terms of the convective velocity for motion of flux surfaces outside the current sheet and the "diffusive velocity" for motion of flux surfaces inside the current sheet.

- (i) Using Eq.(9.42) show that the MHD force acting on the plasma is

$$\mathbf{F}_{MHD} = - \frac{\nabla \psi}{(2\pi)^2 \mu_0} \nabla \cdot \left(\frac{1}{r^2} \nabla \psi \right)$$

Sketch the direction of this force and indicate where this force is finite (hint: consider where \mathbf{J} is finite). Estimate the work $\int \mathbf{F} \cdot d\mathbf{l}$ done on plasma accelerated through the current sheet by using relationships involving B_{in} , B_{out} , δ , and L . Use this estimate to show that

$$U_{out} \simeq v_{A,in} \quad (12.101)$$

where $v_{A,in} = B_{in} / \sqrt{\mu_0 \rho}$ is the Alfvén velocity at the input. (Hint: Let $\Delta\psi$ be the jump in flux experienced by a fluid element as it moves across the current

sheet. Note that $B_{out} \sim \Delta\psi/2\pi rL$ and $B_{in} \sim \Delta\psi/2\pi r\delta$; also note that $\nabla \cdot (r^{-2}\nabla\psi)$ can be expressed in terms of B_{in} and δ .)

- (j) By eliminating U_{in} and U_{out} between Eqs.(12.99), (12.100), and (12.101) show that

$$\frac{\delta}{L} = \frac{U_{in}}{v_{a,in}} = \frac{1}{\sqrt{S_{in}}}$$

where the inflow region Lundquist number S_{in} is defined as

$$S_{in} = \frac{\mu_0 v_{a,in} L}{\eta}$$

- (k) If the initial separation between the two current loops is also of the order of L , how much time is required for the two loops to merge, thus completing the reconnection process? Structures in the solar corona have scale lengths $L \sim 1$ -100 megameters (10^8 m) and it is observed that Alfvén wave disturbances propagate with velocities $v_A \sim 10^6$ m/s. The temperature of these structures is 10-100 eV. Assuming a nominal temperature of 50 eV, use Spitzer resistivity to calculate the nominal value of S_{in} . How long would it take for two solar current loops to merge if they are governed by the mechanism discussed here (what is the appropriate time unit to use seconds, days, weeks, years, ...?). Actual current loops change topology on time scales ranging from minutes to hours – how does this compare with the predictions of this model?

Fokker-Planck theory of collisions

13.1 Introduction

Logically, this chapter ought to be located at the beginning of Chapter 2, just after phase-space concepts had been introduced. The reason this chapter is not located there is that the theory in this chapter is too involved to be at the beginning of the book and would have delayed the introduction of important other topics that do not need the detail of this chapter.

The discussion of collisions in Chapter 1 was very approximate. Collisions were shown to scale as an inverse power of temperature, but this was based on a “one size fits all” analysis since it was assumed that the collision frequency of both slow and fast particles were nominally the same as that of a particle going at the thermal velocity. Because the collision frequency scales as v^{-3} , it is dubious to assume that the collision rates of both super-thermal and subthermal particles can be reasonably represented by a single collision frequency. A more careful averaging over velocities is clearly warranted. This is provided by a Fokker-Planck analysis due to Rosenbluth, Macdonald and Judd (1957) but if all this analysis provided was more accuracy for collision calculations, it would not be worth the considerable effort except possibly for exceptional situations where high accuracy is important. However, it turns out that more than increased accuracy results from this theory, because some new and important phenomena become evident from the analysis.

We begin the analysis by reviewing collisions between two particles. Suppose a test particle having mass m_T and charge q_T collides with a field particle having mass m_F and charge q_F . Since the electric field associated with a charge q is $\mathbf{E} = \hat{r}q/4\pi\epsilon_0r^2$ where r is the distance from the charge, the equations of motion for the respective test and field particles are

$$m_T\ddot{\mathbf{r}}_T = \frac{q_Tq_F}{4\pi\epsilon_0|\mathbf{r}_T - \mathbf{r}_F|^3}(\mathbf{r}_T - \mathbf{r}_F) \quad (13.1a)$$

$$m_F\ddot{\mathbf{r}}_F = \frac{q_Tq_F}{4\pi\epsilon_0|\mathbf{r}_T - \mathbf{r}_F|^3}(\mathbf{r}_F - \mathbf{r}_T). \quad (13.1b)$$

The center of mass vector is defined to be

$$\mathbf{R} = \frac{m_T\mathbf{r}_T + m_F\mathbf{r}_F}{m_T + m_F}. \quad (13.2)$$

Adding Eqs.(13.1a) and (13.1b) gives

$$(m_T + m_F)\dot{\mathbf{R}} = m_T\dot{\mathbf{r}}_T + m_F\dot{\mathbf{r}}_F = 0 \quad (13.3)$$

showing that the center of mass velocity $\dot{\mathbf{R}}$ is a constant of the motion and so does not change as a result of the collision. If $\Delta\dot{\mathbf{r}}_T$ and $\Delta\dot{\mathbf{r}}_F$ are defined as the change in respective velocities of the two particles during a collision, then it is seen that these changes are not independent, but are related by

$$(m_T + m_F)\Delta\dot{\mathbf{R}} = 0 = m_T\Delta\dot{\mathbf{r}}_T + m_F\Delta\dot{\mathbf{r}}_F. \quad (13.4)$$

It is useful to define the relative position vector

$$\mathbf{r} = \mathbf{r}_T - \mathbf{r}_F \quad (13.5)$$

and the reduced mass

$$\frac{1}{\mu} = \frac{1}{m_T} + \frac{1}{m_F}. \quad (13.6)$$

Then, dividing Eqs.(13.1a) and (13.1b) by their respective masses and taking the difference between the resulting equations gives an equation of motion for the relative velocity

$$\mu\ddot{\mathbf{r}} = \frac{q_T q_F}{4\pi\epsilon_0 r^2} \hat{r}. \quad (13.7)$$

Solving Eqs.(13.2) and (13.5) for \mathbf{r}_T and \mathbf{r}_F gives

$$\mathbf{r}_F = \mathbf{R} - \frac{\mu}{m_F} \mathbf{r} \quad (13.8)$$

$$\mathbf{r}_T = \mathbf{R} + \frac{\mu}{m_T} \mathbf{r}$$

and so the respective test and field velocities are

$$\dot{\mathbf{r}}_F = \dot{\mathbf{R}} - \frac{\mu}{m_F} \dot{\mathbf{r}} \quad (13.9)$$

$$\dot{\mathbf{r}}_T = \dot{\mathbf{R}} + \frac{\mu}{m_T} \dot{\mathbf{r}}. \quad (13.10)$$

Since $\Delta\dot{\mathbf{R}} = 0$ the change of the test and field particle velocities as measured in the lab frame can be related to the change in the relative velocity by

$$\Delta\dot{\mathbf{r}}_F = -\frac{\mu}{m_F} \Delta\dot{\mathbf{r}} \quad (13.11)$$

$$\Delta\dot{\mathbf{r}}_T = +\frac{\mu}{m_T} \Delta\dot{\mathbf{r}}. \quad (13.12)$$

The collision problem is first solved in the center of mass frame to find the change in the relative velocity and then the center of mass result is transformed to the lab-frame to determine the change in the lab-frame velocity of the particles.

Let us now consider a many-particle point of view. Suppose a mono-energetic beam of particles impinges upon a background plasma. Several effects are expected to occur due to collisions between the beam and the background plasma. First, there will be a slowing down of the beam as it loses momentum due to collisions. Second, there should be a spreading out of the velocity distribution of the particles in the beam since collisions will tend to diffuse the velocity of the particles in the beam. Meantime, the background plasma should be heated and also should gain momentum due to the collisions. Eventually, the beam should be so slowed down and so spread out that it becomes indistinguishable from the background plasma which will be warmer because of the energy transferred from the beam.

13.2 Statistical argument for the development of the Fokker-Planck equation

The Fokker-Planck theory (Rosenbluth et al. 1957) is based on a logical argument on how a distribution function attains its present form due to collisions at some earlier time. Consider a particle with velocity \mathbf{v} at time t that is subject to random collisions which change its velocity. We define $F(\mathbf{v}, \Delta\mathbf{v})$ as the conditional probability that if a particle has a velocity \mathbf{v} at time t , then at some later time $t + \Delta t$, collisions will have caused the particle to have velocity $\mathbf{v} + \Delta\mathbf{v}$.

Clearly at time $t + \Delta t$ the particle must have some velocity, so the sum of all the conditional probabilities must be unity, i.e., F must be normalized such that

$$\int F(\mathbf{v}, \Delta\mathbf{v}) d\Delta\mathbf{v} = 1. \quad (13.13)$$

This definition of conditional probability can be used to show how a present distribution function $f(\mathbf{v}, t)$ comes to be the way it is because of the way it was at time $t - \Delta t$. This can be expressed as

$$f(\mathbf{v}, t) = \int f(\mathbf{v} - \Delta\mathbf{v}, t - \Delta t) F(\mathbf{v} - \Delta\mathbf{v}, \Delta\mathbf{v}) d\Delta\mathbf{v} \quad (13.14)$$

which sums up all the possible ways for obtaining a given present velocity weighted by the probability of each of these ways occurring. This analysis presumes that the present status depends only on what happened during the previous collision and is independent of all events before that previous collision. A partial differential equation for f can be constructed by Taylor expanding the integrand as follows:

$$\begin{aligned} f(\mathbf{v} - \Delta\mathbf{v}, t - \Delta t) F(\mathbf{v} - \Delta\mathbf{v}, \Delta\mathbf{v}) &= f(\mathbf{v}, t) F(\mathbf{v}, \Delta\mathbf{v}) - \Delta t \frac{\partial f}{\partial t} F(\mathbf{v}, \Delta\mathbf{v}) \\ &\quad - \Delta\mathbf{v} \cdot \frac{\partial}{\partial \mathbf{v}} (f(\mathbf{v}, t) F(\mathbf{v}, \Delta\mathbf{v})) \\ &\quad + \frac{1}{2} \Delta\mathbf{v} \Delta\mathbf{v} : \frac{\partial}{\partial \mathbf{v}} \frac{\partial}{\partial \mathbf{v}} (f(\mathbf{v}, t) F(\mathbf{v}, \Delta\mathbf{v})). \end{aligned} \quad (13.15)$$

Substitution of Eq.(13.15) into Eq.(13.14) gives

$$\begin{aligned} f(\mathbf{v}, t) &= f(\mathbf{v}, t) \int F(\mathbf{v}, \Delta\mathbf{v}) d\Delta\mathbf{v} - \Delta t \frac{\partial f}{\partial t} \int F(\mathbf{v}, \Delta\mathbf{v}) d\Delta\mathbf{v} \\ &\quad - \int \Delta\mathbf{v} \cdot \frac{\partial}{\partial \mathbf{v}} (f(\mathbf{v}, t) F(\mathbf{v}, \Delta\mathbf{v})) d\Delta\mathbf{v} \\ &\quad + \frac{1}{2} \int \Delta\mathbf{v} \Delta\mathbf{v} : \frac{\partial}{\partial \mathbf{v}} \frac{\partial}{\partial \mathbf{v}} (f(\mathbf{v}, t) F(\mathbf{v}, \Delta\mathbf{v})) d\Delta\mathbf{v} \end{aligned} \quad (13.16)$$

where in the top line advantage has been taken of $f(\mathbf{v}, t)$ not depending on $\Delta\mathbf{v}$. Upon

invoking Eq.(13.13) this can be recast as

$$\frac{\partial f}{\partial t} = \left[\begin{array}{l} -\frac{\partial}{\partial \mathbf{v}} \cdot \left(\frac{\int \Delta \mathbf{v} F(\mathbf{v}, \Delta \mathbf{v}) d\Delta \mathbf{v}}{\Delta t} f(\mathbf{v}, t) \right) \\ + \frac{1}{2} \frac{\partial}{\partial \mathbf{v}} \frac{\partial}{\partial \mathbf{v}} : \left(\frac{\int \Delta \mathbf{v} \Delta \mathbf{v} F(\mathbf{v}, \Delta \mathbf{v}) d\Delta \mathbf{v}}{\Delta t} f(\mathbf{v}, t) \right) \end{array} \right]. \quad (13.17)$$

By defining

$$\left\langle \frac{\Delta \mathbf{v}}{\Delta t} \right\rangle = \frac{\int \Delta \mathbf{v} F(\mathbf{v}, \Delta \mathbf{v}) d\Delta \mathbf{v}}{\Delta t} \quad (13.18)$$

and

$$\left\langle \frac{\Delta \mathbf{v} \Delta \mathbf{v}}{\Delta t} \right\rangle = \frac{\int \Delta \mathbf{v} \Delta \mathbf{v} F(\mathbf{v}, \Delta \mathbf{v}) d\Delta \mathbf{v}}{\Delta t} \quad (13.19)$$

the standard form of the Fokker-Planck equation is obtained,

$$\frac{\partial f}{\partial t} = -\frac{\partial}{\partial \mathbf{v}} \cdot \left(\left\langle \frac{\Delta \mathbf{v}}{\Delta t} \right\rangle f(\mathbf{v}, t) \right) + \frac{1}{2} \frac{\partial}{\partial \mathbf{v}} \frac{\partial}{\partial \mathbf{v}} : \left(\left\langle \frac{\Delta \mathbf{v} \Delta \mathbf{v}}{\Delta t} \right\rangle f(\mathbf{v}, t) \right). \quad (13.20)$$

The first term gives the slowing down of a beam and is called the frictional term while the second term gives the spreading out of a beam and is called the diffusive term.

The goal now is to compute $\langle \Delta \mathbf{v} / \Delta t \rangle$ and $\langle \Delta \mathbf{v} \Delta \mathbf{v} / \Delta t \rangle$. To do this, it is necessary to consider all possible ways there can be a change in velocity $\Delta \mathbf{v}$ in time Δt and then average all values of $\Delta \mathbf{v}$ and $\Delta \mathbf{v} \Delta \mathbf{v}$ weighted according to their respective probability of occurrence. We will first evaluate $\langle \Delta \mathbf{v} / \Delta t \rangle$ and then later use the same method to evaluate $\langle \Delta \mathbf{v} \Delta \mathbf{v} / \Delta t \rangle$. The problem will first be solved in the center of mass frame and so involves a particle with reduced mass μ , speed $v_{rel} = |\mathbf{v}_T - \mathbf{v}_F|$, and impact parameter b colliding with a stationary scattering center at the origin. This was discussed in Chapter 1 and the geometry was sketched in Fig.1.3. The deflection angle θ for small angle scattering was shown to be

$$\theta = \frac{q_T q_F}{2\pi \epsilon_0 b \mu v_{rel}^2}. \quad (13.21)$$

The averaging procedure is done in two stages:

1. The effect of collisions in time Δt is calculated. The functional dependence of $\Delta \mathbf{v}$ on the scattering angle θ is determined and then used to calculate the weighted average $\Delta \mathbf{v}$ for all possible impact parameters and all possible azimuthal angles of incidence. This result is then used to calculate the weighted average change in target particle velocity in the lab frame.
2. An averaging is then performed over all possible field particle velocities weighted according to their probability, i.e., weighted according to the field particle distribution function $f_F(\mathbf{v}_F)$.

Energy is conserved in the center of mass frame and since the energy before and after the collision is entirely composed of kinetic energy, the magnitude of v_{rel}^2 must be the same before and after the collision. The collision thus has the effect of causing a simple rotation of the relative velocity vector by the angle θ . Let z be the direction of the relative velocity before the collision and let \hat{b} be the direction of the impact parameter. If $\mathbf{v}_{rel1}, \mathbf{v}_{rel2}$ are

the respective relative velocities before and after the collision, then

$$\begin{aligned}\mathbf{v}_{rel1} &= v_{rel}\hat{z} \\ \mathbf{v}_{rel2} &= v_{rel}\cos\theta\hat{z} + v_{rel}\sin\theta\hat{b}.\end{aligned}\quad (13.22)$$

Thus

$$\begin{aligned}\Delta\mathbf{v}_{rel} &= \mathbf{v}_{rel2} - \mathbf{v}_{rel1} \\ &= v_{rel}(\cos\theta - 1)\hat{z} + v_{rel}\sin\theta\hat{b} \\ &\simeq -\frac{v_{rel}\theta^2}{2}\hat{z} + v_{rel}\theta(\hat{x}\cos\phi + \hat{y}\sin\phi)\end{aligned}\quad (13.23)$$

where ϕ is the angle between the impact parameter and the x axis and the scattering angle θ is assumed to be small. The fact that the z component is negative reflects the slowing down of the particle in its initial direction of motion.

The cross section associated with impact parameter b and the range of azimuthal impact angle $d\phi$ is $bd\phi db$. In time Δt the incident particle moves a distance $v\Delta t$ and so the volume swept out for this cross-section is $bd\phi db v\Delta t$. The number of relevant field particles encountered in time Δt will be the density $f_F(\mathbf{v}_F)d\mathbf{v}_F$ of relevant field particles multiplied by this volume, i.e., $f_F(\mathbf{v}_F)d\mathbf{v}_F bd\phi db v\Delta t$ and so the change in relative velocity for all possible impact parameters and all possible azimuthal angles for a given \mathbf{v}_F will be

$$\Delta\mathbf{v}_{|all\ b, all\ \phi} = v\Delta t f_F(\mathbf{v}_F)d\mathbf{v}_F \int d\phi \int \Delta\mathbf{v} b db. \quad (13.24)$$

The limits of integration for the azimuthal angle are from 0 to 2π and the limits of integration of the impact parameter are from the 90° impact parameter to the Debye length. On writing $\Delta\mathbf{v}$ in component form, this becomes

$$\Delta\mathbf{v}_{rel|all\ b, all\ \phi} = v_{rel}\Delta t f_F(\mathbf{v}_F)d\mathbf{v}_F \int_0^{2\pi} d\phi \int_{b_{\pi/2}}^{\lambda_D} v_{rel}(\theta\cos\phi, \theta\sin\phi, -\theta^2/2) b db. \quad (13.25)$$

The x and y integrals vanish upon integration over ϕ and so

$$\begin{aligned}\Delta\mathbf{v}_{rel|all\ b, all\ \phi} &= -\hat{z}v_{rel}^2\Delta t f_F(\mathbf{v}_F)d\mathbf{v}_F \pi \int_{b_{\pi/2}}^{\lambda_D} \theta^2 b db \\ &= -\hat{z}v_{rel}^2\Delta t f_F(\mathbf{v}_F)d\mathbf{v}_F \pi \int_{b_{\pi/2}}^{\lambda_D} \left(\frac{q_T q_F}{2\pi\epsilon_0 b \mu v_{rel}^2}\right)^2 b db \\ &= -\hat{z}\Delta t f_F(\mathbf{v}_F)d\mathbf{v}_F \frac{q_T^2 q_F^2}{4\pi\epsilon_0^2 \mu^2 v_{rel}^2} \ln\Lambda\end{aligned}\quad (13.26)$$

where $\Lambda = \lambda_D/b_{\pi/2}$.

Using Eq.(13.12) the above expression can be transformed to give the test particle velocity change to be

$$\begin{aligned}\Delta\mathbf{v}_T|all\ b, all\ \phi &= -\hat{z}\Delta t f_F(\mathbf{v}_F)d\mathbf{v}_F \frac{q_T^2 q_F^2}{4\pi\epsilon_0^2 \mu m_T v_{rel}^2} \ln\Lambda \\ &= -\Delta t \frac{q_T^2 q_F^2 \ln\Lambda}{4\pi\epsilon_0^2 \mu m_T} \frac{(\mathbf{v}_T - \mathbf{v}_F)}{|\mathbf{v}_T - \mathbf{v}_F|^3} f_F(\mathbf{v}_F)d\mathbf{v}_F.\end{aligned}\quad (13.27)$$

This result was for a particular value of \mathbf{v}_F and summing over all possible \mathbf{v}_F weighted according to their probability, gives

$$\Delta \mathbf{v}_T |_{\text{all } b, \text{ all } \phi, \text{ all } \mathbf{v}_F} = -\Delta t \frac{q_T^2 q_F^2 \ln \Lambda}{4\pi \varepsilon_0^2 \mu m_T} \int \frac{\mathbf{v}_{rel}}{v_{rel}^3} f_F(\mathbf{v}_F) d\mathbf{v}_F. \quad (13.28)$$

The integrand can be expressed in a simpler form by considering that

$$\frac{\partial r}{\partial \mathbf{r}} = \left(\hat{x} \frac{\partial}{\partial x} + \hat{y} \frac{\partial}{\partial y} + \hat{z} \frac{\partial}{\partial z} \right) \sqrt{x^2 + y^2 + z^2} = \frac{\mathbf{r}}{r} \quad (13.29)$$

and also $\partial/\partial \mathbf{v}_T = \partial/\partial \mathbf{v}_{rel}$. Thus

$$\frac{\partial v_{rel}}{\partial \mathbf{v}_T} = \frac{\mathbf{v}_{rel}}{v_{rel}} \quad (13.30)$$

and

$$\frac{\partial}{\partial \mathbf{v}_T} \frac{1}{v_{rel}} = -\frac{1}{v_{rel}^2} \frac{\mathbf{v}_{rel}}{v_{rel}}. \quad (13.31)$$

Equation (13.28) can therefore be written as

$$\Delta \mathbf{v}_T |_{\text{all } b, \text{ all } \phi, \text{ all } \mathbf{v}_F} = \Delta t \frac{q_T^2 q_F^2 \ln \Lambda}{4\pi \varepsilon_0^2 \mu m_T} \frac{\partial}{\partial \mathbf{v}_T} \int \frac{1}{v_{rel}} f_F(\mathbf{v}_F) d\mathbf{v}_F. \quad (13.32)$$

The $\partial/\partial \mathbf{v}_T$ has been factored out of the integral because \mathbf{v}_T is independent of \mathbf{v}_F , the variable of integration. Since \mathbf{v}_F is a dummy variable, it can be replaced by \mathbf{v}' and since \mathbf{v}_T is the velocity of the given incident particle, the subscript T can be dropped. After making these re-arrangements we obtain the desired result,

$$\left\langle \frac{\Delta \mathbf{v}}{\Delta t} \right\rangle = \frac{q_T^2 q_F^2 \ln \Lambda}{4\pi \varepsilon_0^2 \mu m_T} \frac{\partial}{\partial \mathbf{v}} \int \frac{f_F(\mathbf{v}')}{|\mathbf{v} - \mathbf{v}'|} d\mathbf{v}'. \quad (13.33)$$

The averaging procedure for $\Delta \mathbf{v} \Delta \mathbf{v}$ is performed in a similar manner, starting by noting that

$$\Delta \mathbf{v} \Delta \mathbf{v} = (\theta \cos \phi, \theta \sin \phi, -\theta^2/2) (\theta \cos \phi, \theta \sin \phi, -\theta^2/2) \quad (13.34)$$

and so Eq.(13.25) is replaced by

$$\begin{aligned} \Delta \mathbf{v}_{rel} \Delta \mathbf{v}_{rel} |_{\text{all } b, \text{ all } \phi} &= v_{rel} \Delta t f_F(\mathbf{v}_F) d\mathbf{v}_F \int_0^{2\pi} d\phi \int_{b_{\pi/2}}^{\lambda_D} b db \times \\ &v_{rel}^2 (\theta \cos \phi, \theta \sin \phi, -\theta^2/2) (\theta \cos \phi, \theta \sin \phi, -\theta^2/2). \end{aligned} \quad (13.35)$$

The terms linear in $\sin \phi$ or $\cos \phi$ vanish upon performing the ϕ integration. Also, the $\hat{z}\hat{z}$ term scales as θ^4 and so may be neglected relative to the $\hat{x}\hat{x}$ and $\hat{y}\hat{y}$ terms which scale as

θ^2 . Thus, we obtain

$$\begin{aligned}
\Delta \mathbf{v}_{rel} \Delta \mathbf{v}_{rel} |_{\text{all } b, \phi} &= v_{rel}^3 \Delta t f_F(\mathbf{v}_F) d\mathbf{v}_F \int_0^{2\pi} d\phi \int_{b_{\pi/2}}^{\lambda_D} \theta^2 (\hat{x}\hat{x} \cos^2 \phi + \hat{y}\hat{y} \sin^2 \phi) b db \\
&= v_{rel}^3 \Delta t f_F(\mathbf{v}_F) d\mathbf{v}_F \pi (\hat{x}\hat{x} + \hat{y}\hat{y}) \int_{b_{\pi/2}}^{\lambda_D} \theta^2 b db \\
&= \Delta t f_F(\mathbf{v}_F) d\mathbf{v}_F (\hat{x}\hat{x} + \hat{y}\hat{y}) \frac{q_T^2 q_F^2 \ln \Lambda}{4\pi \varepsilon_0^2 \mu^2 v_{rel}}. \tag{13.36}
\end{aligned}$$

Since \mathbf{v}_{rel} defines the z direction, we may write

$$\hat{x}\hat{x} + \hat{y}\hat{y} = \mathbf{I} - \frac{\mathbf{v}_{rel} \mathbf{v}_{rel}}{v_{rel}^2} \tag{13.37}$$

where \mathbf{I} is the unit tensor. Thus,

$$\Delta \mathbf{v}_{rel} \Delta \mathbf{v}_{rel} |_{\text{all } b, \text{ all } \phi} = \Delta t \frac{q_T^2 q_F^2 \ln \Lambda}{4\pi \varepsilon_0^2 \mu^2} f_F(\mathbf{v}_F) d\mathbf{v}_F \left(\frac{v_{rel}^2 \mathbf{I} - \mathbf{v}_{rel} \mathbf{v}_{rel}}{v_{rel}^3} \right). \tag{13.38}$$

Using Eq.(13.12) this can be transformed to give

$$\Delta \mathbf{v}_T \Delta \mathbf{v}_T |_{\text{all } b, \text{ all } \phi} = \Delta t \frac{q_T^2 q_F^2 \ln \Lambda}{4\pi \varepsilon_0^2 m_T^2} f_F(\mathbf{v}_F) d\mathbf{v}_F \left(\frac{v_{rel}^2 \mathbf{I} - \mathbf{v}_{rel} \mathbf{v}_{rel}}{v_{rel}^3} \right). \tag{13.39}$$

The tensor may be expressed in a simpler form by noting

$$\begin{aligned}
\frac{\partial}{\partial \mathbf{v}_T} \frac{\partial v_{rel}}{\partial \mathbf{v}_T} &= \frac{\partial}{\partial \mathbf{v}_T} \frac{\mathbf{v}_{rel}}{v_{rel}} \\
&= \frac{\mathbf{I}}{v_{rel}} - \frac{\mathbf{v}_{rel} \mathbf{v}_{rel}}{v_{rel}^3} \\
&= \frac{v_{rel}^2 \mathbf{I} - \mathbf{v}_{rel} \mathbf{v}_{rel}}{v_{rel}^3}. \tag{13.40}
\end{aligned}$$

Inserting Eq.(13.40) in Eq.(13.39) and then integrating over all the field particles shows that

$$\left\langle \frac{\Delta \mathbf{v}_T \Delta \mathbf{v}_T}{\Delta t} \right\rangle = \frac{q_T^2 q_F^2 \ln \Lambda}{4\pi \varepsilon_0^2 m_T^2} \int f_F(\mathbf{v}_F) d\mathbf{v}_F \frac{\partial}{\partial \mathbf{v}_T} \frac{\partial}{\partial \mathbf{v}_T} |\mathbf{v}_T - \mathbf{v}_F|. \tag{13.41}$$

However, \mathbf{v}_T is constant in the integrand and so $\partial/\partial \mathbf{v}_T$ may be factored from the integral. Dropping the subscript T from the velocity and changing \mathbf{v}_F to be the integration variable \mathbf{v}' this can be re-written as

$$\left\langle \frac{\Delta \mathbf{v} \Delta \mathbf{v}}{\Delta t} \right\rangle = \frac{q_T^2 q_F^2 \ln \Lambda}{4\pi \varepsilon_0^2 m_T^2} \frac{\partial}{\partial \mathbf{v}} \frac{\partial}{\partial \mathbf{v}} \int |\mathbf{v} - \mathbf{v}'| f_F(\mathbf{v}') d\mathbf{v}'. \tag{13.42}$$

It is convenient to define the Rosenbluth potentials

$$g_F(\mathbf{v}) = \int |\mathbf{v} - \mathbf{v}'| f_F(\mathbf{v}') d\mathbf{v}' \tag{13.43}$$

$$h_F(\mathbf{v}) = \frac{m_T}{\mu} \int \frac{f_F(\mathbf{v}')}{|\mathbf{v} - \mathbf{v}'|} d\mathbf{v}' \tag{13.44}$$

in which case

$$\begin{aligned}\left\langle \frac{\Delta \mathbf{v}}{\Delta t} \right\rangle &= \frac{q_T^2 q_F^2 \ln \Lambda}{4\pi \varepsilon_0^2 m_T^2} \frac{\partial h_F}{\partial \mathbf{v}} \\ \left\langle \frac{\Delta \mathbf{v} \Delta \mathbf{v}}{\Delta t} \right\rangle &= \frac{q_T^2 q_F^2 \ln \Lambda}{4\pi \varepsilon_0^2 m_T^2} \frac{\partial^2 g_F}{\partial \mathbf{v} \partial \mathbf{v}}.\end{aligned}\quad (13.45)$$

The Fokker-Planck equation, Eq.(13.20) thus becomes

$$\frac{\partial f_T}{\partial t} = \sum_{F=i,e} \frac{q_T^2 q_F^2 \ln \Lambda}{4\pi \varepsilon_0^2 m_T^2} \left[-\frac{\partial}{\partial \mathbf{v}} \cdot \left(f_T \frac{\partial h_F}{\partial \mathbf{v}} \right) + \frac{1}{2} \frac{\partial}{\partial \mathbf{v}} \frac{\partial}{\partial \mathbf{v}} : \left(f_T \frac{\partial^2 g_F}{\partial \mathbf{v} \partial \mathbf{v}} \right) \right]. \quad (13.46)$$

The first term on the right hand side is a friction term which slows down the mean velocity associated with f_T while the second term is an isotropization term which spreads out (i.e., diffuses) the velocity distribution described by f_T . The right hand side of Eq.(13.46) thus gives the rate of change of the distribution function due to collisions and so is the correct quantity to put on the right hand side of Eq.(2.12).

13.2.1 Slowing down

Mean velocity is defined by

$$\mathbf{u} = \frac{\int \mathbf{v} f d\mathbf{v}}{n} \quad (13.47)$$

where $n = \int f d\mathbf{v}$. The rate of change of the mean velocity of species T is thus found by taking the first velocity moment of Eq.(13.46). Integration by parts on the right hand side terms respectively give

$$-\int \mathbf{v} \frac{\partial}{\partial \mathbf{v}} \cdot \left(f_T \frac{\partial h_F}{\partial \mathbf{v}} \right) d\mathbf{v} = \int f_T \frac{\partial h_F}{\partial \mathbf{v}} d\mathbf{v} \quad (13.48)$$

and

$$\int \mathbf{v} \frac{\partial}{\partial \mathbf{v}} \frac{\partial}{\partial \mathbf{v}} : \left(f_T \frac{\partial^2 g_F}{\partial \mathbf{v} \partial \mathbf{v}} \right) d\mathbf{v} = -\int \frac{\partial}{\partial \mathbf{v}} \cdot \left(f_T \frac{\partial^2 g_F}{\partial \mathbf{v} \partial \mathbf{v}} \right) d\mathbf{v} = 0 \quad (13.49)$$

where Gauss's theorem has been used in Eq.(13.49). The first velocity moment of Eq.(13.46) is therefore

$$\frac{\partial \mathbf{u}_T}{\partial t} = \sum_{F=i,e} \frac{q_T^2 q_F^2 \ln \Lambda}{4\pi \varepsilon_0^2 n_T m_T^2} \int f_T \frac{\partial h_F}{\partial \mathbf{v}} d\mathbf{v}. \quad (13.50)$$

Let us now suppose that the test particles consist of a mono-energetic beam so that

$$f_T(\mathbf{v}) = n_T \delta(\mathbf{v} - \mathbf{u}_0). \quad (13.51)$$

In this case Eq.(13.50) becomes

$$\frac{\partial \mathbf{u}_T}{\partial t} = \sum_{F=i,e} \frac{q_T^2 q_F^2 \ln \Lambda}{4\pi \varepsilon_0^2 m_T^2} \left(\frac{\partial h_F}{\partial \mathbf{v}} \right)_{\mathbf{v}=\mathbf{u}_0}. \quad (13.52)$$

Let us further suppose that the field particles have a Maxwellian distribution so that

$$f_F(\mathbf{v}) = n_F \left(\frac{m_F}{2\pi \kappa T_F} \right)^{3/2} \exp(-m_F v^2 / 2\kappa T_F) \quad (13.53)$$

and so, using Eq.(13.44),

$$h_F(\mathbf{v}) = \frac{n_F m_T}{\mu} \left(\frac{m_F}{2\pi\kappa T_F} \right)^{3/2} \int \frac{\exp(-m_F v'^2/2\kappa T_F)}{|\mathbf{v} - \mathbf{v}'|} d\mathbf{v}'. \quad (13.54)$$

The velocity integral in Eq.(13.54) can be evaluated using standard means (see assignments) to obtain

$$h_F(\mathbf{v}) = \frac{n_F m_T}{\mu v} \operatorname{erf} \left(\sqrt{\frac{m_F}{2\kappa T_F}} v \right) \quad (13.55)$$

where

$$\operatorname{erf}(x) = \frac{2}{\sqrt{\pi}} \int_0^x \exp(-w^2) dw \quad (13.56)$$

is the Error Function.

Thus, Eq.(13.52) becomes

$$\begin{aligned} \frac{\partial \mathbf{u}_T}{\partial t} = & \frac{n_i q_T^2 q_i^2 \ln \Lambda}{4\pi\epsilon_0^2 m_T^2} \frac{m_T}{\mu_i} \left\{ \frac{\partial}{\partial \mathbf{v}} \left[v^{-1} \operatorname{erf} \left(\sqrt{\frac{m_i}{2\kappa T_i}} v \right) \right] \right\}_{\mathbf{v}=\mathbf{u}_0} \\ & + \frac{n_e q_T^2 q_e^2 \ln \Lambda}{4\pi\epsilon_0^2 m_T^2} \frac{m_T}{\mu_e} \left\{ \frac{\partial}{\partial \mathbf{v}} \left[v^{-1} \operatorname{erf} \left(\sqrt{\frac{m_e}{2\kappa T_e}} v \right) \right] \right\}_{\mathbf{v}=\mathbf{u}_0} \end{aligned} \quad (13.57)$$

where $\mu_{i,e}^{-1} = m_{i,e}^{-1} + m_T^{-1}$.

This can be further simplified by noting (i) quasi-neutrality implies

$$n_i Z q_i + n_e q_e = 0 \quad (13.58)$$

where Z is the charge of the ions, (ii) the masses are related by

$$\frac{m_T}{\mu_{i,e}} = 1 + \frac{m_T}{m_{i,e}}, \quad (13.59)$$

and (iii) the velocity gradient of the Error Function must be in the direction of \mathbf{u}_0 because that is the only direction there is in the problem. Using these relationships and realizing that both the left and right sides are in the direction of \mathbf{u} , Eq.(13.57) becomes

$$\begin{aligned} \frac{\partial u}{\partial t} = & \frac{n_e e^2 \ln \Lambda}{4\pi\epsilon_0^2} \frac{q_T^2}{m_T^2} \left[Z \left(1 + \frac{m_T}{m_i} \right) \frac{d}{du} \left(\frac{\operatorname{erf} \left(\sqrt{\frac{m_i}{2\kappa T_i}} u \right)}{u} \right) \right. \\ & \left. + \left(1 + \frac{m_T}{m_e} \right) \frac{d}{du} \left(\frac{\operatorname{erf} \left(\sqrt{\frac{m_e}{2\kappa T_e}} u \right)}{u} \right) \right]. \end{aligned} \quad (13.60)$$

Let us define

$$\xi_{i,e} = \sqrt{\frac{m_{i,e}}{2\kappa T_{i,e}}} u \quad (13.61)$$

which is the ratio of the beam velocity to the thermal velocity of the ions or electrons. The slowing down relationship can then be expressed as

$$\begin{aligned} \frac{\partial u}{\partial t} = & \frac{n_e e^2 \ln \Lambda}{4\pi \epsilon_0^2} \frac{q_T^2}{m_T^2} \left[Z \left(1 + \frac{m_T}{m_i} \right) \frac{m_i}{2\kappa T_i} \frac{d}{d\xi_i} \left(\frac{\text{erf}(\xi_i)}{\xi_i} \right) \right. \\ & \left. + \left(1 + \frac{m_T}{m_e} \right) \frac{m_e}{2\kappa T_e} \frac{d}{d\xi_e} \left(\frac{\text{erf}(\xi_e)}{\xi_e} \right) \right]. \end{aligned} \quad (13.62)$$

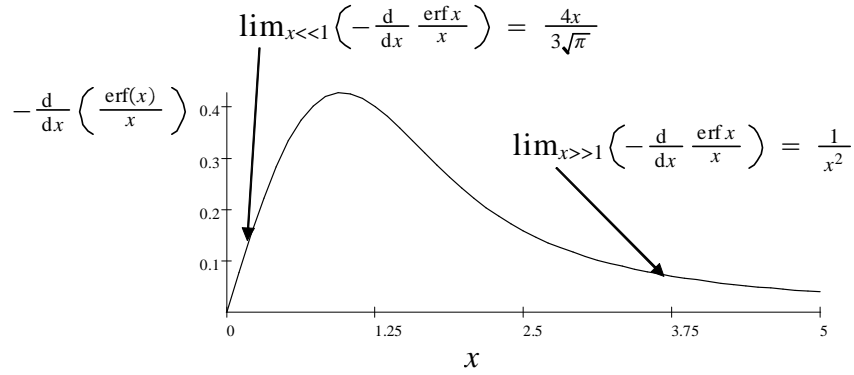


Figure 13.1: Plot of $-(x^{-1} \text{erf } x)'$ v. x .

Figure 13.1 plots $-(\text{erf}(x)/x)'$ as a function of x ; this quantity has a maximum when $x = 0.9$ indicating that the friction increases with respect to x when x is less than 0.9 but decreases with respect to x when x exceeds this value. Examination of this figure suggests that the function has a linear dependence for x well to the left of the maximum and varies as some inverse power of x well to the right of the maximum.

This conjecture is verified by noting that Eq.(13.56) has the limiting values

$$\begin{aligned} \lim_{x \ll 1} \text{erf}(x) & \simeq \frac{2}{\sqrt{\pi}} \int_0^x (1-w^2)dw = \frac{2}{\sqrt{\pi}} \left(x - \frac{x^3}{3} \right) \\ \lim_{x \gg 1} \text{erf}(x) & \simeq 1 \end{aligned} \quad (13.63)$$

and so

$$\lim_{x \ll 1} \left(-\frac{d}{dx} \frac{\text{erf } x}{x} \right) = \frac{4x}{3\sqrt{\pi}} \quad (13.64a)$$

$$\lim_{x \gg 1} \left(-\frac{d}{dx} \frac{\text{erf } x}{x} \right) = \frac{1}{x^2} \quad (13.64b)$$

which is consistent with the figure.

The existence of these two different asymptotic limits according to the ratio of the test particle velocity (i.e., beam velocity) to the thermal velocity indicates three distinct regimes can occur, namely:

1. Test particle is much faster than both ion and electron thermal velocities, that is $\xi_i, \xi_e \gg 1$.
2. Test particle is much slower than both ion and electron thermal velocities, that is $\xi_i, \xi_e \ll 1$.
3. Test particle is much faster than the ion thermal velocity, but much slower than the electron thermal velocity, i.e., $\xi_i \gg 1$ and $\xi_e \ll 1$.

A nominal slowing down time can be defined by writing the generic slowing down equation

$$\frac{\partial u}{\partial t} = -\frac{u}{\tau_s} \quad (13.65)$$

so

$$\tau_s = -\frac{u}{\partial u / \partial t} \quad (13.66)$$

this can be used to compare slowing down of test particles in the three situations listed above.

Test particle faster than both electrons, ions

Here the limit given by Eq.(13.64b) is used for both electrons and ions so that the slowing down becomes

$$\frac{\partial u}{\partial t} = -\frac{n_e e^2 \ln \Lambda}{4\pi \varepsilon_0^2} \frac{q_T^2}{m_T^2} \frac{Z \left(1 + \frac{m_T}{m_i}\right) + \left(1 + \frac{m_T}{m_e}\right)}{u^2} \quad (13.67)$$

and so

$$\tau_s \simeq \frac{4\pi \varepsilon_0^2}{n_e e^2 \ln \Lambda} \frac{m_T^2}{q_T^2} \frac{u^3}{Z + 1 + \frac{m_T}{m_e}} \quad (13.68)$$

since $1/m_e \gg 1/m_i$. Equation (13.67) shows that if the test particle beam is composed of electrons, the ion friction scales as $Z/(Z+2)$ of the total friction while the electron friction scales as $2/(2+Z)$ of the total friction. In contrast, if the test particle is an ion, the friction is almost entirely from collisions with electrons. The slowing down time is insensitive to the plasma temperature except for the weak $\ln \Lambda$ dependence. The slowing down time for ions is of the order of m_i/m_e times longer than the slowing down time for electrons having the same velocity.

Test particle slower than both electrons, ions

Here the limit given by Eq.(13.64a) is used for both electrons and ions so that the slowing down equation becomes

$$\frac{\partial u}{\partial t} = -\frac{u}{3\sqrt{\pi}} \frac{n_e e^2 \ln \Lambda}{\pi \varepsilon_0^2} \frac{q_T^2}{m_T^2} \left(Z \left(1 + \frac{m_T}{m_i}\right) \left(\frac{m_i}{2\kappa T_i}\right)^{3/2} + \left(1 + \frac{m_T}{m_e}\right) \left(\frac{m_e}{2\kappa T_e}\right)^{3/2} \right) \quad (13.69)$$

and the slowing down time becomes

$$\tau_s = \frac{3\sqrt{\pi}\pi\epsilon_0^2 m_T^2}{n_e e^2 \ln \Lambda q_T^2} \frac{1}{\left(Z \left(1 + \frac{m_T}{m_i} \right) \left(\frac{m_i}{2\kappa T_i} \right)^{3/2} + \left(1 + \frac{m_T}{m_e} \right) \left(\frac{m_e}{2\kappa T_e} \right)^{3/2} \right)}. \quad (13.70)$$

The temperature terms scale as the inverse cube of the thermal velocity and so if the ion and electron temperatures are the same order of magnitude, then the ion contribution dominates. Thus, the slowing down is mainly done by collisions with ions and the slowing down time is

$$\tau_s \simeq \frac{3\sqrt{\pi}\pi\epsilon_0^2 m_T^2 (2\kappa T_i/m_i)^{3/2}}{n_e e^2 \ln \Lambda q_T^2 Z \left(1 + \frac{m_T}{m_i} \right)}. \quad (13.71)$$

The beam takes a longer time to slow down in hotter plasmas.

Intermediate case: beam faster than ions, slower than electrons

In this case, the slowing down equation becomes

$$\frac{\partial u}{\partial t} = -\frac{n_e e^2 \ln \Lambda q_T^2}{4\pi\epsilon_0^2 m_T^2} \left(Z \left(1 + \frac{m_T}{m_i} \right) \frac{1}{u^2} + \left(1 + \frac{m_T}{m_e} \right) \left(\frac{m_e}{2\kappa T_e} \right)^{3/2} \frac{4u}{3\sqrt{\pi}} \right) \quad (13.72)$$

and the slowing down time is

$$\tau_s = \frac{4\pi\epsilon_0^2 m_T^2}{n_e q_T^2 e^2 \ln \Lambda \left(Z \left(1 + \frac{m_T}{m_i} \right) \frac{1}{u^3} + \frac{4}{3\sqrt{\pi}} \left(1 + \frac{m_T}{m_e} \right) \left(\frac{m_e}{2\kappa T_e} \right)^{3/2} \right)}. \quad (13.73)$$

13.3 Electrical resistivity

If a uniform steady electric field is imposed on a plasma this electric field will accelerate the ions and electrons in opposite directions. The accelerated particles will collide with other particles and this frictional drag will oppose the acceleration so that a steady state might be achieved where the accelerating force balances the drag force. The electric field causes equal and opposite momentum gains by the electrons and ions and therefore does not change the net momentum of the entire plasma. Furthermore, electron-electron collisions cannot change the total momentum of all the electrons and ion-ion collisions cannot change the momentum of all the ions. The only way for the entirety of electrons to lose momentum is by collisions with ions.

Let us assume that an equilibrium is attained where the electrons and ions have shifted Maxwellian distribution functions

$$\begin{aligned} f_i(\mathbf{v}) &= \frac{n_i}{\pi^{3/2} (2\kappa T_i/m_i)^{3/2}} \exp\left(-m_i (\mathbf{v} - \mathbf{u}_i)^2 / 2\kappa T_i\right) \\ f_e(\mathbf{v}) &= \frac{n_e}{\pi^{3/2} (2\kappa T_e/m_e)^{3/2}} \exp\left(-m_e (\mathbf{v} - \mathbf{u}_e)^2 / 2\kappa T_e\right). \end{aligned} \quad (13.74)$$

The current density will be

$$\mathbf{J} = n_i q_i \mathbf{u}_i + n_e q_e \mathbf{u}_e. \quad (13.75)$$

It is convenient to transform to a frame moving with the electrons, i.e., with the velocity \mathbf{u}_e . In this frame the electron mean velocity will be zero and the ion mean velocity will be $\mathbf{u}_{rel} = \mathbf{u}_i - \mathbf{u}_e$. The current density remains the same because it is proportional to \mathbf{u}_{rel} which is frame-independent. The distribution functions in this frame will be

$$\begin{aligned} f_i(\mathbf{v}) &= \frac{n_i}{\pi^{3/2} (2\kappa T_i / m_i)^{3/2}} \exp\left(-m_i (\mathbf{v} - \mathbf{u}_{rel})^2 / 2\kappa T_i\right) \\ f_e(\mathbf{v}) &= \frac{n_e}{\pi^{3/2} (2\kappa T_e / m_e)^{3/2}} \exp(-m_e v^2 / 2\kappa T_e). \end{aligned} \quad (13.76)$$

Since the ion thermal velocity is much smaller than the electron thermal velocity, the ion distribution function is much narrower than the electron distribution function and the ions can be considered as a mono-energetic beam impinging upon the electrons. Using Eq.(13.57), the net force on this ion beam due to the combination of frictional drag on electrons and acceleration due to the electric field is

$$m_i \frac{\partial \mathbf{u}_{rel}}{\partial t} = \frac{n_e q_i^2 q_e^2 \ln \Lambda}{4\pi \epsilon_0^2 \mu_e} \left\{ \frac{\partial}{\partial \mathbf{v}} \left[v^{-1} \operatorname{erf} \left(\sqrt{\frac{m_e}{2\kappa T_e}} v \right) \right] \right\}_{\mathbf{v}=\mathbf{u}_{rel}} + q_i \mathbf{E}. \quad (13.77)$$

In steady-state the two terms on the right hand side balance each other in which case

$$\mathbf{E} = -\frac{n_e q_i \epsilon^2 \ln \Lambda}{4\pi \epsilon_0^2 \mu_e} \left\{ \frac{\partial}{\partial \mathbf{v}} \left[v^{-1} \operatorname{erf} \left(\sqrt{\frac{m_e}{2\kappa T_e}} v \right) \right] \right\}_{\mathbf{v}=\mathbf{u}_{rel}}. \quad (13.78)$$

If u_{rel} is much smaller than the electron thermal velocity, then Eq.(13.64a) can be used to obtain

$$\mathbf{E} = \frac{n_e q_i \epsilon^2 \ln \Lambda}{3\sqrt{\pi} \pi \epsilon_0^2 m_e} \frac{\mathbf{u}_{rel}}{(2\kappa T_e / m_e)^{3/2}} = \frac{Z e^2 m_e^{1/2} \ln \Lambda}{3\sqrt{\pi} \pi \epsilon_0^2} \frac{\mathbf{J}}{(2\kappa T_e)^{3/2}} \quad (13.79)$$

where $\mathbf{u}_{rel} = \mathbf{J} / n_e e$ and $\mu_e^{-1} = 1/m_i + 1/m_e \simeq 1/m_e$ have been used. Equation (13.79) can be used to define the electrical resistivity

$$\eta = \frac{Z e^2 m_e^{1/2} \ln \Lambda}{3\sqrt{\pi} \pi \epsilon_0^2 (2\kappa T_e)^{3/2}} \quad (13.80)$$

so that

$$\mathbf{E} = \eta \mathbf{J}. \quad (13.81)$$

If the temperature is expressed in terms of electron volts then $\kappa = e$ and the resistivity is

$$\eta = 1.03 \times 10^{-4} \frac{Z \ln \Lambda}{T_e^{3/2}} \text{ Ohm-m.} \quad (13.82)$$

13.4 Runaway electric field

The evaluation of the error function in Eq.(13.78) involved the assumption that u_{rel} , the relative drift between the electron and ion mean velocities, is much smaller than the electron thermal velocity. This assumption implies that $-(x^{-1} \operatorname{erf} x)' \simeq 4x/3\sqrt{\pi}$, so that x lies well to the left of 0.9 in the curve plotted in Fig.13.1. Consideration of Fig.13.1 shows that $-(x^{-1} \operatorname{erf} x)'$ has a maximum value of 0.43 which occurs when $x = 0.9$ so that Eq.(13.78) cannot be satisfied if (Dreicer 1959)

$$E > \max \left\{ -\frac{n_e q_i e^2 \ln \Lambda}{4\pi\epsilon_0^2 m_e} \frac{\partial}{\partial v} \left[v^{-1} \operatorname{erf} \left(\sqrt{\frac{m_e}{2\kappa T_e}} v \right) \right] \right\} = 0.43 \frac{n_e Z e^3 \ln \Lambda}{8\pi\epsilon_0^2 \kappa T_e}. \quad (13.83)$$

If the electron temperature is expressed in terms of electron volts, attaining a balance between the acceleration due to the electric field and frictional drag due becomes impossible if

$$E > E_{Dreicer} \quad (13.84)$$

where the Dreicer electric field is defined by

$$\begin{aligned} E_{Dreicer} &= 0.43 \frac{n_e Z e^3 \ln \Lambda}{8\pi\epsilon_0^2 \kappa T_e} \\ &= 5.6 \times 10^{-18} n_e Z \frac{\ln \Lambda}{T_e} \text{ V/m}. \end{aligned} \quad (13.85)$$

If the electric field exceeds $E_{Dreicer}$ then the frictional drag lies to the right of the maximum in Fig. 13.1. No equilibrium is possible in this case as can be seen by considering the sequence of collisions of a nominal particle. The acceleration due to E between collisions causes the particle to go faster, but since it is to the right of the maximum, the particle has less drag when it goes faster. If the particle has less drag, then it will have a longer mean free path between collisions and so be accelerated to an even higher velocity. The particle velocity will therefore increase without bound if the system is infinite and uniform. In reality, the particle might exit the system if the system is finite or it might radiate energy. Very high, even relativistic velocities can easily develop in runaway situations.

13.5 Assignments

1. Evaluate the integral in Eq.(13.54) and show that it leads to Eq.(13.55). *Hint:* Since \mathbf{v} is a fixed parameter in the integral, let the direction of \mathbf{v} define the axis of a spherical polar coordinate system. Let $\boldsymbol{\xi} = \mathbf{v}' - \mathbf{v}$ and let θ be the angle between $\boldsymbol{\xi}$ and \mathbf{v} . Then note that $(v')^2 = \xi^2 + 2\boldsymbol{\xi} \cdot \mathbf{v} + v^2$ and that $d\mathbf{v}' = d\boldsymbol{\xi}$. Express $d\boldsymbol{\xi}$ in spherical polar coordinates and let $x = \cos \theta$.
2. Interaction of a low density, fast electron beam with a cold background plasma. Assume that the velocity of a beam of electrons impinging on a plasma is much faster than the velocities of the background electrons and ions. The ions have charge Z so that, ignoring the beam density, the quasineutrality condition is $Zn_i = n_e$.

- (a) Show that the Rosenbluth
- h
- potential can be approximated as

$$h_F(\mathbf{v}) = \frac{m_T}{\mu} \int \frac{f_F(\mathbf{v}')}{|\mathbf{v} - \mathbf{v}'|} d\mathbf{v}'$$

$$\simeq \frac{m_e n_F}{v\mu}$$

where

$$\frac{1}{\mu} = \frac{1}{m_e} + \frac{1}{m_F}.$$

What is the form of $h_F(\mathbf{v})$ for beam electrons interacting with background plasma (i) electrons and (ii) ions?

- (b) By approximating

$$(v^2 - 2\mathbf{v} \cdot \mathbf{v}' + v'^2)^{1/2} = v \left(1 - \frac{\mathbf{v} \cdot \mathbf{v}'}{v^2} + \frac{v'^2}{2v^2} \right)$$

where the beam velocity v is much larger than the background species velocity v' , show that the Rosenbluth g potential can be approximated as

$$g_F(\mathbf{v}) = \int |\mathbf{v} - \mathbf{v}'| f_F(\mathbf{v}') d\mathbf{v}'$$

$$\simeq \left(v + \frac{1}{v} \frac{3\kappa T_F}{2m_F} \right) n_F.$$

Hint: use symmetry arguments when considering the term involving $\mathbf{v} \cdot \mathbf{v}'$.

- (c) Assume that the beam velocity is
- z
- directed and let
- $F_T = \int d^2v_\perp f_T$
- so that
- F_T
- describes the projection of the 3-D beam distribution onto the
- z
- axis of velocity space. Since
- $v = v_z$
- and
- $v_y = v_x \approx 0$
- show that it is possible to write

$$h_F(\mathbf{v}) \simeq \frac{m_e n_F}{v_z \mu}$$

$$g_F(\mathbf{v}) \simeq \left(v_z + \frac{1}{v_z} \frac{3\kappa T_F}{2m_F} \right) n_F.$$

Show that the Fokker-Planck equation can be written as

$$\frac{\partial F_T}{\partial t} \simeq \sum_{F=i,e} \frac{n_F q_T^2 q_F^2 \ln \Lambda}{4\pi \epsilon_0^2 m_T^2} \left[\frac{\partial}{\partial v_z} \left(F_T \frac{m_T}{\mu v_z^2} \right) + \frac{1}{2} \frac{\partial^2}{\partial v_z^2} \left(F_T \frac{\partial^2}{\partial v_z^2} \left(v_z + \frac{3\kappa T_F}{2m_F v_z} \right) \right) \right]$$

$$\simeq \sum_{F=i,e} \frac{n_F q_T^2 q_F^2 \ln \Lambda}{4\pi \epsilon_0^2 m_T^2} \frac{\partial}{\partial v_z} \left[F_T \frac{m_T}{\mu v_z^2} + \frac{3}{2v_z^3} \frac{\kappa T_F}{m_F} \frac{\partial F_T}{\partial v_z} \right].$$

- (d) Taking into account charge neutrality and
- $v_z \gg v_{Ti}$
- show that this can be recast as

$$\frac{\partial F_T}{\partial t} \simeq \frac{n_e e^4 \ln \Lambda}{4\pi \epsilon_0^2 m_e^2} \frac{\partial}{\partial v_z} \left[F_T \frac{2+Z}{v_z^2} + \frac{3}{2v_z^3} \frac{\kappa T_e}{m_e} \frac{\partial F_T}{\partial v_z} \right]$$

- (e) Show that a steady-state equilibrium can develop where, because of collisions with background electrons and ions, the fast beam distribution has the form

$$F_T \sim \exp\left(-\frac{(2+Z)m_e v_z^2}{3\kappa T_e}\right).$$

Is this consistent with the original assumption that the beam is fast compared to the background plasma?

3. An axisymmetric plasma has a magnetic field which can be expressed as

$$\mathbf{B} = \frac{1}{2\pi} (\nabla\psi \times \nabla\phi + \mu_0 I \nabla\phi)$$

where ϕ is the toroidal angle, $\psi(r, z)$ is the poloidal flux, and I is the current flowing through a circle of radius r at axial position z .

- (a) Show that the toroidal component of the vector potential is

$$A_\phi(r, z, t) = \frac{1}{2\pi r} \psi(r, z, t)$$

- (b) Assume that the plasma obeys the resistive Ohm's law

$$\mathbf{E} + \mathbf{U} \times \mathbf{B} = \eta \mathbf{J}$$

and assume that the plasma is stationary so that the toroidal component is simply

$$E_\phi = \eta J_\phi.$$

and Eq.(9.42) to show that

$$J_\phi = -\frac{r}{2\pi\mu_0} \nabla \cdot \left(\frac{1}{r^2} \nabla\psi \right)$$

so that the toroidal component of Ohm's law is

$$E_\phi = -\frac{r\eta}{2\pi\mu_0} \nabla \cdot \left(\frac{1}{r^2} \nabla\psi \right).$$

- (c) Assuming classical resistivity $\eta \sim T_e^{-3/2}$ sketch the temperature dependence of $|E_\phi|$ as given above and also sketch the temperature dependence of $E_{Dreicer}$ as given by Eq.(13.85). For a plasma with given ψ and physical dimensions, in what electron temperature limit do runaway electrons develop (high or low temperature)? For a given temperature, do runaways develop with high ψ or low ψ ? For a given temperature and flux, do runaways develop in a large device or in a small device? If the plasma density decays, will runaways develop?

Wave-particle nonlinearities

14.1 Introduction

Linear models are straightforward and rich in descriptive power because they are based on a powerful, integrated set of concepts and tools consisting of eigenmodes, eigenvalues, eigenvectors, orthogonality, and integral transforms. These concepts and tools ultimately depend on the very essence of linearity, namely the principle of superposition.

While many important phenomena are well characterized by linear models there nevertheless exist other important phenomena where the principle of superposition breaks down either partially or completely. The phenomenon in question becomes amplitude-dependent above some critical amplitude threshold and then nonlinearity becomes important. Break-down of the superposition principle means that modes with different eigenvalues (to the extent eigenvalues still exist) are no longer orthogonal and start to interact with each other. These interactions result from non-linear terms in the system of equations, i.e., terms involving products of dependent variables. As an example of this, consider the product of two modes having respective frequencies ω_1 and ω_2 . This product can be decomposed into sum and difference frequencies according to standard trigonometric identities, e.g.,

$$\cos \omega_1 t \cos \omega_2 t = \frac{\cos [(\omega_1 + \omega_2)t] + \cos [(\omega_1 - \omega_2)t]}{2}. \quad (14.1)$$

The beat waves at frequencies $\omega_1 \pm \omega_2$ can act as source terms driving oscillations at $\omega_1 \pm \omega_2$. In the special case where $\omega_1 = \omega_2$, the difference frequency is zero and the non-linear product can act as a source term which modulates equilibrium parameters and thereby changes the mode dynamics. In particular, feedback loops can develop where modes affect their own stability properties. Another possibility occurs when the nonlinear product is very small, but happens to resonantly drive a linear mode. In this case even a weak non-linear coupling between two modes can resonantly drive another linear mode to large amplitude. Similar beating can occur with spatial factors $\sim \exp(i\mathbf{k} \cdot \mathbf{x})$ so that the non-linear product of modes with wavevectors \mathbf{k}_1 and \mathbf{k}_2 drive spatial oscillations with wavevectors $\mathbf{k}_1 \pm \mathbf{k}_2$. In analogy to quantum mechanics the momentum associated with a wave is found to be proportional to \mathbf{k} and the energy proportional to ω . The beating together of two waves with respective space-time dependence $\exp(i\mathbf{k}_1 \cdot \mathbf{x} - i\omega_1 t)$ and $\exp(i\mathbf{k}_2 \cdot \mathbf{x} - i\omega_2 t)$ can then be

interpreted in terms of conservation of wave energy and momentum,

$$\begin{aligned}\omega_3 &= \omega_1 + \omega_2 \\ \mathbf{k}_3 &= \mathbf{k}_1 + \mathbf{k}_2\end{aligned}\tag{14.2}$$

where wave 3 is what results from beating together waves 1 and 2.

Because of the large variety of possible nonlinear effects, there are many ways to categorize nonlinear behavior. For example, one categorization is according to whether the non-linearity involves velocity space (Vlasov non-linearity) or position space (fluid non-linearity). Vlasov nonlinearities are characterized by energy exchange between wave electric fields, resonant particles, and non-resonant particles. Fluid instabilities involve nonlinear mixing of two or more fluid modes and can be interpreted as one wave modulating the equilibrium seen by another wave. Another categorization is according to whether the non-linearity is weak or strong. In weak nonlinear situations, linear theory is invoked as a reasonable first approximation and then used as a building block for developing the non-linear model. In strong non-linear situations, linear assumptions fail completely and the non-linear behavior must be addressed directly without any help from linear theory. Weak non-linear theories can be further categorized into (i) mode-coupling models where a small number of modes mutually interact in a coherent manner and (ii) weak turbulence models where a statistically large number of modes mutually interact with random phase so that some sort of averaging is required.

An important feature of non-linear theory concerns energy. Because energy is a quadratic function of amplitude, energy does not satisfy the principle of superposition and so energy cannot be properly accounted for in linear models. Thus, non-linear models are essential for tracking the flow of energy between modes and also between modes and the equilibrium.

14.2 Vlasov non-linearity and quasi-linear velocity space diffusion

14.2.1 Derivation of the quasilinear diffusion equation

Quasilinear theory (Vedenov, Velikhov and Sagdeev 1962, Drummond and Pines 1962, Bernstein and Engelmann 1966), a surprisingly complete extension to the Landau model of plasma waves, shows how plasma waves can alter the equilibrium velocity distribution. In order to focus attention on the most essential features of this theory, a simplified situation will be considered where the plasma is assumed to be one dimensional, uniform, and unmagnetized. Furthermore, only electrostatic modes will be considered and ion motion will be neglected. Thus the plasma is characterized by the coupled Vlasov and Poisson equations for electrons and the only role for the ions is to provide a static, uniform neutralizing background. It is assumed that the electron velocity distribution function can be decomposed into (i) a spatially independent equilibrium term which is allowed to have a slow temporal variation and (ii) a small, high frequency perturbation having a space-time dependence and which is associated with a spectrum of linear plasma waves of the sort discussed in Section 5.2. Thus, it is assumed that the electron velocity distribution has the form

$$f(x, v, t) = f_0(v, t) + f_1(x, v, t) + f_2(x, v, t) + \dots\tag{14.3}$$

where it is implicit that the magnitude of terms with subscript n is of order ϵ^n where $\epsilon \ll 1$. At $t = 0$, the terms f_n where $n \geq 2$ all vanish because the perturbation was prescribed to be f_1 at $t = 0$. Other variables such as the electric field will have some kind of nonlinear dependence on the distribution function and so, for example, the electric field will have the form

$$E = E_0 + E_1 + E_2 + E_3 + \dots$$

where it is implicit that the n^{th} term is of order ϵ^n .

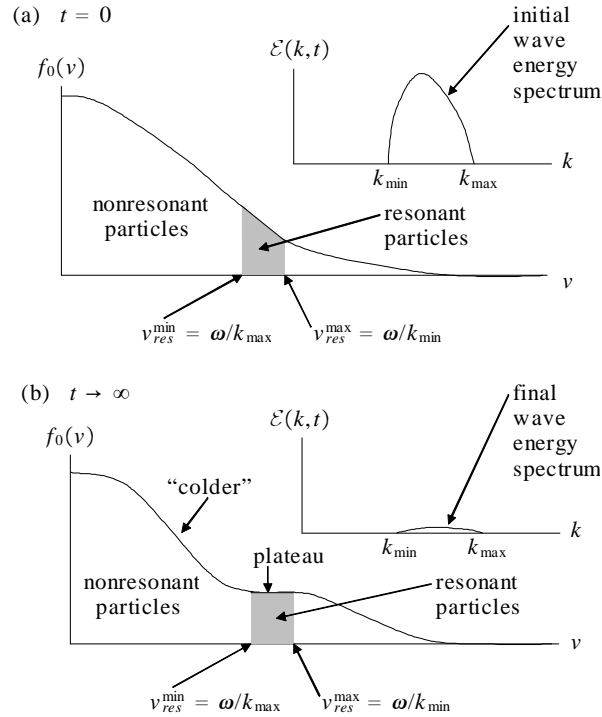


Figure 14.1: (a) At $t = 0$ the equilibrium distribution function $f_0(v)$ is monotonically decreasing resulting in Landau damping of any waves and there is a wave spectrum (insert) with wave energy in the spectral range $k_{min} < k < k_{max}$. Resonant particles are shown as shaded in distribution function and lie in velocity range $v_{res}^{min} < v < v_{res}^{max}$. (b) As $t \rightarrow \infty$ the resonant particles develop a plateau (corresponding to absorbing energy from the wave), the wave spectrum goes to zero, and the non-resonant particles appear to become colder.

Since by assumption, $f_0(v, t)$ does not depend on position, it is convenient to define a velocity-normalized order zero distribution function

$$f_0(v, t) = n_0 \bar{f}_0(v, t) \quad (14.4)$$

so that

$$\int \bar{f}_0(v, t) dv = 1. \quad (14.5)$$

This definition causes n_0 to show up explicitly so that terms such as $(e^2/m\epsilon_0) \partial f_0/\partial v$ can be written as $\omega_p^2 \partial \bar{f}_0/\partial v$. A possible initial condition for $f_0(v, t)$, namely a monotonically decreasing velocity distribution, is shown in Fig.14.1(a).

Spatial averaging will be used in the mathematical procedure to filter out some types of terms while retaining others. This averaging will be denoted by $\langle \rangle$ so that, for example, the average of f_1 is

$$\langle f_1(x, v, t) \rangle = \frac{1}{L} \int dx f_1(x, t) \quad (14.6)$$

where L is the length of the one-dimensional system and the integration is over this length. The spatial average of a quantity is independent of x and so, since f_0 is assumed to be independent of position, $\langle f_0 \rangle = f_0$. (In an alternate version of the theory, the averaging is instead understood to be over a statistically large ensemble of systems containing turbulent waves and in this version, the averaged quantity can be position-dependent.)

The 1-D electron Vlasov equation is

$$\begin{aligned} \frac{\partial}{\partial t} (f_0 + f_1 + f_2 + \dots) + v \frac{\partial}{\partial x} (f_1 + f_2 + \dots) \\ - \frac{e}{m} (E_1 + E_2 + \dots) \frac{\partial}{\partial v} (f_0 + f_1 + f_2 + \dots) = 0; \end{aligned} \quad (14.7)$$

note that there is no $\partial f_0/\partial x$ term because f_0 is assumed to be spatially independent and also there is no E_0 term because the system is assumed to be neutral in equilibrium. The linear portion of this equation

$$\frac{\partial f_1}{\partial t} + v \frac{\partial f_1}{\partial x} - \frac{e}{m} E_1 \frac{\partial f_0}{\partial v} = 0, \quad (14.8)$$

forms the basis for the linear Landau theory of plasma waves discussed in Section 4.5. Subtracting Eq.(14.8) from Eq.(14.7) leaves the remainder equation

$$\begin{aligned} \frac{\partial}{\partial t} (f_0 + f_2 + \dots) + v \frac{\partial}{\partial x} (f_2 + \dots) - \frac{e}{m} (E_2 + \dots) \frac{\partial}{\partial v} (f_0 + f_1 + f_2 + \dots) \\ - \frac{e}{m} E_1 \frac{\partial}{\partial v} (f_1 + f_2 + \dots) = 0. \end{aligned} \quad (14.9)$$

We assume that the quantities with subscripts $n \geq 1$ are waves and therefore have spatial averages which vanish, i.e., $\langle f_1 \rangle = 0$, $\langle E_1 \rangle = 0$, etc. Also, since f_0 is independent of position, it is seen that $\langle E_2 f_0 \rangle = f_0 \langle E_2 \rangle = 0$, etc. Spatial averaging of Eq.(14.9) thus annihilates many terms, leaving

$$\frac{\partial f_0}{\partial t} - \frac{e}{m} \frac{\partial}{\partial v} [\langle E_1 f_1 \rangle + \langle E_2 f_1 \rangle + \dots] \quad (14.10)$$

where $\partial/\partial v$ has been factored out of the spatial averaging because v is an independent variable in phase-space. The term $\langle E_1 f_1 \rangle$ is of order ϵ^2 whereas $\langle E_2 f_1 \rangle$ is of order ϵ^3 and the terms represented by the $+\dots$ are of still higher order. The essential postulate of quasi-linear theory is that all terms of order ϵ^3 and higher may be neglected because ϵ is small.

On applying this postulate, Eq.(14.10) reduces to the *quasi-linear velocity-space diffusion equation*

$$\frac{\partial f_0}{\partial t} = \frac{e}{m} \frac{\partial}{\partial v} \langle E_1 f_1 \rangle. \quad (14.11)$$

This implies that even though f_0 is of order ϵ^0 , the time derivative of f_0 is of order ϵ^2 so that f_0 is a very slowly changing equilibrium.

The nonlinear term $\langle E_1 f_1 \rangle$ can be explicitly calculated by first expressing the perturbations as a sum (i.e., integral) over spatial Fourier modes, for example the first order electric field can be expressed as

$$E_1(x, t) = \frac{1}{2\pi} \int dk \tilde{E}_1(k, t) e^{ikx}. \quad (14.12)$$

This allows the product on the right hand side of Eq.(14.11) to be evaluated as

$$\begin{aligned} \langle E_1 f_1 \rangle &= \frac{1}{L} \int dx \left[\left(\frac{1}{2\pi} \int dk \tilde{E}_1(k, t) e^{ikx} \right) \left(\frac{1}{2\pi} \int dk' \tilde{f}_1(k', v, t) e^{ik'x} \right) \right] \\ &= \frac{1}{2\pi L} \int dk \int dk' \tilde{E}_1(k, t) \tilde{f}_1(k', v, t) \frac{1}{2\pi} \int dx e^{i(k+k')x} \end{aligned} \quad (14.13)$$

where the order of integration has been changed in the second line. Then, invoking the representation of the Dirac delta function

$$\delta(k) = \frac{1}{2\pi} \int dx e^{ikx}, \quad (14.14)$$

Eq.(14.13) reduces to

$$\langle E_1 f_1 \rangle = \frac{1}{2\pi L} \int dk \tilde{E}_1(-k, t) \tilde{f}_1(k, v, t). \quad (14.15)$$

The linear perturbations E_1 and f_1 are governed by the system of linear equations discussed in Section 4.5. This means that associated with each wavevector k there is a complex frequency $\omega(k)$ which is determined by the linear dispersion relation $\mathcal{D}(\omega(k), k) = 0$. This gives the explicit time dependence of the modes,

$$\tilde{E}_1(k, t) = \tilde{E}_1(k) e^{-i\omega(k)t} \quad (14.16a)$$

$$\tilde{f}_1(k, v, t) = \tilde{f}_1(k, v) e^{-i\omega(k)t}. \quad (14.16b)$$

Furthermore, Eq.(14.8) provides a relationship between $\tilde{E}_1(k)$ and $\tilde{f}_1(k, v)$ since the spatial Fourier transform of this equation is

$$-i\omega f_1 + ikv f_1 - \frac{e}{m} E_1 \frac{\partial f_0}{\partial v} = 0 \quad (14.17)$$

which leads to the familiar linear relationship

$$\tilde{f}_1(k, v) = i \frac{e}{m} \tilde{E}_1(k) \frac{\partial f_0 / \partial v}{\omega - kv}. \quad (14.18)$$

Inserting Eqs.(14.18) and (14.16a) into Eq.(14.15) shows that

$$\langle E_1 f_1 \rangle = \frac{i}{2\pi L} \frac{e}{m} \int dk \tilde{E}_1(-k) \tilde{E}_1(k) \frac{\partial f_0 / \partial v}{\omega - kv} e^{-i[\omega(-k) + \omega(k)]t}. \quad (14.19)$$

This expression can be further evaluated by invoking the parity properties of $\tilde{E}_1(k)$ and $\omega(k)$. These parity properties are established by writing

$$E_1(x, t) = \frac{1}{2\pi} \int dk \tilde{E}_1(k) e^{ikx - i\omega(k)t} \quad (14.20)$$

and noting that the left hand side is real because it describes a physical quantity. Taking the complex conjugate of Eq.(14.20) gives

$$E_1(x, t) = \frac{1}{2\pi} \int dk \tilde{E}_1^*(k) e^{-ikx + i\omega^*(k)t}. \quad (14.21)$$

The parity properties are determined by defining a temporary new integration variable $k' = -k$ and noting that $\int_{-\infty}^{\infty} dk$ corresponds to $\int_{\infty}^{-\infty} dk'$ since $dk' = -dk$ and the k limits $(-\infty, \infty)$ correspond to the k' limits $(\infty, -\infty)$. Thus Eq.(14.21) can be recast as

$$\begin{aligned} E_1(x, t) &= \frac{1}{2\pi} \int dk' \tilde{E}_1^*(-k') e^{ik'x + i\omega^*(-k')t} \\ &= \frac{1}{2\pi} \int dk \tilde{E}_1^*(-k) e^{ikx + i\omega^*(-k)t} \end{aligned} \quad (14.22)$$

where the primes have now been removed in the second line. Since Eq.(14.20) and (14.22) have the same left hand sides, the right hand sides must also be the same. Because $\tilde{E}_1(k)$ and $\omega(k)$ are arbitrary, they must individually satisfy the respective parity conditions

$$\begin{aligned} \tilde{E}_1(k) &= \tilde{E}_1^*(-k) \\ \omega(k) &= -\omega^*(-k) \end{aligned} \quad (14.23)$$

or equivalently

$$\begin{aligned} \tilde{E}_1(-k) &= \tilde{E}_1^*(k) \\ \omega(-k) &= -\omega^*(k). \end{aligned} \quad (14.24)$$

If the complex frequency is written in terms of explicit real and imaginary parts $\omega(k) = \omega_r(k) + i\omega_i(k)$ then the frequency parity condition becomes

$$\begin{aligned} \omega_r(-k) + i\omega_i(-k) &= -[\omega_r(k) + i\omega_i(k)]^* \\ &= -\omega_r(k) + i\omega_i(k) \end{aligned} \quad (14.25)$$

from which it can be concluded that

$$\begin{aligned} \omega_r(-k) &= -\omega_r(k) \\ \omega_i(-k) &= \omega_i(k). \end{aligned} \quad (14.26)$$

The real part of ω is therefore an odd function of k whereas the imaginary part is an even function of k .

Application of the parity conditions gives

$$\tilde{E}_1(-k) \tilde{E}_1(k) = \tilde{E}_1^*(k) \tilde{E}_1(k) = \left| \tilde{E}_1(k) \right|^2 \quad (14.27)$$

and

$$\omega(-k) + \omega(k) = 2i\omega_i(k) \quad (14.28)$$

in which case Eq.(14.19) reduces to

$$\langle E_1 f_1 \rangle = \frac{i}{2\pi L} \frac{e}{m} \int dk \frac{|\tilde{E}_1(k)|^2 e^{2\omega_i(k)t}}{\omega - kv} \frac{\partial f_0}{\partial v}. \quad (14.29)$$

Substitution of $\langle E_1 f_1 \rangle$ into Eq.(14.10) gives the time evolution of the equilibrium distribution function,

$$\frac{\partial f_0}{\partial t} = \frac{i}{2\pi L} \frac{e^2}{m^2} \frac{\partial}{\partial v} \int dk \frac{|\tilde{E}_1(k)|^2 e^{2\omega_i(k)t}}{\omega - kv} \frac{\partial f_0}{\partial v}. \quad (14.30)$$

The quantity $|\tilde{E}_1(k)|^2$ has a physical meaning that is made evident by considering the volume average of the electric field energy

$$\begin{aligned} \langle W_E \rangle &= \left\langle \frac{\varepsilon_0 E_1^2}{2} \right\rangle \\ &= \frac{\varepsilon_0}{2L} \int dx \left(\frac{1}{2\pi} \int dk \tilde{E}_1(k) e^{ikx - i\omega(k)t} \right) \left(\frac{1}{2\pi} \int dk' \tilde{E}_1(k') e^{ik'x - i\omega(k')t} \right) \\ &= \frac{\varepsilon_0}{4\pi L} \int dk \int dk' \tilde{E}_1(k) \tilde{E}_1(k') e^{-i[\omega(k) + \omega(k')]t} \frac{1}{2\pi} \int dx e^{i(k+k')x}. \end{aligned} \quad (14.31)$$

However, using Eq.(14.14) this can be written as

$$\begin{aligned} \langle W_E \rangle &= \frac{\varepsilon_0}{4\pi L} \int dk \tilde{E}_1(k) \tilde{E}_1(-k) e^{-i[\omega(k) + \omega(-k)]t} \\ &= \int dk \mathcal{E}(k, t) \end{aligned} \quad (14.32)$$

where

$$\mathcal{E}(k, t) = \frac{\varepsilon_0}{4\pi L} |\tilde{E}_1(k)|^2 e^{2\omega_i(k)t} \quad (14.33)$$

is the time-dependent electric field energy density associated with the wavevector k . A possible initial condition for the distribution function and wave energy spectrum is shown in Fig.14.1(a); the wave energy spectrum is shown in the insert and is finite in the range $k_{\min} < k < k_{\max}$ and the distribution function is monotonically decreasing so as to cause Landau damping of the waves.

Combination of Eqs.(14.30) and (14.33) shows that the evolution of the equilibrium distribution function is given by

$$\frac{\partial f_0}{\partial t} = \frac{2i}{\varepsilon_0} \frac{e^2}{m^2} \frac{\partial}{\partial v} \int dk \frac{\mathcal{E}(k, t)}{\omega - kv} \frac{\partial f_0}{\partial v}. \quad (14.34)$$

This can be summarized as a velocity space-diffusion equation

$$\frac{\partial f_0}{\partial t} = \frac{\partial}{\partial v} \left(D_{QL} \frac{\partial f_0}{\partial v} \right) \quad (14.35)$$

where the *quasi-linear velocity space diffusion coefficient* is

$$D_{QL} = \frac{2ie^2}{\varepsilon_0 m^2} \int dk \frac{\mathcal{E}(k,t)}{\omega - kv}. \quad (14.36)$$

The factor i in the velocity diffusion tensor seems surprising at first because f_0 is a real quantity. However, the i factor is entirely appropriate and is intimately related to the parity properties of $\omega(k)$ since

$$\frac{i}{\omega(k) - kv} = \frac{i[\omega_r(k) - kv] + \omega_i(k)}{[\omega_r(k) - kv]^2 + \omega_i^2(k)}. \quad (14.37)$$

The denominator in this expression is an even function of k , the term $[\omega_r(k) - kv]$ in the numerator is an odd function of k , and $\omega_i(k)$ is an even function of k . Since $\mathcal{E}(k,t)$ is an even function of k , integration over k in Eq.(14.36) annihilates the imaginary component (this component is an odd function of k) and so

$$D_{QL} = \frac{e^2}{\varepsilon_0 m^2} \int dk \frac{2\omega_i(k)\mathcal{E}(k,t)}{[\omega_r(k) - kv]^2 + \omega_i^2(k)}. \quad (14.38)$$

In summary, the self-consistent coupled system of equations for the non-linear evolution of the equilibrium consists of Eq.(14.35), (14.38), and

$$\frac{\partial}{\partial t} \mathcal{E}(k,t) = 2\omega_i(k)\mathcal{E}(k,t) \quad (14.39)$$

which is obtained from Eq.(14.33). The real and imaginary parts of the frequency $\omega_r(k)$, $\omega_i(k)$ appear as parameters in these equations and are determined from the linear wave dispersion relation which in turn depends on f_0 . This linear wave dispersion relation is obtained as in Section 4.5 by writing $E_1 = -\partial\phi_1/\partial x$ and then combining Eq.(14.18) with Poisson's equation

$$k^2 \tilde{\phi}_1(k) = -\frac{e}{\varepsilon_0} \int dv \tilde{f}_1 \quad (14.40)$$

to obtain

$$k^2 \tilde{\phi}_1(k) = -\frac{e^2}{\varepsilon_0 m} \int dv \frac{\partial f_{\sigma 0}}{\partial v} \frac{k \tilde{\phi}_1(k)}{\omega - kv} \quad (14.41)$$

which can be expressed as

$$1 + \frac{\omega_p^2}{k} \int dv \frac{\partial \bar{f}_0 / \partial v}{\omega - kv} = 0 \quad (14.42)$$

using Eq.(14.4). Thus, given the instantaneous value of $f_0(v, t) = n_0 \bar{f}_0(v, t)$, the complex frequency is determined from Eq.(14.42) and then, given the instantaneous value of the wave spectral energy, both the evolution of f_0 and the wave spectral energy are determined from Eqs.(14.35) and (14.39).

14.2.2 Conservation properties of the quasilinear diffusion equation

Conservation of particles

Conservation of particles occurs automatically because Eq.(14.35) has the form of a derivative in velocity space. Thus, the zeroth moment of Eq.(14.35) is simply

$$\frac{\partial}{\partial t} \int dv f_0 = \int dv \frac{\partial}{\partial v} \left(D_{QL} \frac{\partial f_0}{\partial v} \right) = \left[D_{QL} \frac{\partial f_0}{\partial v} \right]_{v=-\infty}^{v=\infty} = 0 \quad (14.43)$$

and so the quasi-linear diffusion equation conserves the density $n = \int dv f_0$.

Conservation of momentum

Examination of momentum conservation requires taking the first moment of Eq.(14.35),

$$\frac{\partial}{\partial t} (nmv) = m \int dv v \frac{\partial}{\partial v} \left(D_{QL} \frac{\partial f_0}{\partial v} \right) = -m \int dv D_{QL} \frac{\partial f_0}{\partial v}. \quad (14.44)$$

Using Eq.(14.36) this becomes

$$\begin{aligned} \frac{\partial}{\partial t} (nmv) &= -m \int dv \frac{2ie^2}{\varepsilon_0 m^2} \int dk \frac{\mathcal{E}(k,t)}{\omega - kv} \frac{\partial f_0}{\partial v} \\ &= -2i\omega_p^2 \int dk \mathcal{E}(k,t) \int dv \frac{1}{\omega - kv} \frac{\partial f_0}{\partial v}. \end{aligned} \quad (14.45)$$

However, the linear dispersion relation Eq.(14.41) shows that

$$\omega_p^2 \int dv \frac{1}{\omega - kv} \frac{\partial f_0}{\partial v} = -k \quad (14.46)$$

and so

$$\frac{\partial}{\partial t} (nmv) = 2i \int dk \mathcal{E}(k,t) k = 0 \quad (14.47)$$

which vanishes because the integrand is an odd function of k . Thus, the constraint provided by the linear dispersion relation shows that the quasi-linear velocity diffusion equation also conserves momentum.

Conservation of energy

Consideration of energy conservation starts out in a similar manner but leads to some interesting, non-trivial results. The mean particle kinetic energy is defined to be

$$W_P = \int dv \frac{mv^2}{2} f_0. \quad (14.48)$$

The time evolution of W_P is obtained by taking the second moment of the quasi-linear diffusion equation, Eq.(14.35),

$$\begin{aligned} \frac{\partial W_P}{\partial t} &= \int dv \frac{mv^2}{2} \frac{\partial}{\partial v} D_{QL} \frac{\partial f_0}{\partial v} \\ &= - \int dv mv D_{QL} \frac{\partial f_0}{\partial v}. \end{aligned} \quad (14.49)$$

Using Eq.(14.36) gives

$$\begin{aligned}
 \frac{\partial W_P}{\partial t} &= - \int dv m v \frac{2ie^2}{\epsilon_0 m^2} \int dk \frac{\mathcal{E}(k,t)}{\omega - kv} \frac{\partial f_0}{\partial v} \\
 &= 2i\omega_p^2 \int dk \frac{\mathcal{E}(k,t)}{k} \int dv \frac{\omega - kv - \omega}{\omega - kv} \frac{\partial \bar{f}_0}{\partial v} \\
 &= -\omega_p^2 \int dk \frac{2i\omega(k)\mathcal{E}(k,t)}{k} \int dv \frac{1}{\omega - kv} \frac{\partial \bar{f}_0}{\partial v}. \quad (14.50)
 \end{aligned}$$

Invoking Eq.(14.42) to substitute for the velocity integral results in

$$\frac{\partial W_P}{\partial t} = \int dk 2i [\omega_r(k) + i\omega_i(k)] \mathcal{E}(k,t). \quad (14.51)$$

Since $\omega_r(k)$ is an odd function of k and $\omega_i(k)$ is an even function of k , only the term involving ω_i survives the k integration and so

$$\frac{\partial W_P}{\partial t} + \int dk 2\omega_i(k)\mathcal{E}(k,t) = 0. \quad (14.52)$$

Using Eq.(14.39) this becomes

$$\frac{\partial}{\partial t} \left[W_P + \int dk \mathcal{E}(k,t) \right] = 0 \quad (14.53)$$

which can now be integrated to give

$$W_P + \int dk \mathcal{E}(k,t) = W_P + W_E = const.$$

showing that the sum of the particle and electric field energies is conserved. The particle energy and the electric field energy therefore need not be individually conserved – only the sum of these two types of energy is conserved. This result allows for energy exchange between the particles and the electric field.

14.2.3 Energy exchange with resonant particles

More detailed insight is obtained by considering the role of resonant particles, i.e., those particles having velocity $v \approx \omega/k$ as indicated by the shaded region in Fig.14.1. This is done by using Eq.(14.37) to re-write the top line of Eq.(14.50) as

$$\begin{aligned}
 \frac{\partial W_P}{\partial t} &= - \frac{2e^2}{\epsilon_0 m} \int dk \mathcal{E}(k,t) \int dv v \frac{i[\omega_r(k) - kv] + \omega_i(k)}{[\omega_r(k) - kv]^2 + \omega_i^2(k)} \frac{\partial f_0}{\partial v} \\
 &= -2\omega_p^2 \int dk \mathcal{E}(k,t) \int dv \frac{v\omega_i(k)}{[\omega_r(k) - kv]^2 + \omega_i^2(k)} \frac{\partial \bar{f}_0}{\partial v} \quad (14.54)
 \end{aligned}$$

where because $\omega_r(k) - kv$ is an odd function of k , only the $\omega_i(k)$ numerator term survives the k integration. The velocity integral can be decomposed into a resonant portion which is the velocity range where $\omega_r \simeq kv$ and the remaining or non-resonant portion. In the resonant portion, it is possible to approximate

$$\frac{\omega_i}{(\omega_r - kv)^2 + \omega_i^2} \simeq \pi \delta(\omega_r - kv) = \frac{\pi}{k} \delta\left(v - \frac{\omega_r}{k}\right) \quad (14.55)$$

while the non-resonant portion can be written as a principle-part integral. Thus, Eq.(14.54) becomes

$$\frac{\partial W_P}{\partial t} = -\omega_p^2 \int dk 2\mathcal{E}(k,t) \left[P \int dv \frac{v\omega_i(k)}{(\omega_r - kv)^2} \frac{\partial \bar{f}_0}{\partial v} + \pi \frac{\omega_r}{k^2} \left(\frac{\partial \bar{f}_0}{\partial v} \right)_{v=\omega_r/k} \right]. \quad (14.56)$$

A relationship between the principle part and resonant terms in this expression can be constructed by similarly decomposing Eq.(14.42) into a resonant portion and a non-resonant or principle part. The principle part is Taylor expanded as a function of $\omega_r + i\omega_i$ where ω_i is assumed to be much smaller than ω_r . This procedure is essentially the scheme discussed in the development of Eq.(5.81), but to emphasize the details the expansion of the principle part is written explicitly here. Thus, the linear dispersion relation Eq.(14.42) can be expanded as

$$\begin{aligned} 0 &= 1 - \frac{\omega_p^2}{k^2} \int dv \frac{\partial \bar{f}_0 / \partial v}{v - \frac{\omega_r}{k} - \frac{i\omega_i}{k}} \\ &= 1 - \frac{\omega_p^2}{k^2} \left[P \int dv \frac{\partial \bar{f}_0 / \partial v}{v - \frac{\omega_r}{k} - \frac{i\omega_i}{k}} + i\pi \left(\frac{\partial \bar{f}_0}{\partial v} \right)_{v=\omega_r/k} \right] \\ &= 1 - \frac{\omega_p^2}{k^2} \left[P \int dv \frac{\partial \bar{f}_0 / \partial v}{v - \frac{\omega_r}{k}} + \frac{i\omega_i}{k} \frac{\partial}{\partial \left(\frac{\omega}{k} \right)} P \int dv \frac{\partial \bar{f}_0 / \partial v}{v - \frac{\omega}{k}} + i\pi \left(\frac{\partial \bar{f}_0}{\partial v} \right)_{v=\omega_r/k} \right] \\ &= 1 - \frac{\omega_p^2}{k^2} \left[P \int dv \frac{\partial \bar{f}_0 / \partial v}{v - \frac{\omega_r}{k}} + \frac{i\omega_i}{k} P \int dv \frac{\partial \bar{f}_0 / \partial v}{\left(v - \frac{\omega}{k} \right)^2} + i\pi \left(\frac{\partial \bar{f}_0}{\partial v} \right)_{v=\omega_r/k} \right]. \end{aligned} \quad (14.57)$$

The imaginary part of the last line must vanish and so

$$\frac{\omega_i}{k} P \int dv \frac{\partial \bar{f}_0 / \partial v}{\left(v - \frac{\omega_r}{k} \right)^2} + \pi \left(\frac{\partial \bar{f}_0}{\partial v} \right)_{v=\omega_r/k} = 0 \quad (14.58)$$

which leads to the usual expression for Landau damping.

If it is assumed that $\omega_r/k \gg v_T$ then the principle part integral in Eq. (3.238) can be approximated as

$$P \int dv \frac{v}{(\omega_r - kv)^2} \frac{\partial \bar{f}_0}{\partial v} \simeq \frac{1}{\omega_r^2} \int dv v \frac{\partial \bar{f}_0}{\partial v} = -\frac{1}{\omega_r^2} \int dv \bar{f}_0 = -\frac{1}{\omega_r^2} \quad (14.59)$$

and the principle part integral in Eq.(14.58) can similarly be approximated as

$$\begin{aligned}
 P \int dv \frac{\partial \bar{f}_0 / \partial v}{(v - \omega_r/k)^2} &= - \int dv \bar{f}_0 \frac{\partial}{\partial v} \frac{1}{(v - \omega_r/k)^2} \\
 &= 2 \int dv \frac{\bar{f}_0}{(v - \omega_r/k)^3} \\
 &\simeq -2 \frac{k^3}{\omega_r^3}.
 \end{aligned} \tag{14.60}$$

Using Eq.(14.59), Eq. (14.56) becomes

$$\frac{\partial W_P}{\partial t} = -\omega_p^2 \int dk 2\mathcal{E}(k,t) \left[-\frac{\omega_i(k)}{\omega_r^2} + \frac{\omega_r}{k^2} \pi \left(\frac{\partial \bar{f}_0}{\partial v} \right)_{v=\omega_r/k} \right] \tag{14.61}$$

and using Eq.(14.60), Eq. (14.58) becomes

$$-2\omega_i \frac{k^2}{\omega_r^3} + \pi \left(\frac{\partial \bar{f}_0}{\partial v} \right)_{v=\omega_r/k} = 0. \tag{14.62}$$

Comparison of the above two expressions shows that the second term in the square brackets of Eq.(14.61) has twice the magnitude of the first term and is of the opposite sign. Since $\omega_r^2 \simeq \omega_p^2$, this means that Eq.(14.61) is of the form

$$\frac{\partial W_P}{\partial t} = \frac{\partial}{\partial t} W_{P,non-resonant} + \frac{\partial}{\partial t} W_{P,resonant} = \int d^3k \mathcal{E}(k,t) [2\omega_i - 4\omega_i] \tag{14.63}$$

where the $2\omega_i$ term prescribes the rate of change of the kinetic energy of the non-resonant particles, and the $-4\omega_i$ term prescribes the rate of change of the kinetic energy of the resonant particles. On the other hand, Eq.(14.52) showed that the rate of change of the total particle kinetic energy was equal and opposite to the total rate of change of the electric field energy. These two statements can be reconciled by asserting that the wave energy consists of equal parts of non-resonant particle kinetic energy and electric field energy and that the resonant particles act as a source or sink for this wave energy. This energy budgeting is shown schematically as

$$\underbrace{\int d^3k 2\omega_i(k) \mathcal{E}(k,t)}_{\substack{\text{kinetic energy} \\ \text{of non-resonant particles}}} + \underbrace{\int d^3k 2\omega_i(k) \mathcal{E}(k,t)}_{\substack{\text{energy stored in} \\ \text{electric field}}} \iff \underbrace{\int d^3k 4\omega_i(k) \mathcal{E}(k,t)}_{\substack{\text{kinetic energy} \\ \text{of resonant particles}}} .$$

$\underbrace{\hspace{15em}}_{\substack{\text{wave} \\ \text{energy}}}$

(14.64)

Behavior of the resonant particles

We define f_{res} as the velocity distribution of the resonant particles, i.e., the particles with velocities $v \simeq \omega/k$ for which $\mathcal{E}(k,t)$ is finite. Since the velocity range $v = \omega(k)/k$ of the resonant particles maps to the spectrum $\mathcal{E}(k,t)$, the upper and lower bounds of the

resonant particle velocity range respectively map to the lower and upper bounds of the values of k for which $\mathcal{E}(k,t)$ is finite. For these particles, the delta function approximation Eq.(14.55) can be used to evaluate the quasilinear diffusion coefficient given by Eq.(14.38) and obtain

$$\begin{aligned} D_{QL,res}(v) &\simeq \frac{2\pi e^2}{\varepsilon_0 m^2} \int dk \delta(\omega_r - kv) \mathcal{E}(k,t) \\ &= \frac{2\pi e^2}{\varepsilon_0 m^2} \int dk \delta(\omega_r/v - k) \frac{\mathcal{E}(k,t)}{v} \\ &= \frac{2\pi e^2}{\varepsilon_0 m^2} \frac{\mathcal{E}(\omega_r/v,t)}{v}. \end{aligned} \quad (14.65)$$

Using this coefficient the quasilinear velocity diffusion for the resonant particles is

$$\frac{\partial f_{0,res}}{\partial t} = \frac{2\pi e^2}{\varepsilon_0 m^2} \frac{\partial}{\partial v} \left(\frac{\mathcal{E}(\omega_r/v,t)}{v} \frac{\partial f_{0,res}}{\partial v} \right). \quad (14.66)$$

It is seen from Eq.(14.62), the generalized formula for Landau damping, that

$$\pi \left(\frac{\partial f_0}{\partial v} \right)_{v=\omega_r/k} = 2\omega_i \frac{k^2}{\omega_r^3} n_0 \quad (14.67)$$

and so Eq.(14.66) becomes

$$\begin{aligned} \frac{\partial f_{0,res}}{\partial t} &= \frac{2e^2}{\varepsilon_0 m^2} \frac{\partial}{\partial v} \left(\frac{\mathcal{E}(\omega_r/v,t)}{v} 2\omega_i \frac{k^2}{\omega_r^3} n_0 \right) \\ &\simeq \frac{2\omega_p}{m} \frac{\partial}{\partial v} \left(\frac{\mathcal{E}(\omega_r/v,t)}{v^3} 2\omega_i \right) \\ &= \frac{2\omega_p}{m} \frac{\partial}{\partial t} \frac{\partial}{\partial v} \left(\frac{\mathcal{E}(\omega_r/v,t)}{v^3} \right) \end{aligned} \quad (14.68)$$

where $\omega_r \simeq \omega_p = \sqrt{n_0 e^2 / \varepsilon_0 m}$ has been used and also, because the particles are resonant, $v \simeq \omega_r/k$. This can be integrated with respect to time to obtain

$$f_{0,res}(v,t) - f_{0,res}(v,0) = \frac{2\omega_p}{m} \frac{\partial}{\partial v} \left(\frac{\mathcal{E}(\omega_r/v,t) - \mathcal{E}(\omega_r/v,0)}{v^3} \right). \quad (14.69)$$

By definition $\mathcal{E}(\omega_r/v,t)$ vanishes for v lying outside the resonant particle velocity range $v_{res}^{\min} < v < v_{res}^{\max}$ because outside this range there is no wave energy with which the particles can resonate (see Fig.14.1). Hence, integration of Eq.(14.69) over the velocity range $v_{res}^{\min} < v < v_{res}^{\max}$ of the resonant particles gives

$$\int_{v_{res}^{\min}}^{v_{res}^{\max}} dv f_{0,res}(v,t) = \int_{v_{res}^{\min}}^{v_{res}^{\max}} dv f_{0,res}(v,0) \quad (14.70)$$

which shows that the number of resonant particles is conserved.

Equation (14.64) showed that the resonant particle energy is not conserved and can be exchanged with the wave energy. Thus, the zeroth moment of the resonant particles is

conserved, but the second moment is not. Change of the resonant particle energy while conserving their number is achieved by adjusting the number of resonant particles that are slightly slower and slightly faster than ω/k . For example, if there is a decrease in the number of resonant particles having $v \simeq (\omega/k)_-$ there must be a corresponding increase in the number of resonant particles having $v \simeq (\omega/k)_+$. This process provides a net transfer of energy from the wave to the resonant particles, involves wave Landau damping, and requires having $\partial f_{0,res}/\partial v < 0$. The result, increasing the number of resonant particles having $v \simeq (\omega/k)_+$ while decreasing the number having $v \simeq (\omega/k)_-$ flattens $f_{0,res}(v)$ and so makes it plateau-like as indicated in Fig.14.1(b).

Behavior of the non-resonant particles

The quasi-linear diffusion coefficient for the non-resonant particles comes from the principle part of the integral in Eq.(14.38), i.e.,

$$D_{QL,non-res} = \frac{e^2}{\epsilon_0 m^2} P \int dk \frac{2\omega_i(k)\mathcal{E}(k,t)}{[\omega_r(k) - kv]^2 + \omega_i^2(k)}. \quad (14.71)$$

The vast majority of the non-resonant particles have velocities much slower than the wave, so for the non-resonant particles it can be assumed $v \ll \omega_r/k$ in which case

$$\begin{aligned} D_{QL,non-res} &\simeq \frac{e^2}{\epsilon_0 m^2} \int dk \frac{2\omega_i(k)\mathcal{E}(k,t)}{\omega_r^2(k)} \\ &\simeq \frac{1}{mn_0} \int dk 2\omega_i(k)\mathcal{E}(k,t). \end{aligned} \quad (14.72)$$

Since this non-resonant particle velocity space diffusion coefficient is velocity-independent, it can be factored from velocity integrals or derivatives. Equation (14.11) showed that the change in f_0 is order ϵ^2 where $\epsilon \ll 1$. This means that changes in f_0 are small compared to f_0 . On the other hand, there is no zero-order wave energy since the wave energy scales as E_1^2 and so is entirely constituted of terms which are order ϵ^2 . Thus, the wave energy spectrum can change substantially (for example, disappear altogether) whereas there is a only slight corresponding change to f_0 . Thus, Eq.(14.35), becomes

$$\begin{aligned} \frac{\partial f_{0,non-res}}{\partial t} &= \frac{1}{mn_0} \frac{\partial}{\partial v} \int dk 2\omega_i(k)\mathcal{E}(k,t) \frac{\partial f_{0,non-res}}{\partial v} \\ &\simeq \frac{1}{mn_0} \left(\frac{d}{dt} \int dk \mathcal{E}(k,t) \right) \frac{\partial^2 f_{0,non-res}}{\partial v^2} \end{aligned} \quad (14.73)$$

which can be integrated to give

$$f_{0,non-res}(v,t) - f_{0,non-res}(v,0) = \frac{1}{mn_0} \left(\int dk [\mathcal{E}(k,t) - \mathcal{E}(k,0)] \right) \frac{\partial^2 f_{0,non-res}}{\partial v^2}. \quad (14.74)$$

Since the number of resonant particles is conserved, the number of non-resonant particles must also be conserved.

If an initial wave spectrum becomes damped at $t = \infty$ then it is possible to write

$$f_{0,non-res}(v, \infty) = f_{0,non-res}(v,0) - \frac{1}{mn_0} \left[\int dk \mathcal{E}(k,0) \right] \frac{\partial^2 f_{0,non-res}(v,0)}{\partial v^2}. \quad (14.75)$$

In the range of velocities where $\partial^2 f_{0,non-res}/\partial v^2 > 0$ there will be a decrease in the number of non-resonant particles and vice versa in the range where $\partial^2 f_{0,non-res}/\partial v^2 < 0$. An initially Maxwellian distribution (which has $\partial^2 f_{0,non-res}/\partial v^2 < 0$ for very small velocities and vice versa for very large velocities) will develop a double-plateau shape (high plateau at low velocities and low plateau at high velocities) with a sharp gradient between the two plateaus. The lower plateau will merge smoothly with the plateau of the resonant particles. The non-resonant portion of the velocity distribution will appear to become colder as the waves damp as indicated in Fig.14.1(b).

This apparent cooling can be quantified by introducing an effective temperature T_{eff} which is defined to have the time derivative

$$\frac{d}{dt} (\kappa T_{eff}) = \frac{2}{n_0} \frac{d}{dt} \int dk \mathcal{E}(k,t). \quad (14.76)$$

This expression can be integrated to obtain

$$\kappa T_{eff}(t) = \kappa T_0 + \frac{2}{n_0} \int dk \mathcal{E}(k,t) \quad (14.77)$$

where T_0 is the temperature for the situation where there are no waves.

Using Eq.(14.76), Eq.(14.73) can be written as

$$\frac{\partial}{\partial t} f_{0,non-res} = \frac{d}{dt} \left(\frac{\kappa T_{eff}}{2m} \right) \frac{\partial^2 f_{0,non-res}}{\partial v^2}. \quad (14.78)$$

If $f_{0,non-res}$ is considered a function of κT_{eff} instead of t , Eq.(14.78) can be written as

$$\frac{\partial}{\partial(\kappa T_{eff})} f_{0,non-res} = \frac{1}{2m} \frac{\partial^2 f_{0,non-res}}{\partial v^2} \quad (14.79)$$

which has the appropriately normalized solution

$$\begin{aligned} f_{0,non-res} &= n_0 \sqrt{\frac{m}{2\pi\kappa T_{eff}(t)}} \exp\left(-\frac{mv^2}{2\kappa T_{eff}(t)}\right) \\ &= n_0 \sqrt{\frac{m/2\pi}{\kappa T_0 + \frac{2}{n_0} \int dk \mathcal{E}(k,t)}} \exp\left(-\frac{mv^2/2}{\kappa T_0 + \frac{2}{n_0} \int dk \mathcal{E}(k,t)}\right). \end{aligned} \quad (14.80)$$

Thus wave damping [i.e., the reduction of $\mathcal{E}(k,t)$] corresponds to an effective cooling of the non-resonant particles. As shown in Eq.(14.64) this kinetic energy reduction is accompanied by an equal reduction in the electric field energy and all this energy is transferred to the resonant particles.

14.3 Echoes

Plasma wave echoes (Gould, O'Neil and Malmberg 1967, Malmberg, Wharton, Gould and O'Neil 1968) are a nonlinear effect that provide some very useful insights into the Landau

damping mechanism and raises some interesting questions about how Landau damping relates to entropy. This arises from consideration of the following two apparently conflicting observations:

1. Wave damping should destroy the information content of the wave by converting ordered motion into heat. Thus, wave damping should increase the entropy of the system.
2. The collisionless Vlasov equation conserves entropy. This is because collisions are the agent that increases randomness and hence entropy. A collisionless system is in principle completely deterministic, so that the future of the system can be predicted with complete precision simply by integrating the system of equations forward in time. This entropy-conserving property of the collisionless Vlasov equation can be seen by direct calculation of the rate of change of the entropy,

$$\begin{aligned}
 \frac{dS}{dt} &= \frac{d}{dt} \int dx \int dv f(x, v, t) \ln f(x, v, t) \\
 &= \int dx \int dv (\ln f + 1) \frac{\partial f}{\partial t} \\
 &= - \int dx \int dv (\ln f + 1) \left(v \frac{\partial f}{\partial x} + \frac{q}{m} E \frac{\partial f}{\partial v} \right) \\
 &= - \int dx \int dv \left(v \frac{\partial}{\partial x} + \frac{q}{m} E \frac{\partial}{\partial v} \right) (f \ln f - f) \\
 &= 0
 \end{aligned} \tag{14.81}$$

since

$$\begin{aligned}
 \int dv \frac{\partial f}{\partial v} &= 0, \quad \int dx \frac{\partial f}{\partial x} = 0 \\
 \int dv \frac{\partial}{\partial v} (f \ln f - f) &= 0, \quad \int dx \frac{\partial}{\partial x} (f \ln f - f) = 0.
 \end{aligned} \tag{14.82}$$

So, what really happens— does Landau damping increase entropy or not? The answer goes right to the heart of what is meant by entropy. In particular, it should be recalled that entropy is defined as the natural logarithm of the number of microscopic states corresponding to a given macroscopic state. The concept “macroscopic state” presumes there exist macroscopic states which are (i) composed of different microscopic states and (ii) for all intents and purposes indistinguishable. Collisions would cause the system to continuously evolve through all the various microscopic states and an observer of the macroscopic system would not be able to distinguish one of these microscopic states from another.

The paradox is resolved because the concept of many microscopic states mapping to a single macroscopic state fails for Landau damping since the physical system for the Landau damping problem is actually in just one well-defined state which can be calculated. The macroscopic state therefore maps to just one microscopic state and so the system does not continuously and randomly evolve through a sequence of microscopic states.

Landau damping does not involve turning ordered information into heat. Instead, macroscopically ordered information is turned into microscopically ordered information. The information is still there, but is encoded in a macroscopically invisible form. A good analogy

to this situation is the process of making a holographic image of an object. The hologram looks blank unless illuminated in such a way to provide the proper decoding. If an observer does not know how to do the decoding, the information is lost to the observer, and the entropy content of the hologram is high compared to a regular photograph. However, if the observer knows how to decode the microscopically stored information, then no information is lost.

The Landau damping process scrambles the phase of the macroscopic information and encodes this as microscopic information which is normally irretrievable. If one does not know the appropriate trick for unscrambling the microscopically encoded information, it would be tempting to state that entropy has increased. However, the appropriate trick exists and has been demonstrated in laboratory experiments. Information that appeared to have been lost is retrieved and so entropy is not increased. The trick involves unscrambling the information encoded in the well-defined microscopic state.

To get an idea for the issues involved, we first consider the simple problem of a one dimensional beam of electrons having initial velocity v_0 . The beam is transiently accelerated by an externally generated, spatially periodic electric field pulse $E = \bar{E} \cos(kx)\delta(t)$ where \bar{E} is considered to be infinitesimal. The equation of motion for the electron beam is

$$m \left(\frac{\partial v}{\partial t} + v \frac{\partial v}{\partial x} \right) = -e\bar{E} \cos(kx)\delta(t) \quad (14.83)$$

and linearization of this equation gives

$$m \left(\frac{\partial v_1}{\partial t} + v_0 \frac{\partial v_1}{\partial x} \right) = -e\bar{E} \cos(kx)\delta(t). \quad (14.84)$$

It is convenient to use complex notation so that $\cos kx \rightarrow e^{ikx}$ and it is understood that eventually, the real part of a complex solution will be used to give the physical solution. It is therefore assumed that $v_1 \sim e^{ikx}$ and so the linearized equation becomes

$$m \left(\frac{\partial v_1}{\partial t} + ikv_0v_1 \right) = -e\bar{E}\delta(t). \quad (14.85)$$

Next it is argued that since the delta function can be considered as the superposition of an infinite spectrum of harmonic oscillations, i.e.,

$$\delta(t) = \frac{1}{2\pi} \int e^{-i\omega t} d\omega \quad (14.86)$$

the response of the beam to each frequency component can be considered. Thus, we consider the equation

$$\frac{\partial \tilde{v}_1}{\partial t} + ikv_0\tilde{v}_1 = -\frac{e\bar{E}}{m} e^{-i\omega t}, \quad (14.87)$$

so that the net velocity is

$$v_1(t) = \frac{1}{2\pi} \int \tilde{v}_1(\omega, t) d\omega. \quad (14.88)$$

Note that $\tilde{v}_1(\omega, t)$ is *not* a Fourier transform because it contains the explicit time dependence.

Since v_0 is the initial beam velocity, $v_1(t)$ must vanish at $t = 0$ providing a boundary condition for Eq.(14.87) at $t = 0$. One way to solve this equation is to first assume that

$\tilde{v}_1(\omega, t)$ consists of a particular solution satisfying the inhomogeneous part of the equation (i.e., balances the driving term on the right hand side) and a homogeneous solution (i.e., a solution of the homogeneous equation (left hand side of Eq.(14.87))). The coefficient of the homogeneous solution is chosen to satisfy the boundary condition at $t = 0$. The particular solution is assumed to vary as $e^{ikx - i\omega t}$ and so is the solution of the equation

$$(-i\omega + ikv_0)\tilde{v}_1 = -\frac{e\bar{E}}{m}e^{-i\omega t}. \quad (14.89)$$

The homogenous solution is the solution of

$$\frac{\partial \tilde{v}_1}{\partial t} + ikv_0\tilde{v}_1 = 0 \quad (14.90)$$

and has the form $\tilde{v}_1^h = \lambda \exp(-ikv_0t)$ where λ is a constant to be determined. Adding the particular and homogeneous solutions together gives the general solution

$$\tilde{v}_1 = -\frac{e\bar{E}}{m} \frac{ie^{-i\omega t}}{(\omega - kv_0)} + \lambda e^{-ikv_0t} \quad (14.91)$$

where λ is chosen to satisfy the initial condition. The initial condition $v_1 = 0$ at $t = 0$ determines λ and gives

$$\tilde{v}_1(\omega, t) = -\frac{ie\bar{E}}{m} \frac{(e^{-i\omega t} - e^{-ikv_0t})}{(\omega - kv_0)} \quad (14.92)$$

as the solution which satisfies both Eq.(14.87) and the initial condition. The term involving e^{-ikv_0t} is called the ballistic term. This term contains information about the initial conditions, is a solution of the homogeneous equation, is missed by Fourier treatments, is incorporated by Laplace transform treatments, and keeps v_1 from diverging when $\omega - kv \rightarrow 0$.

If we wished to revert to the time domain, then the contributions of all the harmonics would have to be summed, giving

$$v_1(t) = -\frac{ie\bar{E}}{2\pi m} \int d\omega \frac{(e^{-i\omega t} - e^{-ikv_0t})}{(\omega - kv_0)}. \quad (14.93)$$

14.3.1 Ballistic terms and Laplace transforms

The discussion above used an approach related to Fourier transforms, but added additional structure to account for the initial condition that $v_1 = 0$ at $t = 0$. This suggests that Laplace transforms ought to be used, since Laplace transforms automatically take into account initial conditions. Let us therefore Laplace transform Eq.(14.87) to see if indeed the particular and ballistic terms are appropriately characterized. The Laplace transform of Eq.(14.85) gives

$$\begin{aligned} p\tilde{v}_1 + ikv_0\tilde{v}_1 &= -\frac{e\bar{E}}{m} \int_0^\infty dt e^{-i\omega t - pt} \\ &= -\frac{e\bar{E}}{m} \frac{1}{i\omega + p} \end{aligned} \quad (14.94)$$

so

$$\tilde{v}_1 = -\frac{e\bar{E}/m}{(p+i\omega)(p+ikv_0)}. \quad (14.95)$$

The inverse Laplace transform gives

$$\tilde{v}_1 = -\frac{1}{2\pi i} \frac{e\bar{E}}{m} \int_{b-i\infty}^{b+i\infty} \frac{e^{pt}}{(p+i\omega)(p+ikv_0)} dp. \quad (14.96)$$

Analytic continuation allows the contour to be completed on the left hand side and it is seen that there are two poles, one at $p = -i\omega$ and the other at $p = -ikv$. Evaluation of the residues for the two poles gives

$$\begin{aligned} \tilde{v}_1 &= -\frac{1}{2\pi i} \frac{e\bar{E}}{m} \left\{ \begin{aligned} &2\pi i \lim_{p \rightarrow -i\omega} (p+i\omega) \left[\frac{e^{pt}}{(p+i\omega)(p+ikv_0)} \right] \\ &+ 2\pi i \lim_{p \rightarrow -ikv} (p+ikv) \left[\frac{e^{pt}}{(p+i\omega)(p+ikv_0)} \right] \end{aligned} \right\} \\ &= -\frac{e\bar{E}}{m} \left\{ \frac{e^{-i\omega t}}{(-i\omega + ikv_0)} + \frac{e^{-ikv_0 t}}{(-ikv_0 + i\omega)} \right\} \end{aligned} \quad (14.97)$$

which is the same as Eq.(14.92). The ballistic term $\sim e^{-ikv_0 t}$ thus results from a pole originating from the Laplace transform of the source term, whereas the homogeneous term $\sim e^{-i\omega t}$ results from the pole originating from the factor $(p+ikv_0)$ that appeared in the left hand side of Eq.(14.94).

14.3.2 Phase mixing of the ballistic term for multiple beams

Now suppose that instead of just one electron beam, there are multiple beams where the density of each beam is proportional to $\exp(-v_0^2/v_T^2)$; this would be one way of characterizing a Maxwellian velocity distribution. Superposition of the ballistic terms from all these beams leads to a vanishing sum, because the ballistic terms each have a velocity-dependent phase and so the superposition would give destructive interference due to phase mixing. In particular, the superposition would involve integrals of the form

$$\int dv_0 e^{-v_0^2/v_T^2 + ikv_0 t} = e^{-k^2 v_T^2 t^2 / 4} \int dv_0 e^{-(v_0/v_T + ikv_T t/2)^2} = \sqrt{\pi} v_T e^{-k^2 v_T^2 t^2 / 4} \quad (14.98)$$

which would quickly become extremely small. This suggests the ballistic term has no enduring macroscopic physical importance and, in fact, this is true for linear problems where the ballistic term is typically ignored. However, the ballistic term can assume importance when nonlinearities are considered.

14.3.3 Beam echoes

The linearized continuity equation corresponding to Eq.(14.84) is

$$\frac{\partial n_1}{\partial t} + v_0 \frac{\partial n_1}{\partial x} + n_0 \frac{\partial v_1}{\partial x} = 0 \quad (14.99)$$

and so, invoking the assumed e^{ikx} dependence, this becomes

$$\frac{\partial n_1}{\partial t} + ikv_0 n_1 + ikn_0 v_1 = 0. \quad (14.100)$$

In analogy to Eq.(14.88) the linearized density can be expressed as

$$n_1(t) = \frac{1}{2\pi} \int \tilde{n}_1(\omega, t) d\omega \quad (14.101)$$

where again $\tilde{n}_1(\omega, t)$ is not a Fourier transform because $\tilde{n}_1(\omega, t)$ contains a ballistic term incorporating information about initial conditions. The equation for each frequency component thus is

$$\frac{\partial \tilde{n}_1}{\partial t} + ikv_0 \tilde{n}_1 + ikn_0 \tilde{v}_1 = 0 \quad (14.102)$$

which may be Laplace transformed to give

$$(p + ikv_0) \tilde{n}_1 + ikn_0 \tilde{v}_1 = 0 \quad (14.103)$$

or, using Eq.(14.95),

$$\tilde{n}_1(p, \omega) = \frac{ikn_0 e \bar{E} / m}{(p + i\omega)(p + ikv_0)^2}. \quad (14.104)$$

There is now a second-order pole at $p = ikv_0$ and so there will be a ballistic term $\sim \exp(ikv_0 t)$ associated with the density perturbation. This ballistic term will also phase mix away if there is a Gaussian velocity distribution of beams.

In order to consider non-linear consequences, we consider the second-order continuity equation

$$\frac{\partial n_2}{\partial t} + v_0 \frac{\partial n_2}{\partial t} + v_1 \frac{\partial n_1}{\partial x} + \frac{\partial}{\partial x} (n_1 v_1) = 0 \quad (14.105)$$

which has inhomogeneous (forcing) terms such as $n_1 v_1$ involving products of linear quantities. Suppose that in addition to the original pulse with spatial wavenumber k at time $t = 0$ an additional pulse is also imposed with wavenumber k' at time $t = \tau$. This additional pulse would introduce ballistic terms having a time dependence $\sim \exp(ik'v_0(t - \tau))$. Thus the nonlinear product $n_1 v_1$ has a dependence

$$n_1 v_1 \sim \text{Re} \exp(ikv_0 t) \times \text{Re} \exp(ik'v_0(t - \tau)) \quad (14.106)$$

which contains terms of the form $\exp(ikv_0 t - k'v_0(t - \tau))$. In general, this product of ballistic terms would phase mix away if there were a Gaussian distribution of beams, just as for the linear ballistic term. However, at the special time given by

$$kt - k'(t - \tau) = 0 \quad (14.107)$$

the phase of the nonlinear ballistic term would be zero for all velocities, and so no phase mixing would occur when the velocity contributions are summed. Thus, at the special time

$$t = \frac{k'\tau}{k' - k} \quad (14.108)$$

the non-linear product is not subject to phase-mixing and the superposition of the non-linear ballistic terms of a Gaussian distribution of beams gives a macroscopic signal. The time at which the phase of the non-linear ballistic term becomes stationary can greatly exceed τ and so a macroscopic nonlinear signal would appear long after both initial pulses have gone. This ghost-like non-linear signal is called the fluid echo.

14.3.4 The self-consistent non-linear Vlasov-Poisson problem

These ideas carry over into the Vlasov-Poisson analysis of plasma waves, but several additional issues occur which complicate and obscure matters. First, the problem takes place in phase-space so instead of having a pair of coupled equations for velocity and density, there is only the Vlasov equation. The Vlasov equation not only contains a convective term analogous to the fluid convective terms but also incorporates an acceleration term which describes how the velocity distribution function is modified when particles undergo acceleration and change their velocity. As in the fluid equations there is a coupling with Poisson's equation. This coupling not only provides the self-consistent interaction giving plasma waves, but it also provides for Landau damping. Landau damping is essentially a phase mixing of the Fourier-like driven terms, each of which scales as $\int dv (\omega - kv)^{-1} \exp(-i\omega t) \partial f_0 / \partial v$. However, linear ballistic terms must also be excited in order to satisfy initial conditions. These ballistic terms scale as $\int dv (\omega - kv)^{-1} \exp(-ikvt) \partial f_0 / \partial v$ and also phase mix away because of the $\exp(-ikvt)$ factor.

If there are two successive pulses, then the non-linear ballistic term will again have a stationary phase (i.e., phase independent of velocity) at the special time given by Eq.(14.108). This time could be arranged to be long after the linear plasma responses to the two pulses have Landau damped away so that the echo would seem to appear from nowhere. Thus, the Vlasov-Poisson analysis contains essentially similar echo physics, but in addition has a self-consistent treatment of the plasma waves and their associated Landau damping.

To proceed with the Vlasov-Poisson analysis, we begin by considering Eq.(14.7) again, which is rewritten below for convenience

$$\begin{aligned} \frac{\partial}{\partial t} (f_0 + f_1 + f_2 + \dots) + v \frac{\partial}{\partial x} (f_0 + f_1 + f_2 + \dots) \\ - \frac{e}{m} (E_0 + E_1 + E_2 + \dots) \frac{\partial}{\partial v} (f_0 + f_1 + f_2 + \dots) = 0. \end{aligned} \quad (14.109)$$

Equilibrium is defined as the solution obtained by balancing all the zeroth order terms, i.e.,

$$\frac{\partial f_0}{\partial t} + v \frac{\partial f_0}{\partial x} - \frac{e}{m} E_0 \frac{\partial f_0}{\partial v} = 0. \quad (14.110)$$

This is trivially satisfied by having $E_0 = 0$, $\partial f_0 / \partial t = 0$, $\partial f_0 / \partial x = 0$ and $f_0(v)$ arbitrary; we will make these assumptions here. This equilibrium solution is then subtracted from Eq.(14.109) leaving

$$\begin{aligned} \frac{\partial}{\partial t} (f_1 + f_2 + \dots) + v \frac{\partial}{\partial x} (f_1 + f_2 + \dots) - \frac{e}{m} E_1 \frac{\partial}{\partial v} (f_0 + f_1 + f_2 + \dots) \\ - \frac{e}{m} (E_2 + \dots) \frac{\partial}{\partial v} (f_0 + f_1 + \dots) = 0. \end{aligned} \quad (14.111)$$

The first-order solution is defined as the solution to

$$\frac{\partial}{\partial t} f_1 + v \frac{\partial f_1}{\partial x} - \frac{e}{m} E_1 \frac{\partial f_0}{\partial v} = 0, \quad (14.112)$$

the equation obtained by retaining all the first-order terms. The first-order solution is then subtracted from Eq.(14.111) and what remains are second and higher order terms. Drop-

ping terms higher than second-order gives the second-order equation

$$\frac{\partial f_2}{\partial t} + v \frac{\partial f_2}{\partial x} - \frac{eE_2}{m} \frac{\partial f_0}{\partial v} - \frac{e}{m} E_1 \frac{\partial f_1}{\partial v} = 0. \quad (14.113)$$

The special case where $E_1 f_1$ has a zero frequency component was discussed in the previous section on quasilinear diffusion and so here only the situation where $E_1 f_1$ has a finite frequency will be considered. Since the first-order system has been solved, the last term in Eq.(14.113) can be considered as a source term and so we re-arrange the equation to be

$$\frac{\partial f_2}{\partial t} + v \frac{\partial f_2}{\partial x} - \frac{eE_2}{m} \frac{\partial f_0}{\partial v} = \frac{e}{m} \frac{\partial}{\partial v} (E_1 f_1) \quad (14.114)$$

where E_1 and f_1 are known and f_2 is to be determined. The specification that $f = f_0 + f_1$ at $t = 0$ provides the boundary condition $f_2 = 0$ at time $t = 0$. Because Eq. (14.114) has both a self-consistent electric field contribution (E_2 term on the left hand side) and a prescribed electric field term (E_1 term on the right hand side), it has aspects of both the self-consistent problem and of the problem where the electric field is prescribed.

The linear problem Suppose periodic grids are inserted into a plasma and the grids are transiently pulsed thereby creating the potential $\phi_{ext}(x, t)$. The charged particles will move in response to this applied potential and the resulting displacement produces a perturbation of the plasma charge density. Poisson's equation must therefore take into account both the charge density on the grid and the resulting plasma charge density and so has the form

$$\nabla^2 \phi_1 = -\frac{1}{\varepsilon_0} (\text{grid charge density} + \text{plasma charge density}). \quad (14.115)$$

Since the grid charge density is related to the grid potential by

$$\nabla^2 \phi_{ext} = -\frac{1}{\varepsilon_0} (\text{grid charge density}) \quad (14.116)$$

Poisson's equation can be recast as

$$\nabla^2 \phi_1 = \nabla^2 \phi_{ext} + \frac{e}{\varepsilon_0} \int f_1 dv. \quad (14.117)$$

A Fourier-Laplace transform operation is then applied to Eq.(14.117) to obtain

$$-k^2 \tilde{\phi}_1 = -k^2 \tilde{\phi}_{ext} + \frac{e}{\varepsilon_0} \int \tilde{f}_1 dv. \quad (14.118)$$

However, using $E_1 = -\nabla \phi_1$ the Fourier Laplace transform of Eq.(14.112) gives

$$\tilde{f}_1 = -i \frac{e}{m} \frac{k \tilde{\phi}_1}{p + ikv} \frac{\partial f_0}{\partial v} \quad (14.119)$$

so that Eq.(14.118) becomes

$$\tilde{\phi}_1(p, k) = \frac{\tilde{\phi}_{ext}(p, k)}{\mathcal{D}(p, k)} \quad (14.120)$$

where

$$\mathcal{D}(p, k) = 1 - i \frac{e^2}{k^2 m \varepsilon_0} \int \frac{k}{p + ikv} \frac{\partial f_0}{\partial v} dv \quad (14.121)$$

is the usual self-consistent linear dielectric response function. Thus, the driven first-order velocity distribution function can be written as

$$\tilde{f}_1 = -i \frac{e}{m} \frac{k}{p + ikv} \frac{\tilde{\phi}_{ext}(p, k)}{\mathcal{D}(p, k)} \frac{\partial f_0}{\partial v}. \quad (14.122)$$

If an inverse transform were to be performed on \tilde{f}_1 , then three issues would have to be taken into account. These are (i) a ballistic term $\sim \exp(ikvt)$ associated with the pole due to $p + ikv$ in the denominator, (ii) a Landau-damped plasma oscillation due to the root of $\mathcal{D}(p, k)$ in the denominator, and (iii) the direct inverse transform of the numerator $\tilde{\phi}_{ext}(p, k)$ which by itself would reproduce the original imposed potential, but which will be modified due to the other factors.

Fourier-Laplace transform of the non-linear equation As discussed in Eq.(14.1) nonlinear quantities provide sum and difference frequencies. For example, an oscillation at frequency ω would result from the nonlinear product of a term oscillating at $\omega - \omega'$ and a term oscillating at ω' since $(\omega - \omega') + \omega' = \omega$. This can be written in a more formal and more general way using convolution integrals for both Fourier and Laplace transforms.

Since Laplace transforms will be used for the temporal dependence and since the right hand side of Eq.(14.114) involves a product term, it is necessary to consider the Laplace transform of a product,

$$\begin{aligned} \mathcal{L}(g(t)h(t)) &= \int_0^\infty g(t)h(t)e^{-pt} dt \\ &= \int_0^\infty \left[\frac{1}{2\pi i} \int_{b-i\infty}^{b+i\infty} \tilde{g}(p')e^{p't} dp' \right] h(t)e^{-pt} dt \\ &= \frac{1}{2\pi i} \int_{b-i\infty}^{b+i\infty} \tilde{g}(p') \left(\int_0^\infty h(t)e^{(p'-p)t} dt \right) dp' \\ &= \frac{1}{2\pi i} \int_{b-i\infty}^{b+i\infty} \tilde{g}(p')\tilde{h}(p-p') dp'. \end{aligned} \quad (14.123)$$

This means that the Laplace transform with argument p results from all possible products of $\tilde{g}(p')$ with $\tilde{h}(p-p')$. If $\exp(\alpha_1 t)$ is the fastest growing term in $g(t)$ and $\exp(\alpha_2 t)$ is the fastest growing term in $h(t)$ then $b > \alpha_1$ is required in order for the Laplace transform of $g(t)$ to be defined. Furthermore, in order for the Laplace transform of $h(t)$ to be defined, it is necessary to have $\text{Re } p - \text{Re } p' > \alpha_2$ or $\text{Re } p > \text{Re } p' + \alpha_2$ which implies $\text{Re } p > b + \alpha_2$. These requirements can be summarized as $\text{Re } p - \alpha_2 > b > \alpha_1$.

Using

$$\tilde{g}(k) = \int_{-\infty}^{\infty} g(x) e^{-ikx} dx \quad (14.124a)$$

$$g(x) = \frac{1}{2\pi} \int_{-\infty}^{\infty} \tilde{g}(k) e^{+ikx} dk, \quad (14.124b)$$

a similar procedure for Fourier transforms gives

$$\begin{aligned}
\mathcal{F}(g(x)h(x)) &= \int_{-\infty}^{\infty} g(x)h(x)e^{ikx} dx \\
&= \int_{-\infty}^{\infty} \left[\frac{1}{2\pi} \int_{-\infty}^{\infty} \tilde{g}(k')e^{-ik'x} dk' \right] h(x)e^{ikx} dx \\
&= \frac{1}{2\pi} \int_{-\infty}^{\infty} dk' \tilde{g}(k') \int_{-\infty}^{\infty} h(x)e^{i(k-k')x} dx \\
&= \frac{1}{2\pi} \int_{-\infty}^{\infty} dk' \tilde{g}(k') \tilde{h}(k-k'). \tag{14.125}
\end{aligned}$$

Thus, the Fourier-Laplace transform of Eq.(14.114) gives

$$\begin{aligned}
&(p + ikv) \tilde{f}_2(p, k) + ik \frac{e}{m} \frac{\partial f_0}{\partial v} \tilde{\phi}_2(p, k) \\
&= -\frac{e}{m} \frac{\partial}{\partial v} \left[\int_{-\infty}^{\infty} \frac{dk'}{2\pi} \int_{b-i\infty}^{b+i\infty} \frac{dp'}{2\pi} k' \tilde{\phi}_1(p', k') \tilde{f}_1(p-p', k-k') \right]. \tag{14.126}
\end{aligned}$$

Because the convolution integrals are notationally unwieldy, to clarify the notation we define the new dummy variables

$$\begin{aligned}
\bar{k}' &= k - k' \\
\bar{p}' &= p - p' \tag{14.127}
\end{aligned}$$

so that Eq.(14.126) becomes

$$\begin{aligned}
&(p + ikv) \tilde{f}_2(p, k) + ik \frac{e}{m} \frac{\partial f_0}{\partial v} \tilde{\phi}_2(p, k) \\
&= -\frac{e}{m} \frac{\partial}{\partial v} \left[\int_{-\infty}^{\infty} \frac{dk'}{2\pi} \int_{b-i\infty}^{b+i\infty} \frac{dp'}{2\pi} k' \tilde{\phi}_1(p', k') \tilde{f}_1(\bar{p}', \bar{k}') \right]. \tag{14.128}
\end{aligned}$$

The factors in the convolution integral can be expressed in terms of the original driving potential using Eqs.(14.120) and (14.122) to obtain

$$(p + ikv) \tilde{f}_2(p, k) + ik \frac{e}{m} \frac{\partial f_0}{\partial v} \tilde{\phi}_2(p, k) = \frac{\partial}{\partial v} \chi(p, k, v) \tag{14.129}$$

where the non-linear convolution term is

$$\begin{aligned}
\chi(p, k, v) &= \left(\frac{e}{m} \right)^2 \int_{-\infty}^{\infty} \frac{dk'}{2\pi} \int_{b-i\infty}^{b+i\infty} \frac{dp'}{2\pi} \left\{ k' \frac{\tilde{\phi}_{ext}(p', k')}{\mathcal{D}(p', k')} \times \right. \\
&\quad \left. \frac{i\bar{k}'}{\bar{p}' + i\bar{k}'v} \frac{\tilde{\phi}_{ext}(\bar{p}', \bar{k}')}{\mathcal{D}(\bar{p}', \bar{k}')} \frac{\partial f_0}{\partial v} \right\}. \tag{14.130}
\end{aligned}$$

Equation (14.129) may be solved for $\tilde{f}_2(p, k)$ to give

$$\tilde{f}_2(p, k) = -i \frac{e}{m} \frac{k}{(p + ikv)} \frac{\partial f_0}{\partial v} \tilde{\phi}_2(p, k) + \frac{1}{(p + ikv)} \frac{\partial}{\partial v} \chi(p, k, v). \quad (14.131)$$

However, the Fourier-Laplace transform of the second-order Poisson's equation gives

$$-k^2 \tilde{\phi}_2(p, k) = \frac{e}{\varepsilon_0} \int \tilde{f}_2(p, k) dv \quad (14.132)$$

and so substituting for $\tilde{f}_2(p, k)$ gives

$$-k^2 \tilde{\phi}_2(p, k) = \frac{e}{\varepsilon_0} \int \left[-i \frac{e}{m} \frac{k}{(p + ikv)} \frac{\partial f_0}{\partial v} \tilde{\phi}_2(p, k) + \frac{1}{(p + ikv)} \frac{\partial \chi}{\partial v} \right] dv \quad (14.133)$$

or

$$\begin{aligned} \tilde{\phi}_2(p, k) &= -\frac{e}{k^2 \varepsilon_0 \mathcal{D}(p, k)} \int \frac{1}{(p + ikv)} \frac{\partial \chi}{\partial v} dv \\ &= \frac{e}{k^2 \varepsilon_0 \mathcal{D}(p, k)} \int \frac{ik\chi}{(p + ikv)^2} dv. \end{aligned} \quad (14.134)$$

Substitution for χ and using the velocity-normalized distribution function $\bar{f}_0 = f_0/n_0$ discussed in Eq.(14.4) gives

$$\begin{aligned} \tilde{\phi}_2(p, k) &= \frac{\omega_p^2}{k^2 \mathcal{D}(p, k)} \frac{e}{m} \int dv \int_{-\infty}^{\infty} \frac{dk'}{2\pi} \int_{b-i\infty}^{b+i\infty} \frac{dp'}{2\pi} \\ &\quad \left\{ \frac{ik}{(p + ikv)^2} \frac{k' \tilde{\phi}_{ext}(p', k')}{\mathcal{D}(p', k')} \frac{i \bar{k}'}{\bar{p}' + i \bar{k}' v} \frac{\tilde{\phi}_{ext}(\bar{p}', \bar{k}')}{\mathcal{D}(\bar{p}', \bar{k}')} \frac{\partial \bar{f}_0}{\partial v} \right\}. \end{aligned} \quad (14.135)$$

Double-impulse source function and its transform

In order to proceed further, the form of the external source must be specified. We assume that the external source consists of two sets of periodic grids which are pulsed sequentially. The first set of grids has wavenumber k_a and is pulsed at $t = 0$ whereas the second set of grids has wavenumber k_b and is pulsed after a delay τ . Thus, the external source has the form

$$\phi_{ext}(x, t) = \phi_a \cos(k_a x) \delta(\omega_p t) + \phi_b \cos(k_b x) \delta(\omega_p(t - \tau)). \quad (14.136)$$

The Fourier-Laplace transform of this source function gives

$$\begin{aligned} \tilde{\phi}_{ext}(p, k) &= \int_{-\infty}^{\infty} \int_0^{\infty} \phi_{ext}(x, t) e^{-ikx - pt} dx dt \\ &= \frac{\pi}{\omega_p} \sum_{\pm} \{ \phi_a \delta(k \pm k_a) + \phi_b \delta(k \pm k_b) e^{-p\tau} \}. \end{aligned} \quad (14.137)$$

Since we are interested in the non-linear interaction between the a and b pulses, only the contribution from the a pulse in the first $\tilde{\phi}_{ext}$ factor in Eq.(14.135) and the contribution

from the b pulse in the second $\tilde{\phi}_{ext}$ factor in Eq.(14.135) will be considered. We therefore substitute the a contribution in Eq.(14.137) for the first $\tilde{\phi}_{ext}$ factor in Eq.(14.135) to obtain

$$\begin{aligned} \tilde{\phi}_2(p, k) &= \frac{\omega_p \pi \phi_a}{k^2 \mathcal{D}(p, k)} \frac{e}{m} \int dv \int_{-\infty}^{\infty} \frac{dk'}{2\pi} \int_{b-i\infty}^{b+i\infty} \frac{dp'}{2\pi} \frac{ik' \delta(k' \pm k_a)}{(p + ikv)^2 \mathcal{D}(p', k')} \\ &\times \frac{i \bar{k}'}{(p - p') + ik'v} \frac{\tilde{\phi}_{ext}((p - p'), \bar{k}')}{\mathcal{D}(p - p', \bar{k}')} \frac{\partial \bar{f}_0}{\partial v}. \end{aligned} \quad (14.138)$$

The effect of the $\delta(k' \pm k_a)$ factor when evaluating the k' integral is to force $k' \rightarrow \pm k_a$ and also $\bar{k}' \rightarrow k \mp k_a$ so that

$$\begin{aligned} \tilde{\phi}_2(p, k) &= \frac{\omega_p}{k^2 \mathcal{D}(p, k)} \frac{e \phi_a}{2m} \sum_{\pm} \int dv \int_{b-i\infty}^{b+i\infty} \frac{dp'}{2\pi} \frac{(\mp ik k_a)}{(p + ikv)^2 \mathcal{D}(p', \mp k_a)} \times \\ &\frac{i (k \mp k_a)}{\bar{p}' + i(k \mp k_a)v} \frac{\tilde{\phi}_{ext}(\bar{p}', (k \mp k_a))}{\mathcal{D}(\bar{p}', k \mp k_a)} \frac{\partial \bar{f}_0}{\partial v}. \end{aligned} \quad (14.139)$$

Now let us substitute for the second $\tilde{\phi}_{ext}$ factor using the contribution from the b pulse to obtain

$$\begin{aligned} \tilde{\phi}_2(p, k) &= \frac{\pi}{2k^2 \mathcal{D}(p, k)} \frac{e}{m} \phi_a \phi_b \sum_{\pm} \sum_{\pm} \int dv \int_{b-i\infty}^{b+i\infty} \frac{dp'}{2\pi} \frac{(\mp ik k_a)}{(p + ikv)^2 \mathcal{D}(p', \mp k_a)} \\ &\times \frac{i (k \mp k_a)}{\bar{p}' + i(k \mp k_a)v} \frac{\delta(k \mp k_a \pm k_b) e^{-\bar{p}' \tau}}{\mathcal{D}(\bar{p}', k \mp k_a)} \frac{\partial \bar{f}_0}{\partial v}. \end{aligned} \quad (14.140)$$

The upper choice of the \pm and \mp signs is selected and the inverse Fourier transform performed to obtain

$$\begin{aligned} \tilde{\phi}_2^{upper}(p, x) &= \frac{\phi_a \phi_b}{4k^2 \mathcal{D}(p, k)} \frac{e}{m} \int_{-\infty}^{\infty} dk \int dv \int_{b-i\infty}^{b+i\infty} \frac{dp'}{2\pi} \frac{(-ik k_a)}{(p + ikv)^2 \mathcal{D}(p', -k_a)} \\ &\times \frac{i (k - k_a)}{\bar{p}' + i(k - k_a)v} \frac{\delta(k - k_a + k_b) e^{-\bar{p}' \tau + ikx}}{\mathcal{D}(\bar{p}', k - k_a)} \frac{\partial \bar{f}_0}{\partial v} \\ &= \frac{\phi_a \phi_b}{4(k_a - k_b)^2 \mathcal{D}(p, k_a - k_b)} \frac{e}{m} \int dv \int_{b-i\infty}^{b+i\infty} \frac{dp'}{2\pi} \times \\ &\frac{i (k_a - k_b)}{(p + i(k_a - k_b)v)^2} \frac{k_a}{\mathcal{D}(p', -k_a)} \frac{i k_b}{\bar{p}' - ik_b v} \frac{e^{-\bar{p}' \tau + i(k_a - k_b)x}}{\mathcal{D}(\bar{p}', -k_b)} \frac{\partial \bar{f}_0}{\partial v}. \end{aligned} \quad (14.141)$$

The lower choice of the \pm and \mp signs means that $k_a \rightarrow -k_a$ and $k_b \rightarrow -k_b$ and so at the end of the calculation $\tilde{\phi}_2^{lower}(p, x)$ can also be determined by simply letting $k_a \rightarrow -k_a$

and $k_b \rightarrow -k_b$. The inverse Laplace transform gives

$$\begin{aligned} \tilde{\phi}_2^{upper}(t, x) &= \frac{\phi_a \phi_b}{4(k_a - k_b)^2} \frac{e}{m} \int_{b-i\infty}^{b+i\infty} \frac{dp}{2\pi i} \frac{1}{\mathcal{D}(p, k_a - k_b)} \int dv \int_{b-i\infty}^{b+i\infty} \frac{dp'}{2\pi} \\ &\quad \times \frac{k_a}{(p + i(k_a - k_b)v)^2} \frac{i k_b}{\mathcal{D}(p', -k_a)} \frac{1}{p - p' - i k_b v} \\ &\quad \times \frac{e^{pt - (p-p')\tau + i(k_a - k_b)x}}{\mathcal{D}(p - p', -k_b)} \frac{\partial \bar{f}_0}{\partial v}. \end{aligned} \quad (14.142)$$

We first consider the p' integral and only retain the ballistic term due to the pole $(p - p') - i k_b v$. Evaluating the residue associated with this pole gives $p' = p - i k_b v$ so

$$\begin{aligned} \tilde{\phi}_2^{upper}(t, x) &= -\frac{\phi_a \phi_b}{4(k_a - k_b)^2} \frac{e}{m} \int_{b-i\infty}^{b+i\infty} dp \frac{1}{\mathcal{D}(p, k_a - k_b)} \int dv \\ &\quad \frac{i(k_a - k_b)}{(p + i(k_a - k_b)v)^2} \frac{i k_a k_b}{\mathcal{D}(p - i k_b v, -k_a)} \frac{e^{pt - i k_b v \tau + i(k_a - k_b)x}}{\mathcal{D}(i k_b v, -k_b)} \frac{\partial \bar{f}_0}{\partial v}. \end{aligned} \quad (14.143)$$

The pole at $(p + i(k_a - k_b)v)^2$ is second-order and so the rule for a second-order residue should be used, i.e.,

$$\oint dp \frac{1}{(p - p_0)^2} g(p) = \pi i \lim_{p \rightarrow p_0} \frac{d}{dp} g(p). \quad (14.144)$$

Thus, we obtain

$$\begin{aligned} \phi_2(t, x) &= -\frac{\phi_a \phi_b \pi i}{4(k_a - k_b)^2} \frac{e}{m} \int dv \lim_{p \rightarrow i(k_b - k_a)v} \frac{d}{dp} \\ &\quad \left(\frac{i(k_a - k_b)}{\mathcal{D}(p, k_a - k_b)} \frac{i k_a k_b}{\mathcal{D}(p - i k_b v, -k_a)} \frac{e^{pt - i k_b v \tau + i(k_a - k_b)x}}{\mathcal{D}(i k_b v, -k_b)} \frac{\partial \bar{f}_0}{\partial v} \right). \end{aligned} \quad (14.145)$$

The strongest dependence on p is in the exponential e^{pt} and so retaining only the contribution of this term to the d/dp operator gives

$$\begin{aligned} \tilde{\phi}_2^{upper}(t, x) &= -\frac{\pi i \phi_a \phi_b}{4(k_a - k_b)^2} \frac{e}{m} \int dv \lim_{p \rightarrow i(k_b - k_a)v} \\ &\quad \left(\frac{t i(k_a - k_b)}{\mathcal{D}(p, k_a - k_b)} \frac{i k_a k_b}{\mathcal{D}(p - i k_b v, -k_a)} \frac{e^{pt - i k_b v \tau + i(k_a - k_b)x}}{\mathcal{D}(i k_b v, -k_b)} \frac{\partial \bar{f}_0}{\partial v} \right) \\ &= \frac{\pi}{4} \frac{k_a k_b}{(k_a - k_b)^2} \frac{e \phi_a \phi_b}{m} e^{i(k_a - k_b)x} \int dv \\ &\quad \frac{i(k_a - k_b)t}{\mathcal{D}(i(k_b - k_a)v, k_a - k_b) \mathcal{D}(-i k_a v, -k_a)} \frac{e^{i(k_b - k_a)v t - i k_b v \tau}}{\mathcal{D}(i k_b v, -k_b)} \frac{\partial \bar{f}_0}{\partial v}. \end{aligned} \quad (14.146)$$

The $\tilde{\phi}^{lower}(t, x)$ term is obtained by letting $k_a - k_b \rightarrow -(k_a - k_b)$ and so

$$\tilde{\phi}_2(t, x) = \tilde{\phi}_2^{upper}(t, x) + \tilde{\phi}^{lower}(t, x). \quad (14.147)$$

If it is assumed that $\bar{f}_0 = (\pi v_T)^{-1/2} \exp(-v^2/v_T^2)$ then the velocity integrals in the upper and lower terms will be

$$\begin{aligned} \frac{1}{\sqrt{\pi}} \int dv e^{-v^2/v_T^2 \pm i[(k_b - k_a)t - k_b \tau]v} &= \exp\left(-[(k_b - k_a)t - k_b \tau]^2 v_T^2/4\right) \\ &= \exp\left(-\left[t - \frac{k_b}{k_b - k_a} \tau\right]^2 \frac{(k_b - k_a)^2 v_T^2}{4}\right). \end{aligned} \quad (14.148)$$

Phase mixing due to the extreme velocity dependence of the $\exp(i(k_b - k_a)vt - ik_b v \tau)$ factor will cause the velocity integral to vanish except at the special time

$$t_{echo} = \frac{k_b}{k_b - k_a} \tau \quad (14.149)$$

when there is no phase mixing and so a finite $\tilde{\phi}_2(t, x)$ signal results. This is the echo. The half-width of the echo can be determined by writing Eq.(14.148) as

$$\frac{1}{\sqrt{\pi}} \int dv e^{-v^2/v_T^2 \pm i[(k_b - k_a)t - k_b \tau]v} = e^{-(t - t_{echo})^2 / (\Delta t)^2} \quad (14.150)$$

where

$$\Delta t = \frac{2}{|k_b - k_a| v_T} \quad (14.151)$$

is the width of the echo.

14.3.5 Spatial echoes

Creating spatially periodic sources with temporal delta functions is experimentally more difficult than creating temporally periodic sources with spatial delta functions. In the latter arrangement, two spatially separated grids are placed in a plasma and each grid is excited at a different frequency. This system is then characterized by a Fourier transform in time and a Laplace transform in space so that the convective derivative in the linearized Vlasov equation has the form $-i\omega f_1 + v \partial f_1 / \partial x$ giving ballistic terms proportional to $\exp(i\omega x/v)$ instead of proportional to $\exp(-ikvt)$. Thus, if two grids separated by a distance L are excited at respective frequencies ω_1 and ω_2 , one grid will excite a ballistic term $\sim \exp(i\omega_1(x-L)/v)$ and the other will excite a ballistic term $\sim \exp(i\omega_2 x/v)$ and so the non-linear product of these two ballistic terms will include a factor $\sim \exp(i\omega_1(x-L)/v - i\omega_2 x/v)$ which will phase mix to zero except at the spatial location

$$x_{echo} = \frac{\omega_1 L}{\omega_1 - \omega_2}. \quad (14.152)$$

If the spatial Landau damping length of the two linear modes is much less than x_{echo} , then the linear modes will appear to damp away spatially and then the echo will appear at $x = x_{echo}$ which will be much further away. This sort of arrangement was used to demonstrate echoes in lab experiments by Malmberg et al. (1968)

14.3.6 Higher order echoes

If one expands the Vlasov equation to higher than second-order, then higher order products of ballistic terms can result. For spatial echoes high order products of the form

$$\left[e^{i\omega_1(x-L)/v} \right]^N \times \left[e^{-i\omega_2 x/v} \right]^M \quad (14.153)$$

will appear and will phase mix away except at locations where

$$N\omega_1(x-L) = M\omega_2 x \quad (14.154)$$

so there will be a higher order echo at the location

$$x_{echo} = \frac{M\omega_2 L}{N\omega_1 - M\omega_2}.$$

14.4 Assignments

1. Competition between collisions and quasilinear diffusion

- (a) Let $v_{Te} = \sqrt{2\kappa T_e/m_e}$ and $w = v_z/v_{Te}$ and show that the Fokker-Planck equation in problem 1 of Chapter 13 can be written in dimensionless form as

$$\frac{\partial F_T}{\partial \tau} \simeq \frac{\partial}{\partial w} \left(F_T \frac{2+Z}{w^2} + \frac{3}{4w^3} \frac{\partial F_T}{\partial w} \right).$$

where $\tau = \nu t$ and

$$\nu = \frac{n_e e^4 \ln \Lambda}{4\pi \epsilon_0^2 m_e^2 v_{Te}^3}$$

is an effective collision frequency.

Now show that the quasilinear diffusion equation can similarly be written in dimensionless form as

$$\frac{\partial F_T}{\partial \tau} = \frac{\partial}{\partial w} \bar{D}_{QL} \frac{\partial F_T}{\partial w}$$

where

$$\bar{D}_{QL}(w) = \frac{D_{QL}}{D_{col}}$$

and

$$D_{col} = \frac{2\nu\kappa T_e}{m_e}$$

is an effective collisional velocity-space diffusion coefficient.

- (b) Suppose that both collisions and quasilinear diffusion are operative so that

$$\frac{\partial F_T}{\partial \tau} = \frac{\partial}{\partial w} \left(\bar{D}_{QL} \frac{\partial F_T}{\partial w} + F_T \frac{2+Z}{w^2} + \frac{3}{4w^3} \frac{\partial F_T}{\partial w} \right).$$

Show that the steady-state solution to this equation has the form (Fisch 1978)

$$F_T \sim \exp \left(- \int^w dw \frac{(2+Z)w}{\left(w^3 \bar{D}_{QL} + \frac{3}{4} \right)} \right)$$

Sketch F_T for the cases where (i) $\bar{D}_{QL} \gg 1$ over a certain range of velocities (i.e., where wave spectrum is resonant with particles) and (ii) $\bar{D}_{QL} \ll 1$. How could this be used to drive a toroidal current in a tokamak? Using the appropriate form of D_{QL} show that the normalized quasilinear diffusion for resonant particles is

$$\bar{D}_{QL}(w) = \frac{8\pi^2 \mathcal{E}(\omega_r/v, t)}{w m_e \omega_{pe}^2 \ln \Lambda}.$$

If the wave is electrostatic then show that

$$\mathcal{E}(\omega_r/v, t) \sim k |\phi|^2$$

where k is the wavenumber of the waves resonantly interacting with the particles so that

$$\bar{D}_{QL}(w) \sim \frac{8\pi^2 k |\phi|^2}{m_e w \omega_{pe}^2 \ln \Lambda}.$$

What sort of waves would be most efficient at driving current, large or small k ? Would this current drive work best in high or low density plasmas?

Wave-wave nonlinearities

15.1 Introduction

Wave non-linearity is a vast subject that is not particularly specific to plasma physics because similar non-nonlinear behavior can occur in any medium that supports wave propagation. However, because of the enormous variety of plasma waves, there is usually at least one plasma context where any given type of wave nonlinearity is an important issue.

Wave nonlinearity occurs when non-linear terms become sufficiently large that they cannot be ignored. Three general types of non-linear wave behavior will be discussed: mode-mode coupling instabilities, self-modulation, and solitons. Before discussing these various behaviors in detail, a qualitative overview will first be presented showing how certain wave nonlinearities typically present themselves.

Mode-mode coupling instabilities

Suppose a linear wave is made to propagate in a plasma by inserting in the plasma an antenna connected to a sine wave generator tuned to an appropriate frequency. As a specific example, suppose the plasma frequency is $\omega_{pe}/2\pi = 100$ MHz and the generator is tuned to $\omega/2\pi = 500$ MHz so as to excite an electromagnetic plasma wave with dispersion relation $\omega^2 = \omega_{pe}^2 + k^2 c^2$. The wave propagates through the plasma and is detected by a distant receiving probe. Instead of connecting the receiving probe to a radio receiver or an oscilloscope, the receiving probe is connected to a spectrum analyzer, a device which provides a graphic display of signal amplitude versus frequency. The signal shows up on this display as a sharp peak at 500 MHz as sketched in Fig.15.1(a). If the signal generator amplitude is increased or decreased, the spectrum analyzer peak goes up or down in proportion, thereby indicating the signal strength.

An odd behavior is observed when the generator amplitude is increased above some critical threshold. At generator amplitudes below this threshold, the spectrum analyzer displays just the single peak at 500 MHz, but above this threshold, two additional peaks abruptly appear at two different frequencies and these new peaks have amplitudes considerably lower than the 500 MHz peak. These two additional peaks are typically at frequencies which sum to 500 MHz and the frequencies of the two additional peaks are typically very different from each other. For example, one of the two additional peaks might be at 1 MHz and the other at 499 MHz. These two peaks are called daughter waves and their spectrum is usually broader and their amplitude “springier” than the 500 MHz “pump” wave. If the

generator amplitude is increased further, the pump wave amplitude no longer increases in proportion to the generator amplitude, and instead the daughter wave amplitudes increase. One gets the impression that the plasma does not like to have too much power in the pump wave and when the above-mentioned threshold is exceeded, excess power spills into the daughter waves at the expense of the pump wave. If the power is increased still more, the daughters become quite large, and then at another threshold, the upper daughter might suddenly spawn its own pair of low and high frequency daughters. The spectrum becomes quite complicated and the amplitudes of the various spectral components depend sensitively on the generator amplitude and on plasma parameters. One gets the impression that energy is sloshing around between the pump wave and the daughter waves.

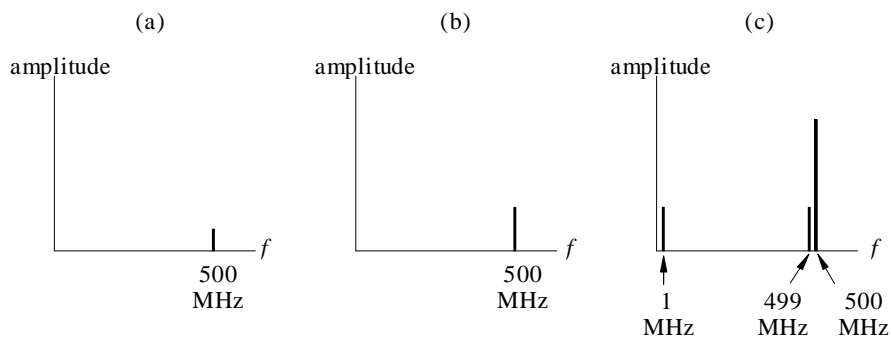


Figure 15.1: Frequency spectrum showing onset of decay instability at high power when a 500 MHz sine wave generator excites a wave in plasma. Low and intermediate generator power as in (a),(b) provide linear response, but high generator power as in (c) results in decay instability with daughter modes appearing at 1 MHz and 499 MHz.

This behavior can occur at surprisingly modest generator power levels where it might have reasonably been expected that nonlinear behavior would be negligible. The springiness of the daughter wave amplitudes suggests that some kind of resonant effect makes the nonlinearities more important than would be expected. The behavior sketched here is sometimes called a parametric decay instability (Silin 1965) because the pump wave is considered as decaying into the daughter waves. It has analogies to photon decay and in a sense can be considered as the classical limit of photon decay. Whether this sort of instability is good or bad depends on the context. If the goal is to propagate a large amplitude wave through a plasma and the wave decays into daughters, then the instability would be bad and efforts would be required to avoid it. On the other hand, if one of the daughter waves is normally difficult to excite and has some beneficial aspects, then the decay instability provides a means to access the desired daughter wave. Another possibility is that the onset of the decay could be used as a diagnostic to provide information about the plasma.

Self-modulation

A closely related situation is where the low-frequency daughter wave is at zero frequency. In this case the pump wave beats with itself and so modulates the equilibrium via a ponderomotive non-linear pressure which acts to expel plasma. If this happens, increasing the generator amplitude above the nonlinear threshold causes the pump wave to dig a

hole in the plasma density. The pump wave can dig itself a channel in the plasma and then this channel can guide, focus, and even trap the pump wave.

Solitons

Plasma waves are dispersive in general so, after propagating some distance, an initially sharp pulse will become less sharp because the various components of the Fourier spectrum constituting the pulse propagate at different phase velocities. However, it is found in certain situations that pulses with an amplitude exceeding some critical value will propagate indefinitely without broadening even though the medium is nominally dispersive. This high amplitude non-dispersive pulse is called a soliton and its existence results from nonlinearities competing against dispersion in a way such that the two effects cancel each other.

15.2 Manley-Rowe relations

Before investigating wave-wave nonlinearities, it is instructive to examine a closely related, but simpler system consisting of three non-linearly coupled harmonic oscillators (Manley and Rowe 1956). This simple system consists of a particle of mass m moving in a three dimensional space with dynamics governed by the Hamiltonian

$$H = \frac{1}{2m} (P_1^2 + P_2^2 + P_3^2) + \frac{1}{2} (\kappa_1 Q_1^2 + \kappa_2 Q_2^2 + \kappa_3 Q_3^2) + \lambda Q_1 Q_2 Q_3. \quad (15.1)$$

In the $\lambda \rightarrow 0$ limit this Hamiltonian describes three independent harmonic oscillators having respective frequencies $\omega_1 = \sqrt{\kappa_1/m}$, $\omega_2 = \sqrt{\kappa_2/m}$ and $\omega_3 = \sqrt{\kappa_3/m}$. In the more general case of finite λ , Hamilton's equations for the P_1, Q_1 conjugate coordinates are

$$\dot{P}_1 = -\frac{\partial H}{\partial Q_1} = -\kappa_1 Q_1 - \lambda Q_2 Q_3, \quad (15.2a)$$

$$\dot{Q}_1 = \frac{\partial H}{\partial P_1} = P_1/m \quad (15.2b)$$

with similar equations for the P_2, Q_2 and P_3, Q_3 conjugates. Using relationships such as $\dot{Q}_1 = P_1/m$, three coupled oscillator equations result, namely

$$\begin{aligned} \ddot{Q}_1 + \omega_1^2 Q_1 &= -\frac{\lambda}{m} Q_2 Q_3 \\ \ddot{Q}_2 + \omega_2^2 Q_2 &= -\frac{\lambda}{m} Q_1 Q_3 \\ \ddot{Q}_3 + \omega_3^2 Q_3 &= -\frac{\lambda}{m} Q_1 Q_2. \end{aligned} \quad (15.3)$$

For small λ , each oscillator may be assumed to oscillate nearly independently so that during each cycle of a given oscillator, the oscillator experiences only slight amplitude and phase changes due to the nonlinear coupling with the other two oscillators. Thus, approximate solutions for the oscillators can be written as

$$\begin{aligned} Q_1(t) &= A_1(t) \cos [\omega_1 t + \delta_1(t)] \\ Q_2(t) &= A_2(t) \cos [\omega_2 t + \delta_2(t)] \\ Q_3(t) &= A_3(t) \cos [\omega_3 t + \delta_3(t)] \end{aligned} \quad (15.4)$$

where it is assumed that

$$\frac{\dot{A}_j}{A_j} \ll \omega_j \text{ and } \dot{\delta}_j \ll \omega_j. \quad (15.5)$$

Each oscillator is considered as a linear mode of the system and, from now on, the term mode will be used interchangeably with oscillator. The energy associated with each mode is

$$W_j = \frac{1}{2m} P_j^2 + \frac{1}{2} \kappa_j Q_j^2 = \frac{m}{2} \dot{Q}_j^2 + \frac{1}{2} \kappa_j Q_j^2 = \frac{m}{2} \omega_j^2 A_j^2 \quad (15.6)$$

and the associated action is

$$\begin{aligned} S &= \oint P_j dQ_j = m \oint \dot{Q}_j dQ_j = -m\omega_j A_j^2 \int_0^{2\pi} \sin \psi_j d \cos \psi_j \\ &= m\omega_j A_j^2 \int_0^{2\pi} \sin^2 \psi_j d\psi_j = \frac{m}{2} \omega_j A_j^2 \end{aligned} \quad (15.7)$$

where $\psi_j = \omega_j t + \delta_j(t)$ is the phase of the mode.

Since \ddot{A}_j and $\ddot{\delta}_j$ are small compared to $\omega_j \dot{A}_j$ and $\omega_j \dot{\delta}_j$ respectively, the former terms may be dropped when calculating the second derivative of Q_j which is therefore

$$\ddot{Q}_j = -\omega_j^2 A_j \cos(\omega_j t + \delta_j) - 2\omega_j \dot{A}_j \sin(\omega_j t + \delta_j) - 2\omega_j A_j \dot{\delta}_j \cos(\omega_j t + \delta_j). \quad (15.8)$$

When the above expression is inserted into Eqs.(15.3) the terms involving ω_j^2 cancel and what remains is

$$\begin{aligned} \left[\begin{array}{l} 2\omega_j \dot{A}_j \sin(\omega_j t + \delta_j) \\ + 2\omega_j A_j \dot{\delta}_j \cos(\omega_j t + \delta_j) \end{array} \right] &= \frac{\lambda}{m} A_k A_l \cos(\omega_k t + \delta_k) \cos(\omega_l t + \delta_l) \\ &= \frac{\lambda}{2m} A_k A_l \left[\begin{array}{l} \cos((\omega_k + \omega_l) t + \delta_k + \delta_l) \\ + \cos((\omega_k - \omega_l) t + \delta_k - \delta_l) \end{array} \right]. \end{aligned} \quad (15.9)$$

It is necessary to write out the three coupled equations explicitly because the coupling terms on the right hand side are not fully symmetric. To identify resonant interactions it is assumed that

$$\omega_3 = \omega_1 + \omega_2 \quad (15.10)$$

$$\theta(t) = \delta_1 + \delta_2 - \delta_3 \quad (15.11)$$

in which case the coupled mode equations can be written

$$\begin{aligned} \left[\begin{array}{l} \dot{A}_1 \sin(\omega_1 t + \delta_1) \\ + A_1 \dot{\delta}_1 \cos(\omega_1 t + \delta_1) \end{array} \right] &= \frac{\lambda A_2 A_3}{4m\omega_1} \left[\begin{array}{l} \cos((\omega_2 + \omega_3) t + \delta_2 + \delta_3) \\ + \underbrace{\cos((\omega_2 - \omega_3) t + \delta_2 - \delta_3)}_{\text{resonant at } -\omega_1} \end{array} \right] \\ \left[\begin{array}{l} \dot{A}_2 \sin(\omega_2 t + \delta_2) \\ + A_2 \dot{\delta}_2 \cos(\omega_2 t + \delta_2) \end{array} \right] &= \frac{\lambda A_1 A_3}{4m\omega_2} \left[\begin{array}{l} \cos((\omega_1 + \omega_3) t + \delta_1 + \delta_3) \\ + \underbrace{\cos((\omega_1 - \omega_3) t + \delta_1 - \delta_3)}_{\text{resonant at } -\omega_2} \end{array} \right] \\ \left[\begin{array}{l} \dot{A}_3 \sin(\omega_3 t + \delta_3) \\ + A_3 \dot{\delta}_3 \cos(\omega_3 t + \delta_3) \end{array} \right] &= \frac{\lambda A_1 A_2}{4m\omega_3} \left[\begin{array}{l} \underbrace{\cos((\omega_1 + \omega_2) t + \delta_1 + \delta_2)}_{\text{resonant at } +\omega_3} \\ + \cos((\omega_1 - \omega_2) t + \delta_1 - \delta_2) \end{array} \right]. \end{aligned} \quad (15.12)$$

Using $\omega_2 - \omega_3 = -\omega_1$, $\delta_2 - \delta_3 = \theta - \delta_1$, $\omega_1 - \omega_3 = -\omega_2$, $\delta_1 - \delta_3 = \theta - \delta_2$ and discarding non-resonant terms, these become

$$\begin{aligned} \dot{A}_1 \sin(\omega_1 t + \delta_1) + A_1 \dot{\delta}_1 \cos(\omega_1 t + \delta_1) &= \frac{\lambda A_2 A_3}{4m\omega_1} \cos(\theta - \omega_1 t - \delta_1) \\ \dot{A}_2 \sin(\omega_2 t + \delta_2) + A_2 \dot{\delta}_2 \cos(\omega_2 t + \delta_2) &= \frac{\lambda A_1 A_3}{4m\omega_2} \cos(\theta - \omega_2 t - \delta_2) \\ \dot{A}_3 \sin(\omega_3 t + \delta_3) + A_3 \dot{\delta}_3 \cos(\omega_3 t + \delta_3) &= \frac{\lambda A_1 A_2}{4m\omega_3} \cos(\theta + \omega_3 t + \delta_3) \end{aligned} \quad (15.13)$$

or

$$\begin{aligned} \begin{bmatrix} \dot{A}_1 \sin(\omega_1 t + \delta_1) \\ + A_1 \dot{\delta}_1 \cos(\omega_1 t + \delta_1) \end{bmatrix} &= \frac{\lambda A_2 A_3}{4m\omega_1} \begin{bmatrix} \cos \theta \cos(\omega_1 t + \delta_1) \\ + \sin \theta \sin(\omega_1 t + \delta_1) \end{bmatrix} \\ \begin{bmatrix} \dot{A}_2 \sin(\omega_2 t + \delta_2) \\ + A_2 \dot{\delta}_2 \cos(\omega_2 t + \delta_2) \end{bmatrix} &= \frac{\lambda A_1 A_3}{4m\omega_2} \begin{bmatrix} \cos \theta \cos(\omega_2 t + \delta_2) \\ + \sin \theta \sin(\omega_2 t + \delta_2) \end{bmatrix} \\ \begin{bmatrix} \dot{A}_3 \sin(\omega_3 t + \delta_3) \\ + A_3 \dot{\delta}_3 \cos(\omega_3 t + \delta_3) \end{bmatrix} &= \frac{\lambda A_1 A_2}{4m\omega_3} \begin{bmatrix} \cos \theta \cos(\omega_3 t + \delta_3) \\ - \sin \theta \sin(\omega_3 t + \delta_3) \end{bmatrix}. \end{aligned} \quad (15.14)$$

Matching the time-dependent sine and cosine terms on both sides gives

$$\dot{A}_1 = \frac{\lambda A_2 A_3}{4m\omega_1} \sin \theta \quad (15.15a)$$

$$\dot{A}_2 = \frac{\lambda A_1 A_3}{4m\omega_2} \sin \theta \quad (15.15b)$$

$$\dot{A}_3 = -\frac{\lambda A_1 A_2}{4m\omega_3} \sin \theta \quad (15.15c)$$

and

$$\begin{aligned} A_1 \dot{\delta}_1 &= \frac{\lambda A_2 A_3}{4m\omega_1} \cos \theta \\ A_2 \dot{\delta}_2 &= \frac{\lambda A_1 A_3}{4m\omega_2} \cos \theta \\ A_3 \dot{\delta}_3 &= \frac{\lambda A_1 A_2}{4m\omega_3} \cos \theta. \end{aligned} \quad (15.16)$$

These equations can be used to establish various conservation relations. Multiplying Eqs.(15.15) by $\omega_j^2 A_j$, and summing gives

$$\frac{1}{2} \frac{d}{dt} (\omega_1^2 A_1^2 + \omega_2^2 A_2^2 + \omega_3^2 A_3^2) = \frac{(\omega_1 + \omega_2 - \omega_3) \lambda A_1 A_2 A_3}{4m} \sin \theta = 0$$

so

$$\omega_1^2 A_1^2 + \omega_2^2 A_2^2 + \omega_3^2 A_3^2 = \text{const.} \quad (15.17)$$

This shows that the sum of the energies of the three modes is constant, but allows for energy transfer back and forth between the three modes.

A corresponding set of relations for the action can be obtained by multiplying pairs of equations in Eq.(15.15) by $\omega_j A_j$ and then either adding or subtracting. For example, multiplying the first pair by $\omega_j A_j$ and subtracting gives

$$\frac{1}{2} \frac{d}{dt} (\omega_1 A_1^2 - \omega_2 A_2^2) = 0. \quad (15.18)$$

Appropriate adding and subtracting in this manner gives

$$\begin{aligned} \omega_1 A_1^2 - \omega_2 A_2^2 &= \text{const.} \\ \omega_1 A_1^2 + \omega_3 A_3^2 &= \text{const.} \\ \omega_2 A_2^2 + \omega_3 A_3^2 &= \text{const.} \end{aligned} \quad (15.19)$$

These relationships can be expressed in a manner analogous to quantum principles by defining the effective "quantum number" of a mode as its ratio of energy to frequency,

$$N_j = \frac{W_j}{\omega_j} = \frac{m}{2} \omega_j A_j^2. \quad (15.20)$$

It is clear that N_j is the same as the action except for an unimportant constant factor. Thus, the action conservation rules can be recast as

$$\begin{aligned} N_1 - N_2 &= \text{const.} \\ N_1 + N_3 &= \text{const.} \\ N_2 + N_3 &= \text{const.} \end{aligned} \quad (15.21)$$

or if changes in action are considered

$$\begin{aligned} \Delta N_1 &= +\Delta N_2 \\ \Delta N_1 &= -\Delta N_3 \\ \Delta N_2 &= -\Delta N_3. \end{aligned} \quad (15.22)$$

This provides an action accounting scheme such that a change $\Delta N_3 = -1$ can be considered as a mode 3 "photon" decaying (or equivalently disintegrating) into a mode 1 photon ($\Delta N_1 = +1$) and a mode 2 photon ($\Delta N_2 = +1$), all the while satisfying conservation of energy; this is sketched in Fig. 15.2.

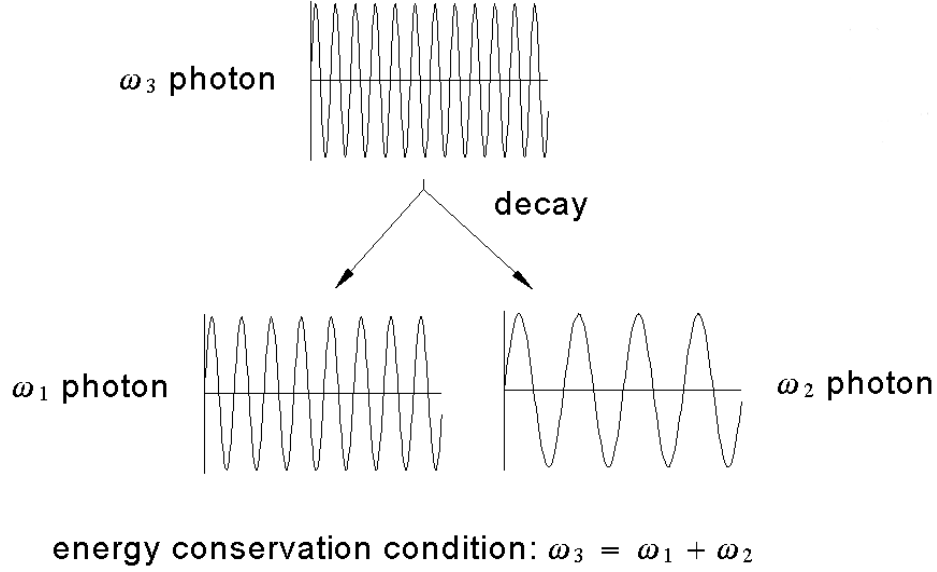


Figure 15.2: Photon at frequency ω_3 decaying into a photon at frequency ω_1 and a photon at frequency ω_2 .

An additional conservation equation can be obtained by subtracting the last of Eqs.(15.16) from the sum of the first two to obtain

$$\begin{aligned}
 \dot{\theta} &= \dot{\delta}_1 + \dot{\delta}_2 - \dot{\delta}_3 \\
 &= \left(\frac{\lambda A_2 A_3}{4m A_1 \omega_1} + \frac{\lambda A_1 A_3}{4m A_2 \omega_2} - \frac{\lambda A_1 A_2}{4m A_3 \omega_3} \right) \cos \theta \\
 &= \left(\frac{\dot{A}_1}{A_1} + \frac{\dot{A}_2}{A_2} + \frac{\dot{A}_3}{A_3} \right) \frac{\cos \theta}{\sin \theta}
 \end{aligned} \tag{15.23}$$

and then integrating to find

$$A_1 A_2 A_3 \cos \theta = \text{const.} \tag{15.24}$$

We now consider some solutions to the system of equations given by Eqs.(15.15b)-(15.15c). Suppose that $A_3 \gg A_2, A_1$ initially. In this case Eq.(15.15c) gives $A_3 \simeq \text{const.}$ Solving Eq.(15.15b) for A_1 and substituting the result in Eq.(15.15a) gives

$$\frac{1}{\sin \theta} \frac{d}{dt} \left(\frac{1}{\sin \theta} \frac{dA_2}{dt} \right) = \frac{\lambda^2 A_3^2}{16m^2 \omega_1 \omega_2} A_2 \tag{15.25}$$

which has exponentially growing solutions if $\omega_1 \omega_2 > 0$. By defining

$$\tau = \int_0^t dt' \sin \theta(t') \tag{15.26}$$

it is seen that

$$\frac{dA_2}{dt} = \frac{d\tau}{dt} \frac{dA_2}{d\tau} = \sin \theta \frac{dA_2}{d\tau} \quad (15.27)$$

and so

$$\frac{d^2 A_2}{d\tau^2} = \frac{\lambda^2 A_3^2}{16m^2 \omega_1 \omega_2} A_2. \quad (15.28)$$

Since $\omega_1 \omega_2 > 0$ and $\omega_1 + \omega_2 = \omega_3$, if ω_3 is chosen to be positive, then both ω_1 and ω_2 must both be positive and therefore $\omega_3 > \omega_1, \omega_2$. If A_2 grows, then because of the action rules, A_1 must grow in the same proportion. Furthermore, as A_1 and A_2 grow, A_3 must decrease until the approximation $A_3 \gg A_1, A_3$ fails. This process can be considered as a high energy “photon” with frequency ω_3 decaying into an ω_1 photon and an ω_2 photon where the latter two photons have lower energy than ω_1 . Equation (15.28) shows that the decay of the mode 3 photon into mode 1,2 photons can be characterized by an exponential growth of the mode 2 amplitude,

$$A_2 \sim e^{\gamma\tau} \quad (15.29)$$

where

$$\gamma = \frac{\lambda A_3}{4m\sqrt{\omega_1 \omega_2}} \quad (15.30)$$

is the instability growth rate. Mode 3 is called the pump mode since it supplies the energy for the instability. Modes 1 and 2 are called the daughter modes.

15.3 Application to waves

Nonlinearities in wave equations give rise to coupled systems of equations similar to Eqs.(15.3). Suppose Q now refers to a plasma parameter, say density, and that the plasma can support three distinct waves (modes) having respective linear density fluctuations

$$\begin{aligned} Q_1(\mathbf{x},t) &= A_1(t) \cos(\mathbf{k}_1 \cdot \mathbf{x} - \omega_1 t - \delta_1(t)) \\ Q_2(\mathbf{x},t) &= A_2(t) \cos(\mathbf{k}_2 \cdot \mathbf{x} - \omega_2 t - \delta_2(t)) \\ Q_3(\mathbf{x},t) &= A_3(t) \cos(\mathbf{k}_3 \cdot \mathbf{x} - \omega_3 t - \delta_3(t)); \end{aligned} \quad (15.31)$$

the density Q therefore has the functional form

$$Q(\mathbf{x},t) = Q_1(\mathbf{x},t) + Q_2(\mathbf{x},t) + Q_3(\mathbf{x},t). \quad (15.32)$$

This situation is mathematically analogous to the coupled oscillator system discussed in Sec.15.2 if the amplitude Q_j of each of the three waves is considered to be an effective canonical coordinate. Each wave satisfies a linear dispersion relation $\omega_j = \omega_j(\mathbf{k})$ and nonlinearities in the wave equations provide a mutual coupling between the modes analogous to the coupling between the different directions of motion for the oscillating mass discussed in Sec.15.2. The $\exp(i\mathbf{k} \cdot \mathbf{x})$ dependence of the waves suggests the need for a wavenumber selection rule

$$\mathbf{k}_3 = \mathbf{k}_1 + \mathbf{k}_2 \quad (15.33)$$

analogous to the frequency selection rule Eq.(15.10). Using the wavenumber selection rule and generalizing the phase offset definition to be $\delta'_j(t) = \delta_j(t) - \mathbf{k}_j \cdot \mathbf{x}$, it is seen that the coupled wave equations become identical to the coupled oscillator equations with δ'_j

replacing δ_j . Hence, so long as the selection rules $\omega_3 = \omega_1 + \omega_2$ and $\mathbf{k}_3 = \mathbf{k}_1 + \mathbf{k}_2$ are satisfied, a high frequency wave ω_3 should decay spontaneously into two low frequency waves ω_1, ω_2 providing there is a suitable coupling coefficient.

15.3.1 Examples of nonlinearities

Nonlinearities can be divided into two general types: (1) two high frequency waves beating together to give a low frequency driving term and (2) a high frequency wave beating with a low frequency wave to give a high frequency driving term. As shown below, the first type of nonlinearity has the form of a radiation pressure (also known as a ponderomotive force) while the second type of nonlinearity has the form of a density modulation.

1. *Beat of two high-frequency waves driving a low frequency wave (ponderomotive force).* Since ion motion is negligible in a high frequency wave, all that is required when considering nonlinearities is the electron equation of motion,

$$\frac{\partial \mathbf{u}_e}{\partial t} = -\mathbf{u}_e \cdot \nabla \mathbf{u}_e + \frac{q_e}{m_e} (\mathbf{E} + \mathbf{u}_e \times \mathbf{B}) - \frac{1}{m_e n_e} \nabla P_e. \quad (15.34)$$

For simplicity, it is assumed no equilibrium magnetic field exists, so the only magnetic field is the wave magnetic field. Tildes are used to denote linear quantities to avoid confusion with the subscripts 1, 2, 3 which denote the low frequency daughter, high frequency daughter and pump wave respectively. Because the pressure gradient term in the electron equation of motion provides only a small correction at high frequencies, the linear motion for either the pump or the high frequency daughter must thus be a solution of

$$\frac{\partial \tilde{\mathbf{u}}_e}{\partial t} = \frac{q_e}{m_e} \tilde{\mathbf{E}}. \quad (15.35)$$

The electron quiver velocity is defined to be

$$\tilde{\mathbf{u}}_e^h = \frac{q_e}{m_e} \int^t \tilde{\mathbf{E}} dt' \quad (15.36)$$

which is the solution to Eq.(15.35) for both electron plasma waves and electromagnetic waves. The main non-linear terms in Eq.(15.34) are $-\tilde{\mathbf{u}}_e \cdot \nabla \tilde{\mathbf{u}}_e + q_e (\tilde{\mathbf{u}}_e \times \tilde{\mathbf{B}}) / m_e$; non-linearity in the pressure gradient is ignored because, by assumption, this term is already small. In order to obtain $\tilde{\mathbf{B}}$, Faraday's law is integrated with respect to time giving

$$\tilde{\mathbf{B}} = -\nabla \times \int^t \tilde{\mathbf{E}} dt' = -\frac{m_e}{q_e} \nabla \times \tilde{\mathbf{u}}_e^h. \quad (15.37)$$

The two nonlinear terms can be combined using Eq.(15.37) to form what is called the ponderomotive force or radiation pressure,

$$\begin{aligned} -\tilde{\mathbf{u}}_e \cdot \nabla \tilde{\mathbf{u}}_e + \frac{q_e}{m_e} (\tilde{\mathbf{u}}_e \times \tilde{\mathbf{B}}) &= -\tilde{\mathbf{u}}_e^h \cdot \nabla \tilde{\mathbf{u}}_e^h - (\tilde{\mathbf{u}}_e^h \times \nabla \times \tilde{\mathbf{u}}_e^h) \\ &= -\frac{1}{2} \nabla (\tilde{u}_e^h)^2. \end{aligned} \quad (15.38)$$

If only one high frequency mode exists and beats with itself, then the ponderomotive force $-\nabla (\tilde{u}_e^h)^2 / 2$ is at zero frequency but if the beating is between two distinct high

frequency modes, then the ponderomotive force contains a term at the difference (i.e., beat) frequency between the frequencies of the two modes. Thus, at low frequencies the electron equation of motion, Eq.(15.34) becomes

$$\frac{\partial \bar{\mathbf{u}}_e}{\partial t} = \frac{q_e}{m_e} \bar{\mathbf{E}} - \frac{1}{m_e n} \nabla \tilde{P}_e - \frac{1}{2} \nabla (\tilde{u}_e^h)^2 \quad (15.39)$$

where only the beat frequency component in $(\tilde{u}_e^h)^2$ is used. The ponderomotive force provides a mechanism for high-frequency waves to couple to low frequency waves. It acts as an effective pressure scaling as $m_e n (\tilde{u}_e^h)^2 / 2$ and so in a sense, the quiver velocity \tilde{u}_e^h acts as a thermal velocity. The ratio of ion radiation pressure to the ion pressure is smaller than the corresponding ratio for electrons by a factor of m_e/m_i because the ion quiver velocity is smaller by this factor. Thus, ion ponderomotive force is ignored since it is so small.

2. *Beating of a low frequency wave with a high frequency wave to drive another high frequency wave (modulation).* By writing Ampere's law as

$$\nabla \times \bar{\mathbf{B}} = \mu_0 \sum_{\sigma} (\tilde{n}_{\sigma} q_{\sigma} \bar{\mathbf{u}}_{\sigma} + n_0 q_{\sigma} \bar{\mathbf{u}}_{\sigma}) + \mu_0 \varepsilon_0 \frac{\partial \bar{\mathbf{E}}}{\partial t} \quad (15.40)$$

it is seen that density fluctuations provide a nonlinear component to the current density. The nonlinear term can be put on the right hand side to emphasize its role as a nonlinear driving term so that Ampere's law becomes

$$\nabla \times \bar{\mathbf{B}} - \mu_0 \varepsilon_0 \frac{\partial \bar{\mathbf{E}}}{\partial t} - \mu_0 \sum_{\sigma} n_0 q_{\sigma} \bar{\mathbf{u}}_{\sigma} = -\mu_0 \sum_{\sigma} \tilde{n}_{\sigma} q_{\sigma} \bar{\mathbf{u}}_{\sigma}. \quad (15.41)$$

The nonlinear term is assumed to be a product of a high frequency wave and a low frequency wave. The linearized continuity equation gives

$$\frac{\partial \tilde{n}_{\sigma}}{\partial t} = -n_{\sigma} \nabla \cdot \bar{\mathbf{u}}_{\sigma} \quad (15.42)$$

showing that $\tilde{n}_{\sigma} \sim \bar{\mathbf{u}}_{\sigma} / \omega$ so that the product $n_{\sigma}^l \mathbf{u}_{\sigma}^h$ is much larger than the product $n_{\sigma}^h \mathbf{u}_{\sigma}^l$ where l and h refer to low and high frequency waves. Thus, the dominant effect of a low frequency wave is to modulate the density profile seen by a high frequency wave.

15.3.2 Possible types of wave interaction

As discussed in Sec.4.2, three distinct types of waves can propagate in an unmagnetized uniform plasma and these waves have the dispersion relations:

$$\begin{aligned} \omega^2 &= \omega_{pe}^2 + k^2 c^2, \text{ electromagnetic wave} \\ \omega^2 &= \omega_{pe}^2 (1 + 3k^2 \lambda_{de}^2), \text{ electron plasma wave} \\ \omega^2 &= \frac{k^2 c_s^2}{1 + k^2 \lambda_{De}^2}, \text{ ion acoustic wave.} \end{aligned} \quad (15.43)$$

If three waves satisfy the selection rules

$$\omega_3 = \omega_1 + \omega_2 \quad (15.44)$$

$$\mathbf{k}_3 = \mathbf{k}_1 + \mathbf{k}_2, \quad (15.45)$$

they can only have the *same* dispersion relation if ω^2 depends linearly on k^2 so that the magnitude of \mathbf{k} is linearly proportional to the magnitude of ω . This is not so for the modes listed in Eq.(15.43) except for the $k^2 \lambda_{De}^2 \ll 1$ limit of the ion acoustic wave; applying the selection rules to this $\omega^2 = k^2 c_s^2$ limit of ion acoustic waves gives nonlinear interactions between various sound wave harmonics, e.g., the first and second harmonic can interact with the third harmonic. Since this limit corresponds to the well-known nonlinear steepening of ordinary sound waves it will not be discussed further.

The situations which are of particular relevance to plasmas are where modes satisfying different types of dispersion relations interact with each other, for example an electromagnetic wave interacting with an electron plasma wave and an ion acoustic wave. The various possibilities for non-linear interactions of the three types of plasma waves are the following:

pump	hf daughter	lf daughter	common name
ω_3	ω_2	ω_1	
em	em	Langmuir	stimulated Raman backscatter
em	em	acoustic	stimulated Brillouin backscatter
em	em	zero frequency	self-focusing
em	Langmuir	Langmuir	two-plasmon decay
em	Langmuir	acoustic	parametric decay instability
Langmuir	Langmuir	acoustic	electron decay instability
Langmuir	Langmuir	zero frequency	caviton

Here the abbreviations em, Langmuir, and acoustic stand for electromagnetic wave, electron plasma wave, and ion acoustic wave respectively and the ordering is by progressively lower frequency, column by column taking into account that $\omega_3 > \omega_2 > \omega_1$ and electromagnetic waves have higher frequencies than Langmuir waves which in turn have higher frequency than ion acoustic waves.

In each case the low frequency daughter modulates the density and beats with either the pump or the high frequency daughter to provide a high frequency nonlinear current as given by Eq.(15.41) while the pump and the high frequency daughter beat together to provide a ponderomotive force that couples to the low frequency wave. Because $c^2 \gg v_{Te}^2 \gg c_s^2$ the electromagnetic wave has a stronger dependence on k^2 than does the electron plasma wave which in turn has a stronger dependence on k^2 than does the ion acoustic wave. This means that if \mathbf{k}_1 , \mathbf{k}_2 , and \mathbf{k}_3 are all in the same direction and Eq.(15.45) is satisfied, Eq.(15.44) cannot be satisfied since $\omega_3(|\mathbf{k}_3|) = \omega_3(|\mathbf{k}_1| + |\mathbf{k}_2|) > \omega_1(|\mathbf{k}_1|) + \omega_2(|\mathbf{k}_2|)$. Thus, the frequency and wavenumber selection rules can only be satisfied if \mathbf{k}_1 , \mathbf{k}_2 , and \mathbf{k}_3 are not all in the same direction. The pump wave direction is taken to define the positive direction, i.e., \mathbf{k}_3 defines the positive direction so one of the daughter waves must propagate in the direction opposite to the pump.

The electromagnetic wave in a given plasma always has a higher frequency than the electron plasma or ion acoustic waves. As a consequence, the low frequency daughter can-

not be an electromagnetic wave because then all three waves would have to be electromagnetic waves which would then violate the requirement that the dispersion relations cannot all be the same. The low frequency daughter must therefore be either an ion acoustic wave or an electron plasma wave. Similarly, the high frequency wave (pump or high frequency daughter) cannot be an ion acoustic wave and so must be either an electromagnetic wave or an electron plasma wave. Thus, the various interactions tabulated above can be accounted for by establishing the appropriate coupling equations for the following four possibilities: high frequency wave is an electromagnetic wave or a Langmuir wave, low frequency wave is a Langmuir wave or an ion acoustic wave.

Low frequency wave is an ion acoustic wave On assuming quasi-neutrality which corresponds to assuming $k^2 \lambda_{De}^2 \ll 1$, the low frequency electron and ion equations of motion may be approximated as

$$\frac{\partial \bar{\mathbf{u}}_e}{\partial t} = \frac{q_e}{m_e} \bar{\mathbf{E}} - \frac{\kappa T_e}{m_e n} \nabla \tilde{n} - \frac{1}{2} \nabla (\tilde{u}_e^h)^2 \quad (15.46)$$

$$\frac{\partial \bar{\mathbf{u}}_i}{\partial t} = \frac{q_i}{m_i} \bar{\mathbf{E}}; \quad (15.47)$$

here only the low frequency beat component of $(\tilde{u}_e^h)^2$ is used. Also, as shown earlier, the ion ponderomotive force is negligible and therefore ignored. Because the electron mass is very small, the left hand side of the electron equation of motion is dropped in which case this equation reduces to the simple force balance relation

$$\frac{q_e}{m_e} \bar{\mathbf{E}} - \frac{\kappa T_e}{m_e n} \nabla \tilde{n} - \frac{1}{2} \nabla (\tilde{u}_e^h)^2 \simeq 0. \quad (15.48)$$

Using Eq.(15.48) to eliminate $\bar{\mathbf{E}}$ from the ion equation gives

$$\frac{\partial \bar{\mathbf{u}}_i}{\partial t} = - \frac{\kappa T_e}{m_i n} \nabla \tilde{n} - \frac{1}{2} \frac{m_e}{m_i} \nabla (\tilde{u}_e^h)^2. \quad (15.49)$$

Because quasi-neutrality is assumed $\tilde{n}_i = \tilde{n}_e = \tilde{n}$, and so the time derivative of the ion continuity equation can be written as

$$\frac{\partial^2 \tilde{n}}{\partial t^2} + n \nabla \cdot \frac{\partial \bar{\mathbf{u}}_i}{\partial t} = 0. \quad (15.50)$$

Substituting for $\partial \bar{\mathbf{u}}_i / \partial t$, the above equation becomes

$$\frac{\partial^2 \tilde{n}}{\partial t^2} - n \nabla \cdot \left(\frac{\kappa T_e}{m_i n} \nabla \tilde{n} + \frac{1}{2} \frac{m_e}{m_i} \nabla (\tilde{u}_e^h)^2 \right) = 0 \quad (15.51)$$

which can be written as an ion acoustic wave equation with a non-linear coupling term due to the electron ponderomotive force,

$$\frac{\partial^2 \tilde{n}}{\partial t^2} - c_s^2 \nabla^2 \tilde{n} = \frac{n}{2} \frac{m_e}{m_i} \nabla^2 (\tilde{u}_e^h)^2. \quad (15.52)$$

If the electron quiver velocity is considered to behave as an effective thermal velocity, then

the low frequency beat component of $(\tilde{u}_e^h)^2$ can be considered as modulating the effective electron temperature. Specifically,

$$\tilde{n}_e \kappa T_e + n \kappa \tilde{T}_e = \tilde{n}_e \kappa T_e + n \frac{m_e (\tilde{u}_e^h)^2}{2} \quad (15.53)$$

and so

$$\tilde{n} c_s^2 \rightarrow \tilde{n} c_s^2 + n \widetilde{(c_s^2)} = \tilde{n} c_s^2 + n \frac{\kappa \tilde{T}_e}{m_i} = \tilde{n} c_s^2 + n \frac{m_e (\tilde{u}_e^h)^2}{2 m_i} \quad (15.54)$$

which is consistent with Eq.(15.52).

Low frequency wave is an electron plasma wave In this case the low frequency wave frequency is above ω_{pe} so that the ions form a stationary background. Now only the electron dynamic response matters and the density perturbation is not quasi-neutral. The electron equation of motion for the low frequency wave is

$$\frac{\partial \tilde{\mathbf{u}}_e}{\partial t} = \frac{q_e}{m_e} \bar{\mathbf{E}} - \frac{3\kappa T_e}{m_e n} \nabla \tilde{n}_e - \frac{1}{2} \nabla (\tilde{u}_e^h)^2 \quad (15.55)$$

where the 3 comes from the adiabatic pressure perturbation. Combining this with the time derivative of the electron continuity equation,

$$\frac{\partial^2 \tilde{n}_e}{\partial t^2} + n \nabla \cdot \left(\frac{\partial \tilde{\mathbf{u}}_e}{\partial t} \right) = 0, \quad (15.56)$$

gives

$$\frac{\partial^2 \tilde{n}_e}{\partial t^2} + n \nabla \cdot \left(\frac{q_e}{m_e} \bar{\mathbf{E}} - \frac{3\kappa T_e}{m_e n} \nabla \tilde{n}_e - \frac{1}{2} \nabla (\tilde{u}_e^h)^2 \right) = 0. \quad (15.57)$$

This may be simplified by invoking Poisson's equation

$$\nabla \cdot \bar{\mathbf{E}} = \frac{1}{\varepsilon_0} \tilde{n}_e q_e \quad (15.58)$$

to obtain

$$\frac{\partial^2 \tilde{n}_e}{\partial t^2} + \omega_{pe}^2 \tilde{n}_e - \frac{3\kappa T_e}{m_e} \nabla^2 \tilde{n}_e = \frac{n}{2} \nabla^2 (\tilde{u}_e^h)^2. \quad (15.59)$$

The left hand side is the electron plasma wave equation (Langmuir wave) and the right hand side provides the nonlinear drive (or coupling) due to ponderomotive force. Again, using Eq.(15.53) it is seen that the ponderomotive force term acts like a modulation of the electron temperature such that $\widetilde{n\kappa T_e} \rightarrow \tilde{n}\kappa T_e + n\kappa \tilde{T}_e$ where \tilde{T}_e is due to the high frequency electron quiver velocity.

High frequency wave is an electron plasma wave In this case the wave is electrostatic and so there is no high frequency oscillating magnetic field. The non-linear continuity equation is

$$\frac{\partial \tilde{n}_e}{\partial t} + n \nabla \cdot \tilde{\mathbf{u}}_e = -\nabla \cdot (\tilde{n}_e \tilde{\mathbf{u}}_e) \quad (15.60)$$

and taking a time derivative this becomes

$$\frac{\partial^2 \tilde{n}_e}{\partial t^2} + n \nabla \cdot \frac{\partial \tilde{\mathbf{u}}_e}{\partial t} = -\frac{\partial}{\partial t} \nabla \cdot (\tilde{n}_e \tilde{\mathbf{u}}_e). \quad (15.61)$$

However, the high frequency linear electron equation of motion is

$$\frac{\partial \bar{\mathbf{u}}_e}{\partial t} = \frac{q_e}{m_e} \bar{\mathbf{E}} - \frac{3\kappa T_e}{m_e n} \nabla \tilde{n}_e \quad (15.62)$$

so Eq.(15.61) becomes

$$\frac{\partial^2 \tilde{n}_e}{\partial t^2} + \omega_{pe}^2 \tilde{n}_e - \frac{3\kappa T_e}{m_e} \nabla^2 \tilde{n}_e = -\frac{\partial}{\partial t} \nabla \cdot (\tilde{n}_e \bar{\mathbf{u}}_e). \quad (15.63)$$

In principle, there are two possible components in the right hand side nonlinear term since $\tilde{n}_e \bar{\mathbf{u}}_e = \tilde{n}_e^l \bar{\mathbf{u}}_e^h + \tilde{n}_e^h \bar{\mathbf{u}}_e^l$ where l and h refer to low and high frequency waves. If both high and low frequency waves are electrostatic, then $\bar{\mathbf{u}}_e \sim \bar{\mathbf{E}} = -i\mathbf{k}\phi$ and $\nabla \cdot \bar{\mathbf{u}}_e = i\mathbf{k} \cdot \bar{\mathbf{u}}_e = i\mathbf{k} \cdot \bar{\mathbf{u}}_e \sim k^2 \phi$ where ϕ is the electrostatic potential. The linearized continuity equation gives

$$\frac{\tilde{n}_e}{n} = -\frac{\mathbf{k} \cdot \bar{\mathbf{u}}_e}{\omega} \sim \frac{k^2 \phi}{\omega} \quad (15.64)$$

and so

$$\left| \frac{\tilde{n}_e^l \bar{\mathbf{u}}_e^h}{\tilde{n}_e^h \bar{\mathbf{u}}_e^l} \right| = \frac{\frac{k_l^2 \phi_l}{\omega_l} k_h \phi_h}{\frac{k_h^2 \phi_h}{\omega_h} k_l \phi_l} = \frac{\omega_h/k_h}{\omega_l/k_l} \gg 1 \quad (15.65)$$

since the phase velocity of the high frequency mode is much higher than the phase velocity of the low frequency mode. Thus, the $\tilde{n}_e^l \bar{\mathbf{u}}_e^h$ term dominates and the other term can be discarded. If the high frequency wave associated with $\bar{\mathbf{u}}_e^h$ is an electromagnetic wave, then the electric field is transverse so $\nabla \cdot \bar{\mathbf{u}}_e^h \sim \nabla \cdot \bar{\mathbf{E}}^h = 0$ in which case there is no high frequency density fluctuation, i.e., $\tilde{n}_e^h = 0$. Again, only the $\tilde{n}_e^l \bar{\mathbf{u}}_e^h$ term is to be retained. Hence, the high frequency wave equation becomes

$$\frac{\partial^2 \tilde{n}_e}{\partial t^2} + \omega_{pe}^2 \tilde{n}_e - \frac{3\kappa T_e}{m_e} \nabla^2 \tilde{n}_e = -\frac{\partial}{\partial t} \nabla \cdot (\tilde{n}_e^l \bar{\mathbf{u}}_e^h). \quad (15.66)$$

If the high frequency wave is electromagnetic, then $\nabla \cdot (\tilde{n}_e^l \bar{\mathbf{u}}_e^h) = \bar{\mathbf{u}}_e^h \cdot \nabla \tilde{n}_e^l$ showing that the non-linearity consists of a density modulation due to the high frequency motion across the density ripples of the low frequency mode. For purposes of consistency, it is worthwhile to express Eq.(15.66) in terms of electric field using

$$\nabla \cdot \tilde{\mathbf{E}} = \frac{1}{\varepsilon_0} \tilde{n}_e q_e \quad (15.67)$$

so

$$\nabla \cdot \left(\frac{\partial^2 \bar{\mathbf{E}}}{\partial t^2} + \omega_{pe}^2 \bar{\mathbf{E}} - \frac{3\kappa T_e}{m_e} \nabla^2 \bar{\mathbf{E}} \right) = -\frac{\partial}{\partial t} \frac{1}{\varepsilon_0} \nabla \cdot (\tilde{n}_e^l q_e \bar{\mathbf{u}}_e^h) \quad (15.68)$$

which can be integrated in space to give the general expression for a high frequency electron plasma wave with nonlinear coupling term,

$$\frac{\partial^2 \bar{\mathbf{E}}}{\partial t^2} + \omega_{pe}^2 \bar{\mathbf{E}} - \frac{3\kappa T_e}{m_e} \nabla^2 \bar{\mathbf{E}} = -\frac{1}{\varepsilon_0} \frac{\partial}{\partial t} (\tilde{n}_e^l q_e \bar{\mathbf{u}}_e^h). \quad (15.69)$$

High frequency wave is an electromagnetic wave Here the wave is transverse so $\nabla \cdot \tilde{\mathbf{E}} = 0$ and the curl of Faraday's law becomes

$$\nabla^2 \tilde{\mathbf{E}} = \frac{\partial \nabla \times \tilde{\mathbf{B}}}{\partial t}. \quad (15.70)$$

Substituting Eq.(15.41) and using the linear equation of motion gives the general expression for a high frequency electromagnetic wave with non-linear coupling term,

$$\frac{\partial^2 \tilde{\mathbf{E}}}{\partial t^2} + \omega_{pe}^2 \tilde{\mathbf{E}} - c^2 \nabla^2 \tilde{\mathbf{E}} = -\frac{1}{\varepsilon_0} \frac{\partial}{\partial t} (\tilde{n}_e^l q_e \tilde{\mathbf{u}}_e^h); \quad (15.71)$$

the term $\tilde{n}_e^h q_e \tilde{\mathbf{u}}_e^l$ has been dropped for the reasons given in the previous paragraph.

Summary of mode interactions Examination of the various combinations considered above shows that the non-linear coupling acting on high frequency modes (either pump and high frequency daughter) is an effective modulation of the density experienced by the high frequency wave, i.e., $\omega_{pe}^2 \rightarrow \omega_{pe}^2 + \omega_{pe}^2 \tilde{n}^l/n$. On the other hand the non-linear coupling acting on the low frequency daughter comes from the electron ponderomotive force which effectively modulates the electron temperature experienced by the low frequency mode, i.e., $\tilde{n} \kappa T_e \rightarrow \tilde{n} \kappa T_e + n \kappa (\tilde{u}_e^h)^2/2$.

Coupled oscillator formulation To see how the coupled wave equations can be expressed in terms of coupled oscillators, the specific situation of an electromagnetic wave interacting with a Langmuir wave and an ion acoustic wave is now considered. In this case, the three coupled equations are

$$\begin{aligned} \frac{\partial^2 \tilde{\mathbf{E}}_3}{\partial t^2} + \omega_{pe}^2 \tilde{\mathbf{E}}_3 - c^2 \nabla^2 \tilde{\mathbf{E}}_3 &= -\frac{q_e}{\varepsilon_0} \frac{\partial}{\partial t} (\tilde{n}_1 \tilde{\mathbf{u}}_2) \\ \frac{\partial^2 \tilde{\mathbf{E}}_2}{\partial t^2} + \omega_{pe}^2 \tilde{\mathbf{E}}_2 - \frac{3\kappa T_e}{m_e} \nabla^2 \tilde{\mathbf{E}}_2 &= -\frac{q_e}{\varepsilon_0} \frac{\partial}{\partial t} (\tilde{n}_1 \tilde{\mathbf{u}}_3) \\ \frac{\partial^2 \tilde{n}_1}{\partial t^2} - c_s^2 \nabla^2 \tilde{n}_1 &= n \frac{m_e}{m_i} \nabla^2 (\tilde{\mathbf{u}}_2 \cdot \tilde{\mathbf{u}}_3) \end{aligned} \quad (15.72)$$

where the relation

$$\left(\frac{1}{2} (\tilde{u}_e^h)^2 \right)_{\omega_1, \mathbf{k}_1} = \frac{1}{2} \langle (\tilde{\mathbf{u}}_2 + \tilde{\mathbf{u}}_3) \cdot (\tilde{\mathbf{u}}_2 + \tilde{\mathbf{u}}_3) \rangle = \langle \tilde{\mathbf{u}}_2 \cdot \tilde{\mathbf{u}}_3 \rangle \quad (15.73)$$

has been used and the angle brackets refer to the component oscillating at the beat frequency $\omega_1 = \omega_3 - \omega_2$ and having the beat wavevector $\mathbf{k}_1 = \mathbf{k}_3 - \mathbf{k}_2$.

The subscript e has been dropped from all dependent variables because they all refer to electrons. Since the acoustic wave frequency is much smaller than ω_{pe} , it is possible to approximate

$$\frac{\partial}{\partial t} (\tilde{n}_1 \tilde{\mathbf{u}}_2) \simeq \tilde{n}_1 \frac{\partial \tilde{\mathbf{u}}_2}{\partial t} = \tilde{n}_1 \frac{q_e}{m_e} \tilde{\mathbf{E}}_2. \quad (15.74)$$

Using the quiver relation Eq.(15.36), the product of the high frequency velocities can be expressed as

$$\langle \tilde{\mathbf{u}}_2 \cdot \tilde{\mathbf{u}}_3 \rangle = \frac{q_e^2}{m_e^2 \omega_2 \omega_3} \langle \tilde{\mathbf{E}}_2 \cdot \tilde{\mathbf{E}}_3 \rangle. \quad (15.75)$$

Although the two velocities are oscillating 90° out of phase relative to their respective electric fields, the non-linear product of the velocities has the same phase behavior as the electric fields. This is because the nonlinear product of the velocities scales as $\langle \cos \omega_2 t \cos \omega_3 t \rangle$ and the nonlinear product of the electric fields scales as $\langle \sin \omega_2 t \sin \omega_3 t \rangle$ so that the difference between these scalings is $\langle \cos \omega_2 t \cos \omega_3 t - \sin \omega_2 t \sin \omega_3 t \rangle = \langle \cos(\omega_2 + \omega_3)t \rangle$ which vanishes because $\omega_2 + \omega_3$ is non-resonant. The system of equations thus becomes

$$\begin{aligned} \left(\frac{\partial^2}{\partial t^2} + \omega_{pe}^2 - c^2 \nabla^2 \right) \bar{\mathbf{E}}_3 &= -\omega_{pe}^2 \frac{\tilde{n}_1}{n} \bar{\mathbf{E}}_2 \\ \left(\frac{\partial^2}{\partial t^2} + \omega_{pe}^2 - \frac{3\kappa T_e}{m_e} \nabla^2 \right) \bar{\mathbf{E}}_2 &= -\omega_{pe}^2 \frac{\tilde{n}_1}{n} \bar{\mathbf{E}}_3 \\ \left(\frac{\partial^2}{\partial t^2} - c_s^2 \nabla^2 \right) \frac{\tilde{n}_1}{n} &= \frac{q_e^2}{m_i m_e \omega_2 \omega_3} \nabla^2 (\bar{\mathbf{E}}_2 \cdot \bar{\mathbf{E}}_3). \end{aligned} \quad (15.76)$$

If different modes are used, e.g., a Langmuir mode decaying into another Langmuir mode or if the low frequency mode is a Langmuir wave, the left hand side wave terms will be changed accordingly, but the right hand coupling terms will stay the same except if the low frequency wave is a Langmuir wave in which case the product $m_i m_e$ must be replaced by m_e^2 in the denominator of the right hand side of the third equation.

The right hand coupling terms can be made identical by defining a renormalized density perturbation

$$\tilde{\psi} = \alpha \frac{\tilde{n}_1}{n} \quad (15.77)$$

so that the equations become

$$\begin{aligned} \left(\frac{\partial^2}{\partial t^2} + \omega_{pe}^2 - c^2 \nabla^2 \right) \bar{\mathbf{E}}_3 &= -\omega_{pe}^2 \frac{\tilde{\psi}}{\alpha} \bar{\mathbf{E}}_2 \\ \left(\frac{\partial^2}{\partial t^2} + \omega_{pe}^2 - \frac{3\kappa T_e}{m_e} \nabla^2 \right) \bar{\mathbf{E}}_2 &= -\omega_{pe}^2 \frac{\tilde{\psi}}{\alpha} \bar{\mathbf{E}}_3 \\ \left(\frac{\partial^2}{\partial t^2} - c_s^2 \nabla^2 \right) \tilde{\psi} &= -\frac{\alpha q_e^2 k_1^2}{m_i m_e \omega_2 \omega_3} \bar{\mathbf{E}}_2 \cdot \bar{\mathbf{E}}_3. \end{aligned} \quad (15.78)$$

Equating the coefficients of the second and third terms gives

$$\alpha = \omega_{pe} \frac{\sqrt{m_i m_e \omega_2 \omega_3}}{q_e k_1} \quad (15.79)$$

so the equations become

$$\begin{aligned} \left(\frac{\partial^2}{\partial t^2} + \omega_{pe}^2 - c^2 \nabla^2 \right) \bar{\mathbf{E}}_3 &= -\lambda \tilde{\psi} \bar{\mathbf{E}}_2 \\ \left(\frac{\partial^2}{\partial t^2} + \omega_{pe}^2 - \frac{3\kappa T_e}{m_e} \nabla^2 \right) \bar{\mathbf{E}}_2 &= -\lambda \tilde{\psi} \bar{\mathbf{E}}_3 \\ \left(\frac{\partial^2}{\partial t^2} - c_s^2 \nabla^2 \right) \tilde{\psi} &= -\lambda \bar{\mathbf{E}}_2 \cdot \bar{\mathbf{E}}_3. \end{aligned} \quad (15.80)$$

where

$$\lambda = \frac{\omega_{pe} q_e k_1}{\sqrt{m_i m_e \omega_2 \omega_3}}. \quad (15.81)$$

Defining the mode frequencies as

$$\begin{aligned} \omega_3^2 &= \omega_{pe}^2 + k_3^2 c^2 \\ \omega_2^2 &= \omega_{pe}^2 + 3k_3^2 \kappa T_e / m_e \\ \omega_1^2 &= k_1^2 c_s^2 \end{aligned} \quad (15.82)$$

the coupled equations become

$$\begin{aligned} \left(\frac{\partial^2}{\partial t^2} + \omega_3^2 \right) \bar{\mathbf{E}}_3 &= -\lambda \tilde{\psi} \bar{\mathbf{E}}_2 \\ \left(\frac{\partial^2}{\partial t^2} + \omega_2^2 \right) \bar{\mathbf{E}}_2 &= -\lambda \tilde{\psi} \bar{\mathbf{E}}_3 \\ \left(\frac{\partial^2}{\partial t^2} + \omega_1^2 \right) \tilde{\psi} &= -\lambda \bar{\mathbf{E}}_2 \cdot \bar{\mathbf{E}}_3 \end{aligned} \quad (15.83)$$

which is identical to the coupled oscillator system described by Eq.(15.3) if m is set to unity in Eq.(15.3) and $\bar{\mathbf{E}}_2$ is parallel to $\bar{\mathbf{E}}_3$. Using Eq.(15.30), the nonlinear growth rate is found to be

$$\begin{aligned} \gamma &= \frac{\lambda E_3}{4 \sqrt{\omega_1 \omega_2}} \\ &= \frac{1}{4} \frac{\omega_{pe}}{\omega_2} \sqrt{\frac{\omega_3}{\omega_1}} k_1 \frac{q_e E_3}{m_e \omega_3}. \end{aligned} \quad (15.84)$$

15.4 Non-linear dispersion formulation and instability threshold

An equivalent way of considering the effect of nonlinearity is to derive a so-called nonlinear dispersion relation (Nishikawa 1968b, Nishikawa 1968a). This method has the virtue that both wave damping and frequency mismatches can easily be incorporated. To see how damping can be introduced, consider an electrical circuit consisting of an inductor, capacitor and resistor all in series. The circuit equation is

$$L \frac{d^2 Q}{dt^2} + R \frac{dQ}{dt} + \frac{Q}{C} = 0 \quad (15.85)$$

where Q is the charge stored in the capacitor and the current is $I = dQ/dt$. The general solution is $Q \sim e^{-i\omega t}$ where ω satisfies

$$\omega^2 + i\omega \frac{R}{L} - \frac{1}{LC} = 0. \quad (15.86)$$

Solving for ω gives the usual damped harmonic oscillator solution

$$\omega = -\frac{iR}{2L} \pm \sqrt{\frac{1}{LC} - \frac{R^2}{4L^2}}. \quad (15.87)$$

Thus, if $1/LC \gg R/L$ the imaginary part of the frequency is $\omega_i = -R/2L$ and the real part of the frequency is $\omega_r = \pm 1/\sqrt{LC}$. This means that the resistor can be identified with damping by the relation $R \rightarrow -2\omega_i L$. Interpreting Q_j now as the dependent variable for oscillation mode j , the appropriate differential equation for the damped mode can be written as

$$\frac{d^2 Q_j}{dt^2} + 2\Gamma_j \frac{dQ_j}{dt} + \omega_j^2 Q_j = 0 \quad (15.88)$$

where $\Gamma_j = |\text{Im } \omega_j|$ is the linear damping rate for mode j . Mode j therefore has the time dependence $\exp(\pm i\omega_j t - \Gamma_j t)$ where both ω_j and Γ_j are positive quantities.

Thus, when dissipation is included, the typical system given by Eq.(15.83) generalizes to

$$\begin{aligned} \left(\frac{\partial^2}{\partial t^2} + 2\Gamma_3 \frac{\partial}{\partial t} + \omega_3^2 \right) \bar{\mathbf{E}}_3 &= -\lambda \tilde{\psi} \bar{\mathbf{E}}_2 \\ \left(\frac{\partial^2}{\partial t^2} + 2\Gamma_2 \frac{\partial}{\partial t} + \omega_2^2 \right) \bar{\mathbf{E}}_2 &= -\lambda \tilde{\psi} \bar{\mathbf{E}}_3 \\ \left(\frac{\partial^2}{\partial t^2} + 2\Gamma_1 \frac{\partial}{\partial t} + \omega_1^2 \right) \tilde{\psi} &= -\lambda \bar{\mathbf{E}}_2 \cdot \bar{\mathbf{E}}_3. \end{aligned} \quad (15.89)$$

Let us now consider again the situation where the pump wave $\bar{\mathbf{E}}_3$ is very large and so may be considered as having approximately constant amplitude. The decay waves then do not grow to sufficient amplitude to deplete the pump energy and so only the last two of the three coupled equations have to be considered. We define \hat{s}_2 as a unit vector in the direction of $\bar{\mathbf{E}}_2$ so that

$$\tilde{E}_2 = \hat{s}_2 \cdot \bar{\mathbf{E}}_2 \quad (15.90)$$

and so the last two of the three coupled equations become

$$\begin{aligned} \left(\frac{\partial^2}{\partial t^2} + 2\Gamma_2 \frac{\partial}{\partial t} + \omega_2^2 \right) \tilde{E}_2 &= -\lambda \tilde{\psi} \hat{s}_2 \cdot \bar{\mathbf{E}}_3 \\ \left(\frac{\partial^2}{\partial t^2} + 2\Gamma_1 \frac{\partial}{\partial t} + \omega_1^2 \right) \tilde{\psi} &= -\lambda \tilde{E}_2 \hat{s}_2 \cdot \bar{\mathbf{E}}_3. \end{aligned} \quad (15.91)$$

The wavevector selection rules are assumed to be satisfied but a slight mismatching in the frequency selection rules will be allowed. The pump wave is now written as

$$\hat{s}_2 \cdot \bar{\mathbf{E}}_3 = Z_3 \cos \omega_3 t \quad (15.92)$$

where Z_3 is the effective pump wave amplitude. The coupled daughter equations then become

$$\begin{aligned} \left(\frac{\partial^2}{\partial t^2} + 2\Gamma_2 \frac{\partial}{\partial t} + \omega_2^2 \right) \tilde{E}_2 &= -\frac{\lambda Z_3}{2} (e^{i\omega_3 t} + e^{-i\omega_3 t}) \tilde{\psi} \\ \left(\frac{\partial^2}{\partial t^2} + 2\Gamma_1 \frac{\partial}{\partial t} + \omega_1^2 \right) \tilde{\psi} &= -\frac{\lambda Z_3}{2} (e^{i\omega_3 t} + e^{-i\omega_3 t}) \tilde{E}_2. \end{aligned} \quad (15.93)$$

The Fourier transform of a quantity $f(t)$ is defined as

$$f(\omega) = \int dt f(t) e^{i\omega t} \quad (15.94)$$

where the sign of the exponent is chosen to be consistent with the convention that a single Fourier mode has the form $\exp(-i\omega t)$. The Fourier transform of $f(t)e^{\pm i\omega_3 t}$ will therefore be

$$\int dt (f(t)e^{\pm i\omega_3 t}) e^{i\omega t} = f(\omega \pm \omega_3) \quad (15.95)$$

and the Fourier transform of $\partial f/\partial t$ will be

$$\int dt \left(\frac{\partial}{\partial t} f(t) \right) e^{i\omega t} = -i\omega \int dt f(t) e^{i\omega t} = -i\omega f(\omega). \quad (15.96)$$

Application of Eqs.(15.95) and (15.96) to Eqs.(15.93) gives

$$\begin{aligned} (-\omega^2 - 2i\omega\Gamma_2 + \omega_2^2) \tilde{E}_2(\omega) &= -\frac{\lambda Z_3}{2} [\tilde{\psi}(\omega + \omega_3) + \tilde{\psi}(\omega - \omega_3)] \\ (-\omega^2 - 2i\omega\Gamma_1 + \omega_1^2) \tilde{\psi}(\omega) &= -\frac{\lambda Z_3}{2} [\tilde{E}_2(\omega + \omega_3) + \tilde{E}_2(\omega - \omega_3)]. \end{aligned} \quad (15.97)$$

By defining a generic linear dispersion relation

$$\varepsilon_j(\omega) = -\omega^2 - 2i\omega\Gamma_j + \omega_j^2, \quad (15.98)$$

these equations can be written as

$$\varepsilon_2(\omega) \tilde{E}_2(\omega) = -\frac{\lambda Z_3}{2} [\tilde{\psi}(\omega + \omega_3) + \tilde{\psi}(\omega - \omega_3)] \quad (15.99)$$

$$\varepsilon_1(\omega) \tilde{\psi}(\omega) = -\frac{\lambda Z_3}{2} [\tilde{E}_2(\omega + \omega_3) + \tilde{E}_2(\omega - \omega_3)]. \quad (15.100)$$

The frequency ω in Eq.(15.100) can be replaced by $\omega \pm \omega_3$ so that

$$\tilde{\psi}(\omega \pm \omega_3) = -\frac{\lambda Z_3}{2\varepsilon_1(\omega \pm \omega_3)} [\tilde{E}_2(\omega) + \tilde{E}_2(\omega \pm 2\omega_3)]$$

which is then substituted into Eq.(15.99) to obtain

$$\varepsilon_2(\omega) \tilde{E}_2(\omega) = \left(\frac{\lambda Z_3}{2} \right)^2 \left[\frac{\tilde{E}_2(\omega) + \tilde{E}_2(\omega + 2\omega_3)}{\varepsilon_1(\omega + \omega_3)} + \frac{\tilde{E}_2(\omega) + \tilde{E}_2(\omega - 2\omega_3)}{\varepsilon_1(\omega - \omega_3)} \right]. \quad (15.101)$$

The terms $\tilde{E}_2(\omega \pm 2\omega_3)$ can be discarded since they are non-resonant and therefore of insignificant amplitude. What remains is

$$\varepsilon_2(\omega) = \left(\frac{\lambda Z_3}{2} \right)^2 \left[\frac{1}{\varepsilon_1(\omega + \omega_3)} + \frac{1}{\varepsilon_1(\omega - \omega_3)} \right] \quad (15.102)$$

which is called the *non-linear dispersion relation* (Nishikawa 1968b, Nishikawa 1968a).

The non-linear dispersion relation is investigated by first writing

$$\omega = x + iy \quad (15.103)$$

where it is assumed that

$$x \simeq \omega_2 \quad (15.104)$$

and also

$$\omega - \omega_3 = x + iy - \omega_3 \simeq -\omega_1. \quad (15.105)$$

These assumptions and definitions have been made so that $\varepsilon_1(\omega - \omega_3)$ is close to zero, $\varepsilon_1(\omega + \omega_3)$ is not close to zero, and positive y corresponds to instability. The term $1/\varepsilon_1(\omega + \omega_3)$ can therefore be discarded as being non-resonant and the nonlinear dispersion relation simplifies to

$$\varepsilon_2(\omega)\varepsilon_1(\omega - \omega_3) = \left(\frac{\lambda Z_3}{2}\right)^2. \quad (15.106)$$

The linear dispersion relations ε_2 and ε_1 on the left hand side are each Taylor-expanded to give

$$\begin{aligned} \varepsilon_2(\omega) &= \varepsilon_2(\omega_2 + x - \omega_2 + iy) \\ &\simeq \varepsilon_2(\omega_2) + (x - \omega_2 + iy) \left. \frac{d\varepsilon_2}{d\omega} \right|_{\omega=\omega_2} \\ &= -2i\omega_2\Gamma_2 - 2\omega_2(x - \omega_2 + iy) \end{aligned} \quad (15.107)$$

and

$$\begin{aligned} \varepsilon_1(\omega - \omega_3) &= \varepsilon_1(-\omega_1 + x + iy + \omega_1 - \omega_3) \\ &\simeq \varepsilon_1(-\omega_1) + (x + iy + \omega_1 - \omega_3) \left. \frac{d\varepsilon_1}{d\omega} \right|_{\omega=-\omega_1} \\ &= 2i\omega_1\Gamma_1 + 2\omega_1(x + iy + \omega_1 - \omega_3). \end{aligned} \quad (15.108)$$

Using these expansions, the nonlinear dispersion relation becomes

$$\{-i(\Gamma_2 + y) - (x - \omega_2)\} \{i(\Gamma_1 + y) + (x + \omega_1 - \omega_3)\} = \frac{1}{\omega_1\omega_2} \left(\frac{\lambda Z_3}{4}\right)^2 \quad (15.109)$$

or, in more compact form,

$$(\bar{x} + i(\Gamma_2 + y))(\bar{x} - \Delta + i(\Gamma_1 + y)) = -\frac{1}{\omega_1\omega_2} \left(\frac{\lambda Z_3}{4}\right)^2 \quad (15.110)$$

where

$$\bar{x} = x - \omega_2 \quad (15.111)$$

and

$$\Delta = \omega_3 - (\omega_1 + \omega_2) \quad (15.112)$$

is the frequency mismatch.

The real and imaginary parts of Eq.(15.110) are

$$(\bar{x} - \Delta)\bar{x} - (\Gamma_2 + y)(\Gamma_1 + y) = -\frac{1}{\omega_1\omega_2} \left(\frac{\lambda Z_3}{4}\right)^2 \quad (15.113)$$

$$\bar{x}(\Gamma_1 + y) + (\bar{x} - \Delta)(\Gamma_2 + y) = 0. \quad (15.114)$$

Solving Eq.(15.114) gives

$$\bar{x} = \frac{(\Gamma_2 + y)}{(2y + \Gamma_1 + \Gamma_2)}\Delta, \quad \bar{x} - \Delta = -\frac{(\Gamma_1 + y)}{(2y + \Gamma_1 + \Gamma_2)}\Delta \quad (15.115)$$

and substitution for \bar{x} and $\bar{x} - \Delta$ in Eq.(15.113) results in the expression for the growth rate

$$(\Gamma_2 + y)(\Gamma_1 + y) \left(1 + \frac{\Delta^2}{(2y + \Gamma_1 + \Gamma_2)^2} \right) = \frac{1}{\omega_1 \omega_2} \left(\frac{\lambda Z_3}{4} \right)^2. \quad (15.116)$$

Onset of instability onset corresponds to y being close to zero and at marginal stability Eq.(15.116) becomes

$$(\Gamma_2 + \Gamma_1)y + \Gamma_1 \Gamma_2 = \frac{\lambda^2 Z_3^2}{16\omega_1 \omega_2 \left(1 + \frac{\Delta^2}{(\Gamma_2 + \Gamma_1)^2} \right)}. \quad (15.117)$$

The growth rate near threshold therefore is

$$y = \frac{1}{(\Gamma_2 + \Gamma_1)} \left(\frac{\lambda^2 Z_3^2}{16\omega_1 \omega_2 \left(1 + \frac{\Delta^2}{(\Gamma_2 + \Gamma_1)^2} \right)} - \Gamma_1 \Gamma_2 \right). \quad (15.118)$$

This shows that the pump amplitude threshold for instability is

$$Z_3 = \frac{4\sqrt{\omega_1 \omega_2 \Gamma_1 \Gamma_2}}{\lambda} \sqrt{1 + \frac{\Delta^2}{(\Gamma_2 + \Gamma_1)^2}}; \quad (15.119)$$

this threshold is proportional to the geometric mean of the linear damping rate of the two modes. If the pump amplitude is below threshold then the nonlinear instability does not occur. The lowest threshold occurs when $\Delta = 0$, i.e., when the frequency selection rule is exactly satisfied. Instability when the pump amplitude exceeds a threshold is routinely observed in actual experimental situations as was discussed earlier, i.e., decay instability of a pump wave is observed to begin only when the pump wave amplitude exceeds threshold (for example, see Stenzel and Wong (1972)). For a pump amplitude well above threshold, Eq.(15.116) becomes

$$y = \sqrt{\frac{1}{\omega_1 \omega_2} \left(\frac{\lambda Z_3}{4} \right)^2 - \frac{\Delta^2}{4}} \quad (15.120)$$

which shows that frequency mismatch reduces the growth rate. The situation reduces to Eqs.(15.84) and (15.30) when $\Delta = 0$. Thus the non-linear dispersion relation formalism extends the Manley-Rowe coupled oscillator model to include the effects of both dissipation and frequency mismatch.

15.5 Digging a hole in the plasma via ponderomotive force

If the low frequency daughter mode is at zero frequency, then the ion acoustic mode ceases to be a wave. Instead, it becomes a density depletion caused by the ponderomotive force

and so Eq.(15.49) reduces to

$$\frac{1}{n} \nabla \tilde{n} = -\frac{1}{2} \frac{m_e}{\kappa T_e} \nabla (\tilde{u}_e^h)^2 \quad (15.121)$$

which can be integrated to give a Boltzmann-like relation

$$\frac{\tilde{n}}{n} = -\frac{1}{2} \frac{m_e}{\kappa T_e} \left\langle (\tilde{u}_e^h)^2 \right\rangle. \quad (15.122)$$

Since the high frequency daughter wave is the same as the pump wave there is now only one high frequency wave and so there is no need to have subscripts distinguishing the modes. The consequence is that the high frequency wave propagates in a plasma having a density depletion dug out by the ponderomotive force. For example the Langmuir wave equation in this case would become

$$\left(\frac{\partial^2}{\partial t^2} + 2\Gamma \frac{\partial}{\partial t} + \omega_{pe}^2 \left(1 - \frac{1}{2} \frac{m_e}{\kappa T_e} \left\langle (\tilde{u}_e^h)^2 \right\rangle \right) - \frac{3\kappa T_e}{m_e} \nabla^2 \right) \tilde{\mathbf{u}}_e^h = 0 \quad (15.123)$$

where $\tilde{\mathbf{u}}_e^h$ has been used as the linear variable instead of $\bar{\mathbf{E}}$ and a linear damping term involving Γ , the linear damping rate has been introduced.

An undamped linear Langmuir wave in a uniform plasma satisfies the dispersion relation $\omega^2 = \omega_{pe}^2 (1 + 3k^2 \lambda_{De}^2)$ where $k\lambda_{De} \ll 1$ so that the wave frequency is very close to ω_{pe} . It is reasonable to presume that the nonlinear wave also oscillates at a frequency very close to ω_{pe} and so what is important is the deviation of the frequency from ω_{pe} . To investigate this, the electron fluid velocity is assumed to be of the form

$$\begin{aligned} \tilde{\mathbf{u}}_e^h(\mathbf{x}, t) &= \text{Re} [\mathbf{A}(x, t) e^{-i\omega_{pe} t}] \\ &= \frac{1}{2} \{ \mathbf{A}(x, t) e^{-i\omega_{pe} t} + \mathbf{A}^*(x, t) e^{i\omega_{pe} t} \} \end{aligned} \quad (15.124)$$

in which case

$$\left\langle (\tilde{\mathbf{u}}_e^h)^2 \right\rangle = \frac{1}{2} |\mathbf{A}|^2 \quad (15.125)$$

and the time dependence of $\mathbf{A}(x, t)$ characterizes the extent to which the wave frequency deviates from ω_{pe} . Because this deviation is small, \mathbf{A} changes slowly compared to ω_{pe} , and so in analogy to Eq.(3.22) it is possible to approximate

$$\frac{\partial^2}{\partial t^2} [\mathbf{A}(x, t) e^{-i\omega_{pe} t}] \simeq -\omega_{pe}^2 \mathbf{A}(x, t) e^{-i\omega_{pe} t} - 2i\omega_{pe} \frac{\partial \mathbf{A}}{\partial t} e^{-i\omega_{pe} t} \quad (15.126)$$

and

$$2\Gamma \frac{\partial}{\partial t} [\mathbf{A}(x, t) e^{-i\omega_{pe} t}] \approx -i2\omega_{pe} \Gamma \mathbf{A} e^{-i\omega_{pe} t}.$$

Substitution of Eq. (15.126) into Eq.(15.123) gives

$$2i\omega_{pe} \frac{\partial \mathbf{A}}{\partial t} + i2\omega_{pe} \Gamma \mathbf{A} + \frac{\omega_{pe}^2}{4} \frac{m_e}{\kappa T_e} |\mathbf{A}|^2 \mathbf{A} + c^2 \nabla^2 \mathbf{A} = 0. \quad (15.127)$$

By defining the normalized variables

$$\begin{aligned}\tau &= \omega_{pe}t/2 \\ \chi &= \frac{\mathbf{A}}{2\sqrt{\kappa T_e/m_e}} \\ \xi &= \mathbf{x}\omega_{pe}/c \\ \eta &= 2\Gamma/\omega_{pe}\end{aligned}\quad (15.128)$$

Eq.(15.127) can be put in the standardized form

$$i\frac{\partial\chi}{\partial\tau} + i\eta\chi + |\chi|^2\chi + \nabla_\xi^2\chi = 0; \quad (15.129)$$

this is called a non-linear Schrödinger equation since if $\eta = 0$, this equation resembles a Schrödinger equation where $|\chi|^2$ plays the role of a potential energy.

In order to exploit this analogy, we recall the relationship between the Schrödinger equation and the classical conservation of energy relation for a particle in a potential well $V(x)$. According to classical mechanics, the sum of the kinetic and potential energies gives the total energy, i.e.,

$$\frac{p^2}{2m} + V(\mathbf{x}) = E. \quad (15.130)$$

However, in quantum mechanics, the momentum and the energy are expressed as spatial and temporal operators, $\mathbf{p} = -i\hbar\nabla$ and $E = i\hbar\partial/\partial t$ which act on a wave function ψ so that Eq.(15.130) becomes

$$-\frac{\hbar^2}{2m}\nabla^2\psi + V\psi = i\hbar\frac{\partial\psi}{\partial t} \quad (15.131)$$

or, after re-arrangement,

$$i\hbar\frac{\partial\psi}{\partial t} - V\psi + \frac{\hbar^2}{2m}\nabla^2\psi = 0. \quad (15.132)$$

Equation (15.130) shows that a particle will be trapped in a potential well if $V(\pm\infty) > E > V_{\min}$ where V_{\min} is the minimum value of V . From the quantum mechanical point of view, $|\psi|^2$ is the probability of finding the particle at position \mathbf{x} . Thus, existence of solutions to Eq.(15.132) localized to the vicinity of V_{\min} is the quantum mechanical way of stating that a particle can be trapped in a potential well. Comparison of Eqs.(15.129) and (15.132) shows that $-|\bar{\mathbf{A}}|^2$ plays the role of V and so a local maximum of $|\bar{\mathbf{A}}|^2$ should act as an effective potential well. This makes physical sense because Langmuir waves reflect from regions of high density and the amplitude-dependent ponderomotive force digs a hole in the plasma. Thus, regions of high wave amplitude create a density depression and the Langmuir wave reflects from the high density regions surrounding this density depression. The Langmuir wave then becomes trapped in a depression of its own making. Formation of this depression can be an unstable process because if a wave is initially trapped in a shallow well, its energy $|\chi|^2$ will concentrate at the bottom of this well, but this concentration of $|\chi|^2$ will make the well deeper and so concentrate the wave energy into a smaller region, making $|\chi|^2$ even larger, and so on.

Caviton instability

The instability outlined above can be described in a quantitative manner using the 1-D version of Eq.(15.129), namely

$$i\frac{\partial\chi}{\partial\tau} + i\eta\chi + |\chi|^2\chi + \frac{\partial^2\chi}{\partial\xi^2} = 0. \quad (15.133)$$

It is assumed that a stable solution $\chi_0(x, t)$ exists initially and satisfies

$$i\frac{\partial\chi_0}{\partial\tau} + i\eta\chi_0 + |\chi_0|^2\chi_0 + \frac{\partial^2\chi_0}{\partial\xi^2} = 0 \quad (15.134)$$

where $|\chi_0(x, t)|$ is bounded in both time and space. Next, a slightly different solution is considered,

$$\chi(x, t) = \chi_0(x, t) + \tilde{\chi}(x, t) \quad (15.135)$$

where the perturbation $\tilde{\chi}(x, t)$ is assumed to be very small compared to $\chi_0(x, t)$. The equation for $\chi(x, t)$ is thus

$$i\frac{\partial}{\partial\tau}(\chi_0 + \tilde{\chi}) + i\eta(\chi_0 + \tilde{\chi}) + |\chi_0 + \tilde{\chi}|^2(\chi_0 + \tilde{\chi}) + \frac{\partial^2}{\partial\xi^2}(\chi_0 + \tilde{\chi}) = 0. \quad (15.136)$$

Subtracting Eq.(15.134) from (15.136) yields

$$i\frac{\partial}{\partial\tau}\tilde{\chi} + i\eta\tilde{\chi} + |\chi_0 + \tilde{\chi}|^2(\chi_0 + \tilde{\chi}) - |\chi_0|^2\chi_0 + \frac{\partial^2}{\partial\xi^2}\tilde{\chi} = 0. \quad (15.137)$$

Expansion of the potential-energy-like terms while keeping only terms linear in the perturbation gives

$$|\chi_0 + \tilde{\chi}|^2(\chi_0 + \tilde{\chi}) - |\chi_0|^2\chi_0 \approx \chi_0^2\tilde{\chi}^* + 2|\chi_0|^2\tilde{\chi} \quad (15.138)$$

so Eq.(15.137) becomes

$$i\frac{\partial}{\partial\tau}\tilde{\chi} + i\eta\tilde{\chi} + \chi_0^2\tilde{\chi}^* + 2|\chi_0|^2\tilde{\chi} + \frac{\partial^2}{\partial\xi^2}\tilde{\chi} = 0. \quad (15.139)$$

It is now assumed that the perturbation is unstable and has the space-time dependence

$$\tilde{\chi} \sim e^{ik\xi + \gamma t} \quad (15.140)$$

in which case Eq.(15.139) becomes

$$(i\gamma + i\eta + 2|\chi_0|^2 - k^2)\tilde{\chi} = -\chi_0^2\tilde{\chi}^* \quad (15.141)$$

which has the complex conjugate

$$(-i\gamma - i\eta + 2|\chi_0|^2 - k^2)\tilde{\chi}^* = -\chi_0^{*2}\tilde{\chi}. \quad (15.142)$$

Combining the above two equations gives a dispersion relation for the growth rate

$$(\gamma + \eta)^2 = -k^4 + 4k^2|\chi_0|^2 - 3|\chi_0|^4. \quad (15.143)$$

The maximum γ is found by taking the derivative of both sides with respect to k^2 and setting this derivative to zero, obtaining

$$k_{\max}^2 = 2 |\chi_0|^2 \quad (15.144)$$

as the value of k^2 giving the maximum for γ . Substitution of k_{\max}^2 into Eq.(15.143) gives

$$\gamma_{\max} = -\eta + |\chi_0|^2. \quad (15.145)$$

Thus, the configuration is unstable when $|\chi_0|^2 > \eta$ or in terms of the original variables when

$$\left(\frac{\mathbf{u}_e^h}{\sqrt{\kappa T_e/m_e}} \right)^2 > \frac{\Gamma}{\omega_{pe}}. \quad (15.146)$$

This is called a caviton instability and it tends to dig a sharp hole. This is because each successive stage of growth can be considered a quasi-equilibrium which is destabilized and from Eq.(15.144) it is seen that the most unstable k becomes progressively larger as the amplitude increases. Another way of seeing this hole-digging tendency is to note that Eqs.(15.141) and (15.142) are coupled by their respective right hand terms and these terms are proportional to the amplitude of the original wave. It is this coupling which leads to instability of the perturbation and so the perturbation is most unstable where the amplitude of the original wave was largest. The digging of a density cavity in a plasma by a Langmuir wave was observed experimentally by Kim, Stenzel and Wong (1974); the density cavity was called a caviton.

Stationary Envelope Soliton

A special, fully nonlinear solution of Eq.(15.133) can be found in the limit where damping is sufficiently small to be neglected so that the non-linear Schrödinger equation reduces to

$$i \frac{\partial \chi}{\partial \tau} + |\chi|^2 \chi + \frac{\partial^2 \chi}{\partial \xi^2} = 0. \quad (15.147)$$

We now search for a solution that vanishes at infinity, propagates at some fixed velocity, and oscillates so that

$$\chi = g(\xi) e^{i\Omega\tau}. \quad (15.148)$$

With this assumption, Eq.(15.147) becomes

$$-\Omega g + g^3 + g'' = 0. \quad (15.149)$$

After multiplying by the integrating factor g' , this becomes

$$\frac{d}{d\xi} \left(-\frac{\Omega}{2} g^2 + \frac{1}{4} g^4 + \frac{1}{2} (g')^2 \right) = 0. \quad (15.150)$$

Since the solution is assumed to vanish at infinity, integration with respect to ξ from $\xi = -\infty$ gives

$$(g')^2 = \Omega g^2 - \frac{1}{2} g^4 \quad (15.151)$$

or

$$\frac{dg}{g\sqrt{\Omega - \frac{1}{2}g^2}} = d\xi. \quad (15.152)$$

By letting

$$g = \frac{\sqrt{2\Omega}}{\cosh \theta} \quad (15.153)$$

it is seen that

$$dg = -\frac{\sqrt{2\Omega}}{\cosh^2 \theta} \sinh \theta d\theta \quad (15.154)$$

in which case

$$\theta = -\sqrt{\Omega}\xi + \delta \quad (15.155)$$

where δ is an arbitrary constant. Thus, the solution is

$$\chi(\xi, \tau) = \frac{\sqrt{2\Omega}e^{i\Omega\tau}}{\cosh(\sqrt{\Omega}\xi - \delta)} \quad (15.156)$$

which is localized in space. For large Ω the oscillation frequency and amplitude both increase, and the localization is more pronounced.

Propagating envelope soliton

One may ask whether the above solution can be generalized to a propagating solution, i.e., can ξ be replaced by $\xi - vt$ where v is a velocity? Making only this replacement is clearly inadequate and so a solution of the form

$$\chi = g(\xi - vt)e^{i\Omega\tau + ih(\xi, \tau)} \quad (15.157)$$

is assumed where $h(\xi, \tau)$ is an unknown function to be determined. Substitution of this assumed solution into Eq.(15.147) gives

$$-ivg' - \Omega g - g\frac{\partial h}{\partial \tau} + g^3 + g'' + 2i\frac{\partial h}{\partial \xi}g' - \left(\frac{\partial h}{\partial \xi}\right)^2 g = 0. \quad (15.158)$$

Setting the imaginary part to zero gives

$$v = 2\frac{\partial h}{\partial \xi} \quad (15.159)$$

which can be integrated to give

$$h = \frac{v\xi}{2} + f(\tau) \quad (15.160)$$

where $f(\tau)$ is to be determined. The real part of the equation becomes

$$-\Omega g - g\frac{\partial h}{\partial \tau} + g^3 + g'' - \frac{v^2}{4}g = 0. \quad (15.161)$$

If we set

$$\frac{\partial h}{\partial \tau} = -\frac{v^2}{4} \quad (15.162)$$

then the terms linear in g vanish, $f(\tau) = -v^2\tau/4$ and so

$$h(\xi, \tau) = \frac{v\xi}{2} - \frac{v^2}{4}\tau. \quad (15.163)$$

Thus, Eq.(15.161) reverts to Eq.(15.149) which is solved as in Eqs.(15.150)-(15.156) to give the propagating envelope soliton

$$\chi(\xi, \tau) = \frac{\sqrt{2\Omega} \exp(i\Omega\tau + iv\xi/2 - iv^2\tau/4)}{\cosh(\sqrt{\Omega}(\xi - vt) - \delta)}. \quad (15.164)$$

15.6 Ion acoustic wave soliton

The ion acoustic wave dispersion relation is

$$\omega^2 = \frac{k^2 c_s^2}{1 + k^2 \lambda_D^2} \quad (15.165)$$

which has the forward propagating solution

$$\omega = k c_s (1 + k^2 \lambda_D^2)^{-1/2} \quad (15.166)$$

or, for small $k \lambda_D$,

$$\omega = k c_s - k^3 \lambda_D^2 c_s / 2 \quad (15.167)$$

where the last term is small. Since $\partial/\partial x \rightarrow ik$ and $\partial/\partial t \rightarrow -i\omega$ the reverse substitution $k \rightarrow -i\partial/\partial x$ and $\omega \rightarrow i\partial/\partial t$ can be invoked so that the forward propagating ion acoustic wave can be written as a partial differential equation for say, the ion velocity

$$i \frac{\partial u_i}{\partial t} = -i \frac{\partial u_i}{\partial x} c_s - (-i)^3 \frac{\partial^3 u_i}{\partial x^3} \frac{\lambda_D^2 c_s}{2}. \quad (15.168)$$

After multiplying by $-i$, this gives the dispersive forward propagating wave equation

$$\frac{\partial u_i}{\partial t} = -c_s \frac{\partial u_i}{\partial x} - \frac{\lambda_D^2 c_s}{2} \frac{\partial^3 u_i}{\partial x^3}. \quad (15.169)$$

This wave equation was derived using a linearized version of the ion fluid equation of motion, namely

$$m_i \frac{\partial u_i}{\partial t} = q_i E. \quad (15.170)$$

If the complete nonlinear ion equation had been used instead, the ion fluid equation of motion would contain a convective nonlinear term and be

$$m_i \left(\frac{\partial u_i}{\partial t} + u_i \frac{\partial u_i}{\partial x} \right) = q_i E. \quad (15.171)$$

This suggests that inclusion of convective ion nonlinearity corresponds to making the generalization

$$\frac{\partial u_i}{\partial t} \rightarrow \frac{\partial u_i}{\partial t} + u_i \frac{\partial u_i}{\partial x} \quad (15.172)$$

and so the forward propagating ion acoustic wave equation with inclusion of ion convective nonlinearity is

$$\frac{\partial u_i}{\partial t} + (u_i + c_s) \frac{\partial u_i}{\partial x} + \frac{\lambda_D^2 c_s}{2} \frac{\partial^3 u_i}{\partial x^3} = 0. \quad (15.173)$$

This suggests defining a new variable

$$U = u_i + c_s \quad (15.174)$$

which differs only by a constant from the ion fluid velocity. The forward propagating nonlinear ion acoustic wave equation can thus be re-written as

$$\frac{\partial U}{\partial t} + U \frac{\partial U}{\partial x} + \frac{\lambda_D^2 c_s}{2} \frac{\partial^3 U}{\partial x^3} = 0. \quad (15.175)$$

We now introduce dimensionless variables by normalizing lengths to the Debye length, velocities to c_s and time to $\omega_{pi} = c_s/\lambda_{de}$. In this case

$$\chi = \frac{U}{c_s}, \quad \xi = \frac{x}{\lambda_D}, \quad \tau = \omega_{pi} t \quad (15.176)$$

so the wave equation becomes

$$\frac{\partial \chi}{\partial \tau} + \chi \frac{\partial \chi}{\partial \xi} + \frac{1}{2} \frac{\partial^3 \chi}{\partial \xi^3} = 0; \quad (15.177)$$

this is called the (KdV) equation (Korteweg 1895) and modern interest in this equation was stimulated with the discovery of a general solution to the soliton problem by Gardner, Greene, Kruskal and Miura (1967).

Because the linear wave is forward traveling with unity velocity in these dimensionless variables, it is reasonable to postulate that the nonlinear solution has the forward propagating form

$$\chi = \chi(\xi - V\tau) \quad (15.178)$$

where V is of order unity. A special solution can be found by introducing the wave-frame position variable

$$\eta = \xi - V\tau \quad (15.179)$$

so the lab frame space and time derivatives can be written as

$$\begin{aligned} \frac{\partial}{\partial \xi} &= \frac{\partial}{\partial \eta} \\ \frac{\partial}{\partial \tau} &= -V \frac{\partial}{\partial \eta} \end{aligned} \quad (15.180)$$

Substitution of these into the wave equation gives an ordinary differential equation in the wave-frame,

$$-V \frac{d\chi}{d\eta} + \frac{1}{2} \frac{d\chi^2}{d\eta} + \frac{1}{2} \frac{d^3 \chi}{d\eta^3} = 0 \quad (15.181)$$

where d has been used instead of ∂ because the equation is an ordinary differential equation. A solution is now sought that vanishes at both plus and minus infinity; such a solution is called a solitary wave. To find this solution, Eq.(15.181) is integrated using the boundary condition that χ vanishes at infinity to obtain

$$-V\chi + \frac{\chi^2}{2} + \frac{1}{2} \frac{d^2 \chi}{d\eta^2} = 0. \quad (15.182)$$

Multiplying by the integration factor $d\chi/d\eta$ allows this to be recast as

$$\frac{d}{d\eta} \left(-\frac{V\chi^2}{2} + \frac{\chi^3}{6} + \frac{1}{4} \left(\frac{d\chi}{d\eta} \right)^2 \right) = 0 \quad (15.183)$$

and then integrating gives

$$\frac{d\chi}{d\eta} = \chi \sqrt{\left(2V - \frac{2}{3}\chi \right)} \quad (15.184)$$

where the boundary condition at infinity has been used again. This can be written as

$$\frac{d(\chi/3)}{2^{1/2} \frac{\chi}{3} \sqrt{V - \frac{\chi}{3}}} = d\eta. \quad (15.185)$$

The substitution

$$\frac{\chi}{3} = \frac{V}{\cosh^2 \theta} \quad (15.186)$$

allows simplification of Eq.(15.185) to

$$d\left(\frac{\chi}{3}\right) = -\frac{2V \sinh \theta}{\cosh^3 \theta} d\theta. \quad (15.187)$$

Thus, Eq.(15.185) becomes

$$\frac{-\frac{2V \sinh \theta}{\cosh^3 \theta} d\theta}{2^{1/2} \frac{V}{\cosh^2 \theta} \sqrt{V - \frac{V}{\cosh^2 \theta}}} = d\eta \quad (15.188)$$

or

$$-\sqrt{\frac{2}{V}} d\theta = d\eta$$

which can be integrated to give

$$\theta = \sqrt{\frac{V}{2}} (\xi_0 - \eta) \quad (15.189)$$

where ξ_0 is a constant. The propagating solitary wave solution to Eq. (15.177) is therefore

$$\chi(\eta) = \frac{3V}{\cosh^2 \left(\sqrt{\frac{V}{2}} (\xi_0 - \eta) \right)} \quad (15.190)$$

or

$$\chi(\xi, \tau) = \frac{3V}{\cosh^2 \left(\sqrt{\frac{V}{2}} (\xi_0 - (\xi - V\tau)) \right)}. \quad (15.191)$$

This solution, called a soliton, has the following properties:

1. It vanishes when $|\xi| \rightarrow \infty$ as required.
2. The spatial profile consists of a solitary pulse centered around the position $\xi = \xi_0 + V\tau$
3. The pulse width scales as $V^{-1/2}$ and the pulse height scales as V so that larger amplitudes are sharper and propagate faster.

An important property of solitons is that they obey a form of superposition principle even though they are essentially nonlinear. In particular, a fast soliton can overtake a slow soliton such that after the collision or interaction, both the fast and slow solitons retain their identity. The underlying mathematical theory explaining this surprising behavior is so complex as to be beyond the scope of this text (the interested reader should consult

Drazin and Johns (1989)). This theory is called inverse scattering (Gardner et al. 1967) and involves mapping the non-linear equation to a special linear equation which is then solved and then mapped back again to give the time evolution of the nonlinear solution. The special linear equation describes a quantum mechanical particle trapped in a potential well where $\chi(\xi, t)$ plays the role of the potential. In particular, the linear equation is of the form $\partial^2 \psi / \partial \xi^2 + (\lambda - \chi(\xi, t)) \psi = 0$ where λ is an eigenvalue and time t is treated as a parameter. When this linear equation is solved for $\chi(\xi, t)$ and the solution is inserted in the KdV equation it is found that $\partial \lambda / \partial t = 0$. This invariance of the eigenvalues is a key feature which makes possible the {nonlinear \rightarrow linear} and then {linear \rightarrow nonlinear} mappings required to construct the solution.

15.7 Assignments

1. Pump depletion for a system of three coupled oscillators.

- (a) Suppose $A_1 = 0$ at $t = 0$ but A_2 and A_3 are finite. What is the value of the constant in Eq.(15.24)?
- (b) Suppose that $\sin \theta$ is not zero. Will A_1 become finite at times $t > 0$? If A_1 becomes finite, what constraint does Eq.(15.24) put on the value of $\cos \theta$ and hence on $\sin \theta$?
- (c) Use Eqs.(15.21) to write $A_1^2(t)$ and $A_2^2(t)$ in terms of $A_3^2(t)$ and the initial conditions $A_0^2(0)$, $A_1^2(0)$, and $A_3^2(0)$.
- (d) Square both sides of Eq.(15.15c) and use the results in (b) (c) above to obtain an equation of the form

$$\frac{1}{2} \left(\frac{dA_3}{dt} \right)^2 + U(A_3) = E \quad (15.192)$$

where E is a constant. Sketch the dependence of $U(A_3)$ on A_3 indicating the locations of maxima and minima.

- (e) Consider Eq.(15.192) as the energy equation for a pseudo-particle with velocity dA_3/dt in a potential well $U(A_3)$. What is the total energy of this pseudo-particle in terms of $A_0^2(0)$, $A_1^2(0)$, and $A_3^2(0)$? What does the position of the pseudo-particle in the potential well correspond to?
- (f) Considering the initial conditions given in (a), where is the pseudo-particle initially located in its potential well? Sketch the qualitative time dependence of A_3 and indicate how features of this time dependence correspond to the location of the pseudo-particle in its potential well.
- (g) Give an integral expression for the time required for A_3 to go to its first zero.
- (h) Solve Eqs.(15.15a)-(15.15c) numerically for the initial conditions given in (a) and use the numerical results to show that the time dependence of A_3 can be interpreted as the position of a pseudo-particle in a potential well prescribed by Eq.(15.192). Note: The reduction of the pump wave amplitude as it transfers energy to the daughter waves is called pump depletion; the mathematical behavior

discussed in this problem can be expressed in terms of Jacobi elliptic functions (Sagdeev and Galeev 1969).

2. Stimulated Raman scattering in laser fusion: Laser fusion is a proposed method for attaining a controlled fusion reaction. This method involves illuminating a millimeter radius pellet with intense laser light so as to ablate the outer layer of the pellet. The radial outflow of the ablating material constitutes a radial outflow of momentum and so, in order to conserve radial momentum, the rest of the pellet accelerates inwards in rocket-like fashion. An important issue is the decay of the incident laser light into other waves because such a decay would reduce the power available to drive the ablation process. For example there could be stimulated Raman scattering where the incident laser light decays into an outward propagating electromagnetic wave (the backscattered light) and an inward propagating Langmuir wave.
 - (a) Let the incident laser beam be denoted by subscript 3, the outward propagating electromagnetic wave be denoted by subscript 2 and the inward propagating Langmuir wave be denoted by subscript 1. Assume that the laser wavelength is much shorter than the characteristic density scale length. Show that if the backward scattered electromagnetic wave has a frequency only slightly above ω_{pe} then it is possible to satisfy the frequency and wavenumber matching conditions at a location where the density is approximately 1/4 of the density where the incident wave would reflect.
 - (b) Draw a sketch of ω versus k for the incident em wave, the backscattered em wave, and the Langmuir wave. Note that $v_{Te} \ll c$ so that if this plot is scaled to show the dispersion of the electromagnetic waves, the Langmuir wave dispersion is almost a horizontal line.
 - (c) Draw vectors on the sketch in (a) with coordinates $\{k, \omega\}$ so that the incident electromagnetic wave is a vector $\mathbf{v}_3 = \{k_3, \omega_3\}$, the backscattered wave is a vector $\mathbf{v}_2 = \{k_2, \omega_2\}$ and the Langmuir wave is a vector $\mathbf{v}_1 = \{k_1, \omega_1\}$. Show on the sketch how the vectors can add up in a manner consistent with the selection rules $\mathbf{v}_3 = \mathbf{v}_1 + \mathbf{v}_2$.
3. Parametric decay instability: The minimum pump amplitude for the parametric decay instability (electromagnetic wave decays into a Langmuir wave and an ion acoustic wave) is given by Eq.(15.119) to be

$$E_3 = 4 \frac{\sqrt{\omega_1 \omega_2 \Gamma_1 \Gamma_2}}{\lambda}$$

where the coupling parameter was defined in Eq.(15.81) to be

$$\lambda = \frac{\omega_{pe} q k_1}{\sqrt{m_i m_e \omega_2 \omega_3}}.$$

- (a) How do the Langmuir wave frequency ω_2 and the ion acoustic wave frequency ω_1 compare to ω_{pe} (nearly same, much larger, or much smaller)?
- (b) Taking into account the selection rules, how does the pump frequency ω_3 compare to ω_{pe} ? What does this imply for k_3 and hence k_1 and k_2 ?

- (c) Using the results from (a) express the instability threshold in a form where $\varepsilon_0 E^2 / n \kappa T_e$ is a function of Γ_1 / ω_1 and Γ_2 / ω_2 .
- (d) Suppose a pump wave with frequency ω_3 propagates into a plasma with a monotonically increasing density. Show the relative locations of stimulated Brillouin and stimulated Raman backscattering in terms of a criterion for the local density. Assume that the wavelengths of the waves are much shorter than the density gradient scale length.
- (e) The National Ignition Facility at the Lawrence Livermore National Lab in the USA, nearing completion in 2004, has an array of 351 nm wavelength lasers which are designed to apply 5×10^{14} watts over the surface of a target with initial radius of 1 mm. If these lasers are considered the pump electromagnetic wave with frequency ω_3 , at what density does $\omega_3 = \omega_{pe}$ occur. Assuming $T_e = 300$ eV, what is the value of $\varepsilon_0 E^2 / n \kappa T_e$ at the location where $\omega_3 = \omega_{pe}$? If $\Gamma_1 / \omega_1 = \Gamma_2 / \omega_2 = 0.1$ will this plasma be susceptible to the parametric decay instability?

Non-neutral plasmas

16.1 Introduction

Conventional plasmas, the main topic of this book, consist of a quasi-neutral collection of mutually interacting ions and electrons. This description applies to the vast majority of entities called plasma (e.g., fusion, industrial, propulsion, ionospheric, magnetospheric, interplanetary, solar, and astrophysical plasmas). Non-neutral plasmas are an exception to this taxonomy and not surprisingly, have certain behaviors which differ from conventional plasmas (Malmberg 1992, Davidson 2001). Applications of non-neutral plasmas include microwave oscillators and amplifiers, simulating the vortex dynamics of ideal two-dimensional hydrodynamics, testing basic non-linear concepts, and confining anti-particles.

16.2 Brillouin flow

Using a cylindrical coordinate system $\{r, \theta, z\}$ we first consider the forces acting on an infinitely long, azimuthally symmetric cylindrical cloud of cold charged particles all having the *same* polarity. Because of the mutual electrostatic repulsion of the same-sign charged particles, the cloud of particles will expand continuously in the r direction and so will not be in radial equilibrium. The cloud would be even further from equilibrium if, in addition, it were to rotate with azimuthal velocity $\mathbf{u} = u_\theta \hat{\theta}$, because rotation would provide a centrifugal force mu_θ^2/r which would add to the radially outwards electrostatic force and so increase the rate of radially outward expansion.

However, if this rotating cloud of same-sign charged particles were immersed in a uniform axial magnetic field $\mathbf{B} = B\hat{z}$, then the magnetic force $\sim q\mathbf{u} \times \mathbf{B}$ would push the charged particles radially inwards, counteracting both the electrostatic repulsion and the centrifugal force. This situation is shown in Fig. 16.1 for the situation where the cloud consists of electrons (Malmberg and de Grassie 1975). Negatively biased electrodes are used at the ends to prevent cloud expansion in the z direction; if the cloud were made of ions, then the end electrodes would be biased positively.

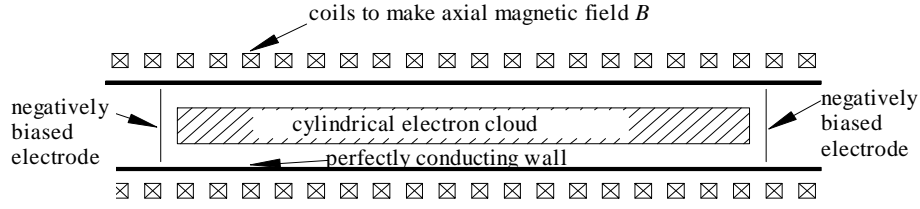


Figure 16.1: Pure electron plasma configuration. Magnetic field $\mathbf{B} = B\hat{z}$ produced by coils, electrodes on ends prevent axial expansion.

Because there is only one charge species, there is no frictional drag due to collisions with a species of opposite polarity, and because the plasma is cold, the pressure is zero. The radial component of the fluid equation of motion Eq.(2.27) thus reduces to a simple competition between the electrostatic, magnetic, and centrifugal forces, namely

$$0 = q(E_r + u_\theta B_z) + \frac{m u_\theta^2}{r}. \quad (16.1)$$

Because of the assumed cylindrical and azimuthal symmetry, Poisson's equation reduces to

$$\frac{1}{r} \frac{\partial}{\partial r} (r E_r) = \frac{n(r)q}{\varepsilon_0} \quad (16.2)$$

which can be integrated to give

$$E_r = \frac{q}{\varepsilon_0} \frac{1}{r} \int_0^r n(r') r' dr'. \quad (16.3)$$

In the special case of uniform density up to the plasma radius r_p , which by assumption is less than the wall radius a , Eq.(16.3) may be evaluated to give

$$E_r = \begin{cases} \frac{nq}{2\varepsilon_0} r & \text{for } r \leq r_p \\ \frac{nq}{2\varepsilon_0} \frac{r_p^2}{r} & \text{for } r_p \leq r \leq a \end{cases} \quad (16.4)$$

so that inside the plasma Eq.(16.1) becomes

$$u_\theta^2 + u_\theta r \omega_c + \frac{\omega_p^2 r^2}{2} = 0. \quad (16.5)$$

This is a quadratic equation for u_θ and it is convenient to express the two roots in terms of angular velocities $\omega_0 = u_\theta/r$ so

$$\omega_0 = \frac{-\omega_c \pm \sqrt{\omega_c^2 - 2\omega_p^2}}{2}. \quad (16.6)$$

Since ω_0 is independent of r , the cloud rotates as a rigid body; this is a special case resulting from the assumption of a uniform density profile (in the more general case of a non-uniform density profile which will be discussed later, the rotation velocity is sheared so that ω_0 is a function of r). The two roots in Eq.(16.6) coalesce at $\omega_p^2 = \omega_c^2/2$; this point of coalescence

is called the and it is seen that real roots ω_0 exist only if the density is sufficiently low for ω_p^2 to be below this limit.

We will consider the situation, typical for non-neutral plasma experiments, where the density is well below the Brillouin limit so that the two roots are well-separated and given by

$$\omega_{0-} \simeq -\omega_c \left(1 + \omega_p^2/2\omega_c^2\right) \quad (16.7)$$

$$\omega_{0+} \simeq \omega_p^2/2\omega_c; \quad (16.8)$$

the plus and minus signs refer to the choice of signs in Eq.(16.6). The large root ω_{0-} is near the cyclotron frequency and the small root ω_{0+} is much smaller than the plasma frequency since $\omega_p \ll \omega_c$. The small root is called the diocotron frequency.

The rotation in the magnetic field provides an inward force balancing the outward radial electrostatic force of the non-neutral plasma. There also exist axial electrostatic forces due to the mutual electrostatic repulsion between the same-sign charges and these forces would cause the plasma to expand axially. Since these axial forces cannot be balanced magnetically, the axial forces are balanced by biased electrodes at the ends of the plasma. The electrodes have the same polarity as the plasma, thereby providing a potential well in the axial direction. Any particle which tries to escape axially is repelled by forces due to the repulsive bias of the end electrode and reflects before reaching the end electrode.

The fast motion of the charged particles in the axial direction smears out axial structure so that the non-neutral plasma can be considered axially uniform to first approximation. A pair of deceptively simple-looking coupled equations relating the electrostatic potential ϕ and the density n govern not only the equilibrium but also the surprisingly rich low-frequency dynamics of a non-neutral plasma. An important feature of these equations is that the $E \times B$ drift

$$\mathbf{u} = \frac{-\nabla\phi \times \mathbf{B}}{B^2} \quad (16.9)$$

describes an incompressible flow, so that when this drift is inserted into the continuity equation

$$\frac{\partial n}{\partial t} + \mathbf{u} \cdot \nabla n + n \nabla \cdot \mathbf{u} = 0, \quad (16.10)$$

the $\nabla \cdot \mathbf{u}$ term vanishes and the density time dependence results from convection only, so that

$$\frac{\partial n}{\partial t} = \frac{\nabla\phi \times \mathbf{B}}{B^2} \cdot \nabla n. \quad (16.11)$$

Equation (16.11) and Poisson's equation

$$\nabla^2 \phi = -\frac{nq}{\epsilon_0} \quad (16.12)$$

provide two coupled equations in n and ϕ and are the governing equations for the configuration. Although Eqs.(16.11) and (16.12) appear simple, they actually allow quite complex behavior which will be discussed in the remainder of this chapter. An interesting feature of these equations is that they have no mass dependence, a consequence of ignoring the centrifugal force term which affects only the high frequency branch, Eq.(16.7). Thus, the low frequency dynamics described by Eqs.(16.11) and (16.12) can be thought of as the dynamics of a massless, incompressible fluid governed by a combination of $E \times B$ drifts and Poisson's equation.

16.3 Isomorphism to incompressible 2D hydrodynamics

Consider now the equations governing an incompressible two-dimensional fluid with velocity $\mathbf{u} = u_r(r, \theta)\hat{r} + u_\theta(r, \theta)\hat{\theta}$. Incompressibility means that the mass density ρ is constant and uniform so that the continuity equation reduces to

$$\nabla \cdot \mathbf{u} = 0. \quad (16.13)$$

Using the vector identity $\mathbf{u} \cdot \nabla \mathbf{u} = \nabla u^2/2 - \mathbf{u} \times \nabla \times \mathbf{u}$ the fluid equation of motion can be written as

$$\rho \left(\frac{\partial \mathbf{u}}{\partial t} + \frac{1}{2} \nabla u^2 - \mathbf{u} \times \nabla \times \mathbf{u} \right) = -\nabla P. \quad (16.14)$$

Taking the curl of this equation and defining the vorticity vector $\boldsymbol{\Omega} = \nabla \times \mathbf{u}$ gives

$$\frac{\partial \boldsymbol{\Omega}}{\partial t} = \nabla \times (\mathbf{u} \times \boldsymbol{\Omega}) \quad (16.15)$$

which has the same form as the ideal MHD induction equation, Eq.(2.81), and so can be interpreted as indicating that the vorticity being frozen into the convecting fluid (Kelvin vorticity theorem). Because

$$\nabla \times \mathbf{u} = \hat{z} \left(\frac{1}{r} \frac{\partial}{\partial r} (r u_\theta) - \frac{1}{r} \frac{\partial u_r}{\partial \theta} \right) \quad (16.16)$$

the vorticity vector lies in the z direction and may be written as

$$\boldsymbol{\Omega} = \Omega \hat{z}. \quad (16.17)$$

The z component of Eq.(16.15) is

$$\begin{aligned} \frac{\partial \Omega}{\partial t} &= \hat{z} \cdot \nabla \times (\mathbf{u} \times \Omega \hat{z}) \\ &= \nabla \cdot ((\mathbf{u} \times \Omega \hat{z}) \times \hat{z}) \\ &= -\nabla \cdot (\mathbf{u} \Omega) \\ &= -\mathbf{u} \cdot \nabla \Omega. \end{aligned} \quad (16.18)$$

The incompressibility condition Eq.(16.13) means that the velocity can be written in terms of a stream-function ψ ,

$$\mathbf{u} = -\nabla \psi \times \hat{z} \quad (16.19)$$

so Eq.(16.18) can be written as

$$\frac{\partial \Omega}{\partial t} = \nabla \psi \times \hat{z} \cdot \nabla \Omega. \quad (16.20)$$

Furthermore, the z component of the curl of Eq.(16.19) can also be expressed in terms of ψ since

$$\begin{aligned} \Omega &= \hat{z} \cdot \nabla \times \mathbf{u} \\ &= -\hat{z} \cdot \nabla \times (\nabla \psi \times \hat{z}) \\ &= -\nabla \cdot ((\nabla \psi \times \hat{z}) \times \hat{z}) \\ &= \nabla^2 \psi. \end{aligned} \quad (16.21)$$

There is thus an exact isomorphism between the non-neutral plasma equations and the equations describing a 2D incompressible fluid; this isomorphism is tabulated below:

<i>Non-neutral plasma</i>	<i>Incompressible 2D fluid</i>
$\frac{\partial n}{\partial t} = \frac{\nabla\phi \times \hat{z}}{B} \cdot \nabla n$	$\frac{\partial \Omega}{\partial t} = \nabla\psi \times \hat{z} \cdot \nabla \Omega$
$\nabla^2 \phi = -\frac{nq}{\epsilon_0}$	$\nabla^2 \psi = \Omega$

These sets of equations can be made identical by setting

$$\psi = \frac{\phi}{B}, \quad \Omega = -\frac{nq}{\epsilon_0 B}. \quad (16.22)$$

Thus density corresponds to vorticity and electrostatic potential corresponds to stream-function.

A non-neutral plasma can therefore be used as an analog computer for investigating the behavior of an inviscid incompressible 2D fluid. This is quite useful because it is difficult to make a real fluid act in a truly two dimensional inviscid fashion whereas it is relatively easy to make a non-neutral plasma. While real fluids are three dimensional, it is nevertheless important to understand 2D dynamics since this understanding can be of considerable help for understanding three dimensional dynamics. The plasma analog contains all the nonlinearities of vortex interactions that characterize the 2D fluid problem. Besides serving as an analog computer for investigations of 2D fluid dynamics, non-neutral plasmas have also been successfully used as a method for trapping antimatter (Surko, Leventhal and Passner 1989).

16.4 Near perfect confinement

An curious feature of non-neutral plasmas is that collisions do not degrade confinement so long as axisymmetry is maintained (O'Neil 1995). Thus, in a pure electron plasma, electron-electron collisions do not cause leakage of the plasma out of the trap (loss of confinement comes only from collisions with neutrals and this can be minimized by using good vacuum techniques). To see this, consider the canonical angular momentum of the i^{th} particle

$$P_{\theta i} = mr_i v_{\theta i} + qr_i A_{\theta i}. \quad (16.23)$$

A collision between two identical charged particles will conserve the total angular momentum of the two particles and so the total angular momentum of all the particles is

$$\sum_{i=1}^N P_{\theta i} = \sum_{i=1}^N (mr_i v_{\theta i} + qr_i A_{\theta i}) = \text{const.} \quad (16.24)$$

even when there are electron-electron collisions. The vector potential for the magnetic field $\mathbf{B} = B\hat{z}$ is $\mathbf{A} = \hat{\theta}Br/2$, and if the magnetic field is sufficiently strong, the inertial term in Eq.(16.24) can be dropped, so that conservation of total canonical angular momentum

reduces to the simple relationship

$$P_\theta = \sum_{i=1}^N P_{\theta i} \simeq \frac{q_e B}{2} \sum_{i=1}^N r_i^2 = \text{const.} \quad (16.25)$$

Equation (16.25) constrains the plasma from moving radially outwards in an axisymmetric fashion. Thus, interparticle collisions cannot make the plasma diffuse to the wall and so a collisional plasma is perfectly confined so long as axisymmetry is maintained.

An alternative interpretation can be developed by considering how collisions cause axisymmetric outward diffusion in a conventional (i.e., electron-ion) plasma. The effect of collisions in this situation can be seen by considering the steady-state azimuthal component of the resistive MHD Ohm's law. This azimuthal component is

$$-U_r B = \eta J_\theta = \left(\frac{m_e \nu_{ei}}{n e^2} \right) n e (u_{i\theta} - u_\theta) = \frac{m_e \nu_{ei}}{e} (u_{i\theta} - u_\theta) \quad (16.26)$$

and shows that axisymmetric radial flow to the wall results from collisions between unlike particles since

$$U_r = -\frac{m_e \nu_{ei}}{e B} (u_{i\theta} - u_\theta). \quad (16.27)$$

Thus, radial transport requires momentum exchange between unlike species and this exchange occurs at a rate dictated by the collision frequency ν_{ei} and by the difference between electron and ion azimuthal velocities. If only one species exists, it is clearly impossible for momentum to be exchanged between unlike species and so there cannot be a net radial motion. A practical consequence of this result is that electron confinement in pure electron plasmas is orders of magnitude larger than confinement in quasi-neutral plasmas (hours/weeks compared to microseconds/seconds).

16.5 Diocotron modes

Non-neutral plasmas support linear waves that differ from those of a quasi-neutral plasma (Gould 1995). The theory of low frequency linear waves in cylindrical non-neutral plasmas can be developed by linearizing the continuity equation Eq.(16.11) to obtain

$$\frac{\partial n_1}{\partial t} + \mathbf{u}_0 \cdot \nabla n_1 + \mathbf{u}_1 \cdot \nabla n_0 = 0. \quad (16.28)$$

Using Eq.(16.9) to give \mathbf{u}_0 , \mathbf{u}_1 and Poisson's equation Eq.(16.12) to give n_0 , n_1 results in the wave equation

$$\frac{\partial \nabla^2 \phi_1}{\partial t} - \frac{\nabla \phi_0 \times \mathbf{B}}{B^2} \cdot \nabla \nabla^2 \phi_1 - \frac{\nabla \phi_1 \times \mathbf{B}}{B^2} \cdot \nabla \nabla^2 \phi_0 = 0. \quad (16.29)$$

Because of the cylindrical geometry, it is convenient to decompose the perturbed potential into azimuthal Fourier modes

$$\phi_1(r, \theta, t) = \sum_{l=-\infty}^{\infty} \tilde{\phi}_l(r, t) e^{il\theta} \quad (16.30)$$

where

$$\tilde{\phi}_l(r, t) = \frac{1}{2\pi} \int_0^{2\pi} d\theta \phi_1(r, \theta, t) e^{-il\theta}. \quad (16.31)$$

The l^{th} azimuthal mode is assumed to have a time dependence $\exp(-i\omega_l t)$ so that

$$\phi_1(r, \theta, t) = \sum_l \tilde{\phi}_l(r) e^{il\theta - i\omega_l t} \quad (16.32)$$

and the Fourier coefficient is given by

$$\tilde{\phi}_l(r) = \frac{1}{2\pi} \int_0^{2\pi} d\theta \phi_1(r, \theta, t) e^{-il\theta + i\omega_l t} . \quad (16.33)$$

Using the equilibrium azimuthal velocity

$$u_{\theta 0}(r) = \frac{-\nabla\phi_0 \times \mathbf{B}}{B^2} \cdot \hat{\theta} \quad (16.34)$$

the temporal-azimuthal Fourier transform of Eq.(16.29) can be written as

$$\left(\omega_l - \frac{lu_{\theta 0}(r)}{r} \right) \nabla^2 \tilde{\phi}_l + \frac{l\tilde{\phi}_l}{rB} \frac{d}{dr} \nabla^2 \phi_0 = 0. \quad (16.35)$$

Using the relations

$$\nabla^2 \tilde{\phi}_l = \frac{1}{r} \frac{d}{dr} \left(r \frac{d\tilde{\phi}_l}{dr} \right) - \frac{l^2}{r^2} \tilde{\phi}_l \quad (16.36)$$

$$\nabla^2 \phi_0 = \frac{1}{r} \frac{d}{dr} \left(r \frac{d\phi_0}{dr} \right) \quad (16.37)$$

this temporal-azimuthal Fourier transform of Eq.(16.29) can be expanded as

$$\left(\omega_l - \frac{lu_{\theta 0}(r)}{r} \right) \left(\frac{1}{r} \frac{d}{dr} \left(r \frac{d\tilde{\phi}_l}{dr} \right) - \frac{l^2}{r^2} \tilde{\phi}_l \right) + \frac{l\tilde{\phi}_l}{rB} \frac{d}{dr} \left(\frac{1}{r} \frac{d}{dr} \left(r \frac{d\phi_0}{dr} \right) \right) = 0 \quad (16.38)$$

The equilibrium angular velocity is

$$\omega_0(r) = \frac{u_{\theta 0}(r)}{r} = \frac{1}{rB} \frac{d\phi_0}{dr} \quad (16.39)$$

and so Eq.(16.38) can be expressed as

$$(\omega - l\omega_0(r)) \left(\frac{1}{r} \frac{d}{dr} \left(r \frac{d\tilde{\phi}_l}{dr} \right) - \frac{l^2}{r^2} \tilde{\phi}_l \right) + \frac{l\tilde{\phi}_l}{r} \frac{d}{dr} \left(\frac{1}{r} \frac{d}{dr} (r^2 \omega_0(r)) \right) = 0 \quad (16.40)$$

where the l subscript has been dropped from ω .

Since Eq.(16.37) gives

$$\frac{d\phi_0}{dr} = -\frac{q}{\varepsilon_0 r} \int_0^r n_0(r') r' dr', \quad (16.41)$$

the equilibrium angular velocity can be evaluated in terms of the equilibrium density to obtain

$$\omega_0(r) = -\frac{q}{\varepsilon_0 B r^2} \int_0^r n_0(r') r' dr'. \quad (16.42)$$

Equation (16.42) reduces to the special case of rigid body rotation when the density is uniform, but in the more general case there is a shear in the angular velocity. It is seen from Eq.(16.39) that

$$\frac{1}{r} \frac{d}{dr} (r^2 \omega_0(r)) = \frac{1}{Br} \frac{d}{dr} \left(r \frac{d\phi_0}{dr} \right) = -\frac{nq}{\varepsilon_0 B} = -\frac{\omega_p^2(r)}{\omega_c}. \quad (16.43)$$

Furthermore, since

$$\frac{d}{dr} \left(\frac{1}{r} \frac{dr^2}{dr} \right) = 0 \quad (16.44)$$

an arbitrary constant can be added to $\omega_0(r)$ in the last term in Eq.(16.40), which consequently can be written as

$$[\omega - l\omega_0(r)] \left(\frac{d}{dr} \left(r \frac{d\tilde{\phi}_l}{dr} \right) - l^2 \tilde{\phi}_l \right) - \tilde{\phi}_l \frac{d}{dr} \left(\frac{1}{r} \frac{d}{dr} [r^2 (\omega - l\omega_0)] \right) = 0; \quad (16.45)$$

this is called the diocotron wave equation.

The diocotron wave equation can be written in a more symmetric form by defining

$$\begin{aligned} \Phi &= r\tilde{\phi}_l \\ G &= r^2 (\omega - l\omega_0(r)) \end{aligned} \quad (16.46)$$

and using

$$\frac{d}{dr} \left(r \frac{d\tilde{\phi}_l}{dr} \right) = r \frac{d}{dr} \left(\frac{1}{r} \frac{d\Phi}{dr} \right) + \frac{\Phi}{r^2} \quad (16.47)$$

to obtain

$$r \frac{d}{dr} \left(\frac{1}{r} \frac{d\Phi}{dr} \right) + (1 - l^2) \Phi - \Phi \frac{r}{G} \frac{d}{dr} \left(\frac{1}{r} \frac{dG}{dr} \right) = 0. \quad (16.48)$$

16.5.1 Wall boundary condition

While the wall boundary condition does not affect the equilibrium of a non-neutral plasma, it plays a critical role for the diocotron modes since these modes are non-axisymmetric. Because the wall is perfectly conducting, the azimuthal electric field must vanish at the wall, i.e., $E_\theta(a) = 0$. This is trivially satisfied for the equilibrium because the equilibrium is axisymmetric and $E_\theta = -r^{-1} \partial\phi/\partial\theta$ vanishes everywhere for an axisymmetric field. However, for a non-axisymmetric perturbation, the azimuthal electric field is $\tilde{E}_{\theta,l} = -il\tilde{\phi}_l/r$ which is, in general, finite. Thus, in order to have the azimuthal electric field vanish at the wall, each finite l mode must satisfy the wall boundary condition $\tilde{\phi}_l(a) = 0$.

16.5.2 The $l = 1$ diocotron mode: a special case

The $l = 1$ mode is a special case and has the exact solution

$$\Phi = \lambda G \quad (16.49)$$

where λ is an arbitrary constant. In terms of the original variables, this solution is (White, Malmberg and Driscoll 1982)

$$\tilde{\phi}_{l=1}(r) = \frac{\omega - \omega_0(r)}{2\omega} S r \quad (16.50)$$

where S is a constant. Since Eq.(16.48) is a second-order ordinary differential equation, it must have two independent solutions and Eq.(16.50) must be one of these solutions. The other solution has a singularity at $r = 0$ and is discarded as being non-physical (this other solution can be found by assuming it is of the form $\Phi = FG$ and substituting this into Eq.(16.48) to find F). It is now evident that rigid body rotation corresponds to having $G = 0$ for all r since $\omega_0(r)$ is a constant and $\omega = \omega_0(a)$ for a rigid body; if $G = 0$ then Eq.(16.48) shows that the form of Φ is unrestricted and so rigid body rotation can have any perturbation profile. On the other hand, if the rotation has even the slightest amount of shear, then G must be non-zero and the solution is restricted to be of the form specified by Eq.(16.50).

The perfectly conducting wall boundary condition $E_\theta = 0$ implies that $\tilde{\phi}_{l=1}(a) = 0$ and so Eq.(16.50) gives the $l = 1$ mode frequency to be

$$\begin{aligned}\omega &= \omega_0(a) \\ &= -\frac{q}{\varepsilon_0 B a^2} \int_0^{r_p} n_0(r') r' dr' \\ &= -\frac{E_r(a)}{B a}\end{aligned}\quad (16.51)$$

which has the interesting feature of depending only on $E_r(a)$, the equilibrium radial field at the wall. Since $E_r(a)$ depends only on the total charge per length, the $l = 1$ mode frequency depends only on the total charge per length and not on the radial profile of the charge density. The coefficient S has been chosen so that the *perturbed* radial electric field at the wall is

$$\tilde{E}_r(a) = -\frac{S a}{2\omega} \left(\frac{d\omega_0(r)}{dr} \right)_{r=a}. \quad (16.52)$$

Since $n_0(a) = 0$ by assumption, Eq.(16.42) shows that

$$\begin{aligned}\left(\frac{d\omega_0(r)}{dr} \right)_{r=a} &= \left(-\frac{2}{r} \omega_0(r) \right)_{r=a} \\ &= -\frac{2\omega}{a}\end{aligned}\quad (16.53)$$

and so

$$S = \tilde{E}_r(a). \quad (16.54)$$

16.5.3 Energy analysis of diocotron modes

The linearized current density of a diocotron mode is

$$\begin{aligned}\mathbf{J}_1 &= n_1 q \mathbf{u}_0 + n_0 q \mathbf{u}_1 \\ &= n_1 q r \omega_0(r) \hat{\theta} + n_0 q \frac{\mathbf{E}_1 \times \mathbf{B}}{B^2}\end{aligned}\quad (16.55)$$

and the $n_1 q r \omega_0(r) \hat{\theta}$ equilibrium flow term enables the wave energy to become negative. The wave is electrostatic so Eq.(7.56) gives the wave energy density to be (Briggs, Daugh-

erty and Levy 1970)

$$\begin{aligned}\bar{w} &= \int_{-\infty}^t dt \left\langle \mathbf{E}_1 \cdot \left(\mathbf{J}_1 + \varepsilon_0 \frac{\partial \mathbf{E}_1}{\partial t} \right) \right\rangle \\ &= \frac{\varepsilon_0}{2} E_1^2 + \int_{-\infty}^t dt \langle \mathbf{E}_1 \cdot \mathbf{J}_1 \rangle .\end{aligned}\quad (16.56)$$

Unlike the uniform plasma analysis in Section 7.4, here both plasma non-uniformity and wall boundary conditions must be taken into account. The change in system energy \bar{W} due to establishment of the diocotron wave is found by integrating \bar{w} over volume and is

$$\begin{aligned}\bar{W} &= \int d^3r \left(\frac{\varepsilon_0}{2} (\nabla \cdot \phi_1 \nabla \phi_1 - \phi_1 \nabla^2 \phi_1) + \int_{-\infty}^t dt n_1 q r \omega_0(r) E_{1\theta} \right) \\ &= q \int d^3r \left(\frac{1}{2} n_1 \phi_1 + r \omega_0(r) \int_{-\infty}^t dt n_1 E_{1\theta} \right)\end{aligned}\quad (16.57)$$

where Eq.(16.55) and the perfectly conducting wall boundary condition $\phi_1(a) = 0$ have been used. Using Eq.(7.62) and (16.32), the energy for a given l mode can be written as

$$W_l = \frac{q}{2} \text{Re} \int d^3r \left(\frac{1}{2} \tilde{n}_l \tilde{\phi}_l^* e^{2\omega_i t} + r \omega_0(r) \int_{-\infty}^t dt \tilde{n}_l \tilde{E}_{1\theta}^* e^{2\omega_i t} \right)\quad (16.58)$$

In order to evaluate this expression, it is necessary to express all fluctuating quantities in terms of the oscillating potential $\tilde{\phi}_l$. Using Poisson's equation in Eq.(16.35) it is seen that

$$\tilde{n}_l = -\frac{l \tilde{\phi}_l}{r B (\omega - l \omega_0(r))} \frac{dn_0}{dr}\quad (16.59)$$

and the complex conjugate of the linearized azimuthal electric field is

$$\tilde{E}_{1\theta}^* = \left(-i \frac{l \tilde{\phi}_l}{r} \right)^* = i \frac{l \tilde{\phi}_l^*}{r} .\quad (16.60)$$

The wave energy is thus

$$\begin{aligned}\delta W_l &= -\frac{q l}{2 B} \text{Re} \int d^3r \left\{ \begin{array}{l} \frac{|\tilde{\phi}_l|^2}{2 r (\omega - l \omega_0(r))} \frac{dn_0}{dr} e^{2\omega_i t} \\ + r \omega_0(r) \int_{-\infty}^t dt \frac{i l |\tilde{\phi}_l|^2 e^{2\omega_i t}}{r^2 (\omega - l \omega_0(r))} \frac{dn_0}{dr} \end{array} \right\} \\ &= -\frac{q L}{4 B} \text{Re} \int_0^{2\pi} d\theta \int_0^a dr \left\{ \left(\begin{array}{l} \frac{e^{2\omega_i t}}{(\omega - l \omega_0(r))} \\ + \omega_0(r) \int_{-\infty}^t \frac{2 i l e^{2\omega_i t} dt}{(\omega - l \omega_0(r))} \end{array} \right) \frac{dn_0}{dr} l |\tilde{\phi}_l|^2 \right\}\end{aligned}\quad (16.61)$$

where L is the axial length of the plasma. The second term above can be directly evaluated as

$$\begin{aligned}
\operatorname{Re} \int_{-\infty}^t dt \frac{2il |\tilde{\phi}_l|^2 e^{2\omega_i t}}{(\omega - l\omega_0(r))} &= \operatorname{Re} \int_{-\infty}^t dt \frac{2il(\omega_r - l\omega_0(r) - i\omega_i)}{(\omega_r - l\omega_0(r))^2 + \omega_i^2} |\tilde{\phi}_l|^2 e^{2\omega_i t} \\
&= \int_{-\infty}^t dt \frac{l2\omega_i}{(\omega_r - l\omega_0(r))^2 + \omega_i^2} |\tilde{\phi}_l(t=0)|^2 e^{2\omega_i t} \\
&= \frac{l}{(\omega_r - l\omega_0(r))^2 + \omega_i^2} |\tilde{\phi}_l|^2 e^{2\omega_i t} \\
&\rightarrow \frac{l}{(\omega_r - l\omega_0(r))^2} |\tilde{\phi}_l|^2 \text{ as } \omega_i \rightarrow 0
\end{aligned} \tag{16.62}$$

Thus, in the limit $\omega_i \rightarrow 0$,

$$\begin{aligned}
\delta W_l &= -\frac{qL}{4B} \int_0^{2\pi} d\theta \int_0^a dr \left[\left(\frac{1}{(\omega - l\omega_0(r))} + \frac{l\omega_0(r)}{(\omega - l\omega_0(r))^2} \right) \frac{dn_0}{dr} l |\tilde{\phi}_l|^2 \right] \\
&= -\frac{\pi qL}{2B} \int_0^a dr \frac{\omega}{(\omega - l\omega_0(r))^2} \frac{dn_0}{dr} l |\tilde{\phi}_l|^2.
\end{aligned} \tag{16.63}$$

For the $l = 1$ mode this can be evaluated using Eq. (16.50) to give

$$\begin{aligned}
\omega &= -\frac{q}{\varepsilon_0 B a^2} \int_0^{r_p} n_0(r') r' dr' \\
\delta W_{l=1} &= -\frac{\pi qL}{2B} \int_0^a dr \frac{\omega}{(\omega - \omega_0(r))^2} \frac{dn_0}{dr} \left[S r \left(\frac{\omega - \omega_0(r)}{2\omega} \right) \right]^2 \\
&= -\frac{\pi qL S^2}{8\omega B} \int_0^a dr \frac{dn_0}{dr} r^2 \\
&= -\frac{\pi qL S^2}{8\omega B} \int_0^a dr \left(-2r n_0(r) + \frac{d}{dr} [r^2 n_0(r)] \right) \\
&= \frac{\pi qL S^2}{4\omega B} \int_0^{r_p} r n_0(r) dr
\end{aligned} \tag{16.64}$$

where $n_0(r) = 0$ for $r_p < r \leq a$ has been used. Finally, using the middle line of Eq.(16.51) this becomes

$$\delta W_{l=1} = -\frac{\varepsilon_0 \pi L a^2 S^2}{4} \tag{16.65}$$

and so the $l = 1$ diocotron mode is seen to be a negative energy mode. This result can also be derived by considering the change in system energy which results when the non-neutral plasma is attracted to a fictitious image charge chosen to maintain the wall as an equipotential when the plasma moves off axis (see assignments).

For $l \geq 2$, the negative energy nature of the diocotron mode can be understood by considering the change in the electrostatic energy stored in an isolated parallel plate capacitor when the distance between the parallel plates is varied. The stored energy is $W = CV^2/2 = Q^2/2C$ and Q is constant because the capacitor is isolated. Increasing the

capacitance at constant Q reduces W , so bringing the plates together makes available free energy which could be used to move the plates even closer together. The system is therefore unstable with respect to perturbations that tend to increase the capacitance. This is the electrostatic analog of the ideal magnetohydrodynamic flux-conserving situation where the energy is $W = \Phi^2/2L$ and Φ is the magnetic flux linked by an isolated inductor L ; any flux-conserving perturbation which increases inductance makes available free energy for driving an instability.

If all the charge of a non-neutral plasma is assumed to be located at the radius r_p , then the combination of the non-neutral plasma and the wall at radius a is effectively a coaxial capacitor. Gauss' law shows that the radial electric field is $2\pi r\epsilon_0 E_r = \lambda$ where λ is the charge per length. The voltage difference between the plasma and the wall is therefore $V = -\int_{r_p}^a E_r dr = \lambda(2\pi\epsilon_0)^{-1} \ln(a/r_p)$ and the capacitance per length is $C' = 2\pi\epsilon_0 [\ln(a/r_p)]^{-1}$. Thus, increasing r_p increases the capacitance and decreases the electrostatic energy associated with the fixed amount of charge. However, such an azimuthally symmetric increase of r_p is forbidden because it would rarefy the plasma, an impossibility since the only allowed motion is an $\mathbf{E} \times \mathbf{B}$ drift which is incompressible for an electrostatic electric field.

The plasma can circumvent this constraint by undergoing an azimuthally periodic incompressible motion that, on average, increases the capacitance. This could be arranged by splitting the system into an even number of equally spaced azimuthally periodic segments and arranging for an incompressible motion where even-numbered segments move towards the wall and odd-numbered segments move away from the wall. The volume between the wall and the plasma would thus be conserved so the system would be incompressible, but because capacitance scales as the inverse of the distance between a segment and the wall, the increase in capacitance due to the segments moving towards the wall would exceed the decrease of the segments moving away from the wall. Thus, the electrostatic energy of the system would decrease and free energy would be available to drive an instability.

16.5.4 Resistive wall

Let us now assume that the conducting wall has an insulated segment of length L_s and angular extent Δ which is connected to ground via a small resistor R . The remainder of the wall is directly connected to ground; this is sketched in Fig.16.2. The wall is thus at or near ground potential and so there are no electric fields exterior to the wall, and in particular there is no radial electric field just outside the wall.

In order for the radial electric field to vanish outside the wall, the wall must have a surface charge density that creates a radial electric field equal and opposite to the radial electric field produced by the plasma so

$$-S = \frac{\tilde{\sigma}_l}{\epsilon_0}. \quad (16.66)$$

The surface charge flows back and forth between the wall segments and ground. The charge on the segment extending from $\theta = -\Delta/2$ to $\Delta/2$ is

$$\begin{aligned} Q_s &= L_s \int_{-\Delta/2}^{\Delta/2} a d\theta \tilde{\sigma}_l e^{il\theta} \\ &= L_s a \tilde{\sigma}_l \frac{e^{il\Delta/2} - e^{-il\Delta/2}}{il} \\ &= -\frac{2}{l} L_s a \varepsilon_0 S \sin \frac{\Delta}{2}. \end{aligned} \quad (16.67)$$

The electric current I flowing through the resistor is the rate of change of this surface charge, i.e., for the $l = 1$ mode this current is

$$I = 2i\omega L_s a \varepsilon_0 S \sin \frac{\Delta}{2}. \quad (16.68)$$

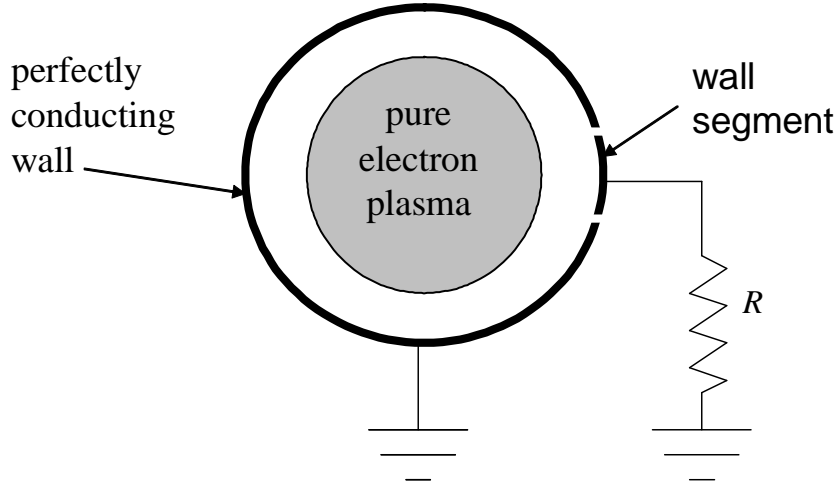


Figure 16.2: Arrangement for resistive wall instability of a non-neutral plasma. Resistor R is connected between ground and an isolated segment of azimuthal extent Δ and axial extent L_s . Remainder of wall is connected directly to ground.

The rate at which energy is dissipated in the resistor is

$$\langle I^2 R \rangle = \frac{1}{2} \left(2\omega L_s a \varepsilon_0 S \sin \frac{\Delta}{2} \right)^2 R. \quad (16.69)$$

If the mode frequency is allowed to have a small imaginary part then the rate of change of electrostatic energy will be

$$P = 2\omega_i \delta W. \quad (16.70)$$

Since the sum of the thermal energy in the resistor and the electrostatic energy in the plasma constitutes the total energy in the system, conservation of this sum gives

$$2\omega_i \delta W + \langle I^2 R \rangle = 0 \quad (16.71)$$

or

$$\omega_i = -\frac{\langle I^2 R \rangle}{2\delta W}. \quad (16.72)$$

Because the mode has negative energy, ω_i is positive corresponding to instability.

Substitution into the RHS gives

$$\omega_i = \frac{4\omega^2 R L_s^2 \varepsilon_0 \sin^2 \frac{\Delta}{2}}{\pi L} \quad (16.73)$$

where L is the axial length of the wall and $L_s \leq L$ is the axial length of the segment. This dependence of the growth rate on resistance has been observed in experiments (White et al. 1982). If the resistor R is replaced by a parallel resonant circuit, then the instability will occur at the resonant frequency of this circuit, because the effective resistance seen by the non-neutral plasma wall segment will be at a maximum at the resonant frequency. This is the basis of the magnetron tube used in radar transmitters and microwave ovens (see assignments).

16.5.5 Diocotron modes with $l \geq 2$

The analysis of $l \geq 2$ diocotron modes resembles the Landau analysis of electron plasma waves but is not exactly the same. In general $l \geq 2$ diocotron modes must be considered using numerical methods because their behavior depends on the equilibrium density profile via coefficients of both the first and last terms in Eq.(16.38). However, some indication of the general behavior can be obtained analytically. An important condition can be obtained (Davidson 2001) by assuming that $\omega = \omega_r + i\omega_i$ and writing Eq.(16.38) as

$$\frac{1}{r} \frac{d}{dr} \left(r \frac{d\tilde{\phi}_l}{dr} \right) - \frac{l^2}{r^2} \tilde{\phi}_l - \frac{(\omega_r - l\omega_0(r)) - i\omega_i}{(\omega_r - l\omega_0(r))^2 + \omega_i^2} \frac{l}{rB} \frac{n'_0 q}{\varepsilon_0} \tilde{\phi}_l = 0. \quad (16.74)$$

After multiplying through by $r\tilde{\phi}_l^*$, integrating from $r = 0$ to $r = a$, and using the perfectly conducting boundary condition $\tilde{\phi}_l(a) = 0$ when integrating the first term by parts, the following integral relation is found:

$$\int_0^a dr \left\{ r \left| \frac{d\tilde{\phi}_l}{dr} \right|^2 + \frac{l^2}{r} |\tilde{\phi}_l|^2 + \frac{(\omega_r - l\omega_0(r)) - i\omega_i}{(\omega_r - l\omega_0(r))^2 + \omega_i^2} |\tilde{\phi}_l|^2 \frac{l}{rB} \frac{n'_0 q}{\varepsilon_0} \right\} = 0. \quad (16.75)$$

The imaginary part of this expression is

$$-\omega_i \frac{lq}{\varepsilon_0 r B} \int_0^{r_p} dr \left\{ \frac{|\tilde{\phi}_l|^2}{(\omega_r - l\omega_0(r))^2 + \omega_i^2} \frac{dn_0}{dr} \right\} = 0; \quad (16.76)$$

the upper limit has been changed to r_p because $n_0(r)$ and dn_0/dr are by assumption zero in the region $r_p < r \leq a$. If dn_0/dr has the same sign throughout the radial interval $0 \leq r \leq r_p$, then the integral would have to be non-zero since the integrand always has the same sign, and so ω_i would have to be zero. Thus, a necessary condition for ω_i to be finite is for dn_0/dr to change signs in the interval $0 \leq r \leq r_p$. This necessary condition corresponds to $n_0(r)$ having a maximum in the interval $0 \leq r \leq r_p$. This sort of profile is commonly called hollow, because $n_0(r)$ starts at some finite value at $r = 0$, increases to a maximum at some finite $r < r_p$, and then decreases to zero at $r = r_p$.

Further progress can be made by expressing the diocotron equations as a pair of coupled equations for the density and potential perturbations, i.e.,

$$\tilde{n}_l = -\frac{l\tilde{\phi}_l}{rB(\omega - l\omega_0(r))} \frac{dn_0}{dr} \quad (16.77)$$

$$\frac{1}{r} \frac{d}{dr} \left(r \frac{d\tilde{\phi}_l}{dr} \right) - \frac{l^2}{r^2} \tilde{\phi}_l = -\frac{\tilde{n}_l q}{\varepsilon_0}. \quad (16.78)$$

Rather than substitute for \tilde{n}_l in order to obtain Eq.(16.38), instead Eq.(16.78) is solved for $\tilde{\phi}_l$ using a Green's function method (Schechter, Dubin, Cass, Driscoll, Lansky and O'Neil 2000). This approach has the virtue of imposing the perfectly conducting wall boundary condition on $\tilde{\phi}_l$ at an earlier stage of the analysis before the entire wave equation is developed. The set of solutions to Eq.(16.78) are then effectively restricted to those satisfying the wall boundary condition, and only this restricted set is used when later combining Eqs.(16.78) and (16.77) to form a wave equation.

The Green's function solution to Eq.(16.78) is obtained by first recasting Eq.(16.78) as

$$\frac{1}{r} \frac{d}{dr} \left(r \frac{d\tilde{\phi}_l}{dr} \right) - \frac{l^2}{r^2} \tilde{\phi}_l = -\frac{q}{\varepsilon_0} \int_0^a ds \delta(r-s) \tilde{n}_l(s). \quad (16.79)$$

Thus, if $\psi(s, r)$ is the solution of

$$\frac{1}{r} \frac{d}{dr} \left(r \frac{d\psi(r, s)}{dr} \right) - \frac{l^2}{r^2} \psi(r, s) = -\delta(r-s) \quad (16.80)$$

where $0 \leq s \leq a$ then

$$\tilde{\phi}_l(r) = \frac{q}{\varepsilon_0} \int_0^a ds \psi(r, s) \tilde{n}_l(s) \quad (16.81)$$

is the solution of Eq.(16.78). The spatial boundary conditions are accounted for when solving Eq.(16.80) for the Green's function $\psi(r, s)$ and so are independent of the form of \tilde{n}_l .

Equation (16.80) is solved by finding separate solutions to its homogeneous counterpart

$$\frac{1}{r} \frac{d}{dr} \left(r \frac{d\psi}{dr} \right) - \frac{l^2}{r^2} \psi = 0 \quad (16.82)$$

for the inner interval $0 \leq r < s$ and for the outer interval $s < r \leq a$ and then appropriately matching these two distinct homogeneous solutions at $r = s$ where they meet. The inner solution must satisfy the regularity condition $\psi(0) = 0$ and the outer solution must satisfy

the wall boundary condition $\psi(a) = 0$. Since the solutions of Eq.(16.82) are $\psi \sim r^{\pm l}$, the inner solution must be

$$\psi = \alpha \left(\frac{r}{a}\right)^l \quad \text{for } 0 \leq r < s \quad (16.83)$$

and the outer solution must be

$$\psi = \beta \left(\left(\frac{r}{a}\right)^l - \left(\frac{r}{a}\right)^{-l} \right) \quad \text{for } s < r \leq a \quad (16.84)$$

where the coefficients α and β are to be determined.

Integration of Eq.(16.80) across the delta function from $r = s_-$ to $r = s_+$ gives the jump condition

$$\left[\frac{d}{dr} \psi(r, s) \right]_{s_-}^{s_+} = -1 \quad (16.85)$$

and integrating a second time shows that ψ must be continuous at $r = s$. These jump and continuity conditions give two coupled equations in α and β ,

$$\frac{\beta l}{a} \left(\left(\frac{s}{a}\right)^{l-1} + \left(\frac{s}{a}\right)^{-l-1} \right) - \frac{\alpha l}{a} \left(\frac{s}{a}\right)^{l-1} = -1 \quad (16.86)$$

$$\beta \left(\left(\frac{s}{a}\right)^l - \left(\frac{s}{a}\right)^{-l} \right) - \alpha \left(\frac{s}{a}\right)^l = 0. \quad (16.87)$$

Solving for α and β gives the Green's function,

$$\psi(r, s) = \begin{cases} -\frac{a}{2l} \left(\frac{s}{a}\right)^{l+1} \left(\left(\frac{r}{a}\right)^l - \left(\frac{r}{a}\right)^{-l} \right) & \text{for } r > s \\ -\frac{a}{2l} \left(\frac{r}{a}\right)^l \left(\left(\frac{s}{a}\right)^{l+1} - \left(\frac{s}{a}\right)^{-l+1} \right) & \text{for } r < s; \end{cases} \quad (16.88)$$

this satisfies Eq.(16.80) and also the boundary conditions at $r = 0$ and $r = a$. Using the Green's function in Eq.(16.81) gives

$$\begin{aligned} \tilde{\phi}_l(r) &= \frac{q}{\varepsilon_0} \left[\int_0^r ds \psi(r, s) \tilde{n}_l(s) + \int_r^a ds \psi(r, s) \tilde{n}_l(s) \right] \\ &= -\frac{a}{2l} \frac{q}{\varepsilon_0} \left[\int_0^r ds \left(\left(\frac{s}{a}\right)^{l+1} \left(\left(\frac{r}{a}\right)^l - \left(\frac{r}{a}\right)^{-l} \right) \right) \tilde{n}_l(s) \right. \\ &\quad \left. + \int_r^a ds \left(\left(\frac{r}{a}\right)^l \left(\left(\frac{s}{a}\right)^{l+1} - \left(\frac{s}{a}\right)^{-l+1} \right) \right) \tilde{n}_l(s) \right] \quad (16.89) \end{aligned}$$

Finally, using Eq.(16.77) to substitute for $\tilde{n}_l(s)$ gives

$$\tilde{\phi}_l(r) = \frac{q}{2\varepsilon_0 B} \left(\int_0^r ds \frac{s^l}{a^l} \left(\frac{r^l}{a^l} - \frac{a^l}{r^l} \right) \frac{\tilde{\phi}_l(s)}{\omega - l\omega_0(s)} \frac{dn_0}{ds} + \int_r^a ds \frac{r^l}{a^l} \left(\frac{s^l}{a^l} - \frac{a^l}{s^l} \right) \frac{\tilde{\phi}_l(s)}{\omega - l\omega_0(s)} \frac{dn_0}{ds} \right). \quad (16.90)$$

This integral equation for $\tilde{\phi}_l(r)$ not only prescribes the mode dynamics, but also explicitly incorporates the spatial boundary conditions. The resonant denominators $\omega - l\omega_0(s)$ in

the s integrals are reminiscent of the resonant denominators occurring in the velocity space integrals of the Landau problem. Stability depends on the sign of dn_0/ds at the location where $\omega = l\omega_0(s)$ in analogy to the dependence of Landau stability on the sign of df_0/dv where $v = \omega/k$. Because these equations are isomorphic to the 2D incompressible hydrodynamic equations, it is seen that phenomena similar to Landau damping or instability should occur in 2D incompressible hydrodynamics.

16.5.6 Phase mixing and relation to Landau damping

The behavior of a localized infinitesimal bump or patch of increased density which is initially off-center provides insight into vortex dynamics. If the equilibrium angular velocity is sheared, then the patch will become sheared because the inner and outer portions of the patch will rotate at different angular velocities. Thus the angular position of different radial positions of the patch will have trajectories scaling as $\theta(r) = t\omega_0(r)$. The angular separation between two points in the patch starting at respective radii r and $r + \delta r$ will scale as $\delta\theta = t\delta r d\omega_0/dr$ and this separation will eventually exceed 2π at sufficiently large t . This gives a sort of spatial phase mixing (Gould 1995), because a localized density patch of increased density will eventually be stretched out to become a multi-turn thin spiral of increased density. The number of turns in the spiral increases linearly with time. The patch is thus smeared out over all angles and so is no longer azimuthally localized. Since the patch is stretched azimuthally and yet is incompressible, the thickness of each turn in the spiral must decrease as the number of turns in the spiral increases. Specifically, the length of the spiral increases with t and the radial thickness of each turn decreases as $1/t$ so that the area remains constant. A graphic demonstration of this stretching and thinning has been obtained by Bachman and Gould (1996) by direct numerical integration of the dynamical equations with an initial condition consisting of a prescribed density patch. Since the decay and eventual disappearance of the patch as it deforms into a nearly infinitely long and nearly infinitely thin spiral is a spatial analog to the velocity space phase mixing underlying Landau damping, it might be expected that the non-linear mixing of two such patches initiated at two successive times might give rise to a spatial echo effect (Gould 1995). This spatial echo effect involving the nonlinear beating of two spatial spirals has been seen experimentally (Yu and Driscoll 2002). In this experiment an $l = 2$ perturbation is applied and then decays as it is stretched into a nearly infinitely long, nearly infinitely thin spiral. Then an $l = 4$ perturbation is applied which similarly decays. Finally, after both of the perturbations have decayed a nonlinear $l = 2$ echo is observed because of nonlinear mixing of the two spirals associated with the respective initial perturbations.

If the patch has a finite amplitude, then its self-electric field will affect the dynamics. This is the non-linear regime and will cause a sigmoidal curling of the patch since azimuthal electric fields associated with the patch will give radial motions in addition to the azimuthal motions.

16.6 Assignments

1. *Relationship between non-neutral and conventional plasma equilibria:*

Compare the following two plasmas, both of which have cylindrical symmetry, axial

uniformity, the same radial electron density profile $n_e(r)$, and are in equilibrium:

- (a) a cylindrical pure electron plasma immersed in a strong magnetic field $\mathbf{B} = B\hat{z}$ where $\omega_{pe}^2 \ll \omega_{ce}^2$
- (b) an *unmagnetized* quasi-neutral electron-ion plasma which has infinitely massive ions.

What is the ion density in the quasi-neutral plasma and what electric field is produced by this ion density? How does the force associated with the electric field produced by the ions in the quasi-neutral plasma compare to the magnetic force associated with electron rotation (finite $u_{e\theta}$) in the pure electron plasma? What is the net equilibrium force on the electrons in the two cases? Assuming that the electrons have zero mass, which plasma has more free energy?

2. *Free energy associated with sheared velocity profile in slab approximation:* Suppose a non-neutral plasma does not rotate as a rigid body and instead has a sheared angular velocity. An observer rotating with the plasma at some radius r_{obs} would conclude that the plasma has positive angular velocity for $r > r_{obs}$ and a negative angular velocity for $r < r_{obs}$. Since the rotational velocity is due to an $\mathbf{E} \times \mathbf{B}$ drift, this means that the effective radial electric field measured in the observer frame must change sign at $r = r_{obs}$.

- (a) Show that this means that there is an effective charge sheet at $r = r_{obs}$.
- (b) Consider the limiting situation where the above situation is modeled using slab geometry so that $r \rightarrow x$ and $\theta \rightarrow y$, $\mathbf{B} = B\hat{z}$ and the non-neutral plasma initially centered about $x = 0$, has width w and a uniform density n for $|x| < w/2$. This equilibrium is sketched in Fig.16.3. There is vacuum in the region between the plasma and perfectly conducting walls at $x = \pm a$ where $a > w/2$. What are the electric field and the plasma flow velocity for $x > 0$ and for $x < 0$?
- (c) Now suppose that the location of the non-neutral plasma charge sheet is perturbed so that instead of being centered at $x = 0$, the location of the center becomes a function of y and is given by $x = \Delta(y) = \bar{\Delta} \cos ky$ where $kd \ll 1$ so that the wavelength in the y direction is very long. What is the boundary condition on E_y and hence on ϕ at the walls?

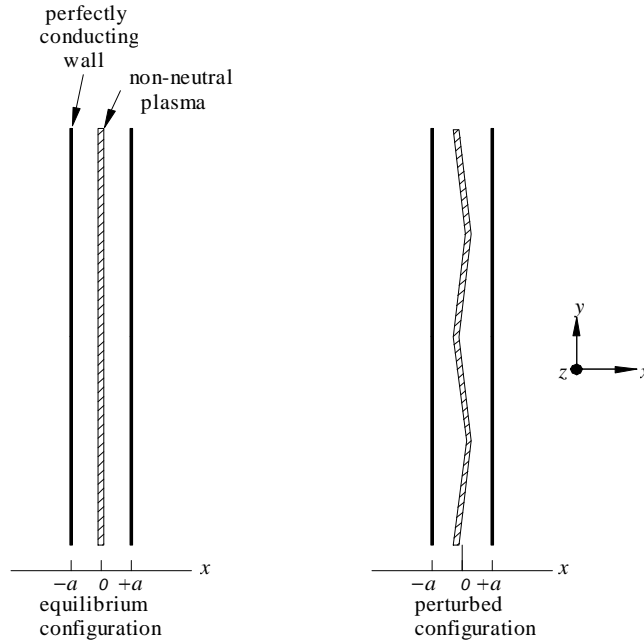


Figure 16.3: Left: equilibrium configuration for non-neutral plasma of width w , centered between pair of perfectly conducting walls at $x = \pm a$. Right: perturbed configuration where position of x -midpoint of plasma is located at $\Delta = \bar{\Delta} \cos ky$.

- (d) Since there is vacuum between the plasma and the wall and $kd \ll 1$, what is the limiting form of Poisson's equation in the regions between the plasma and the walls?
- (e) Assume that w is small, so that the non-neutral plasma can be approximated as being a thin sheet of charge. Being perfectly conducting, the walls must be equipotentials, and so without loss of generality, this potential can be defined to be zero. Show that the potential to the right of the charge sheet must be of the form

$$\phi_r = \alpha(a - x) \quad (16.91)$$

and the potential to the left of the charge sheet must be of the form

$$\phi_l = \beta(a + x) \quad (16.92)$$

where α and β are coefficients to be determined by considering the jump in electric field at the charge sheet.

- (f) Taking into account the jump in the potential at the charge sheet and the continuity in the potential at the charge sheet, solve for α and β . Assume that $w \ll a$ consistent with the assumption that the non-neutral plasma can be considered as a thin charge sheet. Which of E_y^2 , E_x^2 is larger?

- (g) Suppose that the length of the plasma in the y direction is L where L is an integral multiple of $2\pi/k$, the wavelength in the y direction. By calculating E_x to the right of the charge sheet and also to the left of the charge sheet, show that the energy stored in the electrostatic electric field is approximately

$$W = \frac{\epsilon_0}{2} h \int_{-L/2}^{L/2} dy \int_{-a}^a dx E_x^2$$

where h is the length in the z direction. How does W change when $\bar{\Delta}$ is increased? What does this suggest about the stability of sheared velocity profiles with respect to perturbations as prescribed in (c)?

3. *Image charge in cylindrical geometry:* Two line charges λ_1 and λ_2 are aligned along the z axis and located at $\mathbf{r}_1 = x_1 \hat{x}$ and $\mathbf{r}_2 = x_2 \hat{x}$ as shown in Fig. 16.4. What values of x_2 and λ_2 are required in order for the cylindrical surface $\sqrt{x^2 + y^2} = a$ to be an equipotential as would be required in order to have a perfectly conducting wall at $r = a$? The following hints should be useful:
- Define a cylindrical coordinate system r, θ, z so that the cylindrical surface is given by $\mathbf{r} = a\hat{r}$. Determine the potential on the cylindrical surface $r = a$.
 - Show that $|\hat{r} - \hat{x}x_1/a| = |\hat{r}a/x_2 - \hat{x}|$ if $a/x_2 = x_1/a$.
 - Show that $\lambda_2 = -\lambda_1$ is required in order for the cylindrical surface $r = a$ to be an equipotential.

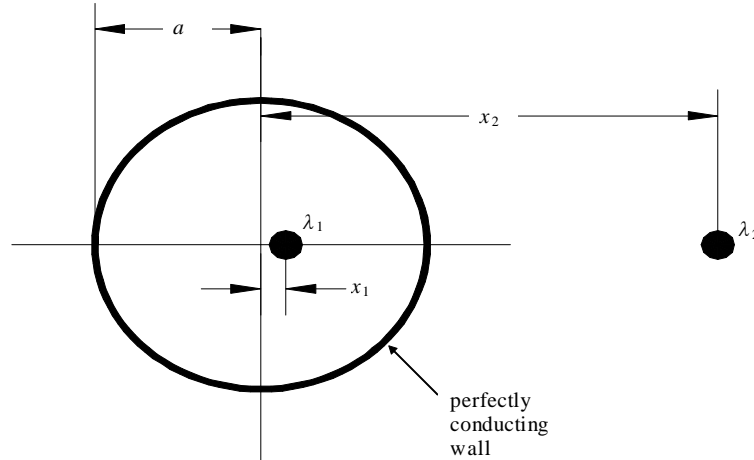


Figure 16.4: Line charge λ_1 is displaced a distance x_1 from axis of perfectly conducting cylindrical wall of radius a . An image charge λ_2 is located at x_2 .

4. *Diocotron mode energy using image charge method:* A cylindrical non-neutral plasma is translationally invariant in the z direction and is bounded by a perfectly conducting

wall at $r = a$. The plasma has an equilibrium density profile $n = n(r)$ for $0 \leq r < r_p$ and $n = 0$ for $r_p < r \leq a$ so there is a finite-size vacuum region between the edge of the plasma r_p and the wall radius a . Calculate the change in system energy if the plasma axis is shifted off the wall axis and compare this result to Eq.(16.65). Hints are given below:

- (a) Show that the electric field outside the plasma is the same as the electric field of a line charge located on the plasma axis.
- (b) Suppose that x denotes the distance the plasma is shifted off the wall axis. What is the location and strength of the image charge required for the wall to be an equipotential? Is the force between the plasma and the image charge attractive or repulsive. How does the image charge move as x increases from zero to some finite value?
- (c) Calculate the force on the image charge. What is the force on the plasma? What work is done by the plasma in order to be displaced by a finite amount x ? Express this work in terms of the radial electric field perturbation at the wall.

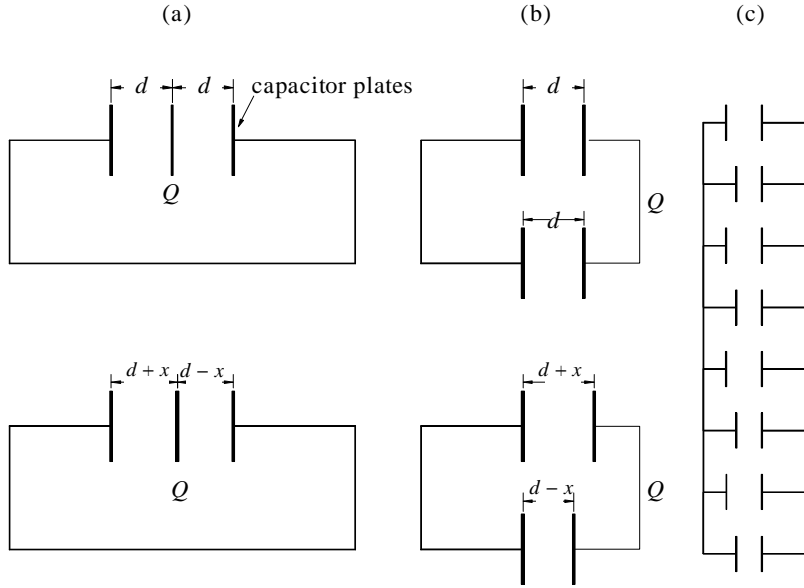


Figure 16.5:

5. *Negative energy in terms of two capacitors with fixed charge:* Consider two situations where a charge Q is stored on the two parallel plate capacitors C_1 and C_2 that deform in such a way as to conserve total system volume; these situations are shown in

Fig.16.5(a) and (b).

- (a) Here the center plate is displaced off center by an amount x so that the volume occupied by the two capacitors is conserved. What is the change in the system energy when the center plate is displaced? Assume that the value of each capacitor is $C_{1,2} = \epsilon_0 A / d_{1,2}$ where $d_{1,2}$ is the distance between the parallel plates and initially $d_1 = d_2$.
- (b) Show that the configuration in Fig.16.5(b) is electrically equivalent to the configuration in Fig.16.5(a). Discuss how the system shown in Fig.16.5(c) would relate to an $l = 4$ diocotron mode (recall that any perturbations to the plasma must be incompressible).

6. *Magnetrons as a generalization of non-neutral plasmas undergoing a resistive wall instability:* The magnetron vacuum tube used in radar transmitters and in microwave ovens can be considered as a non-neutral plasma undergoing a negative energy diocotron instability. These tubes are simple, rugged, and efficient. The relation between the non-neutral plasma resistive wall instability and the magnetron is shown in the sequence of sketches Figs.16.6(a)-(d). The magnetron has a cylindrical geometry with an electron emitting filament (cathode) on the z axis, a segmented cylindrical wall (anode) and a z -directed magnetic field produced by permanent magnets. Instead of having a resistor R connected across the gap of a segmented wall as in Fig.16.6(a), the magnetron has a set of cavities connected across the gap as in Fig.16.6(d). The cavities function as a resonant circuit and the output circuit loading provides an effective resistance at the cavity resonant frequency. From the point of view of the plasma, the power appears to be dissipated in a resistor across the wall gap. However, since the cavity is coupled to an output waveguide, the power is actually transported away from the magnetron via a waveguide to some external location where the power is used to transmit a radar pulse or cook a meal. If the cavities in Fig.16.6(d) are phased $0, \pi$ then the ten cavities provide five complete azimuthal wave periods or $l = 5$. If the electrons have near Brillouin flow, and $l = 5$, what axial magnetic field should be used in order to have an output frequency $f = 2450$ MHz, the frequency used in a home microwave oven. Why would the electron density increase to the point that the flow is nearly Brillouin, and why is the electron density not higher than this value? If the voltage drop between anode and cathode is 4 kV and the electron density is uniform, what nominal wall radius (distance between cathode and anode) should be used? Show that a parallel resonant circuit with a small resistance in series with the coil as 16.6(b) has an effective resistance which peaks at the resonant frequency; why does one want the effective resistance to peak at the resonant frequency?

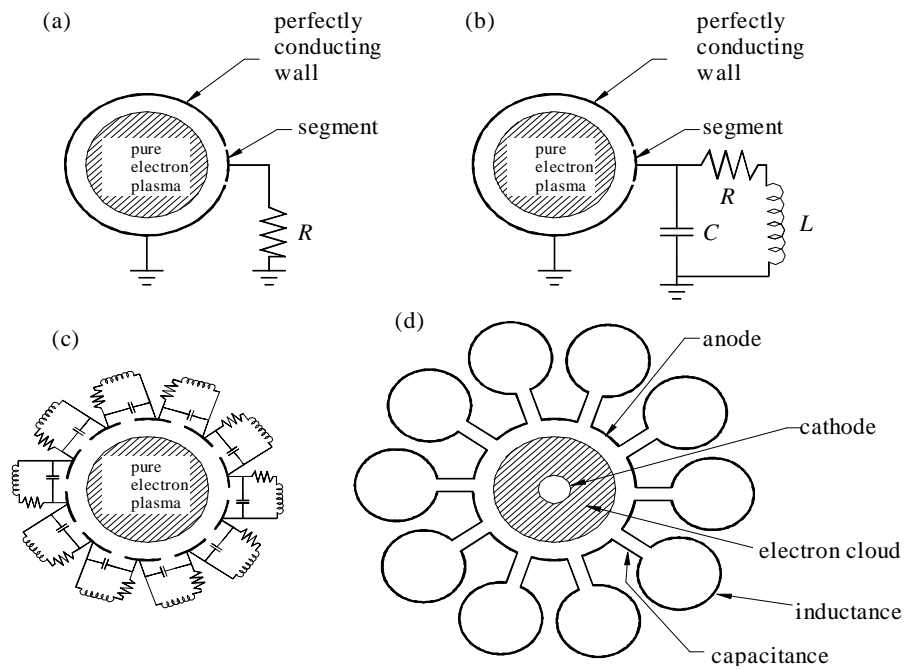


Figure 16.6: (a) Pure electron plasma with one wall segment connected to ground via a resistor R , (b) same, but now connected to ground via a resonant circuit consisting of a capacitor C in parallel with a coil L and a resistor R , (c) same, but now a set of 10 resonant circuits connected across 10 gaps, (d) same, but now the coil is a single turn and the capacitance is in the leads connecting to the coil (the resistor is the loading of the coupler to the output circuit, typically a loop inserted into a coil).

7. *Spiral due to sheared rotation:* Suppose that a non-neutral plasma has a sheared angular velocity so that $\omega_0 = \omega_0(r)$. Suppose that a radial line is painted onto the plasma at $t = 0$ extending from $x = r_p/4, y = 0$ to $x = r_p/2, y = 0$ where r_p is the plasma radius. Suppose that $\omega_0 = \bar{\omega}_0 r / r_p$. Calculate the trajectory of points on the painted line and plot this for successive times using a computer. If the initial line had finite thickness and hence finite area, what would happen to the thickness of the line with increasing time?

Dusty plasmas

17.1 Introduction

Non-neutral plasmas had one less species than a conventional plasma (one species instead of two); dusty plasmas have one more species (three species instead of two). Not surprisingly, the addition of another species provides new freedoms which give rise to new behaviors.

The third species in a dusty plasma, electrically charged dust grains, typically have a charge to mass ratio quite different from that of electrons or ions. Several methods for charging dust grains are possible. Electron bombardment is the usual means for charging laboratory dusty plasmas, but photoionization or radioactive decay could also be operative mechanisms and may be important for certain space and astrophysical situations. Photoionization would make dust grains positive because photoionization causes electrons to leave dust grains. Radioactive decay of dust grains would make the dust grains develop a polarity opposite to that of the particle emitted in the decay process, e.g., alpha particle emission by dust grains would make the dust grains negative.

We shall consider here only the typical laboratory dusty plasma situation where the plasma is weakly ionized and dust grain charging is due to electron bombardment. Negative charging occurs because the electrons, being much lighter than the ions and usually much hotter, have a much larger thermal velocity than the ions. As a result, when a dust grain is inserted into the plasma, it is initially subject to a greater flux of impacting electrons than impacting ions, thereby causing the dust grain to become negatively charged. This negative charge eventually becomes sufficiently large to repel incident electrons and thus attenuate the incoming electron flux. On the other hand, the negative charge of the dust grain accelerates incident ions thereby increasing the ion flux to the dust grain. The net charge on the dust grain reaches equilibrium when the electron and ion fluxes intercepting the dust grain become equal. This is a dynamic equilibrium because it involves a continuous flow of plasma to the dust grain. Some kind of external source is thus required to replenish the plasma electrons and ions continuously, because otherwise all the plasma electrons and ions would eventually collect on the dust grain. The dust grain charging process is quite similar to the development of a floating potential on an insulated probe immersed in a plasma (see Eq.(2.124)).

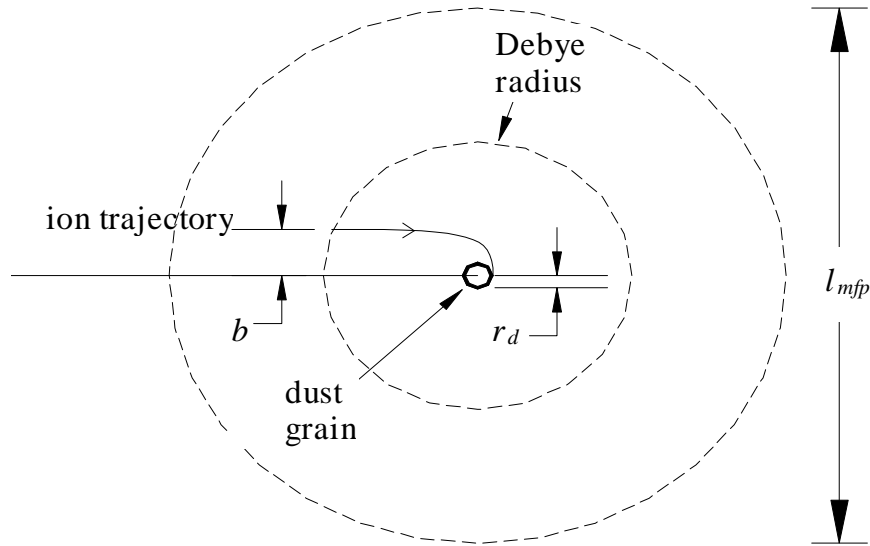


Figure 17.1: Electrons and ions may be considered as being collisionless inside a sphere of diameter l_{mfp} surrounding a dust grain. The trajectory an ion making a grazing collision is shown; this ion has an impact parameter b .

17.2 Electron and ion current flow to a dust grain

Because an individual dust grain is much heavier than an electron or an ion, it can be approximated as an infinitely massive scattering center for the electrons and ions colliding with it. In typical dusty plasma laboratory experiments the collisional mean free path l_{mfp} greatly exceeds the Debye length. This situation is sketched in Fig.17.1 where a dust grain with radius r_d is surrounded by an imaginary sphere with diameter l_{mfp} and the Debye radius is much smaller than l_{mfp} . Electrons and ions are collisionless inside the l_{mfp} sphere and so have Keplerian orbits associated with the electrostatic central force produced by the charge on the dust grain. Because the dust grain is shielded by other particles, the electrons and ions only experience the central force when inside a sphere having the nominal Debye radius.

Dust grain charging involves calculating effective collision cross-sections for the electrons and ions colliding with the dust grain. A useful benchmark reference for this calculation is the cross-section of charged particles colliding with a neutral dust grain. Because charged particles incident on a neutral dust grain have straight line trajectories, the cross-section of a neutral dust grain is just the geometrical area it projects onto a plane, i.e., $\sigma_{geometric} = \pi r_d^2$. The cross-section of a *charged* dust grain differs from $\sigma_{geometric}$ because incident electrons and ions are deflected from straight line trajectories by the electrostatic central force produced by the charge on the dust grain. The respective cross-sections for ions and electrons will now be calculated and related to $\sigma_{geometric}$.

Fig.17.1 shows the impact parameter b and trajectory of an ion colliding with a nega-

tively charged dust grain; the corresponding trajectory of an electron would curl outwards instead of inwards and so the electron would require a much smaller impact parameter b in order to hit the dust grain. We define v to be the initial velocity of an incident particle having mass m and charge q , and define v_{impact} as the velocity of this particle at the instant it makes a grazing impact with the dust grain. Using these definitions it is seen that conservation of angular momentum imposes the requirement

$$vb = v_{impact}r_d \quad (17.1)$$

and conservation of energy impose the requirement

$$\frac{1}{2}mv^2 = \frac{1}{2}mv_{impact}^2 + q\phi_d \quad (17.2)$$

where ϕ_d is the potential on the surface of the dust grain. Figure 17.1 shows that b is larger than r_d for an ion. Because the repulsive force between the negatively charged dust grain and an electron causes the trajectory of an electron to swerve in the opposite sense from an ion, b is smaller than r_d for an electron; that is the electron has to be more 'on-target' than a neutral particle to hit the dust grain whereas an ion can be less 'on-target' than a neutral particle to hit the dust grain.

Eliminating v_{impact} between Eqs.(17.1) and (17.2) gives

$$\frac{1}{2}mv^2 = \frac{1}{2}mv^2\frac{b^2}{r_d^2} + q\phi_d \quad (17.3)$$

so the effective scattering cross-section is (Allen, Boyd and Reynolds 1957)

$$\sigma(v) = \pi b^2 = \left(1 - \frac{2q\phi_d}{mv^2}\right) \sigma_{geometric}. \quad (17.4)$$

For $q\phi_d > 0$ the interaction is repulsive and the cross-section is smaller than $\sigma_{geometric}$, whereas for $q\phi_d < 0$ the interaction is attractive and the cross-section is larger than $\sigma_{geometric}$. The former case applies to electrons and the latter case applies to ions.

The total current flowing to the dust grain for attractive interactions is

$$I_{attractive} = q \int_0^\infty \sigma(v)vf(v)4\pi v^2 dv. \quad (17.5)$$

However, because in the repulsive situation incident particles having $v < \sqrt{2q\phi_d/m}$ are reflected and do not hit the dust grain, the repulsive situation cross-section is zero for all particles having $v < \sqrt{2q\phi_d/m}$. Thus, the total current for repulsive interactions is

$$I_{repulsive} = q \int_{\sqrt{2q\phi_d/m}}^\infty \sigma(v)vf(v)4\pi v^2 dv. \quad (17.6)$$

Since the region outside the l_{mfp} sphere sketched in Fig.17.1 extends to infinity, particles can be considered to have made many collisions before entering the l_{mfp} sphere, and so the velocity distribution of particles incident upon the l_{mfp} sphere will be Maxwellian, i.e.,

$$f(v) = \frac{n_0}{\pi^{3/2}v_T^3} e^{-v^2/v_T^2} \quad (17.7)$$

where $v_T = \sqrt{2\kappa T/m}$ is the thermal velocity. The incident particles will be collisionless as they travel inside the l_{mfp} sphere. Integration of Eqs.(17.5) and (17.6) gives

$$\begin{aligned}
 I_{attractive} &= q \int_0^\infty \pi r_d^2 \left(1 - \frac{2q\phi_d}{mv^2}\right) v f(v) 4\pi v^2 dv \\
 &= 2\pi^{1/2} r_d^2 n_0 q v_T \int_0^\infty \left(1 - \frac{2q\phi_d}{mv_T^2 x}\right) e^{-x} x dx \\
 &= \frac{2}{\pi^{1/2}} \left(1 - \frac{q\phi_d}{\kappa T}\right) n_0 q v_T \sigma_{geometric} \quad (17.8)
 \end{aligned}$$

and

$$\begin{aligned}
 I_{repulsive} &= 2\pi^{1/2} r_d^2 n_0 q v_T \int_{q\phi_d/\kappa T}^\infty \left(1 - \frac{q\phi_d}{\kappa T x}\right) e^{-x} x dx \\
 &= \frac{2}{\pi^{1/2}} e^{-q\phi_d/\kappa T} n_0 q v_T \sigma_{geometric}. \quad (17.9)
 \end{aligned}$$

17.3 Dust charge

As discussed above, a neutral dust grain inserted into a plasma will become negatively charged because $v_{Te} \gg v_{Ti}$. The electron current I_e is thus a repulsive-type current and the ion current I_i is an attractive-type current. As the dust grain becomes more negatively charged, $|I_e|$ decreases and $|I_i|$ increases until $I_i + I_e = 0$ at which time dust grain charging ceases.

The presence of negatively charged dust grains affects the quasi-neutrality condition. Assuming singly charged ions and a charge of Z_d on the negatively charged dust grains, the quasineutrality condition generalizes to

$$n_{i0} = n_{e0} + Z_d n_{d0}. \quad (17.10)$$

Since the ion density is unaffected by the charging process, it is convenient to normalize all densities to the ion density and define

$$\alpha = \frac{Z_d n_{d0}}{n_{i0}} \quad (17.11)$$

so that

$$\frac{n_{e0}}{n_{i0}} = 1 - \alpha \quad (17.12)$$

where n_{e0} , n_{i0} , and n_{d0} are the volume-averaged electron, ion, and dust grain densities. Furthermore, if r_d is small compared to the effective shielding length λ_d , then the dust grain charge Z_d is related to the dust grain surface potential and the dust grain radius r_d via the vacuum Coulomb relationship, i.e.,

$$\begin{aligned}
 \phi_d &= -\frac{Z_d e \exp(-r_d/\lambda_d)}{4\pi\epsilon_0 r_d} \\
 &\simeq -\frac{Z_d e}{4\pi\epsilon_0 r_d} \text{ if } r_d \ll \lambda_d. \quad (17.13)
 \end{aligned}$$

Equation (17.11) can then be written in terms of the dust grain surface potential as

$$\alpha = -\frac{4\pi\varepsilon_0 r_d n_{d0}}{n_{i0}e} \phi_d. \quad (17.14)$$

It is now convenient to introduce the dimensionless variable

$$\psi = -\frac{e\phi}{\kappa T_i} \quad (17.15)$$

so that α becomes

$$\alpha = 4\pi n_{d0} r_d \lambda_{di}^2 \psi_d \quad (17.16)$$

where

$$\lambda_{di} = \sqrt{\frac{\varepsilon_0 \kappa T_i}{n_{i0} e^2}} \quad (17.17)$$

is the ion Debye length. Large ψ_d means that ions fall into a potential energy well much deeper than their thermal energy.

It is also useful to introduce the Wigner-Seitz radius a , a measure of the nominal spacing between adjacent dust grains. This spacing is defined by dividing the total volume of the system V by the total number of dust grains N to find a nominal volume surrounding each dust grain. It is then imagined that this nominal volume is spherical with radius a so that

$$N \frac{4\pi a^3}{3} = V \quad (17.18)$$

in which case

$$n_{d0} = \frac{3}{4\pi a^3} \quad (17.19)$$

and

$$\alpha = \frac{3r_d \lambda_{di}^2}{a^3} \psi_d. \quad (17.20)$$

It is also convenient to normalize lengths to the ion Debye length so

$$\alpha = P \psi_d \quad (17.21)$$

where

$$P = 3 \frac{\bar{r}_d}{a^3} \quad (17.22)$$

and the bar means normalized to an ion Debye length.

The dust charge can also be expressed in a non-dimensional fashion using Eq.(17.13) to give

$$\frac{Z_d}{4\pi n_{i0} \lambda_{di}^3} = \bar{r}_d \psi_d. \quad (17.23)$$

The floating condition $I_i + I_e = 0$ shows that the equilibrium dust potential is given by

$$0 = n_{i0} v_{Ti} \left(1 - \frac{e\phi_d}{\kappa T_i} \right) - n_{e0} v_{Te} \exp(e\phi_d / \kappa T_e) \quad (17.24)$$

which can be re-arranged as

$$(1 + \psi_d) \sqrt{\frac{m_e T_i}{m_i T_e}} \exp(\psi_d T_i / T_e) = 1 - \alpha. \quad (17.25)$$

However, using Eq.(17.21) this becomes

$$(1 + \psi_d) \sqrt{\frac{m_e T_i}{m_i T_e}} \exp(\psi_d T_i / T_e) = 1 - P \psi_d, \quad (17.26)$$

a transcendental equation relating ψ_d and P .

Equation (17.26) shows that, for a given temperature ratio T_i/T_e and given mass ratio m_e/m_i , the normalized dust grain surface potential ψ_d is a function of P , a dimensionless parameter incorporating the geometrical information characterizing the dust grains in the dusty plasma. Because ψ_d appears non-algebraically in Eq.(17.26), it is not possible to solve for $\psi_d(P)$ without resorting to numerical methods. However, solving the inverse relation, namely $P(\psi_d)$, is straightforward because P occurs only once in Eq.(17.26). Solving for P gives (Havnes, Goertz, Morfill, Grun and Ip 1987)

$$P = \frac{1}{\psi_d} - \left(1 + \frac{1}{\psi_d}\right) \sqrt{\frac{m_e T_i}{m_i T_e}} \exp(\psi_d T_i / T_e). \quad (17.27)$$

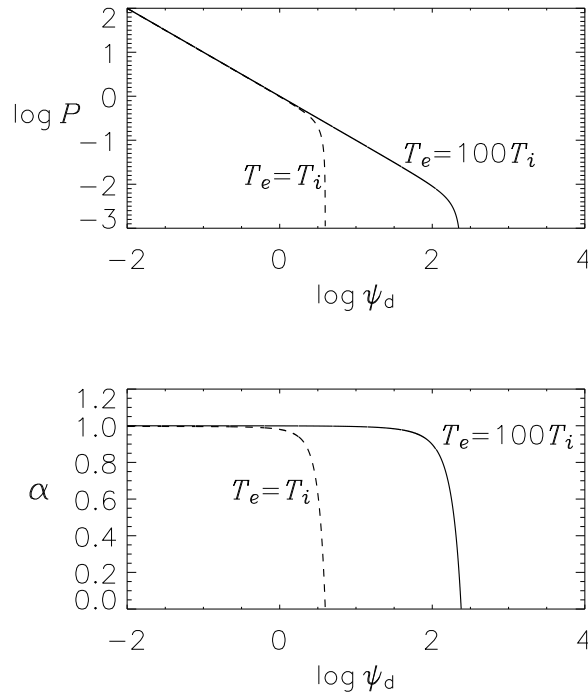


Figure 17.2: Plots of $\log P$ and α v. $\log \psi_d$ for $T_e = 100 T_i$ and $T_e = T_i$. Logarithms are base 10 and ion mass is 40 amu. Since P is proportional to the dust grain density the right hand side of these curves, i.e., small P , corresponds to the limit of low dust grain density.

The upper plot in Fig. 17.2 shows $\log P$ plotted versus $\log \psi_d$ for two cases corresponding to two typical laboratory configurations where dusty plasma experiments have been conducted; the lower plot shows the corresponding dependence of α on ψ_d . The $T_e = T_i$ configuration corresponds to a potassium Q-machine plasma while the $T_e = 100T_i$ configuration corresponds to an argon rf discharge. An ion of 40 atomic mass units has been assumed for both cases. Figure 17.2 shows that P varies inversely with ψ_d up to some critical value and then, for ψ_d above this critical value, P heads sharply to zero for modest increases in ψ_d . The lower plot shows that α is near unity to the left of the knee and then drops sharply to zero to the right of the knee. Comparison of the solid and dashed curves shows that the saturated value of ψ_d is an increasing function of T_e/T_i . The saturation value of ψ_d is 2.5 for the Q-machine parameters whereas the saturated value of ψ_d for the rf discharge is $\sim 2 \times 10^2$. Since P is proportional to \bar{n}^{-3} and hence to the dust grain density, the right hand side of these plots (i.e., where P is small) correspond to the limit of small dust grain density. Also, comparison of the solid and dashed plots shows that ψ_d increases with T_e/T_i . Since Eq.(17.23) shows that Z_d is proportional to ψ_d , it is seen that Z_d also saturates on moving to the right in the plots and largest Z_d occurs at high T_e/T_i and small dust grain density.

The downward sloping segment on the left of Fig. 17.2 corresponds to the $\alpha \simeq 1$ regime which is the situation where the dust grain density is large, nearly all the electrons are attached to the dust grains, and the plasma has almost no free electrons. On the other hand, the saturated limit of ψ_d on the right of Fig. 17.2 corresponds to the $\alpha \ll 1$ regime which is where there is minimal depletion of free electrons, the dust grain density is low, and there is a very high charge on each of the relatively small number of dust grains.

There are thus three regimes:

1. *The regime well to the left of the knee in the curves.* Here $\alpha \simeq 1$ and nearly all electrons are attached to the dust grains. To the extent that α approaches unity, the dust grains replace the electrons as the negative charge carriers.
2. *The regime to the right of the knee in the curves.* Here $\alpha \ll 1$, most electrons are free, and the potential of an individual dust grain is very high and near at its saturation value (right hand side of plots). This regime corresponds to small P and a very small dust grain density.
3. *The regime in the vicinity of the knee in the curves.* If $T_e \gg T_i$ then it is possible to have both α of order unity and ψ_d large even though ψ_d is not quite at its saturation level. In this regime the majority of electrons reside on the dust grains, the dust grains are highly charged, and the dust grain density is appreciable. Crystallization of the dust grains can occur in this regime since crystallization requires a combination of high dust grain charge and small separation between dust grains.

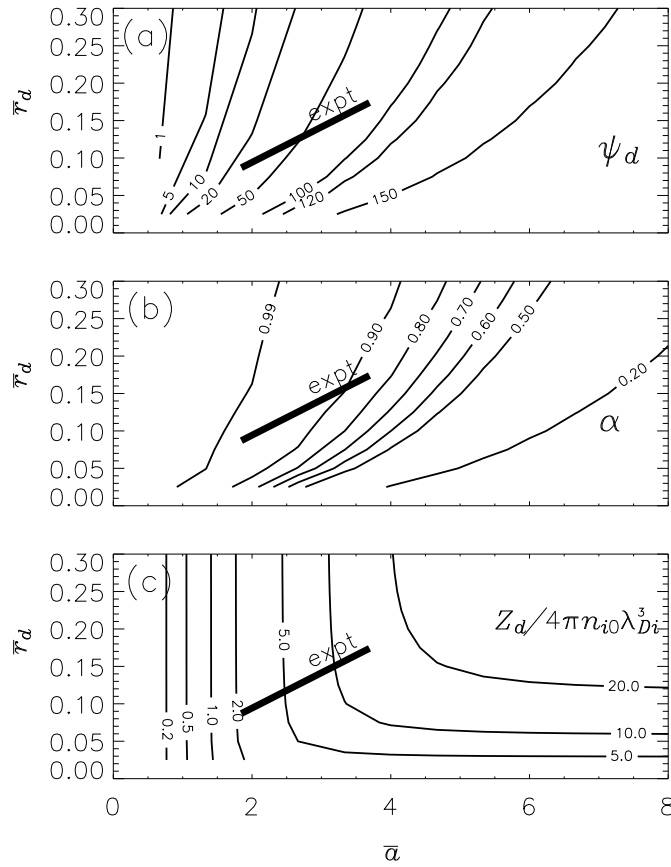


Figure 17.3: Dusty plasma parameter space showing contours of constant ψ_d , α , and $Z_d/4\pi n_{i0}\lambda_{Di}^3$ for an argon plasma with $T_e/T_i = 100$. The experimental line corresponds to the density range of the Chu and I experiment (Chu and I 1994); these plots are from Bellan (2004).

17.4 Dusty plasma parameter space

A dusty plasma is characterized by its normalized dust radius \bar{r}_d and normalized dust interparticle spacing \bar{a} . These quantities determine P and, given P , the normalized dust surface potential ψ_d is obtained by solving Eq.(17.27). Knowing P and ψ_d gives α using Eq.(17.21). The consequence of this logical chain of argument is that α can be considered to be a function of \bar{r}_d and \bar{a} .

A dusty plasma parameter space can thus be constructed where \bar{a} is the horizontal com-

ponent and \bar{r}_d is the vertical component so that a given dusty plasma would correspond to a point in this parameter space. The quantities ψ_d , α , and $Z_d/4\pi n_{i0}\lambda_{di}^3$ are all functions of \bar{a} and \bar{r}_d and so contours of these three quantities can be drawn in the \bar{a}, \bar{r}_d parameter space for specified m_e/m_i and T_e/T_i . Examples of these contours are shown in Fig.17.3 for an argon plasma with $T_e = 100T_i$. An actual experiment would have specific values of \bar{a} and \bar{r}_d and so would be represented as a point in this parameter space. Variation of the ion density in the experiment would change the value of λ_{di} while keeping the ratio \bar{r}_d/\bar{a} fixed and so would correspond to moving along a sloped line in parameter space. The short sloped line in Fig.17.3 represents the density in the dusty plasma experiment by Chu and I (1994) to be discussed later (the finite length of this line corresponds to the error bars for the density measurement).

17.5 Large P limit: dust acoustic waves

The large P limit (i.e., regime 1 discussed above) has nearly all the electrons attached to the dust grains so that the plasma effectively consists of negatively charged dust grains and positive ions. A wave similar to the conventional ion acoustic wave can propagate in this regime, but the role played by positive and negative particles is reversed: here the ions are the light species and the dust grains are the heavy species. In order to appreciate the consequence of this role reversal, consider the conventional ion acoustic wave from the most simplistic point of view. The wave phase velocity ω/k is assumed to be much faster than the ion thermal velocity v_{Ti} (i.e., cold ion regime) but much slower than the electron thermal velocity v_{Te} (i.e., isothermal electron regime) so the respective approximations of the electron and ion equations of motion are

$$0 = -n_e e \mathbf{E} - \nabla (n_e \kappa T_e) \quad (17.28)$$

$$n_i m_i \frac{d\mathbf{u}_i}{dt} = n_i Z e \mathbf{E}. \quad (17.29)$$

Adding the electron and ion equations and assuming quasineutrality $n_e \simeq n_i Z$, gives

$$n_i m_i \frac{d\mathbf{u}_i}{dt} = -\nabla (n_e \kappa T_e) \quad (17.30)$$

showing that the effective force acting on the ions is the electron pressure gradient. This force is coupled to the ions via the electric field. In effect, the electron pressure gradient pushes against the electric field which in turn pushes the ions. Linearizing Eq.(17.30) gives a result similar to a conventional sound wave, except that the system is isothermal with respect to the electron temperature (in a normal neutral gas sound wave, the gas temperature would appear in the right hand side, the gas would be adiabatic, and so a γ would appear upon linearizing the gas pressure). Linearization of Eq.(17.30) and invoking the linearized quasineutrality relation $n_{e1} \simeq n_{i1} Z$, gives

$$n_{i0} m_i \frac{\partial \mathbf{u}_{i1}}{\partial t} = -Z \kappa T_e \nabla n_{i1}. \quad (17.31)$$

The linearized ion equation of continuity is

$$\frac{\partial n_{i1}}{\partial t} + n_{i0} \nabla \cdot \mathbf{u}_{i1} = 0. \quad (17.32)$$

The equations are combined by taking the divergence of Eq.(17.31) and then substituting Eq.(17.32) to obtain

$$\frac{\partial^2 n_{i1}}{\partial t^2} = \frac{Z\kappa T_e}{m_i} \nabla^2 n_{i1} \quad (17.33)$$

which is a wave equation with wave velocity $c_s^2 = Z\kappa T_e/m_i$.

This method can now be generalized to a plasma consisting of ions with charge $+e$, free electrons with charge $-e$, and dust grains with charge $-Z_d e$. The free electron density is assumed to be small so that $P \gg 1$ in which case the configuration is on the left of Fig.17.2. The wave phase velocity is assumed to be much faster than the dust grain thermal velocity, but much slower than the ion/electron thermal velocities so the respective electron, ion and dust grain equations of motion are

$$0 = -n_e e \mathbf{E} - \nabla (n_e \kappa T_e) \quad (17.34)$$

$$0 = +n_i e \mathbf{E} - \nabla (n_i \kappa T_i) \quad (17.35)$$

$$n_d m_d \frac{d\mathbf{u}_d}{dt} = -n_d Z_d e \mathbf{E}. \quad (17.36)$$

Adding the above three equations and invoking quasineutrality (i.e., $n_i = n_d Z_d + n_e$) results in

$$n_d m_d \frac{d\mathbf{u}_d}{dt} = -\nabla (n_i \kappa T_i + n_e \kappa T_e). \quad (17.37)$$

In analogy to the conventional ion acoustic wave, here the ion and electron pressures couple to the dust via the electric field. Linearization of Eq.(17.37) gives

$$n_{d0} m_d \frac{\partial \mathbf{u}_{d1}}{\partial t} = -\kappa T_i \nabla n_{i1} - \kappa T_e \nabla n_{e1} \quad (17.38)$$

while linearization of Eqs.(17.34) and (17.35) gives

$$0 = -n_{e0} e \mathbf{E}_1 - \kappa T_e \nabla n_{e1} \quad (17.39)$$

$$0 = +n_{i0} e \mathbf{E}_1 - \kappa T_i \nabla n_{i1}. \quad (17.40)$$

Eliminating \mathbf{E}_1 between these last two equations shows that

$$\kappa T_e \nabla n_{e1} = -\frac{n_{e0}}{n_{i0}} \kappa T_i \nabla n_{i1} \quad (17.41)$$

which can be integrated to give

$$n_{e1} = -\frac{n_{e0} T_i}{n_{i0} T_e} n_{i1}. \quad (17.42)$$

Inserting Eq.(17.42) into the linearized quasineutrality expression $n_{i1} = n_{d1} Z_d + n_{e1}$ gives

$$n_{i1} = \frac{1}{1 + \frac{n_{e0} T_i}{n_{i0} T_e}} Z_d n_{d1} \quad (17.43)$$

and hence

$$n_{e1} = -\frac{n_{e0} T_i / n_{i0} T_e}{1 + \frac{n_{e0} T_i}{n_{i0} T_e}} Z_d n_{d1}. \quad (17.44)$$

Substitution for n_{i1} and n_{e1} in Eq.(17.38) gives

$$\begin{aligned} n_{d0}m_d \frac{\partial \mathbf{u}_{d1}}{\partial t} &= -\kappa T_i \frac{1 - n_{e0}/n_{i0}}{1 + \frac{n_{e0}T_i}{n_{i0}T_e}} Z_d \nabla n_{d1} \\ &\simeq -\kappa T_i Z_d \nabla n_{d1} \end{aligned} \quad (17.45)$$

since $n_{e0} \ll n_{i0}$ and typically $T_i/T_e \ll n_{i0}/n_{e0}$.

The linearized dust continuity equation is

$$\frac{\partial n_{d1}}{\partial t} + n_{d0} \nabla \cdot \mathbf{u}_{d1} = 0 \quad (17.46)$$

so taking the divergence of Eq.(17.45) and substituting Eq.(17.46) gives

$$\frac{\partial^2 n_{d1}}{\partial t^2} = \frac{Z_d \kappa T_i}{m_d} \nabla^2 n_{d1} \quad (17.47)$$

which is a wave with phase velocity

$$c_{da}^2 = \frac{Z_d \kappa T_i}{m_d}. \quad (17.48)$$

This wave is called the dust acoustic wave and its phase velocity is extremely low because of the large dust grain mass.

This analysis could be extended to include finite $k\lambda_D$ terms as obtained by using the full Poisson's equation instead of making the simplifying assumption of perfect neutrality. A Vlasov approach could also be invoked to demonstrate the effect of Landau damping. Rather than work through the details of these extensions, one can argue that the $\alpha \simeq 1$ dusty plasma is effectively a two-component plasma where the heavy particles are the negatively charged dust grains and the light particles are the positively charged ions. The previously derived results from both two-fluid theory and Vlasov theory could then be invoked by simply identifying the heavy and light particles in the manner stated above. Thus by making the identification,

	ion acoustic wave	dust acoustic wave
inertia provided by	ions	dust grains
restoring force provided by	electron pressure	ion pressure

taking into account finite $k^2\lambda_D^2$ terms will result in a dispersive dust acoustic wave

$$\omega^2 = \frac{k^2 c_{da}^2}{1 + k^2 \lambda_{Di}^2}. \quad (17.49)$$

Similarly, just as an electron flow velocity faster than the ion acoustic phase velocity would destabilize ion acoustic waves via inverse Landau damping, a Landau analysis would show that an ion flow velocity faster than the dust acoustic phase velocity would destabilize dust acoustic waves.

Destabilized dust acoustic waves have been observed in an experiment by Barkan, Merlino and D'Angelo (1995). The phase velocity of these waves was of the order of 10 cm/s which is an order of magnitude less than a human walking speed.

17.6 Dust ion acoustic waves

The presence of dust grains can also substantially modify the propagation properties of conventional ion acoustic waves. In a conventional electron-ion plasma, ion acoustic waves can propagate only if $T_e \gg T_i$. This is because strong ion Landau damping occurs when the wave phase velocity is of the order of the ion thermal velocity and this is impossible to avoid unless $T_e \gg T_i$ since the conventional ion acoustic phase velocity scales as $c_s^2 = (\gamma\kappa T_i + \kappa T_e)/m_i$.

As in the conventional ion acoustic wave, the derivation of dust ion acoustic waves involves the linearized electron and ion equations

$$0 = -n_{e0}e\mathbf{E}_1 - \kappa T_e \nabla n_{e1} \quad (17.50)$$

$$n_{i0}m_i \frac{\partial \mathbf{u}_i}{\partial t} = +n_{i0}e\mathbf{E}_1 - \gamma\kappa T_i \nabla n_{i1} \quad (17.51)$$

but here the possibility of finite T_i has been retained in order to allow consideration of the $T_e \sim T_i$ regime. The wave frequency is assumed to be sufficiently high so that the dust grains are unable to respond to the wave; the dust grains are effectively considered as being infinitely massive and therefore stationary. In this limit the dust grains contribute to the equilibrium quasineutrality condition $n_{i0} = n_{e0} + Z_d n_{d0}$ but since the dust grains are assumed stationary their density cannot change and so the linearized quasi-neutrality condition is $n_{i1} = n_{e1}$. Thus, infinitely massive dust grains affect the equilibrium electron density, but not the perturbed electron density.

Eliminating \mathbf{E}_1 between Eqs.(17.50) and (17.51) gives

$$n_{i0}m_i \frac{\partial \mathbf{u}_i}{\partial t} = -\frac{n_{i0}}{n_{e0}}\kappa T_e \nabla n_{e1} - \gamma\kappa T_i \nabla n_{i1}. \quad (17.52)$$

Since $n_{i1} = n_{e1}$ and $n_{i0}/n_{e0} = n_{i0}/(n_{i0} - Z_d n_{d0})$, Eq.(17.52) becomes

$$n_i m_i \frac{\partial \mathbf{u}_i}{\partial t} = -\frac{1}{1 - Z_d n_{d0}/n_{i0}} \kappa T_e \nabla n_i - \gamma\kappa T_i \nabla n_i. \quad (17.53)$$

Taking the divergence and using Eqs. (17.11) and (17.32) gives

$$m_i \frac{\partial^2 n_{i1}}{\partial t^2} = \left(\frac{1}{1 - \alpha} \kappa T_e + \gamma\kappa T_i \right) \nabla^2 n_{i1} \quad (17.54)$$

which gives the dust ion acoustic wave (Shukla and Silin 1992), a wave with phase velocity

$$c_{DIA}^2 = \frac{1}{1 - \alpha} \frac{\kappa T_e}{m_i} + \gamma \frac{\kappa T_i}{m_i}. \quad (17.55)$$

As α approaches unity, the dust ion acoustic wave phase velocity becomes much greater than the ion thermal velocity even in a plasma having $T_i = T_e$. The dust ion acoustic wave thus propagates without being attenuated by ion Landau damping in a $T_i = T_e$ plasma having $\alpha \simeq 1$, which corresponds to the left side of Fig.17.2. Thus, the presence of a large dust grain density enables the propagation of ion acoustic waves that normally would be damped in a $T_e = T_i$ plasma; this has been observed in experiments by Barkan, D'Angelo and Merlino (1996).

17.7 The strongly coupled regime: crystallization of a dusty plasma

The mutual repulsive force between two negatively charged dust grains scales as Z_d^2 and so will be very large for highly charged dust grains. In the extreme limit of this situation the electrostatic potential energy between dust grains might exceed their kinetic energy so that the grains would tend to form an ordered, crystallized state. The possibility that dust grains might crystallize was first suggested by Ikezi (1986) and has since been demonstrated in a number of experiments (Chu and I 1994, Melzer, Trottenberg and Piel 1994, Thomas, Morfill, Demmel, Goree, Feuerbacher and Mohlmann 1994, Hayashi and Tachibana 1994, Nefedov, Morfill, Fortov, Thomas, Rothermel, Hagl, Ivlev, Zuzic, Klumov, Lipaev, Molotkov, Petrov, Gidzenko, Krikalev, Shepherd, Ivanov, Roth, Binnenbruck, Goree and Semenov 2003, Morfill, Annaratone, Bryant, Ivlev, Thomas, Zuzic and Fortov 2002). The threshold criterion for crystallization will be discussed in this section following a model by Bellan (2004b). The threshold is determined by considering certain issues relating to the validity of the conventional Debye shielding model and the Boltzmann relation.

Large Z_d corresponds to large ψ_d which in turn corresponds to operating towards the right of Fig. 17.2. Since the location of the saturation value of ψ_d increases with T_e/T_i , very large ψ_d can occur if $T_e \gg T_i$. The repulsive force also scales inversely with the square of the distance separating the two dust grains, i.e., the repulsive force also scales as $n_{d0}^{2/3}$. Since P is proportional to n_{d0} , the maximum repulsive force would be obtained around the knee in the $T_e \gg T_i$ curves in Fig. 17.2 since at this location it is possible to have large ψ_d without n_{d0} becoming infinitesimal.

The repulsive electrostatic force between two dust grains is attenuated by Debye shielding. This shielding can be calculated by considering a single dust grain to be a test particle immersed in a plasma consisting of electrons, ions, and other dust grains which will be referred to as “field” dust grains. The test particle will be completely shielded beyond some critical radius. A field dust grain located beyond this critical radius will experience no interaction with the test particle dust grain whereas if the field dust grain is located within the shielding radius, it will experience an enormous repulsive force. The test particle dust grain thus acts like a finite-radius hard sphere in its interactions with field particle dust grains.

A quantitative model for these interactions between dust grains can be developed by considering Poisson’s equation for a dusty plasma,

$$\nabla^2\phi = -\frac{1}{\varepsilon_0} (n_i e - n_e e - Z_d n_d e). \quad (17.56)$$

The usual test-particle argument (see p.8) involves linearization of the Boltzmann relation for each species to obtain a linearized density for each species. These linearized densities are then substituted into Poisson’s equation resulting in the Yukawa-type solution,

$$\phi = -\frac{q_t}{4\pi\varepsilon_0 r} \exp(-r/\lambda_D) \quad (17.57)$$

where $\lambda_D^{-2} = \sum \lambda_{D\sigma}^{-2}$. However, this linearization is based on the assumption $|q_t\phi/\kappa T_\sigma| \ll 1$ which is clearly not true in the vicinity of a highly charged dust grain. This inconsis-

tency cannot be resolved in fluid theory and it is necessary to revert to the more fundamental Vlasov description.

Particles are characterized by a velocity distribution function $f(r, \mathbf{v})$ in the Vlasov description and the Vlasov equation describes the time evolution of f . The test particle location is defined to be at the origin of a spherical coordinate system and the system is assumed to be spherically symmetric so that the only spatial dependence of ϕ and f is on the spherical radius r . The nominal location of the last collision made by a particle incident upon the test particle is the collision mean free path λ_{mfp} and since any particle incident upon the test particle will have traveled many mean free paths, the velocity distribution of particles entering a sphere of order l_{mfp} will be Maxwellian. Because the incident particles are collisionless within the λ_{mfp} sphere, their velocity distribution function must be a solution to the collisionless Vlasov equation inside the sphere. The boundary condition this solution must satisfy is that its large r limit should correspond to the collisional (i.e., Maxwellian) distribution.

Solutions to the collisionless Vlasov equation are functions of constants of the motion as was shown in Sec.2.2 and the appropriate constant of the motion here is the particle energy $W = m_\sigma v^2/2 + q_\sigma \phi(r)$. Hence the distribution function in the collisionless region near the test particle must be

$$f_\sigma(r, \mathbf{v}) = n_{\sigma 0} \left(\frac{m_\sigma}{2\pi\kappa T_\sigma} \right)^{3/2} \exp\left(-\frac{m_\sigma v^2/2 + q_\sigma \phi(r)}{\kappa T_\sigma}\right) \quad (17.58)$$

since this maps to a Maxwellian distribution at large distances r where $\phi(r) \rightarrow 0$.

A negatively charged particle such as a dust grain or an electron experiences a repulsive force upon approaching the dust grain test particle and so slows down. Some approaching negatively charged particles reflect and so the minimum velocity of electrons or dust grains approaching the dust grain test particle is zero. The density of these particles will thus be

$$\begin{aligned} n_\sigma &= \int_0^\infty f_\sigma(r, \mathbf{v}) d^3v \\ &= n_{\sigma 0} \exp\left(-\frac{q_\sigma \phi(r)}{\kappa T_\sigma}\right) \end{aligned} \quad (17.59)$$

which is the same as the fluid theory Boltzmann relation. It is useful at this point to change over to the non-dimensional scalar ψ defined in Eq.(17.15). Since the dust grains are negatively charged, ψ is large and positive in the vicinity of a dust grain. The respective normalized electron and field dust grain densities are thus

$$\frac{n_e}{n_{e0}} = \exp(-\psi T_i/T_e) \quad (17.60)$$

$$\frac{n_d}{n_{d0}} = \exp(-\bar{Z}\psi) \quad (17.61)$$

where

$$\bar{Z} = Z_d T_i/T_d. \quad (17.62)$$

Both the electron and field dust grain densities decrease in the vicinity of the dust grain test particle. However, because \bar{Z} is typically very large and T_i/T_e is assumed to be very small, the field dust density scale length is much shorter than the electron density scale length.

Ion dynamics are qualitatively different because all ions approaching the dust grain are accelerated, leading to the situation that no zero velocity ions exist near the dust grain. In particular, an ion starting with infinitesimal inward velocity at infinity where $\psi = 0$ has nearly zero energy, i.e., $W \simeq 0$. The energy conservation equation for this slowest ion is

$$m_i v^2/2 + e\phi(r) = 0 \quad (17.63)$$

and so the velocity for this slowest ion has the spatial dependence

$$v_{\min} = \sqrt{-\frac{2e\phi(r)}{m_i}}. \quad (17.64)$$

The ion density is thus

$$\begin{aligned} n_i(r) &= \int_{v_{\min}}^{\infty} f_i(r, \mathbf{v}) d^3v \\ &= n_{i0} \left(\frac{m_i}{2\pi\kappa T_i} \right)^{3/2} \exp\left(-\frac{q_i\phi(r)}{\kappa T_i}\right) \int_{v_{\min}}^{\infty} \exp\left(-\frac{mv^2/2}{\kappa T_i}\right) d^3v \\ &= n_{i0} \frac{4}{\sqrt{\pi}} \exp(\psi) \int_{\sqrt{\psi}}^{\infty} \exp(-\xi^2) \xi^2 d\xi. \end{aligned} \quad (17.65)$$

This can be expressed in terms of the Error Function

$$\operatorname{erf} z = \frac{2}{\sqrt{\pi}} \int_0^z \exp(-\xi^2) d\xi \quad (17.66)$$

and, in particular, using the identity

$$\frac{4}{\sqrt{\pi}} \int_z^{\infty} \exp(-\xi^2) \xi^2 d\xi = \frac{2}{\sqrt{\pi}} \int_z^{\infty} d\xi \exp(-\xi^2) - \frac{2}{\sqrt{\pi}} \int_z^{\infty} d\xi \frac{d}{d\xi} (\xi \exp(-\xi^2)) \quad (17.67)$$

it is seen that (Laframboise and Parker 1973)

$$\frac{n_i}{n_{i0}} = \exp(\psi) \left(1 - \operatorname{erf} \sqrt{\psi} \right) + \frac{2}{\sqrt{\pi}} \sqrt{\psi}. \quad (17.68)$$

The error function has the small-argument limit

$$\lim_{z \rightarrow 0} \operatorname{erf} z \simeq \frac{2z}{\sqrt{\pi}} \quad (17.69)$$

and so for $\psi \ll 1$

$$\frac{n_i}{n_{i0}} = 1 + \psi \quad (17.70)$$

which is identical to the Boltzmann result given by fluid theory.

However, because

$$\lim_{z \rightarrow \infty} e^{-z^2} (1 - \operatorname{erf} z) = 0, \quad (17.71)$$

when $\psi \gg 1$ the ion density has a non-Boltzmann dependence

$$\frac{n_i}{n_{i0}} = \frac{2}{\sqrt{\pi}} \sqrt{\psi} \quad (17.72)$$

which is much smaller than the $\exp(\psi)$ dependence predicted by the Boltzmann relation. Poisson's equation can be written non-dimensionally as

$$\begin{aligned} \frac{1}{\bar{r}^2} \frac{\partial}{\partial \bar{r}} \left(\bar{r}^2 \frac{\partial \psi}{\partial \bar{r}} \right) &= \frac{n_i}{n_{i0}} - \frac{n_e}{n_{e0}} - \frac{Z_d n_d}{n_{d0}} \\ &= \frac{n_i}{n_{i0}} - (1 - \alpha) \frac{n_e}{n_{e0}} - \alpha \frac{n_d}{n_{d0}} \end{aligned} \quad (17.73)$$

where, following the normalization convention introduced earlier, $\bar{r} = r/\lambda_{di}$. Upon substituting for the normalized densities, Poisson's equation becomes

$$\begin{aligned} \underbrace{\frac{1}{\bar{r}^2} \frac{\partial}{\partial \bar{r}} \left(\bar{r}^2 \frac{\partial \psi}{\partial \bar{r}} \right)}_{\text{vacuum}} &= \underbrace{e^\psi \left(1 - \operatorname{erf}(\sqrt{\psi}) \right)}_{\text{ions}} + \frac{2}{\sqrt{\pi}} \sqrt{\psi} \\ &\quad - \underbrace{(1 - \alpha) \exp\left(-\frac{\psi T_i}{T_e}\right)}_{\text{electrons}} \\ &\quad - \underbrace{\alpha \exp(-Z\psi)}_{\text{dust}}. \end{aligned} \quad (17.74)$$

Because ψ becomes large near the dust grain, this equation is highly non-linear and so the linearization technique used on p. 8 for the conventional Debye shielding derivation cannot be invoked. Instead, an approximate solution to Poisson's equation is obtained by separating the collisionless region around the dust grain test particle into three concentric layers (regions) according to the magnitude of ψ :

	Region 1	Region 2	Region 3
Definition	$\psi_d > \psi > 1$	$1 > \psi > 1/Z$	$1/Z > \psi$
Location	adjacent to dust grain	middle spherical layer	outer layer
Ions	non-Boltzmann, fast	Boltzmann	Boltzmann
Electrons	Boltzmann	Boltzmann	Boltzmann
Dust	zero density	zero density	Boltzmann
Dependence	vacuum-like w/const.	growing/decaying Yukawa	decaying Yukawa

Poisson's equation has the following approximations in the three regions

$$\text{Region 1 : } \frac{1}{\bar{r}^2} \frac{\partial}{\partial \bar{r}} \left(\bar{r}^2 \frac{\partial \psi}{\partial \bar{r}} \right) = 0 \quad (17.75)$$

$$\text{Region 2 : } \frac{1}{\bar{r}^2} \frac{\partial}{\partial \bar{r}} \left(\bar{r}^2 \frac{\partial \psi}{\partial \bar{r}} \right) = \psi + \alpha \quad (17.76)$$

$$\text{Region 3 : } \frac{1}{\bar{r}^2} \frac{\partial}{\partial \bar{r}} \left(\bar{r}^2 \frac{\partial \psi}{\partial \bar{r}} \right) = (1 + \alpha Z) \psi. \quad (17.77)$$

The reasons for these approximations are as follows:

In region 1, $\psi \gg 1$ so that the ion density is given in principle by Eq.(17.72) which would give a right hand side scaling as $\sqrt{\psi}$. This ion term would dominate the electron and dust terms since the latter are always less than unity in this region. Thus, keeping just the ion term on the right hand side, Poisson's equation in region 1 reduces to

$$\underbrace{\frac{1}{\bar{r}^2} \frac{\partial}{\partial \bar{r}} \left(\bar{r}^2 \frac{\partial \psi}{\partial \bar{r}} \right)}_{\text{vacuum}} \simeq \underbrace{\frac{2}{\sqrt{\pi \psi}} \psi}_{\text{ion}}; \quad (17.78)$$

however, the ion term above can be neglected compared to the vacuum term because $\sqrt{\psi} \gg 1$ since $\psi \gg 1$. Thus Poisson's equation can be approximated in region 1 by just the vacuum term. This assumption is quite good near the dust grain surface where ψ is indeed very large compared to unity, but becomes marginal when ψ approaches unity at the outer limit of region 1.

In region 2, the ions have a Boltzmann distribution so $n_i/n_{e0} = 1 + \psi$. Since $T_i/T_e \ll 1$, the normalized electron density is $n_e/n_{e0} = \exp(-\psi T_i/T_e) \simeq 1$. Because $\bar{Z}\psi \gg 1$, the dust density is nearly zero in this region.

In region 3, Eq.(17.74) approximates to

$$\underbrace{\frac{1}{\bar{r}^2} \frac{\partial}{\partial \bar{r}} \left(\bar{r}^2 \frac{\partial \psi}{\partial \bar{r}} \right)}_{\text{vacuum}} \simeq \underbrace{1 + \psi}_{\text{ions}} - \underbrace{(1 - \alpha) \left(1 - \frac{\psi T_i}{T_e} \right)}_{\text{electrons}} - \underbrace{(1 - \bar{Z}\psi) \alpha}_{\text{dust}} \\ \simeq (1 + \alpha \bar{Z}) \psi \quad (17.79)$$

where $T_i/T_e \ll 1$ has been used. For finite α , the dust term dominates because $\alpha \bar{Z} \gg 1$.

The system has two boundary conditions, one at the dust grain surface and the other at infinity. The former occurs in region 1 and is set by the radial electric field on the dust grain surface. This boundary condition is obtained from Gauss' law which relates $\partial\psi/\partial\bar{r}$ at the dust grain surface to the dust grain charge and radius. The boundary condition at infinity can be considered as the large \bar{r} limit for region 3 and requires ψ to vanish as \bar{r} goes to infinity.

If the same form of Poisson's equation were to characterize regions 1, 2, and 3, then the system would be governed by a single second-order ordinary differential equation and the two boundary conditions described in the previous paragraph would suffice to give a unique solution. However, the equations in regions 1, 2, and 3 differ from each other and so must be solved separately with appropriate matching at the two interfaces between these three regions. The criteria for matching at the interfaces, determined by integrating Poisson's equation twice across each interface, are that both ψ and its radial derivative must be continuous at each interface. An important feature of this analysis is that the locations of the two interfaces are unknowns to be determined by solving the matching problem. Since regions 1 and 2 are of finite extent, both decaying and non-decaying ψ solutions are allowed in these regions. However, only a decaying solution is allowed in region 3.

Region 1, which is governed by Eq.(17.75), has vacuum-like solutions of the form $\psi \sim c\bar{r}^{-1} + d$ where c and d are constants. The constant c is chosen to give the correct radial electric field at the surface of the dust grain test charge and d is chosen so that $\psi = 1$ at \bar{r}_i which is the as-yet undetermined location of the interface between regions 1 and 2.

Using Gauss's law to prescribe the radial electric field at the dust grain surface and also choosing d so that $\psi = 1$ at $\bar{r} = \bar{r}_o$ gives

$$\psi_1(\bar{r}) = \frac{\frac{\alpha \bar{a}^3}{3} + \left(1 - \frac{1}{\bar{r}_i} \frac{\alpha \bar{a}^3}{3}\right) \bar{r}}{\bar{r}}. \quad (17.80)$$

In region 2, which is governed by Eq.(17.76), the effective dependent variable is $\psi + \alpha$ which has growing and decaying Yukawa-like solutions $\sim \exp(\pm \bar{r})/\bar{r}$. It is convenient to write the region 2 solution as

$$\psi_2(\bar{r}) = \frac{\bar{r}_o \left(\frac{1}{\bar{Z}} + \alpha\right) \cosh(\bar{r} - \bar{r}_o) + B \sinh(\bar{r} - \bar{r}_o) - \alpha \bar{r}}{\bar{r}} \quad (17.81)$$

where the coefficients have been chosen so that $\psi = 1/\bar{Z}$ at \bar{r}_o , the as-yet undetermined location of the interface between regions 2 and 3. The coefficient B is also undetermined for now, and it should be noted that ψ is independent of B at $\bar{r} = \bar{r}_o$.

Region 3, governed by Eq.(17.77), has a solution which can be expressed as

$$\psi_3(\bar{r}) = \frac{\bar{r}_o}{\bar{Z}\bar{r}} \exp\left(-\sqrt{\alpha\bar{Z} + 1}(\bar{r} - \bar{r}_o)\right) \quad (17.82)$$

where the coefficients have been chosen to give $\psi = 1/\bar{Z}$ at \bar{r}_o , the interface between regions 2 and 3.

The condition that $\partial\psi/\partial\bar{r}$ is continuous at \bar{r}_o gives

$$B = \alpha - \frac{\bar{r}_o}{\bar{Z}} \sqrt{\alpha\bar{Z} + 1} \quad (17.83)$$

and this result completes the matching process at \bar{r}_o since both ψ and $\partial\psi/\partial\bar{r}$ have now been arranged to be continuous at \bar{r}_o . Since $\psi_1 = 1$ has already been arranged at \bar{r}_i , in order to have continuity of ψ at \bar{r}_i it is necessary to set $\psi_2 = 1$ at \bar{r}_i , i.e.,

$$\bar{r}_i = \bar{r}_o \left(\frac{1}{\bar{Z}} + \alpha\right) \cosh(\bar{r}_i - \bar{r}_o) + B \sinh(\bar{r}_i - \bar{r}_o) - \alpha \bar{r}_i. \quad (17.84)$$

All that remains to be done is to arrange for continuity of $\partial\psi/\partial\bar{r}$ at $\bar{r} = \bar{r}_i$. Since ψ has already been arranged to be continuous at $\bar{r} = \bar{r}_i$, continuity of $\partial(\bar{r}\psi)/\partial\bar{r}$ at $\bar{r} = \bar{r}_i$ implies continuity of $\partial\psi/\partial\bar{r}$. This means that continuity of $\partial\psi/\partial\bar{r}$ at $\bar{r} = \bar{r}_i$ is attained by equating the derivatives of the numerators of the right hand sides of Eqs.(17.80) and (17.81) at \bar{r}_i , i.e., continuity of $\partial\psi/\partial\bar{r}$ at $\bar{r} = \bar{r}_i$ is attained by setting

$$1 - \frac{1}{\bar{r}_i} \frac{\alpha \bar{a}^3}{3} = \bar{r}_o \left(\frac{1}{\bar{Z}} + \alpha\right) \sinh(\bar{r}_i - \bar{r}_o) + B \cosh(\bar{r}_i - \bar{r}_o) - \alpha. \quad (17.85)$$

Since $\bar{Z} \gg 1$ and α is of order unity, Eqs.(17.84) and (17.85) can be approximated as

$$(1 + \alpha) \bar{r}_i = \alpha \bar{r}_o \cosh(\bar{r}_i - \bar{r}_o) + \alpha \sinh(\bar{r}_i - \bar{r}_o) \quad (17.86)$$

$$1 + \alpha - \frac{1}{\bar{r}_i} \frac{\alpha \bar{a}^3}{3} = \alpha \bar{r}_o \sinh(\bar{r}_i - \bar{r}_o) + \alpha \cosh(\bar{r}_i - \bar{r}_o). \quad (17.87)$$

These constitute two coupled nonlinear equations in the unknowns \bar{r}_i and \bar{r}_o and can be solved numerically. Since the parameters α and \bar{a} in these equations are functions of position in dusty plasma parameter space, Eqs.(17.86) and (17.87) can be solved for \bar{r}_i and \bar{r}_o at any point in dusty plasma parameter space. Because a different solution set $\{\bar{r}_i, \bar{r}_o\}$ exists at each point in dusty plasma parameter space, \bar{r}_i and \bar{r}_o may be considered as functions of position in dusty plasma parameter space, i.e., $\bar{r}_i = \bar{r}_i(\bar{a}, \bar{r}_d)$ and $\bar{r}_o = \bar{r}_o(\bar{a}, \bar{r}_d)$.

Now consider the density of the field dust grains in the vicinity of $\bar{r} = \bar{r}_o$. For $\bar{r} > \bar{r}_o$ the normalized potential is prescribed by Eq.(17.82) and decays at the dust Debye length which is an extremely short length because $\bar{Z} \gg 1$. This precipitous spatial attenuation of ψ for $\bar{r} > \bar{r}_o$ means that dust grains are completely shielded from each other when their separation distance slightly exceeds \bar{r}_o . If this is the case, then the dust grains will not interact with each other; i.e., they can be considered as a gas of non-interacting particles. On the other hand, if $\bar{r} < \bar{r}_o$, the normalized potential ψ then exceeds $1/\bar{Z}$ and the dust grains will experience a strong mutual repulsion. This abrupt change-over is implicit in Eq.(17.61) which indicates that n_d/n_{d0} is near unity when $\psi \ll 1/\bar{Z}$ (i.e., just outside $\bar{r} = \bar{r}_o$) but near zero when ψ becomes significantly larger than $1/\bar{Z}$ (i.e., just inside $\bar{r} = \bar{r}_o$). Hence, a dust grain test particle can be considered as a hard sphere of radius \bar{r}_o when interacting with field dust grains.

Since the nominal separation between dust grains is \bar{a} , if $\bar{a} > \bar{r}_o$ then each dust grain is completely shielded from its neighbors in which case the dust grains behave as an ideal gas of non-interacting particles. However, if $\bar{a} < \bar{r}_o$ is attempted, each dust grain experiences the full, unshielded repulsive force of its neighbors. This extreme repulsive force means that it is not possible for \bar{a} to become less than \bar{r}_o . In effect, each dust grain sees its neighbor as a hard sphere of radius \bar{r}_o . Thus, when $\bar{a} = \bar{r}_o$ the collection of pressed-together dust grains should form a regularly spaced lattice structure with lattice spacing of order $\bar{a} = \bar{r}_o$. The dusty plasma has thus crystallized.

The condition for crystallization of a dusty plasma is thus

$$\bar{a} \leq \bar{r}_o(\bar{a}, \bar{r}_d) \quad (17.88)$$

which defines a curve in dusty plasma parameter space. Figure 17.4 shows a plot of contours of \bar{r}_o/\bar{a} in dusty plasma parameter space; for reference the region in parameter space associated with the Chu and I dusty plasma crystallization experiment is indicated as a bold line (as mentioned before, the finite length of this line corresponds to the density measurement error bars). The contour $\bar{r}_o(\bar{a}, \bar{r}_d)/\bar{a} = 1$ gives the crystallization condition; above this contour the dust grains are crystallized. It is also necessary to have \bar{r}_d small as was specified in Eq.(17.13) so that ψ_d is not attenuated from its vacuum value by the effect of the shielding cloud.

Figure 17.5 shows plots of $\log_{10} \psi$, ψ , $10^4 \psi$, n_e/n_{e0} , n_i/n_{i0} , and n_d/n_{d0} as functions of \bar{r} for a dusty plasma on the verge of condensation. The functional form of ψ is obtained from the \bar{r}_i and \bar{r}_o values determined by solving Eqs.(17.86) and (17.87). The extremely rapid cutoff of the potential at \bar{r}_o , the interface between regions 2 and 3 is evident; the characteristic scale of this cut-off is the dust Debye length. The normalized densities are plotted using Eqs.(17.60), (17.68), and (17.61). The field dust grain density vanishes for \bar{r}

inside \bar{r}_o , consistent with the hard-sphere behavior of the dust grain test particle. Although ψ is tiny at the interface between regions 2 and 3, it nevertheless affects the average dust grain density profile at this location because of the extremely large charge on the dust grains.

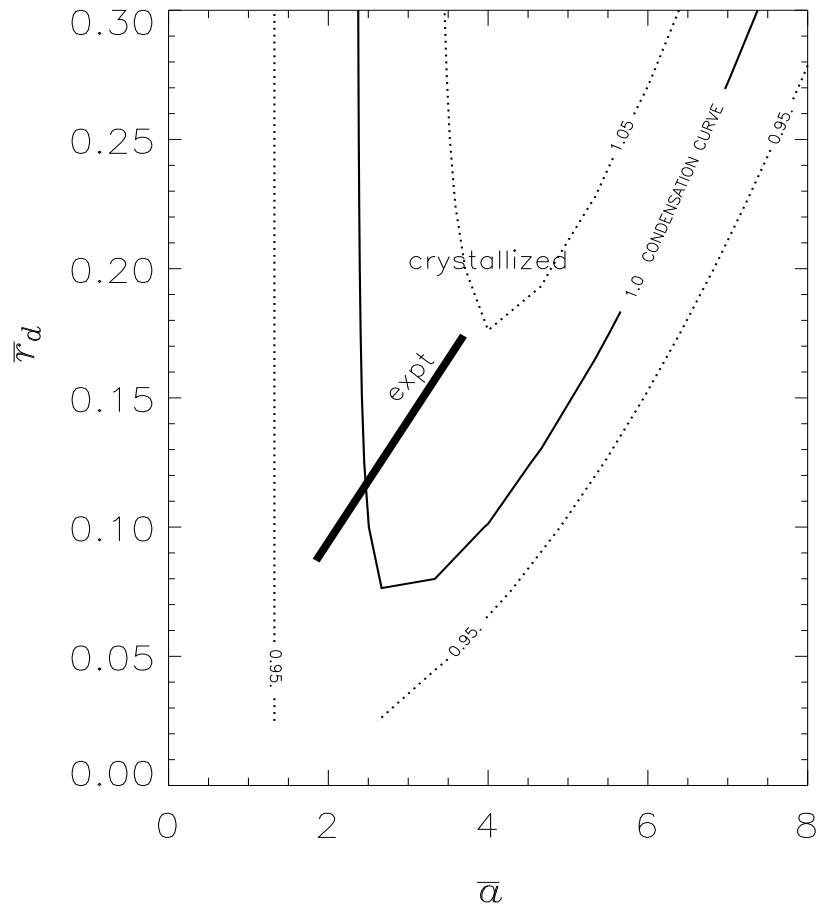


Figure 17.4: Contours of \bar{r}_o/\bar{a} as determined from solution to matching problem. Condensation (crystallization) is predicted to occur above the $\bar{r}_o/\bar{a} = 1$ line. Chu and I (1994) crystallization experiment, shown as bold line, is seen to lie in the condensation region.

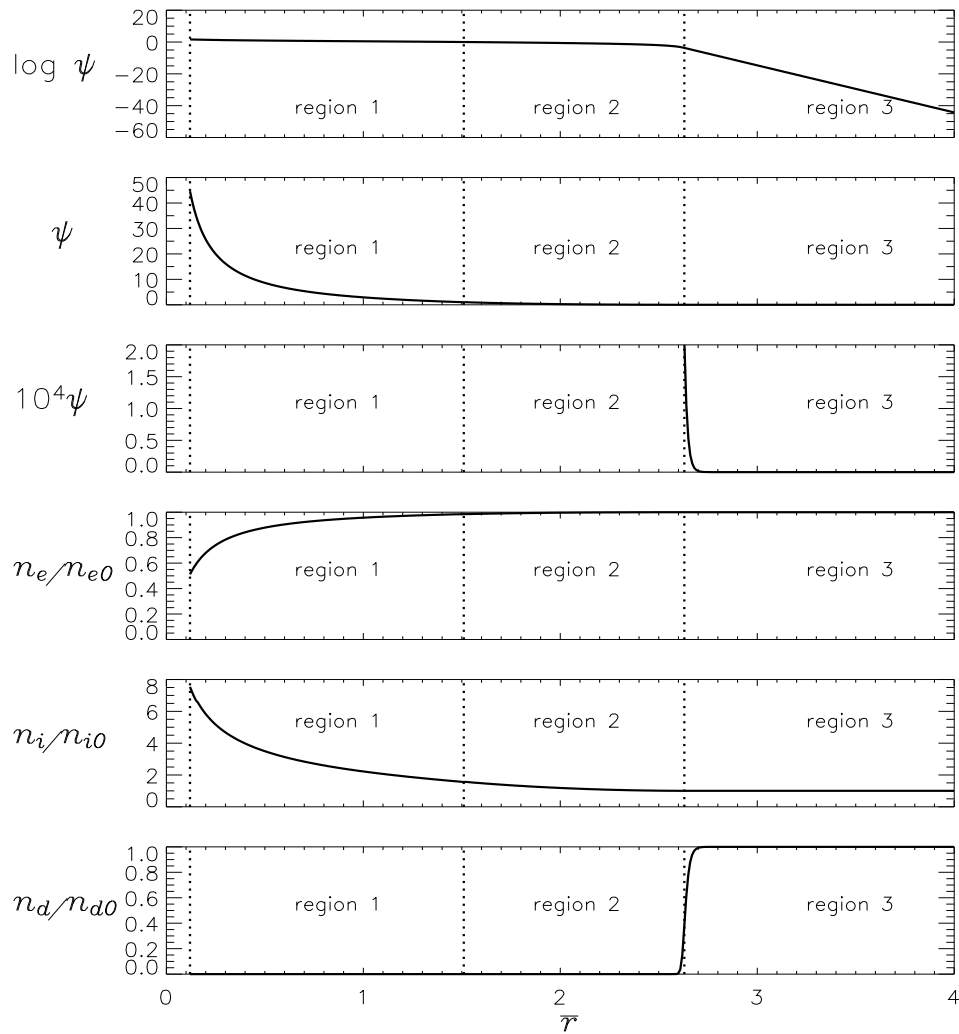


Figure 17.5: Plots of $\log_{10} \psi$, ψ , $10^4 \psi$, n_e/n_{e0} , n_i/n_{i0} , and n_d/n_{d0} as functions of \bar{r} for a dusty plasma on the verge of condensation. Dust grain radius is at left of region 1, parameters are from Bellan (2004b).

17.8 Assignments

1. Assuming $T_e = 3$ eV, $T_i = 0.03$ eV, and $n_i = 10^9$ cm⁻³, estimate to within an order of magnitude how long it would take for 5 μ m dust grains with density $n_d = 10^5$ cm⁻³ to become fully charged. Hint- estimate the initial electron current impinging on a dust grain and compare this to the final charge on the dust grain. Use Fig. 17.3 to estimate Z_d .
2. Orbital motion limit and angular momentum: The (OML) approximation ignores the effective potential resulting from centrifugal force. The validity of this approximation is examined here for the cases of an algebraically decaying central force and an exponentially decaying central force.

- (a) Show that when centrifugal force is taken into account, the radial equation of motion for a particle in a spherically symmetric electrostatic potential $\phi(r)$ is

$$m\ddot{r} = -\frac{\partial\chi}{\partial r}$$

where the effective potential χ is given by

$$\chi = q\phi(r) + \frac{mb^2v^2}{2r^2}$$

and m, b , and v are defined as in Sec. 17.2.

- (b) Show that if $q\phi$ is negative, a local minimum of the effective potential exists at some radial position r_1 ; compare this situation to planetary motion in the solar system.
- (c) Show that if $q\phi \sim -r^{-n}$ there can also be a local maximum at a radius r_2 where $r_2 > r_1$ providing n satisfies a certain condition. What is this condition for n ? Plot $\chi(r)$ for the situation where there is a local maximum. Can a particle incident from infinity reach r_1 if its energy is less than $\chi(r_2)$. What sort of condition does this place m, v , and b . Under what circumstances is the OML approximation valid? Plot trajectories for the situations where the OML approximation is valid and situations where it fails. Comment on whether OML is a reasonable approximation for dust charging.
- (d) Repeat (c) above for the situation where $q\phi \sim -\exp(-r/\lambda)$.
3. Assume the OML approximation is valid so that the effective potential can be considered to have a minimum in the vicinity of a negatively charged dust particle. Show that, if an incident ion does not hit the dust grain, it will reflect back to infinity. Show that a collision could cause an incident ion to be trapped in the effective potential well at r_1 as discussed in problem 1b. Once an ion becomes trapped how long would it stay trapped?
4. Dust Alfvén waves: Show that for waves with frequency below the dust grain cyclotron frequency, a dusty plasma will support MHD Alfvén waves with dispersion $\omega^2 = k_z^2 v_A^2$ where $v_A^2 = B^2/n_d m_d$.

5. Dust whistler waves: Show that a dusty plasma with $\alpha \simeq 1$ will support whistler-like waves with dispersion $\omega \simeq \omega_{ci} \cos \theta$ where $\omega_{cd} \ll \omega \ll \omega_{ci}$.
6. Make a plot like Fig. 17.3 for a dusty plasma with $T_e = T_i$ and discuss whether such a plasma could condense and form crystals.
7. Consider a methane plasma consisting of CH_4 ions and electrons. Assume that there exist some infinitesimal dust nuclei at $t = 0$ and that these become negatively charged as discussed in Sec. 17.2.
Further assume that any methane ion hitting the dust grain sticks to the dust grain so that the mass of the dust grain increases with time. Plot the dust grain radius as a function of time. How long would it take for the dust grains to become sufficiently large to form a crystal (assume that $n_d = 10^5 \text{ cm}^{-3}$, $T_e/T_i = 100$, $\lambda_{di} = 100 \text{ } \mu\text{m}$)?
8. Consider a weakly ionized dusty plasma with $5 \text{ } \mu\text{m}$ diameter dust grains, 3 eV electrons and room temperature (0.025 eV) argon ions. The dusty plasma is located above a horizontal metal plate lying in the $z = 0$ plane. Because electrons move faster than ions and dust grains, the electron flux to the metal plate is initially much larger than the ion or dust grain flux. The faster rate of loss for electrons causes the dusty plasma to become positively charged so that an electric field develops which tends to retard the electrons and accelerate the ions towards the metal plate. Thus, the plasma potential is positive with respect to the metal plate and if the plasma potential is defined to be zero, then the metal plate has a negative potential, say ϕ_{plate} . The electron flux to the plate will thus be

$$\Gamma_e = nv_{Te} \exp(-q_e \phi_{plate} / \kappa T_e)$$

and, using a sheath analysis as in Section 2.7, the ion flux to the plate is

$$\Gamma_i = nc_s$$

where $c_s = \sqrt{\kappa T_e / m_i}$ is the ion acoustic velocity. In equilibrium, the electron and ion fluxes will balance so that

$$\exp(-q_e \phi_{plate} / \kappa T_e) = \sqrt{\frac{m_e}{m_i}}$$

or

$$\phi_{plate} = -\frac{T_e}{2} \ln \frac{m_i}{m_e}$$

where the temperature is expressed in electron volts. The change in potential will occur over a distance of the order of the electron Debye length going from the plate to the bulk plasma so that

$$\phi(z) = -\frac{T_e}{2} \exp(-z/\lambda_{De}) \ln \frac{m_i}{m_e}$$

where z is the distance above the metal plate. By considering the combined effect of the vertical electric field associated with this potential and of gravity acting on a dust grain show that dust grains will tend to levitate above the metal plate. Plot the potential energy of dust grains in the combination of the electrostatic and gravitational

potential fields. Assume that $Z_d = 10^4$ and that the dust grains are made of a material which has a mass density of 1 gm/cc.

9. Suppose a negatively charged dust grain has a charge Z_d and a radius r_d . Show that the potential on the surface of the dust grain is much less than $Z_d/4\pi\epsilon_0 r_d$ if $r_d \gg \lambda_D$ where λ_D is the nominal shielding length for the shielding cloud around the dust grain. What implication does this have for dust charging theory and why do interesting dusty plasmas typically have $r_d \ll \lambda_D$?

Bibliography and suggested reading

- Bateman G 1978 *MHD instabilities* MIT Press Cambridge, Mass.
- Bellan P M 2000 *Spheromaks : a practical application of magnetohydrodynamic dynamos and plasma self-organization* Imperial College Press London.
- Birdsall C K & Langdon A B 1985 *Plasma physics via computer simulation* McGraw Hill New York.
- Boyd T J M & Sanderson J J 2003 *The physics of plasmas* Cambridge University Press Cambridge, U.K.; New York.
- Chen F F 1984 *Introduction to plasma physics and controlled fusion* 2nd edn: Plenum Press New York.
- Cramer N F 2001 *The physics of Alfvén waves* Wiley-VCH Berlin; New York.
- Davidson R C 1972 *Methods in nonlinear plasma theory* Academic Press New York,.
- Davidson R C 2001 *Physics of nonneutral plasmas* Imperial College Press ; World Scientific London Singapore ; River Edge, NJ.
- Drazin P & Johns R 1989 *Solitons: an Introduction* Cambridge University Press Cambridge [England].
- Freidberg J P 1987 *Ideal magnetohydrodynamics* Plenum Press New York.
- Goldston R J & Rutherford P H 1995 *Introduction to plasma physics* Institute of Physics Publishing.
- Hasegawa A & Uberoi C 1982 *The Alfvén Wave* National Technical Information Service, U.S. Department of Commerce, 1982 Oak Ridge, Tenn.
- Hutchison I H 2002 *Principles of plasma diagnostics* 2nd edn Cambridge University Press Cambridge [England]; New York.
- Kadomtsev B B 1965 *Plasma turbulence* Academic Press London, New York,.
- Kivelson M G & Russell C T 1995 *Introduction to space physics* Cambridge University Press Cambridge [England]; New York.
- Krall N A & Trivelpiece A W 1973 *Principles of plasma physics* McGraw-Hill New York.
- Landau L D & Lifshits E M 1989 *Mechanics* Teoreticheskaya fizika (Izd. 3-e). v. 1. 3rd rev. english, repr. with corrections. edn Pergamon Press Oxford; New York.
- Mathews J & Walker R L 1965 *Mathematical methods of physics* W.A. Benjamin New York.
- Melrose D B 1986 *Instabilities in space and laboratory plasmas* Cambridge University Press Cambridge [England]; New York.
- Miyamoto K 1989 *Plasma physics for nuclear fusion* rev. edn MIT Press Cambridge, Mass.
- Moffatt H K 1978 *Magnetic field generation in electrically conducting fluids* Cambridge University Press Cambridge [England]; New York.
- Nicholson D R 1992 *Introduction to plasma theory* Krieger Pub. Co. Malabar, Fla.
- Sagdeev R Z & Galeev A 1969 *Nonlinear plasma theory* Frontiers in physics; v. 34. W. A. Benjamin New York,.

- Schmidt G 1979 *Physics of high temperature plasmas* Academic Press New York.
- Shukla P K & Mamun A A 2002 *Introduction to dusty plasma physics* Institute of Physics Publishing Bristol.
- Stix T H 1992 *Waves in plasmas* American Institute of Physics New York.
- Storey L R O 1956 *Scientific American* **194**, 34.
- Sturrock P A 1994 *Plasma physics : an introduction to the theory of astrophysical, geophysical, and laboratory plasmas* Cambridge University Press Cambridge [England]; New York.
- Swanson D G 2003 *Plasma waves* Series in plasma physics. 2nd edn Institute of Physics Publishing Bristol; Philadelphia.

References

- Alfven, H.: 1943, On the existence of electromagnetic-hydrodynamic waves, *Arkiv Mat. Astron. Fysik* **B29**, 2.
- Allen, J., Boyd, R. and Reynolds, P.: 1957, The collection of positive ions by a probe immersed in a plasma, *Proceedings of the Physical Society of London Section B* **70**, 297.
- Allis, W. P.: 1955, Waves in a plasma, *MIT Res. Lab Electronics Quarterly Report*, Vol. 54, p. 5.
- Appleton, E. V.: 1932, Wireless studies of the ionosphere, *J. Inst. Elec. Engrs.* **71**, 642.
- Bachman, D. and Gould, R.: 1996, Landau-like damping in rotating pure electron plasmas, *IEEE Trans. Plasma Science* **24**, 14.
- Barkan, A., D'Angelo, N. and Merlino, R.: 1996, Experiments on ion-acoustic waves in dusty plasmas, *Planetary and Space Science* **44**, 239.
- Barkan, A., Merlino, R. and D'Angelo, N.: 1995, Laboratory observation of the dust-acoustic wave mode, *Physics of Plasmas* **2**, 3563.
- Barkhausen, H.: 1930, Whistling tones from the Earth, *Proc. Inst. Radio Engrs.* **18**, 1115.
- Barnes, A.: 1977, Geometrical meaning of curl operation when $\mathbf{A} \cdot \text{curl } \mathbf{A} \neq 0$, *American Journal of Physics* **45**, 371.
- Bateman, G.: 1978, *MHD Instabilities*, MIT Press, Cambridge, Mass.
- Bellan, P.: 1992, Vorticity model of flow driven by purely poloidal currents, *Physical Review Letters* **69**, 3515.
- Bellan, P. M.: 2003, Why current-carrying magnetic flux tubes gobble up plasma and become thin as a result, *Physics of Plasmas* **10**, 1999.
- Bellan, P. M.: 2004a, A microscopic, mechanical derivation of the adiabatic gas relation, *American Journal of Physics* **72**, 679.
- Bellan, P. M.: 2004b, A model for the condensation of a dusty plasma, *Physics of Plasmas* **11**, 3368.
- Bellan, P. and Porkolab, M.: 1975, Excitation of lower-hybrid waves by a slow-wave structure, *Physical Review Letters* **34**, 124.
- Bennett, W. H.: 1934, Magnetically self-focussing streams, *Physical Review* **45**, 890.
- Berger, M. and Field, G.: 1984, The topological properties of magnetic helicity, *Journal of Fluid Mechanics* **147**, 133.
- Bernstein, I.: 1958, Waves in a plasma in a magnetic field, *Physical Review* **109**, 10.
- Bernstein, I. B. and Engelmann, F.: 1966, Quasi-linear theory of plasma waves, *Physics of Fluids* **9**, 937.
- Bernstein, I., Frieman, E., Kruskal, M. and Kuslud, R.: 1958, An energy principle for hydromagnetic stability problems, *Proceedings of the Royal Society of London Series A-Mathematical and Physical Sciences* **244**, 17.

- Birdsall, C. K. and Langdon, A. B.: 1985, *Plasma physics via computer simulation*, McGraw Hill, New York.
- Bohm, D. and Gross, E.: 1949, Theory of plasma oscillations. A. Origin of medium-like behavior, *Physical Review* **75**, 1851.
- Braginskii, S. I.: 1965, Transport processes in a plasma, *Reviews of Plasma Physics* **1**, 205.
- Briggs, R. J., Daugherty, J. and Levy, R.: 1970, Role of Landau damping in crossed-field electron beams and inviscid shear flow, *Physics of Fluids* **13**, 421.
- Brillouin, L.: 1926, La mecanique ondulatoire de Schrodinger, une methode generale de resolution par approximations successives, *Compt. Rend.* **183**, 24.
- Calugareanu, G.: 1959, L'intégrale de Gauss et l'analyse des nuds tridimensionnels, *Rev. Math. Pures Appl.* **4**, 5.
- Chew, G., Goldberger, M. and Low, F.: 1956, The Boltzmann equation and the one-fluid hydromagnetic equations in the absence of particle collisions, *Proceedings of the Royal Society of London Series A-Mathematical and Physical Sciences* **236**, 112.
- Chu, J. and I, L.: 1994, Direct observation of Coulomb crystals and liquids in strongly coupled rf dusty plasmas, *Physical Review Letters* **72**, 4009.
- Clemmow, P. C. and Mullaly, R. F.: 1955, Dependence of the refractive index in magneto-ionic theory on the direction of the wave normal, *Physics of the ionosphere: Report of Phys. Soc. Conf. Cavendish Lab.*, Physical Society, London, p. 340.
- Crawford, F.: 1965, Cyclotron harmonic waves in warm plasmas, *Journal of Research of the National Bureau of Standards, Section D- Radio Science* **D 69**, 789.
- Davidson, R. C.: 2001, *Physics of nonneutral plasmas*, Imperial College Press; World Scientific, London Singapore; River Edge, NJ.
- Debye, P. and Huckel, E.: 1923, *Physik. Zeits.* **24**, 185.
- Drazin, P. and Johns, R.: 1989, *Solitons: an Introduction*, Cambridge University Press, Cambridge.
- Drecier, H.: 1959, Electron and ion runaway in a fully ionized gas. 1., *Physical Review* **115**, 238.
- Drummond, W. and Pines, D.: 1962, Non-linear stability of plasma oscillations, *Nuclear Fusion* p. 1049.
- Eckersley, T. L.: 1935, Musical atmospherics, *Nature* **135**, 104.
- Fermi, E.: 1954, Galactic magnetic fields and the origin of cosmic radiation, *Astrophysical Journal* **119**, 1.
- Fisch, N.: 1978, Confining a tokamak plasma with rf-driven currents, *Physical Review Letters* **41**, 873.
- Fisher, R. and Gould, R.: 1969, Resonance cones in field pattern of a short antenna in an anisotropic plasma, *Physical Review Letters* **22**, 1093.
- Fisher, R. and Gould, R.: 1971, Resonance cones in field pattern of a radio frequency probe in a warm anisotropic plasma, *Physics of Fluids* **14**, 857.
- Furth, H., Killeen, J. and Rosenbluth, M.: 1963, Finite-resistivity instabilities of a sheet pinch, *Physics of Fluids* **6**, 459.
- Gardner, C., Greene, J., Kruskal, M. and Miura, R.: 1967, Method for solving Korteweg-deVries equation, *Physical Review Letters* **19**, 1095.
- Gould, R.: 1995, Dynamics of nonneutral plasmas, *Physics of Plasmas* **2**, 2151.

- Gould, R., O'Neil, T. and Malmberg, J.: 1967, Plasma wave echo, *Physical Review Letters* **19**, 219.
- Grad, H. and Rubin, H.: 1958, MHD equilibrium in an axisymmetric toroid, *Proceedings of the 2nd U.N. Conf. on the Peaceful uses of Atomic Energy*, Vol. 31, IAEA, Vienna, p. 190.
- Hansen, J. F. and Bellan, P. M.: 2001, Experimental demonstration of how strapping fields can inhibit solar prominence eruptions, *Astrophysical Journal* **563**, L183.
- Havnes, O., Goertz, C., Morfill, G., Grun, E. and Ip, W.: 1987, Dust charges, cloud potential, and instabilities in a dust cloud embedded in a plasma, *Journal of Geophysical Research - Space Physics* **92**, 2281.
- Hayashi, Y. and Tachibana, K.: 1994, Observation of Coulomb-crystal formation from carbon particles grown in a methane plasma, *Japanese Journal of Applied Physics Part 2 - Letters* **33**, L804.
- Hudgings, D., Meger, R., Striffler, C., Destler, W., Kim, H., Reiser, M. and Rhee, M.: 1978, Trapping of cusp-injected, nonneutral, electron-rings with resistive walls and static mirror coils, *Physical Review Letters* **40**, 764.
- Ikezi, H.: 1986, Coulomb solid of small particles in plasmas, *Physics of Fluids* **29**, 1764.
- Jackson, J.: 1998, *Classical Electrodynamics*, Wiley, New York. Third Edition.
- Jeans, J. H.: 1915, *Monthly Notices of the Royal Astronomical Society* **76**, 70.
- Kim, H., Stenzel, R. and Wong, A.: 1974, Development of cavitons and trappings of rf field, *Physical Review Letters* **33**, 886.
- Klimchuk, J.: 2000, Cross-sectional properties of coronal loops, *Solar Physics* **193**, 53.
- Korteweg, D.: 1895, On the change of form of long waves advancing in a rectangular canal and on a new type of long stationary waves, *Philos. Mag.* **39**, 422.
- Kramers, H. A.: 1926, Wellenmechanik und halbzahlige quantisierung, *Z. Physik.* **39**, 828.
- Kribel, R., Shinsky, K., Phelps, D. and Fleischmann, H.: 1974, Generation of field-reversing electron rings by neutralized-cusp injection into a magnetic-mirror trap, *Plasma Physics and Controlled Fusion* **16**, 113.
- Kruskal, M. D. and Schwarzschild, M.: 1954, Some instabilities of a completely ionized plasma, *Proceedings of the Royal Society of London. Series A, Mathematical and Physical Sciences* **223**, 348.
- Kruskal, M., Johnson, J., Gottlieb, M. and Goldman, L.: 1958, Hydromagnetic instability in a stellarator, *Physics of Fluids* **1**, 421.
- Laframboise, J. and Parker, L.: 1973, Probe design for orbit-limited current collection, *Physics of Fluids* **16**, 629.
- Landau, L.: 1946, On the vibrations of the electronic plasma, *J. Physics (U.S.S.R.)* **10**, 25.
- Langmuir, I.: 1928, Oscillations in ionized gases, *Proceedings of the National Academy of Sciences* **14**, 627.
- Leuterer, F.: 1969, Forward and backward Bernstein waves, *Plasma Physics* **11**, 615.
- Livio, M.: 1999, Astrophysical jets: a phenomenological examination of acceleration and collimation, *Physics Reports - Review Section of Physics Letters* **311**, 225.
- Lundquist, S.: 1950, A, *Arkiv for Fysik* **B2**, 361.

- Maecker, H.: 1955, Plasmastromungen in lichtbogen infolge eigenmagnetischer kompression, *Z. Physik* **141**, 198.
- Malmberg, J.: 1992, Some recent results with nonneutral plasmas, *Plasma Physics and Controlled Fusion* **34**, 1767.
- Malmberg, J. and de Grassie, J.: 1975, Properties of nonneutral plasma, *Physical Review Letters* **35**, 577.
- Malmberg, J. and Wharton, C.: 1964, Collisionless damping of electrostatic plasma waves, *Physical Review Letters* **13**, 184.
- Malmberg, J., Wharton, C., Gould, R. and O'Neil, T.: 1968, Plasma wave echo experiment, *Physical Review Letters* p. 95.
- Manley, J. and Rowe, H.: 1956, Some general properties of nonlinear elements .1. General energy relations, *Proceedings of the Institute of Radio Engineers* **44**, 904.
- Marshall, J.: 1960, Performance of a hydromagnetic plasma gun, *Physics of Fluids* **3**, 134.
- McChesney, J., Stern, R. and Bellan, P.: 1987, Observations of fast stochastic ion heating by drift waves, *Physical Review Letters* **59**, 1436.
- Melzer, A., Trottenberg, T. and Piel, A.: 1994, Experimental-determination of the charge on dust particles forming Coulomb lattices, *Physics Letters A* **191**, 301.
- Moffatt, H. K.: 1978, *Magnetic field generation in electrically conducting fluids*, Cambridge University Press, Cambridge.
- Moffatt, H. and Ricca, R.: 1992, Helicity and the Calugareanu invariant, *Proceedings of the Royal Society of London Series A-Mathematical Physical and Engineering Sciences* **439**, 411.
- Moncuquet, M., Meyervernet, N. and Hoang, S.: 1995, Dispersion of electrostatic-waves in the Io plasma torus and derived electron-temperature, *Journal of Geophysical Research - Space Physics* **100**, 21697.
- Morfill, G., Annaratone, B., Bryant, P., Ivlev, A., Thomas, H., Zuzic, M. and Fortov, V.: 2002, A review of liquid and crystalline plasmas - new physical states of matter?, *Plasma Physics and Controlled Fusion* **44**, B263.
- Nefedov, A., Morfill, G., Fortov, V., Thomas, H., Rothermel, H., Hagl, T., Ivlev, A., Zuzic, M., Klumov, B., Lipaev, A., Molotkov, V., Petrov, O., Gidzenko, Y., Krikalev, S., Shepherd, W., Ivanov, A., Roth, M., Binnenbruck, H., Goree, J. and Semenov, Y.: 2003, PKE-Nefedov: plasma crystal experiments on the International Space Station, *New Journal of Physics* **5**, art. no.-33.
- Nishikawa, K.: 1968a, Parametric excitation of coupled waves .2. Parametric plasmon-photon interaction, *Journal of the Physical Society of Japan* **24**, 1152.
- Nishikawa, K.: 1968b, Parametric excitation of coupled waves .I. General formulation, *Journal of the Physical Society of Japan* **24**, 916.
- O'Neil, T.: 1995, Plasmas with a single sign of charge (an overview), *Physica Scripta* **T59**, 341.
- Parker, E. N.: 1957, Sweet's mechanism for merging magnetic fields in conducting fluids, *Journal of Geophys. Research* **62**, 509.
- Penrose, O.: 1960, Electrostatic instabilities of a uniform non-maxwellian plasma, *Physics of Fluids* **3**, 258.
- Rosenbluth, M., Macdonald, W. and Judd, D.: 1957, Fokker-Planck equation for an inverse-

- square force, *Physical Review* **107**, 1.
- Sagdeev, R. Z. and Galeev, A.: 1969, *Nonlinear plasma theory*, W. A. Benjamin, New York,.
- Schechter, D., Dubin, D., Cass, A., Driscoll, C., Lansky, I. and O'Neil, T.: 2000, Inviscid damping of asymmetries on a two-dimensional vortex, *Physics of Fluids* **12**, 2397.
- Schmitt, J.: 1973, Dispersion and cyclotron damping of pure ion Bernstein waves, *Physical Review Letters* **31**, 982.
- Shafranov, V. D.: 1958, On magnetohydrodynamical equilibrium configurations, *Soviet Physics - JETP* **6**, 545.
- Shafranov, V. D.: 1966, Plasma equilibrium in a magnetic field, *Reviews of Plasma Physics*, Vol. 2, Consultants Bureau, New York, p. 103.
- Shukla, P. and Silin, V.: 1992, Dust ion-acoustic-wave, *Physica Scripta* **45**, 508.
- Silin, V.: 1965, Parametric resonance in a plasma, *Soviet Physics- JETP* **21**, 1127.
- Solovov, L. S.: 1976, *Reviews of Plasma Physics* **6**, 239.
- Spitzer, L. and Harm, R.: 1953, Transport phenomena in a completely ionized gas, *Physical Review* **89**, 977.
- Stasiewicz, K., Bellan, P., Chaston, C., Kletzing, C., Lysak, R., Maggs, J., Pokhotelov, O., Seyler, C., Shukla, P., Stenflo, L., Streltsov, A. and Wahlund, J.: 2000, Small scale Alfvénic structure in the aurora, *Space Science Reviews* **92**, 423.
- Stasiewicz, K., Lundin, R. and Marklund, G.: 2000, Stochastic ion heating by orbit chaotization on electrostatic waves and nonlinear structures, *Physica Scripta* **T84**, 60.
- Stenzel, R. and Wong, A.: 1972, Threshold and saturation of parametric decay instability, *Physical Review Letters* **28**, 274.
- Stix, T.: 1965, Radiation and absorption via mode conversion in an inhomogeneous collision-free plasma, *Physical Review Letters* **15**, 878.
- Stix, T. H.: 1962, *The theory of plasma waves*, McGraw-Hill, New York.
- Stix, T. H.: 1992, *Waves in plasmas*, American Institute of Physics, New York.
- Storey, L. R. O.: 1953, An investigation of whistling atmospherics, *Philosophical transactions of the Royal Society of London*. **246**, 113.
- Surko, C., Leventhal, M. and Passner, A.: 1989, Positron plasma in the laboratory, *Physical Review Letters* **62**, 901.
- Swanson, D. G.: 1989, *Plasma waves*, Academic Press, San Diego. see p.24 for discussion regarding Altar.
- Swanson, D. G.: 2003, *Plasma waves*, Series in plasma physics., 2nd edn, Institute of Physics Publishing, Bristol.
- Sweet, P. A.: 1958, The neutral point theory of solar flares, in B. Lehnert (ed.), *Electromagnetic Phenomena in Cosmical Physics*, Cambridge University Press.
- Taylor, J. B.: 1974, Relaxation of toroidal plasma and generation of reverse magnetic-fields, *Physical Review Letters* **33**, 1139.
- Thomas, H., Morfill, G., Demmel, V., Goree, J., Feuerbacher, B. and Mohlmann, D.: 1994, Plasma crystal - Coulomb crystallization in a dusty plasma, *Physical Review Letters* **73**, 652.
- Trivelpiece, A. and Gould, R.: 1959, Space charge waves in cylindrical plasma columns, *J.*

- Applied Phys.* **30**, 1784.
- Vedenov, A., Velikhov, E. and Sagdeev, R.: 1962, Quasi-linear theory of plasma oscillations, *Nuclear Fusion* p. 465.
- Watson, G. N.: 1922, *A Treatise on the Theory of Bessel Functions*, Cambridge University Press, Cambridge.
- Watson, K.: 1956, Use of the Boltzmann equation for the study of ionized gases of low density .1., *Physical Review* **102**, 12.
- Wentzel, G.: 1926, Eine verallgemeinerung der quantenbedingungen fur die zwecke der wellenmechanik, *Z. Physik.* **38**, 518.
- White, R., Chen, L. and Lin, Z.: 2002, Resonant plasma heating below the cyclotron frequency, *Physics of Plasmas* **9**, 1890.
- White, W., Malmberg, J. and Driscoll, C.: 1982, Resistive-wall destabilization of diocotron waves, *Physical Review Letters* **49**, 1822.
- Woltjer, L.: 1958, A theorem on force-free magnetic fields, *Proceedings of the National Academy of Sciences* **44**, 489.
- Wong, A., Motley, R. and D'Angelo, N.: 1964, Landau damping of ion acoustic waves in highly ionized plasmas, *Physical Review A* **133**, A436.
- Yu, J. H. and Driscoll, C.: 2002, Diocotron wave echoes in a pure electron plasma, *IEEE Trans. Plasma Science* **30**, 24.

Appendix A

Intuitive method for vector calculus identities

Instead of providing the traditional ‘back of the book’ list of vector calculus identities, an intuitive method⁵ for deriving these identities will now be presented.

The building blocks for this are the rules for the vector algebra triple product and for the dot-cross product. These two vector rules will first be reviewed and then the method for combining the vector rules with the rules of calculus will be presented.

Vector algebra triple product

There are two forms for the vector triple product, depending on the location of the parenthesis on the left hand side, namely:

$$\mathbf{A} \times \left(\underbrace{\mathbf{B}}_{\text{middle}} \times \underbrace{\mathbf{C}}_{\text{outer}} \right) = \underbrace{\mathbf{B}}_{\text{middle}} \left(\underbrace{\mathbf{A} \cdot \mathbf{C}}_{\substack{\text{other two} \\ \text{dotted together}}} \right) - \underbrace{\mathbf{C}}_{\text{outer}} \left(\underbrace{\mathbf{A} \cdot \mathbf{B}}_{\substack{\text{other two} \\ \text{dotted together}}} \right) \quad (\text{A.1})$$

$$\left(\underbrace{\mathbf{A}}_{\text{outer}} \times \underbrace{\mathbf{B}}_{\text{middle}} \right) \times \mathbf{C} = \underbrace{\mathbf{B}}_{\text{middle}} \left(\underbrace{\mathbf{A} \cdot \mathbf{C}}_{\substack{\text{other two} \\ \text{dotted together}}} \right) - \underbrace{\mathbf{A}}_{\text{outer}} \left(\underbrace{\mathbf{B} \cdot \mathbf{C}}_{\substack{\text{other two} \\ \text{dotted together}}} \right). \quad (\text{A.2})$$

Both of these distinct forms can be remembered by the two-word mnemonic “middle-outer”. The words middle and outer are defined with reference to the left hand side of both equations; middle refers to the middle vector in the group of three and outer refers to the outer vector in the parentheses. The first term on the right hand side is in the vector direction of the “middle” vector with the other two vectors dotted together; the second term on the right hand side is in the direction of the “outer” vector with the other two vectors dotted together.

Dot-Cross product

Now consider the combination of dot and cross, $\mathbf{A} \cdot \mathbf{B} \times \mathbf{C}$. Here the rules are that the dot and cross can be interchanged without changing the result and the order can be cyclically permuted without changing the result, but if the cyclic order is changed then the

⁵This method was explained to the author by the late C. Oberman.

sign changes. Thus

$$\mathbf{A} \cdot \mathbf{B} \times \mathbf{C} = \mathbf{A} \times \mathbf{B} \cdot \mathbf{C} \quad \text{interchange dot and cross,} \quad (\text{A.3})$$

$$\mathbf{A} \cdot \mathbf{B} \times \mathbf{C} = \mathbf{B} \times \mathbf{C} \cdot \mathbf{A} \quad \text{permutation maintaining cyclic order,} \quad (\text{A.4})$$

$$\mathbf{A} \cdot \mathbf{B} \times \mathbf{C} = -\mathbf{A} \cdot \mathbf{C} \times \mathbf{B} \quad \text{permutation changing cyclic order.} \quad (\text{A.5})$$

Derivation of the vector calculus identities

The basic idea is to replace one of the vectors by the ∇ operator and then rearrange terms and if necessary add terms. The criterion for these maneuvers is that, just like getting the right piece placed in a jigsaw puzzle, here all applicable rules of vector algebra and of calculus must be simultaneously satisfied. The simple example

$$\nabla \cdot (\psi \mathbf{Q}) = \psi \nabla \cdot \mathbf{Q} + \mathbf{Q} \cdot \nabla \psi \quad (\text{A.6})$$

illustrates this principle of satisfying the vector algebra and the calculus rules simultaneously. Here the dot always goes between the ∇ and the \mathbf{Q} in order to satisfy the rules of vector algebra and the ∇ operates once on \mathbf{Q} and once on ψ in order to satisfy the product rule $(ab)' = ab' + a'b$ of calculus.

A less trivial example is $\nabla \cdot (\mathbf{B} \times \mathbf{C})$. Here the ∇ must operate on both \mathbf{B} and \mathbf{C} according to the product rule so, neglecting vector issues for now, the result must be of the form $\mathbf{B} \nabla \mathbf{C} + \mathbf{C} \nabla \mathbf{B}$. This basic product rule result is then adjusted to satisfy the vector dot-cross rules. In particular, the dots and crosses may be interchanged at will and the sign is plus if the cyclic order is $\nabla \mathbf{B} \mathbf{C}$, $\mathbf{B} \mathbf{C} \nabla$, or $\mathbf{C} \nabla \mathbf{B}$ and the sign is minus if the cyclic order is $\nabla \mathbf{C} \mathbf{B}$, $\mathbf{C} \mathbf{B} \nabla$, or $\mathbf{B} \nabla \mathbf{C}$. Since the ∇ is supposed to operate on only one vector at a time, we pick the arrangement where the ∇ is in the middle and either \mathbf{B} or \mathbf{C} is to its right so that each of \mathbf{B} or \mathbf{C} has a turn at being acted on by the ∇ operator. The arrangements of interest are thus $\mathbf{C} \cdot \nabla \times \mathbf{B}$ and $-\mathbf{B} \cdot \nabla \times \mathbf{C}$ where the minus sign has been inserted to account for the change in cyclic order. The result is

$$\nabla \cdot (\mathbf{B} \times \mathbf{C}) = \mathbf{C} \cdot \nabla \times \mathbf{B} - \mathbf{B} \cdot \nabla \times \mathbf{C} \quad (\text{A.7})$$

which satisfies both the vector algebra dot-cross rule and the product rule of calculus.

Next consider the triple product $\mathbf{A} \times (\nabla \times \mathbf{C})$. Here the ∇ operates only on the \mathbf{C} and the vector triple product generates two terms as indicated by Eq.(A.1). Expanding the triple product according to Eq.(A.1) while arranging an ordering of terms where the ∇ operates only on \mathbf{C} gives

$$\mathbf{A} \times \left(\underbrace{\nabla}_{\text{middle}} \times \underbrace{\mathbf{C}}_{\text{outer}} \right) = \left(\underbrace{\nabla}_{\text{middle}} \underbrace{\mathbf{C}}_{\text{outer}} \right) \cdot \mathbf{A} - \left(\underbrace{\mathbf{A} \cdot \nabla}_{\text{middle}} \right) \underbrace{\mathbf{C}}_{\text{outer}}. \quad (\text{A.8})$$

Thus, the first term on the right hand side has its vector direction determined by ∇ with the other two terms dotted together, and the parenthesis indicates that the ∇ operates only on \mathbf{C} . The second term on the right hand side has its vector direction determined by \mathbf{C} with the other two terms dotted together and again the ∇ operates only on \mathbf{C} .

This can be rearranged as

$$(\nabla \mathbf{C}) \cdot \mathbf{A} = \mathbf{A} \times (\nabla \times \mathbf{C}) + \mathbf{A} \cdot \nabla \mathbf{C}. \quad (\text{A.9})$$

Interchanging \mathbf{A} and \mathbf{C} gives

$$(\nabla \mathbf{A}) \cdot \mathbf{C} = \mathbf{C} \times (\nabla \times \mathbf{A}) + \mathbf{C} \cdot \nabla \mathbf{A}. \quad (\text{A.10})$$

Adding these last two expressions gives

$$(\nabla \mathbf{C}) \cdot \mathbf{A} + (\nabla \mathbf{A}) \cdot \mathbf{C} = \mathbf{A} \times (\nabla \times \mathbf{C}) + \mathbf{A} \cdot \nabla \mathbf{C} + \mathbf{C} \times (\nabla \times \mathbf{A}) + \mathbf{C} \cdot \nabla \mathbf{A}. \quad (\text{A.11})$$

However, using the same arguments about maintaining the dot and satisfying the product rule shows that

$$\begin{aligned}\nabla(\mathbf{A} \cdot \mathbf{C}) &= \nabla(\mathbf{C} \cdot \mathbf{A}) \\ &= (\nabla\mathbf{A}) \cdot \mathbf{C} + (\nabla\mathbf{C}) \cdot \mathbf{A}.\end{aligned}\quad (\text{A.12})$$

Here the ∇ operates once on the \mathbf{A} and once on the \mathbf{C} according to the product rule and the dot is always between the \mathbf{A} and the \mathbf{C} . Combining Eqs.(A.11) and (A.12) gives the standard vector identity

$$\nabla(\mathbf{A} \cdot \mathbf{C}) = \mathbf{A} \times (\nabla \times \mathbf{C}) + \mathbf{A} \cdot \nabla\mathbf{C} + \mathbf{C} \times (\nabla \times \mathbf{A}) + \mathbf{C} \cdot \nabla\mathbf{A}.\quad (\text{A.13})$$

Finally, the triple product with two ∇ 's can be expressed as

$$\nabla \times \left(\underbrace{\nabla}_{\text{middle}} \times \underbrace{\mathbf{A}}_{\text{outer}} \right) = \underbrace{\nabla}_{\text{middle}} \left(\underbrace{\nabla \cdot \mathbf{A}}_{\substack{\text{other two} \\ \text{dotted together}}} \right) - \underbrace{\nabla^2}_{\substack{\text{other two} \\ \text{dotted together}}} \underbrace{\mathbf{A}}_{\text{outer}} \quad (\text{A.14})$$

or, without the labeling, as

$$\nabla \times \nabla \times \mathbf{A} = \nabla \nabla \cdot \mathbf{A} - \nabla^2 \mathbf{A}.\quad (\text{A.15})$$

The relationships $\nabla \cdot \nabla \times \mathbf{A} = 0$ and $\nabla \times \nabla \psi = 0$ can be proved by direct evaluation using Cartesian coordinates.

Summary of vector identities

$$\begin{aligned}\mathbf{A} \times (\mathbf{B} \times \mathbf{C}) &= \mathbf{B}(\mathbf{A} \cdot \mathbf{C}) - \mathbf{C}(\mathbf{A} \cdot \mathbf{B}) \\ (\mathbf{A} \times \mathbf{B}) \times \mathbf{C} &= \mathbf{B}(\mathbf{A} \cdot \mathbf{C}) - \mathbf{A}(\mathbf{B} \cdot \mathbf{C}) \\ \mathbf{A} \cdot \mathbf{B} \times \mathbf{C} &= \mathbf{A} \times \mathbf{B} \cdot \mathbf{C}, \text{ interchange dot and cross} \\ \mathbf{A} \cdot \mathbf{B} \times \mathbf{C} &= \mathbf{B} \times \mathbf{C} \cdot \mathbf{A}, \text{ cyclic permutation, cyclic order maintained} \\ \mathbf{A} \cdot \mathbf{B} \times \mathbf{C} &= -\mathbf{A} \cdot \mathbf{C} \times \mathbf{B}, \text{ cyclic permutation, cyclic order changed} \\ \nabla \cdot (\psi \mathbf{A}) &= \psi \nabla \cdot \mathbf{A} + \mathbf{A} \cdot \nabla \psi \\ \nabla \cdot (\mathbf{A} \times \mathbf{B}) &= \mathbf{B} \cdot \nabla \times \mathbf{A} - \mathbf{A} \cdot \nabla \times \mathbf{B} \\ (\nabla \mathbf{B}) \cdot \mathbf{A} &= \mathbf{A} \times (\nabla \times \mathbf{B}) + \mathbf{A} \cdot \nabla \mathbf{B} \\ \nabla(\mathbf{A} \cdot \mathbf{B}) &= \mathbf{A} \times (\nabla \times \mathbf{B}) + \mathbf{A} \cdot \nabla \mathbf{B} + \mathbf{B} \times (\nabla \times \mathbf{A}) + \mathbf{B} \cdot \nabla \mathbf{A} \\ \nabla \times \nabla \times \mathbf{A} &= \nabla(\nabla \cdot \mathbf{A}) - \nabla^2 \mathbf{A} \\ \nabla \cdot \nabla \times \mathbf{A} &= 0 \\ \nabla \times \nabla \psi &= 0\end{aligned}$$

Appendix B

Vector calculus in orthogonal curvilinear coordinates

Derivation of generalized relations

Let x_1, x_2, x_3 be a right-handed set of orthogonal coordinates and let s be the distance along a curve in three dimensional space. Let h_i be the scale factor relating an increment in the i^{th} coordinate to an increment in length in that direction so

$$dl_i = h_i dx_i; \tag{B.1}$$

an example is the ϕ direction of cylindrical coordinates where $dl_\phi = r d\phi$. Since the coordinates are assumed to be orthogonal, the increment in distance along a curve in three dimensional space is

$$(ds)^2 = h_1^2 (dx_1)^2 + h_2^2 (dx_2)^2 + h_3^2 (dx_3)^2. \tag{B.2}$$

The $\{x_1, x_2, x_3\}$ coordinates and corresponding $\{h_1, h_2, h_3\}$ scale factors for Cartesian, cylindrical, and spherical coordinate systems are listed in Table B.1 below.

coordinate system	distance along a curve	$\{x_1, x_2, x_3\}$	$\{h_1, h_2, h_3\}$
Cartesian	$(dx)^2 + (dy)^2 + (dz)^2$	$\{x, y, z\}$	$\{1, 1, 1\}$
cylindrical	$(dr)^2 + (rd\phi)^2 + (dz)^2$	$\{r, \phi, z\}$	$\{1, r, 1\}$
spherical	$(dr)^2 + (rd\theta)^2 + (r \sin \theta d\phi)^2$	$\{r, \theta, \phi\}$	$\{1, r, r \sin \theta\}$

Table B.1: Coordinate systems and their scale factors

The differential of the scalar ψ for a displacement by dl_1 of the coordinate x_1 is

$$d\psi = dl_1 \hat{x}_1 \cdot \nabla \psi \tag{B.3}$$

so the component of the gradient operator in the direction of \hat{x}_1 is

$$\hat{x}_1 \cdot \nabla \psi = \frac{d\psi}{dl_1} = \frac{1}{h_1} \frac{\partial \psi}{\partial x_1}. \tag{B.4}$$

The partial derivative notation is invoked in the right-most expression because the displacement is just in the direction of x_1 .

Generalized gradient operator

Because the coordinates are independent, a displacement in the direction of one coordinate does not affect the dependence on the other coordinates and so the gradient operator is just the sum of its components in the three orthogonal directions, i.e.,

$$\nabla = \frac{\hat{x}_1}{h_1} \frac{\partial}{\partial x_1} + \frac{\hat{x}_2}{h_2} \frac{\partial}{\partial x_2} + \frac{\hat{x}_3}{h_3} \frac{\partial}{\partial x_3}. \tag{B.5}$$

Since $\nabla x_1 = \hat{x}_1/h_1$, the unit vector in the x_1 direction is

$$\hat{x}_1 = h_1 \nabla x_1. \quad (\text{B.6})$$

Also, because the coordinates form a right-handed orthogonal system the unit vectors are related by

$$\hat{x}_1 \times \hat{x}_2 = \hat{x}_3, \quad \hat{x}_2 \times \hat{x}_3 = \hat{x}_1, \quad \hat{x}_3 \times \hat{x}_1 = \hat{x}_2. \quad (\text{B.7})$$

Generalized divergence and curl

Let \mathbf{V} be an arbitrary vector

$$\mathbf{V} = V_1 \hat{x}_1 + V_2 \hat{x}_2 + V_3 \hat{x}_3 \quad (\text{B.8})$$

and consider the divergence of the first term,

$$\begin{aligned} \nabla \cdot (V_1 \hat{x}_1) &= \nabla \cdot (V_1 \hat{x}_2 \times \hat{x}_3) \\ &= \nabla \cdot (V_1 h_2 \nabla x_2 \times h_3 \nabla x_3) \\ &= \nabla (h_2 h_3 V_1) \cdot \nabla x_2 \times \nabla x_3 \\ &= \nabla (h_2 h_3 V_1) \cdot \frac{\hat{x}_2 \times \hat{x}_3}{h_2 h_3} \\ &= \frac{\hat{x}_1}{h_2 h_3} \cdot \nabla (h_2 h_3 V_1) \\ &= \frac{1}{h_1 h_2 h_3} \frac{\partial}{\partial x_1} (h_2 h_3 V_1). \end{aligned} \quad (\text{B.9})$$

Extending this to all three terms gives the general form for the divergence to be

$$\nabla \cdot \mathbf{V} = \frac{1}{h_1 h_2 h_3} \left(\frac{\partial}{\partial x_1} (h_2 h_3 V_1) + \frac{\partial}{\partial x_2} (h_1 h_3 V_2) + \frac{\partial}{\partial x_3} (h_1 h_2 V_3) \right). \quad (\text{B.10})$$

Now consider the curl of the first term of the arbitrary vector, namely

$$\begin{aligned} \nabla \times (V_1 \hat{x}_1) &= \nabla \times (V_1 h_1 \nabla x_1) \\ &= \nabla (V_1 h_1) \times \nabla x_1 \\ &= \frac{1}{h_1} \nabla (V_1 h_1) \times \hat{x}_1 \end{aligned} \quad (\text{B.11})$$

and so

$$\nabla \times \mathbf{V} = \frac{1}{h_1} \nabla (V_1 h_1) \times \hat{x}_1 + \frac{1}{h_2} \nabla (V_2 h_2) \times \hat{x}_2 + \frac{1}{h_3} \nabla (V_3 h_3) \times \hat{x}_3. \quad (\text{B.12})$$

The component in the direction of \hat{x}_1 is

$$\begin{aligned} \hat{x}_1 \cdot \nabla \times \mathbf{V} &= \frac{1}{h_2} \nabla (V_2 h_2) \times \hat{x}_2 \cdot \hat{x}_1 + \frac{1}{h_3} \nabla (V_3 h_3) \times \hat{x}_3 \cdot \hat{x}_1 \\ &= \frac{1}{h_2} \nabla (V_2 h_2) \cdot \hat{x}_2 \times \hat{x}_1 + \frac{1}{h_3} \nabla (V_3 h_3) \cdot \hat{x}_3 \times \hat{x}_1 \\ &= \frac{1}{h_3} \hat{x}_2 \cdot \nabla (V_3 h_3) - \frac{1}{h_2} \hat{x}_3 \cdot \nabla (V_2 h_2) \\ &= \frac{1}{h_2 h_3} \frac{\partial}{\partial x_2} (V_3 h_3) - \frac{1}{h_2 h_3} \frac{\partial}{\partial x_3} (V_2 h_2) \end{aligned} \quad (\text{B.13})$$

Thus the general form of the curl of the arbitrary vector is

$$\begin{aligned}\nabla \times \mathbf{V} &= \frac{1}{h_2 h_3} \left(\frac{\partial}{\partial x_2} (V_3 h_3) - \frac{\partial}{\partial x_3} (V_2 h_2) \right) \hat{x}_1 \\ &\quad + \frac{1}{h_1 h_3} \left(\frac{\partial}{\partial x_3} (V_1 h_1) - \frac{\partial}{\partial x_1} (V_3 h_3) \right) \hat{x}_2 \\ &\quad + \frac{1}{h_1 h_2} \left(\frac{\partial}{\partial x_1} (V_2 h_2) - \frac{\partial}{\partial x_2} (V_1 h_1) \right) \hat{x}_3 \\ &= \frac{1}{h_1 h_2 h_3} \begin{vmatrix} h_1 \hat{x}_1 & h_2 \hat{x}_2 & h_3 \hat{x}_3 \\ \partial/\partial x_1 & \partial/\partial x_2 & \partial/\partial x_3 \\ h_1 V_1 & h_2 V_2 & h_3 V_3 \end{vmatrix}.\end{aligned}\quad (\text{B.14})$$

Generalized Laplacian of a scalar

The Laplacian of a scalar is

$$\nabla^2 \psi = \nabla \cdot \left(\frac{\hat{x}_1}{h_1} \frac{\partial \psi}{\partial x_1} + \frac{\hat{x}_2}{h_2} \frac{\partial \psi}{\partial x_2} + \frac{\hat{x}_3}{h_3} \frac{\partial \psi}{\partial x_3} \right).\quad (\text{B.15})$$

Using Eq.(B.10) this becomes

$$\nabla^2 \psi = \frac{1}{h_1 h_2 h_3} \left(\frac{\partial}{\partial x_1} \left(\frac{h_2 h_3}{h_1} \frac{\partial \psi}{\partial x_1} \right) + \frac{\partial}{\partial x_2} \left(\frac{h_3 h_1}{h_2} \frac{\partial \psi}{\partial x_2} \right) + \frac{\partial}{\partial x_3} \left(\frac{h_1 h_2}{h_3} \frac{\partial \psi}{\partial x_3} \right) \right).\quad (\text{B.16})$$

The Laplacian of a vector in general differs from the Laplacian of a scalar because there are derivatives of unit vectors. However the general formula is overly complex and so the Laplacian of a vector will only be calculated for cylindrical coordinates which are typically of most interest.

Application to Cartesian coordinates

$$\{x_1, x_2, x_3\} = \{x, y, z\}; \{h_1, h_2, h_3\} = \{1, 1, 1\}$$

$$\nabla \psi = \hat{x} \frac{\partial \psi}{\partial x} + \hat{y} \frac{\partial \psi}{\partial y} + \hat{z} \frac{\partial \psi}{\partial z}\quad (\text{B.17})$$

$$\nabla \cdot \mathbf{V} = \frac{\partial V_x}{\partial x} + \frac{\partial V_y}{\partial y} + \frac{\partial V_z}{\partial z}\quad (\text{B.18})$$

$$\begin{aligned}\nabla \times \mathbf{V} &= \left(\frac{\partial V_z}{\partial y} - \frac{\partial V_y}{\partial z} \right) \hat{x} + \left(\frac{\partial V_x}{\partial z} - \frac{\partial V_z}{\partial x} \right) \hat{y} \\ &\quad + \left(\frac{\partial V_y}{\partial x} - \frac{\partial V_x}{\partial y} \right) \hat{z}\end{aligned}\quad (\text{B.19})$$

$$\nabla^2 \psi = \frac{\partial^2 \psi}{\partial x^2} + \frac{\partial^2 \psi}{\partial y^2} + \frac{\partial^2 \psi}{\partial z^2}\quad (\text{B.20})$$

$$\nabla^2 \mathbf{V} = \frac{\partial^2 \mathbf{V}}{\partial x^2} + \frac{\partial^2 \mathbf{V}}{\partial y^2} + \frac{\partial^2 \mathbf{V}}{\partial z^2}\quad (\text{B.21})$$

Application to cylindrical coordinates

$$\{x_1, x_2, x_3\} = \{r, \phi, z\}; \{h_1, h_2, h_3\} = \{1, r, 1\}$$

$$\nabla\psi = \hat{r} \frac{\partial\psi}{\partial r} + \frac{\hat{\phi}}{r} \frac{\partial\psi}{\partial\phi} + \hat{z} \frac{\partial\psi}{\partial z} \quad (\text{B.22})$$

$$\nabla \cdot \mathbf{V} = \frac{1}{r} \frac{\partial}{\partial r} (rV_r) + \frac{1}{r} \frac{\partial V_\phi}{\partial\phi} + \frac{\partial V_z}{\partial z} \quad (\text{B.23})$$

$$\begin{aligned} \nabla \times \mathbf{V} &= \left(\frac{1}{r} \frac{\partial V_z}{\partial\phi} - \frac{\partial V_\phi}{\partial z} \right) \hat{r} + \left(\frac{\partial V_r}{\partial z} - \frac{\partial V_z}{\partial r} \right) \hat{\phi} \\ &\quad + \frac{1}{r} \left(\frac{\partial}{\partial r} (rV_\phi) - \frac{\partial V_r}{\partial\phi} \right) \hat{z} \end{aligned} \quad (\text{B.24})$$

$$\nabla^2\psi = \frac{1}{r} \frac{\partial}{\partial r} \left(r \frac{\partial\psi}{\partial r} \right) + \frac{1}{r^2} \frac{\partial^2\psi}{\partial\phi^2} + \frac{\partial^2\psi}{\partial z^2} \quad (\text{B.25})$$

Laplacian of a vector in cylindrical coordinates

Before proceeding, note that the cylindrical coordinate unit vectors can be expressed in terms Cartesian unit vectors as

$$\hat{r} = \hat{x} \cos \phi + \hat{y} \sin \phi \quad (\text{B.26})$$

$$\hat{\phi} = -\hat{x} \sin \phi + \hat{y} \cos \phi \quad (\text{B.27})$$

so

$$\frac{\partial}{\partial\phi} \hat{r} = \hat{\phi}, \quad \frac{\partial}{\partial\phi} \hat{\phi} = -\hat{r}. \quad (\text{B.28})$$

Thus

$$\nabla \hat{r} = \left(\hat{r} \frac{\partial}{\partial r} + \frac{\hat{\phi}}{r} \frac{\partial}{\partial\phi} + \hat{z} \frac{\partial}{\partial z} \right) \hat{r} = \frac{\hat{\phi}\hat{\phi}}{r} \quad (\text{B.29})$$

$$\nabla \hat{\phi} = \left(\hat{r} \frac{\partial}{\partial r} + \frac{\hat{\phi}}{r} \frac{\partial}{\partial\phi} + \hat{z} \frac{\partial}{\partial z} \right) \hat{\phi} = -\frac{\hat{\phi}\hat{r}}{r} \quad (\text{B.30})$$

and

$$\nabla^2 \hat{r} = -\frac{1}{r^2} \hat{r} \quad (\text{B.31})$$

$$\nabla^2 \hat{\phi} = -\frac{1}{r^2} \hat{\phi}. \quad (\text{B.32})$$

These results can now be used to calculate $\nabla^2 (V_r \hat{r})$ and $\nabla^2 (V_\phi \hat{\phi})$ which can then be

used to construct the full Laplacian. The first calculation gives

$$\begin{aligned}
\nabla^2 (V_r \hat{r}) &= \nabla \cdot \nabla (V_r \hat{r}) \\
&= \nabla \cdot ((\nabla V_r) \hat{r} + V_r \nabla \hat{r}) \\
&= \hat{r} \nabla^2 V_r + (\nabla V_r) \cdot \nabla \hat{r} + \nabla \cdot (V_r \nabla \hat{r}) \\
&= \hat{r} \nabla^2 V_r + 2 \nabla V_r \cdot \nabla \hat{r} + V_r \nabla^2 \hat{r} \\
&= \hat{r} \nabla^2 V_r + \frac{2 \hat{\phi}}{r} \cdot \nabla V_r + \frac{V_r}{r^2} \frac{\partial^2}{\partial \phi^2} \hat{r} \\
&= \hat{r} \nabla^2 V_r + \frac{2 \hat{\phi}}{r^2} \frac{\partial V_r}{\partial \phi} - \frac{V_r}{r^2} \hat{r}
\end{aligned} \tag{B.33}$$

while the second calculation gives

$$\begin{aligned}
\nabla^2 (V_\phi \hat{\phi}) &= \nabla \cdot \nabla (V_\phi \hat{\phi}) \\
&= \nabla \cdot ((\nabla V_\phi) \hat{\phi} + V_\phi \nabla \hat{\phi}) \\
&= \hat{\phi} \nabla^2 V_\phi + 2 \nabla V_\phi \cdot \nabla \hat{\phi} + V_\phi \nabla^2 \hat{\phi} \\
&= \hat{\phi} \nabla^2 V_\phi - \frac{2 \hat{r}}{r^2} \frac{\partial V_\phi}{\partial \phi} - \frac{V_\phi}{r^2} \hat{\phi}.
\end{aligned} \tag{B.34}$$

Since $\nabla^2 (V_z \hat{z}) = \hat{z} \nabla^2 V_z$ it is seen that the Laplacian of a vector in cylindrical coordinates is

$$\begin{aligned}
\nabla^2 \mathbf{V} &= \hat{r} \left(\nabla^2 V_r - \frac{2}{r^2} \frac{\partial V_\phi}{\partial \phi} - \frac{V_r}{r^2} \right) \\
&\quad + \hat{\phi} \left(\nabla^2 V_\phi + \frac{2}{r^2} \frac{\partial V_r}{\partial \phi} - \frac{V_\phi}{r^2} \right) \\
&\quad + \hat{z} \nabla^2 V_z.
\end{aligned} \tag{B.35}$$

Equation (B.28) can also be used to calculate $\mathbf{V} \cdot \nabla \mathbf{V}$ giving

$$\begin{aligned}
\mathbf{V} \cdot \nabla \mathbf{V} &= \left(V_r \frac{\partial}{\partial r} + \frac{V_\phi}{r} \frac{\partial}{\partial \phi} + V_z \frac{\partial}{\partial z} \right) (V_r \hat{r} + V_\phi \hat{\phi} + V_z \hat{z}) \\
&= \hat{r} \left(V_r \frac{\partial V_r}{\partial r} + \frac{V_\phi}{r} \frac{\partial V_r}{\partial \phi} + V_z \frac{\partial V_r}{\partial z} - \frac{V_\phi^2}{r} \right) \\
&\quad + \hat{\phi} \left(V_r \frac{\partial V_\phi}{\partial r} + \frac{V_\phi}{r} \frac{\partial V_\phi}{\partial \phi} + V_z \frac{\partial V_\phi}{\partial z} + \frac{V_\phi V_r}{r} \right) \\
&\quad + \hat{z} \left(V_r \frac{\partial V_z}{\partial r} + \frac{V_\phi}{r} \frac{\partial V_z}{\partial \phi} + V_z \frac{\partial V_z}{\partial z} \right).
\end{aligned} \tag{B.36}$$

Application to spherical coordinates

$$\{x_1, x_2, x_3\} = \{r, \theta, \phi\}; \{h_1, h_2, h_3\} = \{1, r, r \sin \theta\}$$

$$\nabla \psi = \hat{r} \frac{\partial \psi}{\partial r} + \frac{\hat{\theta}}{r} \frac{\partial \psi}{\partial \theta} + \frac{\hat{\phi}}{r \sin \theta} \frac{\partial \psi}{\partial \phi} \quad (\text{B.37})$$

$$\nabla \cdot \mathbf{V} = \frac{1}{r^2} \frac{\partial}{\partial r} (r^2 V_r) + \frac{1}{r \sin \theta} \frac{\partial}{\partial \theta} (\sin \theta V_\theta) + \frac{1}{r \sin \theta} \frac{\partial}{\partial \phi} (V_\phi) \quad (\text{B.38})$$

$$\begin{aligned} \nabla \times \mathbf{V} &= \frac{1}{r \sin \theta} \left(\frac{\partial}{\partial \theta} (V_\phi \sin \theta) - \frac{\partial V_\theta}{\partial \phi} \right) \hat{r} \\ &+ \frac{1}{r \sin \theta} \left(\frac{\partial V_r}{\partial \phi} - \frac{\partial}{\partial r} (V_\phi r \sin \theta) \right) \hat{\theta} \\ &+ \frac{1}{r} \left(\frac{\partial}{\partial r} (V_\theta r) - \frac{\partial V_r}{\partial \theta} \right) \hat{\phi} \end{aligned} \quad (\text{B.39})$$

$$\nabla^2 \psi = \frac{1}{r^2} \frac{\partial}{\partial r} \left(r^2 \frac{\partial \psi}{\partial r} \right) + \frac{1}{r^2 \sin \theta} \frac{\partial}{\partial \theta} \left(\sin \theta \frac{\partial \psi}{\partial \theta} \right) + \frac{1}{r^2 \sin^2 \theta} \frac{\partial^2 \psi}{\partial \phi^2} \quad (\text{B.40})$$

Appendix C

Frequently used physical constants and formulae

Physical constants (to 3 significant figures)

	symbol	value	unit
electron mass	m_e	9.11×10^{-31}	kg
proton mass	m_p	1.67×10^{-27}	kg
vacuum permeability	μ_0	$4\pi \times 10^{-7}$	N A ⁻²
vacuum permittivity	ϵ_0	8.85×10^{-12}	F m ⁻¹
speed of light	c	3.00×10^8	m s ⁻¹
electron charge	e	1.60×10^{-19}	C
Avogadro's number		6.02×10^{23}	mol ⁻¹
Boltzmann constant	κ	1.60×10^{-19}	J eV ⁻¹

Formulae

(all quantities in SI units, temperatures in eV, A is ion atomic mass number)

Lengths

Debye length (p.7)

$$\frac{1}{\lambda_D^2} = \sum_{\sigma} \frac{1}{\lambda_{\sigma}^2}$$

where σ is over all species participating in shielding and

$$\lambda_{\sigma} = \sqrt{\frac{\epsilon_0 \kappa T_{\sigma}}{n_{0\sigma} q_{\sigma}^2}} = 7.4 \times 10^3 \sqrt{\frac{T_{\sigma}}{n_{0\sigma}}} \text{ m}$$

Electron Larmor radius (p.234)

$$r_{Le} = \frac{\sqrt{\kappa T_e / m_e}}{|\omega_{ce}|} = 2.4 \times 10^{-6} \frac{\sqrt{T_e}}{B} \text{ m}$$

Ion Larmor radius (p.234)

$$r_{Li} = \frac{\sqrt{\kappa T_i / m_i}}{|\omega_{ci}|} = 1.0 \times 10^{-4} \frac{\sqrt{AT_i}}{B\sqrt{Z}} \text{ m}$$

where A is atomic mass and Z is ion charge.

Electron collisionless skin depth (p.145)

$$\frac{c}{\omega_{pe}} = \frac{5.3 \times 10^6}{\sqrt{n_e}} \text{ m}$$

Ion collisionless skin depth (assuming quasi-neutral plasma so $n_i Z = n_e$)

$$\frac{c}{\omega_{pi}} = 2.3 \times 10^8 \sqrt{\frac{A}{Z n_e}} \text{ m}$$

Frequencies

Electron plasma frequency (p.126)

$$f_{pe} = \frac{\omega_{pe}}{2\pi} = \frac{1}{2\pi} \sqrt{\frac{n_e e^2}{\epsilon_0 m_e}} = 9 \sqrt{n_e} \text{ Hz}$$

Ion plasma frequency (p.126)

$$f_{pi} = \omega_{pi} = \frac{1}{2\pi} \sqrt{\frac{n_i q_i^2}{\epsilon_0 m_i}} = 0.21 \sqrt{\frac{Z n_e}{A}} \text{ Hz}$$

Electron cyclotron frequency (p.79)

$$f_{ce} = \frac{1}{2\pi} |\omega_{ce}| = \frac{eB}{2\pi m_e} = 2.8 \times 10^{10} B \text{ Hz}$$

Ion cyclotron frequency (p.79)

$$f_{ci} = \frac{1}{2\pi} |\omega_{ci}| = \frac{ZeB}{2\pi m_i} = 1.55 \times 10^7 \frac{ZB}{A} \text{ Hz}$$

Upper hybrid frequency (p.186)

$$f_{uh} = \sqrt{f_{pe}^2 + f_{ce}^2}$$

Lower hybrid frequency (p.186)

$$f_{lh} = \sqrt{f_{ci}^2 + \frac{f_{pi}^2}{1 + \frac{f_{pe}^2}{f_{ce}^2}}}$$

Diocotron frequency (pure electron plasma, p.462)

$$f_{dioc} \simeq f_{pe}^2 / 2f_{ce}$$

Velocities

Electron thermal velocity (p.154)

$$v_{Te} = \sqrt{\frac{2\kappa T_e}{m_e}} = 5.9 \times 10^5 \sqrt{T_e} \text{ m s}^{-1}$$

Ion thermal velocity (p.154)

$$v_{Ti} = \sqrt{\frac{2\kappa T_i}{m_i}} = 1.4 \times 10^4 \sqrt{\frac{T_i}{A}} \text{ m s}^{-1}$$

Ion acoustic velocity (p.(4.33))

$$c_s = \sqrt{\frac{\kappa T_e}{m_i}} = 9.8 \times 10^3 \sqrt{\frac{T_e}{A}} \text{ m s}^{-1}$$

Electron diamagnetic drift velocity (p.250)

$$u_{d,e} = \frac{\kappa T}{eB} \left| \frac{1}{n} \nabla n \right| = \frac{T_e}{B} \left| \frac{1}{n} \nabla n \right| \text{ m s}^{-1}$$

Ion diamagnetic drift velocity (flow in opposite direction from electrons, (p.250))

$$u_{d,i} = \frac{\kappa T_i}{q_i B} \left| \frac{1}{n} \nabla n \right| = \frac{T_i}{ZB} \left| \frac{1}{n} \nabla n \right| \text{ m s}^{-1}$$

Alfvén velocity (p.132)

$$v_A = \frac{B}{\sqrt{\mu_0 n_i m_i}} = \frac{B}{\sqrt{\mu_0 n_e A m_p / Z}} = 2.2 \times 10^{16} B \sqrt{\frac{Z}{n_e A}} \text{ m s}^{-1}$$

Wave phase velocity (p.202)

$$v_{ph} = \frac{\omega}{k} = f\lambda$$

Dimensionless

Plasma beta (p.319)

$$\beta = \frac{2\mu_0 n \kappa T}{B^2} = \frac{4.0267 \times 10^{-25}}{B^2} n T$$

Lundquist number (p.381)

$$S = \frac{\mu_0 v_A L}{\eta}$$

Collisions, resistivity, and runaways

Electron-electron collision rate (p.21)

$$\nu_{ee} = 4 \times 10^{-12} \frac{n \ln \Lambda}{T_e^{3/2}} \text{ s}^{-1}$$

where $\ln \Lambda \sim 10$, electron-ion rate same magnitude, ion-ion slower by $\sqrt{m_e/m_i}$

Spitzer resistivity (p.394)

$$\eta = 1.03 \times 10^{-4} \frac{Z \ln \Lambda}{T_e^{3/2}} \text{ Ohm-m}$$

Dreicer runaway electric field (p.395)

$$E_{Dreicer} = 5.6 \times 10^{-18} n_e Z \frac{\ln \Lambda}{T_e} \text{ V/m.}$$

Typical neutral cross-section (p.16)

$$\sigma_{\text{neut}} \sim 3 \times 10^{-20} \text{ m}^2$$

Warm plasma waves

Electrostatic susceptibility (p.165)

$$\chi_\sigma = \frac{1}{k^2 \lambda_{D\sigma}^2} [1 + \alpha Z(\alpha)]$$

where $\alpha = \omega / kv_{T\sigma}$

Plasma dispersion function (p.165)

$$Z(\alpha) = \frac{1}{\pi^{1/2}} \int_{-\infty}^{\infty} d\xi \frac{\exp(-\xi^2)}{(\xi - \alpha)}$$

$$\lim_{\alpha \ll 1} Z(\alpha) = -2\alpha \left(1 - \frac{2\alpha^2}{3} + \dots \right) + i\pi^{1/2} \exp(-\alpha^2)$$

$$\lim_{\alpha \gg 1} Z(\alpha) = -\frac{1}{\alpha} \left[1 + \frac{1}{2\alpha^2} + \frac{3}{4\alpha^4} + \dots \right] + i\pi^{1/2} \exp(-\alpha^2)$$

Index

- action
 - integral in Lagrangian formalism, 63
 - in wave-wave coupling, 433
 - relation to quantum number, 433
- action integral, 67
- adiabatic invariance
 - breakdown of, 95
 - pendulum, 66
- adiabatic invariant
 - general proof for Hamiltonian system, 70
 - J, second adiabatic invariant, 88
 - mu conservation, 81
 - relation to quantum number, 68
 - third adiabatic invariant, 89
- adiabatic limit of energy equation, 40
- Airy equation, 241
- Alfven time, 370
- Alfven velocity, 183
- Alfven wave, 131
 - compressional (fast), 134, 136
 - in parameter space, 196
 - inertial Alfven wave, 187, 207
 - shear (slow), 137
 - two-fluid model, 138
 - compressional mode, 146
 - inertial Alfven wave, 144
 - kinetic Alfven wave, 145
- alpha particle, 296
- Altar-Appleton-Hartree dispersion relation, 197
- ambipolar diffusion, 18
- analytic continuation, 160
- antenna, 193
- Appleton-Hartree dispersion relation, 197
- arc, 290
- astrophysical jet, 295
- axisymmetry, 280
- bad curvature, 305
- ballistic term, 415
- beam echo, 416
- beat waves, 398
- Bennett pinch, 275, 295
- Bernstein waves, 236
- Bessel function model, 358
- Bessel relationships, 233
- beta, 319
- bilinear function, 311
- Bohm-Gross wave, 129
- Boltzmann relation
 - difficulties with, 498
 - in Debye shielding, 7
 - limitations of, 495
- bounded volume, 190
- bounding surface, 190
- break-even
 - fusion, 297
- break-even, fusion, 296
- Brillouin backscatter, 438
- Brillouin flow, 460
- Brillouin limit, 462
- Bromwich contour, 156
- Calugareanu theorem, 356
- canonical angular momentum, 99
 - in non-neutral plasma, 464
 - toroidal confinement, 285
- canonical momentum, 259
 - definition of, 64
- cathode emission, 27
- caviton, 214, 451
- center of mass frame dynamics, 382

- Child-Langmuir space charge limited emission, 29
- CMA diagram, 188
- coalescence
 - mode, 240
- coalescence, mode, 212
- cold plasma wave energy equation, 221
- collimation, 294
- collision
 - frequencies, 14
 - relations between cross-section, mean-free-path, 27
- collisions
 - and quasi-linear diffusion, 426
 - Coulomb, 11
 - Fokker-Planck model, 389
 - qualitative treatment in Vlasov equation, 34
 - with neutrals, 16
- condensation
 - of dusty plasma, 495
- confinement time, 296
- constant of the motion
 - definition of, 64
- convective derivative
 - definition of, 38
- coronal loop, 295
- correspondence of drift equations with MHD, 91
- coupled oscillator, 442
- cross-section
 - effective, for dust grain charging, 484
 - fusion, 297
 - neutral, 17
 - small-angle scattering, 13
- crystallization, 495
- crystallization criterion, dusty plasma, 501
- current
 - curvature, 93
 - diamagnetic, 91, 250
 - force-free in Grad-Shafranov equation, 281
 - grad B, 93
 - parallel, 268
 - polarization, 93
 - poloidal, 280
 - sheet, 362
 - sheet, in Sweet-Parker reconnection, 380
 - toroidal, 280
- curvature
 - good v. bad, 305, 318
 - magnetic field, 271
- curvature current, 93
- curvature drift, 80
- curved magnetic field, 79
- cusplike field, 103
- cutoff, 131, 185, 190
- cyclotron motion
 - sense of rotation, 29
- daughter wave, 429
- Debye shielding, 129
 - derivation of, 7
 - solution of pde for, 24
- decay instability, 428, 438
- delta W
 - in MHD energy principle, 313
- destructive interference, 202
- deuterium, 296
- diamagnetic, 282
 - current, 91
 - drift velocity, 250
- dielectric constant, 95
- dielectric tensor, 179
- dielectric tensor elements, 181
 - right, left hand polarization, 183
- diffusion
 - ambipolar, 18
 - magnetic, 364
 - quasi-linear velocity space, 405
- diocotron mode, 465
 - resistive wall, image charge method, 479
- distribution function
 - definition of, 31
 - for collisionless drift wave, 260
 - moments of, 33

- double adiabatic laws
 - derivation of, 49
- Dreicer electric field, 395
- drift equations, 73
 - curvature drift, 80
 - derivation of, 75
 - drift in arbitrary force field, 78
 - grad B drift, 80
 - grad B force, 78
 - polarization drift, 78
- drift wave, 249
 - collisional, 253
 - collisionless, 258
 - destabilization of, 257, 262
 - features, 257
 - nonlinear pumping of plasma, 257
- drifts
 - curvature, 80
 - $E \times B$, 73, 75
 - force, 75
 - generalization to arbitrary frequency, 110
 - grad B, 80
 - polarization, 78, 80
- dumbell wave normal surface, 191
- dust
 - charge on grain, 486
 - charging of grains, 485
 - levitation, 505
- dust acoustic waves, 491
- dust charging, 504
- dust ion acoustic waves, 494
- dusty plasma, 483
 - crystalization criterion, 501
 - crystallization (condensation), 495
 - parameter space, 490
- dynamic equilibria, 274, 286
- E cross B drift, 73, 80
- echoes, 412
 - higher order, 426
 - spatial, 425
- effective potential, 99
- electric field
 - runaway (Dreicer), 395
- electromagnetic plasma wave
 - in inhomogeneous plasma, 211
- electromagnetic wave
 - derivation of, 130
 - in decay instability, 442
- electron plasma wave, 129
 - in decay instability, 440
- electrostatic ion cyclotron wave, 263
- ellipsoid wave normal surface, 191
- energy
 - inductive, 273
 - per helicity, 344
 - wave, 219
- energy conservation
 - in nonlinear waves, 399
- energy equation
 - adiabatic limit, 40
 - isothermal limit, 40
 - wave, 219
- energy equation, two-fluid, 40
- energy principle, 306
- energy transfer between waves and particles, 114
- entropy
 - collisions, 43
 - conservation of, 413
 - of a distribution function, 41
- equilibrium
 - impossibility of spherically symmetric MHD, 295
 - stable v. unstable, 298
- extraordinary wave, 186
- fast mode, 134, 192
- Fermi acceleration, 88
- first adiabatic invariant, 82
- floating potential, 57
- flow (MHD accelerated), 286
 - compressible, 291
 - incompressible, 286
 - stagnation of, 294
- flux
 - accumulation of toroidal flux in flow, 294
 - frozen-in, inductance, 272
 - poloidal, 97
 - private and public, 379

- relation to vector potential, 97
 - volume per unit, 334
- flux linkage, 346
- flux preservation, 272
- flux surface, 96
 - in mirror, 91
- flux tube
 - Grad-Shafranov solution for, 295
- Fokker-Planck theory, 382
- force
 - axial MHD force, 287
 - between parallel currents, 268
 - centrifugal, 79
 - flux-conserving, 273
 - hoop, 270
 - non-conservative, 286
 - pinch, 269
- force-free
 - magnetic field, 344
- force-free equilibrium, 322, 335
 - Bessel function model, 358
 - Lundquist solution, 358
- force-free magnetic field, 268
- free-energy
 - in sheared non-neutral plasma, 477
- frequently used formulae, 524
- frictional drag, 391
 - qualitative derivation of, 37
- frozen-in flux
 - proof of, 48
- fusion
 - break-even, 297
 - criteria for, 296
- Gaussian integrals, 59
- geometric optics, 213
- good curvature, 305
- grad B
 - current, 93
 - drift, 80
 - force, 78
- Grad-Shafranov equation, 278
- Green's function in diocotron mode, 474
- group velocity, 201
- guiding center
 - definition of, 76
- Hall term, 48
- Hamilton-Lagrange formalism, 62
- Hamiltonian, 64, 65
 - coupled harmonic oscillator, 430
 - geometric optics, 213
- Helmholtz equation, 358
- Hermitian part, 223
- hollow profile, 474
- hoop force, 270
- ignitron, 29
- ignorable coordinate, 64
- image charge, line, 479
- inductance, 272
- induction equation, 49
 - in magnetic reconnection, 366
- inhomogeneous plasmas, 210
- initial condition
 - Poisson's equation as, 179
- initial value, 158
- instability
 - caviton, 451
 - decay, 428
 - free-boundary, 323, 326
 - kink, 325, 331
 - parametric, 428
 - positron-electron streaming, 150
 - Rayleigh-Taylor, 299
 - resistive wall, 471
 - sausage, 323, 331
 - streaming, 149
- ion acoustic velocity
 - in sheath, 56
- ion acoustic wave, 129
 - in decay instability, 439
 - Landau damping of, 170
 - Landau instability, 176
- ion saturation current, 56
- ion-ion resonance, 208
- isothermal limit of energy equation, 40
- J, second adiabatic invariant, 87

- jet
 - astrophysical, 295
- joining, in mode conversion, 249
- kappa
 - magnetic curvature, 271
- Kelvin vorticity theorem, 463
- kink, 323
- kink instability, 325, 331
 - diamagnetic or paramagnetic?, 335
- Korteweg-de Vries equation, 455
- Kruskal-Shafranov stability criterion, 333
- Lagrange multipliers, 58
- Lagrange's equation, 64
- Lagrangian
 - electromagnetic, 64
- Landau damping, 169
 - and entropy, 413
- Landau problem, 153
- Langmuir probe, 56
- Langmuir wave, 129
- Laplace transform, 155
 - and ballistic term, 415
- Laplace's equation, 265
- Larmor radius
 - poloidal, 285
- laser fusion, 458
- Lawson criterion, 296
- leap-frog numerical integration, 25
- lightning bolt, 200
- line-averaged density, 131
- linear mode conversion, 241
- linearization, general method, 123
- loss-cone, 87
- lower hybrid frequency, 186
- Lundquist number, 381
- Lundquist solution, 358
- magnetic
 - axis, 283
 - diffusion, 364
 - islands, 376
 - reconnection, 360
 - shear, 305
- magnetic field
 - force-free, 268
 - minimum energy, 343
 - most general axisymmetric, 279
 - pressure, 268
 - reconnection in sheared field, 371
 - Solov'ev solution, 282
 - tension, 268
 - vacuum, 265
- magnetic field curvature, 271
- magnetic helicity, 320, 336, 345
 - association with current-driven instability, 319
 - conservation equation, 321, 357
 - conservation of, 341
 - global, 322
 - linkage, 336
 - linked ribbons, 358
 - twist, 338
- magnetic mirror, 84
- magnetic moments
 - density of, 92
- magnetic pressure, 268
- magnetic stress tensor, 271
- magnetic tension, 268
- magnetization, 92
- magnetofluid, definition of, 306
- magnetoplasma dynamic thruster, 290
- magnetron, 481
- Manley-Rowe relations, 430
- Maxwellian distribution
 - definition of, 44
- MHD equations
 - derivation of, 46
 - Ohm's law, derivation of, 47
- MHD with neutrals, 60
- minimum energy
 - frozen-in flux, 272
- minimum energy magnetic field, 343
- moments of distribution function, 33
- momentum conservation
 - in nonlinear waves, 399
- mu conservation, 81
- mu, definition of, 82
- National Ignition Facility, 459

- negative energy wave, 225
- neutron, 296
- nominal plasma parameters, 21
- non-adiabatic motion, 95
- non-linear dispersion relation, 444
- non-neutral plasma, 460
 - relation to Landau damping, 476
- non-resonant particles
 - in quasilinear velocity space diffusion, 411
- numerical integration of particle trajectory, 25

- orbital motion limited model, 485, 504
- ordinary wave, 186
- orthogonal curvilinear coordinates, 518
- overdense, 197

- parallel current, 268
- paramagnetic, 282
- parameter space, 195
- parametric decay instability, 428, 458
- Parker reconnection model, 378
- Penrose criterion, 172
- phase integral, 232
- phase mixing, 202
 - and echoes, 416
- phase space, 30
- physical constants, 524
- pinch
 - Bennett, 295
- pinch force, 269
- plasma dispersion function
 - definition of, 165
 - large argument limit of, 167
 - small argument limit of, 167
- plasma frequency
 - definition of, 126
- plateau velocity distribution, 412
- Plemelj formula, 171
- polarization current, 93
 - relation to capacitance, 95
- polarization drift, 78, 80
 - change in particle energy, 120
 - in Alfvén wave, 132
 - relation to MHD equation of motion, 93
 - stochastic motion, 106
- poles, 160
- poloidal
 - definition of, 279
- poloidal flux, 279
- poloidal Larmor radius, 285
- poloidal magnetic field, 280
- ponderomotive force, 436, 448
- Poynting flux, 220, 309
- Poynting theorem, 357
- pressure
 - magnetic, 268
- pressure tensor, definition of, 37
- principal resonances, 190
- private flux, 379
- product rule for oscillating physical quantities, 221
- public flux, 379
- pump
 - MHD acceleration of fluid, 290
- pump depletion, 457
- pump wave, 429
- pure electron plasma, 460

- QL modes, 199
- QT modes, 199
- quantum mechanics, 323
- quantum mechanics, correspondence to, 214
- quasi-linear velocity space diffusion, 399
- quasi-neutrality, 9
- quasilinear diffusion
 - and collisions, 426
- quiver velocity, 436

- radiation pressure, 436
- radius of curvature, 79
- Raman backscatter, 438
- random velocity, 37
- reduced mass, 383
- redundancy of Poisson's equation, 178

refractive index
 definition of, 181
 relaxation, 341
 relaxed state, 344
 residues, 160
 resistive mode, 360
 resistive time, 371
 resistive wall instability, 471, 479
 resistivity
 Fokker-Planck model, 393
 simple derivation of, 17
 resonance, 185, 190
 ion cyclotron, 193
 ion-ion, 208
 resonance cones, 204
 resonant particles
 in quasilinear velocity space diffusion, 407, 409
 reversal of magnetic field
 spatial (cusp), 103
 temporal, 102
 reversed field pinch, 285, 344
 ribbon, gift-wrapping, 358
 Richardson-Dushman temperature
 limited emission, 29
 Rosenbluth potentials, 388, 395
 runaway electric field, 395, 397
 Rutherford scattering
 derivation, 22

 saddle point, 243
 safety factor, 333
 tokamak, 375
 sausage instability, 323, 331
 scale factor, 518
 scattering
 energy transfer, 23
 large angle, 12
 Rutherford, 11, 22
 small angle, 13
 second adiabatic invariant, 87
 self-adjointness, 310
 self-confinement
 impossibility of, 276
 self-focusing, 438
 separatrix, 284

 sheath physics, 53
 sheet current, 362
 short wave radio transmission, 228
 slow mode, 192
 slow wave, 133
 Snell's law, 211
 solar corona loop, 295, 381
 soliton
 interaction, 456
 ion acoustic wave, 454
 propagating envelope, 453
 stationary envelope, 452
 Solov'ev solution, 282
 orbits in, 295
 space-charge-limited current, 27
 spheromak, 285, 344
 stagnation of flow, 294
 static equilibria, 274
 steepest-descent contour, 242
 stellarator, 285
 stimulated Raman scattering, 458
 Stirling's formula, 58
 stochastic motion, 106
 streaming instability, 149
 stress tensor
 magnetic, 271
 strongly-coupled plasma, 495
 surface wave, 214
 susceptibility
 definition of, 126
 Sweet-Parker
 reconnection, 378
 symmetry
 assumption in MHD jet, 286
 canonical angular momentum & toroidal confinement, 285
 in Grad-Shafranov equation, 280
 in Lagrangian formalism, 64
 in solution of Grad-Shafranov equation, 280

 taxonomy of cold plasma waves, 188
 Taylor relaxation, 341
 TE mode, 216
 tearing, 364
 temperature limited current, 27

- tension
 - magnetic, 268
- thermal force, 59
- third adiabatic invariant, 89
- thruster, 290
- TM mode, 216
- tokamak, 285, 333
- topology
 - minimum energy, 273
- torque, 286
- trapped particle
 - in mirror, 87
- tritium, 296
- twist and writhe, 351, 356
- two-fluid equations
 - derivation of, 36
- underdense, 197
- unperturbed orbit, 232
- untrapped particle
 - in mirror, 87
- upper hybrid frequency, 186
- vacuum magnetic field, 265
- vector calculus identities, 515
- vector potential, 320
 - relation to flux, 97
- velocity
 - Alfven, 132, 183
 - bounce-averaged, 90
 - definitions of ‘average’ velocity, 110
 - diamagnetic drift, 250
 - group, 201
 - in sawtooth wave, 111
 - in small amplitude oscillatory field, 108
 - quiver, 436
- virial theorem, 276
- viscosity, 274, 286
- Vlasov equation
 - derivation of, 31
 - moments of, 34
 - treatment of collisions, 34
- volume per unit flux, 334
- vortices
 - magnetic reconnection, 364
- vorticity, 286
 - source for, 289
- wall stabilization, 326
- warm plasma dispersion relation
 - (electrostatic), 234
- water beading, 362
- wave
 - Alfven, 131
 - beating, 398
 - Bernstein, 236
 - definition of cold plasma wave, 178
 - drift, 249
 - dust acoustic, 491
 - dust Alfven, 504
 - dust ion acoustic, 494
 - dust whistler, 505
 - electron-plasma, 129
 - electrostatic ion cyclotron, 263
 - energy equation, 219, 221
 - energy, finite temperature wave, 224
 - extraordinary, 186
 - frequency dispersion, 201
 - ion acoustic, 129
 - magnetized cold plasma dispersion, 181
 - negative energy, 225
 - ordinary, 186
 - quasi-electrostatic cold plasma, 203
 - surface, 214
 - whistler, 200
- wave energy
 - in diocotron mode, 468
- wave normal surface, 188, 191
- wave-wave nonlinearity, 428
- waveguide, plasma, 214
- wheel wave normal surface, 191
- whistler wave, 200, 207
- Wigner-Seitz radius, 487
- WKB approximation, 66
- WKB criterion, 212
- WKB mode

correspondence to saddle point, 245
WKB solution, 211
WKB solutions
 of mode conversion problem, 249
Woltjer-Taylor relaxation, 341

work function, 29
writhe and twist, 351, 356

X-point, 379

Yukawa solution, 9, 24, 495, 498